Total Synthesis and Study of Myrmicarin Alkaloids

by

Alison Evelynn Ondrus

BSc, Chemistry (2004)

University of Alberta

Submitted to the Department of Chemistry
in Partial Fulfillment of the Requirements for the Degree of
Doctor of Philosophy in Chemistry

at the

Massachusetts Institute of Technology

June 2009

Signature of Author.....
Department of Chemistry
May 13, 2009

Certified by.....
Mohammad Movassaghi
Associate Professor of Chemistry
Thesis Supervisor

Accepted by.....
Robert W. Field
Chairman, Department Committee on Graduate Students

This doctoral thesis has been examined by a committee in the Department of Chemistry as follows:

Professor Rick L. Danheiser..... .....
Chairman

Associate Professor Mohammad Movassaghi.....
Thesis Supervisor

Professor Timothy F. Jamison.....

To my family, and to PJ

Preface

Portions of this work have been adapted from the following articles that were co-written by the author and are reproduced in part with permission from:

Movassaghi, M.; Ondrus, A. E. "Palladium-Catalyzed Synthesis of *N*-Vinyl Pyrroles and Indoles" *J. Org. Chem.* **2005**, *70*, 8638–8641. Copyright 2005 American Chemical Society.

Movassaghi, M.; Ondrus, A. E. "Enantioselective Total Synthesis of Tricyclic Myrmicarin Alkaloids" *Org. Lett.* **2005**, *7*, 4423–4426. Copyright 2005 American Chemical Society.

Ondrus, A. E.; Movassaghi, M. "Dimerization of (+)-Myrmicarin 215B. A Potential Biomimetic Approach to Complex Myrmicarin Alkaloids" *Tetrahedron* **2006**, *62*, 5287–5297. Copyright 2006 Elsevier Ltd.

Movassaghi, M.; Ondrus, A. E.; Chen, B. "Efficient and Stereoselective Dimerization of Pyrroloindolizine Derivatives Inspired by a Hypothesis for the Biosynthesis of Complex Myrmicarin Alkaloids." *J. Org. Chem.* **2007**, *72*, 10065–10074. Copyright 2007 American Chemical Society.

Ondrus. A. E.; Movassaghi, M. "Total Synthesis and Study of Myrmicarin Alkaloids" *Chem. Commun.* **2009**, *accepted*. Copyright 2009 The Royal Society of Chemistry.

Ondrus, A. E.; Movassaghi, M. "Reversible Dimerization of (+)-Myrmicarin 215B" *Org. Lett.* **2009**, *submitted*.

Total Synthesis and Study of Myrmicarin Alkaloids

by

Alison Evelynn Ondrus

Submitted to the Department of Chemistry
on May 13th, 2009 in Partial Fulfillment of the
Requirements for the Degree of Doctor of Philosophy in
Organic Chemistry

ABSTRACT

I. Enantioselective Total Synthesis of Tricyclic Myrmicarin Alkaloids

An enantioselective gram-scale synthesis of a key dihydroindolizine intermediate for the preparation of myrmicarin alkaloids is described. Key transformations in this convergent approach include a stereospecific palladium-catalyzed *N*-vinylation of a pyrrole with a vinyl triflate, a copper-catalyzed enantioselective conjugate reduction of a β-pyrrolyl enoate, and a regioselective Friedel-Crafts reaction. The synthesis of optically active and isomerically pure samples of (4a*R*)-myrmicarins 215A, 215B, and 217 in addition to their respective C4a epimers is presented.

II. Palladium Catalyzed Synthesis of *N*-Vinyl Pyrroles and Indoles

A stereospecific palladium catalyzed *N*-vinylation of azaheterocycles with vinyl triflates is described. Cyclic and acyclic vinyl triflates along with non-nucleophilic azaheterocycles were found to be substrates for this palladium catalyzed synthesis of *N*-vinyl pyrrole and indole derivatives.

III. Dimerization of (+)-Myrmicarin 215B. A Potential Biomimetic Approach to Complex Myrmicarin Alkaloids

The acid promoted diastereoselective dimerization of myrmicarin 215B is described. The reactivity of these sensitive alkaloids, structural assignment, and a possible mechanism for the observed dimerization are discussed. These finding raise the intriguing possibility of the synthesis of the highly sensitive myrmicarin alkaloids based on a strategy involving the direct dimerization of functional tricyclic myrmicarin derivatives.

IV. Efficient and Stereoselective Dimerization of Pyrroloindolizine Derivatives Inspired by a Hypothesis for the Biosynthesis of Complex Myrmicarin Alkaloids

Pyrroloindolizine derivatives participate in efficient and stereoselective homo- and heterodimerization reactions upon treatment with Brønsted or Lewis acids. The distinctive ability of pyrroloindolizines to act as azafulvenium ion precursors provides direct access to both heptacyclic and hexacyclic dimeric products. The inherent reactivity of these structures suggests a concise synthesis of complex myrmicarin alkaloids *via* dimerization of pyrroloindolizines, and may have implications for the biosynthesis of these intriguing alkaloids.

V. Reversible Dimerization of (+)-Myrmicarin 215B

Brønsted acid-promoted reversible dimerization of myrmicarin 215B leads to formation of a new heptacyclic product, isomyrmicarin 430B, that possesses a C1,C2-*trans*, C2,C3-*trans* substituted cyclopentane ring. Mechanistic studies illustrate that isomyrmicarin 430B arises by isomerization of isomyrmicarin 430A *via* fragmentation to tricyclic azafulvenium ions. Factors influencing the structure of heptacyclic isomyrmicarin products and potential relevance of this reversible vinyl pyrroloindolizine dimerization to the biosynthesis of complex myrmicarins are discussed.

Thesis Supervisor: Mohammad Movassaghi
Title: Associate Professor of Chemistry

Table of Contents

Abbreviations

Å	angstrom
[α]	specific rotation
Ac	acetyl
AIBN	2,2'-azobisisobutyronitrile
anis	anisaldehyde
aq	aqueous
atm	atmosphere
B3LYP	3-parameter hybrid Becke exchange/Lee–Yang–Parr correlation functional
BEMP	2-*tert*-butylimino-2-diethylamino-1,3-dimethyl-perhydro-1,3,2-diazaphosphorine
BINAP	2,2′-bis(diphenylphosphino)-1,1′-binaphthyl
br	broad
brsm	yield based on recovered starting material
Bu	butyl
°C	degree Celsius
calcd	calculated
CAM	ceric ammonium molybdate
cm	centimeter
cm^{-1}	wavenumber
COSY	correlation spectroscopy
d	doublet
d	deuterium
δ	parts per million
DEAD	diethyl azodicarboxylate
DFT	density functional theory
diam	diameter
DMAP	4-dimethylaminopyridine
DMF	*N*,*N*-dimethylformamide
DMSO	dimethylsulfoxide
dr	diastereomeric ratio
E	entgegen
ee	enantiomeric excess
EI	electron ionization
equiv	equivalent
ESI	electrospray ionization
Et	ethyl
FMO	fronteir molecular orbital
FT	Fourier transform
g	gram
g	gradient
GC	gas chromatography
h	hour
ht	height
hν	photochemical irradiation

FT	Fourier transform
HMBC	heteronuclear multiple bond correlation
HOMO	highest occupied molecular orbital
HPLC	high performance liquid chromatography
HRMS	high resolution mass spectroscopy
HSQC	heteronuclear single quantum correlation
Hz	Hertz
i	iso
IBX	2-iodoxybenzoic acid
IR	infrared
isoM430A	isomyrmicarin 430A
isoM430B	isomyrmicarin 430B
J	coupling constant
kcal	kilocalorie
KHMDS	potassium hexamethyldisilylamide
L	liter
LAH	lithium aluminum hydride
LDA	lithium diisopropylamide
LHMDS	lithium hexamethyldisilylamide
lit.	literature value
LUMO	lowest unoccupied molecular orbital
m	medium
m	multiplet
M	molar
μ	micro
M215A	myrmicarin 215A
M215B	myrmicarin 215B
M217	myrmicarin 217
M237A	myrmicarin 237A
M237B	myrmicarin 237B
M430A	myrmicarin 430A
M645	myrmicarin 645
M663	myrmicarin 663
Me	methyl
mg	milligram
MHz	megahertz
min	minute
mL	milliliter
mm	millimeter
mmol	millimole
μmol	micromole
mol	mole
MO	molecular orbital
MS	mass spectrometry
m/z	mass to charge ratio
n	normal

nm	nanometer
NMR	nuclear magnetic resonance
nOe	nuclear Overhauser effect
NOESY	nuclear Overhauser effect spectroscopy
o.d.	outer diameter
OTf	trifluoromethanesulfonate
p	*para*
Pd_2dba_3	palladium dibenzylideneacetone
Ph	phenyl
pH	hydrogen ion concentration
PMA	phosphomolybdic acid
PMHS	polymethylhydrosiloxane
ppm	parts per million
PPTS	pyridinium *p*-toluenesulfonate
Pr	propyl
psi	pounds per square inch
Pyr	pyridine
q	quartet
R_f	retention factor
ROESY	rotating frame Overhauser effect spectroscopy
s	secondary
s	singlet
s	strong
SPhos	dicyclohexyl(2',6'-dimethoxybiphenyl-2-yl)phosphine
str	stretch
t	triplet
t	tertiary
TBAF	tetra-*n*-butylammonium fluoride
TES	triethylsilyl
TFA	trifluoroacetic acid
Tf_2O	trifluoromethanesulfonic anhydride
THF	tetrahydrofuran
TIPS	triisopropylsilyl
TLC	thin layer chromatography
TMS	trimethylsilyl
Torr	1/760 atmosphere
UV	ultraviolet
v/v	volume per unit volume
w	weak
XPhos	dicyclohexyl(2',4',6'-triisopropylbiphenyl-2-yl)phosphine
Z	zusammen

Chapter I.

Enantioselective Total Synthesis of Tricyclic Myrmicarin Alkaloids

Introduction and Background

The myrmicarins are a family of structurally fascinating alkaloids found in the poison gland secretion of the African ant species *Myrmicaria opaciventris* (Figure 1).[1,2] Of the alkaloids produced by ants of the *myrmicinae* group, the higher molecular weight myrmicarins display an unprecedented level of complexity.[3] In addition to challenges presented by their elaborate molecular architectures, the isolation and structure elucidation of the complex myrmicarins has been complicated by their air sensitivity.[4] While the bicyclic and tricyclic myrmicarins can be purified chromatographically, myrmicarin 663 (**1**) is the only complex member that has been isolated and characterized as a single component.[5] By contrast, the extreme sensitivity of myrmicarin 430A (**3**) necessitated its characterization as a mixture with the tricyclic myrmicarins in a sample taken directly from the poison gland. Structural assignments for both myrmicarin 430A (**3**) and myrmicarin 663 (**1**) have been achieved using a combination of phase-sensitive two-dimensional NMR techniques. Although submilligram samples of myrmicarin 645 (**2**) have been obtained, the scarcity and oxidative sensitivity of this compound have prevented assignment of its relative stereochemistry.[1,6] Interestingly, while another alkaloid with a molecular weight of 430 was identified during mass spectrometric analysis of the poison gland secretion,[1b,c] no structural information on this compound was obtained.

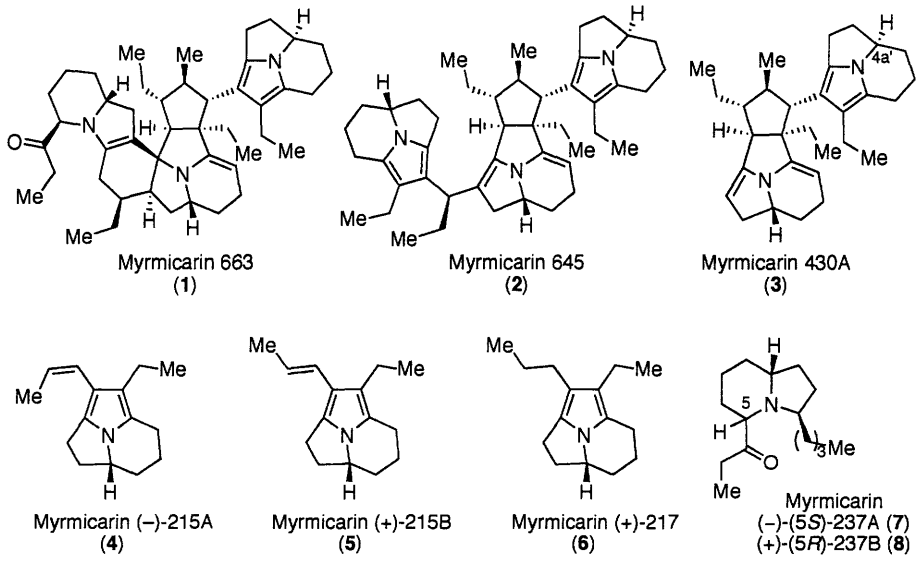

Figure 1. The Myrmicarin alkaloid family.

The intriguing molecular structures of these poisonous alkaloids combined with challenges associated with their sensitivity provide an exciting arena to test and discover new methodologies for organic synthesis. Herein we describe a convergent synthesis of all naturally occurring tricyclic myrmicarin alkaloids employing an efficient approach to a pivotal optically active dihydroindolizine intermediate. The first preparation of isomerically pure samples of myrmicarins 215A (**4**) and myrmicarin 215B (**5**) is discussed. Key steps of the synthesis include an efficient palladium-catalyzed fragment coupling reaction, a copper catalyzed asymmetric conjugate reduction and a regioselective Friedel-Crafts reaction.

Previous Syntheses of Tricyclic Myrmicarins

Motivated by the prominent role of the poison gland secretion in the ecology of the *Myrmicaria* ants and the potent toxicity of the previously unidentified alkaloid constituents, Schröder, Francke, and coworkers embarked on elegant studies to identify the alkaloid poisons produced by *Myrmicaria eumenoides*. A series of detailed structure correlation studies enabled them to access enantioenriched samples of myrmicarin 237A (**7**) and myrmicarin 237B (**8**), establishing the absolute stereochemistry of these bicyclic myrmicarins.[1d] In 1996, Schröder, Francke, and coworkers disclosed the isolation and structure assignment of the tricyclic myrmicarins 215A (**4**), myrmicarin 215B (**5**), and myrmicarin 217 (**6**).[1c] Two years later they reported the first synthesis of myrmicarin 217 (**6**) (Scheme 1).[7] In line with a biomimetic proposal presented in the isolation paper, the key step of this synthesis involved dehydrative cyclization of an unsaturated derivative of myrmicarin 237A (**7**) or myrmicarin 237B (**8**) to provide myrmicarin 217 (**6**). Commencing with piperidine **9**, available in four steps from a reported intermediate in their synthesis of myrmicarin 237A (**7**) and myrmicarin 237B (**8**),[1d] gentle heating of a benzene solution of **9** under dinitrogen atmosphere resulted in efficient conversion to myrmicarin 217 (**6**). *In situ* ^{1}H NMR monitoring revealed that condensation between the amine and the C3 ketone initially produced the C5,C9-*cis* indolizidine **10**, the proposed unsaturated derivative of myrmicarin 237A (**7**). Rapid epimerization at C5 provided a mixture of stereoisomers. In a slower process, intramolecular addition of the C3-C1" enamine to the C1' ketone and dehydration of the resulting alcohol afforded the pyrroloindolizine structure of myrmicarin 217 (**6**).

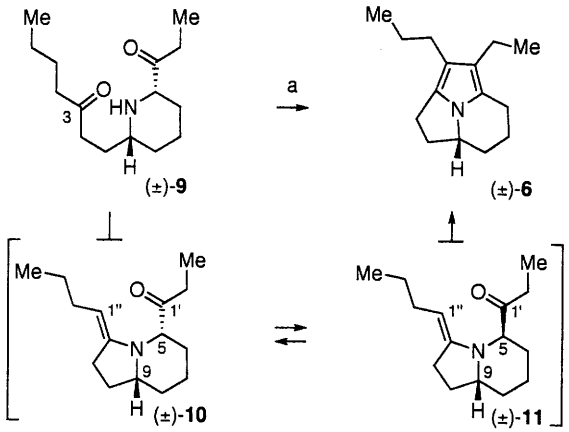

Scheme 1. Schröder and Francke's synthesis of racemic myrmicarin 217 (**6**). Conditions: a) C_6H_6, 40 °C, 53%.

Schröder and Francke note that formation of myrmicarin 237A (**7**), myrmicarin 237B (**8**), and myrmicarin 217 (**6**) from related monocyclic precursors provides support for an analogous biosynthetic relationship. They postulate that myrmicarin 215A (**4**) and myrmicarin 215B (**5**) might likewise arise *via* cyclization of a doubly unsaturated analogue of myrmicarin 237A (**7**) or myrmicarin 237B (**8**), citing the presence of trace amounts of alkaloids with mass 233 in the poison gland secretion as potential evidence for the existence of this intermediate. The corresponding bicylic and tricyclic substructures in the complex myrmicarins prompt them to propose a doubly unsaturated derivative of myrmicarin 237A (**7**) or myrmicarin 237B (**8**) as a common biogenetic precursor to these alkaloids.

The first enantioselective synthesis of (+)-(*R*)-myrmicarin 217 (**6**) was disclosed by Vallée *et al* in 2000 (Scheme 2).[8] Condensation between the D-glutamic acid diethyl ester and tetrahydro-2,5-dimethoxyfuran furnished the enantioenriched *N*-alkylpyrrole **12**. Lewis acid-induced intramolecular Friedel-Crafts cyclization of diester **12** yielded bicycle **13**.[9] Exhaustive reduction of the C7 ketone with sodium cyanoborohydride in the presence of zinc diiodide followed by ester reduction with lithium aluminum hydride generated alcohol **14**. Elaboration to the mixed anhydride **15** and boron trifluoride-induced cyclization yielded the tricylic ketone **16**. Under the directing influence of the C3 carbonyl substituent, completely regioselective acylation at C1 provided diketone **17**. Reduction of both carbonyl groups using lithium aluminum hydride and Vilsmeier-Haak acylation at the remaining unsubstituted pyrrole position generated ketone **19**. Finally, lithium aluminum hydride reduction of the C8 carbonyl substituent furnished (+)-(*R*)-myrmicarin 217 (**6**).

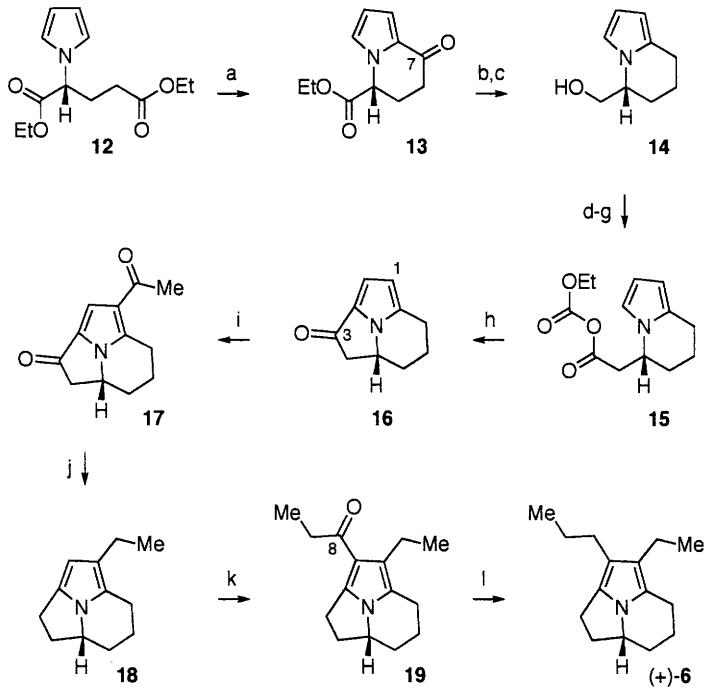

Scheme 2. Vallée's synthesis of (+)-myrmicarin 217 (**6**). Conditions: a) BBr_3, CH_2Cl_2, 5→23 °C. b) $NaBH_3CN$, ZnI_2, CH_2Cl_2, 40 °C. c) $LiAlH_4$, THF, 0→23 °C, 72% (2-steps). d) MsCl, pyridine, CH_2Cl_2, 0 °C. e) NaCN, DMF, 90 °C, 90% (2-steps). f) NaOH, H_2O, MeOH, 65 °C, 90%. g) EtOC(O)Cl, Et_3N, THF, 0 °C. h) BF_3OEt_2, CH_2Cl_2, 40 °C, 57% (2-steps). i) MeC(O)Cl, $AlCl_3$, CH_2Cl_2, 40 °C, 93%. j) $LiAlH_4$, THF, 65 °C, 60%. k) $MeCH_2C(O)NMe_2$, $POCl_3$, toluene, 90 °C, 68%. l) $LiAlH_4$, 1,4-dioxane, 100 °C, 60%.

Intercepting Vallée's synthesis at intermediate **14** (Scheme 2), in 2000 Lazzaroni *et al* reported a formal synthesis of (–)-(*S*)-*ent*-myrmicarin 217 ((–)-*ent*-**6**) (Scheme 3).[10] Cyclodehydration of the aldehyde **20**[11] provided bicycle **21**, whereupon hydrogenation of the alkene and ester reduction provided alcohol *ent*-**14**.

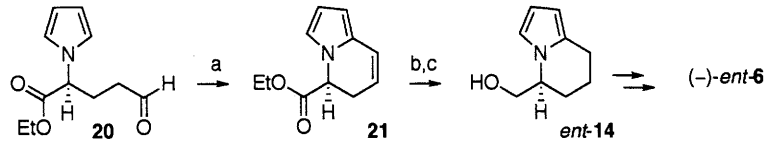

Scheme 3. Lazzaroni's formal synthesis of (–)-*ent*-myrmicarin 217 (*ent*-(–)-**6**). Conditions: a) DMSO, 100 °C, 2 h, 55%. b) H_2, Rh/C, Et_2O, 75%. c) $LiAlH_4$, THF, 23 °C, 80%.

In 2001 Vallée reported the synthesis of myrmicarin 215A (**4**) and myrmicarin 215B (**5**) as a mixture of geometric isomers (Scheme 4).[12] For the purpose of investigating the regioselectivity of acylation in tricycle **22**, they employed lithium aluminum hydride reduction to remove the electron withdrawing C3 ketone in **16**. Careful optimization of acylating agent,

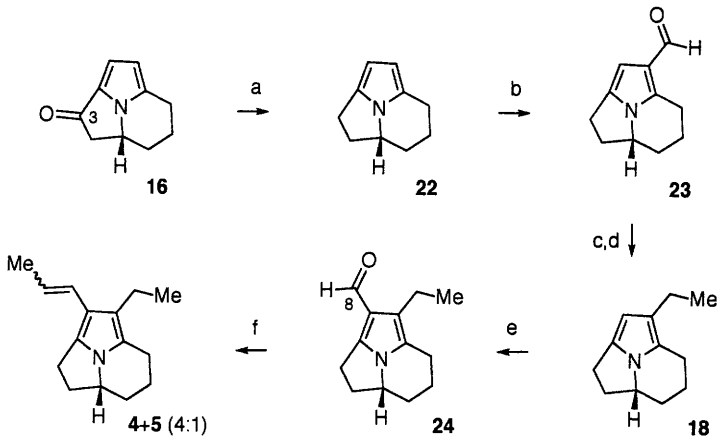

Scheme 4. Vallée's synthesis of enantioenriched myrmicarin 215A (**4**) and myrmicarin 215B (**5**) as a mixture of alkene isomers. Conditions: a) $LiAlH_4$, 1,4-dioxane, 100 °C, 86%. b) DMF, $POCl_3$, toluene, 83 °C, 2 h, 53%. c) MeLi, THF, 0 °C. d) $LiAlH_4$, 1,4-dioxane, 88 °C, 72% (2-steps). e) DMF, $POCl_3$, CH_2Cl_2, 40 °C, 80%. f) Ph_3PEtBr, NaH, THF, 65 °C, 78%, 4:1 **4**:**5**.

reaction solvent, and reaction temperature revealed that formylation of **22** under Vilsmeier conditions in toluene at 83 °C afforded **23** as the exclusive monoformylation product in 53% yield. Elaboration to **18** followed by a second Vilsmeier-Haack reaction and Wittig homologation of the resulting C8 aldehyde provided myrmicarin 215A (**4**) and myrmicarin 215B (**5**) as a 4:1 mixture.

Results and Discussion

We envisioned utilization of optically active dihydroindolizine **25** as a key intermediate for the preparation of myrmicarin alkaloids (Scheme 1). A regioselective Friedel-Crafts reaction of the pyrrole ring (C7a-alkylation) upon Brønsted–acid activation of dimethoxyacetal **26** and elimination of methanol was expected to afford bicyclic vinyl pyrrole **25**. We planned to use a metal-catalyzed enantioselective conjugate reduction of the β-pyrrolyl enoate **27** to introduce the C4a-stereochemistry.[13,14] A convergent synthesis of the pyrrolylenoate **27** was envisioned *via* a metal–catalyzed union of pyrrole **29** and readily available *Z*-vinyl triflate **28** (Scheme 5).

The synthesis of the required β-pyrrolylenoate **27** began with the Claisen condensation of lithium enolate **30** and methyl 4-(dimethoxy)-butyrate (**31**)[15] to give β-ketoester **32** (Scheme 6). The lithium *tert*-butoxide additive was crucial to ensure rapid deprotonation of product **32**, thus preventing the addition of a second equivalent of the lithium enolate **30**.[16] The trapping of the sodium enolate of β-ketoester **32** with Comins reagent (2-[*N*,*N*- bis(trifluoromethylsulfonyl)-

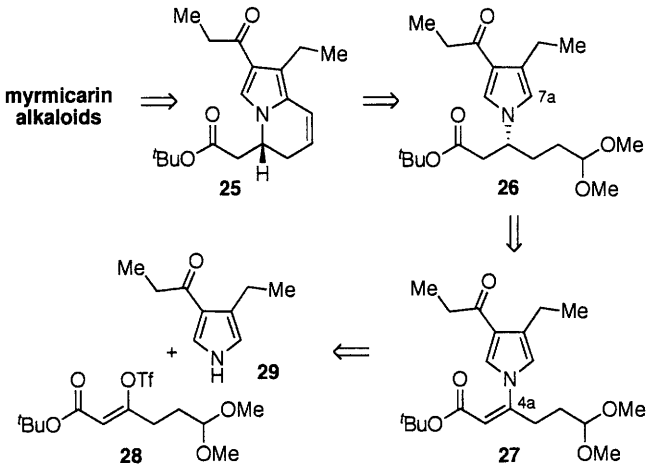

Scheme 5. Our retrosynthetic analysis of the tricyclic myrmicarins.

amino]-5-chloropyridine) gave vinyl triflate **28** in 82% yield with high *Z*-alkene selectivity (*Z*:*E*, >20:1).[17] Early in our studies, we relied on the use of a copper–catalyzed *N*-vinylation of pyrroles for the synthesis of the requisite β-pyrrolyl enoates.[14,18] However, due to difficulties associated with the synthesis of the necessary *Z*-β-iodoenoates[19] containing acid sensitive functional groups, we turned our attention to the use of configurationally defined vinyl triflates.[20]

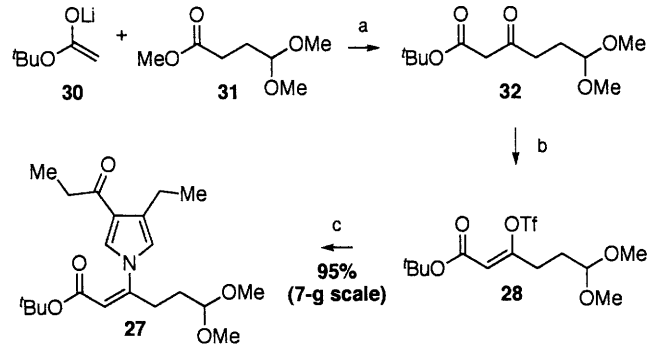

Scheme 6. Synthesis of enoate **27**. Conditions: a) ^{t}BuOLi, THF, –40 °C, 60%. b) NaH, THF, Comins reagent, 0→23 °C, 82%, >20:1 dr. c) **29**, Pd_2dba_3, XPhos, **29**, K_3PO_4, 18 h, toluene, 60 °C, 95%.

While copper-based catalyst systems were not effective, the use of palladium dibenzylideneacetone (Pd_2dba_3) and 2-dicyclohexyl-phosphino-2′,4′,6′-triisopropyl-1,1′-biphenyl (XPhos)[21] provided a highly active catalyst system for the desired coupling reaction.[22] Under optimal conditions, stereospecific coupling of pyrrole **29** and *Z*-vinyl triflate **28** provided the desired *Z*-β-pyrrolyl enoate **27** in 95% yield on multi–gram scale (Scheme 6). This represents the first example of a palladium–catalyzed *N*-vinylation of an azaheterocycle by a vinyl triflate.

The convergent assembly of enoate **27** provides all of the carbons necessary for preparation of the tricyclic myrmicarins.

We planned to introduce the C4a-stereochemistry of the myrmicarin alkaloids through an enantioselective conjugate reduction of enoate **27** (Scheme 5). A variety of efficient catalytic methods have been reported for the synthesis of optically active β-amino acid derivatives.[23] In particular, we were interested in the utilization of a recently reported methodology for the catalytic asymmetric reduction of β-azaheterocyclic enoates.[14] Gratifyingly, the copper-catalyzed reduction of enoate **27** in the presence of (*S*)-2,2′-bis(diphenylphosphino)-1,1′-binaphthyl (BINAP) and the stoichiometric reductant polymethylhydrosiloxane (PMHS) proceeded efficiently to provide optically active β-pyrrolyl ester **26**. After minor optimization for the isolation of the substrate at hand, the reduction of enoate **27** proceeded to give (*R*)-β-pyrrolyl ester **26** in 89% yield and 85% ee on a 2-gram scale (Scheme 7).[24,25] It should be noted that upon completion of our total synthesis of myrmicarin 217 (**6**) from β-pyrrolyl ester **26** prepared using (*R*)-BINAP, we discovered that the conjugate reduction of enoate **27** had proceeded unexpectedly[14] to give (*S*)-β-pyrrolyl ester **26**.[26]

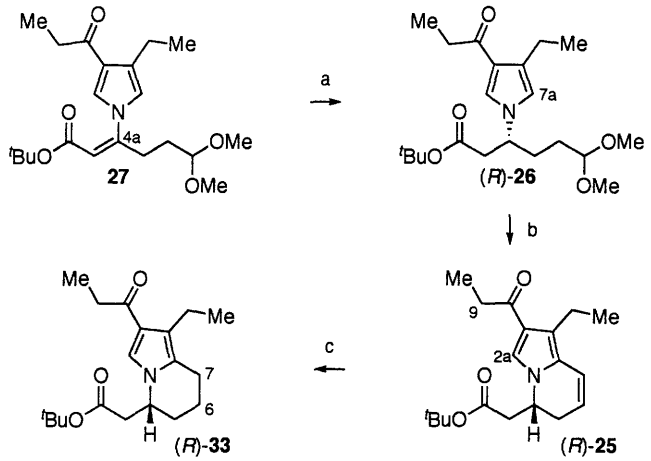

Scheme 7. Enantioselective synthesis of tetrahydroindolizine **33**. Conditions: a) $Cu(OAc)_2 \cdot H_2O$, (*S*)-BINAP, THF, PMHS, ^{t}BuOH, 23 °C, 3 h, 89%, 85% ee. b) Acetone–H_2O–AcOH (2:1:1), 40 °C, 100%, >10:1 dr. c) H_2 (1 atm), Pd/C, EtOAc, 96%.

With a multi-gram enantioselective synthesis of both enantiomers of β-pyrroly ester **26** at hand, we turned our attention to the synthesis of the dihydroindolizine **25**, a key intermediate for the synthesis of the myrmicarin alkaloids (Scheme 1). Optimal conditions (acetone–acetic acid–

water, 2:1:1, 40 °C) were identified for the quantitative conversion of β-pyrrolyl ester **26** to the bicyclic vinyl pyrrole with good regioselectivity (>10:1) for the desired C7a-cyclization product **25** (Scheme 7).[27] The formation of desired dihydroindolizine **25** as the major regioisomer was confirmed by a 9.2% nOe between the C9-methylene of the propanoyl group and the pyrrole C2a-methine upon irradiation of the C2a-methine. Compared to earlier studies employing *N*-alkylpyrrole derivatives, the use of acyl pyrrole **29** in the preparation of **25** not only provided a more convergent synthesis, but the C8-carbonyl also afforded greater stability for isolation and storage of key intermediates towards myrmicarin alkaloids.[28] Hydrogenation of dihydroindolizine (*R*)-**25** gave the tetrahydroindolizine (*R*)-**33** in 96% yield. The corresponding tetrahydroindolizine (*S*)-**33** was prepared with the same efficiency starting with (*S*)-**26**.

The introduction of the third ring of the pyrroloindolizine structure required the reduction of the C3-ester **33** to the corresponding C3-alcohol **34** (Scheme 8). Selective reduction of the C3-ester **33** was accomplished in a single operation by transiently protecting the C8-ketone as a silyl enol ether. In this sequence, conversion of C8-ketone (*R*)-**33** to the corresponding triisopropylsilyl enol ether derivative, reduction of the *tert*-butyl ester by lithium aluminum hydride, and protodesilylation by addition of aqueous hydrochloric acid (pH 1) provided the desired alcohol (*R*)-**34** in 91% yield. That this sequence could be executed in a single flask greatly simplified the preparation of alcohol **34**.[25] Treatment of alcohol (*R*)-**34** with a mixture of triphenylphosphine, iodine, and imidazole led to the conversion of the primary alcohol to the primary iodide (*R*)-**35** in 91% yield. Based on prior literature precedent[29] for cyclization of *N*-(ω-alkyl) radicals onto pyrroles containing an electron–withdrawing group, we first chose to explore free–radical cyclization strategies for the conversion of iodide **35** to tricyclic ketone **19**. Accordingly, treatment of iodide **35** with tri-*n*-butyltin hydride and 2,2′-azobisisobutyronitrile (AIBN) in toluene at reflux did provided tricycle **19**, albeit in low yields and with poor mass recovery (ca. 30–40%). Further attempts using oxidative radical cyclization[30] conditions did not lead to a significant improvement. Ultimately, the optimal conditions for the synthesis of tricyclic ketone **19** were found to involve an intramolecular C2-alkylation of the pyrrole nucleus by activation of the primary iodide in **35**.[31] Under strictly anhydrous conditions, treatment of (*R*)-**35** with silver tetrafluoroborate in a dichloromethane–benzene (3:1) solvent mixture at ambient temperature furnished tricyclic ketone (*R*)-**19** in 75% yield (Scheme 4). The identical sequence starting with ketoester (*S*)-**33** furnished the corresponding alcohol (*S*)-**34**, primary

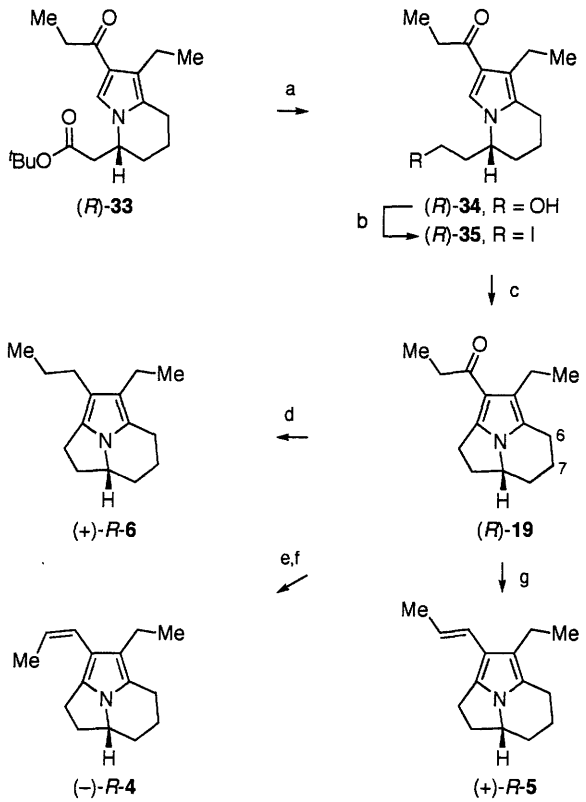

Scheme 8. Our enantioselective synthesis of the tricyclic myrmicarins. Conditions: a) TIPSOTf, Et_3N, CH_2Cl_2, –78 °C; $LiAlH_4$, Et_2O, –78→0 °C; HCl , 91%. b) I_2, Ph_3P, Imidazole, CH_2Cl_2, 0 °C, 91%. c) $AgBF_4$, CH_2Cl_2–benzene (3:1), 75%. d) $LiAlH_4$, 1,4-dioxane, 100 °C, 85%. e) 2-chloro-3-ethylbenzoxazolium tetrafluoroborate, Et_3N, CH_2Cl_2, 12% (80% brsm). f) H_2, Lindlar cat, EtOAc, pyr, 74%. g) $LiAlH_4$, Et_2O, –78→0 °C; NH_4Cl, 61% (2-steps).

iodide (*S*)-**35**, and ketone (*S*)-**19** in 87%, 86%, and 73% yield, respectively.

Enantiomerically enriched tricyclic ketone **19** provided expedient access to isomerically pure samples of tricyclic myrmicarins **4-6** (Scheme 8). As noted during isolation studies,[1c] myrmicarins **4–6** were found to be sensitive to air oxidation, giving the corresponding C6-C7 alkene derivatives[32] followed by rapid decomposition.[25] It should be noted that the propensity toward air oxidation in these pyrroloindolizine derivatives is higher in the absence of the C8-carbonyl. According to literature precedent, heating a mixture of ketone (*R*)-**19** and lithium aluminum hydride in 1,4-dioxane gave (+)-(*R*)-myrmicarin 217 ((+)-**6**, $[\alpha]^{20}_D$ = +72.1 (*c* 0.050, CH_2Cl_2), lit.: $[\alpha]^{20}_D$ = +88 (*c* 1, CH_2Cl_2), Scheme 8) in 85% yield.[8] The enantiomeric (–)-(*R*)-myrmicarin 217 ((–)-**6**, $[\alpha]^{20}_D$ = –67.4 (*c* 0.074, CH_2Cl_2)) was prepared *via* the same procedure in 99% yield.[25]

The stereospecific synthesis of the sensitive myrmicarin 215A (**4**) was achieved *via* a two–step sequence from ketone **19** (Scheme 8). Dehydration of the C8–ketone in (*R*)-**19** using 2-

chloro-3-ethylbenzoxazolium tetrafluoroborate[33] gave the corresponding C8-C9–alkyne, which proved to be a particularly sensitive intermediate.[34] Successful isolation of pure material was only possible by an immediate isolation and purification of the alkyne at less than 30% conversion (12–19%, 75–80% based on recovered starting material). Partial reduction with Lindlar catalyst under an atmosphere of dihydrogen provided exclusively (–)-(*R*)-myrmicarin 215A ((–)-**4**, $[\alpha]^{20}_D = -53.8$ (*c* 0.045, CH_2Cl_2), Scheme 8) in 74% yield. Similarly, ketone (*S*)-**19** was converted to (+)-(*S*)-myrmicarin 215A ((+)-**4**, $[\alpha]^{20}_D = +49.8$ (*c* 0.090, CH_2Cl_2)).

Synthesis of (+)-(*R*)-myrmicarin 215B commenced with the reduction of the ketone in (*R*)-**19** with lithium aluminum hydride to the corresponding C8–alcohol as a mixture of diastereomers (~1:1). Acid catalyzed dehydration then afforded isomerically pure (+)-(*R*)-myrmicarin 215B ((+)-**5**, $[\alpha]^{20}_D = +60.4$ (*c* 0.044, CH_2Cl_2), Scheme 8) in 61% yield.[35] Starting with ketone (*S*)-**19** the corresponding (–)-(*S*)-myrmicarin 215B ((–)-**5**, $[\alpha]^{20}_D = -58.5$ (*c* 0.085, CH_2Cl_2)) was prepared in 74% yield. Interestingly, (4a*R*)-myrmicarins 215A (**4**) and 215B (**5**) rotate plane–polarized light in opposite directions. While myrmicarins 215A (**4**) and 215B (**5**) were isolated and characterized as a mixture, our analysis of the isomerically pure samples has confirmed the previously reported ^1H and ^{13}C NMR assignments of the mixture.[25,36]

Conclusion

A convergent gram-scale synthesis of the key dihydroindolizine **25** for the synthesis of myrmicarin alkaloids in optically active form is described. The enantioselective synthesis of myrmicarins (–)-215A (**4**), (+)-215B (**5**), and (+)-217 (**6**) in addition to their respective enantiomers is described. Central to the success of this approach was the use of an efficient and stereospecific palladium–catalyzed fragment coupling of a *Z*-vinyl triflate and a pyrrole, a copper–catalyzed enantioselective conjugate reduction and two Friedel-Crafts reactions to form the pyrroloindolizine core of myrmicarins. The chemistry described here sets the stage for the synthesis of more complex members of this family of alkaloids.

---

[1] For isolation of **1** and **2**, see: (a) Schröder, F.; Sinnwell, V.; Baumann, H.; Kaib, M.; Francke, W. *Angew. Chem. Int. Ed.* **1997**, *36*, 77–80. For structure assignment of **3**, see: (b) Schröder, F.; Sinnwell, V.; Baumann, H.; Kaib, M. *Chem. Commun.* **1996**, *18*, 2139–2140. For isolation of **4**, **5**, and **6**, see: (c) Schröder, F.; Franke, S.; Francke, W.; Baumann, H.; Kaib, M.; Pasteels, J. M.; Daloze, D. *Tetrahedron* **1996**, *52*, 13539–13546. For isolation and total synthesis of **7** and **8**, see: (d) Francke, W.; Schröder, F.; Walter, F.; Sinnwell, V.; Baumann, H.; Kaib, M. *Liebigs Ann.* **1995**, *6*, 965–977. For a review of the synthesis and study of myrmicarin alkaloids, see: (e) Ondrus, A. E.; Movassaghi, M. *Chem. Commun.* **2009**, *accepted.*

[2] Biological assays show that the toxicity of this secretion is associated with the myrmicarin alkaloids (see refs. 1c, 1d, and 1e).

[3] For reviews on ant alkaloid toxins, see: (a) Leclercq, S.; Braekman, J. C.; Daloze, D.; Pasteels, J. M. in *Progress in the Chemistry of Organic Natural Products*, ed. Herz, W.; Falk, H.; Kirby, G. W.; Moore, R. E. SpringerWienNewYork, Austria, 2000, vol. 79, pp. 115–229. (b) Braekman, J. C.; Daloze, D. *J. Braz. Chem. Soc.* **1996**, *7*, 251–256. (c) Numata, A.; Ibuka, T. in *The Alkaloids: Chemistry and Pharmacology*, ed. Brossi, A. Academic Press, San Diego, 1987, vol. 31, ch. 6, pp. 194–315. (d) Attygalle, A. B.; Morgan, E. D. *Chem. Soc. Rev.* **1984**, *13*, 245–278.

[4] Exposure of a pure sample of **1** to air for two hours results in 50% decomposition, while exposure of fresh poison gland secretion containing **3** to air for one hour results in greater than 90% decomposition of **3** (see refs. 1b and 1c). Due to overlap with the crosspeak signals of the tricyclic myrmicarins, the relative stereochemistry of C4a′ in **3** could not be determined from the NOESY spectrum (see ref. 1b).

[5] Alkaloids **6**, **7**, and **8** were isolated as pure components by neutral alumina gel chromatography (see refs. 1c and 1d). Alkaloids **4** and **5** were isolated as a 2:1 mixture by neutral alumina gel chromatography (see ref. 1c).

[6] The stereochemistry illustrated for **2** in Figure 1 is based on analogy to the other complex myrmicarin structures.

[7] Schröder, F.; Francke, W. *Tetrahedron* **1998**, *54*, 5259–5264.

[8] Sayah, B.; Pelloux-Léon, N.; Valleé, Y. *J. Org. Chem.* **2000**, *65*, 2824–2826.

[9] Jefford, C. W.; Sienkiewicz, K.; Thornton, S. R. *Helv. Chim. Acta* **1995**, *78*, 1511–1524.

[10] Settambolo, R.; Guazzelli, G.; Lazzaroni, R. *Tetrahedron: Asymmetry* **2003**, *14*, 1447–1449.

[11] Synthesized in two steps from L-glutamic acid diethylester hydrochloride.

[12] (a) Sayah, B.; Pelloux-Léon, N.; Milet, A.; Pardillos-Guindet, J.; Vallée, Y. *J. Org. Chem.* **2001**, *66*, 2522–2525. For synthesis of an unnatural derivative of **5**, see: (b) Angle, S. R.; Qian, X. L.; Pletnev, A. A.; Chinn, J. *J. Org. Chem.* **2007**, *72*, 2015–2020.

[13] For reports on CuH-catalyzed asymmetric conjugate reduction, see: (a) Lipshutz, B. H.; Servesko, J. M. *Angew. Chem. Int. Ed.* **2003**, *42*, 4789–4792. (b) Hughes, G.; Kimura, M.; Buchwald, S. L. *J. Am. Chem. Soc.* **2003**, *126*, 11253–11258, and references sited therein. For related references, see: (c) Mahoney, W. S.; Stryker, J. M. *J. Am. Chem. Soc.* **1989**, *111*, 8818–8823 and (d) Mori, A.; Fujita, A.; Kajiro, H.; Nishihara, Y.; Hiyama, T. *Tetrahedron* **1999**, *55*, 4573–4582.

[14] Rainka, M. P.; Aye, Y.; Buchwald, S. L. *Proc. Nat. Acad. Sci., USA* **2004**, *101*, 5821–5823.

[15] Ester **31** is commercially available and can be prepared on >30-g scale; see: Drinan, M. A.; Lash, T. D. *J. Heterocyclic Chem.* **1994**, *31*, 255–257.

[16] Ohta, S.; Shimabayashi, A.; Hayakawa, S.; Sumino, M.; Okamoto, M. *Synthesis* **1985**, 45–48.

[17] Comins, D. L.; Dehghani, A. *Tetrahedron Lett.* **1992**, *33*, 6299–6302.

[18] For reviews, see: (a) Wolfe, J. P.; Wagaw, S.; Marcoux, J.-F.; Buchwald, S. L. *Acc. Chem. Res.* **1998**, *31*, 805–818. (b) Hartwig, J. F. *Acc. Chem. Res.* **1998**, *31*, 852–860. (c) Hartwig, J. F. *Angew. Chem Int. Ed.* **1998**, *37*, 2046–2067. (d) Muci, A. R.; Buchwald, S. L. *Top. Curr. Chem.* **2002**, *219*, 131–209.

[19] For the synthesis of *Z*-β-iodoenoates, see: (a) Piers, E.; Wong, T.; Coish, P. D.; Rogers, C. *Can. J. Chem.* **1994**, *72*, 1816–1819, and (b) Rossi, R.; Bellina, F.; Mannina, L. *Tetrahedron* **1997**, *53*, 1025–1044.

[20] For reviews on the preparation and use of vinyl triflates, see: (a) Ritter, K. *Synthesis* **1993**, 735–762, and (b) Baraznenok, I. L.; Nenajdenko, V. G.; Balenkova, E. S. *Tetrahedron* **2000**, *56*, 3077–3119.

[21] (a) Tomori, H.; Fox, J. M.; Buchwald, S. L. *J. Org. Chem.* **2000**, *65*, 5334–5341. (b) XPhos is available from Strem Chemicals, Inc.

[22] For palladium-catalyzed *N*-vinylation of lithiated azoles, see: (a) Lebedev, A. Y.; Izmer, V. V.; Kazyul'kin, D. N.; Beletskaya, I. P.; Voskoboynikov, A. Z. *Org. Lett.* **2002**, *4*, 623–626. For reports on palladium catalyzed *N*-vinylation, see: (b) Wallace, D. J.; Klauber, D. J.; Chen, C.-y.; Volante, R. P. *Org. Lett.* **2003**, *5*, 4749–4752, and (c) Klapars, A.; Campos, K. R.; Chen, C.-y.; Volante, R. P. *Org. Lett.* **2005**, *7*, 1185–1188.

[23] For reviews on the synthesis of β-amino acids, see: (a) *Enantioselective Synthesis of β-Amino Acids*; Juaristi, E., Ed.; Wiley-VCH: New York, 1997. (b) Liu, M.; Sibi, M. P. *Tetrahedron* **2002**, *58*, 7997–8035. (c) Ma, J.-A. *Angew. Chem Int. Ed.* **2003**, *42*, 4290–4299. (d) Drexler, H.-J.; You, J.; Zhang, S.; Fischer, C.; Baumann, W.; Spannenberg, A.; Heller, D. *Org. Process. Res. Dev.* **2003**, *7*, 355–361. (e) Córdova, A. *Acc. Chem. Res.* **2004**, *37*, 102–112.

[24] The ee was determined by chiral HPLC analysis of a more advanced intermediate.

[25] Please see the Experimental Section for details.

[26] The absolute stereochemical assignment of the conjugate reduction is made by comparison of the sign of optical rotation of our synthetic **19** and *ent*-**19** with that reported for an optically active sample of **19** prepared from D-glutamic acid (ref. 8).

[27] For reviews on the chemistry of pyrroles, see: (a) *Pyrroles*; Jones, A., Ed.; Wiley: New York, 1990, (b) Alan, J. R.; Bean, G. P. *The Chemistry of Pyrroles*,; Academic Press: London, 1977. (c) Baltazzi, E.; Krimen, L. I. *Chem. Rev.* **1963**, *63*, 511–556.

[28] Compounds not containing the C8-carbonyl in this series were found to be less stable toward storage due to decomposition and polymerization.

[29] (a) Aldabbagh, F.; Bowman, W. R.; Mann, E. *Tetrahedron Lett.* **1997**, *38*, 7937–7940. (b) Miranda, L. D.; Cruz-Almanza, R.; Pavón, M.; Alva, E.; Muchowski, J. M. *Tetrahedron Lett.* **1999**, *40*, 7153–7157. (c) Allin, S. M.; Barton, W. R. S.; Bowman, R.; McInally, T. *Tetrahedron Lett.* **2001**, *42*, 7887–7890.

[30] (a) Nakamura, E.; Inubushi, T.; Aoki, S.; Machii, D. *J. Am. Chem. Soc.* **1991**, *113*, 8980–8982. (b) Menes-Arzate, M.; Martínez, R.; Cruz-Almanza, R.; Muchowski, J. M.; Osonio, Y. M.; Miranda, L. D. *J. Org. Chem.* **2004**, *69*, 4001–4004.

[31] Merlic, C. A.; Miller, M. M. *Organometallics* **2001**, *20*, 373–375.

[32] The immediate air oxidation product of **4**, **5**, and **6** corresponds to myrmicarins 213A, 213B, and 215C, respectively (see ref 1c).

[33] Tsuji, T.; Watanabe, Y.; Mukaiyama, T. *Tetrahedron Lett.* **1979**, 481–482.

[34] More forcing dehydration conditions and longer reaction times resulted in lower mass recovery and complications involving C6-C7 oxidation.

[35] Direct acidification of the reaction mixture can also provide **5**. See the Experimental Section for details.

[36] Ketone (*S*)-**19** was converted to (+)-*ent*-**4** (–)-*ent*-**5**, and (–)-*ent*-**6** in 50% brsm (2-steps), 74%, and 99% yield, respectively.

Experimental Section

General Procedures. All reactions were performed in oven-dried or flame-dried round bottomed flasks, modified Schlenk (Kjeldahl shape) flasks, or NMR tubes (Wilmad Glass Co., Inc. cat. no. 528-PP8). The flasks were fitted with rubber septa and reactions were conducted under a positive pressure of argon. Stainless steel syringes or cannulae were used to transfer air- and moisture-sensitive liquids. Flash column chromatography was performed as described by Still et al. using silica gel (60-Å pore size, 32–63 μm, standard grade, Sorbent Technologies) or non-activated alumina gel (80–325 mesh, chromatographic grade, EM Science).[1] Analytical thin–layer chromatography was performed using glass plates pre-coated with 0.25 mm 230–400 mesh silica gel or neutral alumina gel impregnated with a fluorescent indicator (254 nm). Thin layer chromatography plates were visualized by exposure to ultraviolet light and/or by exposure to an ethanolic phosphomolybdic acid (PMA), an acidic solution of *p*-anisaldehyde (anis), an aqueous solution of ceric ammonium molybdate (CAM), an aqueous solution of potassium permanganate ($KMnO_4$) or an ethanolic solution of ninhydrin followed by heating (<1 min) on a hot plate (~250 °C). Organic solutions were concentrated on Büchi R-200 rotary evaporators at ~20 Torr (house vacuum) at 25–35 °C, then at ~1 Torr (vacuum pump) unless otherwise indicated.

Materials. Commercial reagents and solvents were used as received unless otherwise noted. Dichloromethane, diethyl ether, tetrahydrofuran, acetonitrile, and toluene were purchased from J.T. Baker (Cycletainer™) and were purified by the method of Grubbs et al. under positive argon pressure.[2] Triethylamine was distilled from calcium hydride at 760 Torr under a nitrogen atmosphere. Methanol was distilled from magnesium methoxide at 760 Torr under a nitrogen atmosphere. 1,4-dioxane was distilled from sodium hydride. Potassium phosphate was dried at 180 °C under vacuum (~1 torr) for 24 h then stored in a glove box. Sodium hydride was purchased from Aldrich Chemicals as a 60% dispersion in oil and then washed four times with hexanes and stored dry in a glove box. All reagents for NMR experiments were degassed via Ar bubbling for at least 10 min. *t*-Butyl acetate and *t*-butyl alcohol were distilled from potassium carbonate. The molarity of *n*-butyllithium solutions was determined by titration using diphenylacetic acid as an indicator (average of three determinations).[3]

Instrumentation. Proton nuclear magnetic resonance (^{1}H NMR) spectra were recorded with a Varian inverse probe 500 INOVA spectrometer. Chemical shifts are reported in parts per million from internal tetramethylsilane on the δ scale and are referenced from the residual protium in the NMR solvent ($CHCl_3$: δ 7.27, C_6H_6: δ7.16). Data is reported as follows: chemical shift [multiplicity (s = singlet, d = doublet, t = triplet, q = quartet, m = multiplet), coupling constant(s) in Hertz, integration, assignment]. Carbon-13 nuclear magnetic resonance spectra were recorded with a Varian 500 INOVA spectrometer and are reported in parts per million from internal tetramethylsilane on the δ scale and are referenced from the carbon resonances of the solvent ($CDCl_3$: δ 77.2, benzene-d_6: δ 128.0). Data is reported as follows: chemical shift [multiplicity (s = singlet, d = doublet, t = triplet, q = quartet, m = multiplet), coupling constant(s) in Hertz, assignment]. The numbering system used for proton and carbon assignments are consistent with

---

[1] Still, W. C.; Kahn, M.; Mitra, A. *J. Org. Chem.* **1978**, *43*, 2923–2925.

[2] Pangborn, A. B.; Giardello, M. A.; Grubbs, R. H.; Rosen, R. K.; Timmers, F. J. *Organometallics* **1996**, *15*, 1518–1520.

[3] Kofron, W. G.; Baclawski, L. M. *J. Org. Chem.* **1976**, *41*, 1879–1880.

those used in the isolation reports.[4] Infrared data were obtained with a Perkin-Elmer 2000 FTIR and are reported as follows: [frequency of absorption (cm^{-1}), intensity of absorption (s = strong, m = medium, w = weak, br = broad), assignment]. Gas chromatography was performed on an Agilent Technologies 6890N Network GC System with a HP-5 5% Phenyl Methyl Siloxane column. Enantiomeric excess was determined by chiral HPLC analysis on Agilent Technologies 1100 Series HPLC system with a Daicel Chiralpak AD-H column. We are grateful to Dr. Li Li for obtaining the mass spectroscopic data at the Department of Chemistry's Instrumentation Facility, Massachusetts Institute of Technology.

[4] Schröder, F.; Franke, S.; Francke, W.; Baumann, H.; Kaib, M.; Pasteels, J. M.; Daloze, D. *Tetrahedron* **1996**, *52*, 13539–13546.

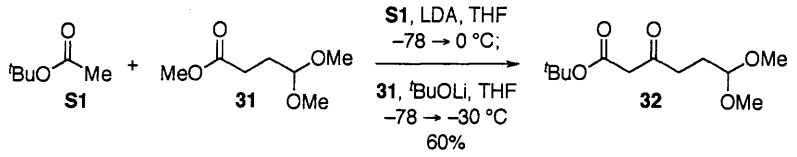

6,6-Dimethoxy-3-oxo-hexanoic acid *tert*-butyl ester (32):

n-Butyllithium (2.50 M in hexanes, 66.1 mL, 165 mmol, 2.00 equiv) was added to a solution of diisopropylamine (23.7 mL, 169 mmol, 2.05 equiv) in THF (330 mL) at –78 °C and the mixture was warmed to 0 °C over 15 min. The resulting lithium diisopropylamide solution was then cooled to –78 °C. After 15 min, *tert*-butyl acetate (**S1**, 24.5 mL, 182 mmol, 2.20 equiv) was added dropwise over 5 min and the mixture was maintained at –78 °C for 20 min to provide the lithium enolate.

In a separate flask, methyl 4-dimethoxybutyrate[5] (**31,** 13.4 g, 82.8 mmol, 1 equiv) was added neat via cannula to a solution of lithium *tert*-butoxide (16.5 g, 207 mmol, 2.50 equiv) in THF (410 mL) at –78 °C. This solution was allowed to warm to –30 °C, at which time the cold (–78 °C) solution of the lithium enolate was added dropwise via cannula over 1.5 h. The resulting pale yellow solution was then maintained at –40 to –30 °C. After 20 min, excess base was quenched at –40 °C by the addition of saturated aqueous ammonium chloride–aqueous hydrogen chloride mixture (3:1, pH 1,500 mL) and the resulting mixture was allowed to warm to 23 °C. The mixture was diluted with EtOAc (600 mL) and the aqueous layer was extracted with additional EtOAc (5 × 250 mL). The combined organic layer was washed with brine (100 mL), was dried over anhydrous sodium sulfate, was filtered, and the volatiles were removed under reduced pressure on a rotary-evaporator. The yellow residue was purified by flash column chromatography on silica gel (7 × 30 cm, 25% EtOAc–hexanes; the residue was split into two equal portions and purified separately by flash column chromatography) to afford the β-ketoester **32** (12.2 g, 60%) as a clear and colorless oil.

^{1}H NMR (500 MHz, C_6D_6, 20 °C, 11:1 mixture of β-ketoester:enol tautomer, β-ketoester denoted by *): 12.94 (s, 1H, C=OCHCOH), 5.01 (s, 1H, C=OCHCOH), 4.20 (t, J = 5.5 Hz, 1H, C**H***$(OCH_3)_2$), 3.06 (s, 6H, CH$(OCH^*_3)_2$), 4.19 (t, J = 5.7 Hz, 1H, C**H**$(OCH_3)_2$), 3.04 (s, 6H, CH$(OCH_3)_2$), 3.00 (s, 2H, CO**CH**$_2$*CO), 2.26 (t, J = 7.2 Hz, 2H, CO**CH**$_2$*CH_2), 2.14 (app t, J = 7.8 Hz, 2H, COHC**H**$_2CH_2$), 1.87 (td, J = 7.2, 5.5 Hz, 2H, C**H**$_2$*CH$(OCH_3)_2$), 1.84 (m, 2H, C**H**$_2$CH$(OCH_3)_2$), 1.37 (s, 9H, OC$(CH_3)_3$, 1.35 (s, 9H, C$(CH_3^*)_3$).

^{13}C NMR (125.8 MHz, C_6D_6, 20 °C): 202.0, 166.8, 104.0, 81.4, 53.0, 50.9, 37.9, 28.3, 27.1.

[5] Ester **31** is commercially available and can be prepared on multi-gram scale according to Drinan, M. A.; Lash, T. D. *J. Heterocyclic Chem.* **1994**, *31*, 255–257.

FTIR (neat) cm^{-1}:	2980 (s, C–H), 2933 (m, C–H), 1746 (s, C=O), 1716 (s, C=O), 1645 (w), 1369 (s), 1128 (s), 1063 (s).
HRMS–ESI (*m/z*):	calcd for $C_{12}H_{22}O_5Na$ $[M+Na]^+$: 269.1359, found: 269.1347.
TLC (5% THF–CH_2Cl_2), *Rf*:	0.31 (UV, anis).

GC (HP-5, 50 °C, 1 min; 25 °C/min to 250 °C; 250 °C, 5.50 min), t_R: 6.81 min.

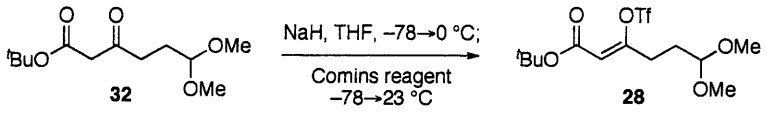

32 **28**

(*Z*)-6,6-Dimethoxy-3-trifluoromethanesulfonyloxy-hex-2-enoic acid *tert*-butyl ester (28):

A solution of β-ketoester **32** (9.50 g, 38.6 mmol, 1 equiv) in THF (16.0 mL + 2 × 2.0 mL rinse) was added to a grey suspension of sodium hydride (1.16 g, 48.3 mmol, 1.25 equiv) in THF (180 mL) at –78 °C. The mixture was warmed to 0 °C over 15 min using an ice–water bath, causing evolution of gas. The resulting yellow mixture was then cooled to –78 °C. After 15 min, a yellow solution of 2-[*N*,*N*- bis(trifluoromethylsulfonyl)amino]-5-chloropyridine (Comins reagent, 19.7 g, 50.1 mmol, 1.30 equiv) in THF (10.0 mL + 2 × 2.0 mL rinse) was added via cannula and the resulting yellow solution was allowed to warm to 0 °C over 30 min. The bath was removed and the solution was allowed to warm to 23 °C over 1 h to give a deep orange solution. Excess base was quenched by the addition of saturated aqueous ammonium chloride (100 mL) to give a neutral (pH 7) aqueous layer. The mixture was diluted with Et_2O (100 mL), the layers were separated, and the aqueous layer was extracted with Et_2O (3 × 75 mL). The combined organic layers were washed with brine (40 mL), were dried over anhydrous sodium sulfate, were filtered, and were concentrated under reduced pressure. The crude yellow residue was added dropwise to a vigorously stirred 100-mL portion of hexanes, was filtered, and was concentrated under reduced pressure to give a faint yellow oil. Dissolution of this residue in hexanes followed by filtration and removal of volatiles under reduced pressure gave a clear and colorless oil. The resulting residue was purified by flash column chromatography (silica gel, 10.5 × 22 cm, 22% EtOAc–hexanes) to yield vinyl triflate **28** as a clear and colorless oil (11.9 g, 82%, >20:1 *Z*:*E*).

^{1}H NMR (500 MHz, C_6D_6, 20 °C):	5.35 (s, 1H, C=OC**H**=COSO$_2$CF$_3$), 3.97 (t, J = 5.6 Hz, 1H, C**H**(OCH$_3$)$_2$), 2.97 (s, 6H, CH(OC**H**$_3$)$_2$), 2.13 (t, J = 7.5 Hz, 2H, COSO$_2$CF$_3$C**H**$_2$CH$_2$), 1.48 (td, J = 7.5, 5.6 Hz, 2H, C**H**$_2$CH(OCH$_3$)$_2$), 1.39 (s, 9H, OC(C**H**$_3$)$_3$).
^{13}C NMR (125.8 MHz, C_6D_6, 20 °C):	161.9, 157.7, 119.4 (q, J = 320.0 Hz, **C**F$_3$), 114.1, 103.2, 82.3, 53.1, 29.9, 29.4, 28.2.
FTIR (neat):	2982 (m, C–H), 2835 (m, C–H), 1727 (s, C=O), 1679 (m), 1427 (s), 1210 (s).
HRMS–ESI (*m/z*):	calcd for $C_{13}H_{21}F_3O_7SNa$ $[M+Na]^+$: 401.0852, found: 401.0855.
TLC (3% Et_2O–CH_2Cl_2), *Rf*:	0.44 (anis).

GC (HP-5, 50 °C, 1 min; 25 °C/min to 250 °C; 250 °C, 5.50 min), t_R: 7.42 min.

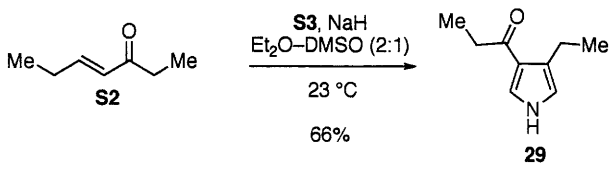

1-(4-Ethyl-1H-pyrrol-3-yl)-propan-1-one (29):[6]

A solution of (*E*)-hept-4-en-3-one (**S2**, 3.10 g, 27.63 mmol, 1 equiv) and tosylmethyl isocyanide (**S3**, 5.13 g, 26.3 mmol, 0.95 equiv) in Et_2O–DMSO (2:1, 150 mL) was added dropwise via cannula over 1 h to a grey suspension of sodium hydride (1.46 g, 60.8 mmol, 2.20 equiv) in Et_2O (55 mL) at 23 °C. The resulting bilayer (colourless layer over a deep brown layer), containing a tan-coloured suspension was vigorously stirred for 1.5 h. The mixture was cooled to and maintained at 0 °C for 10 min, at which time excess base was quenched by the addition of a 50-mL portion of water. Vigorous gas evolution and the formation of a clear yellow organic layer above a deep orange aqueous layer was observed. The aqueous layer was separated and extracted with Et_2O (5 × 50 mL), and the combined organic layers were washed with brine (15 mL), were dried over anhydrous sodium sulfate, were filtered, and were concentrated to give a pale yellow solid. The residue was purified by flash column chromatography on silica gel (3→5 % EtOAc–CH_2Cl_2) to afford the acyl pyrrole **29** (2.62 g, 66%) as a white powder.

^{1}H NMR (500 MHz, $CDCl_3$, 20 °C):	8.61–8.91 (br s, 1H, N**H**), 7.39 (dd, J = 3.2, 2.1 Hz, 1H, NHC**H**CO), 6.59 (tt, J = 2.1, 1.1 Hz, 1H, NHC**H**CCH_2), 2.82 (qd, J = 7.4, 1.1 Hz, 2H, CC**H**$_2$CH$_3$), 2.78 (q, J = 7.4 Hz, 2H, COC**H**$_2$CH$_3$), 1.21 (t, J = 7.4 Hz, 3H, CCH$_2$C**H**$_3$), 1.19 (t, J = 7.4 Hz, 3H, COCH$_2$C**H**$_3$).
^{13}C NMR (125.8 MHz, $CDCl_3$, 20 °C):	198.5, 128.6, 125.5, 123.5, 117.5, 33.6, 20.7, 15.0, 9.6.
FTIR (neat):	3206 (s, N–H), 2909 (w, C–H), 1637 (s, C=O), 1520 (m), 1301 (m), 1162 (m), 1077 (m), 1009 (m), 923 (m).
HRMS–ESI (*m/z*):	calcd for $C_9H_{13}NONa$ $[M+Na]^+$: 174.0889 found: 174.0887.
TLC (5% EtOAc–CH_2Cl_2), *Rf*:	0.56 (UV, anis).

[6] For the synthesis of pyrroles using tosylmethylisocyanide, see: (a) van Leusen, A. M.; Siderius, H.; Hoogenboom, B. E.; van Leusen, D. *Tetrahedron Lett.* **1972**, *52*, 5337–5340 and (b) Chamberlin, K. S.; LeGoff, E. *Heterocycles* **1979**, *12*, 1567–1570.

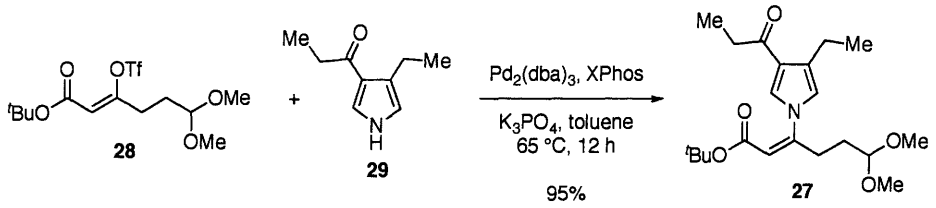

(*Z*)-3-(3-Ethyl-4-propionyl-pyrrol-1-yl)-6,6-dimethoxy-hex-2-enoic acid *tert*-butyl ester (27):

Toluene (82.5 mL) was added to an argon–purged mixture of acyl pyrrole **29** (4.20 g, 27.8 mmol, 1.50 equiv), $Pd_2(dba)_3$ (1.27 g, 1.39 mmol, 0.075 equiv), XPhos (1.41 g, 2.96 mmol, 0.15 equiv), and rigorously anhydrous K_3PO_4 (5.50 g, 25.9 mmol, 1.40 equiv), and the resulting deep red mixture was stirred at 23 °C for 30 min. A solution of vinyl triflate **28** (7.00 g, 18.5 mmol, 1 equiv) in toluene (7.0 mL + 2 × 1.0 mL rinse) was added via cannula and the mixture was heated to 65 °C, producing a color change to brown within 15 minutes. After 12 h at 65 °C, the mixture was allowed to cool to 23 °C and diluted by the addition of saturated aqueous ammonium chloride (150 mL). The mixture (aqueous phase ~ pH 7) was further diluted with EtOAc (150 mL), the layers were separated, and the aqueous layer was extracted with EtOAc (4 × 100 mL). The combined organic phases were washed with brine (20 mL), were dried over anhydrous sodium sulfate, were filtered, and were concentrated under reduced pressure to a deep brown oil. The crude residue was purified by flash column chromatography (silica gel: 8 × 30 cm, 5% EtOAc–CH_2Cl_2) to provide the vinyl pyrrole **27** (6.70 g, 95%) as a yellow oil.

^{1}H NMR (500 MHz, C_6D_6, 20 °C):	7.15 (d, J = 2.4 Hz, 1H, NC**H**=CC=O), 6.35 (m, 1H, NC**H**=CCH_2CH_3), 5.51 (s, 1H, NC=C**H**CO_2), 4.05 (t, J = 5.3 Hz, 1H, C**H**$(OCH_3)_2$), 3.01 (s, 6H, CH$(OCH_3)_2$), 3.08 (dq, J = 7.6, 1.1 Hz, 2H, NCH=CC**H**$_2CH_3$), 2.50 (q, J = 7.3 Hz, 2H, CO**CH**$_2CH_3$), 2.21 (app-t, J = 7.6 Hz, 2H, C**H**$_2CH_2CH(OCH_3)_2$), 1.48 (m, 2H, CH_2C**H**$_2CH(OCH_3)_2$), 1.29 (t, J = 7.6 Hz, 3H, NCH=CCH_2C**H**$_3$), 1.29 (s, 9H, OC$(CH_3)_3$), 1.18 (t, J = 7.3 Hz, 3H, COCH_2C**H**$_3$).
^{13}C NMR (125.8 MHz, C_6D_6, 20 °C):	195.9, 164.1, 149.5, 129.7, 127.9, 124.5, 119.9, 114.1, 103.7, 80.9, 53.1, 33.4, 32.4, 30.4, 28.2, 20.9, 15.1, 9.2.
FTIR (neat):	2975 (m, C–H), 2936 (m, C–H), 1709 (s, C=O), 1662 (s, C=O), 1516 (s), 1368 (m), 1152 (s).
HRMS–ESI (*m/z*):	calcd for $C_{21}H_{33}NO_5Na$ $[M+Na]^+$: 402.2251, found: 402.2241.
TLC (5% EtOAc–CH_2Cl_2), *Rf*:	0.23 (UV, CAM).

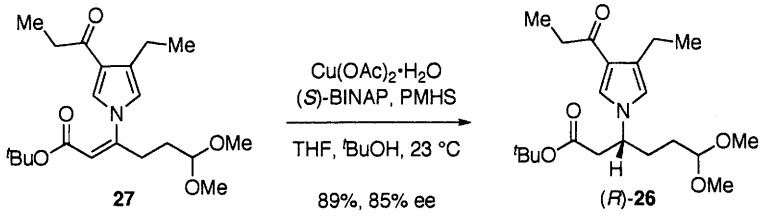

(3*R*)-3-(3-Ethyl-4-propionyl-pyrrol-1-yl)-6,6-dimethoxy-hexanoic acid *tert*-butyl ester (26):

A deep blue solution resulting from the addition of THF (25.5 mL) to an argon-purged mixture of $Cu(OAc)_2 \cdot H_2O$ (236 mg, 1.18 mmol, 0.20 equiv) and (*S*)-BINAP (735 mg, 1.18 mmol, 0.20 equiv) was stirred at 23 °C for 10 min. PMHS (9.74 mL, 38.4 mmol, 6.50 equiv) was added and the mixture was stirred until it attained a bright lime–green color (~5 min), whereupon a solution of the vinyl pyrrole **27** (2.24 g, 5.90 mmol, 1 equiv) and ^{t}BuOH (3.60 mL, 38.4 mmol, 6.50 equiv) in THF (3.60 mL + 2 × 0.75 mL rinse) was added via cannula. After the resulting deep red solution had stirred for 5.5 h, a 125-mL volume of Et_2O was added, the flask was cooled to 0 °C, and aqueous sodium hydroxide (1N, 175 mL) was added slowly, producing vigorous bubbling. An additional 75-mL portion of each Et_2O and aqueous sodium hydroxide (1N) were added sequentially, and the two–phase mixture was vigorously stirred for 2 days. The resulting tan–colored aqueous phase was separated from the deep red organic phase and was extracted with Et_2O (3 × 100 mL). The combined organic layers were washed with saturated aqueous ammonium chloride (120 mL), then with brine (100 mL), were dried over anhydrous sodium sulfate, were filtered, and were concentrated under reduced pressure to a tan-colored oil. Purification of the crude residue by flash column chromatography (silica gel: diam. 8 cm, ht. 12.5 cm, 35% EtOAc–hexanes) provided the (*R*)-β-pyrrolyl ester **26** (2.01 g, 89%, 85% ee) as a pale yellow oil. The ee of the product was determined by chiral HPLC analysis of a more advanced intermediate. Optimum separation between enantiomers was observed using the iodide **35**. See page 41 for full details. The β-pyrrolyl ester (*S*)-**26** was obtained using (*R*)-BINAP according to the above procedure, with the exception that 8.00 instead of 6.50 equivalents of PMHS and ^{t}BuOH were used (3.21 g, 89%, 81% ee).

^{1}H NMR (500 MHz, C_6D_6, 20 °C): 6.95 (d, J = 2.1 Hz, 1H, NC**H**=CC=O), 6.11 (m, 1H, NC**H**=CCH_2CH_3), 4.03–4.09 (m, 1H, NC**H**CH_2), 4.06 (t, J = 5.3 Hz, 1H, C**H**$(OCH_3)_2$), 3.11 (q, J = 7.5 Hz, 2H, NCH=CC**H**$_2CH_3$), 3.06 (s, 3H, OC**H**$_3$), 3.04 (s, 3H, OC**H**$_3$), 2.52 (q, J = 7.4 Hz, 2H, COC**H**$_2CH_3$), 2.33 (dd, J = 15.3, 8.7 Hz, 1H, NCHC**H**$_2CO_2$), 2.23 (dd, J = 15.3, 6.1 Hz, 1H, NCHC**H**$_2CO_2$), 1.49–1.62 (m, 2H, CH_2C**H**$_2$), 1.28–1.44 (m, 2H, C**H**$_2CH_2$), 1.34 (t, J = 7.3 Hz, 3H, NCH=CCH_2C**H**$_3$), 1.26 (s, 9H, OC(C**H**$_3)_3$), 1.22 (t, J = 7.3 Hz, 3H, $COCH_2$C**H**$_3$).

^{13}C NMR (125.8 MHz, C_6D_6, 20 °C): 195.2, 169.3, 128.9, 125.7, 122.8, 117.4, 103.8, 80.5, 57.3, 52.7, 52.2, 42.5, 32.8, 30.5, 29.1, 27.7, 20.6, 15.0, 9.0.

FTIR (neat):	2974 (m, C–H), 1728 (s, C=O), 1656 (s, C=O), 1458 (m), 1368 (s), 1151 (s).
HRMS–ESI (*m/z*):	calcd for $C_{21}H_{35}NO_5Na$ $[M+Na]^+$: 404.2407, found: 404.2405.
TLC (5% EtOAc–CH_2Cl_2), *Rf*:	0.22 (UV, anis).

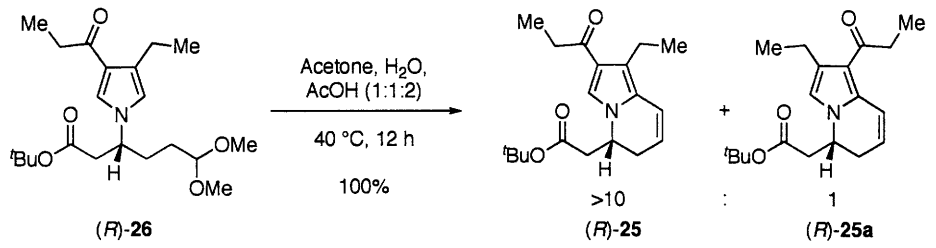

(*R*)-**26**

(4a*R*)-(1-Ethyl-2-propionyl-5,6-dihydro-indolizin-5-yl)-acetic acid *tert*-butyl ester (25):

Acetic acid (58.0 mL, 50 vol %) was added to a solution of *N*-alkyl pyrrole (*R*)-**26** (1.55 g, 4.06 mmol, 1 equiv) in acetone–H_2O (1:1, 58.0 mL) and the colourless transluscent mixture was heated to 40 °C. After 12 h, the resulting yellow mixture was allowed to cool to 23 °C and was diluted with Et_2O (220 mL). The acetic acid was quenched by the slow addition of an aqueous sodium hydroxide solution (3N, 250 mL) to give a neutral (pH 7) aqueous layer. The layers were separated and the aqueous layer was extracted with Et_2O (3 × 100 mL). The combined organic layers were washed with saturated aqueous sodium bicarbonate solution (100 mL) and brine (75 mL) sequentially, were dried over anhydrous sodium sulfate, were filtered, and were concentrated to give the desired product as a bright yellow oil (1.29 g, 100%). ^{1}H NMR analysis of this material showed the presence of clean bicyclic product (*R*)-**25** accompanied by the minor regioisomeric vinylpyrrole (*R*)-**25a** with a selectivity of >10:1 (**25**:**25a**) for the desired regioisomer. For characterization, the two regioisomers were separated and the data presented is for the pure bicycle (*R*)-**25**. However, on larger preparative–scale this vinyl pyrrole product was used without further purification.

Using the same procedure (*S*)-**26** was converted to the corresponding dihydroindolizine (1.42 g, 100%) with >10:1 selectivity for the (*S*)-**25** regioisomer.

^{1}H NMR (500 MHz, C_6D_6, 20 °C): 6.89 (s, 1H, NC**H**=C), 6.26 (dd, J = 9.7, 3.1 Hz, 1H, NCC**H**=CHCH$_2$), 5.22 (ddd, J = 9.7, 6.0, 3.1 Hz, 1H, NCCH=C**H**CH$_2$), 4.18 (qd, J = 6.8, 3.2 Hz, 1H, NC**H**CH$_2$), 3.13 (dt, J = 13.0, 7.3 Hz, 1H, NC=CC**H**$_2$CH$_3$), 2.94 (dt, J = 13.0, 7.3 Hz, 1H, NC=CC **H**$_2$CH$_3$), 2.56 (q, J = 7.3 Hz, 1H, COC**H**$_2$CH$_3$), 2.56 (q, J = 7.3 Hz, 1H, COC**H**$_2$CH$_3$), 2.33 (dd, J = 15.7, 6.8 Hz, 1H, NCHC**H**$_2$CO$_2$), 2.21 (ddt, J = 15.5, 6.8, 3.1 Hz, 1H, NCHC**H**$_2$CH=CH), 2.13 (dd, J = 15.7, 6.8 Hz, 1H, NCHC**H**$_2$CO$_2$), 1.80 (ddt, J = 15.5, 6.0, 3.2 Hz, 1H, NCHC**H**$_2$CH=CH), 1.40 (t, J = 7.3 Hz, 3H, CCH$_2$C**H**$_3$), 1.27 (s, 9H, OC(C**H**$_3$)$_3$), 1.25 (t, J = 7.3 Hz, 3H, COCH$_2$C**H**$_3$).

^{13}C NMR (125.8 MHz, C_6D_6, 20 °C): 195.5, 170.3, 126.8, 126.4, 125.4, 123.4, 118.7, 117.3, 81.0, 51.7, 40.9, 33.3, 29.4, 28.2, 18.9, 16.9, 9.6.

FTIR (neat): 2975 (s, C–H), 2935 (s, C–H), 1727 (s, C=O), 1658 (s, C=O), 1507 (s), 1393 (s), 1368 (s), 1152 (s).

HRMS–ESI (*m/z*):	calcd for $C_{19}H_{27}NO_3Na$ $[M+Na]^+$: 340.1883, found: 340.1888.
TLC (3% EtOAc–CH_2Cl_2), *Rf*:	0.41 (UV, anis).

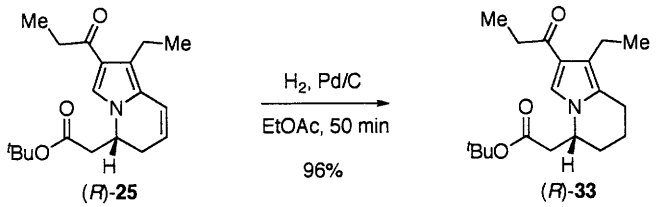

(4a*R*)-(1-Ethyl-2-propionyl-5,6,7,8-tetrahydro-indolizin-5-yl)-acetic acid *tert*-butyl ester (33):

To a solution of alkene (*R*)-**25** (1.24 g, 3.91 mmol, 1 equiv) in EtOAc (56.0 mL) was added 5% palladium on carbon (1.24 g, 100 wt %) in a single portion. The flask was flushed with dihyrogen gas for 5 min, then maintained under a balloon pressure of dihydrogen gas. After 45 min, the balloon was removed and the flask flushed with argon for 5 min. The black suspension was filtered through a short plug of celite (diam. 7 cm, ht. 5 cm, Büchner–funnel under slight vacuum). The reaction flask and celite plug were rinsed with EtOAc (4 × 50 mL) and the combined filtrate was concentrated to afford ketoester (*R*)-**33** (1.20 g, 96%). ^{1}H NMR analysis of this material showed the presence of pure tetrahydroindolizine. On larger preparative–scale, this product was sufficiently pure to be used without further purification. For characterization, the trace amount of minor regioisomer generated during formation of bicyclic alkene **25** was separated and the data presented is for the pure ketoester **33**.

Using the same procedure (*S*)-**25** was reduced to the corresponding tetrahydroindolizine (*S*)-**33** (1.32 g, 100%).

^{1}H NMR (500 MHz, C_6D_6, 20 °C):	6.98 (s, 1H, NC**H**=C), 4.16 (quintet, J = 6.3, 1H, NC**H**CH_2), 2.93–3.08 (m, 2H, CC**H**$_2$$CH_3$), 2.62 (q, J = 7.3 Hz, 2H, COC**H**$_2$$CH_3$), 2.40 (dd, J = 15.9, 6.3 Hz, 1H, NCHC**H**$_2$$CO_2$), 2.24 (t, J = 6.4 Hz, 2H, NCHC**H**$_2$$CH_2$), 2.12 (dd, J = 15.9, 6.3 Hz, 1H, NCHC**H**$_2$$CO_2$), 1.45–1.55 (m, 2H, NCHC**H**$_2$$CH_2$), 1.42 (t, J = 7.3 Hz, 3H, CCH_2C**H**$_3$), 1.33 (s, 9H, $OC(CH_3)_3$), 1.28 (t, J = 7.3 Hz, 3H, $COCH_2$C**H**$_3$), 1.10–1.21 (m, 2H, $NCHCH_2$C**H**$_2$).
^{13}C NMR (125.8 MHz, C_6D_6, 20 °C):	195.9, 170.4, 127.2, 123.7, 123.5, 122.6, 81.1, 51.9, 42.8, 33.2, 29.3, 28.3, 21.6, 19.0, 18.6, 16.1, 9.8.
FTIR (neat):	2974 (s, C–H), 1727 (s, C=O) 1657 (br–s, C=O), 1516 (s), 1368 (s), 1153 (s).
HRMS–ESI (*m/z*):	calcd for $C_{19}H_{29}NO_3Na$ $[M+Na]^+$: 342.2040, found: 342.2037.
TLC (3% EtOAc–CH_2Cl_2), *Rf*:	0.38 (UV, anis).

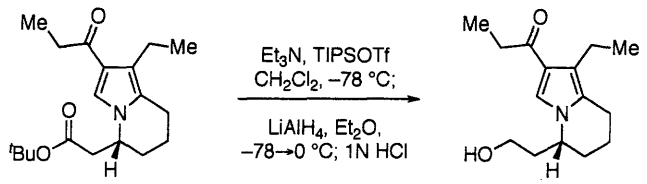

(4a*R*)-1-[1-Ethyl-5-(2-hydroxy-ethyl)-5,6,7,8-tetrahydro-indolizin-2-yl]-propan-1-one (34):

To a faint tan solution of ketoester (*R*)-**33** (990 mg, 3.10 mmol, 1 equiv) and Et_3N (562 mL, 4.03 mmol, 1.30 equiv) in CH_2Cl_2 (15.5 mL) at –78 °C was added triisopropylsilyl trifluoromethane-sulfonate (957 mL, 3.56 mmol, 1.15 equiv), producing an immediate color change to intense yellow. After 15 min, at –78 °C, TLC–analysis (alumina gel, 10% EtOAc–hexanes) indicated that silyl enol ether formation was incomplete, whereupon additional portions of Et_3N (187 mL, 1.34 mmol, 0.43 equiv) and triisopropylsilyl trifluoromethanesulfonate (319 mL, 1.19 mmol, 0.38 equiv) were added sequentially. After a further 15 min, TLC indicated that silyl enol ether formation was complete. The reaction mixture was diluted by the addition of Et_2O (15.5 mL) via syringe over 5 min to maintain the temperature at –78 °C. The flask was opened momentarily, lithium aluminum hydride (706 mg, 18.6 mmol, 6.00 equiv) was added in a single portion as a solid, and the reaction vessel was immediately flushed and sealed under an argon atmosphere. Exchange of the dry-ice–acetone bath with an ice-water bath caused vigorous gas evolution within one minute. After 15 min, TLC-analysis (alumina gel, 30% EtOAc–hexanes) of the reaction mixture indicated that the reduction was complete. The grey reaction mixture was then cooled to –78 °C using a dry-ice–acetone bath. After 5 min, excess lithium aluminum hydride was quenched by the slow addition of water (10 mL) via syringe and the cold bath was removed immediately, allowing the pale grey suspension to warm. Once the mixture had reached 23 °C, it was diluted with a 200-mL portion of Et_2O and a 200-mL volume of aqueous hydrogen chloride solution (1N) to afford an acidic (pH 1) aqueous layer. After thorough mixing of the two layers, the aqueous layer was separated and extracted with Et_2O (4 × 110 mL). The combined organic phases were washed with saturated aqueous sodium hydrogen bicarbonate (120 mL) and brine (60 mL) sequentially, were dried over anhydrous sodium sulfate, were filtered, and were concentrated under reduced pressure to a faint pink oil. Purification of the crude oil by flash column chromatography (silica gel: diam. 5.0 cm, ht. 15.0 cm, 72.5% EtOAc–hex) provided the pure ketoalcohol (*R*)-**34** (695 mg, 91%) as a faint tan oil. For characterization, the corresponding minor regioisomer generated during formation of bicyclic alkene **25** was separated and the data presented is for the pure bicyclic alcohol **34**.

Using the same procedure (*S*)-**33** was converted to the corresponding ketoalcohol (*S*)-**34** (440 mg, 87%).

^1H NMR (500 MHz, C_6D_6, 20 °C): 7.01 (s, 1H, NC**H**=C), 3.77 (dt, J = 13.1, 6.3, 1H, NC**H**CH_2), 3.13–3.22 (m, 2H, $CH_2C\mathbf{H_2}OH$), 2.97–3.09 (m, 2H, $CC\mathbf{H_2}CH_3$), 2.62 (q, J = 7.4 Hz, 2H, $COC\mathbf{H_2}CH_3$), 2.32 (t, J = 6.3 Hz, 2H, $NC{=}C\mathbf{H_2}CH_2$), 1.66 (dt, J = 14.0, 6.6 Hz, 1H, $NCHC\mathbf{H_2}CH_2OH$), 1.45–1.52 (m, 1H, $C\mathbf{H_2}$), 1.44 (t, J = 7.4 Hz, 3H, $CCH_2C\mathbf{H_3}$), 1.31–1.41 (m, 2H,

	CH_2, CH_2'), 1.17–1.25 (m, 2H, CH_2, CH_2'), 1.28 (t, J = 7.3 Hz, 2H, $COCH_2CH_3$), 0.62 (br-s, 1H, OH).
^{13}C NMR (125.8 MHz, C_6D_6, 20 °C):	196.1, 127.2, 123.9, 123.2, 122.6, 59.3, 52.1, 38.8, 33.3, 28.6, 21.7, 19.1, 18.5, 16.2, 9.8.
FTIR (neat):	3420 (s, O–H), 2937 (s, C–H), 1635 (br–s, C=O), 1516 (s), 1382 (s), 1225 (s), 1075 (s).
HRMS–ESI (*m/z*):	calcd for $C_{15}H_{23}NO_2Na$ $[M+Na]^+$: 272.1621, found: 272.1620.
TLC (silica gel, 65% EtOAc–hex), *Rf*:	0.18 (UV, CAM).

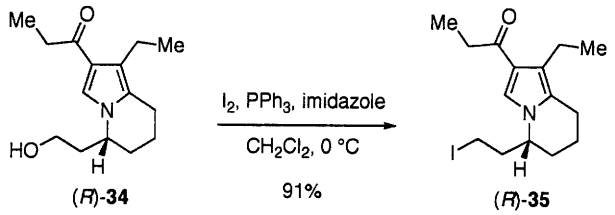

(4a*R*)-1-[1-Ethyl-5-(2-iodo-ethyl)-5,6,7,8-tetrahydro-indolizin-2-yl]-propan-1-one (35):

To a pale yellow solution of PPh_3 (1.64 g, 6.26 mmol, 3.00 equiv) and imidazole (464 mg, 6.82 mmol, 3.27 equiv) in CH_2Cl_2 (8.0 mL) at 0 °C in the dark was added solid iodine (1.59 g, 6.25 mmol, 3.00 equiv), producing a dark yellow slurry. After 15 min, a solution of the alcohol (*R*)-**34** (520 mg, 2.09 mmol, 1 equiv; dried azeotropically by concentration from toluene under reduced pressure, 3 × 1.00 mL) in CH_2Cl_2 (1.50 mL + 2 × 0.50 mL rinse) was added via cannula while the temperature was maintained at 0 °C. After an additional 45 min at 0 °C, the resulting deep orange mixture was diluted with a 5-mL portion of Et_2O followed by the addition of a 10-mL portion of saturated aqueous sodium thiosulfate solution–saturated aqueous sodium bicarbonate solution (1:1) (10 mL). The mixture was immediately allowed to warm to 23 °C and further diluted by the addition of Et_2O (145 mL) and a second portion of saturated aqueous sodium thiosulfate solution (130 mL). The cloudy white aqueous phase was separated and extracted with Et_2O (3 × 90 mL). The combined organic layers were washed with brine (45 mL), were dried over anhydrous sodium sulfate, were filtered, and were concentrated under reduced pressure to a residue consisting of a white solid coated with a tan oil. The crude residue was dissolved in a minimal amount of CH_2Cl_2 and purified by flash column chromatography (silica gel: diam. 4.0 cm, ht. 16.5 cm, 10→12.5% EtOAc–hexane) to give iodide (*R*)-**35** (685 mg, 91%, 85% ee) as a faint yellow oil. At this stage, the corresponding minor regioisomer generated during formation of bicyclic alkene **25** was readily separated. The regioisomerically pure iodide **35** was found to be 85% ee by chiral HPLC analysis [Chiralpak AD-H; 3.0 mL/min; 2.5% *i*-PrOH in hexanes; t_R(major) = 4.44 min, t_R(minor) = 5.03 min].

Using the same procedure (*S*)-**34** was converted to the corresponding iodide (*S*)-**35** (683 mg, 86%, 81% ee).

^{1}H NMR (500 MHz, C_6D_6, 20 °C): 6.83 (s, 1H, NC**H**=C), 3.45 (dt, *J* = 12.9, 5.7 Hz, 1H, NC**H**CH_2), 2.95–3.06 (m, 2H, CC$\mathbf{H_2}CH_3$), 2.57 (q, *J* = 7.3 Hz, 2H, COC$\mathbf{H_2}CH_3$), 2.50–2.56 (m, 1H, NHCH_2C$\mathbf{H_2}$I), 2.43 (dt, 1H, *J* = 10.1, 7.5 Hz, NHCH_2C$\mathbf{H_2}$I), 2.23 (m, 2H, NCC$\mathbf{H_2}CH_2$), 1.77 (dtd, *J* = 14.6, 7.5, 5.7 Hz, 1H, NCHC$\mathbf{H_2}CH_2$I), 1.43 (m, 1H, C$\mathbf{H_2}$), 1.43 (t, *J* = 7.3 Hz, 3H, C=CCH_2C$\mathbf{H_3}$), 1.27 (t, *J* =7.3 Hz, 3H, C(=O)CH_2C$\mathbf{H_3}$), 1.16–1.27 (m, 2H, C$\mathbf{H_2}$, C$\mathbf{H_2}$'), 1.03–1.14 (m, 1H, C$\mathbf{H_2}$), 0.85–0.92 (m, 1H, C$\mathbf{H_2}$).

^{13}C NMR (125.8 MHz, C_6D_6, 20 °C): 195.8, 127.1, 123.5, 122.9, 122.8, 55.2, 39.5, 33.2, 27.4, 21.5, 19.0, 18.4, 16.1, 9.6, 1.5.

FTIR (neat):	2934 (s, C–H), 1651 (br–s, C=O), 1515 (s), 1381 (s), 1193 (s).
HRMS–ESI (*m/z*):	calcd for $C_{15}H_{22}INONa$ $[M+Na]^+$: 382.0638, found: 382.0628.

TLC (silica gel, 15% EtOAc–hexanes), *Rf*: 0.36 (UV, CAM).

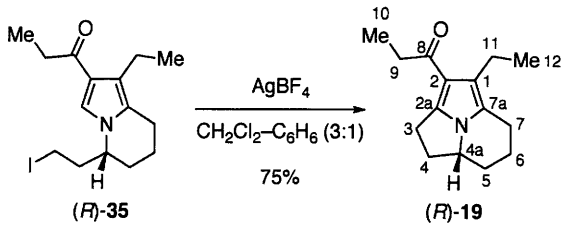

(*R*)-**35** (*R*)-**19**

(4a*R*)-1-(1-Ethyl-3,4,4a,5,6,7-hexahydro-pyrrolo[2,1,5-*cd*]indolizin-2-yl)-propan-1-one (19):[7]

A solution of iodide (*R*)-**35** (509 mg, 1.40 mmol, 1 equiv; dried azeotropically by concentration from toluene under reduced pressure, 3 × 1.00 mL) in CH_2Cl_2 (1.20 mL + 2 × 0.40 mL rinse) was added via cannula to a vigorously stirred pale yellow suspension of silver tetrafluoroborate (690 mg, 3.54 mmol, 2.50 equiv) in CH_2Cl_2–benzene (2:1, 43.0 mL) at 23 °C in the dark. The solution changed to a slightly opaque tan suspension within 5 min. After 2.5 h, the resulting mixture, consisting of a brown solid suspended in a rose colored solution, was diluted with an 80-mL portion of a saturated aqueous sodium thiosulfate solution–saturated aqueous sodium bicarbonate solution (1:1) and a 100-mL volume of Et_2O, such that the rose colored organic layer became tan coloured. The aqueous layer was separated and was extracted with Et_2O (3 × 75 mL). The combined organic layers were washed with brine (40 mL) and were filtered through a plug of celite (diam. 7.0 cm, ht. 8.0 cm, Büchner funnel using slight vacuum). The plug of celite was rinsed with three additional 125-mL portions of Et_2O, and the pale yellow filtrate was concentrated under reduced pressure to afford a yellow semi-solid residue. Purification of the residue by flash column chromatography (silica gel: diam. 4.0 cm, ht. 15.0 cm, 20% EtOAc–hexanes) gave the tricyclic ketone (*R*)-**19** (247 mg, 75%) as a white crystalline solid. (*R*)-**19**: $[\alpha]^{20}_D$ = +58.0 (*c* 0.202, CH_2Cl_2) [lit.:[7] $[\alpha]^{20}_D$ = +64.8 (*c* 0.5, CH_2Cl_2)].

Using the same procedure (*S*)-**35** was converted to the corresponding tricyclic ketone (*S*)-**19** (238 mg, 73%). (*S*)-**19**: $[\alpha]^{20}_D$ = –55.8 (*c* 0.202, CH_2Cl_2).

^{1}H NMR (500 MHz, C_6D_6, 20 °C):	3.01–3.19 (m, 3H, C11–H, C11–H', C4a–H), 2.58 (q, *J* = 7.3 Hz, 2H, C9–H, C9–H'), 2.36–2.51 (m, 3H, C3–H_c, C3–H_t, C7–H_c), 2.18 (ddd, 1H, *J* = 16.5, 12.6, 7.2 Hz, C7–H_t), 1.79 (dt, 1H, *J* = 11.9, 6.0 Hz, C4–H_c), 1.57 (dddd, 1H, *J* = 12.4, 7.2, 3.3, 2.7 Hz, C6–H_t), 1.52 (t, 3H, *J* = 7.5 Hz, C12–H), 1.43 (dq, *J* = 12.4, 3.3 Hz, C5–H_c), 1.32–1.39 (m, 1H, C4–H_t), 1.34 (t, 3H, *J* = 7.5 Hz, C10–H), 1.20 (qdd, 1H, *J* = 12.4, 6.6, 3.3, C6–H_c), 0.73 (qd, 1H, *J* = 12.4, 2.7 Hz, C5–H_t).
^{13}C NMR (125.8 MHz, C_6D_6, 20 °C):	195.2, 137.1, 125.8, 120.7, 117.4, 55.9, 36.2, 34.8, 29.8, 28.3, 22.7, 20.2, 20.0, 16.5, 9.4.
FTIR (neat):	2928 (m, C–H), 1650 (br, s, C=O), 1497 (s), 1450 (s), 1323 (m), 1040 (m).

[7] Sayah, B.; Pelloux-Léon, N.; Vallée, Y. *J. Org. Chem.* **2000**, *65*, 2824–2826.

HRMS–ESI (*m/z*):	calcd for $C_{15}H_{21}NONa$ $[M+Na]^+$: 254.1515, found: 254.1513.
TLC (silica gel, 35% EtOAc–hexanes), *Rf*:	0.45 (UV, CAM).

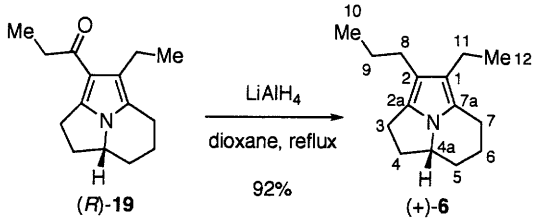

(+)-(4a*R*)-Myrmicarin 217 (6):

To a solution of tricyclic ketone (*R*)-**19** (5.1 mg, 21.9 μmol, 1 equiv) in dioxane (750 μL) at 23 °C was added lithium aluminum hydride (4.1 mg, 109 μmol, 5.00 equiv) in a single portion, and the suspension was warmed to a gentle reflux, during which time slight gas evolution was observed. After 30 min, the mixture was allowed to cool to 23 °C and then cooled further to 0 °C in an ice/water bath. After 5 min, the excess hydride was quenched by the slow addition of water (3.0 mL) via syringe. The cold bath was removed and the grey suspension was allowed to warm to 23 °C, whereupon the aqueous layer was separated and extracted with Et_2O (3 × 4 mL). The combined organic layers were washed with brine (5 mL), were dried over anhydrous sodium sulfate, and were concentrated under reduced pressure to give a yellow oil. The residue was purified by flash column chromatography (alumina gel: diam. 0.6 cm, ht. 4.0 cm, 50% Et_2O–pentane) to provide myrmicarin 217 (**6**, 4.1 mg, 85%) as a clear, colourless oil. Pure samples of myrmicarin 217 may be stored under an argon atmosphere with minimal decomposition for 3 days. Exposure to air results in conversion to myrmicarin 215C and decomposition. Samples of pure myrmicarin 217 retained high purity for up to 7 days when stored at –10 °C as argon-purged solutions in pentane–C_6H_6 (6:1). (*R*)-**6**: $[\alpha]^{20}_D$ = +72.1 (*c* 0.050, CH_2Cl_2) [lit.:[7] $[\alpha]^{20}_D$ = +88 (*c* 1, CH_2Cl_2)].

Using the same procedure (*S*)-**19** was converted to *ent*-myrmicarin 217 ((*S*)-**6**, 13.3 mg, 99%). (*S*)-**6**: $[\alpha]^{20}_D$ = –67.4 (*c* 0.074, CH_2Cl_2).

^{1}H NMR (500 MHz, C_6D_6, 20 °C): 3.33 (tdd, 1H, *J* = 10.8, 4.6, 3.7 Hz, C4a–H), 2.54–2.67 (m, 7H, C3–H_c, C3–H_t, C7–H_c, C8–H, C8–H', C11–H, C11–H'), 2.44 (ddd, 1H, *J* = 17.2, 11.0, 6.6 Hz, C7–H_t), 2.01 (dddd, 1H, *J* = 11.3, 5.5, 4.6, 1.3 Hz, C4–H_c), 1.69–1.82 (m, 3H, C9–H, C9–H', C6–H_t), 1.54–1.63 (m, 2H, C4–H_t, C5–H_c), 1.41 (tddd, 1H, *J* = 13.2, 11.0, 6.7, 2.8 Hz, C6–H_c), 1.31 (t, 3H, *J* = 7.5 Hz, C12–H), 1.07 (t, 3H, *J* = 7.3 Hz, C10–H), 0.88 (tdd, 1H, *J* = 13.2, 10.8, 2.6 Hz, C5–H_t).

^{13}C NMR (125.8 MHz, C_6D_6, 20 °C): 127.7 (C2a), 121.5 (C1), 118.3 (C7a), 114.1 (C2), 55.3 (C4a), 37.6 (C4), 30.4 (C5), 28.5 (C3), 25.4 (C8), 25.4 (C9), 23.3 (C6), 21.1 (C7), 19.2 (C11), 16.9 (C12), 14.9 (C10).

FTIR (neat): 2956 (s, C–H), 2851 (s, C–H), 1656 (w), 1456 (m), 1390 (m), 1321 (m), 1076 (w).

HRMS–ESI (*m/z*):	calcd for $C_{15}H_{24}N$ $[M+H]^+$: 218.1903, found: 218.1916.
TLC (alumina gel, 1% Et_2O–pentane), *Rf*:	0.43 (UV, PMA).

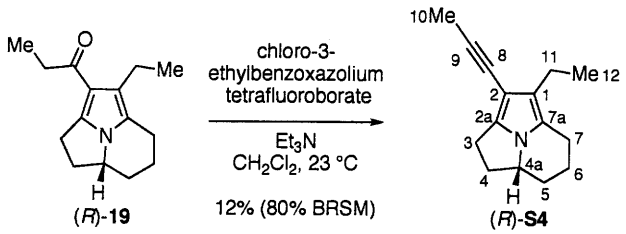

(4a*R*)-1-Ethyl-2-(prop-1-ynyl)-3,4,4a,5,6,7-hexahydro-pyrrolo[2,1,5-*cd*]indolizine (S4):

A solution of tricyclic ketone (*R*)-**19** (30.2 mg, 131 μmol, 1 equiv) and Et_3N (171 μL, 1.23 μmol, 9.38 equiv) in CH_2Cl_2 (400 μL + 2 × 2 μL rinse) was added via cannula to a suspension of 2-chloro-3-ethylbenzoxazolium tetrafluoroborate (44.1 mg, 164 μmol, 1.25 equiv) in CH_2Cl_2 (900 μL) at 0 °C, causing a color change to bright yellow. The mixture was allowed to warm slowly to 23 °C over 2.5 h by slow warming of the cold bath, at which time the resulting deep–brown and opaque mixture was diluted sequentially with Et_2O (6 mL) and brine (4 mL). The aqueous layer was separated and was extracted with Et_2O (3 × 4 mL), and the combined organic layers were washed with $NaHCO_3$ (3 × 4 mL), such that the final brine wash did not appear green. The organic layer was dried over anhydrous sodium sulfate, was filtered, and was concentrated under reduced pressure to afford a deep–brown oil. Purification of the residue by flash column chromatography (alumina gel: diam. 1.5 cm, ht. 5.5 cm, 7.5% Et_2O–pentane) gave the alkyne (*R*)-**S4** (5.8 mg, 12%; 80% based on recovered starting material) as a faint yellow oil. Alkyne **S4** is extremely sensitive to C6-C7 oxidation and must be stored and handled with minimal exposure to air. Samples of alkyne **S4** were used in subsequent reactions within 24 h of preparation.

Using the same procedure (*S*)-**19** was converted to the corresponding alkyne (*S*)-**S4** (5.8 mg, 19%; 72% based on recovered starting material).

^{1}H NMR (500 MHz, C_6D_6, 20 °C): 3.14 (tdd, 1H, J = 10.8, 5.8, 3.7 Hz, C4a–H), 2.71–2.91 (m, 3H, C3–H_t, C11–H, C11–H'), 2.61 (ddd, 1H, J = 15.1, 10.6, 5.8 Hz, C3–H_c), 2.50 (ddd, 1H, J = 16.3, 6.2, 0.8 Hz, C7–H_c), 2.30 (ddd, 1H, J = 16.3, 11.9, 6.7 Hz, C7–H_t), 1.94 (s, 3H, C10–H), 1.82 (dt, 1H, J = 12.0, 5.8 Hz, C4–H_c), 1.61 (ddddd, 1H, J = 13.3, 6.7, 4.1, 2.4, 0.8 Hz, C6–H_t), 1.47 (t, 3H, J = 7.5 Hz, C12–H), 1.36–1.48 (m, 2H, C5–H_c, C4–H_t), 1.27 (tddd, 1H, J = 13.3, 11.9, 6.2, 2.9 Hz, C6–H_c), 0.74 (tdd, 1H, J = 13.3, 10.8, 2.4 Hz, C5–H_t).

^{13}C NMR (125.8 MHz, C_6D_6, 20 °C): 134.6, 125.6, 118.5, 98.1, 85.3, 76.4, 55.8, 37.1, 30.0, 25.7, 22.9, 20.7, 20.0, 16.3, 5.1.

FTIR (neat): 2927 (s, C–H), 2851 (s, C–H), 2222 (w, C≡C), 1597 (w), 1430 (s), 1321 (s), 1022 (w).

HRMS–ESI (*m/z*):	calcd for $C_{15}H_{20}N$ $[M+H]^+$: 214.1590, found: 214.1598.
TLC (silica gel, 30% EtOAc-hexanes), *Rf*:	0.53 (UV, ninhydrin).

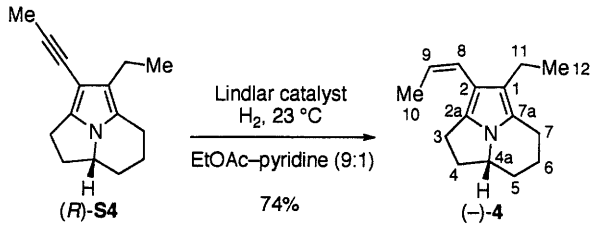

(–)-(4a*R*)-Myrmicarin 215A (4):

A sample of Lindar catalyst (0.7 mg, 30 wt %) was added to a solution of alkyne (*R*)-**S4** (2.3 mg, 10.8 μmol, 1 equiv) in EtOAc–pyridine (4:1, 2.00 mL) at 23 °C and the flask was flushed with a stream of dihyrdogen for 2 min using a balloon. The grey suspension was then maintained under a balloon pressure of dihydrogen. After 1.5 h and again after 3 h total stirring time, additional 0.7-mg portions of Lindlar catalyst were added and the flask was purged with balloon pressure dihydrogen for 3 min. After an additional 2.5 h, the flask was flushed with argon for 3 min to remove the remaining dihydrogen, and the mixture was diluted with Et_2O (5 mL). The resulting suspension was filtered through a plug of celite (diam. 0.6 cm, ht. 5.5 cm) and the plug was rinsed with an 10-mL portion of Et_2O. After concentrating to approximately 1 mL, the clear and colourless filtrate was filtered through a plug of activated basic alumina (diam. 0.6 cm, ht. 4.0 cm) and concentrated under reduced pressure to give (–)-myrmicarin 215A (**4**) as a white crystalline solid (1.7 mg, 74%). Myrmicarin 215A (**4**) was found to isomerize to myrmicarin 215B (**5**) upon exposure to silica gel for TLC analysis (with and without neutralization using triethylamine). Furthermore, significant decomposition upon exposure to silica gel was apparent. ^{1}H NMR analysis of the direct reduction product showed only the presence of myrmicarin 215A. Exposure to air results in conversion to myrmicarin 213A and decomposition, which is complete within approximately 1 day. Samples of myrmicarin 215A retained purity for up to 7 days when stored at –10 °C as argon-purged solutions in pentane–C_6H_6 (6:1). (*R*)-**4**: $[\alpha]^{20}_D = -53.8$ (*c* 0.045, CH_2Cl_2).

Using the same procedure (*S*)-**S4** was converted to *ent*-myrmicarin 215A ((*S*)-**4**, 3.9 mg, 70%). (*S*)-**4**: $[\alpha]^{20}_D = +49.8$ (*c* 0.090, CH_2Cl_2).

^{1}H NMR (500 MHz, C_6D_6, 20 °C): 6.66 (dqd, 1H, *J* = 10.8, 1.8, 0.6 Hz, C8–H), 5.65 (dq, *J* = 10.8, 6.9 Hz, C9–H), 3.33 (tdd, 1H, *J* = 10.7, 5.5, 3.7 Hz, C4a–H), 2.54–2.67 (m, 4H, C3–H_c, C7–H_c, C11–H, C11–H'), 2.49 (dd, 1H, *J* = 14.8, 8.1 Hz, 3–H_t), 2.39 (ddd, 1H, *J* = 16.2, 11.8, 6.8 Hz, 7–H_t), 1.96 (dt, *J* = 11.5, 5.5 Hz, 1H, 4–H_c), 1.90 (dd, 3H, *J* = 6.9, 1.8 Hz, 10–H), 1.68 (ddddd, 1H, *J* = 13.3, 6.8, 4.1, 2.5, 1.4 Hz, 6–H_t), 1.46–1.59 (m, 2H, 4–H_t, 5–H_c), 1.36 (tddd, *J* = 13.3, 11.8, 6.7, 2.7 Hz, 1H, 6–H_c), 1.30 (t, 3H, *J* = 7.5 Hz, 12–H), 0.82 (tdd, 1H, *J* = 13.3, 10.7, 2.5 Hz, 5–H_t).

^{13}C NMR (125.8 MHz, C_6D_6, 20 °C): 129.2 (C2a), 124.7 (C8), 122.3 (C1), 120.8 (C9), 119.4 (C7a), 112.8 (C2), 55.8 (C4a), 37.8 (C4), 30.4

	(C5), 27.6 (C3), 22.9 (C6), 20.9 (C7), 19.3 (C11), 16.7 (C12), 15.8 (C10).
FTIR (neat):	3010 (m, C–H), 2929 (s, C–H), 1727 (w), 1639 (m), 1443 (m), 1321 (m), 1167 (w).
HRMS–ESI (*m/z*):	calcd for $C_{15}H_{22}N$ $[M+H]^+$: 216.1747 found: 216.1753.
TLC (alumina gel, 30% Et_2O–pentane), *Rf*:	0.28 (UV, PMA).

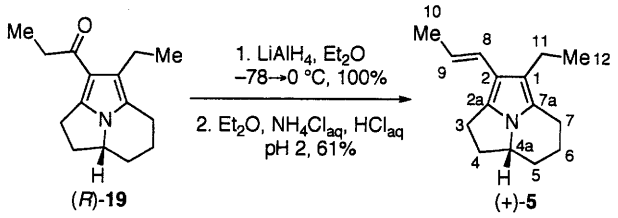

(+)-(4a*R*)-Myrmicarin 215B (5):

To a solution of tricyclic ketone (*R*)-**19** (11.8 mg, 51.0 μmol, 1 equiv) in Et_2O (950 μL) at –78 °C was added solid lithium aluminum hydride (11.6 mg, 306 μmol, 6.00 equiv) in a single portion. The mixture was then allowed to warmed to 0 °C using an ice–water bath. After 40 min at 0 °C, the grey suspension was cooled on a dry-ice–acetone bath for 5 min and the excess hydride was quenched by the slow addition of water (1.20 mL) via syringe. The cold bath was immediately removed and the mixture allowed to warm to 23 °C. The pale grey suspension was diluted sequentially with a 6-mL portion of Et_2O and a saturated aqueous solution of Rochelle salt (6 mL), and the two–phase mixture was vigorously stirred. After 3 h, the resulting slightly opaque aqueous layer was separated from the clear and colourless organic layer and was extracted with EtOAc (3 × 5 mL). The combined organic layers were washed with a 5-mL protion of brine, were dried over anhydrous sodium sulfate, were filtered, and were concentrated under reduced pressure to give the corresponding alcohols as a colourless oil (11.9 mg, 100%) and a mixture of C8-epimers (~3:2).

A solution of the C8-alcohols (21.9 mg, 93.9 μmol, 1 equiv) in 15.0 mL Et_2O was washed sequentially with 3-mL portions of a saturated aqueous ammonium chloride solution–aqueous hydrochloric acid solution (9 × 3 mL pH 2 aqueous NH_4Cl) until TLC indicated that elimination was complete. The organic solution was then washed with saturated aqueous sodium bicarbonate solution (4 mL), then with brine (4 mL), was dried over anhydrous sodium sulfate, was filtered, and was concentrated under reduced pressure to give myrmicarin 215B (**5**) as fine white needles (12.4 mg, 61%). Although stable to chromatography on neutral alumina gel, ^1H NMR analysis showed that further purification was unnecessary. Exposure to air results in conversion to myrmicarin 213B and decomposition, which is complete within approximately 1 day. Samples of myrmicarin 215B retained high purity for up to 5 days when stored at –10 °C as argon-purged solutions in pentane–C_6H_6 (6:1). (*R*)-**5**: $[\alpha]^{20}_D$ = +60.4 (*c* 0.044, CH_2Cl_2).

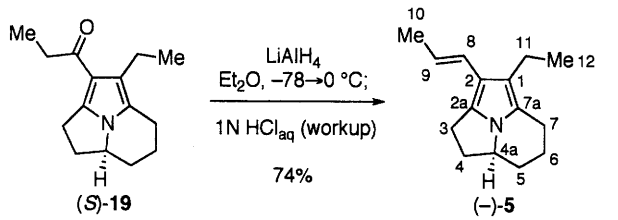

(–)-(4a*S*)-Myrmicarin 215B (5):

To a solution of tricyclic ketone (*S*)-**19** (16.1 mg, 69.6 μmol, 1 equiv) in Et_2O (1.40 mL) at –78 °C was added lithium aluminum hydride (15.9 mg, 418 μmol, 6.00 equiv) in a single portion. The mixture was then allowed to warm to 0 °C using an ice-water bath. After 35 min at 0 °C, the grey suspension was cooled on a dry-ice–acetone bath for 5 min and the excess hydride

was quenched by addition of water (1.40 mL) via syringe. The cold bath was removed immediately and the mixture allowed to warm to 23 °C. A 10-mL portion of Et_2O was added and the mixture was washed with a saturated aqueous ammonium chloride solution–aqueous hydrochloric acid solution (10 mL + 3 × 2 mL pH 2 aqueous NH_4Cl), at which point TLC indicated that elimination was complete. The organic solution was washed with saturated aqueous sodium bicarbonate solution (3 mL), was dried over anhydrous sodium sulfate, was filtered, and was concentrated under reduced pressure to give *ent*-myrmicarin 215B (**5**) as fine white needles (11.1 mg, 74%). (*S*)-**5**: $[\alpha]^{20}_D = -58.5$ (*c* 0.085, CH_2Cl_2).

^{1}H NMR (500 MHz, C_6D_6, 20 °C):	6.67 (dq, 1H, *J* = 15.6, 1.7 Hz, C8–H), 5.89 (dq, *J* = 15.6, 6.5 Hz, C9–H), 3.25 (tdd, 1H, *J* = 10.8, 5.3, 3.7 Hz, C4a–H), 2.62–2.72 (m, 4H, C3–H_c, C3–H_t, C11–H, C11–H'), 2.57 (ddd, 1H, *J* = 16.2, 6.5, 1.3 Hz, C7–H_c), 2.37 (ddd, 1H, *J* = 16.2, 11.9, 6.8 Hz, C7–H_t), 1.91–1.96 (m, 1H, C4–H_c), 1.94 (dd, 3H, *J* = 6.5, 1.7 Hz, C10–H), 1.68 (ddddd, 1H, *J* = 13.7, 6.8, 4.1, 2.6, 1.3 Hz, C6–H_t), 1.44–1.51 (m, 2H, C4–H_t, C5–H_c), 1.27–1.40 (m, 1H, C6–H_c), 1.32 (t, 3H, *J* = 7.5 Hz, C12–H), 0.82 (tdd, 1H, *J* = 12.9, 10.8, 2.6 Hz, C5–H_t).
^{13}C NMR (125.8 MHz, C_6D_6, 20 °C):	128.7 (C2a), 126.0 (C8), 121.4 (C1), 119.2 (C9), 118.7 (C7a), 113.9 (C2), 55.3 (C4a), 37.1 (C4), 30.2 (C5), 26.2 (C3), 23.1 (C6), 20.8 (C7), 19.6 (C10), 19.2 (C11), 17.0 (C12).
FTIR (neat):	2928 (s, C–H), 1659 (s), 1506 (w), 1452 (s), 1321 (m), 1062 (w), 961 (m).
HRMS–ESI (*m/z*):	calcd for $C_{15}H_{22}N$ $[M+H]^+$: 216.1747 found: 216.1754.
TLC(alumina gel, 30% Et_2O–pentane), *Rf*:	0.28 (UV, PMA).

Table S1. ^{1}H and ^{13}C NMR data in ppm for myrmicarin 215A (**4**), myrmicarin 215B (**5**), and myrmicarin 217 (**6**).[a,b]

	Myrmicarin 215A (**4**)				Myrmicarin 215B (**5**)				Myrmicarin 217 (**6**)			
	Isolation report[c,d] C_6D_6 (^{13}C rel. TMS) C_6D_5H (^{1}H rel. TMS)		**This report**[e] C_6D_6 (^{13}C δ128.0) C_6D_5H (^{1}H δ7.16)		**Isolation report**[c,d] C_6D_6 (^{13}C rel. TMS) C_6D_5H (^{1}H rel. TMS)		**This report**[e] C_6D_6 (^{13}C δ128.0) C_6D_5H (^{1}H δ7.16)		**Isolation report**[c,f] C_6D_6 (^{13}C rel. TMS) C_6D_5H (^{1}H rel. TMS)		**This report**[e] C_6D_6 (^{13}C δ128.0) C_6D_5H (^{1}H δ7.16)	
	δ_C	δ_H	δ_C	δ_H	δ_C	δ_H	δ_C	δ_H	δ_C	δ_H	δ_C	δ_H
1	121.9	-	122.3	-	121.0	-	121.4	-	121.2	-	121.5	-
2	112.5	-	112.8	-	113.5	-	113.9	-	113.8	-	114.1	-
2a	128.8	-	129.2	-	128.2	-	128.7	-	127.4	-	127.7	-
3	27.2	2.62[c]	27.6	2.54–2.67[c]	27.2	2.63–2.66[c,t]	26.2	2.63–2.72[c,t]	28.1	2.62[c]	28.5	2.54–2.67[c,t]
		2.49[t]		2.49[t]						2.60[t]		
4	37.4	1.97[c]	37.8	1.96[c]	36.8	1.95[c]	37.1	1.91–1.96[c]	37.3	2.03[c]	37.6	2.01[c]
		1.51[t]		1.46–1.59[t]		1.51[t]		1.44–1.51[t]		1.59[t]		1.54–1.63[t]
4a	55.2	3.34	55.8	3.33	54.9	3.26	55.3	3.25	55.0	3.33	55.3	3.33
5	30.0	1.55[c]	30.4	1.46–1.59[c]	29.9	1.53[c]	30.2	1.44–1.51[c]	30.1	1.58[c]	30.4	1.54–1.63[c]
		0.83[t]		0.82[t]		0.83[t]		0.82[t]		0.89[t]		0.88[t]
6	22.5	1.37[c]	22.9	1.36[c]	22.5	1.36[c]	23.1	1.27–1.40[c]	23.0	1.42[c]	23.3	1.41[c]
		1.69[t]		1.68[t]		1.69[t]		1.68[t]		1.73[t]		1.69–1.82[t]
7	20.5	2.59[c]	20.9	2.54–2.67[c]	20.4	2.57[c]	20.8	2.57[c]	20.8	2.64[c]	21.1	2.54–2.67[c]
		2.39[t]		2.39[t]		2.37[t]		2.37[t]		2.44[t]		2.44[t]
7a	119.0	-	119.4	-	118.3	-	118.7	-	118.0	-	118.3	-
8	124.3	6.65	124.7	6.66	125.6	6.66	126.0	6.67	25.0	2.56, 2.64	25.4	2.54–2.67
9	120.4	5.64	120.8	5.65	118.9	5.88	119.2	5.89	25.0	1.76	25.4	1.69–1.82
10	15.4	1.90	15.8	1.90	19.2	1.94	19.6	1.94	14.6	1.07	14.9	1.07
11	18.9	2.54–2.66	19.3	2.54–2.67	18.8	2.59–2.71	19.2	2.62–2.72	18.9	2.57, 2.61	19.2	2.54–2.67
12	16.3	1.29	16.7	1.30	16.6	1.31	17.0	1.32	16.5	1.30	16.9	1.31

[a]The superscripts 'c' and 't refer to the protons *cis* and *trans*, respectively, to the C4a methine in each spin system. [b]Proton chemical shifts for multiplets are reported as a range. [c]From reference 1c. ^{1}H and ^{13}C spectra were obtained in benzene-d_6 at 500 MHz and 125 MHz, respectively, and chemical shifts were assigned relative to tetramethylsilane as an internal standard. [d]Myrmicarins 215A (**4**) and 215B (**5**) were isolated and characterized as a 2:1 mixture. ^{1}H NMR assignments for each separate ^{1}H spin set were achieved using phase sensitive (^{1}H,^{1}H)-DQ-COSY and *E*-COSY analysis. ^{13}C NMR assignments were achieved using HMQC analysis. [e]Myrmicarins 215A (**4**), 215B (**5**), and 217 (**6**) were isolated and characterized as single components. ^{1}H and ^{13}C spectra were obtained in benzene-d_6 at 500 MHz and 125 MHz, respectively. ^{1}H NMR chemical shifts were assigned relative to residual protium in the solvent C_6D_5H, δ7.16 ppm. ^{13}C NMR chemical shifts were assigned relative to carbon resonances in the solvent C_6D_6, δ128.0 ppm. [f]Myrmicarin 217 (**6**) was isolated and characterized as a single component.

Table S2. Coupling constants in Hz for myrmicarin 215A (**4**), myrmicarin 215B (**5**), and myrmicarin 217 (**6**).[a,b]

	Isolation report[c]	**This report**[d]		
	Myrmicarin 215A (**4**), 215B (**5**), 217 (**6**)	Myrmicarin 215A (**4**)	Myrmicarin 215B (**5**)	Myrmicarin 217 (**6**)
3–H_c	14.9, 10.7, 6.2	-	-	-
3–H_t	14.9, 8.0, 0.5	14.8, 8.1	-	-
4–H_c	11.7, 6.2, 5.3, 0.5	11.5, 5.5, 5.5	-	11.3, 5.5, 4.6, 1.3
4–H_t	11.7, 10.7, 10.3, 8.0	-	-	-
4a	11.1, 10.3, 5.4, 3.8	10.7, 10.7, 5.5, 3.7	10.8, 10.8, 5.3, 3.7	10.8, 10.8, 4.6, 3.7
5–H_c	12.7, 4.0, 3.8, 2.9	-	-	-
5–H_t	13.1, 12.7, 11.1, 2.7	13.3, 13.3, 10.7, 2.5	12.9, 12.9, 10.8, 2.6	13.2, 13.2, 10.8, 2.6
6–H_c	13.5, 13.1, 11.9, 6.6, 2.9	13.3, 13.3, 11.8, 6.7, 2.7	-	13.2, 13.2, 11.0, 6.7, 2.8
6–H_t	13.5, 6.9, 4.0, 2.7, 1.2	13.3, 6.8, 4.1, 2.5, 1.4	13.7, 6.8, 4.1, 2.6, 1.3	-
7–H_c	15.9, 6.6, 1.2	-	16.2, 6.5, 1.3	-
7–H_t	15.9, 11.9, 6.9	16.2, 11.8, 6.8	16.2, 11.9, 6.8	16.2, 11.0, 6.6
8	11.0[e], 15.6[f], 1.7[e,f]; 6.5[g]	10.8, 1.8, 0.6	15.6, 1.7	-
9[h]	11.0[e], 6.9[e]; 15.6[f], 6.6[f]	10.8, 6.9	15.6, 6.5	-
10	6.9[e], 6.6[f], 1.7[e,f]; 7.2[g]	6.9, 1.8	6.5, 1.7	7.3
12	7.5	7.5	7.5	7.5

[a]The subscripts 'c' and 't refer to the protons *cis* and *trans*, respectively, to the C4a methine in each spin system. [b]Coupling constants for signals that appear as multiplets are not reported. [c]From reference 1c. Myrmicarins 215A (**4**) and 215B (**5**) were isolated and characterized as a 2:1 mixture; myrmicarin 217 (**6**) was isolated and characterized as a single component. Coupling constants were extracted using phase sensitive (^{1}H,^{1}H)-DQ-COSY and *E*-COSY analysis and are reported as an averaged value for myrmicarins 215A (**4**), 215B (**5**), and 217 (**6**). [d]Myrmicarins 215A (**4**), 215B (**5**), and 217 (**6**) were isolated and characterized as single components. Coupling constants were extracted from the one-dimensional ^{1}H NMR spectrum. [e]Coupling constant for myrmicarin 215A (**4**). [f]Coupling constant for myrmicarin 215B (**5**). [g]Coupling constant for myrmicarin 217 (**6**). [h]The C9–H protons in myrmicarin 217 (**6**) couple to the C8–H protons with a coupling constant of 6.5 Hz and to the C10–H protons with a coupling constant of 7.2 Hz.

Chapter II.

Palladium Catalyzed Synthesis of *N*-Vinyl Pyrroles and Indoles

Introduction and Background

Transition metal catalyzed carbon–nitrogen bond formation has become a powerful methodology in organic synthesis.[1] A variety of highly active palladium and copper catalyst systems have been reported for the *N*-arylation of amines, amides, azoles, and carbamates.[2,3] However, there exist fewer examples of C–N bond formation as a method of *N*-vinylation.1[,4,5] Reports concerning the *N*-vinylation of dialkyl amines and azoles are even more rare as compared to *N*-vinylation of amides and carbamates.[6,7] A single study on the palladium catalyzed coupling of lithiated azoles with vinyl bromides has been reported.[6c] Herein we describe a palladium catalyzed stereospecific coupling of vinyl triflates with pyrroles and indoles.

Results and Discussion

In 2004, Buchwald reported the efficient copper catalyzed asymmetric conjugate reduction of a variety of 3-aza-2-enoates (**2**) to give the corresponding 3-aza-alkanoates (**3**, Equation 1).[7] The necessary 3-aza-2-enoate (**2**) substrates were prepared *via* a copper catalyzed *N*-vinylation of azaheterocycles and lactams with *Z*-3-iodoenoates (**1**).

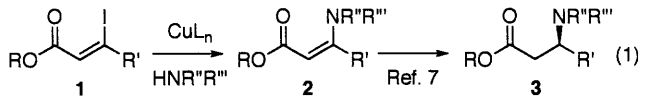

(1)

We were particularly interested in the use of this chemistry for the synthesis of optically active β-azolyl carboxylic acid building blocks for complex alkaloid synthesis. However, the reaction conditions for generating the necessary *Z*-3-iodoenoates (**1**), namely treatment of the corresponding ynoates with sodium iodide in acetic acid at elevated temperatures (60→150 °C),[8] were not compatible with several substrates of interest. Furthermore, a similar direct synthesis of the isomeric *E*-3-iodoenoates[9] is not available. We envisioned the use of readily available β-ketoesters as precursors for the stereospecific synthesis of both *Z*- and *E*-β-pyrrolyl enoates **4** (Scheme 1). Specifically, we sought a catalytic method for the stereospecific *N*-vinylation of pyrroles with configurationally defined vinyl triflates.[10]

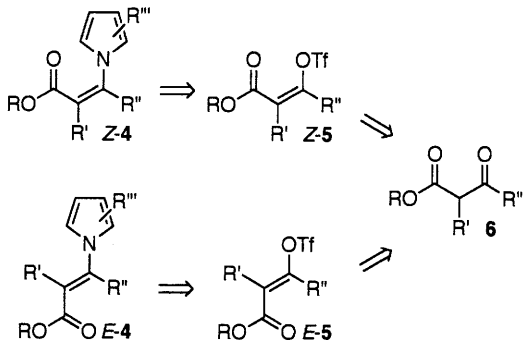

Scheme 1. Stereospecific synthesis of β-pyrrolyl enoates.

Initial experiments on the coupling of pyrrole (**7a**) and vinyl triflates **5a-b** (Equation 2) revealed that copper-based catalyst systems were not effective, typically returning the unreacted triflates. However, the combination of palladium dibenzylideneacetone ($Pd_2(dba)_3$) and 2-dicyclohexyl-phosphino-2′,4′,6′-triisopropyl-1,1′-biphenyl (XPhos)[11,12] provided a highly active catalyst system for the efficient and selective synthesis of the desired *N*-vinyl pyrroles. Under optimal conditions, the coupling of the vinyl triflate **5a** (1 equiv) with pyrrole (**7a**, 1.5 equiv) using Pd_2dba_3 (5 mol%), XPhos (10 mol%) as ligand in the presence of anhydrous potassium phosphate (1.40 equiv) in toluene at 60 °C proceeded to give the desired *Z*-β-pyrrolyl enoate **4aa** with complete stereospecificity in 84% yield after 3.5 h (Table 1, entry 1). Under identical conditions, the coupling of the more sensitive dimethoxy–acetal containing vinyl triflate **5b** afforded the corresponding *N*-vinyl pyrrole **4ba** (Equation 2) in 79% isolated yield.[13]

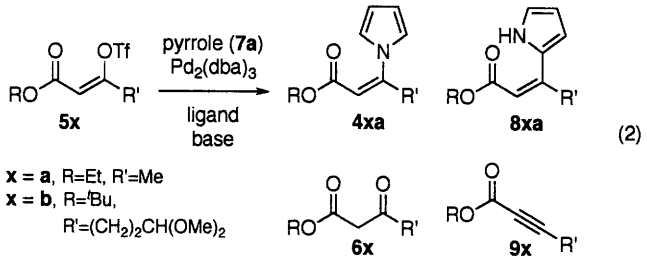

(2)

Two commonly observed side products in these coupling reactions were the β-ketoesters **6a-b** and the ynoates **9a-b** (Equation 2). Potassium phosphate tribasic was most effective as the base–additive compared to potassium phosphate dibasic, cesium carbonate, triethylamine and 1,8-diazabicyclo[5.4.0]undec-7-ene, the latter giving predominantly the undesired ynoate byproduct. The use of rigorously dried anhydrous potassium phosphate was found to minimize

the formation of both the β-ketoester and the ynoate byproducts.[14,15] Attempted palladium catalyzed coupling of preformed pyrrolyllithium with vinyl triflate **5b** gave predominantly (~80%) the undesired elimination product **9b** (Equation 2).[6c] Furthermore, when *N*-tributylstannylpyrrole[16] was used in place of pyrrole (**7a**) for the synthesis of *N*-vinyl pyrrole **4ba**, in the absence of anhydrous potassium phosphate, the product mixture contained as much as 50% *C*-coupled product **8ba** (Equation 2).[17] Interestingly, this undesired *C*-coupled byproduct was not observed using pyrrole (**7a**) with the optimal conditions described above.

Considering the synthetic utility of *N*-vinyl pyrroles and indoles and encouraged by these early results, we sought to explore the generality of this catalytic *N*-vinylation reaction (Table 1). Representative vinyl triflates[18] and azaheterocycles used as substrates in these studies are shown in Chart 1.

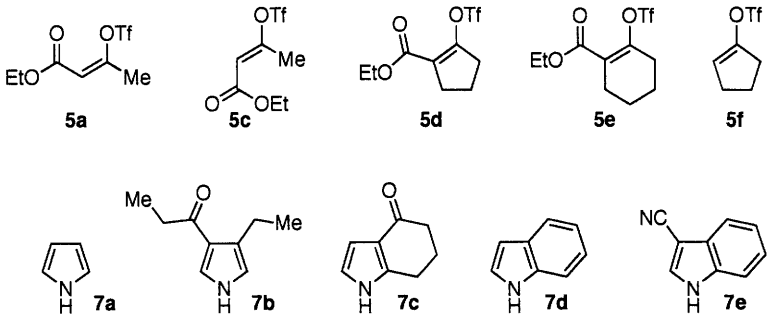

Chart 1. Representative vinyl triflate and heterocycle substrates.

The coupling of *Z*-vinyl triflate **5a** with the less nucleophilic acyl pyrrole **7b** at 60 °C affords the desired product **4ab** in 70% yield after 7 h (Table 1, entry 2). An enhancement in the rate of this coupling reaction was noted using dioxane as a co-solvent, affording *N*-vinyl pyrrole derivative **4ab** in 91% isolated yield after 1 h at 60 °C (Table 1, entry 3). Alternatively, increasing the reaction temperature to 80 °C gave **4ab** in 81% yield after complete consumption of starting material (Table 1, entry 4). The coupling of *Z*-vinyl triflate **5a** with the more sterically hindered tetrahydroindolone **7c** was found to be more difficult as compared to the acyl pyrrole **7b** (Table 1, compare entries 2 and 5). The use of toluene–dioxane solvent mixture and higher reaction temperatures slightly increased the yield of this coupling reaction to afford **4ac** in 50% isolated yield (Table 1, entry 7). The coupling of the cyanoindole **7e**, the least reactive azole examined in this study, with *Z*-vinyl triflate **5a** gave only 24% yield of the *N*-vinyl

Table 1. Palladium catalyzed *N*-vinylation of azaheterocycles with vinyl triflates.

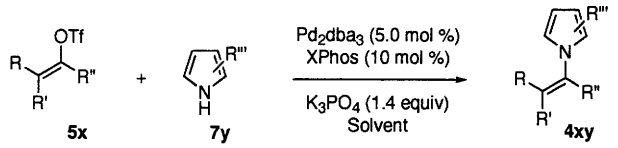

entry	product	temperature (time)[a]	solvent[b]	yield[c]
1	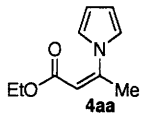 **4aa**	**60 (3.5)**	**A**	**84**
2	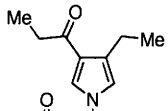	60 (7)	A	70
3	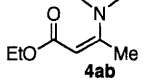 **4ab**	**60 (1)**	**B**	**91**
4		80 (1.5)	A	81
5	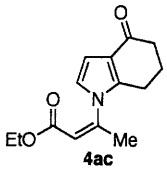	60 (25)	A	29[d]
6		60 (1); 80 (6)	B	44
7	**4ac**	**60 (2.5); 80 (7)**	**A**	**50[d]**
8	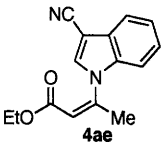	60 (48)	A	24[d]
9		60 (1); 80 (6)	B	9[e]
10	**4ae**	60 (2.5); 80 (7)	A	17
11	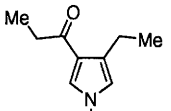	60 (2.5); 80 (3)	A	52
12	**4cb**	**60 (0.5); 80 (1.5)**	**B**	**60[f]**
13	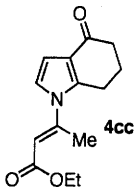 **4cc**	60 (2.5); 80 (3)	A	29
14		**60 (0.5); 80 (1.5)**	**B**	**73**
15	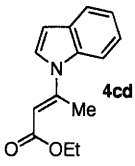 **4cd**	**60 (5)**	**A**	**74**

entry	product	temperature (time)[a]	solvent[b]	yield[c]
16	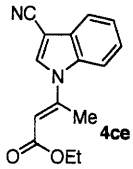 **4ce**	**60 (2.5); 80 (3)**	**A**	**74**
17		60 (0.5); 80 (2.5)	B	71
18	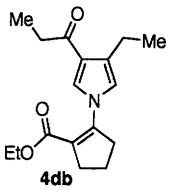 **4db**	**60 (0.5); 80 (2)**	**B**	**70**
19	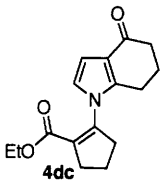	60 (0.5); 80 (3); 95 (3.5)	B	53
20	**4dc**	**60 (0.5); 95 (3.5)**	**B**	**62**
21	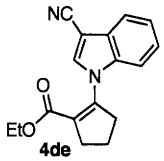	60 (0.5); 80 (3); 95 (3.5)	B	18[g]
22	**4de**	60 (0.5); 95 (2.5)	B	17[g]
23	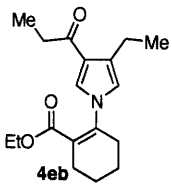	60 (6); 80 (8)	A	55
24	**4eb**	**60 (2.5); 110 (2.5)**	**A**	**91**
25	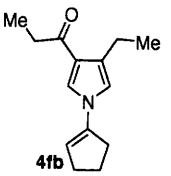	60 (5.5); 80 (18.5)	A	43[d]
26	**4fb**	**60 (1); 110 (16)**	**A**	**72**

[a] Reaction temperature in °C; reaction time in h. [b] Solvent: A = toluene, B = toluene–1,4-dioxane (3:1). [c] Isolated yield after purification. [d] Remaining vinyl triflate: entry 5, 38%; entry 7, 13%; entry 8, 65%; entry 25, 25%. [e] Complete consumption of **5a**; the ynoate **9a** constitutes the mass balance. [f] Complete conversion to product **4cb** (>90% yield) prior to chromatographic purification. [g] Ethyl 2-oxo-cyclopentanecarboxylate was formed (~50%).

azaheterocycle **4ae** after 48 h (Table 1, entry 8). Both the use of toluene–dioxane solvent mixture and higher reaction temperatures were found to increase the formation of the ynoate **9a** (Equation 2) without a net increase in the yield of the coupled product **4ae** (Table 1, entries 9 and 10).[15,19]

To highlight the stereospecificity of this transformation, we examined the coupling between *E*-vinyl triflate **5c** and various azaheterocycles (Table 1, entries 11–17). In every case, the palladium catalyzed stereospecific C–N bond formation proceeded to afford the desired *E*-enoate. Acyl pyrrole **7b**, tetrahydroindolone (**7c**), indole (**7d**), and 3-cyanoindole (**7e**) were successfully coupled with *E*-vinyl triflate **5c** to give the corresponding *N*-vinyl azaheterocycle in 60, 73, 74, and 74% yield, respectively (Table 1, entries 12, 14, 15, and 16). Interestingly, the *E*-vinyl triflate **5c** demonstrated an enhanced rate of coupling relative to the *Z*-vinyl triflate **5a** in all cases examined. Additionally, the coupling reactions employing *E*-vinyl triflate **5c** exhibited a much slower rate of ynoate formation as compared to those using *Z*-vinyl triflate **5a**. Where possible, the use of 1,4-dioxane as a co-solvent and higher reaction temperatures for a shorter reaction time afforded more efficient palladium catalyzed *N*-vinylation.[20] An initial short incubation of the reaction components at 60 °C followed by warming to higher temperatures provided the best results.[21]

The palladium catalyzed *N*-vinylation reactions with cyclic vinyl triflates **5d** and **5e** were found to be slower than the vinyl triflates **5a** and **5c**. However, the greater thermal stability and the absence of the competing base-induced triflate elimination allowed the use of higher reaction temperatures with these substrates. The coupling of azaheterocycles **7b**, **7c** and **7e** with triflate **5d** gave the corresponding *N*-vinyl products in 70, 62 and 17% yield, respectively (Table 1, entries 18, 20, and 22). In the latter case a significant quantity (~50%) of ethyl 2-oxo-cyclopentanecarboxylate was isolated, suggesting a competitive sulfonyl transfer reaction.15 The coupling of the vinyl triflate **5e** with the acyl pyrrole **7b** proceeded efficiently at 110 °C to give the *N*-vinyl pyrrole **4eb** in 91% yield (Table 1, entry 24). Neither of the less reactive azaheterocycles **7c** nor **7e** gave appreciable amounts of the corresponding coupling products with vinyl triflate **5e**.

The coupling of vinyl triflate **5f** with acyl pyrrole **7b** afforded the desired *N*-vinyl azole **4fb** in 72% yield (Table 1, entry 26), demonstrating the possible extension of this chemistry to unactivated vinyl triflates. However, the longer reaction time and the higher reaction

temperature needed for the synthesis of product **4fb** should be noted. The reduction of the steric bulk of the vinyl triflate and the presence of the electron withdrawing ester each have a beneficial effect on the rate of the coupling reaction. The relative rate of coupling for the vinyl triflates discussed here was found to be: **5c** > **5a** > **5d** > **5e** > **5f** (Chart 1). Similarly, the azaheterocycles used in this study may be ranked from most reactive to the least reactive: **7a** > **7b** > **7d** > **7c** > **7e** (Chart 1). While the deprotonation of the heterocycle is facilitated by the presence of an electron-withdrawing substituent, these less nucleophilic heterocycles exhibit a slower overall rate of coupling. Hence, undesired reactions including triflate elimination and sulfonyl transfer reactions may compete when very non-nucleophilic azaheterocycles are used as substrates.[22]

Conclusion

In conclusion, a catalytic method for the stereospecific *N*-vinylation of azaheterocycles using vinyl triflates was described. Both cyclic and acyclic vinyl triflates were found to be substrates for this palladium catalyzed synthesis of *N*-vinyl pyrrole and indole derivatives. Successful use of non-nucleophilic azaheterocycles in this coupling reaction is noteworthy. The ready availability of both *E*- and *Z*-vinyl triflates[23] in conjunction with the herein described chemistry offers an attractive method for the synthesis of *N*-vinyl azaheterocycles.

---

[1] (a) Wolfe, J. P.; Wagaw, S.; Marcoux, J.-F.; Buchwald, S. L. *Acc. Chem. Res.* **1998**, *31*, 805–818. (b) Hartwig, J. F. *Acc. Chem. Res.* **1998**, *31*, 852–860. (c) Hartwig, J. F. *Angew. Chem. Int. Ed.* **1998**, *37*, 2046–2067. (d) Yang, B. H.; Buchwald, S. L. *J. Organomet. Chem.* **1999**, *576*, 125–146. (e) Muci, A. R.; Buchwald, S. L. *Top. Curr. Chem.* **2002**, *219*, 131–209. (f) Hartwig, J. F. In *Handbook of Organopalladium Chemistry for Organic Synthesis*; Negishi, E., Ed.; Wiley-Interscience: New York, 2002; p. 1051.

[2] (a) Wolfe, J. P.; Wagaw, S.; Buchwald, S. L. *J. Am. Chem. Soc.* **1996**, *118*, 7215–7216. (b) Driver, M. S.; Hartwig, J. F. *J. Am. Chem. Soc.* **1996**, *118*, 7217–7218. For examples of palladium catalyzed *N*-arylation of azoles, see: (c) Mann, G.; Hartwig, J. F.; Driver, M. S.; Fernández-Rivas, C. *J. Am. Chem. Soc.* **1998**, *120*, 827–828, (d) Old, D. W.; Harris, M. C.; Buchwald, S. L. *Org. Lett.* **2000**, *2*, 1403–1406, and (e) Watanabe, M.; Nishiyama, M.; Yamamoto, T.; Koie, Y. *Tetrahedron Lett.* **2000**, *41*, 481–483.

[3] For examples of copper-catalyzed *N*-arylation, see: (a) Kiyomori, A.; Marcoux, J.-F.; Buchwald, S. L. *Tetrahedron Lett.* **1999**, *40*, 2657–2660, (b) Collman, J. P.; Zhong, M. *Org. Lett.* **2000**, *2*, 1233–1236, (c) Gujadhur, R. K.; Bates, C. G.; Venkataraman, D. *Org. Lett.* **2001**, *3*, 4315–4317, (d) Klapars, A.; Antilla, J. C.; Huang, X.; Buchwald, S. L. *J. Am. Chem. Soc.* **2001**, *123*, 7727–7729, (e) Klapars, A.; Huang, X.; Buchwald, S. L. *J. Am. Chem. Soc.* **2002**, *124*, 7421–7428, (f) Kwong, F. Y.; Buchwald, S. L. *Org. Lett.* **2003**, *5*, 793–796, (g) Ma, D.; Cai, Q.; Zhang, H. *Org. Lett.* **2003**, *5*, 2453–2455, (h) Padwa, A.; Crawford, K. R.; Rashatasakhon, P.; Rose, M. *J. Org. Chem.* **2003**, *68*, 2609–2617, and (i) Antilla, J. C.; Baskin, J. M.; Barder, T. E.; Buchwald, S. L. *J. Org. Chem.* **2004**, *69*, 5578–5587.

[4] For intramolecular palladium catalyzed *N*-vinylation of amides, see: (a) Palomo, C.; Aizpurua, J. M.; Legido, M.; Picard, J. P.; Dunogues, J.; Constantieux, T. *Tetrahedron Lett.* **1992**, *33*, 3903–3906, (b) Cuevas, J.-c.; Patil, P.; Snieckus, V. *Tetrahedron Lett.* **1989**, *30*, 5841–5844, and (c) Kozawa, Y.; Mori, M. *Tetrahedron Lett.* **2002**, *43*, 111–114. For reports on palladium catalyzed *N*-vinylation, see: (d) Wallace, D. J.; Klauber, D. J.; Chen, C.-y.;

Volante, R. P. *Org. Lett.* **2003**, *5*, 4749–4752, and (e) Klapars, A.; Campos, K. R.; Chen, C.-y.; Volante, R. P. *Org. Lett.* **2005**, *7*, 1185–1188.

[5] (a) For a review on the use of copper in cross-coupling reaction, see: Beletskaya, I. P.; Cheprakov, A. V. *Coord. Chem. Rev.* **2004**, *248*, 2337–2364. For amidation of vinyl halides with copper as the catalyst or promoter, see: (b) Ogawa, T.; Kiji, T.; Hayami, K.; Suzuki, H. *Chem. Lett.* **1991**, 1443–1446, (c) Shen, R.; Porco, J. A., Jr. *Org. Lett.* **2000**, *2*, 1333–1336, (d) Shen, R.; Lin, C. T.; Porco, J. A., Jr. *J. Am. Chem. Soc.* **2002**, *124*, 5650–5651, (e) Jiang, L.; Job, G. E.; Klapars, A.; Buchwald, S. L. *Org. Lett.* **2003**, *5*, 3667–3669, (f) Han, C.; Shen, R.; Su, S.; Porco, J. A., Jr. *Org. Lett.* **2004**, *6*, 27–30, (g) Pan, X.; Cai, Q.; Ma, D. *Org. Lett.* **2004**, *6*, 1809–1812, and (h) Hu, T.; Li, C. *Org. Lett.* **2005**, *7*, 2035–2038. For copper catalyzed and promoted *N*-alkynylation, respectively, see: (i) Frederick, M. O.; Mulder, J. A.; Tracey, M. R.; Hsung, R. P.; Huang, J.; Kurtz, K. C. M.; Shen, L.; Douglas, C. J. *J. Am. Chem. Soc.* **2003**, *125*, 2368–2369, and (j) Dunetz, J. R.; Danheiser, R. L. *Org. Lett.* **2003**, *5*, 4011–4014. For a copper catalyzed C–N bond formation using allenyl halides, see: (k) Trost, B. M.; Stiles, D. T. *Org. Lett.* **2005**, *7*, 2117–2120.

[6] For palladium catalyzed *N*-vinylation of amines, see: (a) Barluenga, J.; Fernández, M. A.; Aznar, F.; Valdés, C. *Chem. Commun.* **2002**, 2362–2363, and (b) Willis, M. C.; Brace, G. N. *Tetrahedron Lett.* **2002**, *43*, 9085–9088. (c) For palladium-catalyzed *N*-vinylation of lithiated azoles, see: Lebedev, A. Y.; Izmer, V. V.; Kazyul'kin, D. N.; Beletskaya, I. P.; Voskoboynikov, A. Z. *Org. Lett.* **2002**, *4*, 623–626.

[7] Rainka, M. P.; Aye, Y.; Buchwald, S. L. *Proc. Nat. Acad. Sci., USA* **2004**, *101*, 5821–5823.

[8] For the synthesis of *Z*-β-iodoenoates, see: Piers, E.; Wong, T.; Coish, P. D.; Rogers, C. *Can. J. Chem.* **1994**, *72*, 1816–1819.

[9] For synthesis of *E*-β-iodoenoates *via* an iododestannylation step, see: (a) Thibonnet, J.; Launay, V.; Abarbri, M.; Duchêne, A.; Parrain, J.-L. *Tetrahedron Lett.* **1998**, *39*, 4277–4280. (b) Maguire, R. J.; Munt, S. P.; Thomas, E. J. *J. Chem. Soc., Perkin Trans. 1* **1998**, 2853–2863, and (c) Dieter, R. K.; Lu, K. *J. Org. Chem.* **2002**, *67*, 847–855. For isomerization of *Z*-β-iodoenoates, see: (d) Ohba, M.; Kawase, N.; Fujii, T. *J. Am. Chem. Soc.* **1996**, *118*, 8250–8257 and (e) Dudley, G. B.; Takaki, K. S.; Cha, D. D.; Danheiser, R. L. *Org. Lett.* **2000**, *2*, 3407–3410.

[10] For reviews on the preparation and use of vinyl triflates, see: (a) Ritter, K. *Synthesis* **1993**, 735–762, and (b) Baraznenok, I. L.; Nenajdenko, V. G.; Balenkova, E. S. *Tetrahedron* **2000**, *56*, 3077–3119. Also, see: (c) Comins, D. L.; Dehghani, A. *Tetrahedron Lett.* **1992**, *33*, 6299–6302.

[11] Use of XPhos gave superior results as compared to tri-(*o*-tolyl)phosphine, 2,2′-bis(diphenylphosphino)-1,1′-binaphthyl (BINAP), and 2-dicyclohexylphosphino-2′,6′-dimethoxy-1,1′-biphenyl (SPhos).

[12] (a) Tomori, H.; Fox, J. M.; Buchwald, S. L. *J. Org. Chem.* **2000**, *65*, 5334–5341. (b) XPhos is commercially available.

[13] In the absence of palladium catalyst none of the coupling products were observed.

[14] Best results were obtained by further drying commercially available anhydrous potassium phosphate (160 °C, 0.1 Torr, 12 h) handling it under inert atmosphere.

[15] For a discussion on the competitive elimination reaction to give ynoates in studies concerning the palladium catalyzed C–O and C–S bond formation, see: Rossi, R.; Bellina, F.; Mannina, L. *Tetrahedron* **1997**, *53*, 1025–1044.

[16] For the synthesis of *N*-(tributylstannyl)-pyrrole, see: Williamson, B. L.; Stang, P. J. *Synlett* **1992**, 199–200.

[17] For use of dialkylaminotributystannanes in *N*-arylation reactions, see: Kosugi, M.; Mameyama, M.; Migita, T. *Chem. Lett.* **1983**, 927–928, Paul, F.; Patt, J.; Hartwig, J. F. *J. Am. Chem. Soc.* **1994**, *116*, 5969–5970, and Guram, A. S.; Buchwald, S. L. *J. Am. Chem. Soc.* **1994**, *116*, 7901–7902.

[18] See the Experimental Section for details.

[19] For a discussion on the competitive loss of triflates *via* nucleophilic attack at the sulfur center during *N*-arylation of amines with electron deficient aryl triflates, see: (a) Wolfe, J. P.; Buchwald, S. L. *J. Org. Chem.* **1997**, *62*, 1264–1267 and (b) Louie, J.; Driver, M. S.; Hamann, B. C.; Hartwig, J. F. *J. Org. Chem.* **1997**, *62*, 1268–1273.

[20] For a discussion on the rate of reductive elimination and C–N bond formation in *N*-arylation of azaheterocycles, see reference 2c.

[21] The immediate heating of the starting reaction components to temperatures above 60 °C is not recommended. In the case of triflate **5a**, omission of this incubation time resulted in a noticeable decrease in the efficiency of the coupling reaction.

[22] Consistent with this observation, no coupling product was observed using 2-formylpyrrole in conjunction with vinyl triflates **5a**, **5c** and **5e**. Formation of unreactive $(\text{azaheterocyclic})_n$–palladium complexes due to higher concentration of the aza-anion may also be in part responsible for the observed lower reactivity of acidic azaheterocycles; see reference 2c.

[23] The ease of stereospecific synthesis of fully substituted vinyl triflates as compared to the corresponding vinyl iodides is noteworthy; see references 8–10.

Experimental Section

General Procedures. All reactions were performed in oven-dried or flame-dried round bottomed flasks or modified Schlenk (Kjeldahl shape) flasks. The flasks were fitted with rubber septa and reactions were conducted under a positive pressure of argon. Stainless steel syringes or cannulae were used to transfer air- and moisture-sensitive liquids. Flash column chromatography was performed as described by Still et al. using silica gel (60-Å pore size, 32–63 μm, standard grade) or non-activated alumina gel (80–325 mesh, chromatographic grade).[1] Analytical thin–layer chromatography was performed using glass plates pre-coated with 0.25 mm 230–400 mesh silica gel or neutral alumina gel impregnated with a fluorescent indicator (254 nm). Thin layer chromatography plates were visualized by exposure to ultraviolet light and/or by exposure to an ethanolic phosphomolybdic acid (PMA), an acidic solution of *p*-anisaldehyde (anis), an aqueous solution of ceric ammonium molybdate (CAM), an aqueous solution of potassium permanganate ($KMnO_4$) or an ethanolic solution of ninhydrin followed by heating (<1 min) on a hot plate (~250 °C). Organic solutions were concentrated on a rotary evaporators at ~20 Torr (house vacuum) at 25–35 °C, then at ~1 Torr (vacuum pump) unless otherwise indicated.

Materials. Commercial reagents and solvents were used as received with the following exceptions: Dichloromethane, diethyl ether, tetrahydrofuran, acetonitrile, and toluene were purified by the method of Grubbs et al. under positive argon pressure,[2] 1,4-dioxane was distilled from sodium hydride. Potassium phosphate was dried at 180 °C under vacuum (~1 torr) for 24 h then stored in a glove box. Sodium hydride was purchased as a 60% dispersion in oil and then washed four times with hexanes and stored dry in a glove box. The molarity of *n*-butyllithium solutions was determined by titration using diphenylacetic acid as an indicator (average of three determinations).[3] Vinyl triflates used in this study were prepared according to literature procedures as noted below. Pyrrole was distilled from calcium hydride and stored at –10 °C in the dark. Commercially available azaheterocycles and XPhos were purchased and used as received.

Instrumentation. Proton nuclear magnetic resonance (^{1}H NMR) spectra were recorded on a 500 MHz spectrometer. Chemical shifts are recorded in parts per million from internal tetramethylsilane on the δ scale and are referenced from the residual protium in the NMR solvent ($CHCl_3$: δ 7.27, C_6H_6: δ7.16). Data is reported as follows: chemical shift [multiplicity (s = singlet, d = doublet, t = triplet, q = quartet, m = multiplet), coupling constant(s) in Hertz, integration, assignment]. Carbon-13 nuclear magnetic resonance spectra were recorded on a 500 MHz spectrometer and are recorded in parts per million from internal tetramethylsilane on the δ scale and are referenced from the carbon resonances of the solvent ($CDCl_3$: δ 77.2, benzene-d_6: δ 128.0). Data is reported as follows: chemical shift [multiplicity (s = singlet, d = doublet, t = triplet, q = quartet, m = multiplet), coupling constant(s) in Hertz, assignment]. Infrared data were on a FT-IR and are reported as follows: [frequency of absorption (cm^{-1}), intensity of absorption (s = strong, m = medium, w = weak, br = broad), assignment]. Gas chromatograpy was performed on a HP-5 5% Phenyl Methyl Siloxane column.

---

[1] Still, W. C.; Kahn, M.; Mitra, A. *J. Org. Chem.* **1978**, *43*, 2923–2925.

[2] Pangborn, A. B.; Giardello, M. A.; Grubbs, R. H.; Rosen, R. K.; Timmers, F. J. *Organometallics* **1996**, *15*, 1518–1520.

[3] Kofron, W. G.; Baclawski, L. M. *J. Org. Chem.* **1976**, *41*, 1879–1880.

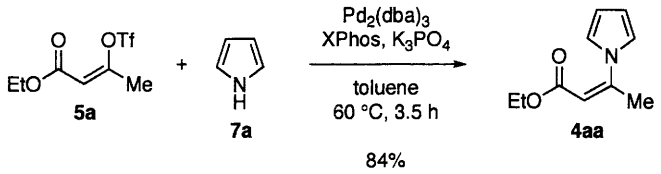

Z-3-Pyrrol-1-yl-but-2-enoic acid ethyl ester (4aa, Table 1, entry 1):

Toluene (1.90 mL) was added to an argon–purged sample of $Pd_2(dba)_3$ (17.5 mg, 19.1 μmol, 0.05 equiv), XPhos (18.2 mg, 38.1 μmol, 0.10 equiv), and rigorously anhydrous K_3PO_4 (113 mg, 534 μmol, 1.40 equiv) in a flame-dried flask. Pyrrole (**7a**, 40.0 μL, 572 μmol, 1.50 equiv) was then added and the deep red mixture was heated to 60 °C. After 30 min, triflate **5a**[4] (100 mg, 381 μmol, 1 equiv) was added via syringe, producing a color change to forest green within approximately 10 min then to brown within an additional 1 h. After 3.5 h TLC analysis indicated that the reaction was complete, whereupon the mixture was allowed to cool to 23 °C, was diluted with EtOAc (10 mL), and was vacuum filtered through a plug of celite (diam. 2.5 cm, ht. 2.5 cm). The celite-plug and flask were rinsed with an additional 15-mL portion of EtOAc, and the combined organic filtrates were washed with water (7.5 mL) and brine (7.5 mL), were dried over anhydrous sodium sulfate, were filtered, and were concentrated under reduced pressure to give a deep brown residue. Purification of the crude material by flash column chromatography (silica gel: diam. 3.0 cm, ht. 22 cm; 60% EtOAc–hexanes) afforded the vinyl pyrrole **4aa**[5] (57.1 mg, 84%) as a yellow oil.

^{1}H NMR (500 MHz, $CDCl_3$, 20 °C):	6.90 (app t, J = 2.2 Hz, 2H), 6.23 (app t, J = 2.2 Hz, 2H), 5.52 (q, J = 1.2 Hz, 1H), 4.10 (q, J = 7.1 Hz, 2H), 2.26 (d, J = 1.3 Hz, 3H), 1.20 (t, J = 7.1 Hz, 3H).
^{13}C NMR (125.7 MHz, $CDCl_3$, 20 °C):	165.2, 147.7, 121.4, 110.1, 107.6, 60.5, 24.5, 14.4.
FTIR (neat):	2982 (w, C–H), 1718 (s, C=O), 1641 (s, C=C), 1481, 1182, 1051.
HRMS–ESI (*m/z*):	calcd for $C_{10}H_{13}NO_2Na$ $[M+Na]^+$: 202.0838, found: 202.0839.
TLC (7.5% EtOAc–hexanes), *Rf*:	0.15 (UV, anis).

[4] For the general procedure used to prepare the vinyl triflate **5a**, see: Kim, H.-O.; Ogbu, C. O.; Nelson, S.; Kahn, M. *Synlett* **1998**, 1059–1060.

[5] For an alternate synthesis of **4aa**, see: Rainka, M. P.; Aye, Y.; Buchwald, S. L. *Proc. Nat. Acad. Sci., USA* **2004**, *101*, 5821–5823.

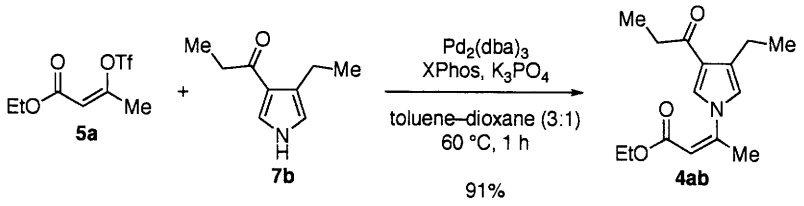

Z-3-(3-Ethyl-4-propionyl-pyrrol-1-yl)-but-2-enoic acid ethyl ester (4ab, Table 1, entry 3):

A mixture of toluene–dioxane (3:1, 1.90 mL) was added to an argon–purged sample of acyl pyrrole **7b**[6] (86.5 mg, 572 μmol, 1.50 equiv), $Pd_2(dba)_3$ (17.5 mg, 19.1 μmol, 0.05 equiv), XPhos (18.2 mg, 38.1 μmol, 0.10 equiv), and rigorously anhydrous K_3PO_4 (113 mg, 534 μmol, 1.40 equiv) in a flame-dried flask and the resulting deep red mixture was heated to 60 °C. After 30 min, triflate **5a** (100 mg, 381 μmol, 1 equiv) was added via syringe, producing a color change to brown within approximately 1 min. After 1 h, GC analysis indicated that the reaction was complete, whereupon the mixture was allowed to cool to 23 °C, was diluted with EtOAc (10 mL), and was vacuum filtered through a plug of celite (diam. 2.5 cm, ht. 2.5 cm). The celite-plug and flask were rinsed with a 15-mL portion of EtOAc, and the combined organic filtrates were washed with water (7.5 mL) and brine (7.5 mL), were dried over anhydrous sodium sulfate, were filtered, and were concentrated under reduced pressure to yield a deep brown residue. Purification of the crude material by flash column chromatography (silica gel: diam. 3.0 cm, ht. 18 cm; 20% EtOAc–hexanes) gave the vinyl pyrrole **4ab** (91.2 mg, 91%) as a yellow oil.

^{1}H NMR (500 MHz, $CDCl_3$, 20 °C):	7.53 (d, J = 2.3 Hz, 1H), 6.60 (dt, J = 2.3, 1.2 Hz, 1H), 5.64 (q, J = 1.2 Hz, 1H), 4.13 (q, J = 7.1 Hz, 2H), 2.78 (qd, J = 7.3, 1.2 Hz, 2H), 2.75 (q, J = 7.3, 2H), 2.29 (d, J = 1.2 Hz, 3H), 1.22 (t, J = 7.1 Hz, 3H), 1.19 (t, J = 7.3 Hz, 3H), 1.17 (t, J = 7.3 Hz, 3H).
^{13}C NMR (125.7 MHz, $CDCl_3$, 20 °C):	197.3, 164.7, 146.9, 129.3, 128.0, 123.8, 119.4, 109.8, 60.7, 33.2, 24.3, 20.2, 14.4, 14.3, 8.8.
FTIR (neat):	2971 (m, C–H), 1705 (m, C=O), 1662 (s, C=O), 1518, 1189, 1047.
HRMS–ESI (*m/z*):	calcd for $C_{15}H_{21}NO_3Na$ $[M+Na]^+$: 286.1414, found: 286.1417.
TLC (40% EtOAc–hexanes), *Rf*:	0.42 (UV, anis).

[6] For the synthesis of pyrroles using tosylmethylisocyanide, see: (a) van Leusen, A. M.; Siderius, H.; Hoogenboom, B. E.; van Leusen, D. *Tetrahedron Lett.* **1972**, *52*, 5337–5340 and (b) Chamberlin, K. S.; LeGoff, E. *Heterocycles* **1979**, *12*, 1567–1570.

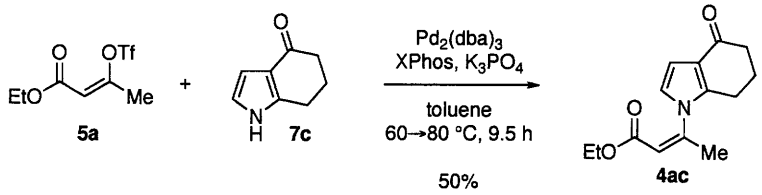

Z-3-(4-Oxo-4,5,6,7-tetrahydro-indol-1-yl)-but-2-enoic acid ethyl ester (4ac, Table 1, entry 7):

A mixture of toluene–dioxane (3:1, 1.90 mL) was added to an argon–purged sample of 1,5,6,7-tetrahydro-4*H*-indol-4-one (**7c**, 77.3 mg, 572 μmol, 1.50 equiv), $Pd_2(dba)_3$ (17.5 mg, 19.1 μmol, 0.05 equiv), XPhos (18.2 mg, 38.1 μmol, 0.10 equiv), and rigorously anhydrous K_3PO_4 (113 mg, 534 μmol, 1.40 equiv) in a flame-dried flask and the resulting deep red mixture was heated to 60 °C. After 30 min, triflate **5a** (100 mg, 381 μmol, 1 equiv) was added via syringe, producing a color change to forest green within approximately 1 min. After 2.5 h, the temperature was increased to 80 °C and the green–brown mixture stirred for 7 h, at which point GC analysis indicated that the reaction was complete. The mixture was then allowed to cool to 23 °C, was diluted with EtOAc (10 mL), and was vacuum filtered through a plug of celite (diam. 2.5 cm, ht. 2.5 cm). The celite-plug and flask were rinsed with an additional 15-mL portion of EtOAc, and the combined organic filtrates were washed with water (7.5 mL) and brine (7.5 mL), were dried over anhydrous sodium sulfate, were filtered, and were concentrated under reduced pressure to give a deep brown residue. Purification of the crude material by flash column chromatography (silica gel: diam. 3.0 cm, ht. 22 cm; 60% EtOAc–hexanes) afforded the vinyl indolone **4ac** (47.3 mg, 50%) as a white solid.

^{1}H NMR (500 MHz, $CDCl_3$, 20 °C):	6.65 (d, J = 1.2 Hz, 1H), 6.55 (d, J = 1.2 Hz, 1H), 6.01 (q, J = 1.2 Hz, 1H), 4.04 (q, J = 7.1 Hz, 2H), 2.63 (t, J = 6.2 Hz, 2H), 2.48 (app t, J = 6.2 Hz, 2H), 2.21 (d, J = 1.3 Hz, 3H), 2.12 (pentet, J = 6.2 Hz, 2H), 1.12 (t, J = 7.1 Hz, 3H).
^{13}C NMR (125.7 MHz, $CDCl_3$, 20 °C):	194.7, 163.7, 147.0, 143.9, 121.6, 121.2, 118.1, 106.9, 60.9, 38.1, 24.9, 24.1, 22.4, 14.2.
FTIR (neat):	2944 (m, C–H), 1722 (s, C=O), 1659 (s, C=O), 1464, 1048.
HRMS–ESI (*m/z*):	calcd for $C_{14}H_{17}NO_3Na$ $[M+Na]^+$: 270.1101, found: 270.1102.
TLC (60% EtOAc–hexanes), *Rf*:	0.29 (UV, anis).

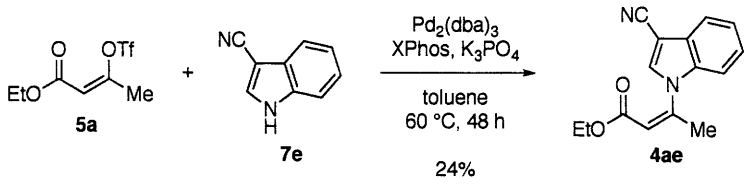

Z-3-(3-Cyano-indol-1-yl)-but-2-enoic acid ethyl ester (4ae, Table 1, entry 8):

Toluene (1.90 mL) was added to an argon–purged sample of 3-cyanoindole (**7e**, 81.3 mg, 572 μmol, 1.50 equiv), $Pd_2(dba)_3$ (17.5 mg, 19.1 μmol, 0.05 equiv), XPhos (18.2 mg, 38.1 μmol, 0.10 equiv), and rigorously anhydrous K_3PO_4 (113 mg, 534 μmol, 1.40 equiv) in a flame-dried flask and the resulting deep red mixture was heated to 60 °C. After 30 min, triflate **5a** (100 mg, 381 μmol, 1 equiv) was added via syringe, producing a color change to olive green within approximately 3 min. After 48 h, GC analysis indicated that the reaction was no longer proceeding at an appreciable rate. The mixture was then allowed to cool to 23 °C, was diluted with EtOAc (10 mL), and was vacuum filtered through a plug of celite (diam. 2.5 cm, ht. 2.5 cm). The celite-plug and flask were rinsed with an additional 15-mL portion of EtOAc and the combined organic filtrates were washed with water (7.5 mL) and brine (7.5 mL), were dried over anhydrous sodium sulfate, were filtered, and were concentrated under reduced pressure to an orange residue. Analysis of the crude product mixture by ^{1}H NMR revealed the presence of unreacted starting triflate **5a**, product **4ae**, and ethyl but-2-ynoate (**5a**:**7ae**:**9a** = 30:17:5). Purification of the crude material by flash column chromatography (silica gel: diam. 3.0 cm, ht. 22 cm; 20% EtOAc–hexanes) provided the vinyl indole **4ae** (23.0 mg, 24%) as an off–white solid.

^{1}H NMR (500 MHz, $CDCl_3$, 20 °C):	7.78 (dd, J = 6.6, 1.5 Hz, 1H), 7.63 (s, 1H), 7.29–7.36 (m, 3H), 6.15 (q, J = 1.2 Hz, 1H), 3.90 (q, J = 7.1 Hz, 2H), 2.36 (d, J = 1.2 Hz, 3H), 0.90 (t, J = 7.1 Hz, 3H).
^{13}C NMR (125.8 MHz, $CDCl_3$, 20 °C):	163.9, 146.1, 135.6, 134.6, 129.0, 128.1, 125.2, 123.4, 120.7, 118.8, 116.0, 112.1, 61.4, 24.5, 14.4.
FTIR (neat):	2983 (w, C–H), 2222 (s, C≡N), 1720 (s, C=O), 1660, 1535, 1217.
HRMS–ESI (*m/z*):	calcd for $C_{15}H_{14}N_2O_2Na$ $[M+Na]^+$: 277.0947, found: 277.0950.
TLC (35% EtOAc–hexanes), *Rf*:	0.33 (UV, CAM).

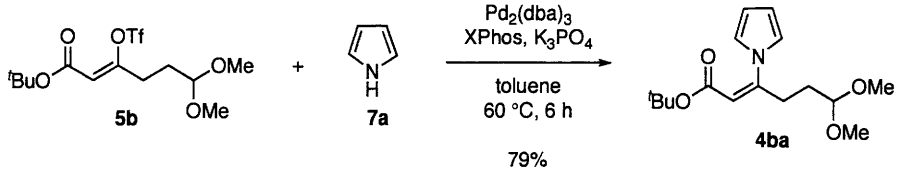

***Z*-3-(3-Ethyl-4-propionyl-pyrrol-1-yl)-but-2-enoic acid ethyl ester (4ba, equation 2):**

Toluene (1.90 mL) was added to an argon–purged sample of $Pd_2(dba)_3$ (17.5 mg, 19.1 μmol, 0.05 equiv), XPhos (18.2 mg, 38.1 μmol, 0.05 equiv), and rigorously anhydrous K_3PO_4 (113 mg, 534 μmol, 1.40 equiv) in a flame-dried flask. Pyrrole (**7a**, 40.0 μL, 572 μmol, 1.50 equiv) was then added via syringe and the deep red mixture was heated to 60 °C. After 30 min, triflate **5b**[7] (100 mg, 381 μmol, 1 equiv) was added via syringe, producing a color change to brown within approximately 10 min. After 6 h, GC analysis indicated that the reaction was complete, whereupon the mixture was allowed to cool to 23 °C, was diluted with EtOAc (10 mL), and was vacuum filtered through a plug of celite (diam. 2.5 cm, ht. 2.5 cm). The celite-plug and flask were rinsed with a 15-mL portion of EtOAc, and the combined organic filtrates were washed with water (7.5 mL) and brine (7.5 mL), were dried over anhydrous sodium sulfate, were filtered, and were concentrated under reduced pressure to yield a deep brown residue. Purification of the crude material by flash column chromatography (silica gel: diam. 2.0 cm, ht. 17 cm; 5% EtOAc–CH_2Cl_2) gave the vinyl pyrrole **4ba** (89.1 mg, 79%) as a yellow oil.

^{1}H NMR (500 MHz, $CDCl_3$, 20 °C):	6.73 (app t, J = 2.2 Hz, 2H), 6.22 (app t, J = 2.2 Hz, 2H), 5.55 (s, 1H), 4.28 (t, J = 5.5 Hz, 1H), 3.27 (s, 6H), 2.53 (t, J = 7.8 Hz, 2H), 1.64 (dt, J = 7.8, 5.5 Hz, 2H), 1.37 (s, 9H).
^{13}C NMR (125.7 MHz, $CDCl_3$, 20 °C):	164.6, 150.1, 121.1, 112.0, 109.9, 103.6, 81.0, 53.3, 32.5, 30.1, 28.1.
FTIR (neat):	2978 (m, C–H), 1704 (m, C=O), 1645 (m, C=C), 1482, 1367, 1154.
HRMS–ESI (*m/z*):	calcd for $C_{16}H_{25}NO_4Na$ $[M+Na]^+$: 318.1676, found: 318.1674.
TLC (20% EtOAc–hexanes), *Rf*:	0.34 (UV, anis).

[7] For general procedures used to prepare the vinyl triflate **5b**, see: Comins, D. L.; Dehghani, A. *Tetrahedron Lett.* **1992**, *33*, 6299–6302 and Kim, H.-O.; Ogbu, C. O.; Nelson, S.; Kahn, M. *Synlett* **1998**, 1059–1060.

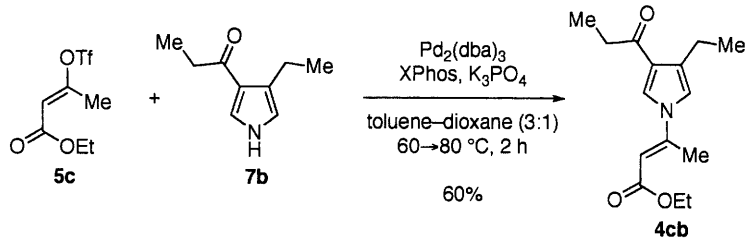

_E_-3-(3-Ethyl-4-propionyl-pyrrol-1-yl)-but-2-enoic acid ethyl ester (4cb, Table 1, entry 12):

A mixture of toluene–dioxane (3:1, 1.90 mL) was added to an argon–purged sample of acyl pyrrole **7b** (86.5 mg, 572 μmol, 1.50 equiv), $Pd_2(dba)_3$ (17.5 mg, 19.1 μmol, 0.05 equiv), XPhos (18.2 mg, 38.1 μmol, 0.10 equiv), and rigorously anhydrous K_3PO_4 (113 mg, 534 μmol, 1.40 equiv) in a flame-dried flask and the resulting deep red mixture was heated to 60 °C. After 30 min, triflate **5c**[8] (100 mg, 381 μmol, 1 equiv) was added via syringe, producing a color change to brown within approximately 5 min. After 30 min, the temperature was increased to 80 °C and the brown mixture stirred for 1.5 h, at which point GC analysis indicated that the reaction was complete. The mixture was then allowed to cool to 23 °C, was diluted with EtOAc (10 mL), and was vacuum filtered through a plug of celite (diam. 2.5 cm, ht. 2.5 cm). The celite-plug and flask were rinsed with a 15-mL portion of EtOAc, and the combined organic filtrates were washed with water (7.5 mL) and brine (7.5 mL), were dried over anhydrous sodium sulfate, were filtered, and were concentrated under reduced pressure to give a deep brown residue. Purification of the crude material by flash column chromatography (silica gel: diam. 3.0 cm, ht. 24 cm; 20% EtOAc–hexanes) afforded the vinyl pyrrole **4cb** (59.8 mg, 60%) as a yellow oil.

^{1}H NMR (500 MHz, $CDCl_3$, 20 °C):	7.56 (d, J = 2.3 Hz, 1H), 6.84 (dt, J = 2.3, 1.3 Hz, 1H), 5.97 (q, J = 0.9 Hz, 1H), 4.22 (q, J = 7.1 Hz, 2H), 2.78 (qd, J = 7.4, 1.3 Hz, 2H), 2.78 (q, J = 7.3, 2H), 2.70 (d, J = 0.9 Hz, 3H), 1.32 (t, J = 7.1 Hz, 3H), 1.20 (t, J = 7.4 Hz, 3H), 1.18 (t, J = 7.3 Hz, 3H).
^{13}C NMR (125.8 MHz, $CDCl_3$, 20 °C):	197.9, 167.2, 150.7, 131.4, 125.8, 124.7, 117.8, 105.9, 60.9, 33.7, 20.7, 16.7, 15.0, 14.7, 9.2.
FTIR (neat):	2976 (m, C–H), 1713 (s, C=O), 1640 (s, C=O), 1516, 1409, 1154.
HRMS–EI (*m/z*):	calcd for $C_{15}H_{21}NO_3Na$ $[M+Na]^+$: 286.1414, found: 286.1419.
TLC (25% EtOAc–hexanes), *Rf*:	0.39 (UV, anis).

[8] For the synthesis of *Z*-vinyl triflate **5c**, see: Ohba, M.; Kawase, N.; Fujii, T. *J. Am. Chem. Soc.* **1996**, *118*, 8250–8257.

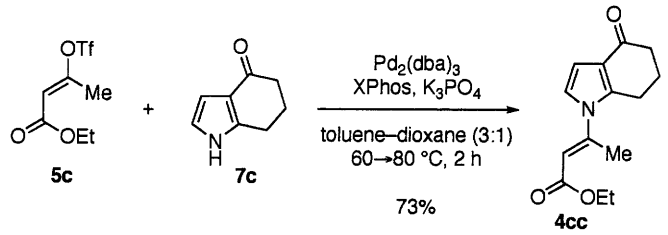

_E_-3-(4-Oxo-4,5,6,7-tetrahydro-indol-1-yl)-but-2-enoic acid ethyl ester (4cc, Table 1, entry 14):

A mixture of toluene–dioxane (3:1, 1.90 mL) was added to an argon–purged sample of 1,5,6,7-tetrahydro-4*H*-indol-4-one (**7c**, 77.3 mg, 572 μmol, 1.50 equiv), $Pd_2(dba)_3$ (17.5 mg, 19.1 μmol, 0.05 equiv), XPhos (18.2 mg, 38.1 μmol, 0.10 equiv), and rigorously anhydrous K_3PO_4 (113 mg, 534 μmol, 1.40 equiv) in a flame-dried flask and the resulting deep red mixture was heated to 60 °C. After 30 min, triflate **5c** (100 mg, 381 μmol, 1 equiv) was added via syringe, producing a color change to forest green within approximately 5 min. After 30 min, the temperature was increased to 80 °C and the brown mixture stirred for 1.5 h, at which point GC analysis indicated that the reaction was complete. The mixture was then allowed to cool to 23 °C, was diluted with EtOAc (10 mL), and was vacuum filtered through a plug of celite (diam. 2.5 cm, ht. 2.5 cm). The celite-plug and flask were rinsed with a 15-mL portion of EtOAc, and the combined organic filtrates were washed with water (7.5 mL) and brine (7.5 mL), were dried over anhydrous sodium sulfate, were filtered, and were concentrated to a deep brown residue. Purification of the crude material by flash column chromatography (silica gel: diam. 3.0 cm, ht. 25 cm; 60% EtOAc–hexanes) gave the vinyl indolone **4cc** (68.7 mg, 73%) as a yellow oil.

^{1}H NMR (500 MHz, $CDCl_3$, 20 °C):	6.76 (d, J = 3.3 Hz, 1H), 6.64 (d, J = 3.3 Hz, 1H), 5.81 (q, J = 1.1 Hz, 1H), 4.32 (q, J = 7.2 Hz, 2H), 2.87 (t, J = 6.2 Hz, 2H), 2.62 (d, J = 1.1 Hz, 3H), 2.51 (app t, J = 6.2 Hz, 2H), 2.15 (pentet, J = 6.2 Hz, 2H), 1.32 (t, J = 7.2 Hz, 3H).
^{13}C NMR (125.8 MHz, $CDCl_3$, 20 °C):	195.3, 166.5, 151.1, 143.4, 129.0, 123.6, 122.0, 114.8, 107.9, 61.2, 38.4, 24.8, 19.7, 15.0.
FTIR (neat):	2943 (w, C–H), 1712 (s, C=O), 1659 (s, C=O), 1461, 1158.
HRMS–ESI (*m/z*):	calcd for $C_{14}H_{17}NO_3Na$ $[M+Na]^+$: 270.1101, found: 270.1106.
TLC (65% EtOAc–hexanes), *Rf*:	0.38 (UV, anis).

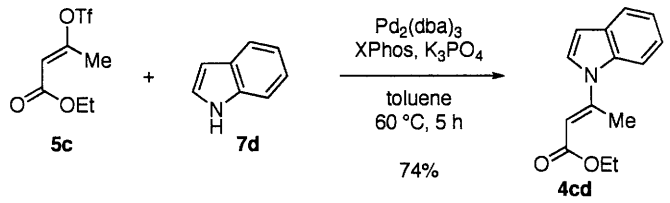

***E*-3-Indol-1-yl-but-2-enoic acid ethyl ester (4cd, Table 1, entry 15):**

Toluene (1.90 mL) was added to an argon–purged sample of indole (**7d**, 67.0 mg, 572 μmol, 1.50 equiv), $Pd_2(dba)_3$ (17.5 mg, 19.1 μmol, 0.05 equiv), XPhos (18.2 mg, 38.1 μmol, 0.10 equiv), and rigorously anhydrous K_3PO_4 (113 mg, 534 μmol, 1.40 equiv) in a flame-dried flask and the resulting deep red mixture was heated to 60 °C. After 30 min, triflate **5c** (100 mg, 381 μmol, 1 equiv) was added via syringe, producing a color change to brown within approximately 5 min. After 5 h at 60 °C GC analysis indicated that the reaction was complete, whereupon the mixture was allowed to cool to 23 °C, was diluted with EtOAc (10 mL), and was vacuum filtered through a plug of celite (diam. 2.5 cm, ht. 2.5 cm). The celite-plug and flask were rinsed with a 15-mL portion of EtOAc, and the combined organic filtrates were washed with water (7.5 mL) and brine (7.5 mL), were dried over anhydrous sodium sulfate, were filtered, and were concentrated under reduced pressure to give a deep brown residue. Purification of the crude material by flash column chromatography (silica gel: diam. 2.0 cm, ht. 24 cm; 3.5→7.5% EtOAc–hexanes) afforded the vinyl indole **4cd** (65.3 mg, 74%) as a colorless oil.

^{1}H NMR (500 MHz, $CDCl_3$, 20 °C):	7.70 (dq, J = 8.4, 0.8 Hz, 1H), 7.62 (dt, J = 7.6, 0.8 Hz, 1H), 7.29 (d, J = 3.4, 1H), 7.27 (ddd, J = 8.4, 7.1, 0.8 Hz, 1H), 7.18 (ddd, J = 7.6, 7.1, 0.8 Hz, 1H), 6.64 (dd, J = 3.4, 0.8 Hz, 1H), 6.12 (q, J = 0.8 Hz, 1H), 4.23 (q, J = 7.1 Hz, 2H), 2.78 (d, J = 0.8 Hz, 3H), 1.32 (t, J = 7.1 Hz, 3H).
^{13}C NMR (125.7 MHz, $CDCl_3$, 20 °C):	167.3, 151.7, 135.4, 130.6, 126.2, 123.4, 121.7, 121.7, 112.9, 109.1, 105.9, 60.3, 19.0, 14.6.
FTIR (neat):	2980 (s, C–H), 1710 (s, C=O), 1633 (s, C=C), 1454, 1151.
HRMS–EI (*m/z*):	calcd for $C_{14}H_{15}NO_2Na$ $[M+Na]^+$: 252.0995, found: 252.1003.
TLC (7.5% EtOAc–hexanes), *Rf*:	0.29 (UV, anis).

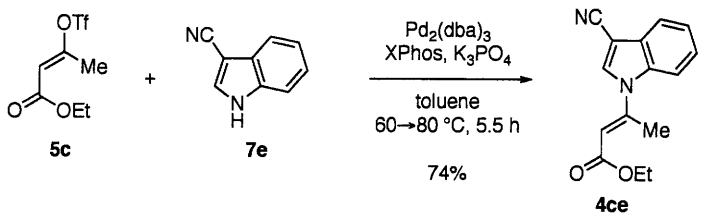

***E*-3-(3-Cyano-indol-1-yl)-but-2-enoic acid ethyl ester (4ce, Table 1, entry 16):**

A mixture of toluene–dioxane (3:1, 1.90 mL) was added to an argon–purged sample of 3-cyanoindole (**7e**, 81.3 mg, 572 μmol, 1.50 equiv), $Pd_2(dba)_3$ (17.5 mg, 19.1 μmol, 0.05 equiv), XPhos (18.2 mg, 38.1 μmol, 0.10 equiv), and rigorously anhydrous K_3PO_4 (113 mg, 534 μmol, 1.40 equiv) in a flame-dried flask and the resulting deep red mixture was heated to 60 °C. After 30 min, triflate **5c** (100 mg, 381 μmol, 1 equiv) was added via syringe, producing a color change to forest green within approximately 5 min. After 2.5 h, the temperature was increased to 80 °C and the brown mixture stirred for an additional 3 h, at which point GC analysis indicated that the reaction was complete. The mixture was then allowed to cool to 23 °C, was diluted with EtOAc (10 mL), and was vacuum filtered through a plug of celite (diam. 2.5 cm, ht. 2.5 cm). The celite-plug and flask were rinsed with a 15-mL portion of EtOAc, and the combined organic filtrates were washed with water (7.5 mL) and brine (7.5 mL), were dried over anhydrous sodium sulfate, were filtered, and were concentrated under reduced pressure to provide an orange residue. Purification of the crude material by flash column chromatography (silica gel: diam. 3.0 cm, ht. 24 cm; 20% EtOAc–hexanes) gave the vinyl indole **4ce** (71.9 mg, 74%) as an off–white solid.

^{1}H NMR (500 MHz, $CDCl_3$, 20 °C):	7.79 (dd, J = 8.2, 1.1 Hz, 1H), 7.78 (s, 1H), 7.67 (dd, J = 8.4, 0.9 Hz, 1H), 7.41 (ddd, J = 8.4, 7.1, 1.1 Hz, 1H), 7.37 (ddd, J = 8.2, 7.1, 0.9 Hz, 1H), 6.19 (q, J = 0.9 Hz, 1H), 4.28 (q, J = 7.2 Hz, 2H), 2.77 (d, J = 0.9 Hz, 3H), 1.35 (t, J = 7.2 Hz, 3H).
^{13}C NMR (125.8 MHz, $CDCl_3$, 20 °C):	166.5, 150.1, 135.2, 133.5, 129.0, 125.8, 124.2, 121.0, 115.5, 114.6, 113.5, 90.6, 61.4, 19.5, 15.0.
FTIR (neat):	2983 (w, C–H), 2225 (s, C≡N), 1717 (s, C=O), 1644, 1551, 1182.
HRMS–ESI (*m/z*):	calcd for $C_{15}H_{14}N_2O_2Na$ $[M+Na]^+$: 277.0947, found: 277.0951.
TLC (25% EtOAc–hexanes), *Rf*:	0.37 (UV, CAM).

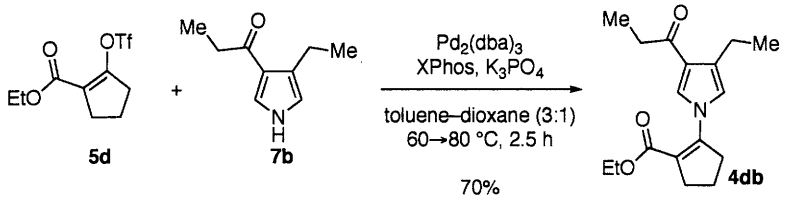

2-(3-Ethyl-4-propionyl-pyrrol-1-yl)-cyclopent-1-enecarboxylic acid ethyl ester (4db, Table 1, entry 18):

A mixture of toluene–dioxane (3:1, 1.90 mL) was added to an argon–purged sample of acyl pyrrole **7b** (86.5 mg, 572 μmol, 1.50 equiv), $Pd_2(dba)_3$ (17.5 mg, 19.1 μmol, 0.05 equiv), XPhos (18.2 mg, 38.1 μmol, 0.10 equiv), and rigorously anhydrous K_3PO_4 (113 mg, 534 μmol, 1.40 equiv) in a flame-dried flask and the resulting deep red mixture was heated to 60 °C. After 30 min, triflate **5d**[9] (110 mg, 381 μmol, 1 equiv) was added via syringe, producing a color change to brown within approximately 5 min. After 30 min, the temperature was increased to 80 °C and the brown mixture stirred for 2 h, at which point GC analysis indicated that the reaction was complete. The mixture was then allowed to cool to 23 °C, was diluted with EtOAc (10 mL), and was vacuum filtered through a plug of celite (diam. 2.5 cm, ht. 2.5 cm). The celite–plug and flask were rinsed with an additional 15-mL portion of EtOAc, then the combined organic filtrates were washed with water (7.5 mL) and brine (7.5 mL), were dried over anhydrous sodium sulfate, were filtered, and were concentrated under reduced pressure to give a deep brown residue. Purification of the crude material by flash column chromatography (silica gel: diam. 3.0 cm, ht. 24 cm; 17.5 →20% EtOAc–hexanes) provided the vinyl pyrrole **4db** (77.3 mg, 70%) as a yellow oil.

^{1}H NMR (500 MHz, $CDCl_3$, 20 °C):	7.84 (d, J = 2.3 Hz, 1H), 6.77 (dt, J = 2.3, 1.1 Hz, 1H), 4.21 (q, J = 7.2 Hz, 2H), 2.93 (app tt, J = 7.6, 2.1 Hz, 2H), 2.84 (app tt, J = 7.6, 2.1 Hz, 2H), 2.78 (qd, J = 7.4, 1.1 Hz, 2H), 2.77 (q, J = 7.3, 2H), 1.99 (pentet, J = 7.6 Hz, 2H), 1.27 (t, J = 7.2 Hz, 3H), 1.19 (t, J = 7.3 Hz, 3H), 1.17 (t, J = 7.4 Hz, 3H).
^{13}C NMR (125.8 MHz, $CDCl_3$, 20 °C):	197.9, 165.5, 146.7, 129.5, 129.0, 124.3, 120.7, 118.1, 61.2, 37.6, 34.4, 33.6, 20.8, 20.6, 14.9, 14.8, 9.3.
FTIR (neat):	2969 (s, C–H), 1708 (s, C=O), 1666 (s, C=O), 1518, 1199, 1063.
HRMS–ESI (*m/z*):	calcd for $C_{17}H_{23}NO_3Na$ $[M+Na]^+$: 312.1570, found: 312.1566.
TLC (25% EtOAc–hexanes), *Rf*:	0.44 (UV, anis).

[9] For the synthesis of vinyl triflate **5d**, see: Jasperse, C. P.; Curran, D. P. *J. Am. Chem. Soc.* **1990**, *112*, 5601–5609.

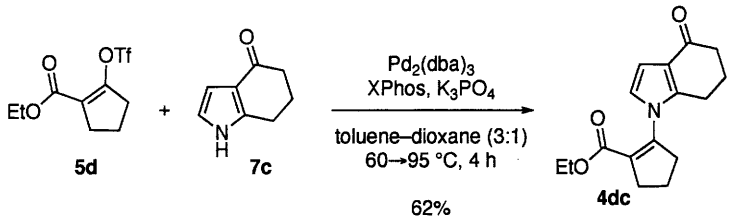

2-(4-Oxo-4,5,6,7-tetrahydro-indol-1-yl)-cyclopent-1-enecarboxylic acid ethyl ester (4dc, Table 1, entry 20):

A mixture of toluene–dioxane (3:1, 1.90 mL) was added to an argon–purged sample of 1,5,6,7-tetrahydro-4*H*-indol-4-one (**7c**, 77.3 mg, 572 μmol, 1.50 equiv), $Pd_2(dba)_3$ (17.5 mg, 19.1 μmol, 0.05 equiv), XPhos (18.2 mg, 38.1 μmol, 0.10 equiv), and rigorously anhydrous K_3PO_4 (113 mg, 534 μmol, 1.40 equiv) in a flame-dried flask and the resulting deep red mixture was heated to 60 °C. After 30 min, triflate **5d** (110 mg, 381 μmol, 1 equiv) was added via syringe, producing a color change to olive green within approximately 10 min. After 30 min, the temperature was increased to 95 °C and the green–brown mixture stirred for 3.5 h, at which point GC analysis indicated that the reaction was complete. The mixture was then allowed to cool to 23 °C, was diluted with EtOAc (10 mL), and was vacuum filtered through a plug of celite (diam. 2.5 cm, ht. 2.5 cm). The celite–plug and flask were rinsed with an additional 15-mL portion of EtOAc, and the combined organic filtrates were washed with water (7.5 mL) and brine (7.5 mL), were dried over anhydrous sodium sulfate, were filtered, and were concentrated under reduced pressure to provide a deep brown residue. Purification of the crude material by flash column chromatography (silica gel: diam. 3.0 cm, ht. 22 cm; 60% EtOAc–hexanes) gave the vinyl indolone **4dc** (63.7 mg, 62%) as an off–white solid.

^{1}H NMR (500 MHz, $CDCl_3$, 20 °C):	6.62 (d, J = 3.4 Hz, 1H), 6.58 (d, J = 3.4 Hz, 1H), 4.08 (q, J = 7.1 Hz, 2H), 2.84 (app tt, J = 7.6, 2.5 Hz, 2H), 2.80 (app tt, J = 7.6, 2.5 Hz, 2H), 2.64 (t, J = 6.3 Hz, 2H), 2.48 (app t, J = 6.3 Hz, 2H), 2.11 (pentet, J = 6.3 Hz, 2H), 2.07 (pentet, J = 7.6 Hz, 2H), 1.11 (t, J = 7.1 Hz, 3H).
^{13}C NMR (125.7 MHz, $CDCl_3$, 20 °C):	194.7, 163.9, 146.7, 144.3, 128.4, 122.1, 121.6, 106.5, 60.9, 38.1, 37.7, 32.4, 24.1, 22.7, 20.5, 14.2.
FTIR (neat):	2948 (m, C–H), 1710 (s, C=O), 1660 (s, C=O), 1499, 1464, 1237.
HRMS–EI (*m/z*):	calcd for $C_{16}H_{19}NO_3Na$ $[M+Na]^+$: 296.1257, found: 296.1248.
TLC (65% EtOAc–hexanes), *Rf*:	0.22 (UV, anis).

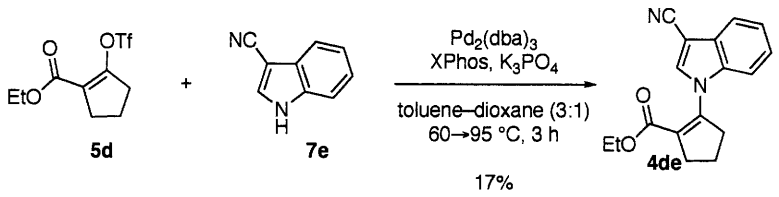

2-(3-Cyano-indol-1-yl)-cyclopent-1-enecarboxylic acid ethyl ester (4de, Table 1, entry 22):

A mixture of toluene–dioxane (3:1, 1.90 mL) was added to an argon–purged sample of 3-cyanoindole (**7e**, 81.3 mg, 572 μmol, 1.50 equiv), $Pd_2(dba)_3$ (17.5 mg, 19.1 μmol, 0.05 equiv), XPhos (18.2 mg, 38.1 μmol, 0.10 equiv), and rigorously anhydrous K_3PO_4 (113 mg, 534 μmol, 1.40 equiv) in a flame-dried flask and the resulting deep red mixture was heated to 60 °C. After 30 min, triflate **5d** (110 mg, 381 μmol, 1 equiv) was added via syringe, producing a color change to olive green within approximately 10 min. After 30 min, the temperature was increased to 95 °C and the green–brown mixture stirred for 2.5 h, at which point GC analysis indicated that the reaction was complete. The mixture was then allowed to cool to 23 °C, was diluted by the addition of EtOAc (10 mL), and was vacuum filtered through a plug of celite (diam. 2.5 cm, ht. 2.5 cm). The celite–plug and flask were rinsed with an additional 15-mL portion of EtOAc, and the combined organic filtrates were washed with water (7.5 mL) and brine (7.5 mL), were dried over anhydrous sodium sulfate, were filtered, and were concentrated to yield a deep brown residue. Purification of the crude material by flash column chromatography (silica gel: diam. 3.0 cm, ht. 22 cm; 25% EtOAc–hexanes) gave the vinyl indole **4de** (18.9 mg, 17%) as an off–white solid.

^{1}H NMR (500 MHz, $CDCl_3$, 20 °C):	7.77 (m, 1H), 7.69 (s, 1H), 7.27–7.37 (m, 3H), 3.97 (q, J = 7.2 Hz, 2H), 2.98 (app tt, J = 7.6, 2.5 Hz, 2H), 2.93 (app tt, J = 7.6, 2.5 Hz, 2H), 2.16 (pentet, J = 7.6 Hz, 2H), 0.89 (t, J = 7.2 Hz, 3H).
^{13}C NMR (125.7 MHz, $CDCl_3$, 20 °C):	163.7, 145.4, 135.5, 135.1, 128.1, 127.7, 124.6, 123.0, 120.2, 115.5, 112.3, 88.4, 61.0, 36.9, 32.5, 20.7, 13.9.
FTIR (neat):	2978 (w, C–H), 2221 (s, C≡N), 1710 (s, C=O), 1536, 1461, 1213.
HRMS–ESI (*m/z*):	calcd for $C_{17}H_{16}N_2O_2Na$ $[M+Na]^+$: 303.1104, found: 303.1095.
TLC (25% EtOAc–hexanes), *Rf*:	0.23 (UV, anis).

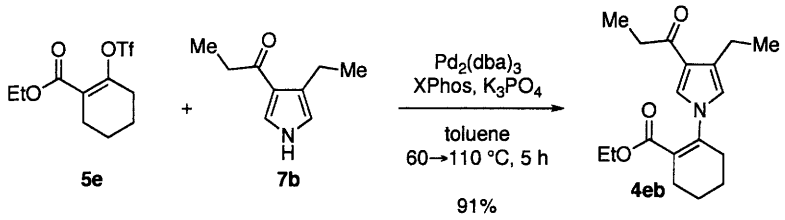

2-(3-Ethyl-4-propionyl-pyrrol-1-yl)-cyclohex-1-enecarboxylic acid ethyl ester (4eb, Table 1, entry 24):

Toluene (1.90 mL) was added to an argon–purged mixture of acyl pyrrole **7b** (86.5 mg, 572 μmol, 1.50 equiv), $Pd_2(dba)_3$ (17.5 mg, 19.1 μmol, 0.05 equiv), XPhos (18.2 mg, 38.1 μmol, 0.10 equiv), and rigorously anhydrous K_3PO_4 (113 mg, 534 μmol, 1.40 equiv) in a flame-dried flask and the resulting deep red mixture was heated to 60 °C. After 30 min, vinyl triflate **5e**[10] (110 mg, 381 μmol, 1 equiv) was added via syringe, producing a color change to burgundy within approximately 15 min. After an additional 2.5 h, the reaction temperature was raised to 110 °C and the deep brown mixture stirred for 2 h, at which point GC analysis indicated that the reaction was complete. The mixture was then allowed to cool to 23 °C, was diluted with EtOAc (10 mL), and was vacuum filtered through a plug of celite (diam. 2.5 cm, ht. 2.5 cm). The celite–plug and flask were rinsed with an additional 15-mL portion of EtOAc, and the combined organic filtrates were washed sequentially with water (7.5 mL) and brine (7.5 mL), were dried over anhydrous sodium sulfate, were filtered, and were concentrated under reduced pressure to give a deep brown residue. Purification of the crude material by flash column chromatography (silica gel: diam. 3.0 cm, ht. 24 cm; 20% EtOAc–hexanes) gave vinyl pyrrole **4eb** (105 mg, 91%) as a yellow oil.

^{1}H NMR (500 MHz, $CDCl_3$, 20 °C):	7.22 (d, J = 2.3 Hz, 1H), 6.77 (dt, J = 2.3, 1.1 Hz, 1H), 3.99 (q, J = 7.1 Hz, 2H), 2.77 (qd, J = 7.5, 1.1 Hz, 2H), 2.71 (q, J = 7.4, 2H), 2.46 (m, 4H), 1.82 (dtd, J = 8.8, 6.0, 2.7 Hz, 2H), 1.73 (dtd, J = 8.8, 6.0, 2.7 Hz, 2H), 1.17 (t, J = 7.5 Hz, 3H), 1.16 (t, J = 7.4 Hz, 3H), 1.01 (t, J = 7.1 Hz, 3H).
^{13}C NMR (125.8 MHz, $CDCl_3$, 20 °C):	197.7, 169.2, 141.0, 129.4, 127.1, 126.1, 123.9, 120.1, 61.7, 33.6, 31.2, 27.1, 22.9, 22.1, 20.6, 14.9, 14.6, 9.5.
FTIR (neat):	2937 (m, C–H), 1710 (s, C=O), 1659 (s, C=O), 1516, 1282.
HRMS–ESI (*m/z*):	calcd for $C_{18}H_{25}NO_3Na$ $[M+Na]^+$: 326.1727, found: 326.1731.
TLC (35% EtOAc–hexanes), *Rf*:	0.38 (UV, anis).

[10] For the synthesis of vinyl triflate **5e**, see: Li, S.-J.; Dieter, R. K. *J. Org. Chem.* **2003**, *68*, 969–973.

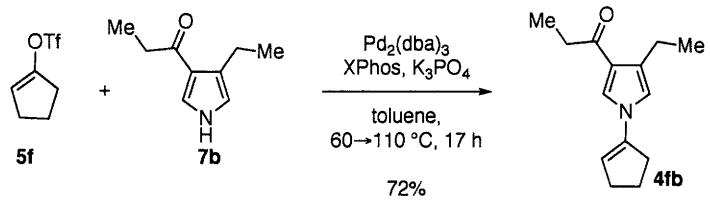

1-(3-Ethyl-4-propionyl-pyrrol-1-yl)-cyclopentene (4fb, Table 1, entry 26):

Toluene (1.90 mL) was added to an argon–purged sample of acyl pyrrole **7b** (86.5 mg, 572 μmol, 1.50 equiv), $Pd_2(dba)_3$ (17.5 mg, 19.1 μmol, 0.05 equiv), XPhos (18.2 mg, 38.1 μmol, 0.10 equiv), and rigorously anhydrous K_3PO_4 (113 mg, 534 μmol, 1.40 equiv) in a flame-dried flask and the resulting deep red mixture was heated to 60 °C. After 30 min, triflate **5f**[11] (82.4 mg, 381 μmol, 1 equiv) was added via syringe, producing a color change to green within approximately 10 min. After 1 h, the temperature was increased to 110 °C and the brown mixture stirred for 16 h, at which point GC analysis indicated that the reaction was complete. The mixture was then allowed to cool to 23 °C, was diluted with EtOAc (10 mL), and was vacuum filtered through a plug of celite (diam. 2.5 cm, ht. 2.5 cm). The celite–plug and flask were rinsed with an additional 15-mL portion of EtOAc, then the combined organic filtrates were washed with water (7.5 mL) and brine (7.5 mL), were dried over anhydrous sodium sulfate, were filtered, and were concentrated under reduced pressure to give a deep brown residue. Purification of the crude material by flash column chromatography (silica gel: diam. 2.0 cm, ht. 23 cm; 7.5% EtOAc–hexanes) provided the vinyl pyrrole **4fb** (60.4 mg, 72%) as a white solid.

^{1}H NMR (500 MHz, $CDCl_3$, 20 °C):	7.35 (d, J = 2.1 Hz, 1H), 6.71 (dt, J = 2.1, 1.0 Hz, 1H), 5.58 (app pentet, J = 2.2 Hz, 1H), 2.77 (qd, J = 7.4, 1.0 Hz, 2H), 2.74 (m, 2H), 2.74 (q, J = 7.4 Hz, 2H), 2.50 (app tq, J = 7.3, 2.2 Hz, 2H), 2.07 (app pentet, J = 7.4, Hz, 2H), 1.18 (t, J = 7.4 Hz, 3H), 1.16 (t, J = 7.4 Hz, 3H).
^{13}C NMR (125.7 MHz, $CDCl_3$, 20 °C):	197.3, 139.6, 129.6, 124.6, 123.4, 117.9, 111.9, 33.1, 31.8, 30.9, 22.3, 20.2, 14.5, 9.0.
FTIR (neat):	2967 (m, C–H), 1648 (s, C=O), 1519 (s, C=C), 1206.
HRMS–ESI (*m/z*):	calcd for $C_{14}H_{19}NONa$ $[M+Na]^+$: 240.1359, found: 240.1367.
TLC (10% EtOAc–hexanes), *Rf*:	0.22 (UV, anis).

[11] For the synthesis of vinyl triflate **5f**, see: (a) Pfeifer, W. D.; Bahn, C. A.; Schleyer, P. v. R.; Bocher, S.; Harding, C. E.; Hummel, K.; Hanack, M.; Stang, P. J. *J. Am. Chem. Soc.* **1971**, *93*, 1513–1516 and (b) Stang, P. J.; Treptow, W. *Synthesis* **1980**, 283–284.

Chapter III.

Dimerization of (+)-Myrmicarin 215B. A Potential Biomimetic Approach to Complex Myrmicarin Alkaloids

Introduction and Background

A family of structurally fascinating alkaloids have been isolated from the poison gland secretion of the African *Myrmicaria opaciventris* ant species (Figure 1).[1] Through a series of elegant spectroscopic studies, the relative stereochemistry of myrmicarins 430A (**1**) and 663 (**2**) has been assigned. These complex alkaloids were found to be highly sensitive to air oxidation, complicating their isolation. The high sensitivity of myrmicarin 430A (**1**) required its structural assignment as a crude mixture using phase-sensitive spectroscopic techniques.[1c] The relative stereochemistry of myrmicarin 645 (**5**) in addition to the absolute stereochemistry of complex myrmicarin alkaloids (i.e., **1**, **2**, and **5**) is unknown. Another isomeric myrmicarin 430 was detected in the poison gland secretion but no structural information was reported. Interestingly, the paralytic activity of the poison gland secretion has been attributed to these intriguing alkaloids.[1b] A combination of their alluring molecular structure and the plethora of challenges associated with their sensitivity has prompted us to initiate a program directed toward the synthesis of the complex myrmicarin alkaloids. Herein we report our findings that raise the possibility of an efficient strategy for the synthesis of complex myrmicarins based on a vinyl pyrrole dimerization strategy.

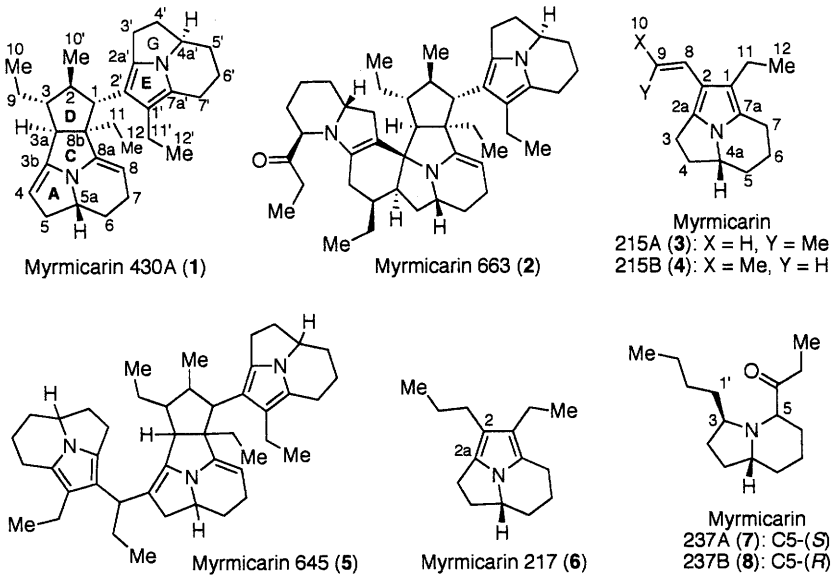

Figure 1. Representative members of the myrmicarin family of alkaloids. The relative stereochemistry of **5** is unknown; see reference 1d.

Hypothesis for the Biosynthesis of Complex Myrmicarins

Schröder and Francke have reported the spontaneous dehydration of a C1'–C3 unsaturated derivative of myrmicarin 237 (Figure 1) to give myrmicarin 217 (**6**),[2] which they cite as strong evidence for the formation of tricyclic myrmicarins from simpler indolizine derivatives. Furthermore, they propose the possible dimerization of a doubly unsaturated indolizine derivative **9** (Scheme 1) to afford myrmicarin 430A (**1**) and other complex myrmicarin alkaloids.[1b]

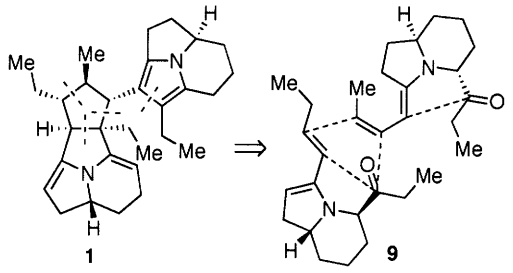

Scheme 1. Francke's proposed dimerization of bicyclic diene **9** to give myrmicarin 430A (**1**).

While the dimerization of **9** to give myrmicarin 430A (**1**) is plausible, we considered the possibility of tricyclic myrmicarin derivatives serving as direct precursors to **1**. We propose that an acid promoted dimerization of a suitable vinyl pyrroloindolizine derivative may lead directly to the fully substituted cyclopentane D-ring of myrmicarin 430A (**1**) as shown in Scheme 2.

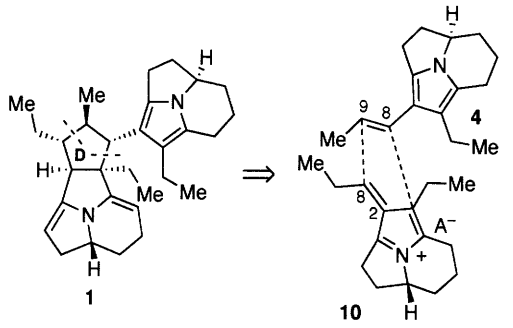

Scheme 2. Our proposed potential biomimetic dimerization of pyrroloindolizines to give myrmicarin 430A (**1**).

Specifically, our approach to the complex myrmicarin alkaloids is based on the hypothesis that C9-protonation of myrmicarin 215B (**4**) by a Brønsted acid (HA) would lead to reversible formation of the highly reactive azafulvenium ion **10** (Schemes 2 and 3).[3] We

envisioned that C9-nucleophilic addition of myrmicarin 215B (**4**) to the C8-electrophilic center of the proposed azafulvenium ion **10** would result in the hexacyclic azafulvenium ion **11** (Scheme 3), exchanging a π-bond for a σ-bond. Intramolecular trapping of the intermediate azafulvenium ion **11** by C8b-nucleophilic[4] addition to C1-electrophilic center *via* transition state structure **12** was envisioned to give the iminium ion **13** as a heptacyclic precursor to myrmicarin 430A (**1**). The C8-deprotonation of iminium ion **13** would afford bis-enamine **14**. Acid catalyzed tautomerization of the C3b-enamine would provide the expected *cis*-azabicyclooctane core (the CD-ring system of **1**) of myrmicarin 430A (**1**). Central to this strategy for the synthesis

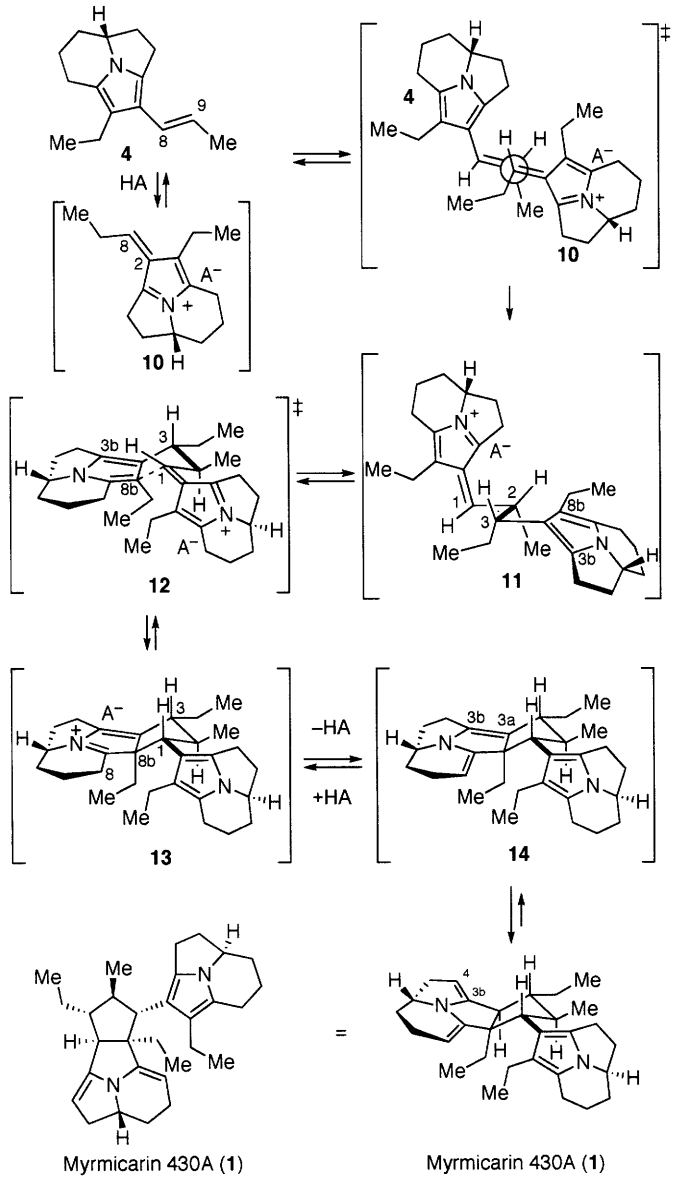

Scheme 3. Our proposed dimerization of myrmicarin 215B (**4**) to give **1**.

of complex myrmicarins was our proposed acid promoted cyclopentane annulation of vinyl pyrroloindolizine **4** (myrmicarin 215B), an unknown mode of reactivity for vinyl pyrroles. We envisioned isolation of the highly unstable myrmicarin 430A (**1**) either as an iminium ion salt (i.e. **13**, Scheme 3) or as an appropriate derivative masking the sensitive enamine functional groups.

Enantioselective Synthesis of the Tricyclic Myrmicarins

The implementation of this strategy for the preparation of complex myrmicarin alkaloids required the development of a versatile synthesis of tricyclic myrmicarin derivatives. We have reported a concise, enantioselective synthesis of all tricyclic myrmicarins (Scheme **4**).[5,6] The key steps involve palladium–catalyzed coupling between triflate **19** and pyrrole **18**,[7,8] copper–catalyzed enantioselective conjugate reduction of the resulting *N*-vinyl pyrrole **17**,[9,10] and a regioselective acid catalyzed Friedel-Crafts cyclization to provide the dihydroindolizine **15** (Scheme 4).[5]

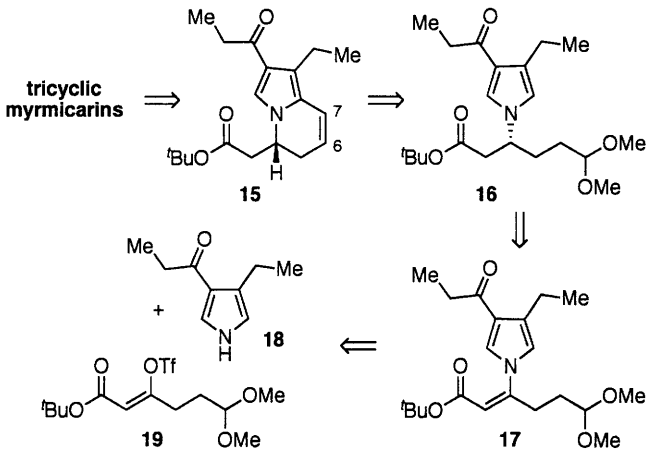

Scheme 4. Synthesis of key bicyclic intermediate **15**.

Hydrogenation of the C6–C7 alkene in **15** (Scheme 4) and selective conversion of the *tert*-butyl ester to the corresponding primary iodide followed by a silver tetrafluoroborate promoted cyclization provides the tricyclic ketone **20** (Scheme 5).[5] The final stages of the synthesis of myrmicarin 215B (**4**) involved reduction of the ketone **20** with lithium aluminum hydride at 0 °C to afford the acid sensitive tricyclic alcohol **21** as an equal mixture of C8-epimers (Scheme 5). Acid catalyzed dehydration of alcohol **21** gave exclusively myrmicarin 215B (**4**).

Alternatively, the reduction of ketone **20** to the C8-alcohol followed by an acidic workup (pH 2) directly gave **4**.[5] The synthesis of the acid sensitive C8-C9 *Z*-alkene of myrmicarin 215A (**3**) was possible by an initial dehydration of ketone **20**, using 2-chloro-3-ethylbenzoxazolium tetrafluoroborate,[11] followed by partial hydrogenation with Lindlar catalyst.[5] These stereoselective routes to the vinyl pyrroloindolizine structure provided access to the first pure samples of myrmicarins 215A (**3**) and 215B (**4**). Complete reduction of the C3-carbonyl of **20** using lithium aluminum hydride at high temperature provided myrmicarin 217 (**6**). The spectroscopic data for the synthetic alkaloids **3**, **4**, and **6** were found to be identical with those reported for natural isolates.[1b]

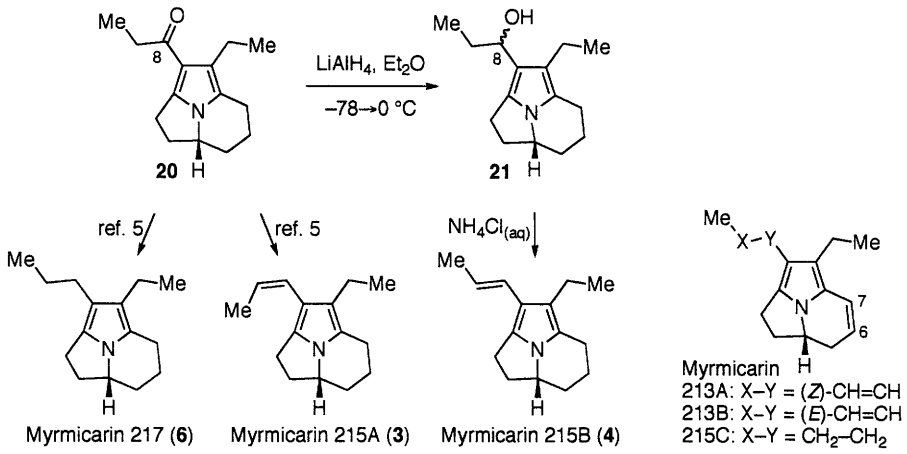

Scheme 5. Enantioselective synthesis of the tricyclic myrmicarin alkaloids.

During the late operations in the synthesis of the tricyclic myrmicarins, we found the intermediates lacking the C8-ketone to be highly sensitive to both air oxidation and acid catalyzed decomposition. As noted in the isolation reports of myrmicarins 215 and 217, these compounds show significant air oxidation to the corresponding C6-C7 didehydro derivatives 213A/B and 215C.[1b] In fact, we observed direct conversion of benzene-d_6 solutions of myrmicarins 215A, 215B, and 217 to myrmicarins 213A, 213B, and 215C, respectively, upon exposure to oxygen. Prolonged exposure to oxygen led to complete decomposition of both the tricyclic myrmicarins and their dehydrogenated derivatives. As a result, all manipulations of the tricyclic myrmicarin derivatives were conducted strictly under an argon atmosphere.[12] Indeed, as a testament to their acid sensitivity, thin layer chromatography showed that brief exposure of myrmicarin 215A (**3**) to silica gel effected partial conversion to myrmicarin 215B (**4**).

Results and Discussion

Acid-Promoted Reactivity of Myrmicarin 215

As an alternative to performing an acid catalyzed C8-C9 dehydration using an acidic aqueous work-up, completely stereoselective conversion of the alcohol **21** (~1:1, C8-epimers) to myrmicarin 215B (**4**) was achieved by treatment of a benzene-d_6 solution (0.05M) of alcohol **21** with acetic acid (1.5 equiv) at ambient temperature. ^{1}H NMR monitoring of the reaction mixture led to the detection of the intermediate C8-acetate **22**, likewise as an approximately equal mixture of C8-epimers. After 1 h, trace amounts of myrmicarin 215B (**4**) were detected. Consumption of approximately 90% of the alcohol **21** occurred in 9 h, at which point an equal mixture of acetate **22** and myrmicarin 215B (**4**) was observed. After an additional 61 h, myrmicarin 215B (**4**) was the only significant component remaining in the sample. Failure to detect the putative azafulvenium ion **23** by ^{1}H NMR is consistent with its expected high reactivity and short lifetime.[3]

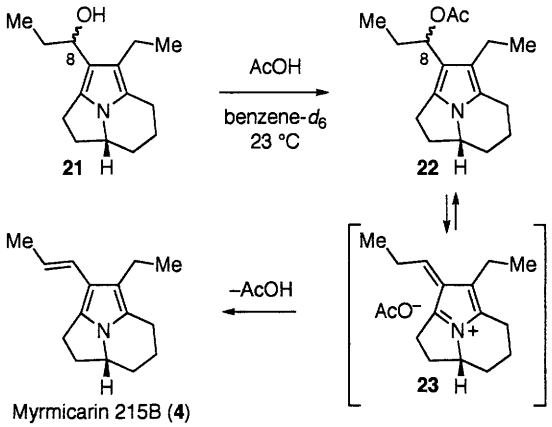

Scheme 6. Acetic acid catalyzed dehydration of alcohol **21** to myrmicarin 215B (**4**).

In contrast, treatment of a benzene-d_6 solution (0.05M) of alcohol **21** with trifluoroacetic acid (TFA, 1.10 equiv) effected full and clean conversion (≥90% by ^{1}H and ^{13}C NMR) to a single new product within 45 min. ^{1}H NMR (500 MHz) monitoring of the reaction mixture revealed that myrmicarin 215B (**4**) was formed immediately upon introduction of TFA and persisted in rapidly diminishing quantities until complete conversion to the new compound had occurred. Attempts to isolate this product after proper work-up or by direct crystallization were not successful due to rapid decomposition. However, under strictly moisture- and oxygen–free

atmosphere the reaction mixture could be stored at subambient temperatures for 24 h without significant decomposition. ^{13}C NMR (125 MHz) showed this compound to possess 30 chemically distinct carbons, the number expected for the desired dimerization product. Importantly, the same dimeric product could be obtained cleanly (≥90% by ^{1}H NMR) by direct treatment of a benzene-d_6 solution (0.05M) of myrmicarin 215B (**4**) with TFA (1.10 equiv). ^{1}H NMR (500 MHz) monitoring of a benzene-d_6 solution (0.05M) of myrmicarin 215B (**4**) with substoichiometric quantities of TFA revealed the extent of the conversion to the dimeric product was approximately equal to the amount of Brønsted acid additive, suggesting an acid promoted dimerization. By comparison, monitoring a dilute benzene-d_6 solution (0.003M) of myrmicarin 215B (**4**) exposed to a large excess of TFA (>100 equiv) gave less than 5% of the dimeric product. Instead we observed a mixture of pyrrole-ring protonated species over a period of several days.[13,14] A basic work-up returned the starting myrmicarin 215B (**4**). Under these conditions, the neutral myrmicarin 215B (**4**) required to serve as the nucleophile in the dimerization process was not present in sufficient concentration for the reaction to occur. Notably, the dimerization of myrmicarin 215B (**4**) proceeds at low concentrations (i.e. 0.005 M) in the presence of stoichiometric quantities of acid.

Significantly, subjection of myrmicarin 215A (**3**) to these dimerization conditions (benzene-d_6, 0.01M, 23 °C, 5.5 h) provided a compound that was identical by ^{1}H NMR to the dimeric product obtained from myrmicarin 215B (**4**). While a trace amount of myrmicarin 215B (**4**) was observed immediately after treatment with TFA, the monomer persisting throughout the reaction was exclusively myrmicarin 215A (**3**), suggesting that the C8-C9–alkene isomerization was slower than the subsequent acid promoted dimerization of myrmicarin 215B (**4**). Interestingly, the major myrmicarin 215 isomer isolated from the poison gland secretion is myrmicarin 215A (**3**) and not myrmicarin 215B (**4**).[1b]

Synthesis and Isolation of Dimeric Myrmicarins

Due to the aforementioned instability of the acid promoted dimerization product of myrmicarin 215B (**4**) toward isolation, we attempted to assign its structure using a combination of gradient correlation (gCOSY) and heteronuclear single quantum correlation (HSQC) NMR experiments. Hence, we found the C_{30}-dimeric compound to possess four methyl, thirteen methylene, and five methine units, as well as eight quaternary carbons. Compellingly, all of the

resonances in the ^{1}H NMR spectrum occurred in the upfield region (<δ3.57 ppm), attesting to the absence of the C8-C9 alkene present in the monomeric myrmicarins 215A (**3**) and 215B (**4**). Furthermore, the ^{1}H and ^{13}C NMR spectra contained one subset of that closely matched those of the tricyclic portion of myrmicarin 217 (**6**). Considering the intermediates in our proposed acid promoted dimerization of myrmicarin 215B (**4**), we speculated that the immediate dimeric product might be related to the iminium ion **13** (Scheme 3), a protonated tautomer of myrmicarin 430A (**1**). As the instability of the immediate dimerization product precluded an aqueous work-up, chromatographic purification, or crystallization, we examined reaction conditions that would provide a more stable, isolable derivative for thorough characterization.

Addition of hydrogen cyanide to a solution of the dimeric product to trap the putative iminium ion did not provide a stable derivative.[15] We reasoned that introduction of mild reducing agents would result in reduction of a reactive iminium ion or enamine functional group(s) that may be present in the dimerization product (i.e., C8a-iminium ion **13** or bis-enamine **14**, Scheme 3). Interestingly, sequential treatment of a benzene solution (0.02 M) of either alcohol **21** or myrmicarin 215B (**4**) with TFA (1.10 equiv) for 4 h at 23 °C followed by addition of sodium triacetoxyborohydride (6.50 equiv) in acetonitrile and mixing of the mixture (3.5:1, benzene:acetonitrile) for 3.5 hours at 23 °C, provided a compound with *sufficient* stability to undergo aqueous work-up (saturated aqueous ammonium hydrogen chloride solution), isolation, and chromatographic purification on silica gel. Significantly, this oxygen–sensitive

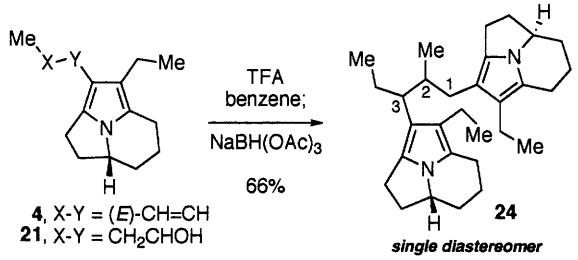

Scheme 7. Acid promoted dimerization of myrmicarin 215B (**4**) followed by immediate reduction to provide the first isolable dimeric product **24**. The C2- and C3-stereochemistry was later assigned; see below.

compound obtained in 66% isolated yield as a *single diastereomer* was consistent in all respects (HR-CIMS, ^{1}H, ^{13}C, gCOSY, HSQC) with the hexacyclic dimer **24** (Scheme 7). The isolation of the dimer **24** as the sole product suggests a highly diastereoselective dimerization of myrmicarin 215B (**4**) in the initial bond forming event. The C2- and C3-stereochemistry was later shown to

be (2*S*,3*R*), as described below. The isolation of compound **24** is consistent with hydride reduction at C1 in either azafulvenium ion **11** (Scheme 3) or iminium ion **13** (Scheme 3).[16]

Although evidence for the first of the two carbon–carbon bond forming events in our proposed dimerization was compelling, we required a means of isolating a suitable derivative of the putative heptacyclic iminium ion to validate the formation of the second carbon–carbon bond, and to secure the presence of the fully substituted cyclopentane. The difficulties in the full structural characterization of the immediate TFA promoted dimerization product (due to its limited longevity) notwithstanding, *in situ* NMR correlation experiments of this compound provided valuable information. Importantly, while the assignment of all thirty signals in the ^{13}C NMR spectrum agreed reasonably well with the predicted values based on those of myrmicarin 430A (**1**), the resonance assigned to position C8b in the putative iminium ion **13** (Scheme 4) occurred at an anomalously high chemical shift (δ96.1 ppm). As this value was higher than expected for a quaternary carbon, we systematically considered alternative structures that would be more consistent with the data for the putative iminium ion (Scheme 8). While the anticipated C1–C8b bond formation would result in the heptacyclic iminium ion **13** (Scheme 8, path A), an alternate bond formation between C1 and C3b would provide the isomeric heptacyclic iminium

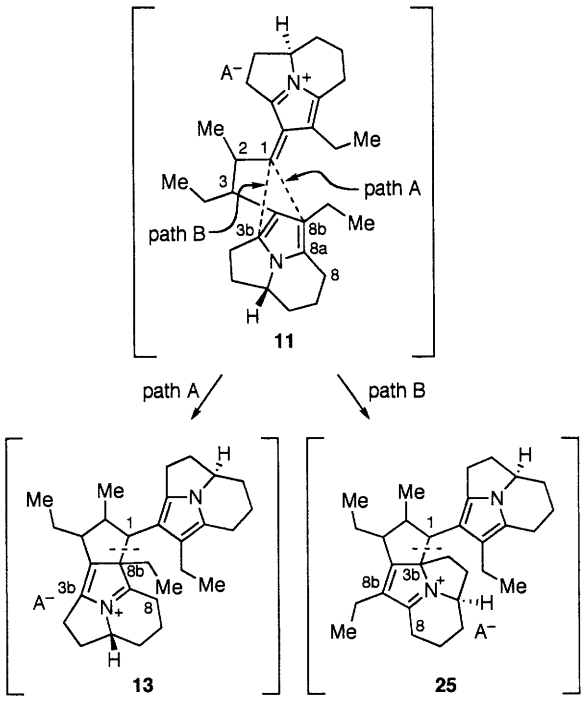

Scheme 8. Two possible modes of intramolecular azafulvenium ion trapping leading to isomeric heptacyclic iminium ions **13** and **25**.

ion **25** (Scheme 8, path B).[17] In this scenario, the signal at δ96.1 ppm would be due to the C3b in the iminium ion **25** (Scheme 8).

The spectroscopic data that we had obtained for the heptacyclic iminium ion was more consistent with a C1–C3b second bond formation to yield **25** (Scheme 8). To firmly establish the connectivity of the heptacyclic dimerization product, we investigated possible derivatives for further spectroscopic analysis. We reasoned that C8-deprotonation of the putative intermediate **25** (Scheme 8) with a strong base would provide the corresponding enamine that may exhibit enhanced stability relative to the iminium ion **25**. Gratifyingly, we found that treatment of a benzene-d_6 solution of the dimeric iminium ion, prepared as described above, with excess resin-bound BEMP (2-*tert*-butylimino-2-diethylamino-1,3-dimethyl-perhydro-1,3,2-diazaphosphorine, 10 equiv) under strictly oxygen–free conditions cleanly yielded a new C_{30}-product as a solution

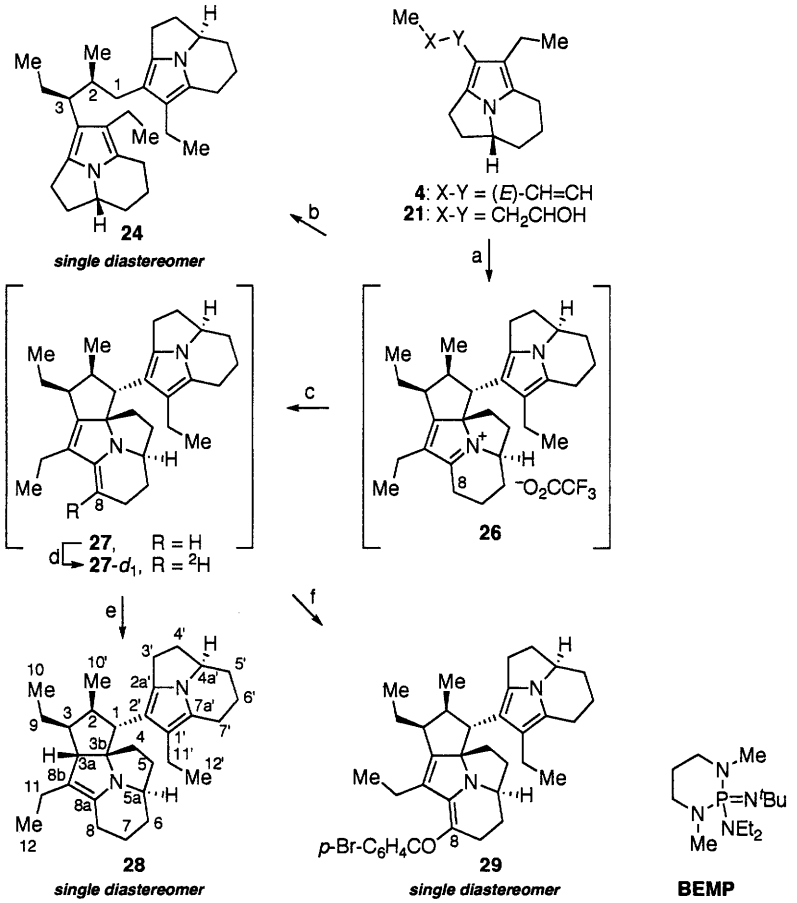

Scheme 9. TFA promoted dimerization of myrmicarin 215B (**4**) and related derivtives. Conditions: a) TFA, benzene-d_6, 23 °C, 3 h, ≥90%. b) $NaBH(OAc)_3$, MeCN-d_3, benzene-d_6, 23 °C, 3.5 h, 66% from **21**. c) resin bound-BEMP, benzene-d_6, 23 °C, 30 min. d) methanol-d_4 (~15 equiv), benzene-d_6, 23 °C, 1.5 h, complete C8 deuterium incorporation. e) Pd/C, H_2, 87% from **21**. f) *p*-BrPhCOCl, 30 min; $^iPr_2NH$, 67% from **21**.

in benzene-d_6. Importantly, the ^{1}H NMR (500 MHz) of this species possessed a single resonance at δ4.72 ppm (1H, dd), which was consistent with an expected C8-methine of enamine **27** (Scheme 9, for stereochemical assignment see Figure 2). Addition of methanol-d_4 (15 equiv) to the solution of enamine **27** resulted in complete disappearance of the resonance at δ4.72 ppm over a period of 1.5 h, consistent with the ^{2}H/H-exchange of an enamine. Unfortunately, the enamine **27** was unstable toward an aqueous work-up or attempted purification. While this presented challenges with regard to isolation or derivatization of enamine **27**, its sensitivity was not surprising based on the reported difficulties associated with the closely related myrmicarin 430A (**1**). However, an isolable derivative could be obtained by hydrogenation (1 atm of dihydrogen over 5% palladium on carbon) of the diene **27** in benzene, which cleanly afforded the enamine **28**.[18] Thus without the need for isolation of sensitive intermediates, alcohol **21** was converted to enamine **28** in a single operation (87%).[19] Enamine **28** was sufficiently stable toward isolation in neat form but required storage under strictly inert atmosphere to avoid oxidative decomposition.

Similar to the previously isolated hexacycle **24** (Scheme 7), the ^{1}H and ^{13}C NMR spectra of both diene **27** and enamine **28** contained one set of resonances that closely resembled those of the tricyclic core of myrmicarin 217 (**6**). Furthermore, the ^{13}C NMR and HSQC spectra of each compound showed the correct number of methine, methylene, methyl, and quaternary carbon units for structures **27** and **28** (Scheme 9). The presence of distinct C4-C8 and C1-C3 spin systems was recognized in the gCOSY spectra of both diene **27** and enamine **28**. However, this data alone was not sufficient to distinguish between the two modes of cyclization (path A versus path B, Scheme 8) in the formation of these heptacyclic products. Additional data obtained using heteronuclear multiple bond correlation (HMBC) and nuclear Overhauser effect spectroscopy (NOESY) NMR (600 MHz) experiments allowed structural verification of products **27-29** (Scheme 9). The HMBC correlations (Figure 2A) in the spectrum of the enamine **28** were entirely consistent with the heptacyclic structure depicted in Scheme 9 (path B, Scheme 8). Correlations between C1–H/C4–H_c, C3a–H/C4–H_t, and C3a–H/C11–H in the NOESY spectrum of enamine **28** validated this structural assignment. Additionally, NOESY correlations between C1-H/C10'-H, C2-H/C3-H, and C3a/C9 provided the relative stereochemistry about the newly formed fully substituted cyclopentane ring (Figure 2B).[20]

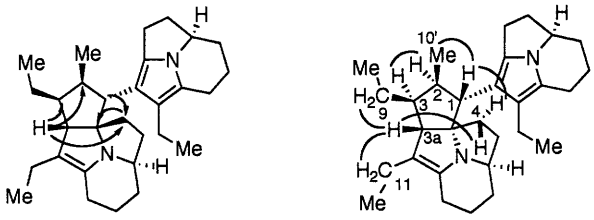

Figure 2. Key HMBC ($^{1}H \rightarrow ^{13}C$) and NOESY correlations for the enamine **28**.

We also sought derivatives that would be amenable to X-ray crystallographic analysis. Unfortunately, numerous attempts to crystallize the enamine **28** were unsuccessful. Even under strictly inert conditions extensive decomposition was observed within two days. Similar complications were present during manipulations of the corresponding protonated salts of enamine **28** formed upon treatment of **28** with a variety of Brønsted acids. In attempts to obtain derivatives with greater stability, we found that treatment of a benzene solution of the enamine **27** (Scheme 9) with benzoyl chlorides in the presence of excess diisopropylethylamine cleanly provided the corresponding C8-benzoylated products, many of which could be purified by silica gel chromatography. For example, in a single operation, the C8-*p*-bromobenzoylated product **29** was obtained in 67% yield starting with the alcohol **21** without isolation of iminium ion **26** or diene **27**. Although the C8-*p*-bromobenzoylated and C8-*p*-iodobenzoylated products were found to be storable in the absence of oxygen, crystallization and co-crystallization attempts did not provide samples suitable for single crystal X-ray analysis. However, 2D-NMR analysis of these samples provided additional data that paralleled our earlier results with the enamine **28** (Figure 2). Specifically, the data obtained using the isolable *p*-bromobenzoylated product **29** (gCOSY, HSQC, HMBC, and NOESY) provided further support for the structural assignment of compounds **26-29**. The signals at 96.1, 86.4, 83.6, and 86.9 ppm in the ^{13}C NMR spectra of **26-29**, respectively, were consistent with the C3b-tertiary amine. Since the hexacyclic dimer **24** is obtained by treatment of the iminium ion intermediate **26** with sodium triacetoxyborohydride, the C2- and C3-stereochemistry of **24** is assignment based on the relative stereochemistry found in the heptacyclic compounds **26-29**.

A possible mechanism for the dimerization of myrmicarin 215B (**4**) to enamine **27** is presented in Scheme 10. The overall process may involve a stepwise C9-C8 bond formation to give **30** followed by C3b-C1 bond formation to provide the iminium ion **31**.[21] The relative

Table 1. ^{1}H and ^{13}C NMR data in ppm for myrmicarin 430A[a] (**1**), iminium salt **26**, heptacyclic diene **27**, heptacyclic enamine **28**, and bromophenyl ketone **29** in benzene-d_6.[b]

	Myrmicarin 430A (**1**)		Iminium salt **26**[c]		Heptacyclic diene **27**[c]		Heptacyclic enamine **28**[c,d]		Bromophenyl ketone **29**[c,d]	
	δ_C	δ_H	δ_C	δ_H	δ_C	δ_H	δ_C	δ_H	δ_C	δ_H
1	55.3	3.21	45.9	2.54	49.4	2.60	51.9	2.85	48.5	2.58
2	43.4	1.97	51.7	2.29[d]	50.3	2.26	40.1	2.68	49.4	2.20
3	54.7	1.66	45.2	2.35	44.8	2.48	50.1	1.72	45.1	2.48
3a	62.1	–	181.0	–	152.3	–	62.0	–	162.6	–
3b	145.8	–	96.1	–	86.4	–	83.6	2.92	86.9	–
4	88.3	4.38	38.0	1.47, 1.54	41.3	1.75, 1.85	38.2	1.90[t], 2.14[c]	41.0	1.61[t], 1.65[c]
5	41.4	2.65[t], 3.10[c]	36.7	1.68, 2.31	36.3	1.68, 2.16	28.0	1.06[c], 1.56[t]	36.7	1.52[c], 2.15[t]
5a	55.1	3.94	55.7	2.73	54.8	3.00	58.8	2.65	54.6	2.80
6	28.1	1.30[t], 1.42[c]	27.0	0.88, 1.35	30.6	1.09, 1.71	27.7	1.51[t], 1.81[c]	30.4	0.82[t], 1.43[c]
7	22.3	1.93[t], 2.16[c]	18.6	1.22, 1.81	22.7	2.15, 2.21	20.6	1.24[t], 1.42[c]	28.8	2.24[c], 2.38[t]
8	90.1	4.39	26.4	2.77, 2.82	88.0	4.72	24.9	1.90[c], 2.38[t]	104.2	–
8a	48.7	2.54	187.1	–	132.9	–	140.5	–	162.6	–
8b	154.1	–	137.2	–	132.7	–	114.8	–	136.6	–
9	27.5	1.35, 1.85	21.0	1.08, 1.29	20.8	1.31, 1.50	22.9	1.25, 1.67	20.8	1.23, 1.44
10	12.8	1.16	13.3	0.81	13.9	1.00	13.6	1.07	13.6	0.93
10'	17.1	0.98	16.7	0.74	16.3	1.04	14.7	1.03	16.3	0.95
11	26.7	1.47, 1.73	18.3	2.24 (2H)	19.4	2.26, 2.34	19.9	2.05, 2.26	20.9	2.25, 3.16
12	17.1	0.99	14.0	1.06	14.8	1.24	14.9	1.14	14.8	1.19
1'	123.6	–	121.7	–	121.9	–	123.2	–	122.0	–
2'	111.7	–	111.3	–	114.2	–	111.2	–	113.6	–
2a'	127.6	–	127.1	–	128	–	128	–	128	–
3'	27.7	2.56[t], 2.69[c]	27.0	2.05, 2.29	27.9	2.70, 3.00	28.6	2.87[t], 3.10	27.5	2.65[t], 2.78[c]
4'	37.1	1.67[t], 2.07[c]	37.7	1.60, 2.34	37.3	1.65, 2.08	37.5	1.70[t], 2.17[c]	37.3	1.63[t], 2.13[c]
4a'	54.8	3.38	55.6	3.57	55.5	3.46	55.5	3.54	55.6	3.48
5'	30.0	0.90[t], 1.57[c]	29.7	0.77, 1.64	30.2	0.88, 1.53	30.5	0.96[t], 1.63[c]	30.1	0.89[t], 1.56[c]
6'	22.9	1.41[c], 1.70[t]	22.7	1.45, 1.68	23.3	1.39, 1.69	23.3	1.41[c], 1.71[t]	23.2	1.38[c], 1.69[t]
7'	21.0	2.46[t], 2.69[c]	20.9	2.29, 2.54	21.3	2.50, 2.68	21.3	2.47[t], 2.64[c]	21.2	2.44[t], 2.62[c]
7a'	118.1	–	119.4	–	116.7	–	117.4	–	117.5	–
11'	18.8	2.68, 2.93	18.6	2.39, 2.45	19.2	2.67	19.3	2.66, 2.68	19.0	2.59
12'	16.6	1.32	17.1	1.19	17.6	1.38	17.3	1.34	17.4	1.32

[a]From reference 1c. [b]The superscripts 'c' and 't' refer to the protons *cis* and *trans*, respectively, to the C4a' or C5a methine in each spin system. [c]Signal assignments were made through analysis of ^{1}H NMR, ^{13}C NMR, gCOSY, and HSQC spectra. [d]Signal assignments were made through analysis of HMBC, and NOESY or ROESY spectra.

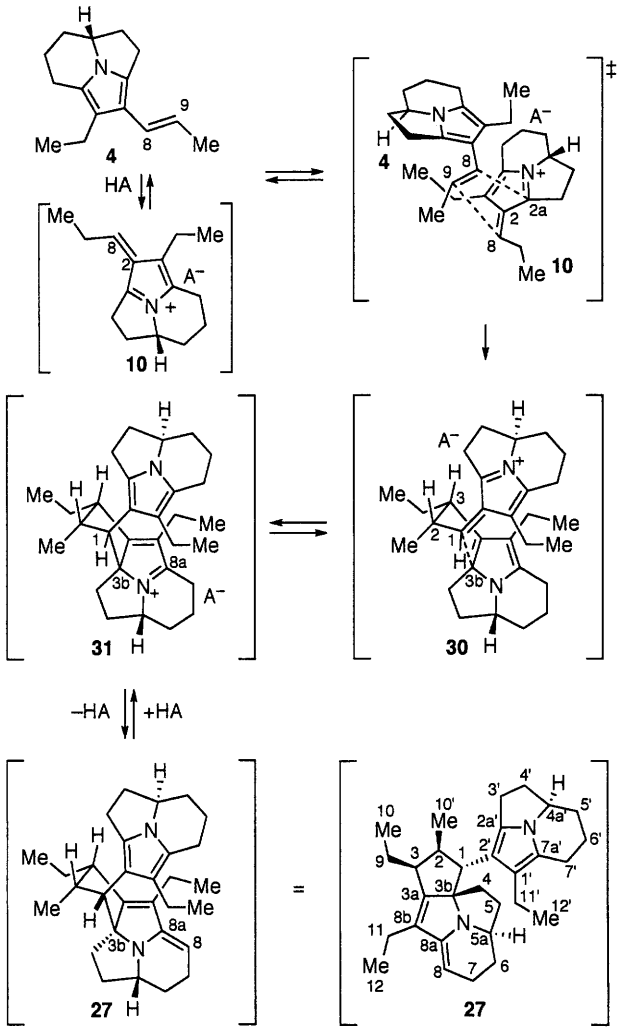

Scheme 10. The proposed mechanism for the diastereoselective dimerization of (+)-myrmicarin 215B (**4**) to an isomer of myrmicarin 430A (**1**), enamine **27** (isomyrmicarin 430A).

stereochemistry of the newly formed cyclopentane ring that is shared in compounds **26-29** suggests a convex face to convex face approach (i.e., **30**, Scheme 10). Under the reaction conditions described above, π-stacking interactions between the putative electron deficient azafulvenium ion **10** and the approaching electron rich vinyl pyrroloindolizine (**4**), or the positioning of the counter ion (A^-, Scheme 10) with respect to the dimerization precursors may be responsible for the observed stereoselectivity. Hence, ongoing efforts are directed at modifying the reaction conditions and identifying an appropriate counter ion (i.e. *formate*) that may influence the mode of dimerization (Scheme 8). While the involvement of any biosynthetic machinery in the dimerization of C15 myrmicarin monomers to the more complex myrmicarins is unknown at this time, the observed high level of diastereoselection and efficiency in our acid

promoted dimerization of myrmicarin 215B (**4**) highlights the possible direct dimerization of a pyrroloindolizine (i.e. **4**) as the first step toward C30 and C45 derivatives.

Conclusion

TFA-promoted dimerization of (+)-myrmicarin 215B (**4**) leads to a sequence of highly efficient and stereoselective carbon–carbon bond forming events, providing the heptacyclic dimeric enamine **27** (Scheme 9). A possible mechanism for the diastereoselective dimerization of myrmicarin 215B (**4**) to this isomer of myrmicarin 430A (**1**), isomyrmicarin 430A (**27**), is presented (Scheme 10). The isolation of a single diastereomer of the heptacyclic products *via* the TFA promoted dimerization of myrmicarin 215 is noteworthy. These observations provide experimental data relevant to our proposed vinyl pyrroloindolizine dimerization strategy for the synthesis of the heptacyclic portion of complex myrmicarin alkaloids. Current efforts are directed at controlling the mode of dimerization (Scheme 8) for implementation of this strategy toward these highly sensitive compounds: a strategy with potential implications regarding the biogenesis of these structurally fascinating alkaloids.

---

[1] (a) Francke, W.; Schröder, F.; Walter, F.; Sinnwell, V.; Baumann, H.; Kaib, M. *Liebigs Ann.* **1995**, 965–977. (b) Schröder, F.; Franke, S.; Francke, W.; Baumann, H.; Kaib, M.; Pasteels, J. M.; Daloze, D. *Tetrahedron* **1996**, *52*, 13539–13546. (c) Schröder, F.; Sinnwell, V.; Baumann, H.; Kaib, M. *J. Chem. Soc. Chem. Commun.* **1996**, 2139–2130. (d) Schröder, F.; Sinnwell, V.; Baumann, H.; Kaib, M.; Francke, W. *Angew. Chem. Int. Ed.* **1997**, *36*, 77–80.

[2] Schröder, F.; Francke, W. *Tetrahedron* **1998**, *54*, 5259–5264.

[3] The C2-C8 olefin geometry of this putative intermediate (i.e. **10**) is not known at this time as we have not directly observed this intermediate spectroscopically.

[4] Upon formation of the first carbon-carbon bond the numbering used for all dimeric compounds is consistent with the numbering system for myrmicarin 430A (**1**) (see ref. 1c).

[5] Movassaghi, M.; Ondrus, A. E. *Org. Lett.* **2005**, *7*, 4423–4426.

[6] For a previous total synthesis of (*R*)-(+)- myrmicarin 217 (**6**), see: Sayah, B.; Pelloux-Léon, N.; Vallée, Y. *J. Org. Chem.* **2000**, *65*, 2824–2826. For a previous total synthesis of (±)-myrmicarin 217 (**6**), see reference 2. For a formal synthesis of (*S*)-(–)- myrmicarin 217 (**6**), see: Settambolo, R.; Guazzelli, G.; Lazzaroni, R. *Tetrahedron: Asymmetry.* **2003**, *14*, 1447–1449. For a previous enantioselective synthesis of myrmicarin 215 as a mixture of alkene isomers, see: Sayah, B.; Pelloux-Léon, N.; Milet, A.; Pardillos-Guindet, J.; Vallée, Y. *J. Org. Chem.* **2001**, *66*, 2522–2525.

[7] Movassaghi, M.; Ondrus, A. E. *J. Org. Chem.* **2005**, *70*, 8638–8641.

[8] For reviews on transition metal catalyzed C-N bond formation, see: (a) Wolfe, J. P.; Wagaw, S.; Marcoux, J.-F.; Buchwald, S. L. *Acc. Chem. Res.* **1998**, *31*, 805–818. (b) Hartwig, J. F. *Acc. Chem. Res.* **1998**, *31*, 852–860. (c) Hartwig, J. F. *Angew. Chem. Int. Ed.* **1998**, *37*, 2046–2067. (d) Yang, B. H.; Buchwald, S. L. *J. Organomet. Chem.* **1999**, *576*, 125–146. (e) Muci, A. R.; Buchwald, S. L. *Top. Curr. Chem.* **2002**, *219*, 131–209. (f) Hartwig, J. F. In *Handbook of Organopalladium Chemistry* for Organic Synthesis. For palladium-catalyzed *N*-vinylation of lithiated azoles, see: (g) Lebedev, A. Y.; Izmer, V. V.; Kazyul'kin, D. N.; Beletskaya, I. P.; Voskoboynikov, A. Z. *Org. Lett.* **2002**, *4*, 623–626. For reports on palladium-catalyzed *N*-vinylation, see: (h) Wallace, D. J.; Klauber, D. J.; Chen, C.-y.; Volante, R. P. *Org. Lett.* **2003**, *5*, 4749–4752, and (i) Klapars, A.; Campos, K. R.; Chen, C.-y.; Volante, R. P. *Org. Lett.* **2005**, *7*, 1185–1188.

[9] Rainka, M. P.; Aye, Y.; Buchwald, S. L. *Proc. Nat. Acad. Sci., USA* **2004**, *101*, 5821–5823.

[10] For reports on CuH-catalyzed asymmetric conjugate reduction, see: (a) Lipshutz, B. H.; Servesko, J. M. *Angew. Chem. Int. Ed.* **2003**, *42*, 4789–4792, (b) Hughes, G.; Kimura, M.; Buchwald, S. L. *J. Am. Chem. Soc.* **2003**, *126*, 11253–11258 and references cited therein. For related references, see: (c) Mahoney, W. S.; Stryker, J. M. *J. Am. Chem. Soc.* **1989**, *111*, 8818–8823. (d) Mori, A.; Fujita, A.; Kajiro, H.; Nishihara, Y.; Hiyama, T. *Tetrahedron* **1999**, *55*, 4573–4582.

[11] Tsuji, T.; Watanabe, Y.; Mukaiyama, T. *Chem. Lett.* **1979**, 481–482.

[12] Owing to their acid sensitivity, none of the tricyclic myrmicarins could be efficiently purified by silica gel chromatography due to poor mass recovery. While spectroscopically pure samples of myrmicarins 215A, 215B, and 217 could be obtained without purification, all of the tricyclic myrmicarins could be subject to alumina gel chromatography without significant loss of material.

[13] While the exact position of protonation was unclear, the resonances corresponding to the C8-C9 vinyl groups of two major pyrrole-ring protonated compounds were visible.

[14] For a study on ring protonation of *N*-phenylpyrroles, see: Chiang, Y.; Hinman, R. L.; Theodoropulos, S.; Whipple, E. B. *Tetrahedron* **1967**, *23*, 745–759.

[15] No stable tricyclic or dimeric cyanide–adducts were observed (^{1}H NMR, TLC) under a variety of reaction conditions.

[16] While an azafulvenium ion is not observed spectroscopically, a potential equilibration between iminium ion **13** and azafulvenium ion **11** (Scheme 3) followed by rapid reduction may provide **25.** Alternatively C1-delivery of a hydride with concomitant displacement of a pyrroloindolizine would not require equilibration to the azafulvenium ion.

[17] For discussions regarding the regioselectivity of electrophilic addition to pyrroles, see: (a) Schofield, K. *Hetero-Aromatic Nitrogen Compounds*; Butterworths: London, 1967. (b) Patterson, J. M. *Synthesis* **1976**, 281–304. (c) *Pyrroles*; Jones, A., Ed.; Wiley: New York, 1990.

[18] The formation of enamine **28** is consistent with hydrogenation of C3a–C8b alkene followed by tautomerization to the tetrasubstituted C8a-enamine.

[19] Hydrogenation of this enamine under forcing conditions (160 psi H_2, 23 °C, 60 h) did provide further reduction of the enamine to the corresponding amine as a single diastereomer with similar chemical lability to **28**.

[20] The designations C4–H_c and C4–H_t refer to the protons *cis* and *trans* to the C4a methine, respectively.

[21] (a) While equilibrium of **30** and **31** is neither supported by spectroscopic data nor by enthalpic considerations, the presence of this equilibrium cannot be ruled out at this time. (b) Alternative cycloaddition type processes for the direct union of **4** and **10** to provide iminium ion **31** have been considered, and as with other possibilities necessarily await further experimental data.

Experimental Section

General Procedures. Reactions were performed in oven-dried or flame-dried round bottomed flasks or modified Schlenk (Kjeldahl shape) flasks. The flasks were fitted with rubber septa and reactions were conducted under a positive pressure of argon. NMR experiments were performed in vacuum-dried Wilmad Glass Co., Inc. 528-PP NMR tubes. Stainless steel syringes or cannulae were used to transfer air- and moisture-sensitive liquids. Flash column chromatography was performed as described by Still[1] using silica gel (60-Å pore size, 32–63 μm, standard grade, Sorbent Technologies) or non-activated alumina gel (80–325 mesh, chromatographic grade, EM Science). Analytical thin–layer chromatography was performed using glass plates pre-coated with 0.25 mm 230–400 mesh silica gel or neutral alumina gel impregnated with a fluorescent indicator (254 nm). Thin layer chromatography plates were visualized by exposure to ultraviolet light and/or by exposure to an ethanolic phosphomolybdic acid (PMA), an acidic solution of *p*-anisaldehyde (anis), an aqueous solution of ceric ammonium molybdate (CAM), an aqueous solution of potassium permanganate ($KMnO_4$) or an ethanolic solution of ninhydrin followed by heating (<1 min) on a hot plate (~250 °C). Organic solutions were concentrated on Büchi R-200 rotary evaporators at ~20 Torr (house vacuum) at 25–35 °C, then at ~1 Torr (vacuum pump) unless otherwise indicated.

Materials. Commercial reagents and solvents were used as received with the following exceptions: Dichloromethane, diethyl ether, tetrahydrofuran, acetonitrile and toluene was purchased from J.T. Baker (Cycletainer™) and were purified by the method of Grubbs et al. under positive argon pressure.[2]

Instrumentation. Proton nuclear magnetic resonance (^{1}H NMR) spectra were recorded with a Varian inverse probe 500 INOVA spectrometer or a Bruker inverse probe 600 Avance spectrometer. Chemical shifts are recorded in parts per million from internal tetramethylsilane on the δ scale and are referenced from the residual protium in the NMR solvent (C_6H_6: δ7.16). Data is reported as follows: chemical shift [multiplicity (s = singlet, d = doublet, q = quartet, m = multiplet), coupling constant(s) in Hertz, integration, assignment]. Carbon-13 nuclear magnetic resonance spectra were recorded with a Varian 500 INOVA spectrometer and are recorded in parts per million from internal tetramethylsilane on the δ scale and are referenced from the carbon resonances of the solvent (benzene-d_6: δ 128.0). We thank Dr. Li Li for obtaining HRMS data at the Department of Chemistry Instrumentation Facility (MIT-DCIF). Infrared data were obtained with a Perkin-Elmer 2000 FTIR and are reported as follows: [frequency of absorption (cm^{-1}), intensity of absorption (s = strong, m = medium, w = weak, br = broad), assignment].

Positional Numbering System. For direct comparison, the numbering scheme used for dimeric compounds is consistent with that used by Schröder and coworkers in the isolation paper for myrmicarin 430A[3] and that used by us for isomyrmicarin 430A.

---

[1] Still, W. C.; Kahn, M.; Mitra, A. *J. Org. Chem.* **1978**, *43*, 2923–2925.

[2] Pangborn, A. B.; Giardello, M. A.; Grubbs, R. H.; Rosen, R. K.; Timmers, F. J. *Organometallics* **1996**, *15*, 1518–1520.

[3] Schröder, F.; Sinnwell, V.; Baumann, H.; Kaib, M. *J. Chem. Soc. Chem. Commun.* **1996**, *18*, 2139–2140.

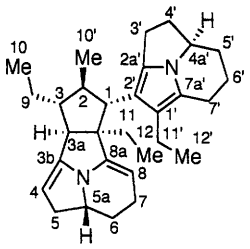

Myrmicarin 430A
(**1**)

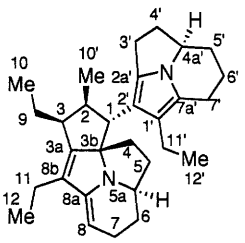

Isomyrmicarin 430A
(**27**)

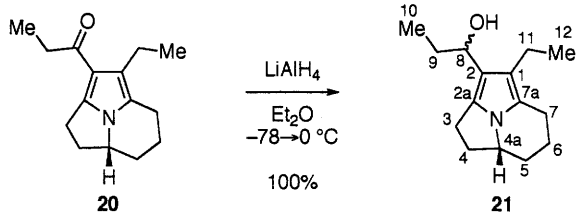

Tricyclic Alcohol 21:

Solid lithium aluminum hydride (11.6 mg, 306 μmol, 6.00 equiv) was added in a single portion to a solution of tricyclic ketone **20** (11.8 mg, 51.0 μmol, 1 equiv) in Et_2O (950 μL) at –78 °C followed by immediate placement of the reaction flask on an ice–water bath. After 40 min, the vigorously stirred grey suspension was cooled to –78 °C and excess hydride was quenched by the slow addition of water (1.20 mL) via syringe. The cold bath was immediately removed and the mixture allowed to warm to 23 °C. The pale grey suspension was diluted sequentially with a 6-mL portion of Et_2O and a saturated aqueous solution of Rochelle salt (6 mL), and the two–phase mixture was vigorously stirred. After 3 h, the resulting slightly opaque aqueous layer was separated from the clear and colorless organic layer and was extracted with EtOAc (3 × 5 mL). The combined organic layers were washed with a 5-mL portion of brine, dried over anhydrous sodium sulfate, filtered, and concentrated under reduced pressure to give exclusively the alcohol **21** as a colorless oil (10.9 mg, 100%). ^{1}H NMR analysis revealed the product to be a mixture of C8-epimers (3:2). The alcohol **21** was found to be exceedingly sensitive toward dehydration and decomposition upon treatment with silica or alumina gel and required storage under an argon atmosphere.

^{1}H NMR (500 MHz, C_6D_6, 20 °C, 3:2 mixture of epimers, major epimer denoted by *): 4.71 (dd, 1H, J = 7.6, 5.8 Hz, C8–H*), 4.70 (dd, 1H, J = 7.2, 6.3 Hz, C8–H), 3.19–3.27 (m, 2H, C4a–H*, C4a–H), 2.74 (dd, 1H, J = 14.6, 7.9 Hz, C7–H*), 2.53–2.70 (m, 9H, C3–H*, C3–H, C3–H*, C3–H, C11–H*, C11–H, C11–H'*, C11–H', C7–H), 2.31–2.41 (m, 2H, C7–H*, C7–H), 2.00–2.09 (m, 2H, C4–H*, C4–H), 1.90–1.99 (m, 4H, C9–H*, C9–H, C9–H'*, C9–H'), 1.65–1.72 (m, 2H, C6–H, C6–H), 1.50–1.60 (m, 4H, C4–H*, C4–H, C5–H*, C5–H), 1.31 (t, 3H, J = 7.5 Hz, C12–H*), 1.28 (t, 3H, J = 7.6 Hz, C12–H), 1.12 (t, 3H, J = 7.3 Hz, C10–H), 1.11 (t, 3H, J = 7.3 Hz, C10–H*), 0.79–0.90 (m, 2H, C5–H*, C5–H).

^{13}C NMR (125 MHz, C_6D_6, 20 °C, 3:2 mixture of epimers, major epimer denoted by *): 127.7*, 127.6, 121.6*, 121.6, 118.9*, 118.5, 118.3*, 118.3, 70.0*, 69.7, 55.3*, 55.2, 37.2*, 37.4, 31.5*, 32.4, 30.2*, 30.2, 26.3*, 26.3, 23.2*, 23.1, 20.9*, 20.9, 19.2*, 19.1, 17.2*, 17.3, 11.8, 11.7*.

FTIR (thin film) cm^{-1}:	3417 (br s, O–H), 2597 (s, C–H), 2854 (s, C–H), 1454, 1320, 1044.
HRMS (ESI):	calcd for $C_{15}H_{23}NONa$ $[M+Na]^+$: 256.1672, found: 256.1677.

TLC (alumina gel, 30% EtOAc–hexanes), *Rf*: 0.26, 0.30 (UV, $KMnO_4$).

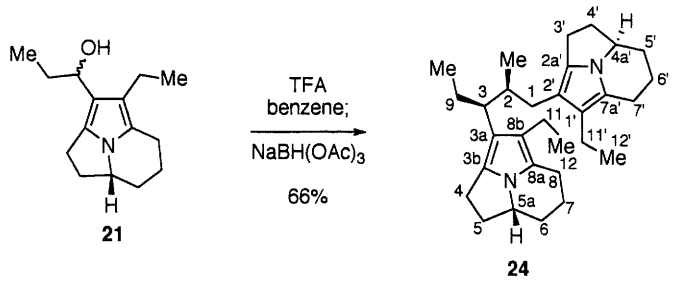

Hexacyclic Dimer 24:

A sample of alcohol **21** (3.4 mg, 14.6 μmol, 1 equiv) was dried by concentration from anhydrous benzene-d_6 (3 × 350 μL). The residue was dissolved in benzene-d_6 (650 μL) and was purged by a stream of argon for 3 min. A solution of TFA (1.2 μL, 16.0 μmol, 1.10 equiv) in benzene-d_6 (51.2 μL) was added drop wise via syringe. The resulting solution became intense yellow immediately upon addition of TFA and faded to a tan color within 2 min. The mixture was mixed and maintained under an argon atmosphere for 4.5 h. A suspension of sodium triacetoxyborohydride (20.1 mg, 94.9 μmol, 6.50 equiv) in acetonitrile-d_3 (200 μL) was then added via syringe and the resulting pale burgundy suspension was stirred under inert atmosphere. After 3.5 h, the suspension was diluted with EtOAc (7.5 mL) and the resulting mixture was washed with saturated aqueous ammonium chloride solution (4 mL). The clear, colorless aqueous layer was separated and extracted with ethyl acetate (3 × 3 mL) and the combined pale yellow organic solution was washed with saturated aqueous sodium bicarbonate (3 mL), and brine (3 mL). The organic layer was dried over anhydrous sodium sulfate, and then concentrated under reduced pressure to give a deep brown residue. Purification of the residue by silica gel column chromatography (5% EtOAc-hexanes; diameter 0.5 cm, height 4.5 cm) gave the hexacyclic dimer **24** as a yellow oil (2.1 mg, 66%).[4]

^{1}H NMR (500 MHz, C_6D_6, 20 °C): 3.36 (m, 2H, C4a'–H, C5a'–H), 3.15 (dd, 1H, J = 13.4, 2.7 Hz, C1–H), 2.80 (m, 1H, C3–H), 2.79 (m, 1H, C3'–H/C4–H), 2.63–2.73 (m, 9H, C3'–H/C4–H, C11–H, C11'–H, C3'–H/C4–H, C7'–H, C8–H, C3'–H/C4–H), 2.46 (m, 2H, C7'–H, C8–H), 2.35 (dd, 1H, J = 13.4, 10.8 Hz, C1–H'), 2.20 (m, 1H, C2–H), 2.06 (m, 1H, C4'–H/C5–H), 2.01 (m, 1H, C4'–H/C5–H), 2.01 (m, 1H, C9–H), 1.93 (m, 1H, C9–H'), 1.71 (m, 2H, C6'–H/C7–H), 1.67 (m, 1H, C4'–H/C5–H), 1.59 (m, 1H, C4'–H/C5–H), 1.57 (m, 2H, C5'–H, C6–H), 1.46 (t, 3H, J = 7.5 Hz, C12–H/C12'–H), 1.43 (t, 3H, J = 7.5 Hz, C12–H/C12'–H), 1.42 (m, 1H, C6'–H/C7–H), 1.35 (m, 1H, C6'–H/C7–H), 1.26 (d, 3H, J = 6.7 Hz, C10'–H), 1.11 (t, 3H, J = 7.3 Hz, C10–H), 0.91 (m, 1H, C5'–H/C6–H), 0.88 (m, 1H, C5'–H/C6–H).

[4] While the critical spin system (C1-C3) was conclusively assigned, the two overlapping pyrroloindolizine spin systems of hexacycle **24** (C4-C8 and C3'-C7') are identified but not assigned.

^{13}C NMR (125 MHz, C_6D_6, 20 °C):	128 (C2a'/C3b), 126.8 (C2a'/C3b), 122.7 (C1'/C8b), 121.8 (C1'/C8b), 118.6 (C7a'/C8a), 118.3 (C7a'/C8a), 116.5 (C2'/C3a), 114.1 (C2'/C3a), 55.4 (C4a'/C5a), 55.2 (C4a'/C5a), 44.9 (C3), 42.1 (C2), 37.6 (C4', C5), 31.3 (C1), 30.6 (C5'/C6), 30.3 (C5'/C6), 27.4 (C3'/C4), 25.6 (C3'/C4), 25.2 (C9), 23.3 (C6'/C7), 23.2 (C6'/C7), 21.3 (C7'/C8), 21.2 (C7'/C8), 19.3 (C11/C11'), 19.3 (C11/C11'), 18.2 (C10'), 17.0 (C12, $C12_2$'), 13.8 (C10).
FTIR (thin film) cm^{-1}:	2928 (s, C–H), 2852 (s, C–H), 1737, 1688, 1458, 1321, 1261, 1197.
HRMS (ESI):	calcd for $C_{30}H_{44}N_2$ $[M+H]^+$: 433.3577, found: 433.3441.

TLC (silica gel, 10% EtOAc–hexanes), *Rf*: 0.53 (UV, anis).

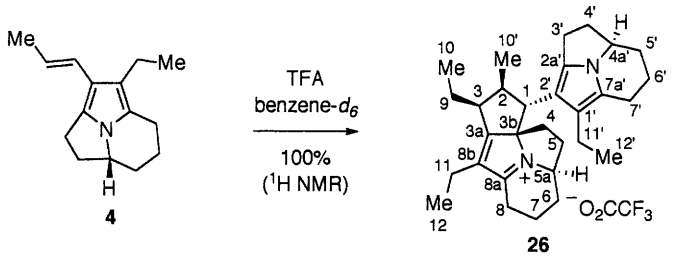

Iminium Salt 26:

A sample of myrmicarin 215B (**4**, 5.5 mg, 25.6 μmol, 1 equiv) was dried by concentration from anhydrous benzene (3 × 350 μL). The residue was dissolved in benzene-d_6 (600 μL) in an NMR tube fitted with a rubber septum and was purged by a gentle stream of argon for 3 min. A solution of TFA (2.2 μL, 29.4 μmol, 1.15 equiv) in benzene-d_6 (52.7 μL) was added drop-wise via syringe. The resulting reaction mixture became intense yellow immediately upon addition of the TFA solution and gradually turned brown over 30 min. The sample was mixed and maintained under an argon atmosphere for 4.5 h at ambient temperature. ^{1}H NMR analysis revealed complete conversion of myrmicarin 215B (**4**) to the highly air-sensitive iminium salt **26**. This compound was found to be unstable toward isolation. The same dimerization product **26** was obtained starting with the alcohol **21** in place of myrmicarin 215B (**4**) following a similar protocol.

^{1}H NMR (500 MHz, C_6D_6, 20 °C): 3.57 (tdd, 1H, J = 10.5, 4.9, 3.7 Hz, C4a'–H), 2.82 (m, 1H, C8–H), 2.77 (m, 1H, C8–H'), 2.73 (m, 1H, C5a–H), 2.54 (m, 1H, C7'–H), 2.54 (d, 1H, J = 9.8 Hz, C1–H), 2.45 (m, 1H, C11'–H), 2.39 (m, 1H, C11'–H'), 2.35 (m, 1H, C3–H), 2.34 (m, 1H, C4'–H), 2.31 (m, 1H, C5–H), 2.29 (m, 1H, C7'–H), 2.29 (m, 1H, C2–H), 2.29 (m, 1H, C3'–H), 2.24 (q, 2H, J = 7.6 Hz, C11–H), 2.05 (tdd, 1H, J = 14.3, 10.7, 6.3 Hz, C3'–H), 1.81 (m, 1H, C7–H), 1.68 (m, 1H, C6'–H), 1.68 (m, 1H, C5–H), 1.64 (m, 1H, C5'–H), 1.60 (m, 1H, C4'–H), 1.54 (m, 1H, C4–H), 1.47 (m, 1H, C4–H'), 1.45 (m, 1H, C6'–H), 1.35 (m, 1H, C6–H), 1.29 (m, 1H, C9–H), 1.22 (m, 1H, C7–H'), 1.19 (t, 3H, J = 7.5 Hz, C12'–H), 1.08 (m, 1H, C9–H'), 1.06 (t, 3H, J = 7.6 Hz, C12–H), 0.88 (m, 1H, C6–H'), 0.81 (t, 3H, J = 7.5 Hz, C10–H), 0.77 (m, 1H, C5'–H), 0.74 (d, 3H, J = 6.7 Hz, C10'–H).

^{13}C NMR (125 MHz, C_6D_6, 20 °C): 187.1 (C8a), 181.0 (C3a), 137.2 (C8b), 127.1 (C2a'), 121.7 (C1'), 119.4 (C7a'), 111.3 (C2'), 96.1 (C3b), 55.7 (C5a), 55.6 (C4a'), 51.7 (C2), 45.9 (C1), 45.2 (C3), 38.0 (C4), 37.7 (C4'), 36.7 (C5), 29.7 (C5'), 27.0 (C6), 27.0 (C3'), 26.4 (C8), 22.7 (C6'), 21.0 (C9), 20.9 (C7'), 18.6 (C7), 18.6 (C11'),

18.3 (C11), 17.1 (C12'), 16.7 (C10'), 14.0 (C12), 13.3 (C10).

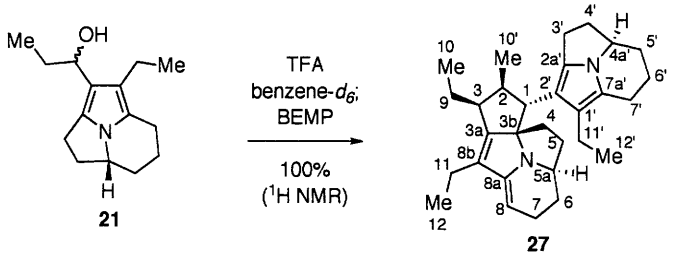

Heptacyclic Diene 27:

A sample of alcohol **21** (5.1 mg, 21.9 μmol, 1 equiv) was dried by concentration from anhydrous benzene (3 × 350 μL). The residue was dissolved in benzene-d_6 (600 μL) in an NMR tube fitted with a rubber septum and was purged by a gentle stream of argon for 3 min. A solution of TFA (1.8 μL, 24.1 μmol, 1.10 equiv) in benzene-d_6 (52.1 μL) was added drop wise via syringe. The resulting reaction mixture became intense yellow immediately upon addition of the TFA and faded to a tan color within 2 min. The sample was mixed and maintained under an argon atmosphere for 4.5 h at ambient temperature. Monitoring of the reaction mixture by ^{1}H NMR revealed complete consumption of alcohol **21** and myrmicarin 215B (**4**, generated *in situ*). The contents of the sample were transferred to a recovery flask under an inert atmosphere (glove-box, nitrogen atmosphere) and the transfer completed with three 350 μL benzene-d_6 rinses. A single portion of resin-bound 2-*tert*-butylimino-2-diethylamino-1,3-dimethyl-perhydro-1,3,2-diazaphosphorine (BEMP, 99.0 mg, 2.2 mmol/mg on 200-400 mesh polystyrene resin, 10.0 equiv) was added to the solution of the iminium salt **26** and the resulting pale yellow suspension was stirred for 30 min under strictly inert conditions. The suspension was filtered through a cotton plug, the filter-cake was rinsed with benzene-d_6 (3 × 350 μL), and the pale yellow solution was sealed in a recovery flask under a nitrogen atmosphere, placed on a vacuum manifold and concentrated to ~350 μL. The transfer of this solution via cannula into a sealed, argon-purged NMR tube and using two additional portions of benzene-d_6 (150 μL) to complete the transfer, provided a clear, faintly yellow solution of the exceedingly air-sensitive diene **27** suitable for ^{1}H NMR and ^{13}C NMR analysis.

^{1}H NMR (500 MHz, C_6D_6, 20 °C): 4.72 (dd, 1H, J = 7.2, 3.2 Hz, C8–H), 3.46 (tdd, 1H, J = 10.9, 5.4, 3.8 Hz, C4a'–H), 3.00 (m, 1H, C3'–H), 3.00 (m, 1H, C5a–H), 2.70 (dd, J = 15.4, 7.5 Hz, 1H, C3'–H), 2.68 (m, 1H, C7'–H), 2.67 (q, 2H, J = 7.6 Hz, C11'–H), 2.60 (d, 1H, J = 10.7 Hz, C1–H), 2.50 (ddd, 1H, J = 16.0, 11.8, 6.3 Hz, C7'–H), 2.48 (m, 1H, C3–H), 2.34 (dq, 1H, J = 13.8, 7.5 Hz, C11–H), 2.26 (dq, 1H, J = 13.8, 7.5 Hz, C11–H'), 2.26 (m, 1H, C2–H), 2.21 (m, 1H, C7–H), 2.16 (m, 1H, C5–H), 2.15 (m, 1H, C7–H'), 2.08 (dt, 1H, J = 11.5, 5.8 Hz, C4'–H), 1.85 (td, 1H, J = 11.5, 7.8 Hz, C4–H), 1.75 (m, 1H, C4–H'), 1.71 (m, 1H, C6–H), 1.69 (m, 1H, C6'–H), 1.68 (m, 1H, C5–H'), 1.65 (m, 1H, C4'–H), 1.53 (m, 1H, C5'–H), 1.50 (m, 1H, C9–H), 1.39 (m, 1H, C6'–H), 1.38 (t, 3H, J = 7.6

	Hz, C12'–H), 1.31 (m, 1H, C9–H'), 1.24 (t, 3H, J = 7.5 Hz, C12–H), 1.09 (tdd, 1H, J = 11.9, 4.9, 1.4 Hz, C6–H'), 1.04 (d, 3H, J = 6.7 Hz, C10'–H), 1.00 (t, 3H, J = 7.3 Hz, C10–H), 0.88 (tdd, 1H, J = 12.8, 10.9, 2.0 Hz, C5'–H).
^{13}C NMR (125 MHz, C_6D_6, 20 °C):	152.9 (C8a), 152.3 (C3a), 132.7 (C8b), 128 (C2a'), 121.9 (C1'), 116.7 (C7a'), 114.2 (C2'), 88.0 (C8), 86.4 (C3b), 55.5 (C4a'), 54.8 (C5a), 50.3 (C2), 49.4 (C1), 44.8 (C3), 41.3 (C4), 37.3 (C4'), 36.2 (C5), 30.6 (C6), 30.2 (C5'), 27.9 (C3'), 23.3 (C6'), 22.7 (C7), 21.3 (C7'), 20.8 (C9), 19.4 (C11), 19.2 (C11'), 17.6 (C12'), 16.3 (C10'), 14.8 (C12), 13.9 (C10).

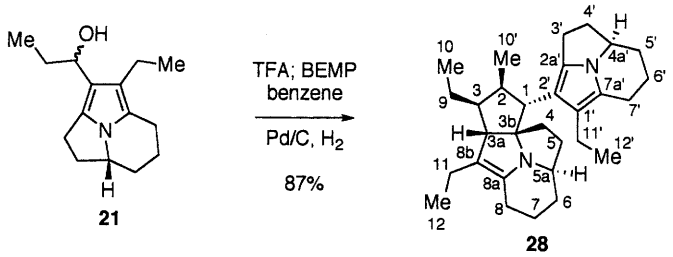

Heptacyclic Enamine 28:

A sample of alcohol **21** (10.0 mg, 42.9 μmol, 1 equiv) was dried by concentration from anhydrous benzene (3 × 350 μL). The residue was dissolved in benzene (1.06 mL) and was purged by a stream of argon for 3 min. A solution of TFA (3.5 μL, 47.2 μmol, 1.10 equiv) in benzene (23.5 μL) was added drop-wise via syringe. The resulting solution became intense yellow immediately upon addition of TFA and faded to a clear tan color within 2 min. The mixture was mixed and maintained under an argon atmosphere for 4.5 h. The contents of the sample were transferred to a recovery flask under an inert atmosphere (glove-box, nitrogen atmosphere) and the transfer completed with three 350-μL benzene-d_6 rinses. A single portion of resin-bound 2-*tert*-butylimino-2-diethylamino-1,3-dimethyl-perhydro-1,3,2-diazaphosphorine (BEMP, 195 mg, 2.2 mmol/mg on 200-400 mesh polystyrene resin, 10.0 equiv) was added to the solution of the iminium ion salt **26** and the resulting pale yellow suspension was stirred for 30 min under strictly inert conditions. The suspension was filtered through a cotton plug and the filter-cake was rinsed with benzene (3 × 450 μL) to give a solution of the diene **27**. Palladium on activated carbon (20.0 mg, 5%-Pd/C) was added and the flask was sealed under nitrogen and removed from the glove-box. The reaction vessel was flushed with dihydrogen (~1 atm) for 5 min and then maintained under a balloon-pressure of dihydrogen for an additional 30 min at ambient temperature. Dilution of the black suspension with EtOAc (2 mL), and filtration of the mixture through a plug of celite (diam 0.6 cm, ht. 4.0 cm), followed by an EtOAc rinse (15 mL), yielded a clear yellow solution of the desired enamine **28**. Removal of the volatiles under reduced pressure gave the pure enamine **28** (8.1 mg, 87%) as a clear yellow oil with marginal stability. This enamine was sufficiently stable toward isolation in neat form but required storage under strictly inert atmosphere to avoid oxidative decomposition; spectroscopic characterization was conducted shortly after isolation.

^{1}H NMR (600 MHz, C_6D_6, 20 °C): 3.54 (tdd, 1H, J = 10.7, 5.5, 3.6 Hz, C4a'–H), 3.10 (ddd, 1H, J = 15.3, 10.9, 5.9 Hz, C3'–H_c), 2.92 (s, 1H, C3a–H), 2.87 (dd, 1H, J = 15.3, 7.6 Hz, C3'–H_t), 2.85 (d, 1H, J = 12.8 Hz, C1–H), 2.68 (m, 1H, C2–H), 2.68 (m, 1H, C11'–H), 2.66 (m, 1H, C11'–H), 2.65 (m, 1H, C5a–H), 2.64 (m, 1H, C7'–H_c), 2.47 (ddd, 1H, J = 15.9, 11.8, 6.4 Hz, C7'–H_t), 2.38 (dt, 1H, J = 14.4, 4.2 Hz, C8–H_t), 2.26 (dq, 1H, J = 14.3, 7.3 Hz, C11–H), 2.17 (dt, 1H, J = 10.7, 5.7 Hz, C4'–H_c), 2.14 (td, 1H, J = 11.9, 7.6 Hz, C4–H_c), 2.05 (dq, 1H, J = 14.3, 7.3 Hz, C11–H'), 1.90 (m, 1H, C4–H_t), 1.90 (m, 1H, C8–H_c), 1.81 (tdd,

	1H, J = 13.6, 5.5, 4.7 Hz, C6–H_c), 1.72 (m, 1H, C3–H), 1.71 (m, 1H, C6'–H_t), 1.70 (m, 1H, C4'–H_t), 1.67 (m, 1H, C9–H), 1.63 (m, 1H, C5'–H_c), 1.56 (td, J =11.7, 3.6 Hz, 1H, C5–H_t), 1.51 (dddd, J = 13.5, 5.2, 3.2, 1.9, 1H, C6–H_t), 1.42 (m, 1H, C7–H_c), 1.41 (m, 1H, C6'–H_c), 1.34 (t, 3H, J = 7.5 Hz, C12'–H), 1.25 (m, 1H, C9–H'), 1.24 (m, 1H, C7–H_t), 1.14 (t, 3H, J = 7.3 Hz, C12–H), 1.07 (t, 3H, J = 7.3 Hz, C10–H), 1.06 (m, 1H, C5–H_c), 1.03 (d, 1H, J = 7.0 Hz, C10'–H), 0.96 (tdd, 1H, J = 12.8, 10.7, 2.4 Hz, C5'–H_t).
^{13}C NMR (125 MHz, C_6D_6, 20 °C):	140.5 (C8a), 128 (C2a'), 123.2 (C1'), 117.4 (C7a'), 114.8 (C8b), 111.2 (C2'), 83.6 (C3b), 62.0 (C3a), 58.8 (C5a), 55.5 (C4a'), 51.9 (C1), 50.1 (C3), 40.1 (C2), 38.2 (C4), 37.5 (C4'), 30.5 (C5'), 28.6 (C3'), 28.0 (C5), 27.7 (C6), 24.9 (C8), 23.3 (C6'), 22.9 (C9), 21.3 (C7'), 20.6 (C7), 19.9 (C11), 19.3 (C11'), 17.3 (C12'), 14.9 (C12), 14.7 (C10'), 13.6 (C10).
HRMS (ESI):	calcd for $C_{30}H_{44}N_2$ $[M+H]^+$: 433.3577, found: 433.3566.

TLC (silica gel pre-treated with Et_3N, 1.5% Et_3N, 2.5% EtOAc–hexanes), R_f: 0.27 (UV, anis).

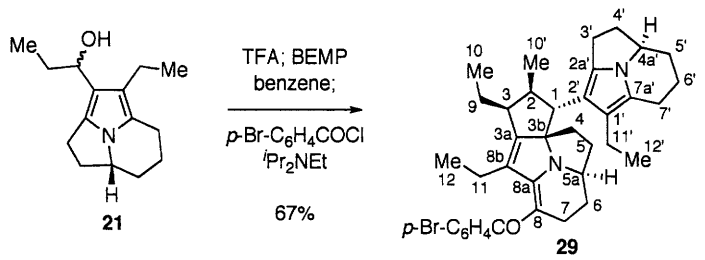

Bromophenyl ketone 29:

A sample of alcohol **21** (9.6 mg, 41.2 μmol, 1 equiv) was dried by concentration from anhydrous benzene (3 × 500 μL). The residue was dissolved in benzene (1.0 mL) and was purged by a stream of argon for 3 min. A solution of TFA (3.4 μL, 45.3 μmol, 1.10 equiv) in benzene (25.0 μL) was added drop-wise via syringe. The pale yellow mixture became intense yellow immediately upon addition of TFA and faded to a clear tan color solution within 2 min. The reaction mixture was mixed and maintained at ambient temperature for 4.5 h under strictly inert atmosphere to allow complete conversion of the myrmicarin 215B (**4**) to the iminium ion **26**. A single portion of resin-bound BEMP (187 mg, 2.2 mmol/mg on 200-400 mesh polystyrene resin, 10.0 equiv) was added under an inert atmosphere (glove-box, nitrogen atmosphere) to the solution of the iminium salt **26** and the resulting pale yellow suspension was stirred under strictly inert conditions. After 30 min, the yellow suspension was filtered through a cotton plug into a recovery flask and the transfer was completed using additional benzene (3 × 450 μL) as a rinse. The flask was sealed under nitrogen and removed from the glove-box. The pale yellow solution was concentrated partially under reduced pressure (to ~750 μL). Diisopropylethyamine (89.7 μL, 515 μmol, 12.5 equiv) was added via syringe at ambient temperature, followed by 4-bromobenzoyl chloride (11.3 mg, 51.5 μmol, 1.25 equiv) as a solid in a single portion and the flask was immediately resealed and flushed with argon. The resulting intense yellow, slightly opaque mixture was vigorously stirred at ambient temperature. After 30 min, diisopropylamine (150 μL, 1.07 mmol, 26.1 equiv) was introduced via syringe to quench the excess acid chloride. After 5 min, the suspension was concentrated under reduced pressure to give the crude product as a bright yellow semi-solid. Purification of the residue by column chromatography on silica gel (5% Et_3N, 5% EtOAc-hexanes, diameter 1.5 cm, height 15 cm) afforded the benzoylated derivative **29** as a bright yellow oil (8.4 mg, 67%).

^{1}H NMR (600 MHz, C_6D_6, 20 °C): 7.67 (d, 2H, J = 8.2 Hz, C15–H, C15'–H), 7.29 (d, 2H, J = 8.2 Hz, C16–H, C16'–H), 3.48 (tdd, 1H, J = 10.7, 5.0, 3.7 Hz, C4a'–H), 3.16 (dq, 1H, J = 14.0, 7.3 Hz, C11–H), 2.80 (m, 1H, C5a–H), 2.78 (m, 1H, C3'–H_c), 2.65 (m, 1H, C3'–H_t), 2.62 (m, 1H, C7'–H_c), 2.59 (m, 2H, C11'–H), 2.48 (m, 1H, C3–H), 2.44 (m, 1H, C7'–H_c), 2.38 (dt, 1H, J = 13.8, 3.3 Hz, C7–H_t), 2.25 (m, 1H, C11–H'), 2.24 (td, 1H, J = 13.8, 2.9 Hz, C7–H_c), 2.20 (m, 1H, C2–H), 2.15 (m, 1H, C5–H_t), 2.13 (m, 1H, C4'–H_c), 1.69 (m, 1H, C6'–H_t), 1.65 (m, 1H, C4–H_c), 1.63 (m, 1H, C4'–H_t), 1.61 (m, 1H, C4–H_t), 1.56 (m, 1H, C5'–

	H_c), 1.52 (m, 1H, C5–H_c), 1.44 (m, 1H, C9–H), 1.43 (m, 1H, C6–H_c), 1.38 (m, 1H, C6'–H_c), 1.32 (t, 3H, J = 7.6 Hz, C12'–H), 1.23 (m, 1H, C9–H'), 1.19 (t, 3H, J = 7.3 Hz, C12–H), 0.95 (d, 3H, J = 6.7 Hz, C10'–H), 0.93 (t, 3H, J = 7.6 Hz, C10–H), 0.89 (tdd, 1H, J = 12.6, 10.4, 2.2 Hz, C5'–H_t), 0.82 (dtd, 1H, J = 13.8, 11.9, 2.9 Hz, C6–H_t).
^{13}C NMR (125 MHz, C_6D_6, 20 °C):	190.4 (C13), 162.6 (C3a), 162.6 (C8a), 141.8 (C14), 136.6 (C8b), 131.8 (C15), 131.4 (C16), 128 (C2a'), 125.2 (C17), 122.0 (C1'), 117.5 (C7a'), 113.6 (C2'), 104.2 (C8), 86.9 (C3b), 55.6 (C4a'), 54.6 (C5a), 49.4 (C2), 48.5 (C1), 45.1 (C3), 41.0 (C4), 37.3 (C4'), 36.7 (C5), 30.4 (C6), 30.1 (C5'), 28.8 (C7), 27.5 (3'), 23.2 (C6'), 21.2 (C7'), 20.9 (C11), 20.8 (C9), 19.0 (C11'), 17.4 (C12'), 16.3 (C10'), 14.8 (C12), 13.6 (C10).
HRMS (ESI):	calcd for $C_{37}H_{45}BrN_2O$ $[M+H]^+$: 613.2788, found: 613.2771.
TLC (silica gel, 20% EtOAc–hexanes), R_f:	0.41 (UV, ninhydrin).

Chapter IV.

Efficient and Stereoselective Dimerization of Pyrroloindolizine Derivatives Inspired by a Hypothesis for the Biosynthesis of Complex Myrmicarin Alkaloids

Introduction and Background

The complex myrmicarins are a family of structurally fascinating and air sensitive alkaloids isolated from the poison gland of the African ant species *Myrmicaria opaciventris* (Figure 1).[1] Detailed spectroscopic studies have been used to assign the relative stereochemistries of the complex myrmicarins 430A (**4**)[1c] and 663 (**5**).[1d] While myrmicarin 663 (**5**) was isolated and fully characterized, the extreme sensitivity of myrmicarin 430A (**4**) required its structural assignment as a crude isolation mixture using phase sensitive 2D NMR techniques. Likewise, the fragility and limited quantities of isolated myrmicarin 645 (**6**) precluded its relative stereochemical assignment. An isomeric myrmicarin 430B was also identified,[1c] but no structural information on this compound has been reported.

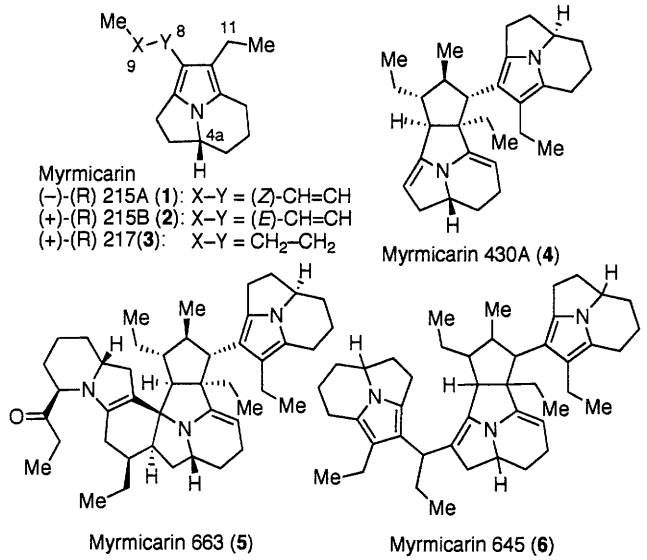

Figure 1. Members of the myrmicarin alkaloids.

Hypothesis for the Biosynthesis of Complex Myrmicarins

The compelling architectures of these toxic alkaloids and the challenges associated with their sensitivity inspired us to initiate a program directed at their study and total synthesis.[2] Our synthetic approach is based on our proposal that these complex molecules could be accessed from activated pyrroloindolizine derivatives (Scheme 1) through a potentially biomimetic dimerization event.[2a] We have considered three possible pathways for the dimerization of myrmicarin 215 (**2**) to provide the heptacyclic structure of myrmicarin 430A (**4**). In the first scenario, we envisioned that protonation of (+)-myrmicarin 215B (**2**) at C9 could initiate a

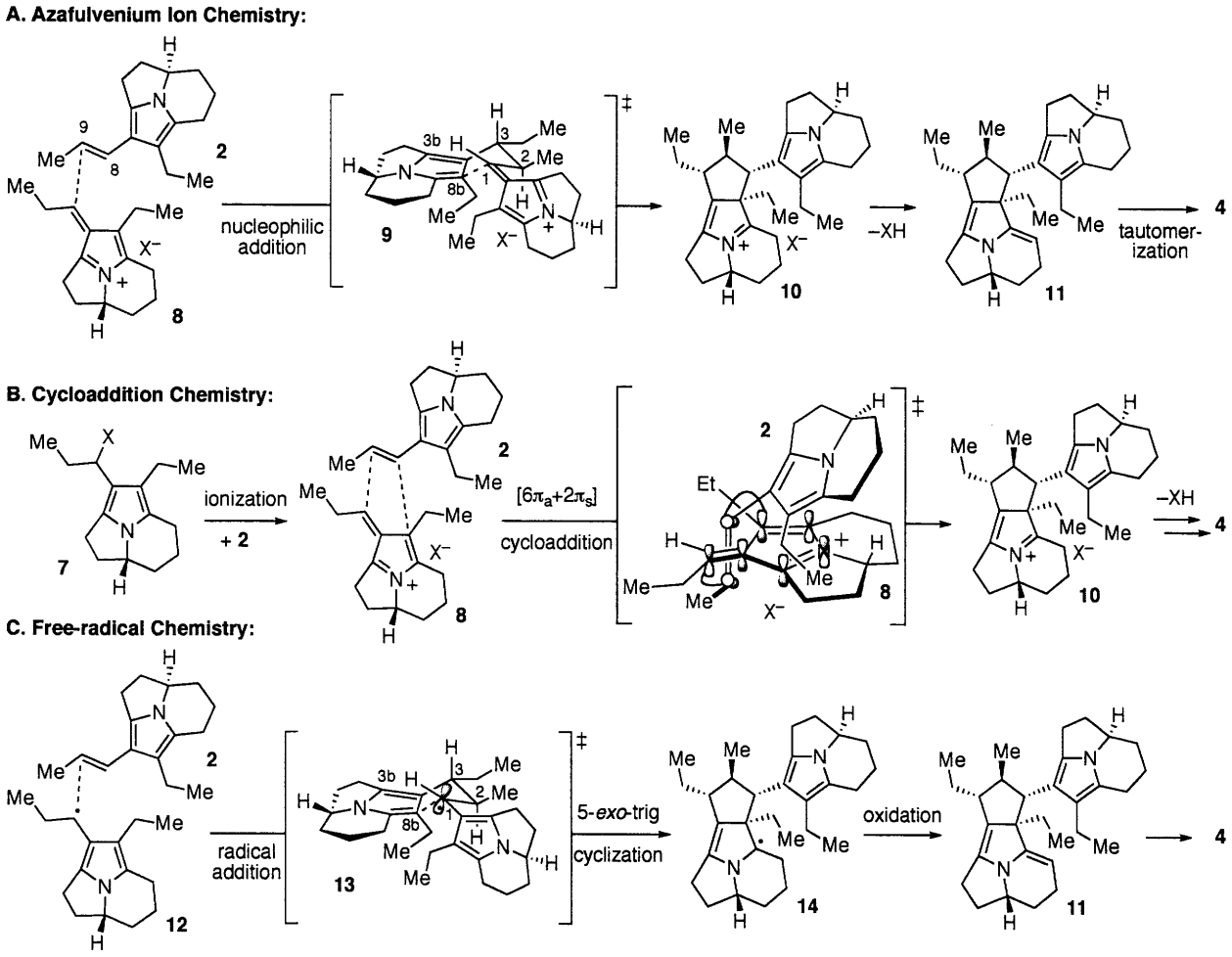

Scheme 1. Our proposed biomimetic dimerization of pyrroloindolizines for the synthesis of myrmicarin 430A (**4**).

sequence of bond forming events mediated by highly electrophilic azafulvenium ion intermediates (i.e. **8**, Scheme 1A).[2a] In this sequence, cyclopentannulation would occur through intermolecular trapping of the tricyclic azafulvenium ion **8** by (+)-myrmicarin 215B (**2**), followed by an intramolecular Friedel-Crafts trapping at C8b of intermediate **9** (Scheme 1A).

Alternatively, the five contiguous stereocenters in myrmicarin 430A (**4**) may be generated in a concerted cycloaddition process involving neutral (+)-myrmicarin 215B (**2**) and the tricyclic azafulvenium ion **8** (Scheme 1B). The reactive intermediate **8** can be generated either by C9-protonation of **2** or by expulsion of a leaving group at C8 of pyrroloindolizine derivative **7**. Consistent with FMO analysis, a $[6\pi_a+2\pi_s]$ cycloaddition[3] would afford the observed stereochemistry at each of the stereocenters of myrmicarin 430A (**4**). Another possible dimerization manifold involves activation of (+)-myrmicarin 215B (**2**) or a tricyclic derivative **7** as the stabilized radical intermediate **12**, which could undergo intermolecular radical addition to

another (+)-myrmicarin 215B (**2**) to give **13** (Scheme 1C). Subsequent 5-*exo*-trig radical cyclization of **13** (C1–C8b bond formation) would provide the heptacycle **14**, which would lead to formation of myrmicarin 430A (**4**) *via* oxidation and tautomerization reactions. Herein we report our studies on the reactivity of functional pyrroloindolizines pertinent to our hypothesis regarding the biosynthesis of these alkaloids. Additionally, relying on the unique reactivity of pyrroloindolizines, we discuss the development of a convergent strategy for the assembly of functional intermediates for the synthesis of complex myrmicarins.

Acid-Promoted Reactivity of Myrmicarin 215

While our initial biosynthetic hypotheses (Scheme 1A) suggested a succinct means of generating these complex alkaloids, the proposed cyclopentannulation reactions required an unprecedented mode of reactivity for vinyl pyrroles.[4] Earlier we reported the direct and highly diastereoselective homodimerization of (+)-myrmicarin 215B (**2**) leading to generation of a single heptacyclic product and introduction of four contiguous stereocenters.[2a] *In situ* ^{1}H NMR monitoring revealed that Brønsted acid (trifluoracetic acid, TFA) treatment of (+)-myrmicarin 215B (**2**) in benzene-d_6 (0.050 M) resulted in complete conversion to a single new dimeric compound, namely the heptacyclic iminium ion **16** (Scheme 2). Deprotonation of **16** gave the air

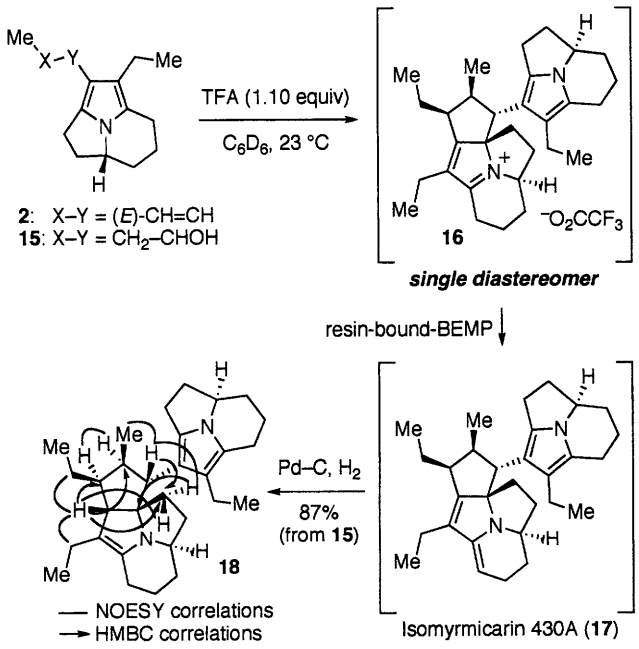

Scheme 2. Our synthesis of isomyrmicarin 430A (**17**) by direct dimerization of (+)-myrmicarin 215B (**2**).[2a]

sensitive isomyrmicarin 430A (**17**). Although the direct dimerization product **16** was unstable to isolation, chemical modification of this compound provided stable derivatives that were amenable to full structural characterization, enabling rigorous assignment of their connectivity and stereochemistry through a combination of high field 2D NMR techniques (Scheme 2).[2a] Our analysis revealed that the obtained dimer was regioisomeric at one bond and epimeric at one stereocenter to myrmicarin 430A (**4**). Significantly, this structure validated our mechanistic hypothesis that acid promoted activation of (+)-myrmicarin 215B (**2**) can provide C8 electrophilic derivatives susceptible to a highly diastereoselective attack by the vinyl group of a second equivalent of (+)-myrmicarin 215B (**2**).

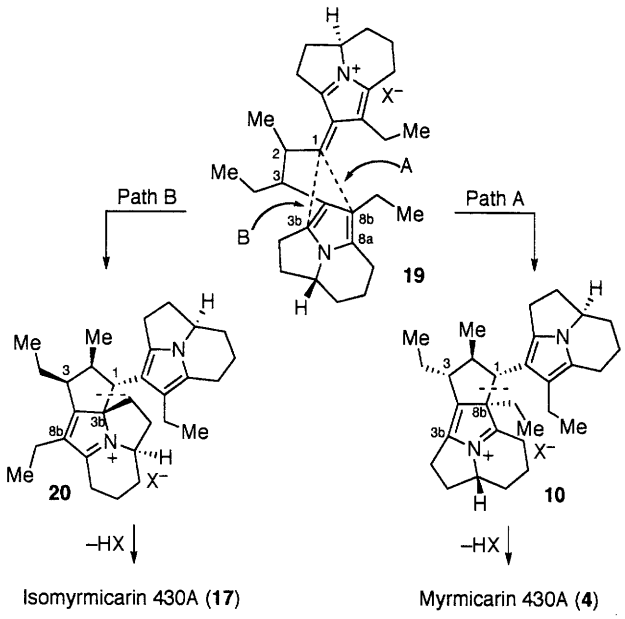

Scheme 3. Bond formation leading to myrmicarin 430A (**4**, Path A) and isomyrmicarin 430A (**17**, Path B).

According to this stepwise mechanism, the regiochemical difference between the myrmicarin 430A (**4**) and isomyrmicarin 430A (**17**) structures arises from the proposed Friedel-Crafts trapping of the hexacyclic iminium ion **19** (Scheme 3), where the observed heptacycle **20** possesses a C1-C3b bond (Path B) instead of the C1-C8b bond (Path A) found in the framework of the natural alkaloid myrmicarin 430A (**4**). Additionally, the isomyrmicarin 430A stereochemistry at C3 is opposite to that found in myrmicarin 430A (**4**).

Results and Discussion

Brønsted Acid Promoted Dimerization Conditions

The homodimerization of (+)-myrmicarin 215B (**2**) provided the basis for a potentially direct formation of myrmicarin 430A (**4**). The nature of the putative azafulvenium ion intermediates in the dimerization suggested that the rate or reversibility of each bond forming event may be influenced by solvent and counter ion effects. In order to address the regio- and stereochemical differences between the heptacycle we had obtained (**20**, Scheme 3) and the desired structure (**10**, Scheme 3), we examined the acid promoted dimerization of (+)-myrmicarin 215B (**2**) under different reaction conditions (Table 1). Due to the known instability of myrmicarin 430A (**4**) and the observed sensitivity of heptacyclic derivatives such as **16**, these experiments were monitored by *in situ* ^{1}H NMR and the structure of air-sensitive final products confirmed by conversion to isolable derivatives. Unless strictly anhydrous conditions were required, the alcohol **15**, which also undergoes TFA induced dimerization[2a] to isomyrmicarin 430A (**17**) *via* (+)-myrmicarin 215B (**2**), was employed in place of **2** due to its enhanced stability.

The stoichiometric trifluoroacetic acid (TFA) induced dimerization behavior of (+)-myrmicarin 215B (**2**) was examined in methanol-d_4, THF-d_8, acetonitrile-d_3, and cyclohexane-d_{12}. In cyclohexane-d_{12} the TFA promoted reactivity of (+)-myrmicarin 215B (**2**, 0.0050M) was similar to that we had observed in benzene-d_6.[2a] Namely, introduction of substoichiometric TFA promoted formation of the dimer **20** ($X^- = F_3CCO_2^-$) to approximately the same extent as the added acid (Table 1, entry 1), while rapid addition of superstoichiometric TFA yielded only pyrrole ring protonated products (Table 1, entry 2). Treatment of a THF-d_8 solution of alcohol **15** (0.026M) with trifluoroacetic acid (1.10 equiv) resulted in immediate and quantitative conversion to (+)-myrmicarin 215B (**2**), which was subsequently consumed to form the dimer **20** (Table 1, entry 3). In this case, the dimerization was substantially slower than the dimerization in benzene-d_6 and only reached 80% conversion to **20** within 24 hours. In contrast, introduction of 1.10 equivalents of TFA to a solution of **15** in acetonitrile-d_3 (0.025M) effected complete conversion to **20** within 30 seconds without a visible accumulation of (+)-myrmicarin 215B (**2**, Table 1, entry 4). In methanol-d_4, treatment of a solution of **15** (0.026M) with TFA (1.10 equiv) did not afford (+)-myrmicarin 215B (**2**) but resulted in complete formation of the C8 methanol adduct **21** within 30 seconds, which underwent 95% conversion to **20** within 45 minutes (Table

1, entry 5) without a visible accumulation of (+)-myrmicarin 215B (**2**). Significantly, no methanol adduct of dimeric products corresponding to trapping of putative intermediates (i.e., **9**, Scheme 1A) or a methanol adduct of **20** were observed.

Table 1. Treatment of (+)-myrmicarin 215B (**2**) and alcohol **15** with Brønsted acids.

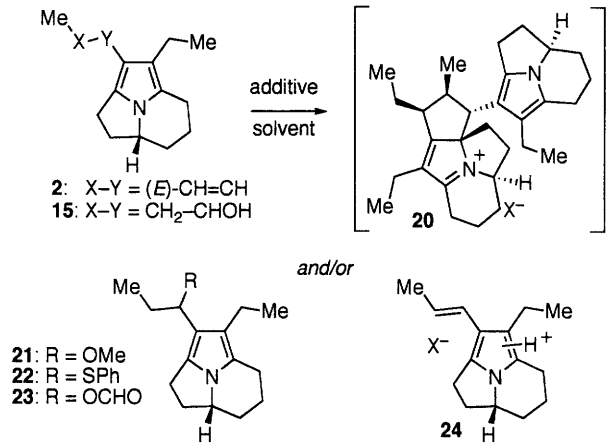

entry	substrate	solvent	acid (equiv)	additive	product(s)[a]
1	**2**	C_6D_{12}	TFA (<1.00)	none	**20**
2	**2**	C_6D_{12}	TFA (>1.00)	none	**24**
3	**15**	THF-d_8	TFA (1.10)	none	**20**
4	**15**	CD_3CN	TFA (1.10)	none	**20**
5	**15**	CD_3OD	TFA (1.10)	none	**21,20**
6	**15**	THF-d_8	TFA (1.10)	LiCl (sat.)	**2,20**
7	**15**	THF-d_8	AcOH (0.20)	LiCl (sat.)	**2**
8	**2**	THF-d_8	TFA (1.10)	$LiClO_4$ (sat.)	**24**
9	**15**	THF-d_8	$HClO_4$ (1.10)	$LiClO_4$ (sat.)	**24**
10	**15**	CD_3OD	$HClO_4$ (1.10)	$LiClO_4$ (sat.)	**21**[b]
11	**15**	CD_3OD	$HClO_4$ (<1.10)	$LiClO_4$ (1.6M)	**21,20**
12	**15**	CD_3OD	TFA (1.10)	*p*-MePhSH (0.60 equiv)	**22+20** (80:20)
13	**15**	DCO_2D	DCO_2D (solvent)	none	**23,24**

[a]Reactions monitored *in situ* by ^{1}H NMR. [b]Pyrrole-ring protonated forms.

To investigate the influence of the ionic strength of the medium and the nature of the counterion on the acid induced chemistry of **2** we examined the effect of salt additives. While addition of TFA (1.10 equiv) to a solution of **15** in THF-d_8 (0.030 M) saturated with anhydrous lithium chloride (LiCl) effected immediate conversion to (+)-myrmicarin 215B (**2**), it substantially reduced the rate of the subsequent dimerization to **20**, yielding a 1:1 ratio of (+)-

myrmicarin 215B (**2**) to **20** after a period of 190 minutes (Table 1, entry 6), whereas the same ratio was obtained in 30 minutes in the absence of LiCl. Consistent with our reported result for benzene–d_6,[2a] the acetic acid (0.20 equiv) treatment of a THF–d_8 solution of **15** (0.054M) saturated with LiCl effected complete conversion to (+)-myrmicarin 215B (**2**), but did not promote dimerization (Table 1, entry 7). By contrast, treatment of a THF-d_8 solution of (+)-myrmicarin 215B (**2**, 0.0065M) saturated with $LiClO_4$ as the salt additive with TFA (1.10 equiv) immediately generated a mixture of pyrrole–ring protonated tricyclic species and produced none of the heptacyclic iminium ion **20** (Table 1, entry 8).

To rule out possible influence of the trifluoroacetate anion in the dimerization process, a THF-d_8 solution of **15** (0.013M) saturated with $LiClO_4$ was treated with $HClO_4$ (1.10 equiv) in place of TFA. Consistent with the observed TFA induced reactivity (Table 1, entry 8), introduction of $HClO_4$ instantly generated a mixture of ring protonated tautomers **24** (Table 1, entry 9). Exposure of a methanol-d_4 solution of **15** (0.013M) saturated with $LiClO_4$ to $HClO_4$ (1.10 equiv) afforded a mixture of ring protonated forms of the C8 methanol adduct **21**, which did not undergo dimerization (Table 1, entry 10). By contrast in an unsaturated methanolic solution of $LiClO_4$ (1.6M), portionwise addition of $HClO_4$ (0.10 equiv/portion) to a solution of **15** (0.026M) effected complete formation of **21**, followed by approximately proportional conversion to **20** (Table 1, entry 11).

In an effort to more efficiently trap possible electrophilic monomeric or dimeric intermediates present in equilibrium with the iminium ion **20**, *p*-methylbenzenethiol (0.60 equiv) was introduced to a methanol–d_4 solution of **15** (0.020M) prior to portionwise substoichiometric addition of TFA. In this case, introduction of TFA resulted in immediate conversion to the C8-methanol adduct **21** followed by progressive formation of the tricyclic C8-sulfide **22**, completely consuming the thiol additive (Table 1, entry 12). Concomitant dimerization of the remaining C8-methanol adduct to **20** consumed the remainder of the tricyclic substrate **15**. Thiol adduct **22** was not subject to dimerization and no other adducts were observed during the reaction.[5] An attempt to use a weaker organic acid as a proton source and solvent by dissolving **15** in neat formic acid-d_2 resulted in immediate conversion to the corresponding epimeric formate esters **23**, followed by slow conversion to a mixture of ring protonated tautomers **24**, with approximately five percent (+)-myrmicarin 215B (**2**) visible throughout (Table 1, entry 13).

In none of these experiments did we visualize any dimeric species other than **20** (X^- =

$F_3CCO_2^-$ or ClO_4^-, Table 1). While the use of strongly acidic conditions favoring ring protonation of (+)-myrmicarin 215B (**2**) prevented dimerization (Table 1, entries 7, 8, and 12), conditions that would enable neutral (+)-myrmicarin 215B (**2**) and an azafulvenium ion to coexist (Table 1, entries 2, 3, 4, 5, 6, 11, and 12) resulted in completely selective and quantitative formation of **20**. Tricyclic C8-adducts were generated as equilibrating compounds in the presence of nucleophilic solvent (Table 1, entries 5 and 11) or irreversibly in the presence of stronger nucleophiles (Table 1, entry 12), however no nucleophilic adducts of the dimeric products were observed. The substantially reduced rate of dimerization in the presence of nucleophilic counterion under saturating conditions (Table 1, entry 6) suggests possible reversible interception of azafulvenium ion intermediates at either of the carbon–carbon bond forming steps (Scheme 1A). These observations collectively suggest that if a dimeric azafulvenium ion existed (i.e., **19**, Scheme 3) it was a fleeting intermediate.

Possible [$6\pi_a+2\pi_s$] Cycloaddition Pathway

The insensitivity of the dimerization reaction described above to variations in the reaction conditions prompted us to consider that the high diastereoselectivity and efficiency of the process might be a consequence of a concerted cycloaddition event instead of a stepwise ionic sequence (Scheme 4). Frontier molecular orbital (FMO) analysis of the proposed event revealed that a thermally allowed [$6\pi_a+2\pi_s$] cycloaddition between the *E*-azafulvenium ion **25** and the *E*-alkene of (+)-myrmicarin 215B (**2**) could provide the isomyrmicarin 430A (**17**) structure with the correct stereochemistry in the cyclopentane ring (Scheme 4B).[3] In this sequence, association between the electron poor azafulvenium ion **25** and the electron rich (+)-myrmicarin 215B (**2**) would bring their convex faces together, whereupon a gearing effect would move the vinyl group of (+)-myrmicarin 215B (**2**) to the more sterically accessible side of azafulvenium ion **25**. Interestingly, preliminary computations show that the *Z*-azafulvenium ion **8** is favored over the *E*-isomer **25** by ~1.3 kcal/mol, consistent with predictions based on molecular models and allylic strain considerations.[6] This would suggest that the observed dimerization may occur by equilibration of **8** and **25** accompanied by a faster cycloaddition involving the high energy isomer **25**.

A persuasive factor in our consideration of this [$6\pi_a+2\pi_s$] cycloaddition was that an analogous process involving the *Z*-azafulvenium ion **8** would provide precisely the connectivity

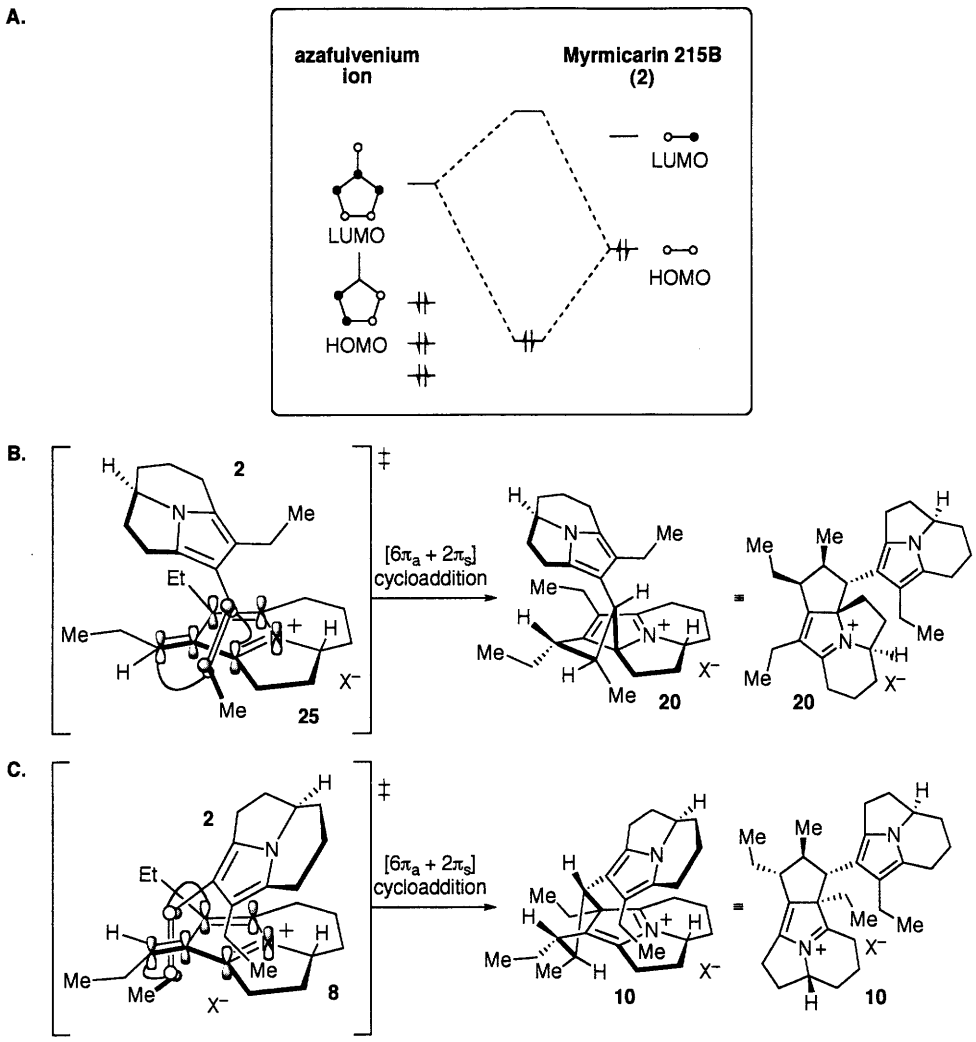

Scheme 4. A) FMO analysis of a concerted $[6\pi_a+2\pi_s]$ cycloaddition between an azafulvenium ion and an alkene. B) Possible cycloaddition involving the *E*-azafulvenium ion **25** and (+)-myrmicarin 215B (**2**) leading to iminium ion **20** en route to isomyrmicarin 430A (**17**). C) Potential cycloaddition leading to iminium ion **10** en route to myrmicarin 430A (**4**).

and stereochemistry found in myrmicarin 430A (**4**, Schemes 1B and 4C). Hence, mutual association of the convex faces of (+)-myrmicarin 215B (**2**) and the *Z*-azafulvenium ion **8** would enable the approach of the C8-C9 alkene of (+)-myrmicarin 215B (**2**) *syn*-coplanar to the C8 methine of *Z*-azafulvenium ion **8**, providing the iminium ion **10** *via* an antarafacial cycloaddition en route to myrmicarin 430A (**4**, Scheme 4C).

Design and Synthesis of Conformationally Restricted Azafulvenium Ion Precursors

While it may be speculated that an enzyme mediated protonation event could be responsible for triggering a cycloaddition reaction and controlling the stereochemistry of an

azafulvenium ion in the biosynthesis of myrmicarin 430A (**4**), we wished to examine this hypothesis experimentally using conformationally restricted substrates. If the dimerization was occurring through a concerted cycloaddition mechanism and the regio- and stereochemical outcome was dictated by the geometry of the azafulvenium ion, then a structure locked in the *Z*-geometry should undergo a cycloaddition with (+)-myrmicarin 215B (**2**) to provide the myrmicarin 430A (**4**) framework (Scheme 5).

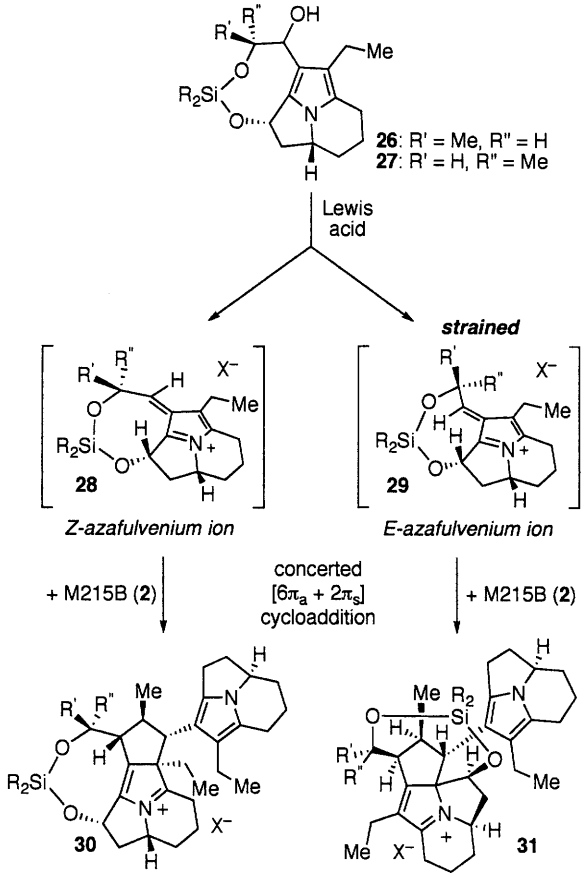

Scheme 5. Expected heptacycles from a $[6\pi_a+2\pi_s]$ cycloaddition between **2** and azafulvenium ions **28** and **29**.

Therefore, we prepared the alcohols **26–27**, in which a siloxy tether favors a *Z*-azafulvenium ion geometry upon ionization of the C8 alcohol (Scheme 5). The *Z*-azafulvenium ion **28**, which is expected to give the desired myrmicarin 430A (**4**) carbon skeleton in a $[6\pi_a+2\pi_s]$ manifold, can better accommodate the azafulvenium ion in the eight-membered ring than the corresponding *E*-azafulvenium ion **29**. Additionally, sterically demanding alkyl groups on silicon would further favor formation and cycloaddition *via* the *Z*-azafulvenium ion **28**.

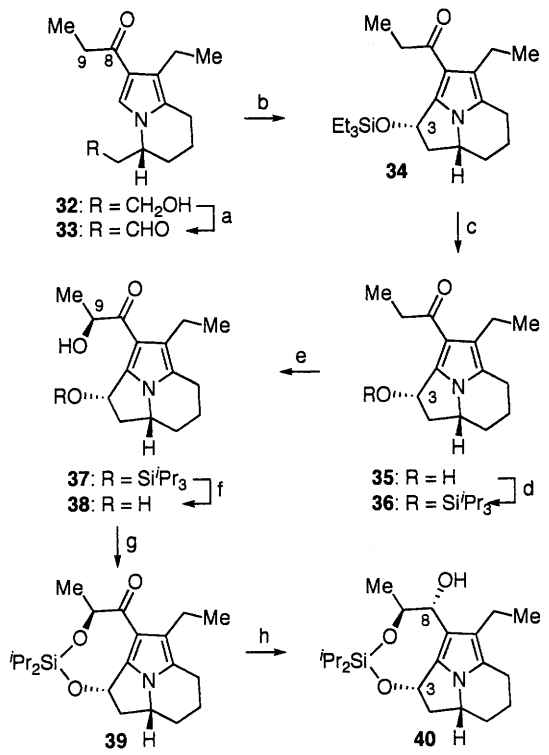

Scheme 6. Synthesis of azafulvenium ion precursor **40**. Conditions: a) IBX, DMSO, 82%. b) TESOTf, 2,6-lutidine, PhH, 23 °C, 4:1 dr. c) TBAF, THF, 81% (2-steps). d) TIPSOTf, 2,6-lutidine, CH_2Cl_2, –40→0 °C. 82%. e) KHMDS, Davis oxaziridine, THF –78 °C, 90%, 5:1 dr. f) TBAF, THF, 92%. g) $^iPr_2SiCl_2$, DMAP, DMF, 77%. h) LAH, Et_2O, –78→0 °C, 77%, 6:1 dr.

The synthesis of the tethered azafulvenium ion precursor **40** commenced with oxidation of our previously reported (*R*)-alcohol **32**[2b] to the aldehyde **33** using 2-iodoxybenzoic acid in dimethylsulfoxide (Scheme 6).[7] Treatment of the aldehyde **33** with excess triisopropylsilyl trifluoromethanesulfonate in benzene at 50 °C for 4 hours effected C8-silyl enol ether formation and Friedel-Crafts cyclization to provided a C3-silyloxy pyrroloindolizine as a 6:1 C3-epimeric mixture. The acidic work up of this mixture and careful chromatographic separation yielded the diastereomerically pure ketone **36** in 81% overall yield. For large–scale preparation, an alternative sequence was employed, which involved subjection of aldehyde **33** to triethylsilyl trifluoromethanesulfonate at 23 °C for 25 min, exhaustive desilylation of the crude mixture, facile chromatographic separation of the C3 epimeric alcohols, and silylation of the major C3 epimer **35** (Scheme 6). In this series, the major C3*S*-hydroxy pyrroloindolizine and related derivatives were found to be far more stable than the minor C3*R*-hydroxy series and were thus employed in subsequent steps. Hydroxylation of the lithium enolate of **36** with (±)-*trans*-2-(phenylsulfonyl)-3-phenyloxaziridine (Davis oxaziridine)[8] generated the α-keto alcohol **37** in

85% yield as a 4:1 mixture of chromatographically separable C8-epimers.[9] Deprotection of the C3-alcohol[10] allowed the introduction of the desired [1,3,2]-dioxasilocine substructure of ketone **39**. Reduction of the C8 ketone provided the C8-alcohol **40** (10:1 dr, major shown, Scheme 6), which was obtained in diastereomerically pure form after flash column chromatography.

To investigate the heterodimerization event of interest (Scheme 5) we required a means of generating the putative azafulvenium ion from the conformationally restricted precursor **40** without activation of (+)-myrmicarin 215B (**2**). To avoid rapid self-dimerization of (+)-myrmicarin 215B (**2**) in the presence of Brønsted acid, we relied on Lewis acid activation of the C8-alcohol **40**. As validation of this strategy, under optimal conditions, treatment of the tricyclic C8-alcohol **15** (1:1 mixture of C8 alcohols) with scandium trifluoromethanesulfonate ($ScOTf_3$, 0.20 equiv) in the presence of the *E*-thiol ketene acetal **41** (2.00 equiv, *E*(O):*Z*(O)=20:1)[11] provided the thiolester **42** in 85% yield (Equation 1).[12]

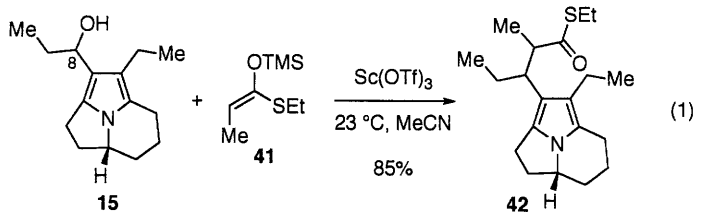

(1)

Based on these observations we sought to substitute an electron rich vinyl pyrroloindolizine derivative in place of the thiol ketene acetal **41** to probe the cycloaddition hypothesis outlined in Scheme 5. *In situ* ^{1}H NMR monitoring showed that portionwise addition of 0.40 equivalents of $Sc(OTf)_3$ to a mixture of (+)-myrmicarin 215B (**2**) and conformationally restricted azafulvenium ion precursor **40** (**2**:**40**, 2:1) in acetonitrile-d_3 selectively and completely produced a single new heterodimeric species (≥90% by ^{1}H NMR)[13] with no visible formation of any isomyrmicarin 430A derivatives. This product proved to be slightly more stable to isolation than isomyrmicarin 430A (**17**). Isolation and structural analysis of this new air-sensitive heterodimerization product by a combination of 2D NMR techniques established the structure of the heterodimer **43** (Equation 2), which possessed connectivity and stereochemistry consistent with that of isomyrmicarin 430A (**17**, Scheme 2). Strong C1–H/C4–H NOESY correlations confirmed the connectivity of the cyclopentane ring, while C1–H/C10′–H and C2–H/C3–H correlations secured the stereochemistry at C1, C2, and C3. A C3–H/C9–H correlation

confirmed that the C9 stereochemistry of the alcohol **40** had been retained.

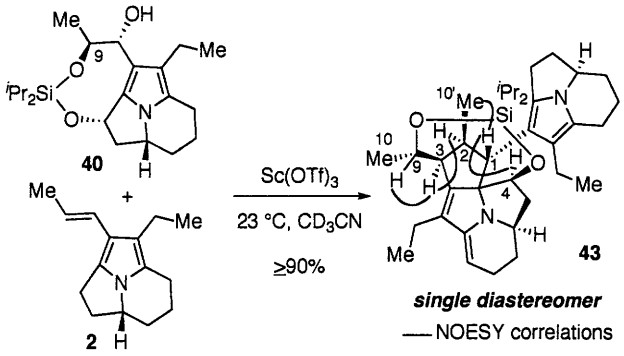

(2)

While molecular model analysis of the *E*-azafulvenium ion **29** (Scheme 5) en route to the isomyrmicarin 430A framework indicated that this compound was significantly more strained than the corresponding *Z*-azafulvenium ion **28**, it remained possible that **29** could be accessed from (9*S*)-alcohol **40** (Equation 2) as a high energy intermediate. By contrast, a similar analysis of the C9-epimer of **40** (i.e., **27**, Scheme 5) clearly showed that the corresponding *E*-azafulvenium ion derivative would suffer a significant allylic strain that was absent in the desired *Z*-azafulvenium ion. Based on the expectation that **27** (Scheme 5) would provide greater preference for formation of **28** over **29**, we embarked on the preparation of the C9-epimer of **40** (Scheme 7). To garner significant quantities of the required C9-epimer, the C9-alcohol **37** was subjected to Mitsunobu inversion[14] with *p*-nitrobenzoic acid (Scheme 7) followed by hydrolysis and desilylation to provide the diol **45**. While introduction of the tether had proceeded efficiently with the C9 epimer **38** (Scheme 6), exposure of diol **45** to the same conditions provided only 29% of the desired product **46** along with a mixture of C9- and C3-mono- and bis-silylated products (Scheme 7), suggesting a more challenging formation of the epimeric [1,3,2]-dioxasilocine substructure. Separation of **46** from the mixture and desilylation of the undesired products allowed recycling to access the target compound **46**. As another testament to the conformational and reactivity differences between the C9-epimers of these pyrroloindolizines, lithium aluminum hydride reduction of the ketone **46** afforded the unstable C3,C8,C9-triol derivative as the major product, along with the desired alcohol **47** and recovered starting material. Despite these challenges, the desired azafulvenium ion precursor **47** was obtained in low yield as a single diastereomer (Scheme 7) in this sequence, allowing its examination as an azafulvenium ion precursor.

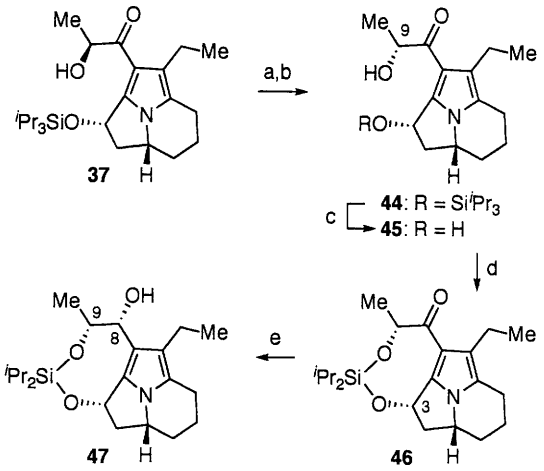

Scheme 7. Synthesis of (9*R*)-alcohol **47**. Conditions: a) PPh_3, DEAD, *p*-$NO_2C_6H_4CO_2H$, THF, 61% (72% brsm). b) LiOH, THF–H_2O, 50 °C, 100%. c) TBAF, THF, 92%. d) $^{i}Pr_2SiCl_2$, DMAP, DMF, 29%. e) LAH, Et_2O, –78→0 °C, 16% (24% brsm).

In the key heterodimerization event, exposure of an equal mixture of (+)-myrmicarin 215B (**2**) and alcohol **47** to the conditions described previously (Equation 2) completely and exclusively afforded a new heterodimeric product (Scheme 8) in ≥90% yield by ^{1}H NMR.[15] Reciprocal C4/C1–H and C1/C4–H HMBC correlations revealed that the dimer **49** again had the same connectivity as isomyrmicarin 430A (Scheme 8). C1–H/C10′–H and C2–H/C3–H NOESY correlations revealed the stereochemistry at C1, C2, and C3 was identical to that of **43** and isomyrmicarin 430A (**17**). Finally, C1–H/C9–H and C9–H/C10′–H correlations confirmed that the heterodimers **49** and **43** differed only in their C9-stereochemistry. It should be noted that the prohibitively strained *E*-azafulvenium ion **48b** is an unlikely intermediate in this dimerization reaction. Additionally, an antarafacial [$6\pi_a+2\pi_s$] cycloaddition involving a *Z*-azafulvenium ion and (+)-myrmicarin 215B (**2**) would furnish a product with the stereochemistry at C3 opposite to that found in **49**. These factors taken together suggest that the observed heterodimerization does not proceed *via* a concerted cycloaddition. Instead, the structure of condensation product **49** is more consistent with a stepwise addition of (+)-myrmicarin 215B (**2**) to the azafulvenium ion **48a**, followed by attack of the pyrrole at to the resulting electrophilic C1 (Scheme 8). While these results did not rule out a concerted [$6\pi_a+2\pi_s$] pathway for the formation of either isomyrmicarin 430A (**17**) or myrmicarin 430A (**4**), they did implicate significant obstacles in implementation of a single step cyclopentannulation employing these azafulvenium ions toward the synthesis of the complex myrmicarins.

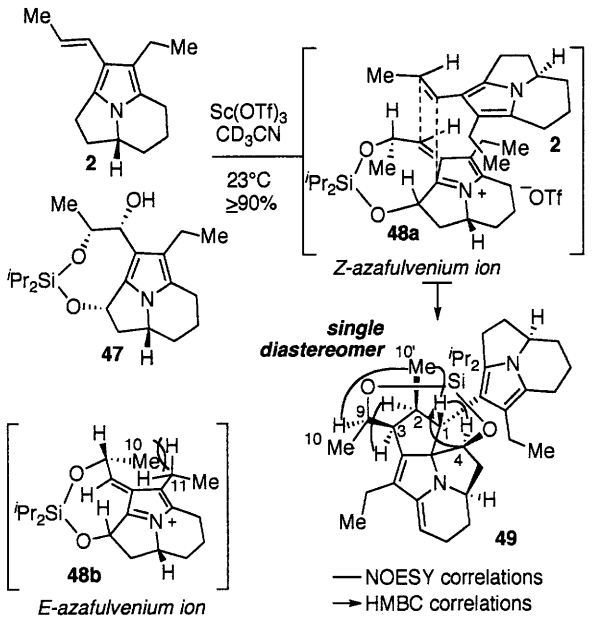

Scheme 8. Diastereoselective condensation of (+)-myrmicarin 215B (**2**) and alcohol **47**.

A Directed Heterodimerization Approach to Functional Dimeric Pyrroloindolizines

To overcome the inherent propensity to form the isomyrmicarin substructure in the observed homo- and hetero-dimerization reactions we required a means of decoupling the two bond-forming events of the cyclopentannulation. Hence, we sought the selective electrophilic activation of a pyrroloindolizine derivative **50** (Scheme 9) followed by nucleophilic trapping by **51** to provide the C2–C3 bond in the heterodimer **53**. We reasoned that the introduction of a 'blocking' functional group (Y) at C8 of the pyrroloindolizine **51** (Scheme 9) should either prevent an intramolecular Friedel-Crafts addition to directly give the desired hexacycle **55**, or promote cleavage of the C1–C3b bond in an isomyrmicarin derivative **54** (Scheme 9). Introduction of a functional handle at C9 of the electrophilic precursor would enable adjustment of the stereochemistry at C3 after dimerization. This strategy could also benefit from the use of tethered azafulvenium ions (i.e., as **40** and **47**) to secure dimeric products with a high level of diastereoselection. Significantly, this approach would provide access to functional hexacyclic derivatives pertinent to alternative late–stage cyclopentannulation chemistries, such as free-radical mediated cyclization as suggested by our proposed radical dimerization of pyrroloindolizines (Scheme 1C). With these considerations in mind, we investigated the directed heterodimerization of pyrroloindolizine derivatives.

The (*R*)-ketone **56**[2b] served as a versatile building block for the preparation of the

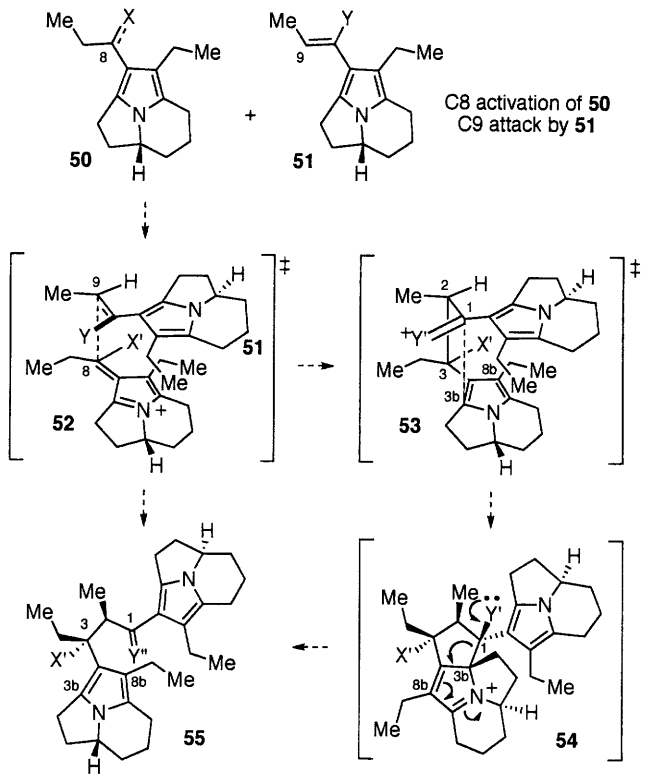

Scheme 9. Directed heterodimerization of functional pyrroloindolizines.

necessary functional pyrroloindolizines (Scheme 10). The silyl enol ether **57** was prepared quantitatively and exclusively as the *Z*-isomer by treatment of the ketone **56** with triisopropyl trifluoromethanesulfonate in the presence of triethylamine at low temperature. Hydroxylation of the lithium enolate of **56** followed by *O*-methylation with methyl iodide and sodium hydride provided the C9-methoxy ketopyrroloindolizine **59** as a mixture of C9-epimers (5:2).[16] As in the synthesis of ketone **37**, strict control over the stoichiometry of the oxidant during the hydroxylation step was necessary to avoid further oxidation of the product **58**. Inspired by our earlier studies, we explored the direct electrophilic activation of the vinylogous amide **58** in the presence of silyl enol ether **57**. Despite pronounced Brønsted acid sensitivity, the silyl enol ether **57** served as a superb nucleophile in trapping the activated derivative of amide **59**. In this event, treatment of an equal mixture of the α-methoxy ketone **59** and the silyl enol ether **57** with trifluoromethanesulfonic anhydride in the presence of 2,6-di-*t*butyl-4-methylpyridine provided the methyl vinyl ether **60** in 70% yield as a mixture of diastereomers.[17] Hydrolysis of **60** to the diketone **61** was achieved by exposure to pyridinium *p*-toluenesulfonate in benzene–acetonitrile–water at 23 °C under strictly oxygen–free conditions.[18] Importantly, this two–step sequence provides a directed condensation between two pyrroloindolizine fragments (i.e., **57** and **59**) while

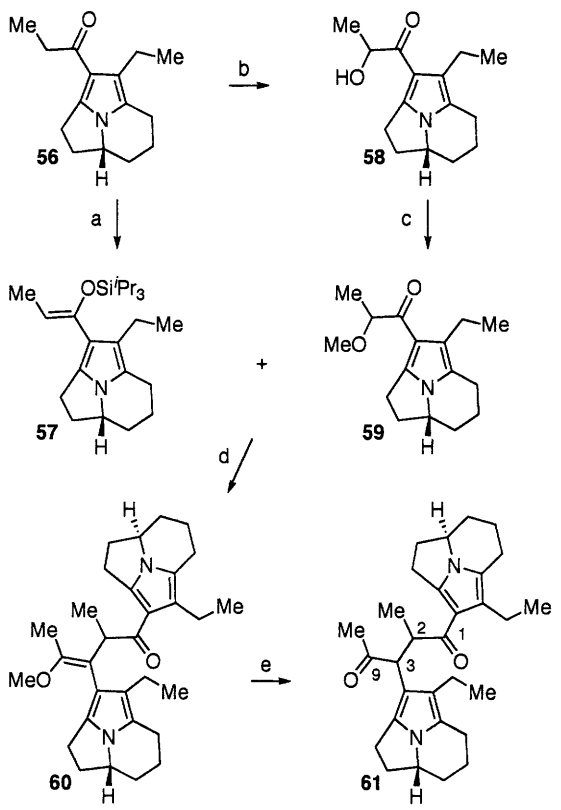

Scheme 10. Synthesis of the hexacycle **61** by directed dimerization of functional pyrroloindolizines. Conditions: a) TIPSOTf, Et_3N, CH_2Cl_2, –40 °C, 100%. b) KHMDS; Davis'–oxaziridine, THF, –78 °C, 86%, 5:2 dr. c) NaH, MeI, DMF, 23 °C, 94%. d) Tf_2O, 2,6-di-^{t}butyl-4-methylpyridine, CH_2Cl_2, –78 °C, 84%. e) PPTS, H_2O, MeCN, C_6H_6, 23 °C, 70%.

at the same time securing the C1-vinylogous amide needed for activation and cyclopentannulation, in addition to the C9-ketone for control of C3-stereochemistry.

In parallel to these efforts, we investigated the use of conformationally restricted pyrroloindolizine electrophiles to gain stereochemical control in the heterodimerization reaction. For example, when the azafulvenium precursor **40** is treated with catalytic scandium trifluromethanesulfonate in the presence of the silyl enol ether **57** (1.56 equiv), heterodimer **62** is obtained in 73% yield as a 5:1 mixture of two diastereomers (Equation 3). Key C2–H/C4–H and C9–H/C3–H NOE correlations clearly secure the structure of the major diastereomer as shown in Equation 3. With these promising initial results, our current efforts are focused on merging of the fragment assembly strategy illustrated in Scheme 10 with the use of conformationally biased azafulvenium ion precursors (i.e., **40** and **47**) to access functional and dimeric pyrroloindolizines with enhanced levels of diastereoselection. Additionally, the C1-carbonyl of dimeric pyrroloindolizines allows investigation of free-radical or azafulvenium ion mediated pathways to

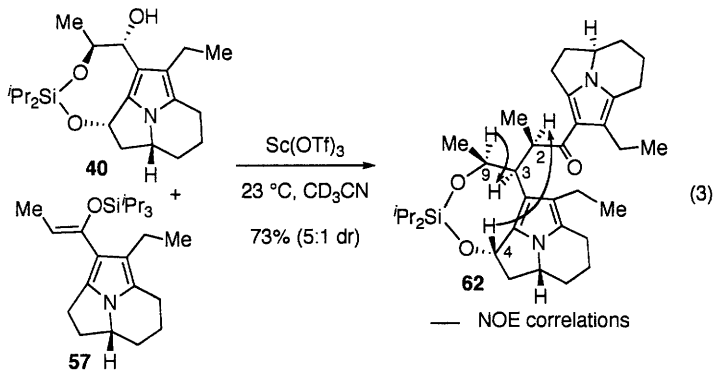

(3)

introduce the C1-C8b bond found in complex myrmicarins guided by the hypotheses outlined in Scheme 1.

Conclusion

Vinyl pyrroloindolizines possess a unique structure that predisposes them to highly efficient activation at C8. This mode of activation enables a variety of activated pyrroloindolizine derivatives to undergo reaction with neutral pyrroloindolizines to afford the corresponding dimeric structures. In an ionic manifold, Brønsted acid activation of the natural alkaloid (+)-myrmicarin 215B (**2**) leads to highly efficient and stereoselective homodimerization to form the heptacyclic isomyrmicarin 430A (**17**) under a variety of reaction conditions. Likewise, Lewis acid activation of the conformationally restricted azafulvenium precursors **40** or **47** in the presence of (+)-myrmicarin 215B (**2**) affords heptacyclic derivatives **43** and **49**, respectively–structures that are consistent with a highly efficient non-concerted ionic heterodimerization process. Through strategic design of the pyrroloindolizine species involved in the dimerization (e.g. **57** and **59**), the two bond forming events of the cyclopentannulation can be decoupled, providing hexacyclic dimers en route to the complex myrmicarin alkaloid structures. Importantly, dimeric products such as **61** and **62** contain functional groups needed to investigate alternative radical or ionic pathways to control the regio- and stereochemistry of the cyclopentannulation process. While representing a concise route to the complex myrmicarins, the dimerization of these pyrroloindolizines offers insight with potential relevance to their biosynthesis. Such considerations continue to guide our study of these structurally fascinating alkaloids.

---

[1] (a) Francke, W.; Schröder, F.; Walter, F.; Sinnwell, V.; Baumann, H.; Kaib, M. *Liebigs Ann. Chem.* **1995**, 965–

977. (b) Schröder, F.; Franke, S.; Francke, W.; Baumann, H.; Kaib, M.; Pasteels, J. M.; Daloze, D. *Tetrahedron* **1996**, *52*, 13539–13546. (c) Schröder, F.; Sinnwell, V.; Baumann, H.; Kaib, M. *Chem. Commun.* **1996**, 2139–2140. (d) Schröder, F.; Sinnwell, V.; Baumann, H.; Kaib, M.; Francke, W. *Angew. Chem. Int. Ed.* **1997**, *36*, 77–80. (e) Schröder, F.; Francke, W. *Tetrahedron* **1998**, *54*, 5259–5264.

[2] (a) Ondrus, A. E.; Movassaghi, M. *Tetrahedron* **2006**, *62*, 5287–5297. (b) Movassaghi, M.; Ondrus, A. E. *Org. Lett.* **2005**, *7*, 4423–4426.

[3] For FMO analysis of cycloadditions involving fulvenes, see: (a) Houk, K. N.; George, J. K.; Duke, R. E. Jr. *Tetrahedron* **1974**, *30*, 523–533. (b) Houk, K. N. *Acc. Chem. Res.* **1975**, *8*, 361–369. For computational analysis of fulvene FMOs, see: (c) Scott, A. P.; Agranat, I.; Biedermann, U. P.; Riggs, N. V.; Radom, L. *J. Org. Chem.* **1997**, *62*, 2026–2038. (d) Havenith, R. W. A.; Fowler, P. W.; Steiner, E. *J. Chem. Soc. Perkin Trans. 2* **2002**, *2*, 502–507. For formal [6+2] cycloadditions involving fulvene species, see: (e) Hong, B.-C.; Shr, Y.-J.; Wu, J.-L.; Gupta, A. K.; Lin, K.-J. *Org. Lett.* **2002**, *4*, 2249–2252. (f) Hafner, K.; Suda, M. *Angew. Chem. Int. Ed.* **1976**, *15*, 314–315.

[4] For a review on the chemistry of *C*-vinyl pyrrole derivatives, see: (a) Trofimov, B. A.; Sobenina, L. N.; Demenev, A. P.; Mikhaleva, A. I. *Chem. Rev.* **2004**, *104*, 2481–2506. For general reviews on the chemistry of pyrroles, see: (b) Pelkey, E. T. In *Progress in Heterocyclic Chemistry*; Gribble, G.; Joule, J., Eds.; Five-Membered Ring Systems: Pyrroles and Benzo Derivatives. Publisher: Elsevier Ltd.: Oxford, UK, 2005; Vol. 17, pp. 109–141. (c) *Pyrroles*; Jones, A., Ed.; Wiley: New York, 1990. (d) Alan, J. R.; Bean, G. P. *The Chemistry of Pyrroles*; Academic Press: London, 1977. (e) Baltazzi, E.; Krimen, L. I. *Chem. Rev.* **1963**, *63*, 511–556.

[5] Heating a solution of this mixture of dimer **20** and sulfide **22** (55 °C) resulted only in decomposition of the dimer.

[6] DFT calculations performed using B3LYP/6-31G; gas phase, energy minimized structure of the free azafulvenium ions.

[7] Frigerio, M.; Santagostino, M. *Tetrahedron Lett.* **1994**, *35*, 8019–8022.

[8] Davis, F. A.; Vishwakarma, L. C.; Billmers, J. G.; Finn, J. *J. Org. Chem.* **1984**, *49*, 3241–3243.

[9] Attempts to introduce the C9-alcohol *via* the C8-C9 silyl enol ether by dihydroxylation or epoxidation failed, likely as a result of the sensitivity of the vinyl pyrrole nucleus toward oxidation.

[10] The presence of a free C3-hydroxyl group significantly complicated the introduction of the C9-hydoxyl group.

[11] For the synthesis of *E*(O)- and *Z*(O)-thiol ketene acetal **41**, see Evans, D. A.; Burgey, C. S.; Kozlowski, M. C.; Tregay, S. W. *J. Am. Chem. Soc.* **1999**, *121*, 686–699, and DeRoy, P. L.; Charette, A. B. *Org. Lett.* **2003**, *5*, 4163–4165, respectively.

[12] Under the conditions described above, thiolester **42** was obtained as an inseparable mixture of diastereomers (dr, 1:17:2.5:13). Use of the corresponding *Z*-thiol keteneacetal (2.00 equiv, *E*(O):*Z*(O)=1:12) gave **42** with a diminished level of diastereoselection (dr, 1:2.1:1.4:2.3).

[13] *In situ* ^{1}H NMR monitoring of the homogeneous reaction mixture showed complete consumption of **40** with concomitant formation of **43** and no other visible compounds except remaining excess **2**.

[14] For a review see Hughes, D. L. *Org. Prep. Proceed. Int.* **1996**, *28*, 127–164.

[15] *In situ* ^{1}H NMR monitoring of the homogeneous reaction mixture showed complete consumption of **47** and **2** with concomitant clean and exclusive formation of **49**.

[16] The C9 stereochemistry of the major and minor diastereomers of **58** and **59** was not determined.

[17] Efforts to rigorously assign the stereochemistry of rotamers and/or diastereomers of **60** and **61** using variable-temperature ^{1}H NMR analysis were unsuccessful. Heating to temperatures above 80 °C led to decomposition.

[18] The oxidation of the more electron rich pyrroloindolozine substructure is greatly accelerated in the presence of acid.

Experimental Section

General Procedures. All reactions were performed in oven-dried or flame-dried round-bottomed flasks or in oven-dried 5 mm o.d. NMR tubes. The flasks were fitted with rubber septa and reactions were conducted under a positive pressure of argon. Stainless steel syringes or cannulae were used to transfer air- and moisture-sensitive liquids. Where necessary (so noted), solutions were deoxygenated by bubbling through with balloon-pressure argon through for the time stated. Where noted, compounds were dried azeotropically by concentrating three times from benzene under high-vacuum (0.1 Torr), refilling the flask with argon between each cycle. Flash column chromatography was performed as described by Still et al. using silica gel (60-Å pore size, 32–63 μm, standard grade).[1] Analytical thin–layer chromatography was performed using glass plates pre-coated with 0.25 mm 230–400 mesh silica gel impregnated with a fluorescent indicator (254 nm). Thin layer chromatography plates were visualized by exposure to ultraviolet light and an aqueous solution of ceric ammonium molybdate (CAM). Organic solutions were concentrated on rotary evaporators at ~20 Torr (house vacuum) at 25–35 °C.

Materials. Commercial reagents and solvents were used as received with the following exceptions: dichloromethane, diethyl ether, tetrahydrofuran, and triethylamine were purified by the method of Grubbs et al. under positive argon pressure.[2] Dimethylsulfoxide (>99.9 % HPLC grade, ≤0.020 % water) was used as received. Benzene and 2,6-lutidine were distilled over calcium hydride, and dimethylformamide was distilled over calcium sulfate under reduced pressure. Triethylsilyl trifluoromethanesulfonate and triisopropyl trifluoromethanesulfonate were distilled under reduced pressure. Deuterated solvents were used as received.

Instrumentation. Proton nuclear magnetic resonance (^{1}H NMR) spectra were recorded with an inverse probe 500 MHz, a 500 MHz, or an inverse probe 600 MHz spectrometer, are recorded in parts per million from internal tetramethylsilane on the δ scale and are referenced from the residual protium in the NMR solvent (C_6D_5H: δ 7.16, $CHCl_3$: δ 7.27). Data is reported as follows: chemical shift [multiplicity (s = singlet, d = doublet, t = triplet, q = quartet, m = multiplet), coupling constant(s) in Hertz, integration, assignment]. Carbon-13 nuclear magnetic resonance (^{13}C NMR) spectra were recorded with a 500 MHz spectrometer, are recorded in parts per million from internal tetramethylsilane on the δ scale, and are referenced from the carbon resonances of the solvent (C_6D_6: δ 128.39, $CDCl_3$: δ 77.23). Infrared data (IR) are reported as follows: frequency of absorption (cm^{-1}), intensity of absorption (s = strong, m = medium, w = weak, br = broad). High resolution mass spectra were obtained using a Fourier transform ion cyclotron resonance mass spectrometer with electrospray ionization.

Compound Numbering. The numbering system for proton and carbon assignments for all pyrroloindolizine structures is consistent with the isolation reports for the naturally occurring tricyclic myrmicarins.[3] The numbering system for proton and carbon assignments for all

---

[1] Still, W. C.; Kahn, M.; Mitra, A. *J. Org. Chem.* **1978**, *43*, 2923–2925.

[2] Pangborn, A. B.; Giardello, M. A.; Grubbs, R. H.; Rosen, R. K.; Timmers, F. J. *Organometallics* **1996**, *15*, 1518–1520.

[3] Schröder, F.; Franke, S.; Francke, W. *Tetrahedron* **1996**, 52, 13539–13546.

heterodimeric structures is consistent with the isolation reports for myrmicarin 430A[4] and the numbering system of isomyrmicarin 430A.[5]

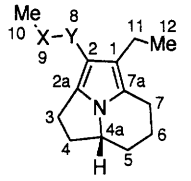

Myrmicarin
(–)-(R) 215A: X-Y = (*Z*)-CH=CH
(+)-(R) 215B: X-Y = (*E*)-CH=CH
(+)-(R) 217: X-Y = CH_2–CH_2

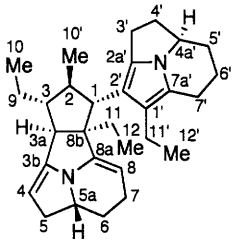

Myrmicarin 430A

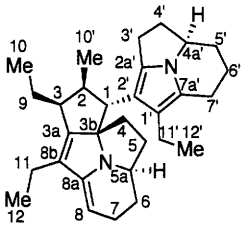

Isomyrmicarin 430A

[4] Schröder, F.; Sinnwell, V.; Baumann, H.; Kaib, M. *Chem. Commun.* **1996**, 2139–2140.
[5] Ondrus, A. E.; Movassaghi, M. *Tetrahedron* **2006**, *62*, 5287–5297.

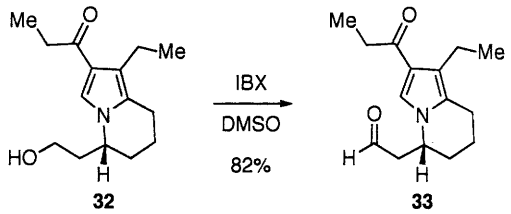

32 33

(1-Ethyl-2-propionyl-5,6,7,8-tetrahydro-indolizin-5-yl)-acetaldehyde (33):

A solution of 2-iodoxybenzoic acid[6] (IBX, 620 mg, 2.21 mmol, 1.10 equiv) in anhydrous dimethylsulfoxide (DMSO, 2.50 mL) was prepared by sonicating the initial suspension for 30 min, and this solution was then degassed (argon purge, 10 min). The solution of IBX was added dropwise via cannula to an anhydrous and degassed (argon purge, 10 min) solution of alcohol **32**[7] (502 mg, 2.01 mmol, 1 equiv) in dimethylsulfoxide (10.0 mL), causing the solution to turn deep rose within 2 min. After 1 h, an additional portion of 2-iodoxybenzoic acid (620 mg, 2.21 mmol, 1.10 equiv) in dimethylsulfoxide (2.50 mL) was prepared and degassed as above and added to the reaction mixture via cannula. After an additional 2 h, the deep rose solution was partitioned between diethyl ether (10 mL) and a mixture of saturated aqueous sodium thiosulfate solution and saturated aqueous sodium bicarbonate solution (10:1, 10 mL). The resulting mixture was diluted with additional portions of diethyl ether (70 mL) and saturated aqueous sodium thiosulfate solution-saturated aqueous sodium bicarbonate solution (10:1, 60 mL), then the aqueous phase was separated from the clear, pale yellow organic phase and extracted with diethyl ether (5 × 60 mL). The combined organic phases were washed with brine (50 mL), were dried over anhydrous sodium sulfate, and were concentrated in vacuo. The resulting brown residue was purified by flash column chromatography on silica gel (eluent: 2.5% triethylamine and 32.5 → 57.5% ethyl acetate in hexanes, diameter: 4.0 cm, height: 6.0 cm) to afford the aldehyde **33** as a pale yellow oil (408 mg, 82%).

^{1}H NMR (500 MHz, C_6D_6, 20 °C):	9.02 (t, J =1.1 Hz, 1H, C**H**O), 6.77 (s, 1H, NC**H**=C), 3.99 (ddd, J = 11.3, 6.7, 5.1 Hz, 1H, NC**H**CH_2), 2.93–3.04 (m, 2H, CC**H**$_2$$CH_3$), 2.23 (m, 2H, NCC**H**$_2$$CH_2$), 2.03 (ddd, J = 18.2, 5.1, 1.1 Hz, 1H, NCHC**H**$_2$CHO), 1.83 (ddd, J = 18.2, 6.7, 1.1 Hz, 1H, NCHC**H**$_2$CHO), 1.41 (t, J = 7.5 Hz, 3H, CCH_2C**H**$_3$), 1.36–1.40 (m, 1H, NCHC**H**$_2$$CH_2$), 1.26 (t, J = 7.4 Hz, 3H, $COCH_2$C**H**$_3$), 1.00–1.24 (m, 3H, NCHC**H**$_2$$CH_2$, $NCHCH_2$C**H**$_2$).
^{13}C NMR (125.8 MHz, C_6D_6, 20 °C):	198.5, 196.1, 128, 127.3, 123.5, 122.7, 50.4, 49.3, 33.3, 29.4, 21.5, 19.0, 18.5, 16.1, 9.7.
FTIR (neat) cm^{-1}:	2936 (s, C–H), 2730 (m, C–H), 1723 (s, C=O), 1688 (s, C=O), 1650 (s), 1516 (m), 1380 (m).

[6] Prepared according to the procedure of Frigerio, M.; Santagostino, M.; Sputore, S. *J. Org. Chem.* **1999**, *64*, 4537-4538.

[7] Movassaghi, M.; Ondrus, A. E. *Org. Lett.* **2005**, *7*, 4423–4426.

HRMS–ESI (*m/z*):	calcd for $C_{15}H_{22}NO_2$ $[M+H]^+$: 248.1645, found: 248.1654.
TLC (silica gel, 50% EtOAc–hexanes), *Rf*:	0.39 (UV, CAM).

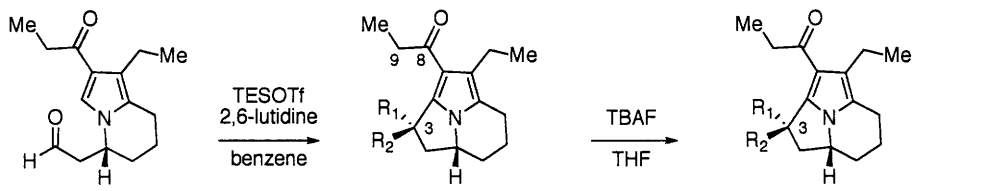

1-(1-Ethyl-3-hydroxy-3,4,4a,5,6,7-hexahydro-pyrrolo[2,1,5-*cd*]indolizin-2-yl)-propan-1-one (35):

Triethylsilyl trifluoromethanesulfonate (TESOTf, 1.08 mL, 4.79 mmol, 3.30 equiv) was added dropwise via syringe to a colorless and anhydrous solution of aldehyde **33** (358 mg, 1.45 mmol, 1 equiv) and 2,6-lutidine (845 μL, 7.25 mmol, 5.00 equiv) in benzene (30.0 mL), producing an intense yellow solution. After 15 min, the reaction flask was placed on an ice-water bath for 3 min, then saturated aqueous sodium bicarbonate solution (35 mL) was added and the reaction flask was immediately removed from the ice-water bath. This mixture was diluted with diethyl ether (60 mL) and the aqueous phase was separated from the yellow organic phase and extracted with diethyl ether (3 × 20 mL). Aqueous hydrochloric acid solution (1N, 100 mL) was added to the combined organic phases and the biphasic mixture was agitated thoroughly (~3 min) in a separatory funnel until TLC analysis indicated that the C8-C9 silyl enol ethers had been completely hydrolyzed to the C8 ketone. The aqueous phase was separated from the yellow organic phase and extracted with diethyl ether (2 × 30 mL), then the combined organic phases were washed sequentially with saturated aqueous sodium bicarbonate solution (35 mL) and brine (35 mL), were dried over anhydrous sodium sulfate, were filtered, and were concentrated under reduced pressure to give crude **34** and **S1**.

Tetrabutylammonium fluoride (TBAF, 1.0 M in tetrahydrofuran, 5.08 mL, 5.08 mmol, 3.50 equiv) was added via syringe to a solution of the crude yellow residue in tetrahydrofuran (THF, 7.25 mL) at 0 °C in an ice-water bath. After 15 min, ethyl acetate (5 mL) and water (5 mL) were added simultaneously and the reaction flask was immediately removed from the ice-water bath. The mixture was diluted with additional portions of ethyl acetate (30 mL), water (10 mL), and brine (1.5 mL). The aqueous phase was separated from the yellow organic phase and extracted with ethyl acetate (5 × 15 mL). The combined organic phases were washed with brine (15 mL), were dried over anhydrous sodium sulfate, were filtered, and were concentrated under reduced pressure to give a yellow residue. This residue was purified by flash column chromatography on silica gel (eluent: 45 → 75% ethyl acetate in hexanes, diameter: 4.0 cm, height: 23 cm) to afford the tricyclic alcohols **35** (237 mg, 66%) and **S2** (52.3 mg, 15%) as white powders.

Ketone 34:

^{1}H NMR (500 MHz, C_6D_6, 20 °C): 5.17 (dd, J = 7.6, 6.1 Hz, 1H, C3–H), 3.32 (dq, J = 16.8, 7.4 Hz, 1H, C9–H), 3.08–3.18 (m, 2H, C11–H, C11–H'), 2.92 (tdd, J = 10.8, 5.4, 3.2 Hz, 1H, C4a–H), 2.86 (dq, J = 16.8, 7.3 Hz, 1H, C9–H'), 2.43 (ddd, J = 16.4, 6.5, 1.1 Hz, 1H, C7–H_c), 2.31 (dt, J = 11.7, 5.7 Hz, 1H, C4–H_c), 2.17 (ddd, J =

16.3, 12.0, 6.9 Hz, 1H, C7–H_t), 1.70 (ddd, J = 11.3, 10.5, 7.8 Hz, 1H, C4–H_t), 1.53–1.58 (m, 1H, C6–H_t), 1.51 (t, J = 7.5 Hz, 3H, C12–H), 1.44 (t, J = 7.3 Hz, 3H, C10–H), 1.39 (dq, J = 12.5, 3.4 Hz, 1H, C5–H_c), 1.17 (tddd, J = 13.4, 12.3, 6.5, 2.8 Hz, 1H, C6–H_c), 0.96 (t, J = 7.9 Hz, 9H, $SiCH_2C\mathbf{H}_3$), 0.77 (tdd, J = 12.9, 11.2, 2.6 Hz, 1H, C5–H_t), 0.59 (q, J = 7.9 Hz, 6H, $SiC\mathbf{H}_2CH_3$).

^{13}C NMR (125.8 MHz, C_6D_6, 20 °C): 196.4, 137.1, 127.3, 120.2, 118.0, 72.4, 53.4, 47.5, 35.7, 29.5, 22.2, 20.2, 19.9, 16.3, 9.3, 7.5, 5.7.

FTIR (neat) cm^{-1}: 2956 (s, C–H), 1650 (s, C=O), 1491 (m), 1321 (m), 1118 (s).

HRMS–ESI (*m/z*): calcd for $C_{21}H_{35}NO_2SiNa$ $[M+Na]^+$: 384.2329, found: 384.2335.

TLC (silica gel, 10% EtOAc–hexanes), *Rf*: 0.28 (UV, CAM).

Tricyclic alcohol 35:

^{1}H NMR (500 MHz, C_6D_6, 20 °C): 6.11 (s, 1H, C3–OH), 5.35 (dd, J = 8.2, 6.4 Hz, 1H, C3–H), 2.92 (dddd, J = 11.2, 10.3, 5.2, 3.9 Hz, 1H, C4a–H), 2.74 (dq, J = 17.2, 7.0 Hz, 1H, C11–H), 2.67 (dq, J = 17.2, 7.0 Hz, 1H, C11–H'), 2.53 (dq, J = 10.7, 7.4 Hz, 1H, C9–H), 2.52 (dq, J = 10.7, 7.4 Hz, 1H, C9–H'), 2.47 (ddd, J = 11.7, 6.3, 5.4 Hz, 1H, C4–H_c), 2.31 (ddd, J = 16.5, 6.7, 1.2 Hz, 1H, C7–H_c), 2.10 (ddd, J = 16.5, 11.9, 7.0 Hz, 1H, C7–H_t), 1.90 (ddd, J = 11.8, 10.2, 8.2 Hz, 1H, C4–H_t), 1.47 (ddddd, J = 13.9, 6.9, 4.1, 2.7, 1.4 Hz, 1H, C6–H_t), 1.24 (t, J = 7.2 Hz, 3H, C12–H), 1.21–1.27 (m, 1H, C5–H_c), 1.13 (t, J = 7.5 Hz, 3H, C10–H), 1.07 (tddd, J = 13.5, 11.8, 6.6, 2.7 Hz, 1H, C6–H_c), 0.66 (tdd, J = 12.9, 11.3, 2.6 Hz, 1H, C5–H_t).

nOe data (500 MHz, C_6D_6, 20 °C):

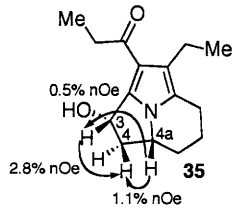

^{13}C NMR (125.8 MHz, $CDCl_3$, 20 °C): 201.0, 142.9, 123.8, 121.6, 118.0, 70.3, 56.0, 46.3, 34.3, 30.1, 22.4, 20.5, 20.1, 16.7, 9.1.

FTIR (neat) cm^{-1}:	3346 (m, O–H), 2942 (m, C–H), 1609 (s, C=O), 1498 (s), 1452 (m), 1253 (m).
HRMS–ESI (*m/z*):	calcd for $C_{15}H_{21}NO_2Na$ $[M+Na]^+$: 270.1464, found: 270.1461.
TLC (silica gel, 60% EtOAc–hexanes), *Rf*:	0.57 (UV, CAM).

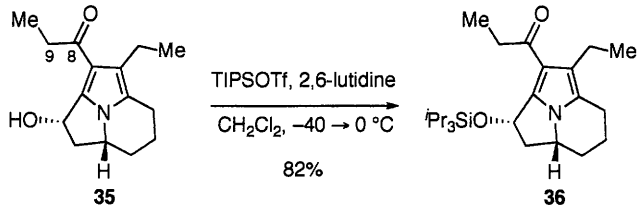

35 36

1-[1-Ethyl-3-(triisopropyl-silanyloxy)-3,4,4a,5,6,7-hexahydro-pyrrolo[2,1,5-*cd*]indolizin-2-yl]-propan-1-one (36):

Triisopropyl trifluoromethanesulfonate (TIPSOTf, 500 μL, 1.86 mmol, 2.26 equiv) was added dropwise via syringe to a clear yellow solution of tricyclic alcohol **35** (204 mg, 825 μmol, 1 equiv) and 2,6-lutidine (480 μL, 4.12 mmol, 5.00 equiv) in dichloromethane (12.0 mL) at –40 °C. The resulting intense yellow solution was maintained at –40 °C for 2 min, and then the reaction flask was placed on an ice-water bath. After 15 min, saturated aqueous sodium bicarbonate solution (15 mL) was added and the reaction flask was removed from the ice water bath. The mixture was diluted with diethyl ether (50 mL) and the layers were separated. The yellow organic phase was extracted with diethyl ether (3 × 15 mL). Aqueous hydrochloric acid solution (1N, 60 mL) was added to the combined organic phases and the biphasic mixture was agitated thoroughly (~8 min) in a separatory funnel until TLC analysis indicated that the C8-C9 silyl enol ether had been completely converted to the C8 ketone **36**. The aqueous phase was extracted with diethyl ether (2 × 30 mL), and the combined organic phases were washed sequentially with saturated aqueous sodium bicarbonate solution (25 mL) and brine (25 mL), were dried over anhydrous sodium sulfate, were filtered, and were concentrated under reduced pressure to a yellow residue. This residue was purified by flash column chromatography on silica gel (eluent: 3.5% triethylamine, 1% ethyl acetate, and 6% dichloromethane in hexanes, diameter: 4.0 cm, height: 19 cm) to afford the triisopropylsilyl ether **36** (273 mg, 82%) as a white powder.

^{1}H NMR (500 MHz, C_6D_6, 20 °C): 5.38 (dd, J = 7.8, 6.1 Hz, 1H, C3–H), 3.38 (dq, J = 17.1, 7.3 Hz, 1H, C9–H), 3.16 (dq, J = 13.7, 7.0 Hz, 1H, C11–H), 3.04 (dq, J = 13.7, 7.1 Hz, 1H, C11–H'), 2.91 (dq, J = 17.1, 7.3 Hz, 1H, C9–H'), 2.89 (tdd, J = 10.7, 5.4, 3.3 Hz, 1H, C4a–H), 2.43 (ddd, J = 16.1, 6.6, 1.1 Hz, 1H, C7–H_c), 2.41 (dt, J = 11.4, 5.7 Hz, 1H, C4–H_c), 2.17 (ddd, J = 16.3, 12.2, 6.9 Hz, 1H, C7–H_t), 1.79 (ddd, J = 11.3, 10.5, 7.8 Hz, 1H, C4–H_t), 1.56 (ddddd, J = 13.7, 6.8, 4.1, 2.7, 1.4 Hz, 1H, C6–H_t), 1.49 (t, J = 7.4 Hz, 3H, C12–H), 1.44 (t, J = 7.3 Hz, 3H, C10–H), 1.40–1.45 (m, 1H, C5–H_c), 1.19 (tddd, J = 13.4, 12.2, 6.5, 2.9 Hz, 1H, C6–H_c), 1.01–1.12 (m, 21H, SiC**H**$(CH_3)_3$, SiCH$(CH_3)_3$), 0.84 (tdd, J = 12.8, 11.2, 2.6 Hz, 1H, C5–H_t).

^{13}C NMR (125.8 MHz, C_6D_6, 20 °C):	196.5, 137.0, 127.0, 120.0, 118.2, 73.3, 53.2, 47.4, 35.8, 29.6, 22.2, 20.1, 20.0, 18.7, 18.6, 16.4, 13.6, 9.1.
FTIR (neat) cm^{-1}:	2867 (s, C–H), 1650 (s, C=O), 1489 (s), 1256 (m), 1123 (m).
HRMS–ESI (*m/z*):	calcd for $C_{24}H_{41}NO_2SiNa$ $[M+Na]^+$: 426.2799, found: 426.2791.

TLC (silica gel, 12.5% EtOAc–hexanes), *Rf*: 0.33 (UV, CAM).

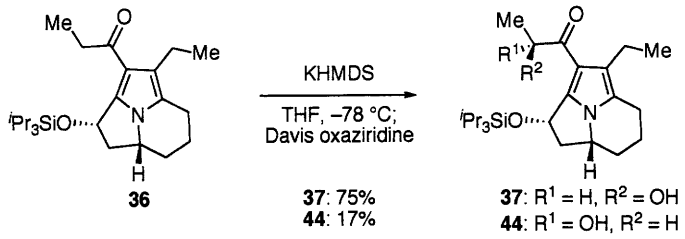

1-[1-Ethyl-3-(triisopropyl-silanyloxy)-3,4,4a,5,6,7-hexahydro-pyrrolo[2,1,5-*cd*]indolizin-2-yl]-2-hydroxy-propan-1-one (37):

An anhydrous solution of triisopropylsilyl ether **36** (99.8 mg, 247 μmol, 1 equiv) in tetrahydrofuran (1050 μL + 2 × 250 μL) was added dropwise via cannula to a solution of potassium hexamethyldisilazane (KHMDS, 173 mg, 865 μmol, 3.50 equiv) in tetrahydrofuran (700 μL) at –78 °C. After the addition was complete, the reaction flask was placed on an ice-water bath for 5 min, and then moved to a dry ice-acetone bath at –78 °C for 5 min. A solution of (±)-*trans*-2-(phenylsulfonyl)-3-phenyloxaziridine[8] (Davis oxaziridine, 32.4 mg, 124 μmol, 0.500 equiv) in tetrahydrofuran (280 μL) was then added dropwise via syringe to the clear yellow reaction mixture. An additional four portions of (±)-*trans*-2-(phenylsulfonyl)-3-phenyloxaziridine (4 × 8.05 mg, 30.9 μmol, 0.125 equiv) in tetrahydrofuran (70.0 μL) were added every 5 min and the progress of the reaction was monitored by TLC analysis after the addition of each portion. Five min after adding the last portion, ethyl acetate (3 mL) and a mixture of saturated aqueous sodium thiosulfate solution and saturated aqueous sodium bicarbonate solution (3:2, 3 mL) were added simultaneously, and the reaction flask was immediately removed from the dry ice-acetone bath. The mixture was diluted with additional portions of ethyl acetate (27 mL) and saturated aqueous sodium thiosulfate solution-satuated aqueous sodium bicarbonate solution (3:2, 22 mL) and the aqueous phase was separated from the yellow organic phase and extracted with ethyl acetate (3 × 22.5 mL). The combined organic phases were washed with a mixture of brine and saturated aqueous sodium thiosulfate solution (10:1, 15 mL), were dried over anhydrous sodium sulfate, were filtered, and were concentrated under reduced pressure to ~500-μL volume. This crude sample was subjected to flash column chromatography on silica gel (eluent: 15% ethyl acetate in hexanes, diameter: 3.0 cm, height: 25 cm) to afford the α-hydroxy ketones **37** (78.0 mg, 75%) and **44** (17.5 mg, 17%) as white powders.

α-Hydroxy Ketone 37:

^{1}H NMR (500 MHz, C_6D_6, 20 °C): 5.47 (dq, J = 7.7, 6.7 Hz, 1H, C9–H), 5.13 (dd, J = 8.6, 5.9 Hz, 1H, C3–H), 4.10 (d, J = 7.8 Hz, 1H, C9-O**H**), 3.08 (dq, J = 13.9, 7.1 Hz, 1H, C11–H), 2.78 (dq, J = 13.9, 7.2 Hz, 1H, C11–H'), 2.64 (tdd, J = 11.0, 5.1, 3.4 Hz, 1H, C4a–H), 2.36 (ddd, J =

[8] (±)-*trans*-2-(phenylsulfonyl)-3-phenyloxaziridine was prepared from *N*-benzylidenebenzenesulfonamide according to the procedure of Ruano, J. L. G.; Aleman, J.; Fajardo, C.; Parra, A. *Org. Lett.* **2005**, *7*, 5493–5496. *N*-benzylidene-benzenesulfonamide was prepared according to the procedure of Vishwakarma, L. C.; Stringer, O. D.; Davis, F. A. *Org. Syn.* **1988**, *66*, 203–210.

16.3, 6.3, 1.1 Hz, 1H, C7–H_c), 2.23 (dt, J = 11.2, 5.5 Hz, 1H, C4–H_c), 2.10 (ddd, J = 16.4, 12.1, 6.7 Hz, 1H, C7–H_t), 1.74 (td, J = 10.9, 8.6 Hz, 1H, C4–H_t), 1.57 (d, J = 6.7 Hz, 3H, C10–H), 1.49 (ddddd, J = 13.7, 6.7, 4.0, 2.8, 1.3 Hz, 1H, C6–H_t), 1.39 (t, J = 7.4 Hz, 3H, C12–H), 1.32 (dq, J = 12.5, 3.3 Hz, 1H, C5–H_c), 1.09–1.17 (m, 1H, C6–H_c), 1.09–1.17 (m, 21H, SiC**H**$(CH_3)_3$, SiCH$(CH_3)_3$), 0.74 (tdd, J = 12.7, 11.5, 2.6 Hz, 1H, C5–H_t).

^{13}C NMR (125.8 MHz, C_6D_6, 20 °C): 201.2, 136.5, 127.5, 120.9, 115.5, 73.4, 71.6, 52.9, 46.3, 29.0, 24.7, 22.1, 20.0, 19.7, 18.8, 18.6, 16.5, 13.7.

FTIR (neat) cm^{-1}: 3459 (m, O–H), 2945 (s, C–H), 1643 (s, C=O), 1461 (m), 1117 (s).

HRMS–ESI (*m/z*): calcd for $C_{24}H_{41}NO_3SiNa$ $[M+Na]^+$: 422.2748, found: 422.2761.

TLC (silica gel, 22.5% EtOAc–hexanes), *Rf*: 0.25 (UV, CAM).

α-Hydroxy Ketone 44:

^{1}H NMR (500 MHz, C_6D_6, 20 °C): 5.47 (dq, J = 7.2, 6.6 Hz, 1H, C9–H), 5.46 (dd, J = 7.8, 6.1 Hz, 1H, C3–H), 4.50 (d, J = 6.4 Hz, 1H, C9-O**H**), 3.11 (dq, J = 14.0, 7.1 Hz, 1H, C11–H), 2.86 (tdd, J = 10.7, 5.2, 3.6 Hz, 1H, C4a–H), 2.80 (dq, J = 13.9, 7.2 Hz, 1H, C11–H'), 2.40 (dt, J = 11.4, 5.7 Hz, 1H, C4–H_c), 2.33 (ddd, J = 16.5, 6.6, 1.1 Hz, 1H, C7–H_c), 2.08 (ddd, J = 16.6, 11.9, 6.9 Hz, 1H, C7–H_t), 1.74 (ddd, J = 11.2, 10.4, 8.0 Hz, 1H, C4–H_t), 1.56 (d, J = 6.9 Hz, 3H, C10–H), 1.49 (ddddd, J = 13.8, 6.9, 4.1, 2.7, 1.3 Hz, 1H, C6–H_t), 1.35 (t, J = 7.5 Hz, 3H, C12–H), 1.33–1.39 (m, 1H, C5–H_c), 1.07–1.15 (m, 1H, C6–H_c), 1.06–1.11 (m, 21H, SiC**H**$(CH_3)_3$, SiCH$(CH_3)_3$), 0.75 (tdd, J = 12.9, 11.3, 2.6 Hz, 1H, C5–H_t).

^{13}C NMR (125.8 MHz, C_6D_6, 20 °C): 199.2, 138.2, 127.4, 120.9, 113.5, 73.3, 70.9, 53.7, 48.0, 29.5, 24.4, 21.9, 20.0, 19.8, 18.7, 18.6, 16.1, 13.6.

FTIR (neat) cm^{-1}: 3450 (m, O–H), 2944 (s, C–H), 1643 (s, C=O), 1462 (m), 1118 (s).

HRMS–ESI (*m/z*): calcd for $C_{24}H_{41}NO_3SiNa$ $[M+Na]^+$: 442.2748, found: 442.2750.

TLC (silica gel, 22.5% EtOAc–hexanes), *Rf*: 0.32 (UV, CAM).

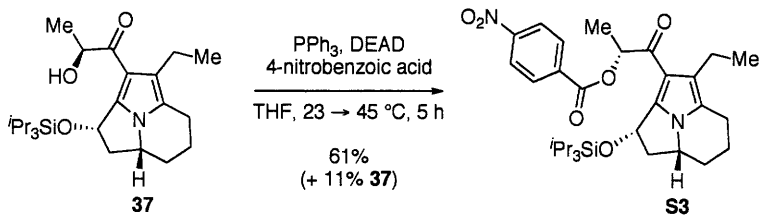

4-Nitro-benzoic acid 2-[1-ethyl-3-(triisopropyl-silanyloxy)-3,4,4a,5,6,7-hexahydro-pyrrolo[2,1,5-*cd*]indolizin-2-yl]-1-methyl-2-oxo-ethyl ester (S3):

Diethyl azodicarboxylate (DEAD, 150 μL, 952 μmol, 20.00 equiv) was added dropwise to a solution of triphenylphosphine (PPh_3, 300 mg, 114 μmol, 20.00 equiv) in tetrahydrofuran (600 μL) at 0 °C. The reaction flask was removed from the cooling bath and the resulting pale yellow solution was stirred for 5 min. This solution was drawn into a syringe and half of it (DEAD: 75.0 μL, 476 μmol, 10.00 equiv, PPh_3: 150 mg, 57.2 μmol, 12.00 equiv, tetrahydrofuran: 300 μL) was transferred to an anhydrous solution of α-hydroxy ketone **37** (20.0 mg, 47.6 μmol, 1 equiv) and 4-nitrobenzoic acid (79.5 mg, 476 μmol, 10.00 equiv) in tetrahydrofuran (600 μL) at 23 °C. The reaction flask was immediately placed on an oil bath at 45 °C. After 5 h, the deep yellow solution was allowed to cool to room temperature and then diluted with ethyl acetate (15 mL), water (10 mL), and brine (1 mL). The aqueous phase was separated from the yellow organic phase and extracted with ethyl acetate (3 × 10 mL). The combined organic phases were washed with brine (7.5 mL), were dried over anhydrous sodium sulfate, were filtered, and were concentrated to a bright yellow residue. This residue was purified by flash column chromatography on silica gel (eluent: 9 → 12.5% ethyl acetate and 18 → 25% dichloromethane in hexanes, diameter: 2.5 cm, height: 22 cm) to afford the 4-nitrobenzoyl ester **S3** (16.4 mg, 61%) as a pale yellow oil, along with recovered α-hydroxy ketone **37** (3.1 mg, 11%).

^{1}H NMR (500 MHz, C_6D_6, 20 °C): 7.94 (d, J = 9.0 Hz, 2H, $NO_2CC\mathbf{H}$), 7.64 (d, J = 9.0 Hz, 2H, $NO_2CCHC\mathbf{H}$), 6.57 (q, J = 7.0 Hz, 1H, C9–H), 5.43 (dd, J = 8.3, 5.8 Hz, 1H, C3–H), 3.03 (dq, J = 13.9, 7.1 Hz, 1H, C11–H), 2.89 (dq, J = 13.9, 7.1 Hz, 1H, C11–H'), 2.84 (tdd, J = 10.9, 5.2, 3.9 Hz, 1H, C4a–H), 2.42 (dt, J = 11.1, 5.6 Hz, 1H, C4–H_c), 2.35 (ddd, J = 16.4, 6.4, 1.6 Hz, 1H, C7–H_c), 2.10 (ddd, J = 16.5, 12.1, 6.6 Hz, 1H, C7–H_t), 1.80 (td, J = 10.9, 8.4 Hz, 1H, C4–H_t), 1.72 (d, J = 6.9 Hz, 3H, C10–H), 1.50–1.56 (m, 1H, C6–H_t), 1.40 (t, J = 7.5 Hz, 3H, C12–H), 1.37–1.43 (m, 1H, C5–H_c), 1.07–1.18 (m, 1H, C6–H_c), 1.05–1.16 (m, 21H, $SiC\mathbf{H}(CH_3)_3$, $SiCH(C\mathbf{H}_3)_3$), 0.81 (tdd, J = 12.9, 11.3, 2.6 Hz, 1H, C5–H_t).

^{13}C NMR (125.8 MHz, C_6D_6, 20 °C): 191.3, 164.4, 150.8, 137.5, 136.3, 131.2, 128.9, 127.7, 123.6, 120.8, 114.4, 75.8, 73.8, 53.3, 47.4, 29.4, 21.9, 20.3, 19.8, 19.2, 18.9, 18.8, 16.1, 13.9.

FTIR (neat) cm^{-1}:	2946 (m, C–H), 1728 (s, C=O), 1660 (s, C=O), 1529 (s), 1276 (s).
HRMS–ESI (*m/z*):	calcd for $C_{31}H_{44}N_2O_6SiNa$ $[M+Na]^+$: 591.2861, found: 591.2867.

TLC (silica gel, 10% EtOAc, 20% CH_2Cl_2–hexanes), *Rf*: 0.42 (UV, CAM).

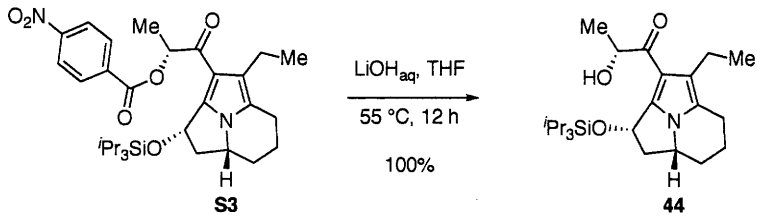

1-[1-Ethyl-3-(triisopropyl-silanyloxy)-3,4,4a,5,6,7-hexahydro-pyrrolo[2,1,5-*cd*]indolizin-2-yl]-2-hydroxy-propan-1-one (44):

Aqueous lithium hydroxide solution (LiOH, 3.5 M, 465 μL, 9.98 equiv) was added via syringe to a solution of 4-nitrobenzoyl ester **S3** (26.5 mg, 46.6 μmol, 1 equiv) in tetrahydrofuran (3.10 mL). The reaction flask was placed on an oil bath at 55 °C and the mixture was stirred vigorously, producing a finely dispersed suspension. After 12 h, the suspension was allowed to cool to room temperature then diluted with ethyl acetate (10 mL), water (6 mL), and brine (0.5 mL). The aqueous phase was separated and extracted with ethyl acetate (3 × 7.5 mL). The combined organic phases were washed with brine (5 mL), were dried over anhydrous sodium sulfate, were filtered, and were concentrated under reduced pressure to provide the α-hydroxy ketone **44** (19.6 mg, 100%) as an off-white solid. See the procedure on page 138 for characterization data.

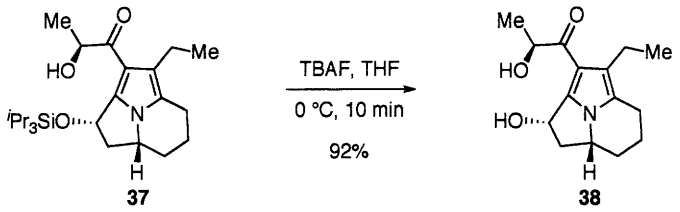

1-(1-Ethyl-3-hydroxy-3,4,4a,5,6,7-hexahydro-pyrrolo[2,1,5-*cd*]indolizin-2-yl)-2-hydroxy-propan-1-one (38):

Tetrabutylammonium fluoride (TBAF, 1.0 M in tetrahydrofuran, 270 μL, 270 μmol, 1.50 equiv) was added via syringe to a solution of α-hydroxy ketone **37** (75.2 mg, 179 μmol, 1 equiv) in tetrahydrofuran (3.60 mL) at 0 °C. After 10 min, chloroform (5 mL) and water (5 mL) were added simultaneously to the pale yellow solution and the reaction flask was immediately removed from the cooling bath. The mixture was diluted with additional portions of chloroform (7.5 mL) and brine (1.5 mL), and the aqueous phase was separated and extracted with chloroform (5 × 4 mL). The combined organic phases were washed with brine (5 mL), were dried over anhydrous sodium sulfate, were filtered, and were concentrated under reduced pressure to a pale yellow residue. This residue was purified by flash column chromatography on silica gel (eluent: 65 → 80% ethyl acetate in hexanes, diameter: 2.5 cm, height: 3.5 cm) to give the diol **38** (43.3 mg, 92%) as a white powder.

^{1}H NMR (500 MHz, $CDCl_3$, 20 °C):	5.52 (s, 1H, C3-O**H**), 5.41 (dd, J = 7.9, 6.5 Hz, 1H, C3–H), 4.87 (pentet, J = 6.8 Hz, 1H, C9–H), 3.98 (d, J = 6.6 Hz, 1H, C9-O**H**), 3.92 (dddd, J = 11.3, 10.2, 5.4, 3.8 Hz, 1H, C4a–H), 3.05 (dt, J = 12.0, 6.0 Hz, 1H, C4–H_c), 2.79 (ddd, J = 16.5, 6.3, 1.1 Hz, 1H, C7–H_c), 2.58 (q, J = 7.6 Hz, 2H, C11–H), 2.52 (ddd, J = 16.6, 11.9, 6.4 Hz, 1H, C7–H_t), 2.15–2.22 (m, 2H, C5–H_c, C6–H_t), 2.12 (ddd, J = 12.0, 10.2, 8.1 Hz, 1H, C4–H_t), 1.76 (tddd, J = 14.2, 9.8, 5.1, 2.1 Hz, 1H, C6–H_c), 1.47 (dtd, J = 17.1, 12.7, 2.8 Hz, 1H, C5–H_t), 1.45 (d, J = 6.9 Hz, 3H, C10–H), 1.15 (t, J = 7.5 Hz, 3H, C12–H).
^{13}C NMR (125.8 MHz, $CDCl_3$, 20 °C):	201.2, 144.6, 123.7, 122.5, 113.8, 70.6, 70.3, 56.2, 46.0, 29.9, 23.7, 22.3, 20.6, 20.1, 16.3.
FTIR (neat) cm^{-1}:	3358 (s, O–H), 2927 (s, C–H), 1638 (s, C=O), 1449 (s), 1089 (s).
HRMS–ESI (*m/z*):	calcd for $C_{15}H_{21}NO_3Na$ $[M+Na]^+$: 286.1414, found: 286.1421.
TLC (silica gel, 75% EtOAc–hexanes), *Rf*:	0.30 (UV, CAM).

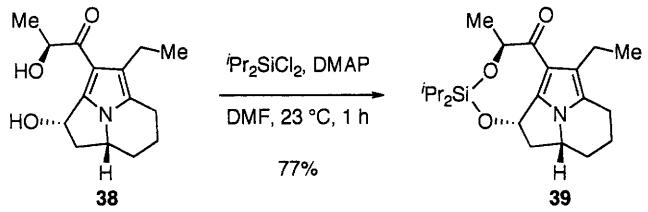

[1,3,2]-Dioxasilocine ketone 39:

Diisopropyldichlorosilane (^{i}Pr$_2$SiCl$_2$, 44.5 μL, 247 μmol, 1.50 equiv) was added dropwise via syringe to a solution of diol **38** (43.3 mg, 164 μmol, 1 equiv) and 4-(dimethylamino)pyridine (DMAP, 70.1 mg, 574 μmol, 3.50 equiv) in dimethylformamide (DMF, 4.30 mL) at 23 °C. After 1 h, diethyl ether (17.5 mL) and a mixture of water and saturated aqueous sodium bicarbonate solution (3:1, 15 mL) were added and the aqueous phase was separated from the organic phase and extracted with diethyl ether (5 × 10 mL). The combined organic phases were washed with brine (10 mL), were dried over anhydrous sodium sulfate, were filtered, and were concentrated under reduced pressure. The crude residue was purified by flash column chromatography on silica gel (eluent: 2.5% triethylamine and 5% ethyl acetate in hexanes, diameter: 3.0 cm, height: 5.5 cm) to provide the diisopropylsilyl tethered diol **39** (47.8 mg, 77%) as a colourless oil.

^{1}H NMR (500 MHz, C_6D_6, 20 °C):	5.45 (dd, J = 8.5, 6.2 Hz, 1H, C3–H), 4.88 (q, J = 6.5 Hz, 1H, C9–H), 3.22 (dq, J = 13.9, 7.0 Hz, 1H, C11–H), 3.01 (dq, J = 13.8, 7.0 Hz, 1H, C11–H'), 2.92 (tdd, J = 10.9, 4.9, 3.7 Hz, 1H, C4a–H), 2.44 (ddd, J = 16.5, 6.5, 1.0 Hz, 1H, C7–H$_c$), 2.38 (dt, J = 11.5, 5.7 Hz, 1H, C4–H$_c$), 2.19 (ddd, J = 16.5, 12.0, 6.9 Hz, 1H, C7–H$_t$), 1.95 (ddd, J = 11.5, 10.7, 8.6 Hz, 1H, C4–H$_t$), 1.71 (d, J = 6.6 Hz, 3H, C10–H), 1.54 (t, J = 7.4 Hz, 3H, C12–H), 1.34–1.39 (m, 1H, C5–H$_c$), 1.51–1.57 (m, 1H, C6–H$_t$), 1.23–1.30 (m, 6H, SiCH(C**H**$_3$)$_3$), 1.14–1.18 (m, 3H, SiCH(C**H**$_3$)$_3$), 1.10–1.18 (m, 1H, C6–H$_c$), 1.10–1.14 (m, 3H, SiCH(C**H**$_3$)$_3$), 1.09–1.25 (m, 2H, SiC**H**(CH$_3$)$_3$), 0.76 (tdd, J = 12.5, 11.5, 2.7 Hz, 1H, C5–H$_t$).
^{13}C NMR (125.8 MHz, C_6D_6, 20 °C):	197.0, 137.9, 128, 120.7, 114.3, 76.1, 72.7, 53.4, 46.0, 29.4, 22.3, 22.1, 20.4, 20.0, 18.4, 18.2, 18.0, 17.9, 16.5, 12.9, 12.5.
FTIR (neat) cm^{-1}:	2946 (s), 1644 (s, C=O), 1463 (s), 1321 (s), 1119 (s).
HRMS–ESI (*m/z*):	calcd for $C_{21}H_{33}NO_3SiNa$ $[M+Na]^+$: 398.2122, found: 398.2128.

TLC (silica gel, 12.5% EtOAc–hexanes), *Rf*: 0.30 (UV, CAM).

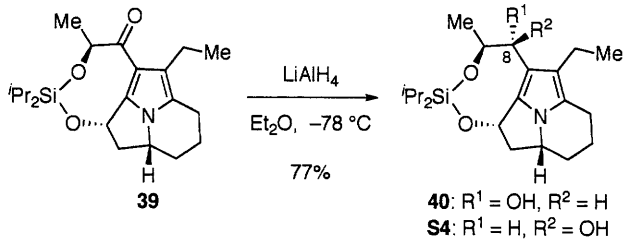

39

40: $R^1 = OH$, $R^2 = H$
S4: $R^1 = H$, $R^2 = OH$

[1,3,2]-Dioxasilocine alcohol 40:

Lithium aluminum hydride (4.6 mg, 121 μmol, 7.00 equiv) was added as a solid in a single portion to a solution of diisopropylsilyl tethered diol **39** (6.5 mg, 17.3 μmol, 1 equiv) in diethyl ether (1.00 mL) at –78 °C and the reaction flask was immediately placed on an ice-water bath. After 15 min, saturated aqueous ammonium chloride solution (3 mL) was added, resulting in vigorous gas evolution. The reaction flask was immediately removed from the cooling bath and the reaction mixture was allowed to warm at room temperature. After 5 min, the mixture was diluted with ethyl acetate (6 mL), saturated aqueous ammonium chloride solution (2 mL), and water (1.5 mL). The opaque grey aqueous phase (pH 8) was separated and extracted with ethyl acetate (4 × 10 mL). The combined organic phases were washed with brine (3.5 mL), were dried over anhydrous sodium sulfate, were filtered, and were concentrated under reduced pressure to a pale yellow residue. The crude dr was determined to be 10:1 by ^{1}H NMR analysis. This crude residue was purified by flash column chromatography on silica gel (eluent: 1.5% triethylamine and 3 → 6% ethyl acetate in hexanes, diameter: 1.5 cm, height: 8.5 cm) to afford the azafulvenium ion precursors (5.0 mg, 77%). Two batches were obtained: one containing diastereomerically pure **40** (3.8 mg, 58%, >98:2 dr), along with a 1:1 mixture of C8 epimers **40** and **S4** (1.2 mg, 18%, 1:1 dr).

^{1}H NMR (500 MHz, C_6D_6, 20 °C): 5.46 (dd, J = 8.8, 6.0 Hz, 1H, C3–H), 4.68 (qd, J = 6.5, 2.4 Hz, 1H, C9–H), 4.53 (dd, J = 4.5, 2.5 Hz, 1H, C8–H), 3.11 (tdd, J = 10.7, 4.6, 3.9 Hz, 1H, C4a–H), 2.50 (dq, J = 14.6, 7.4 Hz, 1H, C11–H), 2.48 (ddd, J = 16.2, 6.5, 1.0 Hz, 1H, C7–H$_c$), 2.44 (dq, J = 14.5, 7.3 Hz, 1H, C11–H'), 2.38 (ddd, J = 11.1, 6.1, 5.0 Hz, 1H, C4–H$_c$), 2.30 (ddd, J = 16.3, 11.7, 6.9 Hz, 1H, C7–H$_t$), 1.86 (ddd, J = 11.2, 10.4, 8.8 Hz, 1H, C4–H$_t$), 1.74 (heptet, J = 7.6 Hz, 1H, SiC**H**(CH$_3$)$_3$), 1.64 (d, J = 4.6 Hz, 1H, C8–O**H**), 1.58 (ddddd, J = 13.7, 6.9, 4.1, 2.7, 1.4 Hz, 1H, C6–H$_t$), 1.37 (dq, J = 12.5, 3.5 Hz, 1H, C5–H$_c$), 1.30–1.32 (m, 6H, C10–H, C12–H), 1.28–1.33 (m, 1H, SiC**H**(CH$_3$)$_3$), 1.28 (d, J = 7.6 Hz, 3H, SiCH(C**H**$_3$)$_3$), 1.26 (d, J = 7.6 Hz, 3H, SiCH(C**H**$_3$)$_3$), 1.18–1.30 (m, 1H, C6–H$_c$), 1.16–1.19 (m, 6H, SiCH(C**H**$_3$)$_3$), 0.79 (tdd, J = 12.9, 11.1, 2.4 Hz, 1H, C5–H$_t$).

^{13}C NMR (125.8 MHz, C_6D_6, 20 °C):	132.4, 123.4, 119.0, 113.7, 74.8, 71.6, 71.4, 53.9, 47.4, 29.9, 22.4, 21.5, 20.7, 19.3, 18.9, 18.8, 18.2, 18.2, 17.6, 13.9, 13.8.
FTIR (neat) cm^{-1}:	3588 (w, O–H), 2928 (s), 1436 (m), 1361 (m), 1094 (s).
HRMS–ESI (*m/z*):	calcd for $C_{21}H_{35}NO_3SiNa$ $[M+Na]^+$: 400.2278, found: 400.2265.
TLC (10% EtOAc–hexanes), *Rf*:	0.25 (CAM).

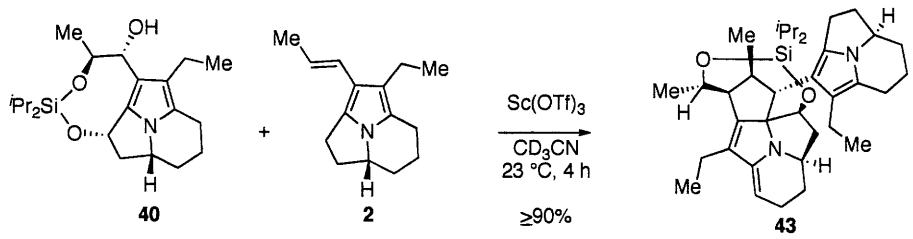

Heterodimer 43:

An anhydrous mixture of (+)-**2** (7.6 mg, 35.3 μmol, 2.00 equiv) and alcohol **40** (6.7 mg, 17.7 μmol, 1 equiv) was transferred in acetonitrile-d_3 (250 + 2 × 150 μL) to a sealed, argon-purged NMR tube. To this solution was added a solution of scandium trifluoromethanesulfonate (0.871 mg, 0.177 μmol, 0.100 equiv) in acetonitrile–d_3 (5.0 μL) via syringe, producing an intense yellow color. After 10 min, an additional portion of scandium trifluoromethanesulfonate (0.871 mg, 0.177 μmol, 0.100 equiv) in acetonitrile–d_3 (5.0 μL) was added, producing a white precipitate. After an additional 1 h, four portions of scandium trifluoromethanesulfonate (0.435 mg, 0.177 μmol, 0.100 equiv) in acetonitrile–d_3 (2.5 μL) were added at 10 min intervals. When 1 h and 20 min had elapsed since the last portion of scandium trifluoromethanesulfonate had been added, ^{1}H NMR analysis showed clean and complete conversion to the desired and air-senstivie heterodimeric product (≥90%, ^{1}H NMR) with only remaining **2** (~45%, ^{1}H NMR). Triethylamine (5.0 μL, 35.4 μmol, 2.00 equiv) was added to the opaque, bright yellow sample, producing additional white precipitate. The mixture was then transferred under argon to a 5-mL pear-shaped flask, the transfer was completed with acetonitrile-d_3 (2 × 250 μL), and the suspension was concentrated under reduced pressure on an argon/high vacuum manifold (final volume approximately 150 μL). This deep orange suspension was immediately purified by flash column chromatography on silica gel (eluent: 2.5% triethylamine and 2.5% ethyl acetate in hexanes, diameter: 1.5 cm, height: 4.0 cm) to yield the sensitive heterodimer **43** and co-eluting **2** (5:1) as a colorless oil that had to be rapidly secured for detailed analysis (including gCOSY, NOESY, and HSQC) due to sensitivity to oxidation.

^{1}H NMR (500 MHz, C_6D_6, 20 °C): 4.74 (t, J = 6.2 Hz, 1H, C4–H), 4.65 (dd, J = 5.6, 3.7 Hz, 1H, C8–H), 4.48 (qd, J = 6.9, 1.4 Hz, 1H, C9–H), 3.32 (tdd, J = 10.7, 5.0, 3.7 Hz, 1H, C4a'–H), 3.18 (d, J = 8.5 Hz, 1H, C1–H), 3.11 (ddd, J = 13.8, 7.3, 6.4 Hz, 1H, C5a–H), 2.93 (ddd, J = 14.9, 11.1, 6.3 Hz, 1H, C3'–H_c), 2.52–2.80 (m, 6H, C11'–H, C11'–H', C3–H, C7'–H_c, C3'–H_t, C2–H), 2.45 (ddd, J = 16.1, 11.7, 6.5 Hz, 1H, C7'–H_t), 2.27 (dq, J = 14.4, 7.3 Hz, 1H, C11–H), 2.25 (dq, J = 14.3, 7.3 Hz, 1H, C11–H'), 2.01–2.14 (m, 4H, C5–H_c, C5–H_t, C7–H_c, C7–H_t), 1.84 (dq, J = 12.7, 6.3 Hz, 1H, C6–H_c), 1.59–1.71 (m, 2H, C6'–H_t, C4'–H_t), 1.56 (d, J = 7.3 Hz, 3H, C10'–H), 1.49–1.54 (m, 1H, C5'–H_c), 1.45 (d, J = 6.9 Hz, 3H, C10–H), 1.41–1.47 (m, 1H, C6–H_t), 1.41 (t, J = 7.5 Hz, 3H, C12'–H), 1.28–1.36 (m, 8H, SiC**H**$(CH_3)_3$,

	$SiCH(CH_3)_3$), 1.21 (t, J = 7.6 Hz, 3H, C12–H), 1.12–1.25 (m, 1H, C6'–H_c), 1.12–1.17 (m, 3H, $SiCH(CH_3)_3$), 0.88 (tdd, J = 13.3, 11.8, 3.0 Hz, 1H, C5'–H_t).
^{13}C NMR (125.8 MHz, C_6D_6, 20 °C):	154.7, 148.5, 136.0, 126.0, 122.4, 119.3, 113.5, 90.2, 89.8, 86.7, 73.4, 55.3, 55.3, 53.3, 49.4, 47.0, 41.4, 37.2, 30.8, 30.2, 27.4, 26.2, 24.6, 23.1, 21.1, 21.0, 19.7, 18.9, 18.6, 18.4, 18.3, 18.1, 17.0, 14.2, 12.8, 12.1.
FTIR (neat) cm^{-1}:	2940 (s), 1730 (m), 1668 (m), 1461 (m), 1095 (m).
HRMS–ESI (*m/z*):	calcd for $C_{36}H_{55}N_2O_2Si$ $[M+H]^+$: 575.4027, found: 575.4043.

TLC (Et_3N–pretreated silica, 2.5% Et_3N, 2.5% EtOAc–hexanes), *Rf*: 0.76 (UV, CAM).

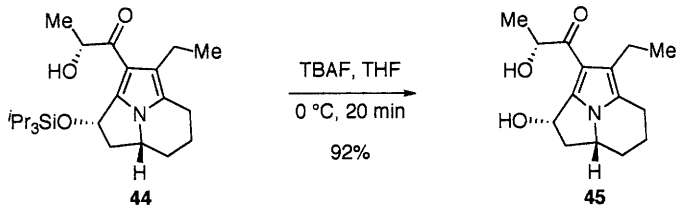

44 **45**

1-(1-Ethyl-3-hydroxy-3,4,4a,5,6,7-hexahydro-pyrrolo[2,1,5-*cd*]indolizin-2-yl)-2-hydroxy-propan-1-one (45):

Tetrabutylammonium fluoride (1.0 M in THF, 100 μL, 100 μmol, 1.67 equiv) was added via syringe to a solution of triisopropylsilyl ether **44** (24.9 mg, 59.3 μmol, 1 equiv) in tetrahydrofuran (2.00 mL) at 0 °C. After 20 min, chloroform (5 mL) and aqueous sodium chloride solution (10 wt %, 5 mL) were added simultaneously to the pale yellow solution and the reaction flask was immediately removed from the cooling bath. The mixture was diluted with additional portions of chloroform (10 mL) and aqueous sodium chloride solution (10 wt %, 5 mL). The aqueous layer was separated and extracted with chloroform (5 × 10 mL), and the combined organic layers were washed with brine (7.5 mL), were dried over anhydrous sodium sulfate, were filtered, and were concentrated under reduced pressure to a pale yellow solution in chloroform (150 μL). This crude solution was purified by flash column chromatography on silica gel (eluent: 65 → 80% ethyl acetate in hexanes, diameter: 2.5 cm, height: 3.5 cm) to provide the diol **45** (14.4 mg, 92%) as a white powder.

^{1}H NMR (500 MHz, $CDCl_3$, 20 °C):	5.46 (dd, J = 8.2, 6.4 Hz, 1H, C3–H), 4.97 (q, J = 6.5 Hz, 1H, C9–H), 4.09 (br s, 1H, C9-O**H**), 3.90 (dddd, J = 11.3, 10.1, 5.2, 3.6 Hz, 1H, C4a–H), 3.08 (ddd, J = 11.9, 6.4, 5.5 Hz, 1H, C4–H_c), 2.97 (br s, 1H, C3–O**H**), 2.78 (ddd, J = 16.7, 6.7, 1.1 Hz, 1H, C7–H_c), 2.66 (dq, J = 14.5, 7.3 Hz, 1H, C11–H), 2.58 (dq, J = 14.4, 7.2 Hz, 1H, C11–H'), 2.56 (ddd, J = 16.2, 11.8, 6.5 Hz, 1H, C7–H_t), 2.15–2.22 (m, 2H, C5–H_c, C6–H_t), 2.05 (ddd, J = 12.0, 10.2, 8.3 Hz, 1H, C4–H_t), 1.71–1.83 (m, 1H, C6–H_c), 1.43 (d, J = 6.7 Hz, 3H, C10–H), 1.37–1.49 (m, 1H, C5–H_t), 1.17 (t, J = 7.5 Hz, 3H, C12–H).
^{13}C NMR (125.8 MHz, $CDCl_3$, 20 °C):	199.6, 142.3, 125.4, 122.3, 113.4, 71.0, 70.6, 55.5, 46.8, 29.8, 23.5, 22.2, 20.3, 20.0, 16.5.
FTIR (neat) cm^{-1}:	3331 (s, O–H), 2929 (s, C–H), 1635 (s, C=O), 1448 (s), 1092 (s).
HRMS–ESI (*m/z*):	calcd for $C_{15}H_{21}NO_3Na$ $[M+Na]^+$: 286.1414, found: 286.1424.
TLC (silica gel, 65% EtOAc–hexanes), *Rf*:	0.20 (UV, CAM).

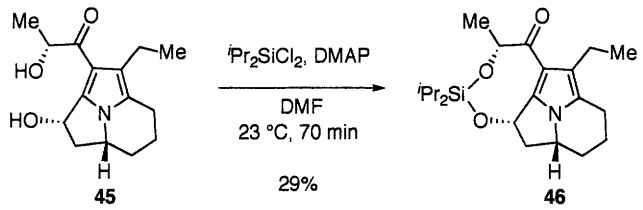

[1,3,2]-Dioxasilocine ketone 46:

Diisopropyldichlorosilane ($^{i}Pr_2SiCl_2$, 13.6 μL, 75.2 μmol, 1.50 equiv) was added dropwise via syringe to a solution of diol **45** (13.2 mg, 50.1 μmol, 1 equiv) and 4-(dimethylamino)pyridine (DMAP, 21.4 mg, 175 μmol, 3.50 equiv) in dimethylformamide (1.00 mL) at 23 °C, producing a white suspension. Additional portions of diisopropyldichlorosilane (6.8 μL, 37.7 μmol, 0.750 equiv) and 4-(dimethylamino)pyridine (21.4 mg, 75.2 μmol, 3.50 equiv) were added after 25 min and 55 min, respectively. After 70 min total reaction time, TLC analysis indicated that the starting material had been completely consumed. Diethyl ether (10 mL) and a mixture of water and saturated aqueous sodium bicarbonate solution (7:1, 8 mL) were added. The aqueous layer was separated and extracted with ethyl acetate (3 × 7.5 mL). The combined organic phases were washed with brine (6 mL), were dried over anhydrous sodium sulfate, were filtered, and were concentrated under reduced pressure. This residue was purified by flash column chromatography on silica gel (eluent: 2.5% triethylamine and 2 → 75% ethyl acetate in hexanes, diameter: 1.5 cm, height: 22 cm) to afford the diisopropylsilyl tethered diol **46** (5.5 mg, 29%) as a colorless oil. The remainder of the material isolated from the column, consisting of a mixture of C3 and C9 mono- and bis-silylated byproducts, was combined and diol **45** was recovered by their treatment with tetrabutylammonium fluoride in tetrahydrofuran at 0 °C.

^{1}H NMR (500 MHz, C_6D_6, 20 °C): 5.29 (dd, J = 7.5, 6.6 Hz, 1H, C3–H), 4.90 (q, J = 6.2 Hz, 1H, C9–H), 3.08 (dq, J = 13.8, 7.1 Hz, 1H, C11–H), 2.94 (dq, J = 13.8, 7.1 Hz, 1H, C11–H'), 2.83 (tdd, J = 10.8, 5.9, 3.5 Hz, 1H, C4a–H), 2.47 (dt, J = 12.1, 6.1 Hz, 1H, C4–H_c), 2.30 (ddd, J = 16.4, 6.6, 1.1 Hz, 1H, C7–H_c), 2.06 (ddd, J = 16.5, 12.0, 6.9 Hz, 1H, C7–H_t), 1.79 (ddd, J = 12.1, 10.4, 7.6 Hz, 1H, C4–H_t), 1.66 (d, J = 6.3 Hz, 3H, C10–H), 1.48 (ddddd, J = 13.7, 6.9, 4.0, 2.7, 1.4 Hz, 1H, C6–H_t), 1.40 (t, J = 7.5 Hz, 3H, C12–H), 1.36 (dq, J = 12.5, 3.4 Hz, 1H, C5–H_c), 1.16 (d, J = 7.1 Hz, 3H, SiCH(C**H**$_3$)$_3$), 1.13 (d, J = 7.0 Hz, 3H, SiCH(C**H**$_3$)$_3$), 1.05–1.12 (m, 1H, C6–H_c), 1.16 (d, J = 7.1 Hz, 3H, SiCH(C**H**$_3$)$_3$), 1.04–1.21 (m, 1H, Si**C**H(CH$_3$)$_3$), 0.90 (d, J = 7.2 Hz, 3H, SiCH(C**H**$_3$)$_3$), 0.87 (d, J = 7.1 Hz, 3H, SiCH(C**H**$_3$)$_3$), 0.77–0.81 (m, 1H, C5–H_t), 0.76–0.86 (m, 1H, Si**C**H(CH$_3$)$_3$).

^{13}C NMR (125.8 MHz, C_6D_6, 20 °C):	192.4, 136.4, 128.9, 121.0, 115.8, 72.5, 71.6, 53.3, 47.3, 29.6, 22.2, 19.9, 19.7, 18.6, 17.8, 17.7, 17.6, 17.4, 16.1, 13.5, 13.3.
FTIR (neat) cm^{-1}:	2931 (s), 2866 (s), 1666 (s, C=O), 1445 (m), 1110 (s).
HRMS–ESI (*m/z*):	calcd for $C_{21}H_{33}NO_3SiNa$ $[M+Na]^+$: 398.2122, found: 398.2112.

TLC (silica gel, 12.5% EtOAc–hexanes), *Rf*: 0.22 (UV, CAM).

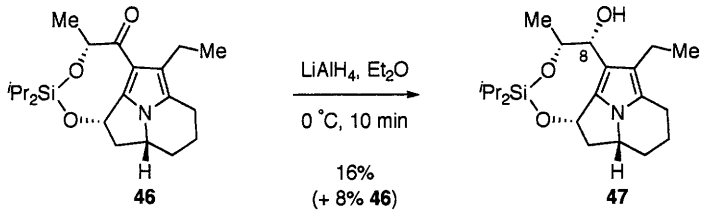

[1,3,2]-Dioxasilocine alcohol 47:

Lithium aluminum hydride (11.9 mg, 313 μmol, 10.00 equiv) was added as a solid in a single portion to a solution of ketone **46** (11.8 mg, 31.3 μmol, 1 equiv) in diethyl ether (Et_2O, 1.60 mL) at 0 °C. After 10 min, the mixture was diluted with saturated aqueous ammonium chloride solution (4 mL) and ethyl acetate (3 mL), and the reaction flask was immediately removed from the cooling bath. The reaction mixture was stirred at room temperature for 5 min, then diluted with additional portions of ethyl acetate (50 mL) and saturated aqueous ammonium chloride solution (50 mL). The opaque grey aqueous phase (pH 7) was separated and extracted with ethyl acetate (4 × 40 mL). The combined organic phases were washed with brine (35 mL), were dried over anhydrous sodium sulfate, were filtered, and were concentrated under reduced pressure. The white residue was purified by flash column chromatography on silica gel (eluent: 2.5% triethylamine and 5% ethyl acetate in hexanes changed gradually to 2.5% triethylamine and 3.5% methanol in ethyl acetate, diameter: 1.5 cm, height: 10 cm) to afford the sensitive alcohol **47** (1.9 mg, 16%) as a colorless oil. The remainder of the material isolated from the column consisted of recovered starting material (1.0 mg, 8.4%) and the fully desilylated C3-C8-C9 triol (2.9 mg, 24%).

^{1}H NMR (500 MHz, C_6D_6, 20 °C): 5.25 (dd, J = 7.3, 6.7 Hz, 1H, C3–H), 4.60 (d, J = 11.4 Hz, 1H, C8–H), 4.48 (q, J = 6.3 Hz, 1H, C9–H), 3.03 (tdd, J = 10.8, 5.4, 3.2 Hz, 1H, C4a–H), 2.97 (dq, J = 14.7, 7.6 Hz, 1H, C11–H), 2.74 (dq, J = 14.3, 7.3 Hz, 1H, C11–H'), 2.51 (ddd, J = 11.7, 6.3, 5.5 Hz, 1H, C4–H_c), 2.49 (d, J = 11.4 Hz, 1H, C8–O**H**), 2.48 (ddd, J = 16.3, 6.7, 1.3 Hz, 1H, C7–H_c), 2.27 (ddd, J = 16.3, 11.9, 6.8 Hz, 1H, C7–H_t), 1.91 (ddd, J = 11.7, 10.6, 7.5 Hz, 1H, C4–H_t), 1.59 (ddddd, J = 13.7, 6.8, 4.0, 2.7, 1.4 Hz, 1H, C6–H_t), 1.46 (d, J = 6.3 Hz, 3H, C10–H), 1.42–1.46 (m, 1H, C5–H_c), 1.40 (t, J = 7.5 Hz, 3H, C12–H), 1.23 (tddd, J = 13.4, 12.1, 6.5, 3.0 Hz, 1H, C6–H_c), 1.12–1.15 (m, 6H, SiCH(CH_3)$_3$), 1.06–1.15 (m, 1H, SiC**H**(CH_3)$_3$), 0.98 (d, J = 7.1 Hz, 3H, SiCH(CH_3)$_3$), 0.85–0.91 (m, 1H, C5–H_t), 0.82–0.95 (m, 1H, SiC**H**(CH_3)$_3$).

^{13}C NMR (125.8 MHz, C_6D_6, 20 °C): 128, 125.2, 119.4, 118.0, 71.5, 71.1, 70.8, 52.7, 47.4, 29.8, 22.8, 22.6, 20.6, 19.4, 18.1, 18.0, 18.0, 17.8, 16.6, 12.8, 12.4.

HRMS–ESI (*m/z*):	calcd for $C_{21}H_{35}NO_3SiNa$ $[M+Na]^+$: 400.2278, found: 400.2281.
TLC (silica gel, 10% EtOAc–hexanes), *Rf*:	0.36 (CAM).

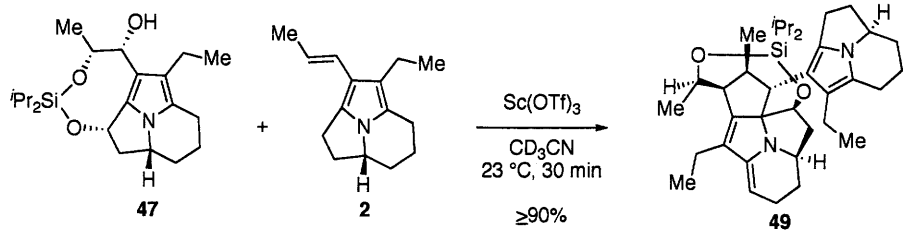

Heterodimer 49:

An anhydrous solution of (+)-myrmicarin 215B (**2**, 1.1 mg, 5.01 μmol, 1.00 equiv) in acetonitrile–d_3 (500 μL) was added portionwise to an anhydrous solution of alcohol **47** (1.9 mg, 5.01 μmol, 1 equiv) in acetonitrile–d_3 (250 μL) until ^{1}H NMR analysis showed that the ratio of the two species was exactly 1:1. This solution was concentrated (final volume 150 μL) and transferred under argon to a sealed, argon-purged NMR tube, followed by an acetonitrile–d_3 (2 × 30 μL) rinse of the transfer flask. To this solution, scandium trifluoromethanesulfonate (0.246 mg, 0.501 μmol, 0.100 equiv) in acetonitrile–d_3 (5.0 μL) was added via syringe, producing an intense yellow color. After 10 min, an additional two portions of scandium trifluoromethanesulfonate (2 × 0.246 mg, 0.501 μmol, 0.100 equiv) were added at 10 min intervals. When 10 min had elapsed since the last portion of scandium trifluoromethanesulfonate was added, ^{1}H NMR analysis showed complete and clean formation of the desired heterodimer **49** (≥90%) as a single diastereomer and trace amount of remaining **2** (<5%). Triethylamine (5.0 μL, 35.9 μmol, 7.16 equiv) was added to the intense yellow solution, producing a small amount of precipitate. The sample was transferred under argon to a 5-mL pear-shaped flask, the NMR tube was rinsed with acetonitrile–d_3 (2 × 100 μL), and the suspension was concentrated under reduced pressure on an argon/high vacuum manifold (final volume ~200 μL). This sample was directly purified by flash column chromatography on a silica gel (eluent: 2.5% triethylamine and 2.5% ethyl acetate in hexanes, diameter: 1.0 cm, height: 2.5 cm) to afford the sensitive heterodimer **49** and myrmicarin 215B (>95:5) as a colorless oil that had to be rapidly secured for detailed analysis (including gCOSY, gHSQC, NOESY, and gHMBC) due to sensitivity to oxidation.

^{1}H NMR (500 MHz, C_6D_6, 20 °C): 4.66 (dd, J = 7.5, 3.0 Hz, 1H, C8–H), 4.28 (d, J = 4.3 Hz, 1H, C4–H), 4.11 (qd, J = 8.9, 5.8 Hz, 1H, C9–H), 3.30 (tdd, J = 10.6, 5.3, 3.5 Hz, 1H, C4a'–H), 3.18 (dddd, J = 11.6, 9.3, 6.4, 2.1 Hz, 1H, C5a–H), 2.95 (ddd, J = 15.2, 11.1, 6.2 Hz, 1H, C3'–H_c), 2.56–2.71 (m, 5H, C3–H, C7'–H_c, C3'–H_t, C11'–H, C11'–H'), 2.53 (d, J = 9.0 Hz, 1H, C1–H), 2.45 (dq, J = 14.6, 7.4 Hz, 1H, C11–H), 2.31–2.49 (m, 3H, C7–H_t, C5–H_c, C2–H), 2.27 (dq, J = 14.6, 7.4 Hz, 1H, C11–H'), 2.16 (ddt, J = 15.2, 11.9, 3.3 Hz, 1H, C7–H_t), 2.06 (dt, J = 11.4, 5.9 Hz, 1H, C4'–H_c), 2.04–2.12 (m, 1H, C2–H), 1.95 (dd, J = 13.7, 1.8 Hz, 1H, C5–H_t), 1.56–1.68 (m, 3H, C6'–H_t, C4'–H_t, C6–H_c), 1.51 (td, J = 11.8, 4.0 Hz, 1H, C6–H_t),

	1.42–1.48 (m, 1H, C5'–H_c), 1.35 (t, J = 7.5 Hz, 3H, C12'–H), 1.32 (d, J = 5.8 Hz, 3H, C10–H), 1.27 (t, J = 7.5 Hz, 3H, C12–H), 1.24–1.32 (m, 2H, C6'–H_c, SiC**H**$(CH_3)_3$), 1.17 (d, J = 7.4 Hz, 3H, SiCH(C**H**$_3)_3$), 1.14 (d, J = 7.4 Hz, 3H, SiCH(C**H**$_3)_3$), 1.09–1.14 (m, 6H, SiCH(C**H**$_3)_3$), 1.08–1.18 (m, 1H, SiC**H**$(CH_3)_3$), 0.99 (d, J = 7.0 Hz, 3H, C10'–H), 0.82 (tdd, J = 13.1, 11.7, 3.3 Hz, 1H, C5'–H_t).
^{13}C NMR (125.8 MHz, C_6D_6, 20 °C):	154.3 (C8a), 145.9 (C3a), 134.1 (C8b), 131.2 (C2a'), 121.9 (C1'), 116.8 (C7a'), 113.4 (C2'), 91.4 (C3b), 87.1 (C8), 84.7 (C4), 67.7 (C9), 55.3 (C4a'), 55.0 (C5a), 50.2 (C3), 49.7 (C2), 48.2 (C1), 43.5 (C5), 37.2 (C4'), 31.1 (C6), 30.1 (C5'), 27.4 (C3'), 25.9 (C10), 23.3 (C7), 23.2 (C6'), 21.3 (C7), 19.6 (C11), 19.2 (C11'), 18.6 (SiCH(**C**$H_3)_3$), 18.5 (SiCH(**C**$H_3)_3$, 18.2 (SiCH(**C**$H_3)_3$, 18.2 (SiCH(**C**$H_3)_3$, 17.8 (C12'), 17.3 (C10'), 14.3 (C12), 12.1 (Si**C**H$(CH_3)_3$, 11.5 (Si**C**H$(CH_3)_3$.
FTIR (neat) cm^{-1}:	2929 (s), 1717 (m), 1653 (m), 1507 (w), 1118 (m).
HRMS–ESI (*m/z*):	calcd for $C_{36}H_{55}N_2O_2Si$ $[M+H]^+$: 575.4027, found: 575.4033.

TLC (Et_3N–pretreated silica, 2.5% Et_3N, 2.5% EtOAc–hexanes), *Rf*: 0.82 (UV, CAM).

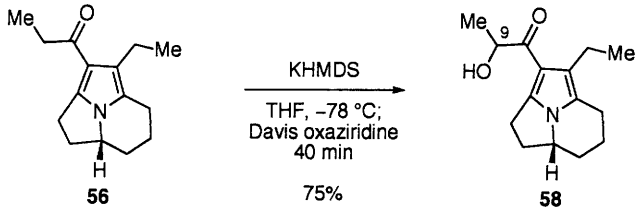

1-(1-Ethyl-3,4,4a,5,6,7-hexahydro-pyrrolo[2,1,5-*cd*]indolizin-2-yl)-2-hydroxy-propan-1-one (58):

An anhydrous solution of ketone **56** (97.3 mg, 421 μmol, 1 equiv) in tetrahydrofuran (2500 + 2 × 250 μL) was added via cannula to a solution of potassium bis(trimethylsilyl)amide (KHMDS, 209 mg, 1.05 mmol, 2.50 equiv) in tetrahydrofuran (750 μL) at –78 °C , producing a clear and pale yellow solution. After 15 min, a solution of (±)-*trans*-2-(phenylsulfonyl)-3-phenyloxaziridine[8] (Davis oxaziridine, 110 mg, 421 μmol, 1.00 equiv) in tetrahydrofuran (440 μL) was added dropwise via syringe. After 5 min, two additional portions of (±)-*trans*-2-(phenylsulfonyl)-3-phenyloxaziridine (11.0 mg, 42.1 μmol, 0.100 equiv) in tetrahydrofuran (44.0 μL) were added at 5 min intervals. When 5 min had elapsed after the last addition, a mixture of saturated aqueous sodium thiosulfate solution and saturated aqueous sodium bicarbonate solution (1:1, 3 mL) was added to the yellow reaction mixture and the reaction flask was immediately removed from the cooling bath. The mixture was diluted with ethyl acetate (20 mL) and an additional portion of saturated aqueous sodium thiosulfate solution-saturated aqueous sodium bicarbonate solution (1:1, 12 mL), and the aqueous phase was extracted with ethyl acetate (4 × 15 mL). The combined organic phases were washed with brine (12.5 mL), were dried over anhydrous sodium sulfate, were filtered, and were concentrated under reduced pressure to a yellow solution in ethyl acetate (approximately 300 μL). This sample was directly purified by flash column chromatography on silica gel (eluent: 2.5% triethylamine, 37.5% ethyl acetate, and 15% dichloromethane in hexanes, diameter: 2.5 cm, height: 17 cm) to afford the α-hydroxy ketone **58** (78.0 mg, 75%, mixture of C9 epimers, 9:5 dr) as a while powder.

^{1}H NMR (500 MHz, C_6D_6, 20 °C, 9:5 dr, major epimer denoted by *): 4.67–4.78 (m, 2H, C9–H*, C9–H), 4.55–4.57 (m, 2H, C9–O**H***, C9–O**H**), 2.85–3.17 (m, 6H, C11–H*, C11–H'*, C11–H, C11–H', C4a–H*, C4a–H), 2.04–2.42 (m, 8H, C3–H_t*, C3–H_t, C7–H_c*, C7–H_c, C3–H_c*, C3–H_c, C7–H_t*, C7–H_t), 1.65–1.71 (m, 2H, C4–H_c*, C4–H_c), 1.47–1.56 (m, 2H, C6–H_t*, C6–H_t), 1.42–1.46 (m, 12H, C12–H*, C12–H, C10–H*, C10–H), 1.19–1.39 (m, 4H, C4–H_t*, C4–H_t, C5–H_c*, C5–H_c), 1.07–1.18 (m, 2H, C6–H_c*, C6–H_c), 0.59–0.69 (C5–H_t*, C5–H_t*).

^{13}C NMR (125.8 MHz, C_6D_6, 20 °C, 9:5 dr, major epimer denoted by *): 197.3*, 197.2, 138.1, 138.1*, 126.7*, 126.5, 121.7, 121.5*, 113.3, 113.2*, 70.5, 70.1*, 56.1*, 56.0, 36.3, 35.9*, 29.5, 29.4*,

	28.3, 28.0*, 23.9*, 23.8, 22.6*, 22.3, 20.1, 20.1*, 19.9*, 19.8, 16.3*, 16.1.
FTIR (neat) cm^{-1}:	3451 (m, O–H), 2921 (s), 1632 (s, C=O), 1460 (m), 1370 (m), 1039 (m).
HRMS–ESI (*m/z*):	calcd for $C_{15}H_{21}NO_2Na$ $[M+Na]^+$: 270.1465, found: 270.1469.

TLC (2.5% Et_3N, 17.5% EtOAc, 20% CH_2Cl_2–hexanes), *Rf*: 0.21 (UV, CAM).

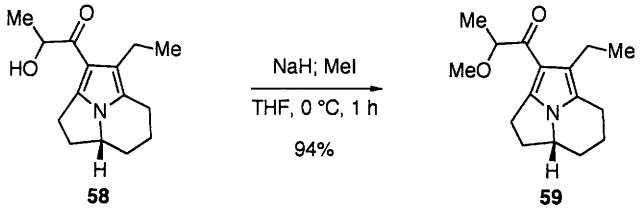

1-(1-Ethyl-3,4,4a,5,6,7-hexahydro-pyrrolo[2,1,5-*cd*]indolizin-2-yl)-2-methoxy-propan-1-one (59):

Sodium hydride (60% dispersion in mineral oil, 56.0 mg, 1.40 mmol, 2.00 equiv) was added in a single portion to an anhydrous solution of the α-hydroxy ketone **58** (173 mg, 700 μmol, 1 equiv) and methyl iodide (131 μL, 2.10 mmol, 3.00 equiv) in dimethylformamide (4.75 mL) at 23 °C. The resulting suspension gradually became a clear and colouress solution within 5 min. After 1 h, the solution was slowly poured into a mixture of water and saturated aqueous ammonium chloride solution (1:1, 20 mL) causing vigorous gas evolution, and this mixture was diluted with a solution of ethyl acetate and hexanes (3:2, 25 mL). The aqueous phase was separated and extracted with ethyl acetate-hexanes (3:2, 4 × 20 mL). The combined organic phases were washed with brine (15 mL), were dried over anhydrous sodium sulfate, were filtered, and were concentrated under reduced pressure. The residue was purified by flash column chromatography on silica gel (eluent: 2.5% triethylamine and 37.5% ethyl acetate in hexanes, diameter: 3.0 cm, height: 10 cm) to afford the α-methoxy ketone **59** (173 mg, 94%, mixture of C9 epimers, 9:5 dr) as a colorless oil.

^{1}H NMR (500 MHz, C_6D_6, 20 °C, 9:5 dr):	4.30 (q, J = 6.8 Hz, 1H), 4.28 (q, J = 6.7 Hz, 1H), 2.94–3.16 (m, 6H), 2.71 (dd, J = 15.8, 8.1 Hz, 1H), 2.70 (dd, J = 15.7, 8.1 Hz, 1H), 2.50 (ddd, J = 16.9, 11.8, 6.7 Hz, 1H), 2.70 (dd, J = 15.7, 8.1 Hz, 1H), 2.50 (ddd, J = 16.0, 10.5, 5.8 Hz, 1H), 2.50 (ddd, J = 16.0, 10.7, 5.2 Hz, 1H), 2.38 (ddd, J = 16.5, 6.4, 0.9 Hz, 2H), 2.13 (ddd, J = 16.9, 11.8, 6.7 Hz, 1H), 2.12 (ddd, J = 16.4, 12.1, 6.3 Hz, 1H), 1.73–1.79 (m, 2H), 1.47–1.55 (m, 2H), 1.45–1.49 (m, 12H), 1.29–1.42 (m, 4H), 0.99–1.20 (m, 2H), 0.62–0.72 (m, 2H).
^{13}C NMR (125 MHz, C_6D_6, 20 °C, 9:5 dr):	195.5, 195.4, 137.5, 137.5, 126.8, 126.8, 121.1, 121.0, 115.3, 115.1, 81.3, 81.1, 56.6, 56.6, 56.1, 56.1, 36.2, 36.2, 29.7, 29.6, 29.3, 29.1, 19.0, 18.5, 16.4, 16.3, 22.6, 22.5, 20.3, 20.3, 19.9, 19.9.
FTIR (neat) cm^{-1}:	2929 (s), 1651 (s, C=O), 1494 (s), 1320 (m), 1037 (w).
HRMS (ESI):	calcd for $C_{16}H_{23}NNaO_2$ $[M+Na]^+$: 284.1621, found: 284.1626.

TLC (2.5% Et_3N, 17.5% EtOAc, 20% CH_2Cl_2–hexanes), *Rf*: 0.26 (UV, CAM).

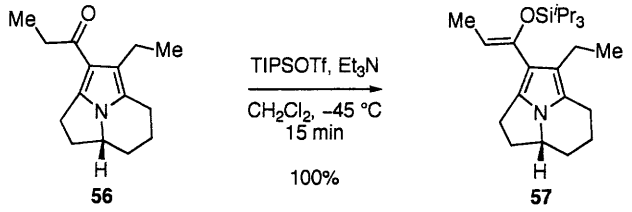

Z-4-Ethyl-3-[1-(triisopropyl-silanyloxy)-propenyl]-1,2,5,6,7,7a-hexahydro-pyrrolo[2,1,5-*cd*]indolizine (57):

Triisopropylsilyl trifluoromethanesulfonate (TIPSOTf, 24.2 μL, 89.9 μmol, 1.05 equiv) was added dropwise to an anhydrous solution of ketone **56** (19.8 mg, 85.6 μmol, 1 equiv) and triethylamine (59.7 μL, 428 μmol, 5.00 equiv) in dichloromethane (1.70 mL) at –45 °C such that the intense yellow color produced upon adding each drop had completely disappeared before the next drop was added. After complete addition of triisopropylsilyl trifluoromethanesulfonate, an ice-cold solution of saturated aqueous sodium bicarbonate solution (3.5 mL) was added. The reaction flask was immediately removed from the cooling bath and the mixture was diluted with an additional portion of ice-cold saturated aqueous sodium bicarbonate solution (1.5 mL) and diethyl ether (7.5 mL). The aqueous layer was separated and extracted with diethyl ether (2 × 6 mL). The combined organic phases were washed with ice-cold brine (3.5 mL), were dried over anhydrous sodium sulfate, were filtered, and were concentrated under reduced pressure to afford the pure *Z*-triisopropylsilyl enol ether **57** (33.2 mg, 100%) as a colorless oil.

^{1}H NMR (500 MHz, C_6D_6, 20 °C):	4.91 (q, 1H, J = 6.7 Hz), 3.31 (tdd, 1H, J = 10.7, 5.5, 3.8 Hz), 2.65–2.88 (m, 4H), 2.57 (ddd, 1H, J = 16.3, 6.0, 0.7 Hz), 2.37 (ddd, 1H, J = 16.3, 11.8, 6.9 Hz), 1.99 (dt, J = 11.6, 5.5 Hz, 1H), 1.92 (d, 3H, J = 6.7 Hz), 1.66 (ddddd, 1H, J = 13.7, 6.7, 4.1, 2.7, 0.7 Hz), 1.49–1.61 (m, 2H), 1.29–1.39 (m, 1H), 1.37 (t, 3H, J = 7.5 Hz), 0.82 (tdd, 1H, J = 12.7, 10.7, 2.7 Hz).
^{13}C NMR (125 MHz, C_6D_6, 20 °C):	148.2, 129.3, 121.7, 119.1, 116.7, 104.6, 55.6, 37.5, 30.4, 25.9, 23.0, 21.1, 19.9, 18.7, 16.2, 14.3, 12.3.
FTIR (neat) cm^{-1}:	2943 (s), 2865 (s), 1661 (s, C=C), 1463 (s), 1060 (s).
HRMS (ESI):	calcd for $C_{24}H_{42}NOSi$ $[M+H]^+$: 388.3030, found: 388.3046.

TLC (alumina gel, 10% EtOAc–hexanes), *Rf*: 0.72 (UV, CAM).

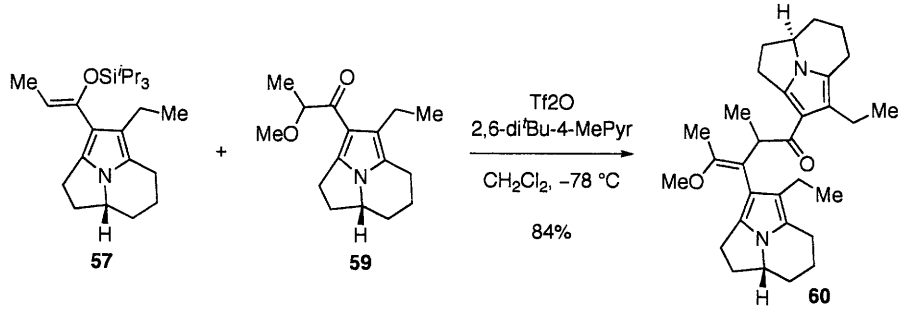

1,3-Bis-(1-ethyl-3,4,4a,5,6,7-hexahydro-pyrrolo[2,1,5-*cd*]indolizin-2-yl)-4-methoxy-2-methyl-pent-3-en-1-one (60):

A solution of 2,6-di-*tert*-butyl-4-methylpyridine (377 mg, 1.84 mmol, 5.00 equiv) in dichloromethane (500 μL + 250 μL rinse) was added to an anhydrous solution of triisopropylsilyl enol ether **57** (160 mg, 413 μmol, 1.13 equiv) and the α-methoxyketone **59** (96.0 mg, 367 μmol, 1 equiv, mixture of C9 epimers, 5:2 dr) in dichloromethane (2.50 mL) at 23 °C and the resulting solution was cooled to –78 °C. Trifluoromethanesulfonic anhydride (Tf_2O, 31.0 μL, 184 μmol, 0.500 equiv) was added dropwise via syringe, causing the solution to become opaque and deep burgundy within 90 seconds. After 30 min, three additional portions of trifluoromethanesulfonic anhydride (31.0 μL, 184 μmol, 0.500 equiv) were added in 30 min intervals. When 40 min had elapsed after the last addition, saturated aqueous sodium bicarbonate solution (1.5 mL) was added and the aqueous phase was allowed to freeze (<5 seconds), and the reaction flask was removed from the cooling bath. After approximately 5 min at 23 °C the biphasic mixture was diluted with ethyl acetate (15 mL) and an additional portion of saturated aqueous sodium bicarbonate solution (5 mL) and water (1.5 mL). The aqueous layer was separated and extracted with ethyl acetate (3 × 7.5 mL). The combined aqueous phases were washed with brine (5 mL), were dried over anhydrous sodium sulfate, and were filtered. Benzene (5 mL) was added to the organic phase and it was concentrated to a deep burgundy solution (final volume approximately 250 μL). This sample was directly subjected to flash column chromatography on silica gel (eluent: 2% triethylamine, 2% ethyl acetate, and 5% dichloromethane in hexanes, then flushed with 5% triethylamine in ethyl acetate to recover any remaining α-methoxy ketone, diameter: 3.0 cm, height: 25 cm) to afford the desired heterodimer **60** (142 mg, 84%, mixture of stereoisomers, 3:2:1 dr) as a pale orange oil.

^{1}H NMR (500 MHz, C_6D_6, 20 °C, 3:2:1 dr) 4.06 (q, J = 7.0 Hz, 1H), 4.04 (q, J = 7.0 Hz, 1H), 4.04 (q, J = 7.0 Hz, 1H), 3.24 (s, 3H), 3.24 (s, 3H), 3.24 (s, 3H), 3.09–3.46 (m, 6H), 2.30–3.09 (m, 36H), 2.14–2.25 (m, 6H), 2.09 (s, 3H), 2.07 (s, 3H), 2.03 (s, 3H), 1.75 (d, J = 7.0 Hz, 3H), 1.74 (d, J = 7.0 Hz, 3H), 1.72 (d, J = 7.0 Hz, 3H), 1.33–1.97 (m, 24H), 1.15–1.30 (m, 18H), 0.73–1.02 (m, 6H).

^{13}C NMR (125 MHz, C_6D_6, 20 °C, 3:2:1 dr): 196.0, 195.6, 195.9, 150.7, 150.6, 150.5, 136.5, 136.3, 136.3, 130.6, 130.3, 129.6, 126.8, 126.6, 126.4, 126.4, 126.4, 126.4, 123.0, 122.9, 122.8, 120.3, 120.3, 120.2, 118.2, 118.2, 118.1, 117.9,

	117.8, 117.7, 113.2, 113.1, 112.4, 56.6, 56.6, 56.5, 56.1, 56.1, 55.9, 55.8, 55.7, 55.7, 48.7, 48.6, 47.9, 37.5, 37.4, 37.4, 36.6, 36.5, 36.3, 30.6, 30.4, 30.3, 30.1, 30.0, 30.0, 28.1, 28.0, 27.6, 26.7, 26.5, 26.3, 23.4, 23.4, 23.3, 22.9, 22.9, 22.8, 21.9, 21.8, 21.8, 20.1, 20.1, 20.0, 20.0, 20.0, 20.0, 20.0, 20.0, 19.9, 17.9, 17.6, 17.6, 16.5, 16.1, 16.0, 16.0, 15.8, 15.8, 15.6, 15.4, 15.2.
FTIR (neat) cm^{-1}:	2928 (s), 1643 (s, C=O), 1496 (s), 1427 (s), 1321 (m).
HRMS (ESI):	calcd for $C_{31}H_{43}N_2O_2$ $[M+H]^+$: 475.3319, found: 475.3316.

TLC (Et_3N–pretreated silica gel, 1% Et_3N, 9% EtOAc–hexanes), *Rf*: 0.31 (UV, CAM).

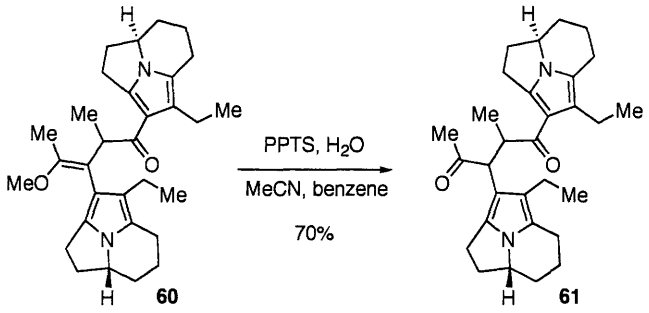

1,3-Bis-(1-ethyl-3,4,4a,5,6,7-hexahydro-pyrrolo[2,1,5-*cd*]indolizin-2-yl)-2-methyl-pentan-1,4-dione (61):

To a degassed solution (argon purge, 15 min) of methyl ether **60** (140 mg, 304 μmol, 1 equiv) in benzene (10.0 mL) was added a degassed solution (argon purge, 15 min) of pyridinium *p*-toluenesulfonic acid (PPTS, 115 mg, 456 μmol, 1.50 equiv) and deionized water (H_2O, 15.0 μL, 832 μmol, 2.74 equiv) in acetonitrile (1.00 mL). The resulting deep orange fine suspension was sonicated for 30 min, then saturated aqueous sodium bicarbonate solution (15 mL) was added and the mixture was diluted with ethyl acetate (25 mL). The aqueous phase was separated and extracted with ethyl acetate (3 × 20 mL). The combined organic phases were washed with brine (12.5 mL) and were dried over anhydrous sodium sulfate, were filtered, and were concentrated under reduced pressure. The red residue was purified by flash column chromatography on silica gel (eluent: 1% triethylamine and 17.5 → 35% ethyl acetate in hexanes, diameter: 2.5 cm, height: 24 cm) to provide the air-sensitive diketone **61** (94.5 mg, 70%, nearly equal mixture of stereoisomers) as an off-white solid.

^{1}H NMR (500 MHz, C_6D_6, 20 °C, mixture of 4 stereoisomers, 1.20:1:1.20:1.22 dr): 4.62 (d, J = 10.9 Hz, 1H, C3–H), 4.56 (d, J = 10.5 Hz, 1H, C3–H), 4.46 (d, J = 10.4 Hz, 1H, C3–H), 4.38 (d, J = 10.4 Hz, 1H, C3–H), 3.95–4.14 (m, 4H), 1.80–3.50 (m, 64H), 2.16 (s, 3H, C10–H), 2.11 (s, 3H, C10–H), 2.08 (s, 3H, C10–H), 2.02 (s, 3H, C10–H), 1.20–1.70 (m, 60H), 0.54–1.18 (m, 16H).

^{13}C NMR (125.8 MHz, C_6D_6, 20 °C, mixture of 4 stereoisomers, 1.20:1:1.20:1.22 dr): 207.8, 207.2, 206.4, 206.3, 200.0, 199.9, 198.1, 198.0, 137.4, 137.4, 136.8, 136.7, 129.3, 129.0, 128.9, 128.0, 126.4, 126.2, 126.2, 125.8, 122.8, 122.6, 122.2, 122.2, 120.9, 120.8, 120.8, 120.7, 119.4, 119.4, 119.3, 119.1, 118.0, 117.4, 117.0, 116.8, 110.8, 110.3, 109.8, 109.4, 56.0, 55.9, 55.9, 55.9, 55.6, 55.4, 55.4, 55.2, 53.1, 52.6, 52.4, 52.4, 46.6, 46.2, 46.0, 45.2, 37.4, 37.4, 37.3, 37.3, 36.7, 36.2, 36.1, 36.0, 30.6, 30.4, 30.1, 30.0, 30.0, 29.9, 29.7, 29.7, 29.6, 29.5, 28.7, 28.6, 28.4, 28.4, 26.5, 25.7, 23.1, 23.1, 23.1, 22.9, 22.9, 22.8, 22.7, 22.7, 22.5, 21.1, 21.0, 21.0, 21.0, 20.3, 20.2, 20.1, 20.1, 20.1,

	19.9, 19.9, 19.9, 19.2, 19.2, 19.0, 19.0, 18.9, 18.7, 18.5, 18.0, 17.8, 17.1, 17.0, 16.7, 16.7, 16.4, 16.4, 16.4, 16.3, 16.2, 16.2.
FTIR (neat) cm^{-1}:	2928 (s, C–H), 1706 (s, C=O), 1641 (s, C=O), 1497 (s), 1428 (s), 1321 (s), 1167 (m).
HRMS–ESI (*m/z*):	calcd for $C_{30}H_{41}N_2O_2$ $[M+H]^+$: 461.3163, found: 461.3149.

TLC (1% Et_3N, 20% EtOAc–hexanes), *Rf*: 0.33 (UV, CAM).

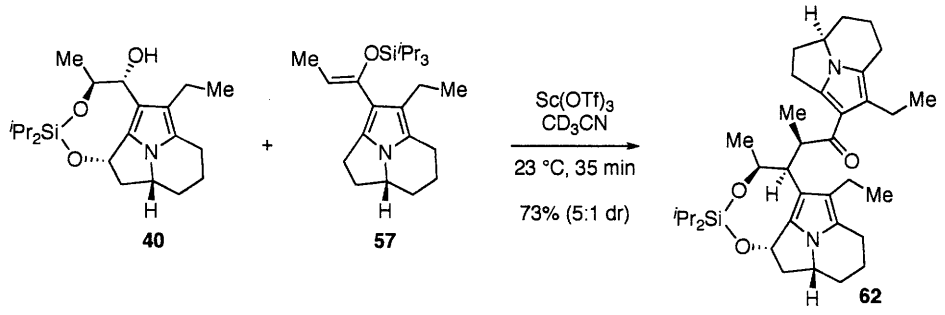

Heterodimer 62:

A solution of scandium trifluoromethanesulfonate ($Sc(OTf)_3$, 0.153 mg, 0.310 μmol, 0.0250 equiv) in acetonitrile–d_3 (35.0 μL) was added to an anhydrous solution of triisopropylsilyl enol ether **57** (7.1 mg, 19.3 μmol, 1.56 equiv) and alcohol **40** (4.7 mg, 12.4 μmol, 1 equiv) in acetonitrile–d_3 (550 μL) in a sealed, argon-purged NMR tube, producing an intense yellow color. After 20 min, an additional portion of scandium trifluoromethanesulfonate (0.305 mg, 0.620 μmol, 0.0500 equiv) was added. When 10 min had elapsed since the last portion of scandium trifluoromethanesulfonate was added, ^{1}H NMR showed complete consumption of alcohol **40**. The sample was poured into a vigorously stirring mixture of water, saturated aqueous sodium bicarbonate solution, and diethyl ether (3:1:5, 9 mL), and the aqueous phase was separated and extracted with diethyl ether (3 × 5 mL). The combined organic phases were washed with brine (5 mL), were dried over anhydrous sodium sulfate, were filtered, and were concentrated under reduced pressure. This crude residue was purified by flash column chromatography on silica gel (eluent: 3.5% triethylamine and 10% ethyl acetate in hexanes, diameter: 1.0 cm, height: 3.5 cm) to give the heterodimer **62** (5.3 mg, 73%) as a pale yellow oil.

^{1}H NMR (500 MHz, C_6D_6, 20 °C, 5:1 dr, values are for the major diastereomer): 5.48 (t, J = 6.7 Hz, 1H, C4–H), 4.59 (qd, J = 6.4, 0.6 Hz, 1H, C9–H), 4.15 (dd, J = 9.1, 0.7 Hz, 1H, C3–H), 4.04 (dq, J = 9.0, 7.3 Hz, 1H, C2–H), 3.13–3.33 (m, 3H, C3'–H_c, C11'–H, C5a–H), 2.91–3.13 (m, 3H, C4a'–H, C11'–H, C11–H), 2.67–2.74 (m, 2H, C5–H_c, C11–H), 2.51 (dd, J = 16.3, 5.9 Hz, 1H, C8–H_t), 2.39–2.45 (m, 2H, C3'–H_t, C7'–H_c), 2.33 (ddd, J = 15.9, 11.8, 6.4 Hz, 1H, C8–H_c), 2.19 (ddd, J = 16.4, 11.8, 6.6 Hz, 1H, C7'–H_t), 2.10 (ddd, J = 12.1, 10.3, 6.7 Hz, 1H, C5–H_t), 1.96–2.01 (m, 2H, C4'–H_c, C5–H_t), 1.60–1.66 (m, 1H, C7–H_t), 1.55 (t, J = 7.4 Hz, 3H, C12'–H), 1.50 (d, J = 6.6 Hz, 3H, C10–H), 1.44–1.57 (m, 3H, C6'–H_t, C6–H_c, C4'–H_t), 1.35 (t, J = 7.5 Hz, 3H, C12–H), 1.26 (d, J = 7.4 Hz, 3H, C10'–H), 1.26–1.37 (m, 2H, C5'–H_c, C7–H_c), 1.09–1.22 (m, 2H, C6'–H_c, C6–H_t), 1.08 (d, J = 7.4 Hz, 3H, $SiCH(CH_3)_3$), 1.00 (d, J = 6.9 Hz, 3H, $SiCH(CH_3)_3$), 0.97 (d, J = 7.5 Hz, 3H,

$SiCH(C\mathbf{H}_3)_3$), 0.87–0.99 (m, 3H, $SiC\mathbf{H}(CH_3)_3$), 0.69–0.77 (m, 1H, C5'–H_t).

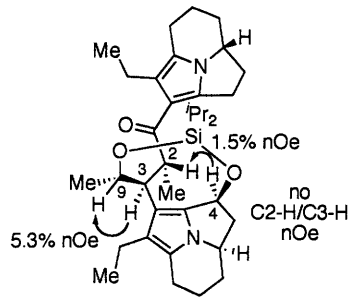

62

nOe data (500 MHz, C_6D_6, 20 °C):

HRMS–ESI (*m/z*): calcd for $C_{36}H_{54}N_2O_3SiNa$ $[M+Na]^+$: 613.3796, found: 613.3777.

TLC (Et_3N–pretreated silica gel, 2.5% Et_3N, 5% EtOAc–hexanes), *Rf*: 0.26 (UV, CAM).

NOESY Correlations for heterodimers **43** and **49**.

Proton signal	NOESY correlations	
	43	**49**
C1–H	C4–H, C10'–CH_3, C11'–CH_2	C4–H, C9–H, C10'–CH_3
C2–H	C3–H, C10'–CH_3	C3–H, C10'–CH_3
C3–H	C2–H, C9–H, C10–CH_3	C2–H, C10–CH_3, C12–CH_3
C4–H	C1–H, C5a–H, C5–H_c/C5–H_t	C1–H, C5–H_c, C9–H
C5–H_c	C4–H, C5a–H[a]	C4–H, C5a–H, C5–H_t
C5–H_t		C4–H, C5–H_t, C6–H_t
C5a–H	C4–H, C5–H_c/C5–H_t	C5–H_c, C6–H_c
C6–H_c	C5a–H, C6–H_t, C7–H_c/C7–H_t	C5a–H, C6–H_t, C7–H_c
C6–H_t	C6–H_c, C7–H_c/C7–H_t	C5–H_t, C6–H_c, C7–H_t
C7–H_c	C6–H_c, C6–H_t, C8–H[b]	C6–H_c, C7–H_t, C8–H
C7–H_t		C6–H_t, C7–H_c
C8–H	C7–H_c/C7–H_t, C11–H	C7–H_c, C11–CH_2, C12–CH_3
C9–H	C3–H, C10–CH_3	C1–H, C4–H, C10–CH_3, C10'–CH_3
C10–CH_3	C3–H, C9–H	C3–H, C9–H, C10'–CH_3
C11–H	C8–H, C12–CH_3	C8–H, C12–CH_3[c]
C11–H'	C12–CH_3	
C12–CH_3	C11–H	C3–H, C11–CH_2
C10'–CH_3	C1–H, C2–H	C1–H, C2–H, C10–CH_3
C3'–H_c	C3'–H_t, C4'–H_c	C3'–H_t, C4'–H_c
C3'–H_t	C3'–H_c, C4'–H_t	C3'–H_c, C4'–H_t
C4'–H_c	C3'–H_c, C4'–H_t, C4a'–H	C3'–H_c, C4a'–H, C4'–H_t
C4'–H_t	C3'–H_t, C4'–H_c	C3'–H_t, C4'–H_c
C4a'–H	C4'–H_c, C5'–H_c, C6'–H_c	C4'–H_c, C5'–H_c, C6'–H_c
C5'–H_c	C4a'–H, C6'–H_c, C6'–H_t	C4a'–H, C6'–H_t
C5'–H_t	C5'–H_c, C6'–H_t	C5'–H_c, C6'–H_t
C6'–H_c	C4a'–H, C6'–H_t, C7'–H_c	C4a'–H, C6'–H_t, C7'–H_c
C6'–H_t	C6'–H_c, C7'–H_t	C5'–H_c, C5'–H_t, C6'–H_c, C7'–H_t
C7'–H_c	C6'–H_c, C7'–H_t	C6'–H_c, C6'–H_t, 7't
C7'–H_t	C6'–H_t, C7'–H_c	C7'–H_c
C11'–CH_2	C1–H, C12'–CH_3	C12'–CH_3
C12'–CH_3	C11'–CH_2	C11'–CH_2

[a]Signals for protons C5–H_c and C5–H_t overlap in the ^{1}H NMR spectrum of **43**. [b]Signals for protons C7–H_c and C7–H_t overlap in the ^{1}H NMR spectrum of **43**. [c]Signals for protons C11–H and C11–H' overlap in the ^{1}H NMR spectrum of **49**.

Summary of key correlations:

Key correlations for assignment of C1, C2, C3 stereochemistry of heterodimer **43**:

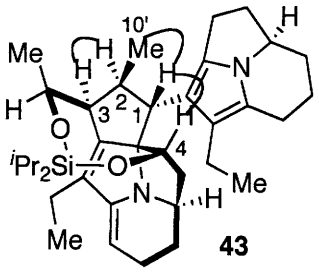

43

Key correlations for assignment of C9 stereochemistry of heterodimer **43**:

no C9–H/C10'–CH_3 correlation

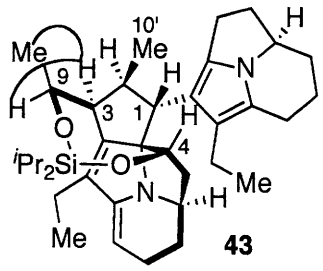

43

Key correlations for assignment of C1, C2, C3 stereochemistry of heterodimer **49**:

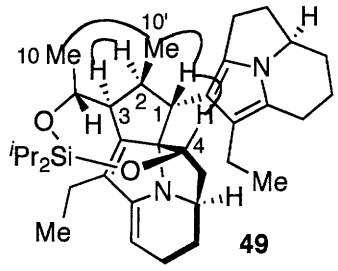

49

Key correlations for assignment of C9 stereochemistry of heterodimer **49**:

no C3–H/C9–H correlation

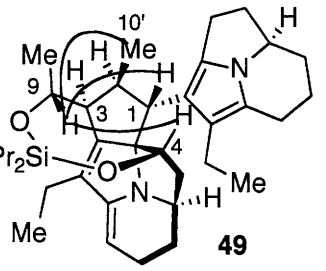

49

Chapter V.

Reversible Dimerization of (+)-Myrmicarin 215B

Introduction and Background

The myrmicarins are a family of air sensitive alkaloids isolated from the poison gland of the African ant species *Myrmicaria opaciventris*. Detailed spectroscopic studies by Schröder, Francke, and coworkers have revealed the relative stereochemistry of myrmicarins 430A and 663 (**M430A** and **M663**, Figure 1), while the stereochemistry of myrmicarin 645 (**M645**) remains unknown.[1] Significantly, the extreme air sensitivity of **M430A** required its characterization as a *crude* isolation mixture using phase-sensitive 2D-NMR techniques.[2] The challenges offered by their elaborate and highly air sensitive structures and the lack of information regarding their specific mode of biological action inspired us to embark on their study. Specifically, we envisioned that the complex myrmicarins could be assembled through potentially biomimetic dimerization or trimerization of the tricyclic myrmicarins. Herein we report the first experimental evidence for the reversible dimerization of (+)-myrmicarin 215B (**M215B**) and discuss mechanistic studies that provide a more detailed understanding of the reactivity of this natural alkaloid toxin.

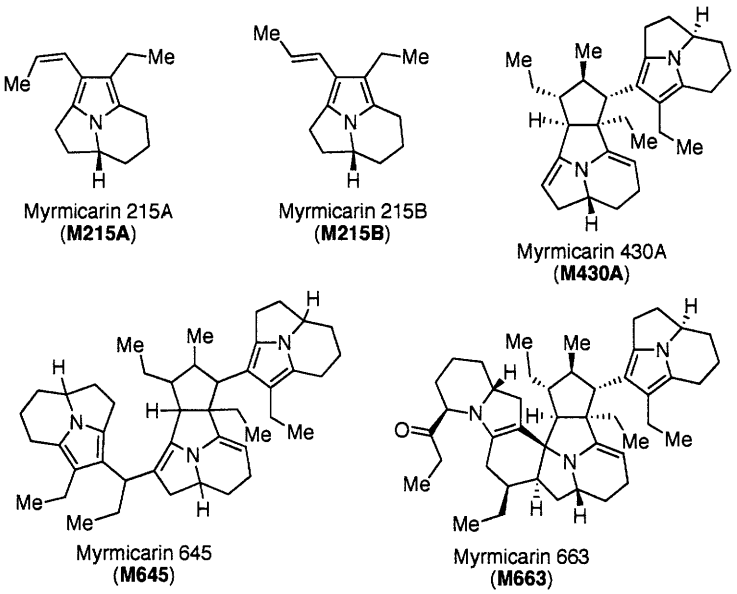

Figure 1. Representative myrmicarin alkaloids.

Results and Discussion

In 2005 we disclosed a highly efficient and diastereoselective Brønsted acid-promoted dimerization of (+)-**M215B** to yield the heptacyclic structure of isomyrmicarin 430A

(**isoM430A**, Equation 1).[3] To determine the influence of the reaction conditions on the rate, reversibility, and products of this dimerization, we examined the acid-promoted chemical reactivity of (+)-**M215B** in a range of different Brønsted acids, solvents, and additives.[4] The

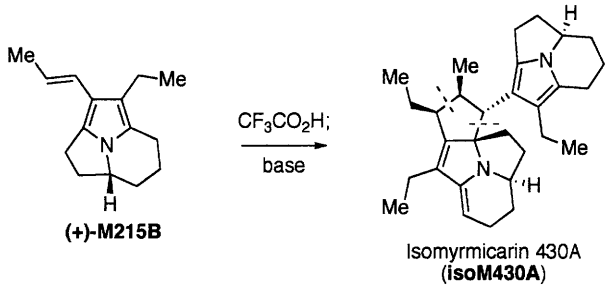

(1)

rapid formation of **isoM430A** as the sole product without visible intermediacy of other dimeric or tricyclic compounds motivated us to identify a gradual, non-invasive method of introducing the Brønsted acid that would be compatible with *in situ* analysis of highly air sensitive dimeric compounds. Reports describing slow photochemical generation of hydrochloric acid from dichloromethane upon ultraviolet irradiation suggested a possible technique that would satisfy these requirements.[5] Use of deuterated dichloromethane as solvent would enable us to use *in situ* ^{1}H NMR monitoring and deuterium incorporation as mechanistic probes to study the Brønsted acid-promoted dimerization of (+)-**M215B**.

An initial experiment demonstrated that irradiation of a sample of water–dichloromethane (7% v/v) using a medium–pressure mercury UV lamp afforded an aqueous layer at a pH of approximately 3, indicating the presence of photochemically generated acid.[6] When we applied this technique in our own study, *in situ* monitoring by ^{1}H NMR revealed that irradiation of a rigorously degassed dichloromethane-d_2 solution of (+)-**M215B** yielded the **isoM430A** precursor **1** (Scheme 1) as the sole product after two hours of irradiation. Irradiation for an additional ten hours caused gradual conversion to the C1, C2 isomeric heptacycle **2**.[7]

In order to perform rigorous structural analysis of this new dimeric compound we attempted to isolate a neutral derivative. We anticipated that use of our reported techniques for isolation and derivatization of highly air sensitive dimeric pyrroloindolizines would provide samples for comparison with reported myrmicarin and isomyrmicarin structures.[8] Rapid filtration of the reaction mixture containing **2** through triethylamine-pretreated silica gel furnished a new heptacyclic structure (Scheme 1). While this exceptionally fragile compound

underwent complete decomposition within approximately four hours,[9] analysis of freshly prepared samples using two-dimensional NMR techniques revealed that the heptacycle had the same connectivity as **isoM430A**.

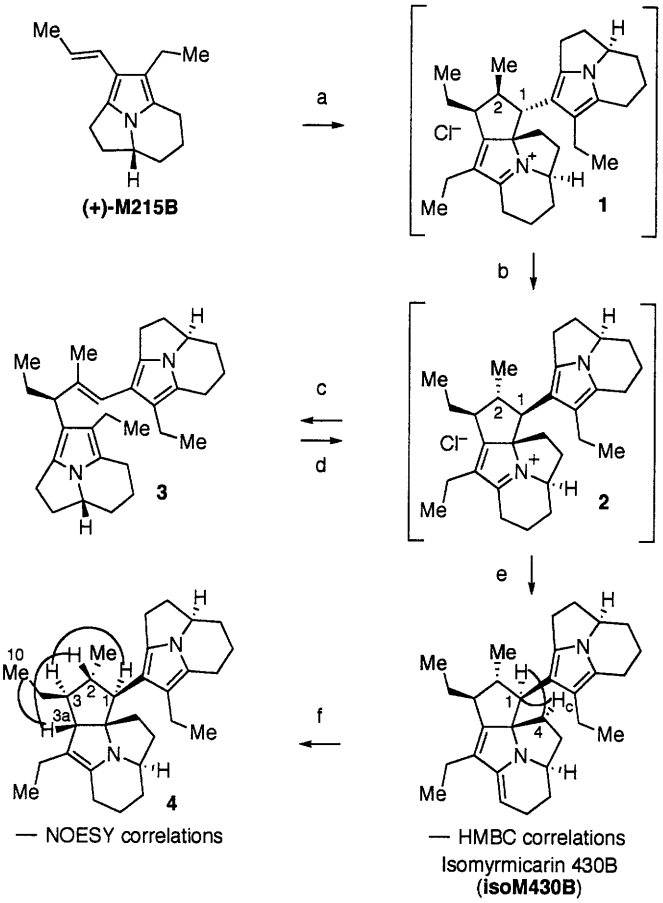

Scheme 1. Dimerization of **M215B** upon photochemical generation of HCl. Conditions: a) hv, CD_2Cl_2, 23 °C, 2 h. b) hv, CD_2Cl_2, 23 °C, 10 h. c) Al_2O_3, 60%, 5:4 *E*:Z. d) hv, CD_2Cl_2, 23 °C, 1 h. e) Et_3N, SiO_2, 66%. f) H_2, Pd/C, C_6H_6, 23 °C, 40%.

Specifically, reciprocal C1/C4–H_c and C4/C1–H HMBC correlations established the regiochemistry of the cyclopentannulation. To emphasize the analogy between the connectivity of this dimer and that of **isoM430A**, we termed this heptacyclic diene isomyrmicarin 430B (**isoM430B**). To confirm the stereochemistry of this exceedingly unstable compound, a freshly generated sample was immediately treated with dihydrogen in the presence of catalytic palladium on carbon, a procedure that we had developed for derivatization of the similarly unstable **isoM430A**.[3a] The resulting enamine **4** could be purified by chromatography and was stable over a period of days in degassed benzene-d_6. Strong C3a–H/C2–H and C1–H/C3–H

correlations revealed that the configuration of the C1 and C2 positions was inverted relative to **isoM430A**, while a C3a–H/C10–H NOESY correlation showed that the **isoM430A** stereochemistry at C3 was maintained.

By contrast, filtration of the reaction mixture containing the iminium ion **2** through basic alumina gel caused fragmentation to alkene **3** as a variable (1:0 to 1:1) mixture of *E*/*Z* isomers in yields of 40-60% (Scheme 1). Interestingly, irradiation of a dichloromethane solution of **3** as a mixture of isomers in any proportion directly produced **2** within one hour (Scheme 1).[7]

As an additional probe to study the mechanism of formation of **isoM430B** we sought to perform deuterium incorporation studies. For this purpose, known quantities of deuterium oxide (D_2O) were included in the reaction medium to override the effect of exchange between photochemically generated deuterium chloride and adventitious protium sources.[10] Under these conditions irradiation of a D_2O–dichloromethane-d_2 (7% v/v) solution of (+)-**M215B** for six hours yielded a dimeric structure showing three sites of deuterium incorporation (Scheme 2).[11]

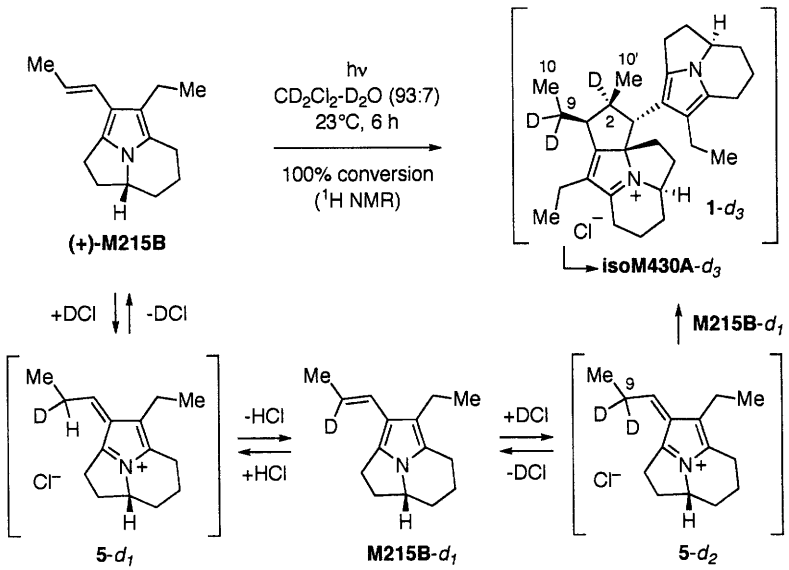

Scheme 2. Deuterium incorporation in **isoM430A**.

While the remainder of the ^{1}H NMR spectrum matched that of the undeuterated iminium ion **1**, the splitting pattern induced by coupling to the C2 and C9 protons in the C10′ and C10 methyl signals, respectively, was absent. This result indicated that rapid equilibrium between (+)-**M215B** and the tricyclic azafulvenium ion **5** had resulted in full deuterium incorporation at C9 in

both of the tricyclic dimerization partners, which appeared as deuterium incorporation at the corresponding C2 and C9 positions in the **isoM430A** heptacycle.

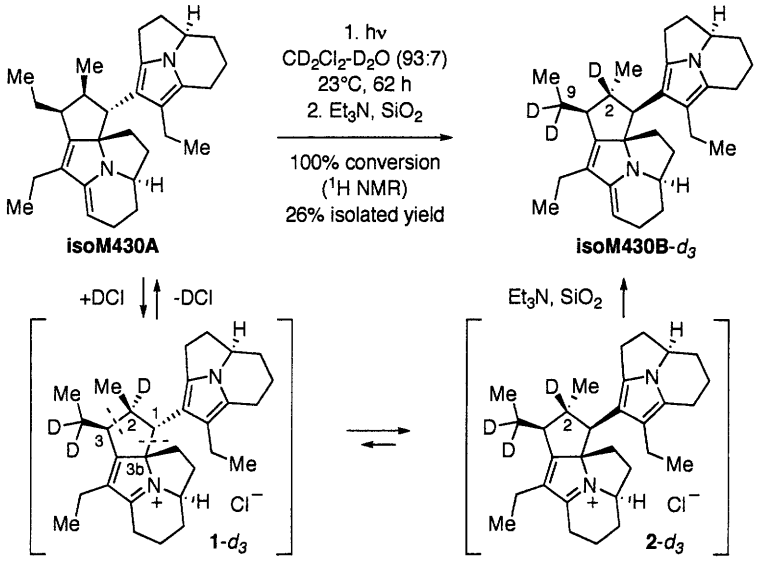

Scheme 3. Deuterium incorporation in **1** and **isoM430B**

Interestingly, irradiation of **isoM430A** in D_2O- dichloromethane-d_2 (7% v/v) for 62 hours resulted in the formation of the **isoM430B** heptacycle showing three sites of deuteration (Scheme 3).[12] In this case, full deuterium incorporation had again occurred at C2 and at both positions of the C9 methylene group. Monitoring of the reaction *in situ* by ^1H NMR showed that the **isoM430A** stereochemistry was maintained throughout full deuterium incorporation at C2 and C9, whereupon slow isomerization yielded **isoM430B**. Deuterium incorporation at C9 in these heptacycles is consistent with fragmentation of the dimeric structure to tricyclic azafulvenium ions, which would again be subject to rapid H/D exchange at C9 (Scheme 2). Significantly, this provided the first evidence that an equilibrium process involving formation of the **isoM430A** heptacycle may encompass reversible formation of both the first and the second bond of the dimerization.

By contrast, irradiation of a dichloromethane-d_2 solution of hexacyclic alkene **3** for 20 hours in the presence of D_2O directly produced the **isoM430B** heptacycle exhibiting complete deuterium incorporation at C2 only (Equation 2). The failure of **3** to incorporate deuterium at C9 suggests that it did not detectably interconvert with tricyclic azafulvenium ions over the period of irradiation.

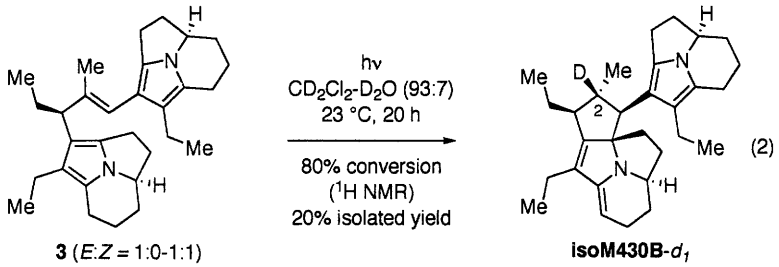

(2)

Furthermore, irradiation of a D_2O-dichloromethane-d_2 solution of **isoM430B** for 67 hours effected no deuterium incorporation at C2 or C9, suggesting that it did not appreciably fragment to either hexacyclic or tricyclic azafulvenium ions on this timescale.

Cumulatively, these results suggest a mechanism in which trace quantities of photochemically generated hydrochloric acid promote reversible dimerization of (+)-**M215B** (Scheme 4). Initial dimerization produces hexacyclic azafulvenium ion **6** with the **isoM430A**

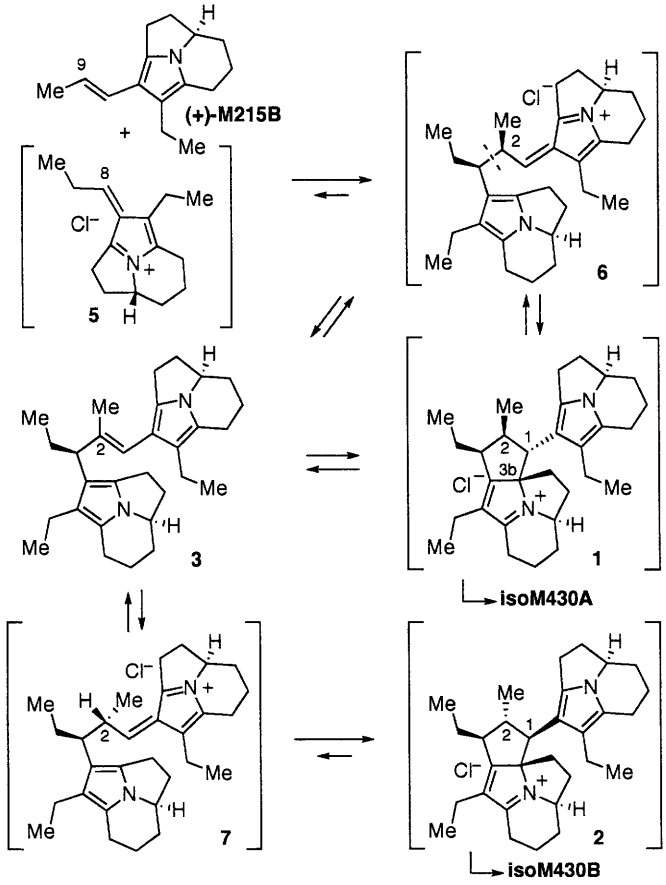

Scheme 4. Proposed mechanism for reversible dimerization of **M215B** in the presence of photochemically generated H(D)Cl.

stereochemistry at C2, which cyclizes to heptacycle **1**. Rupture of the C1-C3b bond of the iminium ion could regenerate azafulvenium ion **6**, and fragmentation of this structure would produce tricyclic azafulvenium ion **5**. Alternatively, **6** may undergo deprotonation at C2 to form alkene **3**. Protonation of this alkene from the opposite face would provide azafulvenium ion **7** with the **isoM430B** configuration at C2. Significantly, the failure of **3** to detectibly interconvert with tricyclic azafulvenium ions suggests that fragmentation is slow relative to interconversion between dimeric structures.[13] Rapid cyclization of **7** would generate the C1,C2-*trans*, C2, C3-*trans* substituted heptacycle **2** as the thermodynamic product. Interestingly, the cyclopentane substituents in **M430A** also exhibit a C1,C2-*trans*, C2,C3-*trans* substitution pattern, consistent with a possibility that **M430A** may also be a thermodynamic product in an equilibrium process.

Although the C1 and C2 stereocenters in the **isoM430A** structure were subject to variation, neither the stereochemistry at C3 nor the connectivity of the cyclopentane ring was altered. The invariance of the **isoM430A** configuration at C3 and the **isoM430A** connectivity raised the possibility that the C3 stereochemistry established in the first bond formation may influence the regiochemistry of subsequent pyrrole alkylation. To examine this possible relationship we prepared the C3 unsubstituted hexacyclic alcohol **8** as a 1:1 mixture of C2 epimers (Scheme 5).

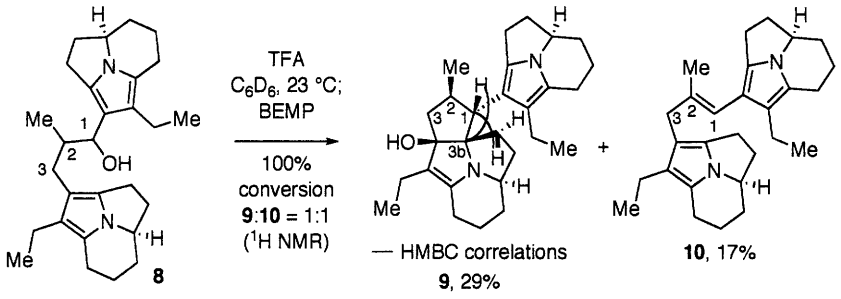

Scheme 5. Cyclization of **8**.

In situ monitoring by ^{1}H NMR demonstrated that ionization of the C1 alcohol upon treatment of a benzene-d_6 solution of **8** with 1.10 equivalents of trifluoroacetic acid followed by addition of 2-*tert*-butylimino-2-diethylamino-1,3-dimethyl-perhydro-1,3,2-diazaphosphorine (BEMP) under inert atmosphere afforded a 1:1 mixture of the **isoM430A** derivative **9** and the alkene **10**. Careful chromatographic separation of these highly sensitive compounds provided pure samples of **9** and **10** for full structural analysis. The generation of a single heptacyclic

structure and the failure to observe products with the **M430A** connectivity in the absence of a C3 substituent strongly indicate that the **isoM430A** configuration at the C3 ethyl group is not necessary to direct C3b alkylation.

Conclusion

Mechanistic investigation into the formation of **isoM430B** yielded the first experimental evidence for fully reversible dimerization of (+)-**M215B**. *In situ* ^{1}H NMR monitoring of the chemistry of highly sensitive dimeric structures, complemented by isolation of pure samples and derivatives for full spectroscopic analysis, provided detailed information about the intermediates involved in this process. Deuterium incorporation studies indicate that interconversion between isomyrmicarin structures can occur *via* fragmentation to tricylic intermediates, and establish that (+)-**M215B** dimerizes to afford distinct kinetic and thermodynamic products.

The sampling of different heptacyclic dimeric myrmicarin structures under equilibrium conditions demonstrates that dimerization of M215B is a dynamic process subject to influence by the reaction conditions. Variation in the structure of dimeric products raises the intriguing possibility that M430A may likewise arise as a component of a reversible equilibrium process involving other dimeric myrmicarins. Studies on the chemical reactivity of M215B may enable the identification of factors that facilitate the formation or trapping of M430A in the natural environment of the poison gland. Powerful techniques for isolation and characterization of dimeric products, combined with the ability to generate strategically functionalized dimeric pyrroloindolizines through directed heterodimerization, provide a means to target specific structural features that influence the products of these potential equilibria. In addition to presenting a succinct approach to the chemical synthesis of the complex myrmicarins, these studies provide key insight into their possible biosynthesis *via* direct dimerization or trimerization of the simple tricyclic structures.

---

[1] **M430A**: (a) Schröder, F.; Sinnwell, V.; Baumann, H.; Kaib, M. *Chem. Commun.* **1996**, *18*, 2139–2140. **M663** and **M645**: (b) Schröder, F.; Sinnwell, V.; Baumann, H.; Kaib, M.; Francke, W. *Angew. Chem. Int. Ed.* **1997**, *36*, 77–80. **M217**, **M215A**, and **M215B**: (c) Schröder, F.; Franke, S.; Francke, W.; Baumann, H.; Kaib, M.; Pasteels, J. M.; Daloze, D. *Tetrahedron* **1996**, *52*, 13539–13546.

[2] An isomeric myrmicarin 430 was identified during these studies but no structural data was reported (ref. 1a).

[3] (a) Ondrus, A. E.; Movassaghi, M. *Tetrahedron* **2005**, *62*, 5287–5297. For our enantioselective synthesis of **M215A**, **M215B**, and **M217**, see: (b) Movassaghi, M.; Ondrus, A. E. *Org. Lett.* **2005**, *7*, 4423–4426.

[4] Movassaghi, M.; Ondrus, A. E.; Chen, B. *J. Org. Chem.* **2007**, *72*, 10065–10074.

[5] For selected studies on the generation of hydrochloric acid from chlorinated solvents upon ultraviolet irradiation, see: (a) Scolaro, L. M.; Romeo, A.; Castriciano, M. A.; De Luca, G.; Patane, S.; Micali, N. *J. Am. Chem. Soc.* **2003**, *125*, 2040–2041. (b) Semeluk, G. P.; Unger, I. *Nature* **1963**, *198*, 853-855. (c) Alapi, T.; Dombi, A. *Chemosphere* **2007**, *67*, 693–701.

[6] Water was added to dissolve photochemically generated hydrochloric acid and maximize its capture.

[7] Irradiation of **M215B** in non-chlorinated solvents resulted in partial isomerization to **M215A**. See the Experimental Section for details.

[8] Attempts to prepare neutral or salt derivatives of complex myrmicarin and isomyrmicarin structures for X-ray crystallographic analysis have been unsuccessful (refs. 1c, 3b).

[9] Although samples of iminium salt **2** could be stored for up to three days without visible decomposition, the corresponding heptacyclic diene (**isoM430B**, Scheme 1) was subject to more rapid decomposition.

[10] For example, H/D exchange with trace moisture or acidic protons in dimeric azafulvenium or iminium structures. This exchange prevented detectable deuterium incorporation in reactions conducted in dichloromethane-d_2 alone.

[11] Rapid H/D exchange at C8 in **isoM430A** and **isoM430B** with trace water during filtration through silica gel prevented observation of potential deuterium incorporation.

[12] Potential intermediacy of **2** possessing deuterium incorporation at C2 alone could not be detected by ^{1}H NMR due to signal overlap.

[13] Although we did not observe evidence for fragmentation of **3**, this possibility (e.g. *via* **6** or **7**) cannot be ruled out.

Experimental Section

General Procedures. All reactions were performed in dry 5 mm o.d. NMR tubes for *in situ* reaction monitoring. The NMR tubes were fitted with rubber septa and reactions were conducted under a positive pressure of argon. Stainless steel syringes or cannulae were used to transfer air- and moisture-sensitive liquids. Flash column chromatography was performed as described by Still et al. using silica gel (60 Å pore size, 40-63 μm, 4-6% H_2O content, Zeochem).[1] Where necessary (noted), silica gel was neutralized by treatment of the silica gel prior to chromatography with the eluent containing 2.5% triethylamine. Analytical thin-layer chromatography was performed using glass plates pre-coated with 0.25 mm 230–400 mesh silica gel or alumina gel impregnated with a fluorescent indicator (254 nm). Where necessary (noted), silica gel plates were neutralized by treatment with a solution of 2.5% triethylamine in ethyl acetate followed by heating on a hot plate (~250 °C). Thin layer chromatography plates were visualized by exposure to ultraviolet light and/or by exposure to an aqueous solution of ceric ammonium molybdate (CAM) followed by heating (<1 min) on a hot plate (~250 °C). Organic solutions were concentrated on Büchi R-200 rotary evaporators at ~20 Torr at 25–35 °C unless otherwise indicated.

Materials. Commercial reagents and solvents were used as received. Dichloromethane-d_2 solutions were deoxygenated by alternate freeze (liquid nitrogen)/evacuation/argon-flush/thaw cycles (FPT, three iterations) and neutralized by stirring over potassium carbonate.

Instrumentation. Solutions were irradiated using a Hanovia 450-watt medium pressure mercury lamp at a distance of 7.0 cm from the lamp and a temperature of 23 °C. Proton nuclear magnetic resonance (^{1}H NMR) spectra were recorded with a Varian inverse probe 500 INOVA spectrometer or a Bruker inverse probe 600 Avance spectrometer. Chemical shifts are recorded in parts per million on the δ scale and are referenced from the residual protium in the NMR solvent (C_6D_5H: δ7.16). Data is reported as follows: chemical shift [multiplicity (s = singlet, d = doublet, t = triplet, q = quartet, m = multiplet, br = broad), coupling constant(s) in Hertz, integration, assignment]. Carbon-13 nuclear magnetic resonance (^{13}C NMR) spectra were recorded with a Varian 500 INOVA spectrometer. Chemical shifts are recorded in parts per million on the δ scale and are referenced from the carbon resonances of the solvent (C_6D_6: δ 128.4). Infrared data were obtained with a Perkin-Elmer 2000 FT-IR and are reported as follows: [frequency of absorption (cm^{-1}), intensity of absorption (s = strong, m = medium, w = weak, br = broad), assignment]. We are grateful to Dr. Li Li for obtaining the mass spectroscopic data at the Department of Chemistry's Instrumentation Facility, Massachusetts Institute of Technology. High-resolution mass spectra (HRMS) were recorded on a Bruker APEX 4.7 Tesler FTMS spectrometer using electronspray ion source (ESI).

Positional Numbering System. For direct comparison, the numbering scheme used for dimeric compounds is consistent with that used by Schröder and coworkers in the isolation paper for myrmicarin 430A[2] and that used previously by us for isomyrmicarin 430A.[3]

---

[1] Still, W. C.; Kahn, M.; Mitra, A. *J. Org. Chem.* **1978**, *43*, 2923–2925.
[2] Schröder, F.; Sinnwell, V.; Baumann, H.; Kaib, M. *Chem. Commun.* **1996**, *18*, 2139–2140.
[3] Ondrus, A. E.; Movassaghi, M. *Tetrahedron* **2005**, *62*, 5287–5297.

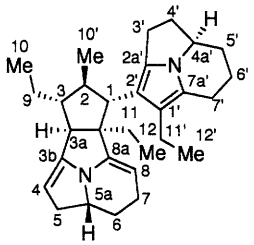

Myrmicarin 430A
(**M430A**)

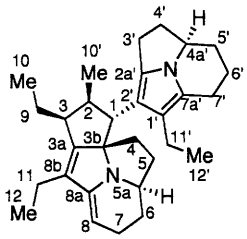

Isomyrmicarin 430A
(**isoM430A**)

Additional Notes.

*A) Supplementary notes on photochemical irradiation of **M215B**:*

- Irradiation of a solution of **M215B** in benzene, acetonitrile, or hexanes using a 450-watt medium-pressure mercury lamp effected partial isomerization to the **M215A** olefin isomer (Table S1).
- Irradiation of a methanolic solution of **M215B** provided both **M215A** and methanol adduct **S1** as a 1:1 mixture of diastereomers (Scheme S1).[4]
- **M215A** was not detected during irradiation of **M215B** in dichloromethane-d_2.

Table S1. Photochemical activation of **M215B**.[a]

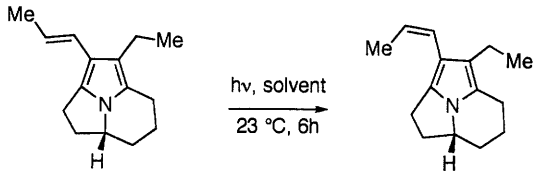

M215B **M215A**

solvent	product ratio M215A : M215B	isolated yield (%)[a]
CH_3CN	16 : 84	76
C_6H_6	33 : 67	93
hexanes	19 : 81	60

[a] Combined isolated yield; ratio determined by ^1H NMR.

Scheme S1.

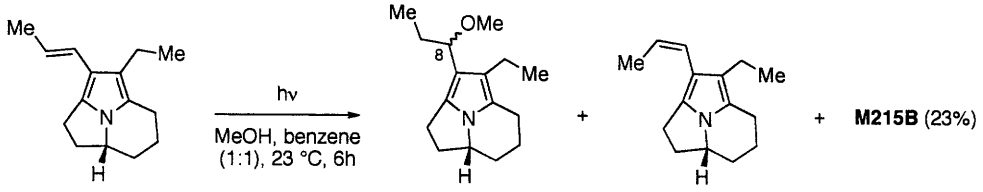

M215B **S1** (41%, 1:1 dr) **M215A** (23%)

*B) Supplementary notes on HCl-induced dimerization of **M215B**:*

Generation of HCl:

- Treatment of a dichloromethane-d_2 solution of **M215B** with hydrochloric acid (1.40 equiv) in the dark for 20 hours followed by filtration of the reaction mixture through triethylamine-pretreated silica gel provided **isoM430B** as the sole product in 30% yield.
- Irradiation of a dichloromethane-d_2 solution of **M215B** containing 1,8-diazabicyclo[5.4.0]undec-7-ene (DBU, 2.60 equiv) for 10 hours returned exclusively **M215B**.

[4] For examples of nucleophile addition to alkenes under photochemical irradiation, see: (a) Moran, J.; Cebrowski, P. H.; Beauchemin, A. R.; *J. Org. Chem.* **2008**, *73*, 1004–1007. (b) Shim, S. C.; Kim, D. S.; Yoo, D. J.; Wada, T.; Inoue, Y. *J. Org. Chem.* **2002**, *67*, 5718–5726. (c) Kropp, Paul J. *J. Am. Chem. Soc.* **1966**, *88*, 4091—4092. (d) Marshall, J. A.; Carroll, R. D. *J. Am. Chem. Soc.* **1966**, *88*, 4092–4093 For a discussion of photochemically induced reactions of cycloalkenes, see: Marshall, J. A. *Science* **1970**, *170*, 137–141.

- Irradiation of a dichloromethane-d_2 solution of **M215B** containing 2,2,6,6-tetramethyl-1-piperidinyloxy (TEMPO, 1.10 equiv) for 6 hours returned exclusively **M215B**.
- Reactions conducted in dichloromethane provided results identical to those conducted in dichloromethane-d_2, indicating that photochemical generation of HCl versus DCl did not influence the outcome or rate of these transformations to an observable extent.

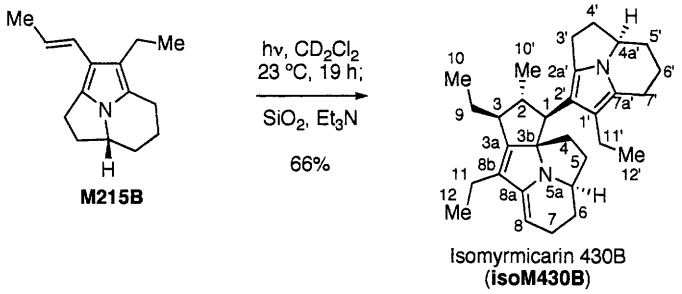

Isomyrmicarin 430B (isoM430B):

A sample of **M215B** (29.5 mg, 137 μmol, 1 equiv) in neutralized, degassed dichloromethane-d_2 was sealed in an NMR tube under an argon atmosphere and was irradiated at 23 °C for 19 h. The resulting deep brown reaction mixture was filtered through silica gel neutralized with triethylamine (2.5% Et_3N and 2.5% EtOAc in hexanes, diam. 1.5 cm, ht. 13 cm) to afford **isoM430B** (19.4 mg, 66%) as a pale yellow oil. Isolated samples of **isoM430B** undergo complete decomposition after approximately four hours in degassed benezene-d_6 at 20 °C.

Samples for spectroscopic analysis were prepared immediately and high quality data was acquired within two hours of isolation. Complete assignment was possible with the aid of additional information from gCOSY, HSQC, gHMBC, and NOESY.

^{1}H NMR (500 MHz, C_6D_6, 20 °C): 4.72 (dd, J = 7.3, 3.2 Hz, 1H, C8-H), 3.45 (dq, J = 9.6, 6.4 Hz, 1H, C5a–H), 3.22 (tdd, J = 10.5, 5.0, 3.6 Hz, 1H, C4a'–H), 3.09 (dq, J = 14.5, 7.3 Hz, 1H, C11'–H), 2.92 (d, J = 11.7 Hz, 1H, C1–H), 2.69 (dd, J = 14.3, 7.8 Hz, 1H, C3'–H_t), 2.54–2.64 (m, 3H, C3'–H_c, C11'–H', C7'–H_c), 2.42 (ddd, J = 15.4, 13.1, 8.1 Hz, 1H, C7'–H_t), 2.18–2.30 (m, 5H, C11–H, C2–H, C7–H_t, C3–H, C11–H'), 2.08–2.15 (m, 1H, C7–H_c), 2.02 (dt, J = 11.5, 5.7 Hz, 1H, C4'–H_c), 1.86 (dt, J = 11.4, 5.6 Hz, 1H, C4–H_c), 1.78–1.86 (m, 1H, C6–H_c), 1.48–1.68 (m, 8H, C9–H, C6'–H_t, C5–H_c, C9–H', C4'–H_t, C5'–H_c, C4–H_t, C5–H_t), 1.26–1.39 (m, 1H, C6'–H_c), 1.24 (t, J = 7.2 Hz, 3H, C12'–H), 1.22 (d, J = 6.8 Hz, 3H, C10'–H), 1.17 (t, J = 7.6 Hz, 3H, C12–H), 1.00–1.12 (m, 1H, C6–H_t), 1.03 (t, J = 7.6 Hz, 3H, C10–H), 0.89 (br q, J = 13.1 Hz, 1H, C5'–H_t).

^{13}C NMR (125 MHz, C_6D_6, 20 °C): 155.7 (C8a), 152.7 (C3a), 132.4 (C8b), 126.7 (C2a'), 124.4 (C1'), 118.6 (C7a'), 112.3 (C2'), 89.1 (C8), 88.2 (C3b), 56.3 (C5a), 55.1 (C4a'), 54.1 (C1), 48.4 (C2), 45.2 (C3), 37.8 (C4'), 36.1 (C5), 31.8 (C4), 30.5 (C5'), 30.4 (C6), 29.5 (C9), 27.5 (C3'), 23.2 (C6'), 22.6 (C7), 20.9 (C7'), 20.2 (C10'), 19.4

	(C11), 18.7 (C11'), 17.4 (C12'), 14.4 (C12), 13.5 (C10).
FTIR (thin film) cm^{-1}:	2929 (s), 1737 (w), 1642 (w), 1454 (m), 1372 (w), 1320 (w), 1167 (w).
HRMS (ESI):	calc'd for $C_{30}H_{43}N_2$ $[M+H]^+$: 431.3421, found: 431.3413.

TLC (2.5% Et_3N in [2.5% EtOAc in hexanes], Et_3N neutralized silica gel), *Rf*: 0.40 (UV, CAM).

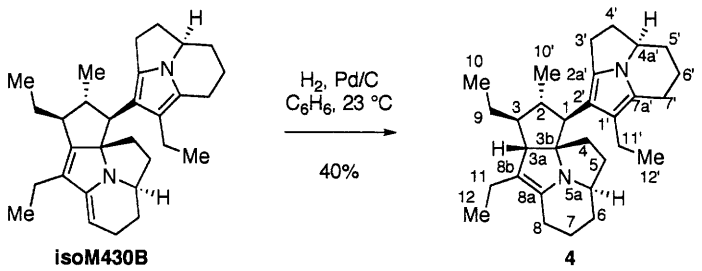

Heptacyclic Enamine 4:

A suspension of **isoM430B** (31.3 mg, 72.7 μmol, 1 equiv) and Pd (10% on activated carbon, 62.6 mg, 200 wt %) in benzene (2.50 mL) was stirred vigorously under a dihydrogen atmosphere (1 atm) at 23 °C for 25 min. The reaction mixture was filtered through a plug of celite (EtOAc, diam. 0.6 cm, ht. 5.5 cm) and the reaction flask and plug were rinsed with additional portions of EtOAc (3 × 3 mL). The clear yellow filtrate was concentrated under reduced pressure and the residue was purified by flash column chromatography (silica gel, 2.5% Et_3N, 1.5% EtOAc, and 1.5% CH_2Cl_2 in hexanes, diam. 1.5 cm, ht. 6 cm) to give **4** (12.7 mg, 40%) as a yellow oil. Samples of **4** in degassed benzene-d_6 undergo complete decomposition within four days at 20 °C.

High quality spectra were acquired within 24 hours of isolation. Complete assignment was possible with the aid of additional information from gCOSY, gHSQC, gHMBC, and gNOESY.

^{1}H NMR (600 MHz, C_6D_6, 20 °C): 3.31–3.37 (m, 1H, C4a'–H), 3.27 (d, J = 12.4 Hz, 1H, C1–H), 3.15 (m, 1H, C5a–H), 3.08 (dq, J = 14.4, 7.4 Hz, 1H, C11'–H), 2.96 (d, J = 8.9 Hz, 1H, C3a–H), 2.57–2.70 (m, 4H, C11'–H', C7'–H_c, C3'–H_c, C3'–H_t), 2.51 (ddd, J = 19.5, 15.3, 10.3 Hz, 1H, C7'–H_t), 2.34 (dt, J = 13.5, 4.5 Hz, 1H, C8–H_t), 2.19–2.28 (m, 2H, C11–H, C11–H'), 1.94–2.12 (m, 3H, C4'–H_c, C4–H_c, C8–H_c), 1.70–1.91 (m, 7H, C6–H_c, C2–H, C4'–H_t, C6'–H_t, C9–H, C9–H'), 1.50–1.70 (m, 3H, C3–H, C5'–H_c, C5–H_t), 1.33–1.46 (m, 4H, C6–H_t, C7–H_c, C4–H_t, C6'–H_c), 1.40 (t, J = 7.2 Hz, 3H, C12'–H), 1.19–1.30 (m, 1H, C7–H_t), 1.05–1.16 (m, 1H, C5–H_c), 1.15 (d, J = 6.6 Hz, 3H, C10'–H), 1.14 (t, J = 7.5 Hz, 3H, C12–H), 1.09 (t, J = 7.5 Hz, 3H, C10–H), 0.93 (br q, J = 12.2 Hz, 1H, C5'–H_t).

^{13}C NMR (125 MHz, C_6D_6, 20 °C): 139.3 (C8a), 127.8 (C2a'), 123.6 (C1'), 118.2 (C7a'), 115.7 (C8b), 115.0 (C2'), 82.5 (C3b), 63.4 (C3a), 59.9 (C5a), 57.0 (C1), 55.2 (C4a'), 54.3 (C3), 44.2 (C2), 38.0 (C4'), 35.8 (C4), 30.3 (C5'), 29.4 (C5), 27.4 (C6), 26.9 (C3'), 25.3 (C9), 24.5 (C8), 23.2

	(C6'), 21.1 (C7'), 21.0 (C7), 19.9 (C11), 19.0 (C11'), 18.2 (C10'), 17.6 (C12'), 14.7 (C12), 10.9 (C10).
FTIR (thin film) cm^{-1}:	2919 (s), 1660 (m), 1456 (m), 1265 (w), 1167 (w), 737 (m).
HRMS (ESI):	calc'd for $C_{30}H_{45}N_2$ $[M+H]^+$: 433.3577, found: 433.3593.

TLC (2.5% Et_3N in [2.5% EtOAc in hexanes], Et_3N neutralized silica gel), *Rf*: 0.42 (UV, CAM).

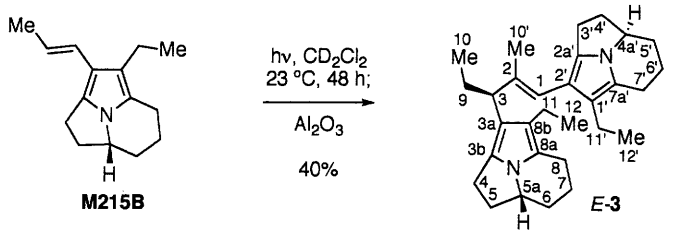

Hexacyclic Alkene 3:

A solution of **M215B** (10.3 mg, 50.2 μmol, 1 equiv) in neutralized, degassed dichloromethane-d_2 was sealed in an NMR tube under an argon atmosphere and was irradiated at 23 °C for 48 h. The resulting deep brown reaction mixture was filtered through neutral alumina gel (10% Et_2O in pentane, diam. 1.5 cm, ht. 8.5 cm) to afford *E*-**3** (4.3 mg, 40%) as a white solid.

Highest quality spectra were obtained by immediate use of samples and complete assignment was possible with the aid of additional information from gCOSY, HSQC, and gHMBC.

Data for *E*-**3**:

^{1}H NMR (500 MHz, C_6D_6, 20 °C): 6.65 (s, 1H, C1–H), 3.60 (dd, J = 8.5, 6.8 Hz, 1H, C3–H), 3.26–3.34 (m, 2H, C4a'–H, C5a–H), 2.54–2.79 (m, 9H, C4–H_c, C4–H_t, C11'–H, C11'–H', C11–H, C11–H', C7'–H_c, C8–H_c, C3'–H_c), 2.38–2.49 (m, 3H, C3'–H_t, C7'–H_t, C8–H_t), 2.06–2.14 (m, 1H, C9–H), 1.98–2.04 (m, 2H, C5–H_c, C9–H'), 1.94 (s, 3H, C10'–H), 1.86–1.91 (m, 1H, C4'–H_c), 1.58–1.69 (m, 3H, C6'–H_t, C7–H_t, C5–H_t), 1.42–1.58 (m, 3H, C5'–H_c, C6–H_c, C4'–H_t), 1.26–1.40 (m, 2H, C6'–H_c, C7–H_c), 1.36 (t, J = 7.5 Hz, 3H, C12–H *or* C12'–H), 1.35 (t, J = 7.5 Hz, 3H, C12–H *or* C12'–H), 1.18 (t, J = 7.3 Hz, 3H, C10–H), 0.88 (br q, J = 11.5 Hz, 1H, C6–H_t), 0.80 (br q, J 12.2 Hz, 1H, C5'–H_t).

nOe data (500 MHz, C_6D_6, 20 °C):

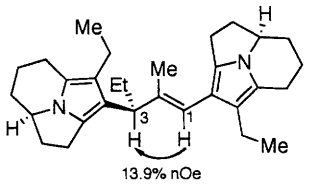

^{13}C NMR (125 MHz, C_6D_6, 20 °C): 137.6 (C2), 128.9 (C2a'), 126.9 (C3b), 122.4 (C8b), 122.3 (C1'), 119.1 (C1), 118.9 (C8a), 118.4 (C7a'), 117.0 (C3a), 114.0 (C2'), 55.5 (C4a' *or* C5a), 55.0 (C4a' *or* C5a), 49.5 (C3), 37.8 (C4'), 37.4 (C5), 30.5 (C5' *or* C6), 30.4 (C5' *or* C6), 27.5 (C3'), 27.2 (C4),

	26.7 (C9), 23.2 (C6' *or* C7), 23.0 (C6' *or* C7), 21.1 (C7' *or* C8), 21.0 (C7' *or* C8), 19.6 (C11'), 19.3 (C11), 17.0 (C12 *or* C12'), 16.9 (C12 *or* C12'), 16.0 (C10'), 13.9 (C10).
FTIR (thin film) cm^{-1}:	2926 (s), 1699 (m), 1457 (m), 1378 (w), 1262 (w), 1089 (w).
HRMS (ESI):	calc'd for $C_{30}H_{43}N_2$ $[M+H]^+$: 431.3421, found: 431.3413.

TLC (15% EtOAc in hexanes, neutral alumina gel), *Rf*: 0.59 (UV, CAM).

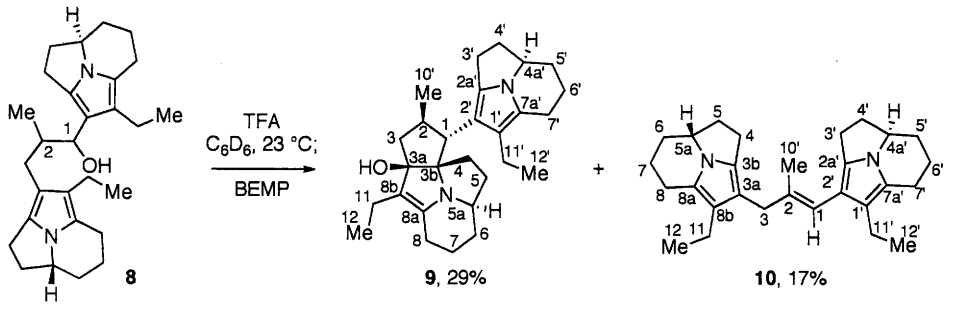

Heptacyclic Alcohol 9 and Hexacyclic Alkene 10:

A solution of alcohol **8**[5] (11.4 mg, 27.0s μmol, 1 equiv) in benzene-d_6 (810 μL) at 23 °C was degassed thoroughly by passage of a stream of argon. A solution of trifluoroacetic acid (TFA, 2.08 μL, 27.0 μmol, 1.00 equiv) in benzene-d_6 (40.0 μL) was added in four equal portions at three minute intervals. After 5 h, the NMR tube was moved into a glovebox and the bright yellow reaction mixture was transferred to a flask containing 2-*tert*-butylimino-2-diethylamino-1,3-dimethyl-perhydro-1,3,2-diazaphosphorine (BEMP, 50.0 mg, 111 μmol, 4.10 equiv) under dinitrogen atmosphere. The resulting suspension was stirred vigorously for 30 min and the reaction mixture was filtered through a plug of cotton. The filtrate was removed from the glovebox and concentrated under reduced pressure, and the yellow residue was purified by flash column chromatography (silica gel, 2.5% Et_3N, 2.5→40% EtOAc in hexanes, diam. 1.5 cm, ht. 18 cm) to give heptacyclic alcohol **9** (3.3 mg, 29%) hexacyclic alkene **10** (1.8 mg, 17%) as pale yellow oils.

Heptacyclic alcohol **9** underwent immediate and complete decomposition upon exposure to neutral alumina gel and partial decomposition upon extended exposure (>15 min) to triethylamine-neutralized silica gel. Hexacyclic alkene **10** also underwent partial decomposition upon extended exposure (>10 min) to triethylamine-neutralized silica gel. Separation of **9** and **10** was achieved by rapid elution of **10** (<1 min) followed by swift progressive increase in the polarity of the eluent (<10 min total for full elution of **9**).

Data for heptacyclic alcohol **9**:
Best spectra were obtained by immediate use of samples and complete assignment was possible with the aid of additional information from gCOSY, gHSQC, gHMBC, and gNOESY.

^{1}H NMR (500 MHz, C_6D_6, 20 °C): 3.39 (tdd, J = 10.7, 5.1, 3.6 Hz, 1H, C4a'–H), 2.96 (ddd, J = 15.3, 11.1, 6.3 Hz, 1H, C3'–H_c), 2.75 (dd, J = 15.2, 7.8 Hz, 1H, C3'–H_t), 2.56–2.63 (m, 4H, C7'–H_c, C11'–H, C11'–H', C5a–H), 2.52 (d, J = 11.7 Hz, 1H, C1–H), 2.38–2.46 (m, 3H, C4–H_t, C7'–H_t, C3–H_c), 2.22–2.26 (m, 1H, C8–H_t), 2.06–2.19 (m, 4H, C11–H, C2–H, C11–H', C4'–H_c), 1.81 (td, J = 12.9, 4.4 Hz, 1H, C8–H_c), 1.54–1.76 (m, 6H, C6–H_c, C4–H_c, C6'–H_t, C4'–H_t, C5'–H_c, C3–H_t), 1.30–1.42 (m, 3H, C6–H_t, C7–H_c, C6'–H_c), 1.27 (t, J =

[5] The corresponding C1 ketone was synthesized as a 1:1 mixture of C2 epimers; lithium aluminum hydride reduction produced **8** as an inseparable mixture of four diastereomers in a ratio of 5:9:5:8.

7.5 Hz, 3H, C12'–H), 1.18–1.27 (m, 2H, C5–H_t, C7–H_t), 1.13 (t, J = 7.6 Hz, 3H, C12–H), 0.98 (d, J = 6.5 Hz, 3H, C10'–H), 0.90–1.00 (m, 1H, C5–H_c), 0.89 (br q, J = 12.2 Hz, 1H, C5'–H_t).

Select gNOESY data (500 MHz, C_6D_6, 20 °C):

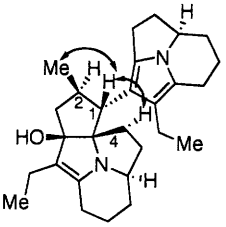

^{13}C NMR (125 MHz, C_6D_6, 20 °C): 145.2 (C8a), 129.7 (C2a'), 123.3 (C1'), 117.4 (C7a'), 115.1 (C8b), 111.1 (C2'), 92.0 (C3a), 86.1 (C3b), 59.4 (C5a), 55.5 (C4a'), 55.0 (C1), 48.7 (C3), 37.5 (C4'), 35.3 (C2), 30.3 (C5'), 29.5 (C4), 28.4 (C3'), 28.4 (C5), 27.7 (C6), 24.8 (C8), 23.2 (C6'), 21.2 (C7'), 20.6 (C7), 19.1 (C11'), 18.4 (C10'), 18.1 (C11), 17.8 (C12), 17.4 (C12').

FTIR (thin film) cm^{-1}: 3455 (br m), 2952 (s), 1727 (m), 1673 (m), 1455 (s), 1025 (m).

HRMS (ESI): calc'd for $C_{28}H_{41}N_2O$ $[M+H]^+$: 421.3213, found: 421.3216.

TLC (2.5% Et_3N in [2.5% EtOAc in hexanes], Et_3N neutralized silica gel), *Rf*: 0.25 (UV, CAM).

Data for hexacyclic alkene **10**:
Best spectra were obtained by immediate use of samples and complete assignment was possible with the aid of additional information from gCOSY, HSQC, and gHMBC.

^{1}H NMR (500 MHz, C_6D_6, 20 °C): 6.63 (s, 1H, C1–H), 3.66 (d, J = 15.2 Hz, 1H, C3–H), 3.52 (d, J = 15.2 Hz, 1H, C3–H'), 3.28–3.35 (m, 2H, C4a'–H, C5a–H), 2.50–2.75 (m, 9H, C4–H_c, C4–H_t, C11–H, C11–H', C11'–H, C11'–H', C7'–H_c, C8–H_c, C3'–H_c), 2.52 (dd, J = 14.7, 8.1 Hz, 1H, C3'–H_t), 2.36–2.47 (m, 2H, C7'–H_t, C8–H_t), 2.04 (s, 3H, C10'–H), 2.01 (dt, J = 11.7, 6.0 Hz, 1H, C5–H_c), 1.94 (dt, J = 11.4, 5.7, 1H, C4'–H_c), 1.56–1.71 (m, 3H, C6'–H_t, C7–H_t, C5–H_t), 1.46–1.56 (m, 3H, C5'–H_c, C6–H_c, C4'–H_t), 1.25–1.42 (m, 2H, C6'–H_c, C7–H_c), 1.35 (t, J = 7.5 Hz, 3H, C12–H *or* C12'–H), 1.33 (t, J = 7.5 Hz, 3H, C12–H *or* C12'–H), 0.87 (br q, J = 12.2 Hz, 1H, C5'–H_t *or* C6–H_t), 0.81 (br q, J = 12.2 Hz, 1H, C5'–H_t *or* C6–H_t).

nOe data (500 MHz, C_6D_6, 20 °C):

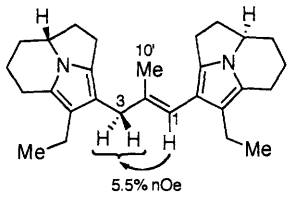

^{13}C NMR (125 MHz, C_6D_6, 20 °C): 134.2 (C2), 128.9 (C2a'), 128.8 (C3b), 122.2 (C8b *or* C1'), 122.2 (C8b *or* C1'), 119.4 (C1), 119.0 (C8a), 118.5 (C7a'), 114.1 (C2'), 112.5 (C3a), 55.5 (C4a'), 55.4 (C5a), 37.8 (C4'), 37.7 (C5), 37.3 (C3), 30.5 (C5' *or* C6), 30.5 (C5' *or* C6), 27.6 (C3'), 25.3 (C4), 23.3 (C6' *or* C7), 23.0 (C6' *or* C7), 21.2 (C7' *or* C8), 21.0 (C7' *or* C8), 19.5 (C11 *or* C11'), 19.3 (C11 *or* C11'), 19.0 (C10'), 16.9 (C12 *or* C12'), 16.8 (C12 *or* C12').

FTIR (thin film) cm^{-1}: 2926 (s), 1651 (m), 1455 (m), 1088 (w), 736 (w).

HRMS (ESI): calc'd for $C_{28}H_{39}N_2$ $[M+H]^+$: 403.3108, found: 403.3107.

TLC (2.5% Et_3N in [2.5% EtOAc in hexanes], Et_3N neutralized silica gel), *Rf*: 0.54 (UV, CAM).

Appendix A.

Spectra for Chapter I

ACQUISITION	
sfrq	499.758
tn	H1
at	3.277
np	65536
sw	9998.8
fb	not used
bs	4
tpwr	56
pw	8.2
d1	3.000
tof	1498.1
nt	24
ct	24
alock	n
gain	not used
FLAGS	
il	n
in	n
dp	y
hs	nn
DISPLAY	
sp	-250.2
wp	6246.5
vs	151
sc	0
wc	250
hzmm	3.89
is	33.57
rfl	4564.4
rfp	3578.2
th	7
ins	2.000
nm	cdc ph

DEC. & VT	
dfrq	125.677
dn	C13
dpwr	34
dof	1498.1
dm	nnn
dmm	w
dmf	10000
dseq	
dres	1.0
homo	n
PROCESSING	
wtfile	
proc	ft
fn	65536
math	f
werr	
wexp	
wbs	
wnt	

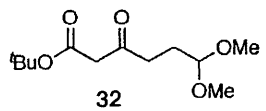

32

ACQUISITION		DEC. & VT	
sfrq	125.796	dfrq	500.233
tn	C13	dn	H1
at	1.736	dpwr	37
np	131010	dof	-500.0
sw	37735.8	dm	y
fb	not used	dmm	w
bs	8	dmf	10000
ss	1	dseq	
tpwr	53	dres	1.0
pw	6.9	homo	n
d1	0.763	PROCESSING	
tof	631.4	lb	0.30
nt	10000	wtfile	
ct	1096	proc	ft
alock	n	fn	131072
gain	not used	math	f
FLAGS			
il	n	werr	
in	n	wexp	
dp	y	wbs	
hs	nn	wnt	
DISPLAY			
sp	-1258.4		
wp	31445.8		
vs	151		
sc	0		
wc	250		
hzmm	125.78		
is	500.00		
rfl	22374.0		
rfp	16149.3		
th	20		
ins	1.000		
nm	ph		

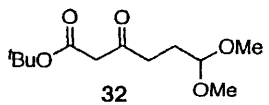

32

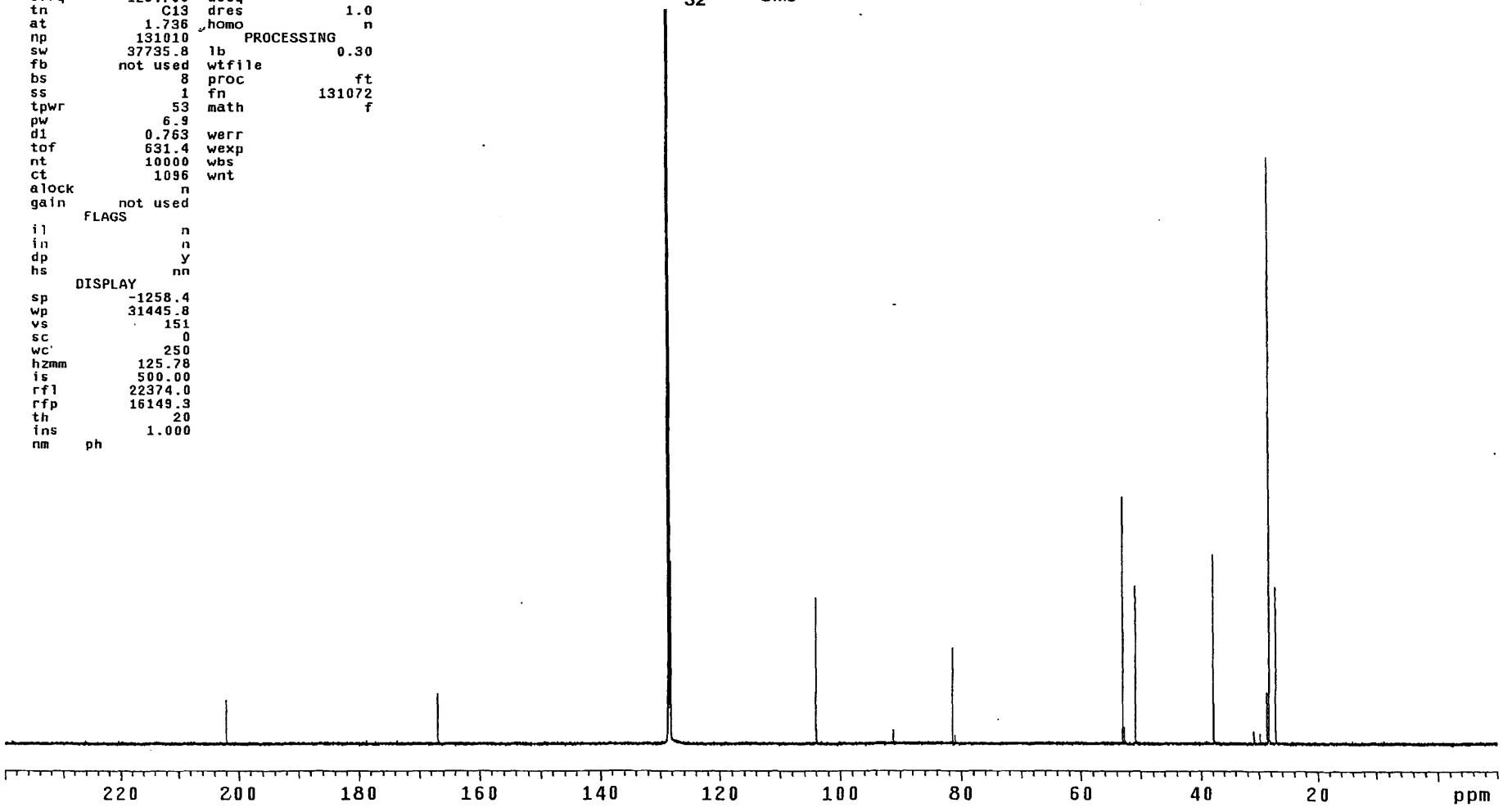

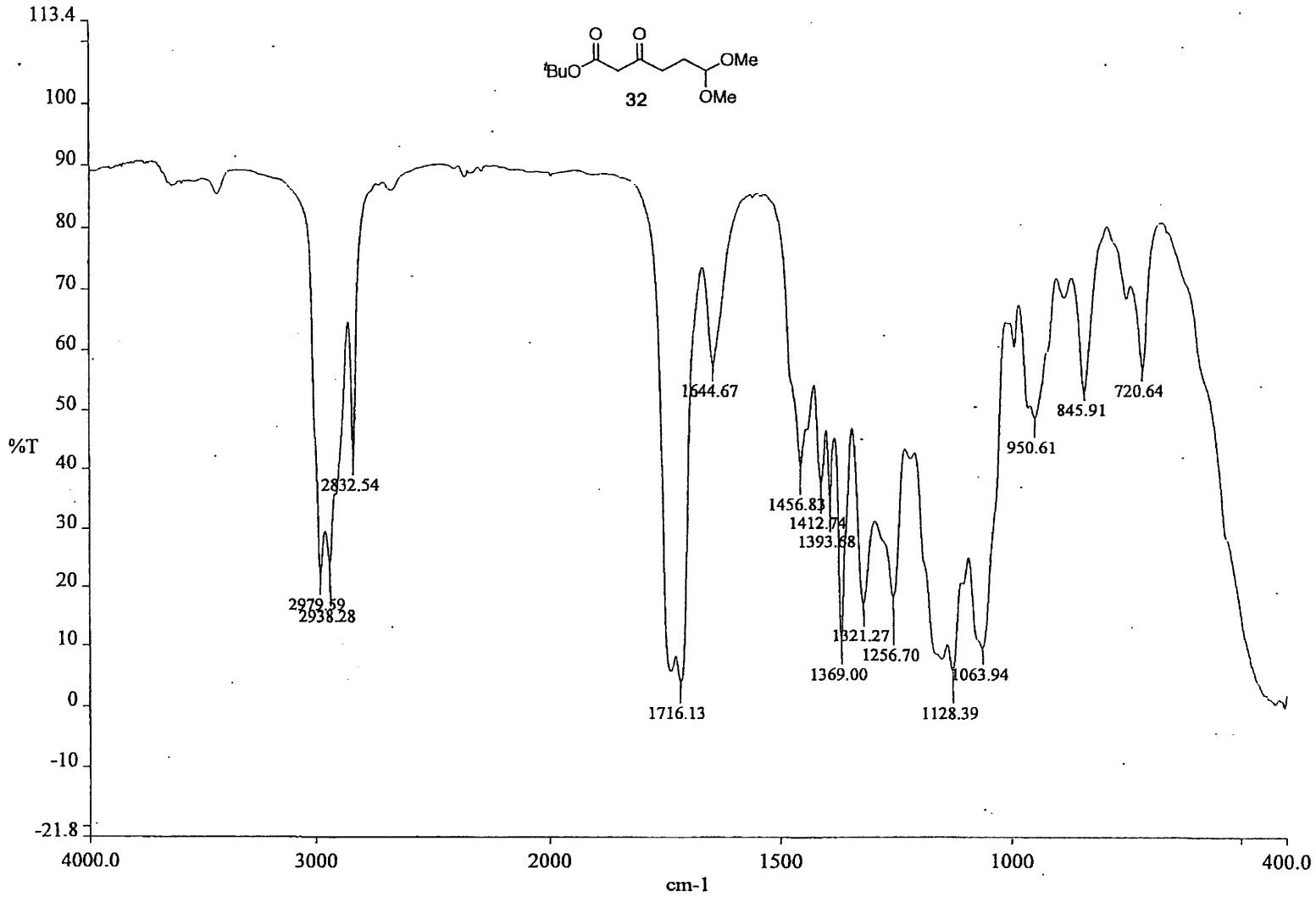
113.4
100
90
80
70
60
50
40
30
20
10
0
-10
-21.8
%T
4000.0
3000
2000
1500
1000
400.0
cm-1
tBuO
O
O
OMe
OMe
32
2979.59
2938.28
2832.54
1716.13
1644.67
1456.83
1412.74
1393.58
1369.00
1321.27
1256.70
1128.39
1063.94
950.61
845.91
720.64

ACQUISITION		DEC. & VT	
sfrq	499.758	dfrq	125.677
tn	H1	dn	C13
at	3.277	dpwr	34
np	65536	dof	1498.1
sw	9998.8	dm	nnn
fb	not used	dmm	w
bs	4	dmf	10000
tpwr	56	dseq	
pw	8.2	dres	1.0
d1	3.000	homo	n
tof	1498.1	PROCESSING	
nt	24	wtfile	
ct	24	proc	ft
alock	n	fn	65536
gain	not used	math	f
FLAGS		werr	
il	n	wexp	
in	n	wbs	
dp	y	wnt	
hs	nn		
DISPLAY			
sp	-250.2		
wp	6246.5		
vs	151		
sc	0		
wc	250		
hzmm	40.00		
is	33.57		
rfl	4563.8		
rfp	3578.2		
th	7		
ins	2.000		
nm cdc ph			

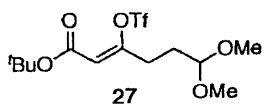

27

ACQUISITION	
sfrq	125.796
tn	C13
at	1.736
np	131010
sw	37735.8
fb	not used
bs	8
ss	1
tpwr	53
pw	6.9
d1	0.763
tof	631.4
nt	10000
ct	2464
alock	n
gain	not used

FLAGS	
il	n
in	n
dp	y
hs	nn

DISPLAY	
sp	-1258.4
wp	31445.8
vs	166
sc	0
wc	250
hzmm	5.14
is	500.00
rfl	22373.4
rfp	16149.3
th	8
ins	1.000
nm	ph

DEC. & VT	
dfrq	500.233
dn	H1
dpwr	37
dof	-500.0
dm	y
dmm	w
dmf	10000
dseq	
dres	1.0
homo	n

PROCESSING	
lb	0.30
wtfile	
proc	ft
fn	131072
math	f
werr	
wexp	
wbs	
wnt	

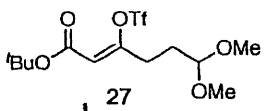

27

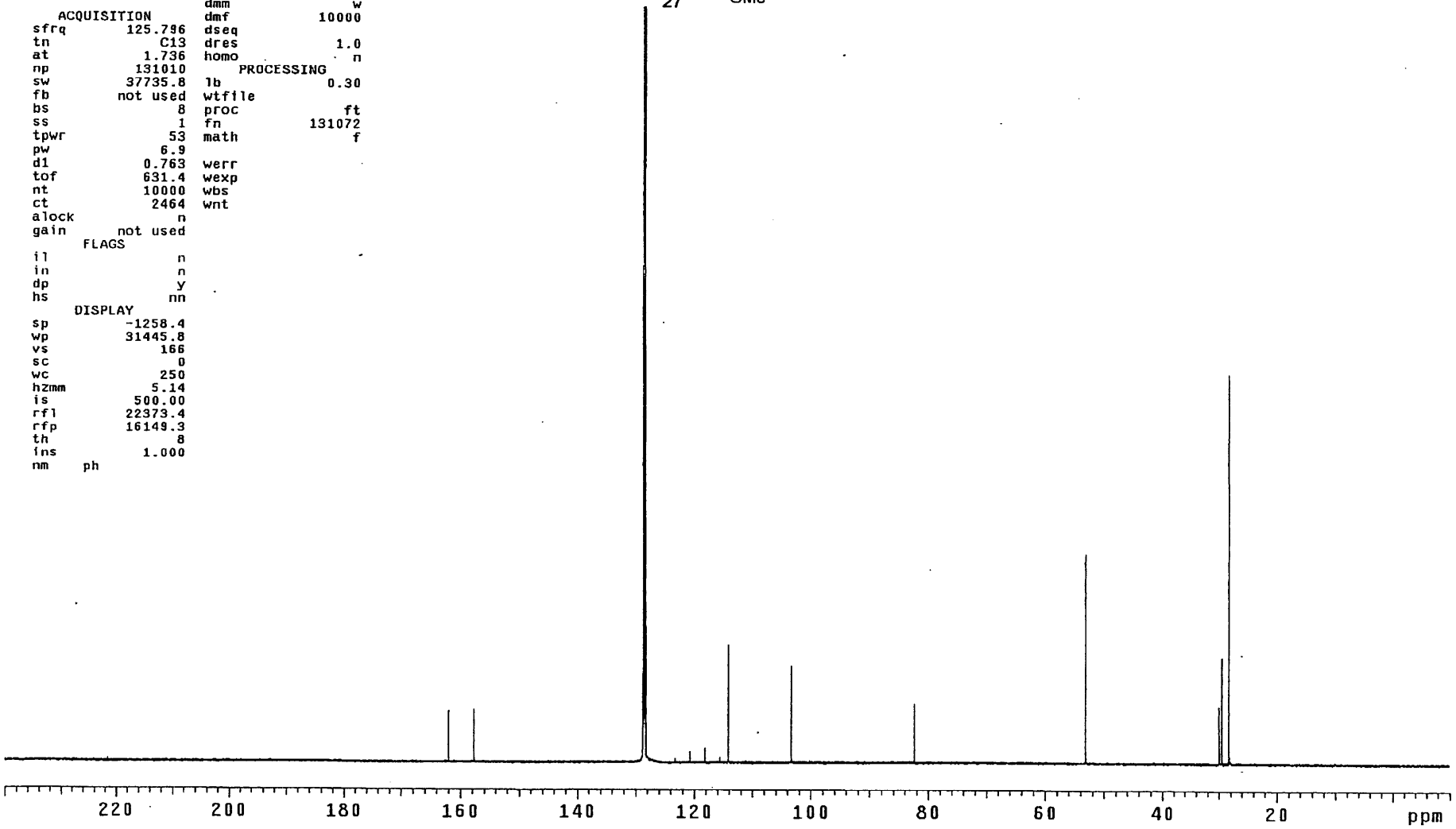

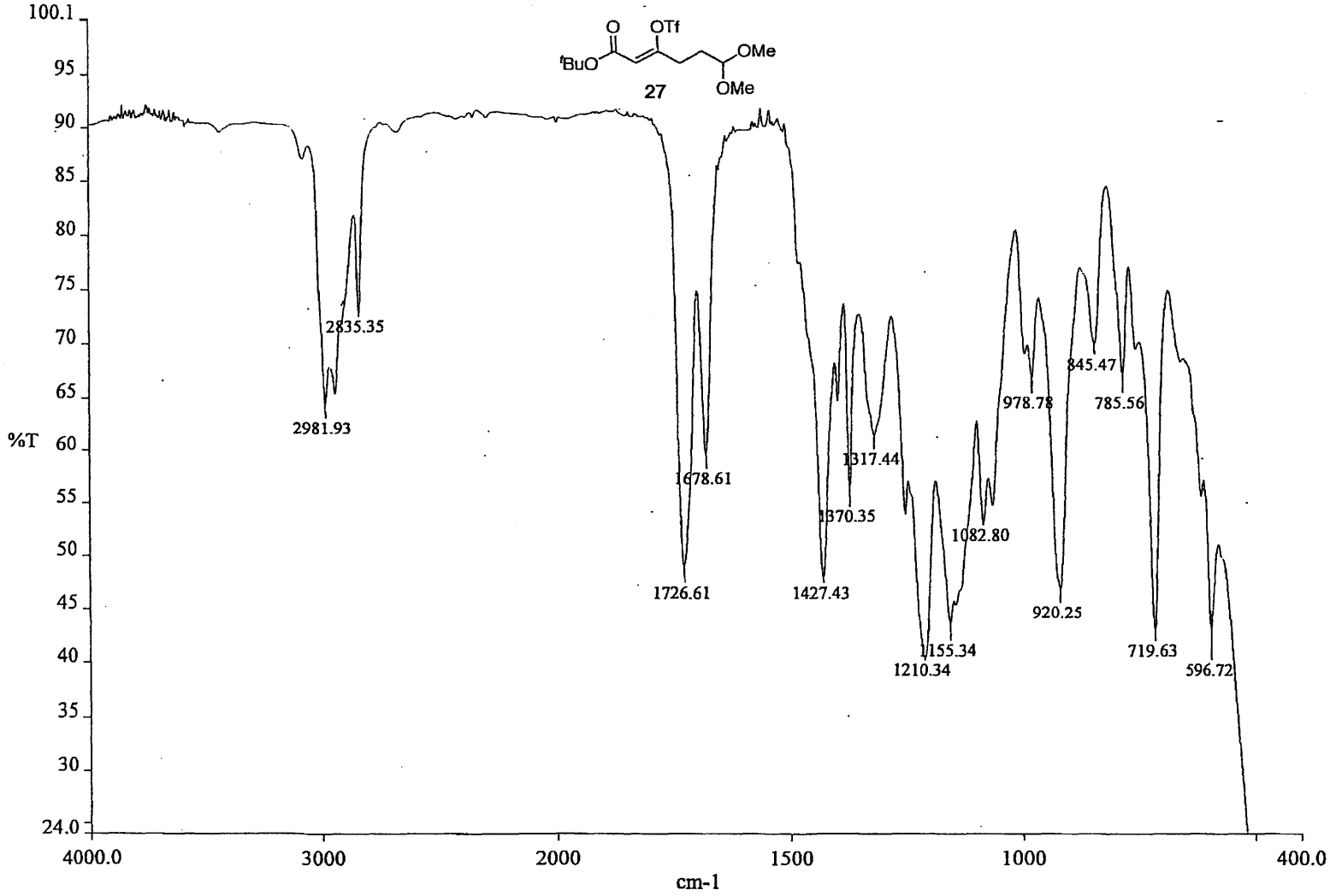
100.1
95
90
85
80
75
70
65
60
55
50
45
40
35
30
24.0
%T
4000.0
3000
2000
1500
1000
400.0
cm-1
O
OTf
tBuO
OMe
OMe
27
2981.93
2835.35
1726.61
1678.61
1427.43
1370.35
1317.44
1210.34
1155.34
1082.80
978.78
920.25
845.47
785.56
719.63
596.72

ACQUISITION	
sfrq	499.758
tn	H1
at	3.277
np	65536
sw	9998.8
fb	not used
bs	4
tpwr	56
pw	8.2
d1	2.000
tof	1498.1
nt	24
ct	24
alock	n
gain	not used

FLAGS	
il	n
in	n
dp	y
hs	nn

DISPLAY	
sp	-249.9
wp	6246.8
vs	90
sc	0
wc	250
hzmm	24.99
is	33.57
rfl	4637.5
rfp	3623.2
th	7
ins	1.000
nm	cdc ph

DEC. & VT	
dfrq	125.677
dn	C13
dpwr	34
dof	1498.1
dm	nnn
dmm	w
dmf	10000
dseq	
dres	1.0
homo	n

PROCESSING	
wtfile	
proc	ft
fn	65536
math	f
werr	
wexp	
wbs	
wnt	

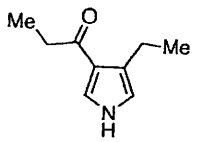

29

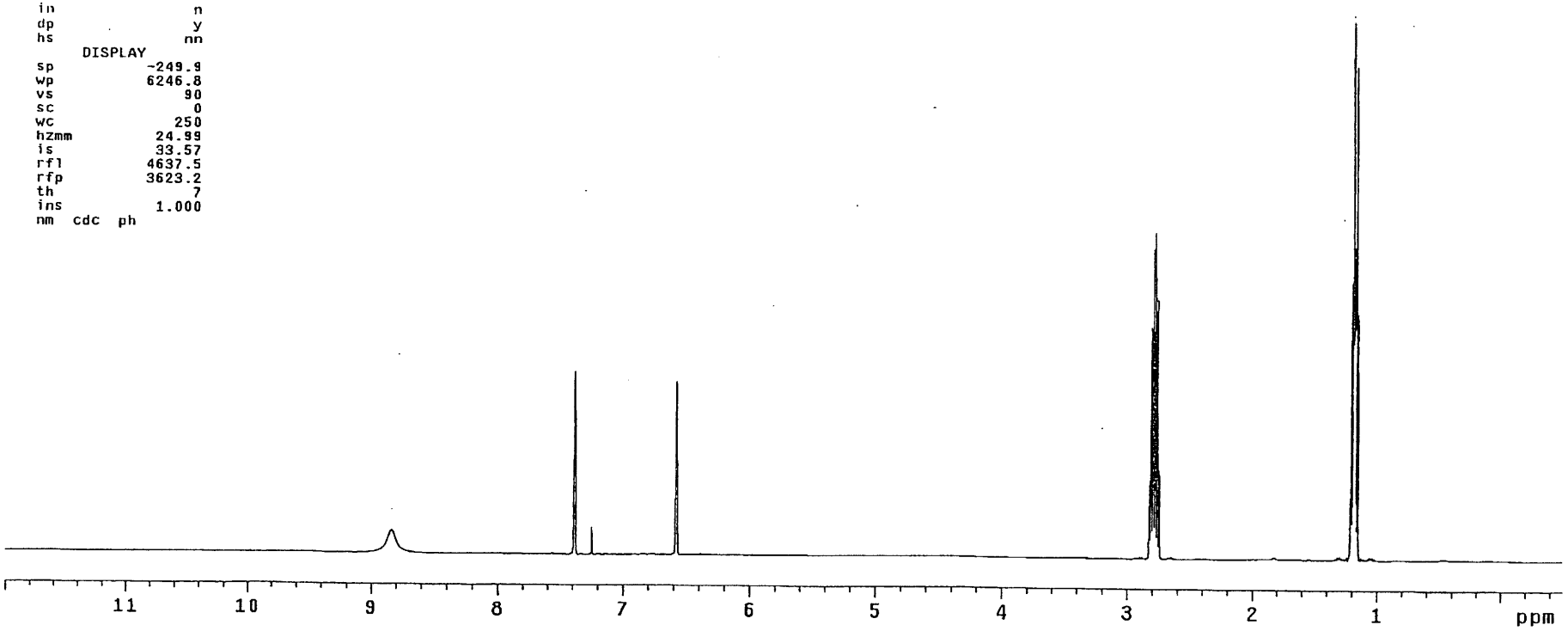

ACQUISITION	
sfrq	125.796
tn	C13
at	1.736
np	131010
sw	37735.8
fb	not used
bs	8
ss	1
tpwr	53
pw	6.9
d1	0.763
tof	631.4
nt	10000
ct	392
alock	n
gain	not used

FLAGS	
il	n
in	n
dp	y
hs	nn

DISPLAY	
sp	-1258.6
wp	31448.1
vs	77
sc	0
wc	250
hzmm	6.19
is	500.00
rfl	16006.2
rfp	9730.6
th	20
ins	1.000
nm	ph

DEC. & VT	
dfrq	500.233
dn	H1
dpwr	37
dof	-500.0
dm	y
dmm	w
dmf	10000
dseq	
dres	1.0
homo	n

PROCESSING	
lb	0.30
wtfile	
proc	ft
fn	131072
math	f
werr	
wexp	
wbs	
wnt	

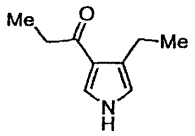

29

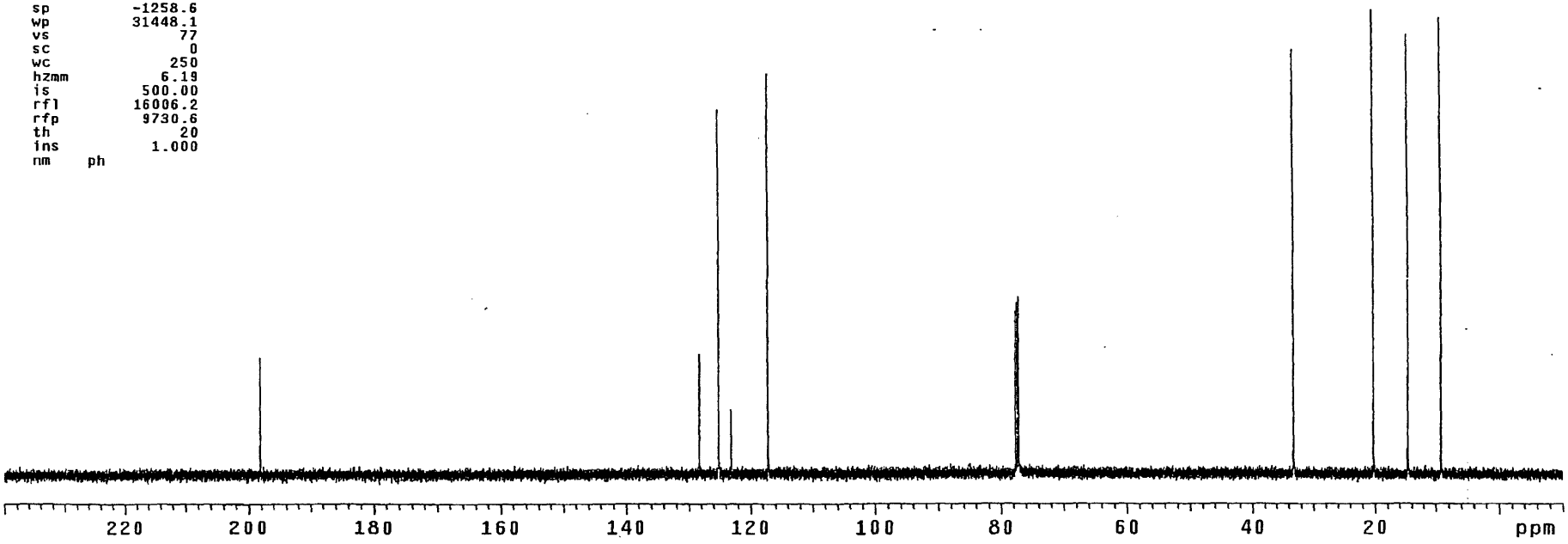

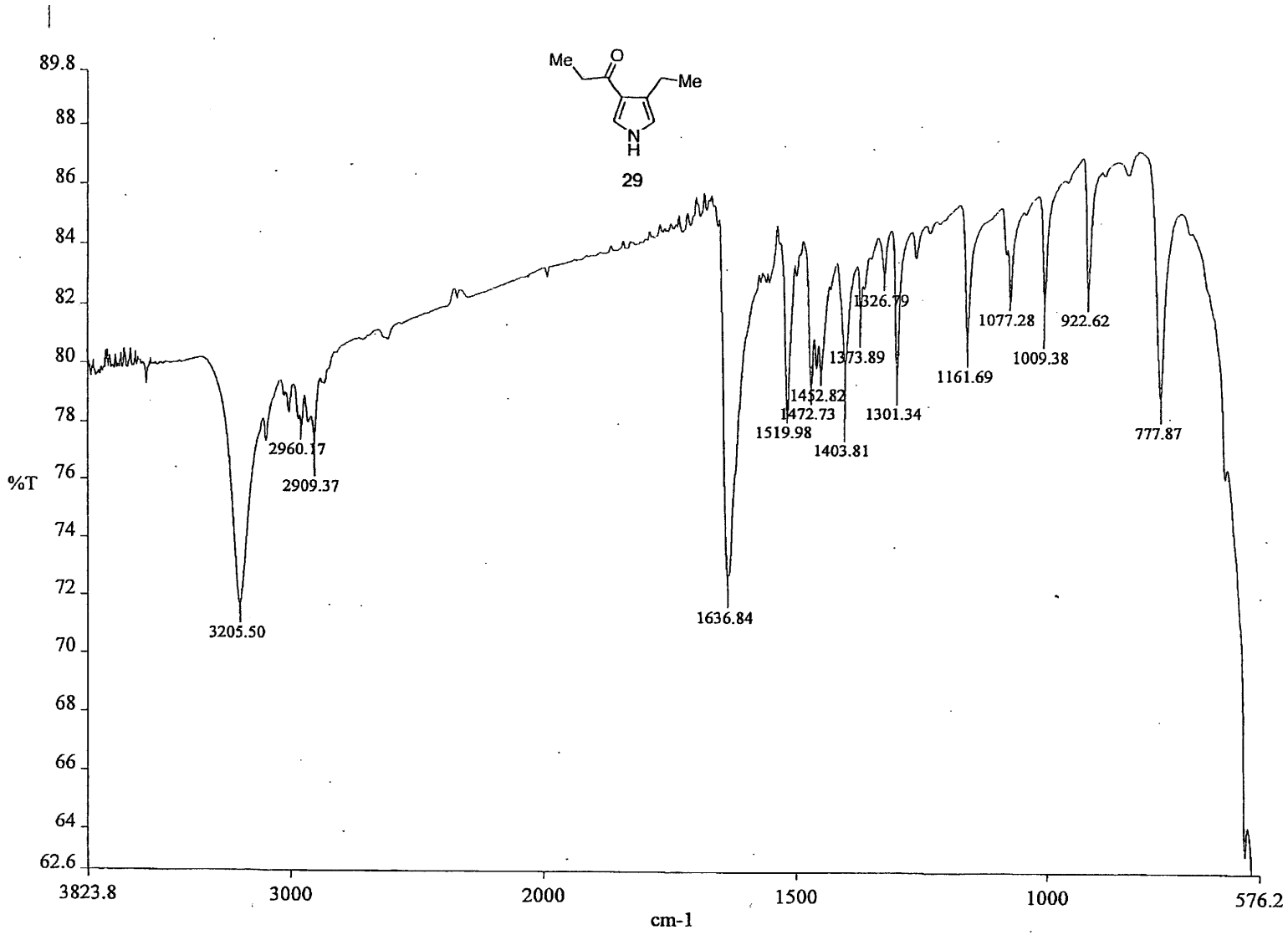
Me
O
Me
N
H
29
89.8
88
86
84
82
80
78
76
74
72
70
68
66
64
62.6
%T
3205.50
2960.17
2909.37
1636.84
1519.98
1472.73
1452.82
1403.81
1373.89
1326.79
1301.34
1161.69
1077.28
1009.38
922.62
777.87
3823.8
3000
2000
1500
1000
576.2
cm-1

ACQUISITION	
sfrq	499.758
tn	H1
at	3.277
np	65536
sw	9998.8
fb	not used
bs	4
tpwr	56
pw	8.2
d1	3.000
tof	1498.1
nt	24
ct	24
alock	n
gain	not used
FLAGS	
il	n
in	n
dp	y
hs	nn
DISPLAY	
sp	-250.0
wp	6246.8
vs	132
sc	0
wc	250
hzmm	2.23
is	33.57
rfl	4557.8
rfp	3578.2
th	7
ins	2.000
nm cdc ph	

DEC. & VT	
dfrq	125.677
dn	C13
dpwr	34
dof	1498.1
dm	nnn
dmm	w
dmf	10000
dseq	
dres	1.0
homo	n
PROCESSING	
wtfile	
proc	ft
fn	65536
math	f
werr	
wexp	
wbs	
wnt	

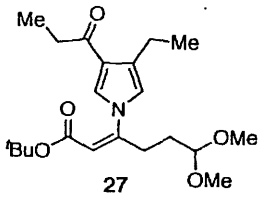

27

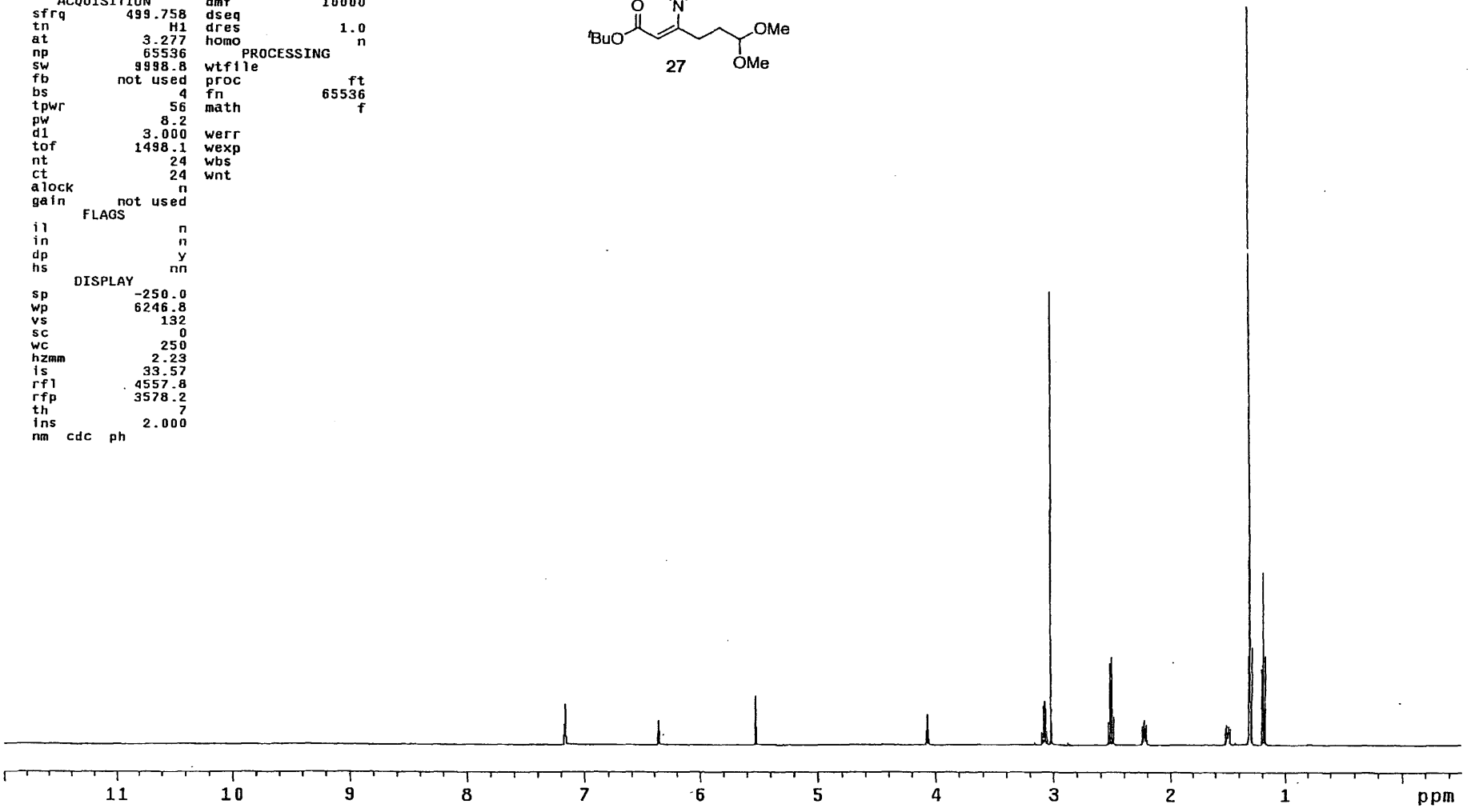

ACQUISITION		DEC. & VT	
sfrq	125.796	dfrq	500.233
tn	C13	dn	H1
at	1.736	dpwr	37
np	131010	dof	-500.0
sw	37735.8	im	y
fb	not used	dmm	w
bs	8	dmf	10000
ss	1	dseq	
tpwr	53	dres	1.0
pw	6.9	homo	n
d1	0.763	PROCESSING	
tof	631.4	lb	0.30
nt	10000	wtfile	
ct	1488	proc	ft
alock	n	fn	131072
gain	not used	math	f
FLAGS		werr	
il	n	wexp	
in	n	wbs	
dp	y	wnt	
hs	nn		
DISPLAY			
sp	-1259.0		
wp	31448.1		
vs	141		
sc	0		
wc	250		
hzmm	3.29		
is	500.00		
rfl	22374.0		
rfp	16149.3		
th	6		
ins	1.000		
nm	ph		

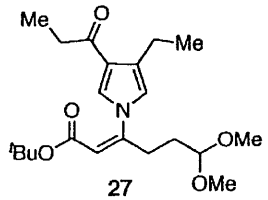

27

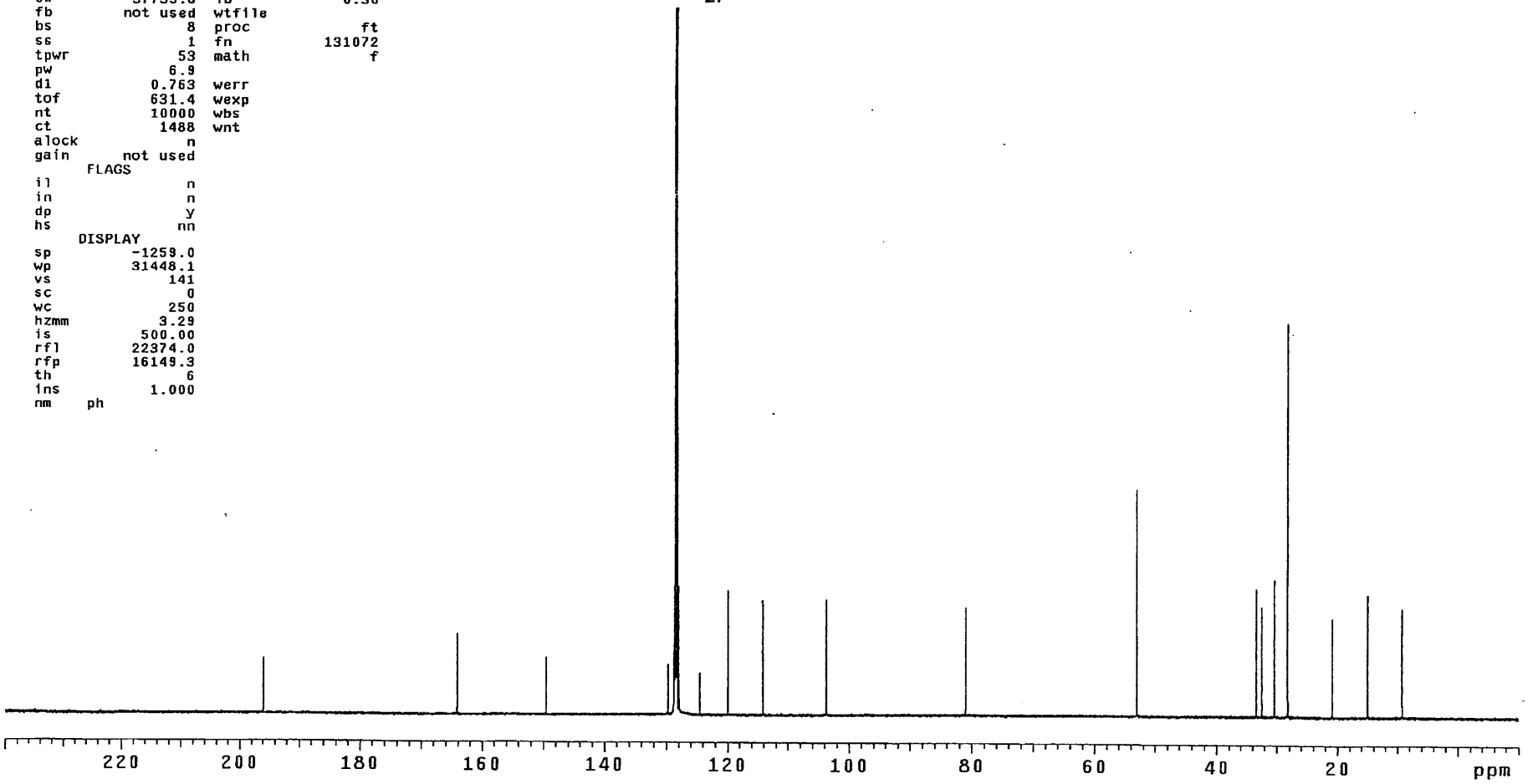

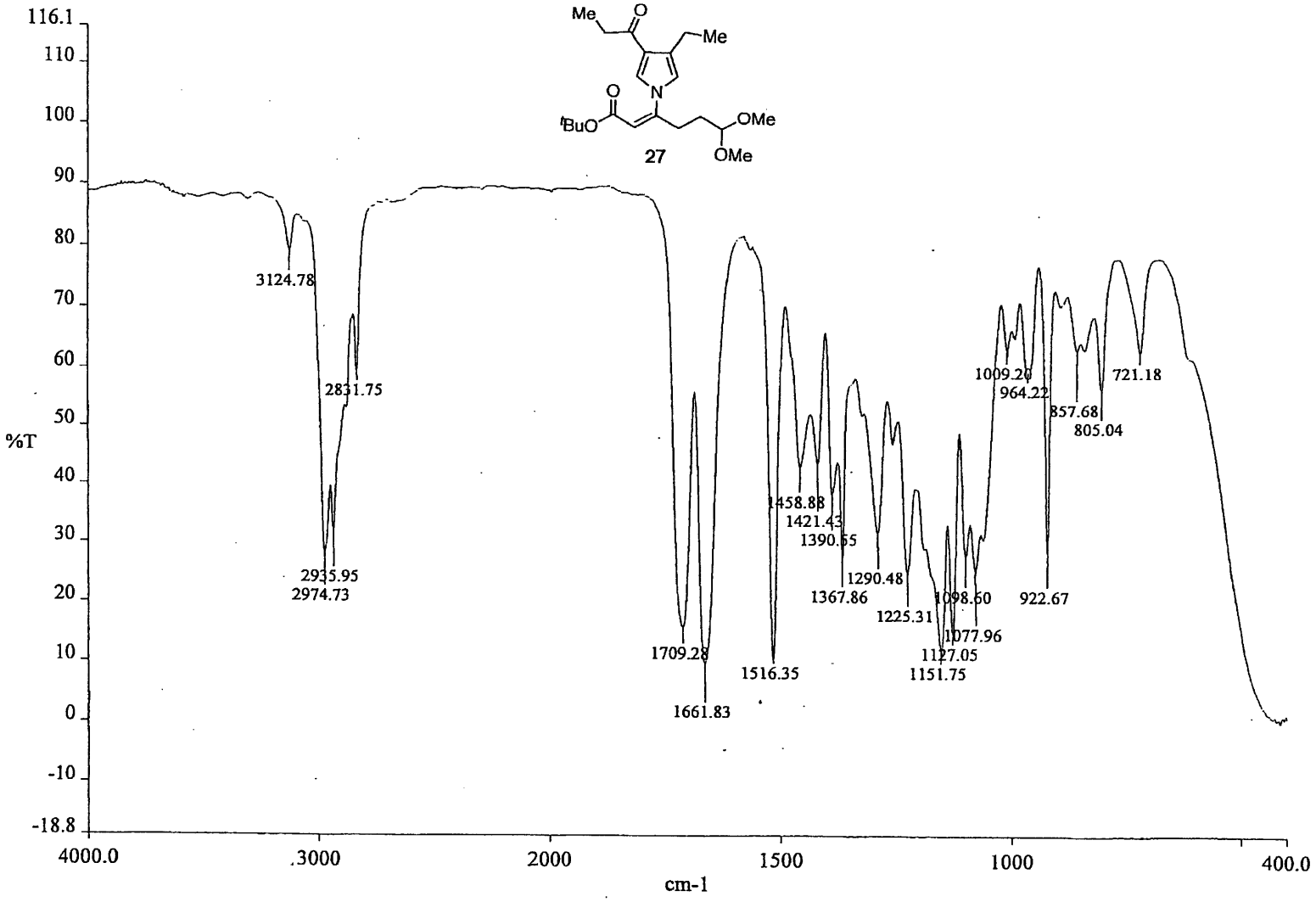
Me
O
Me
N
O
tBuO
OMe
OMe
27
116.1
110
100
90
80
70
60
50
40
30
20
10
0
-10
-18.8
%T
3124.78
2831.75
2935.95
2974.73
1709.28
1661.83
1516.35
1458.88
1421.43
1390.65
1367.86
1290.48
1225.31
1151.75
1127.05
1098.60
1077.96
1009.20
964.22
922.67
857.68
805.04
721.18
4000.0
3000
2000
1500
1000
400.0
cm-1

ACQUISITION	
sfrq	499.758
tn	H1
at	3.277
np	65536
sw	9998.8
fb	not used
bs	4
tpwr	56
pw	8.2
d1	2.000
tof	1498.1
nt	24
ct	24
alock	n
gain	not used

FLAGS	
il	n
in	n
dp	y
hs	nn

DISPLAY	
sp	-250.5
wp	6246.5
vs	163
sc	0
wc	250
hzmm	1.89
is	33.57
rfl	4563.2
rfp	3578.2
th	7
ins	2.000
nm	cdc ph

DEC. & VT	
dfrq	125.677
dn	C13
dpwr	34
dof	1498.1
dm	nnn
dmm	w
dmf	10000
dseq	
dres	1.0
homo	n

PROCESSING	
wtfile	
proc	ft
fn	65536
math	f
werr	
wexp	
wbs	
wnt	

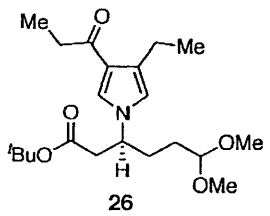

26

ACQUISITION	
sfrq	125.796
tn	C13
at	1.736
np	131010
sw	37735.8
fb	not used
bs	8
ss	1
tpwr	53
pw	6.9
d1	0.763
tof	631.4
nt	100000
ct	1056
alock	n
gain	not used

FLAGS	
il	n
in	n
dp	y
hs	nn

DISPLAY	
sp	-1259.0
wp	31448.1
vs	159
sc	0
wc	250
hzmm	3.82
is	500.00
rfl	22374.0
rfp	16149.3
th	4
ins	1.000
nm	ph

DEC. & VT	
dfrq	500.233
dn	H1
dpwr	37
dof	-500.0
dm	y
dmm	w
dmf	10000
dseq	
dres	1.0
homo	n

PROCESSING	
lb	0.30
wtfile	
proc	ft
fn	131072
math	f
werr	
wexp	
wbs	
wnt	

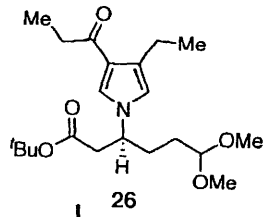

26

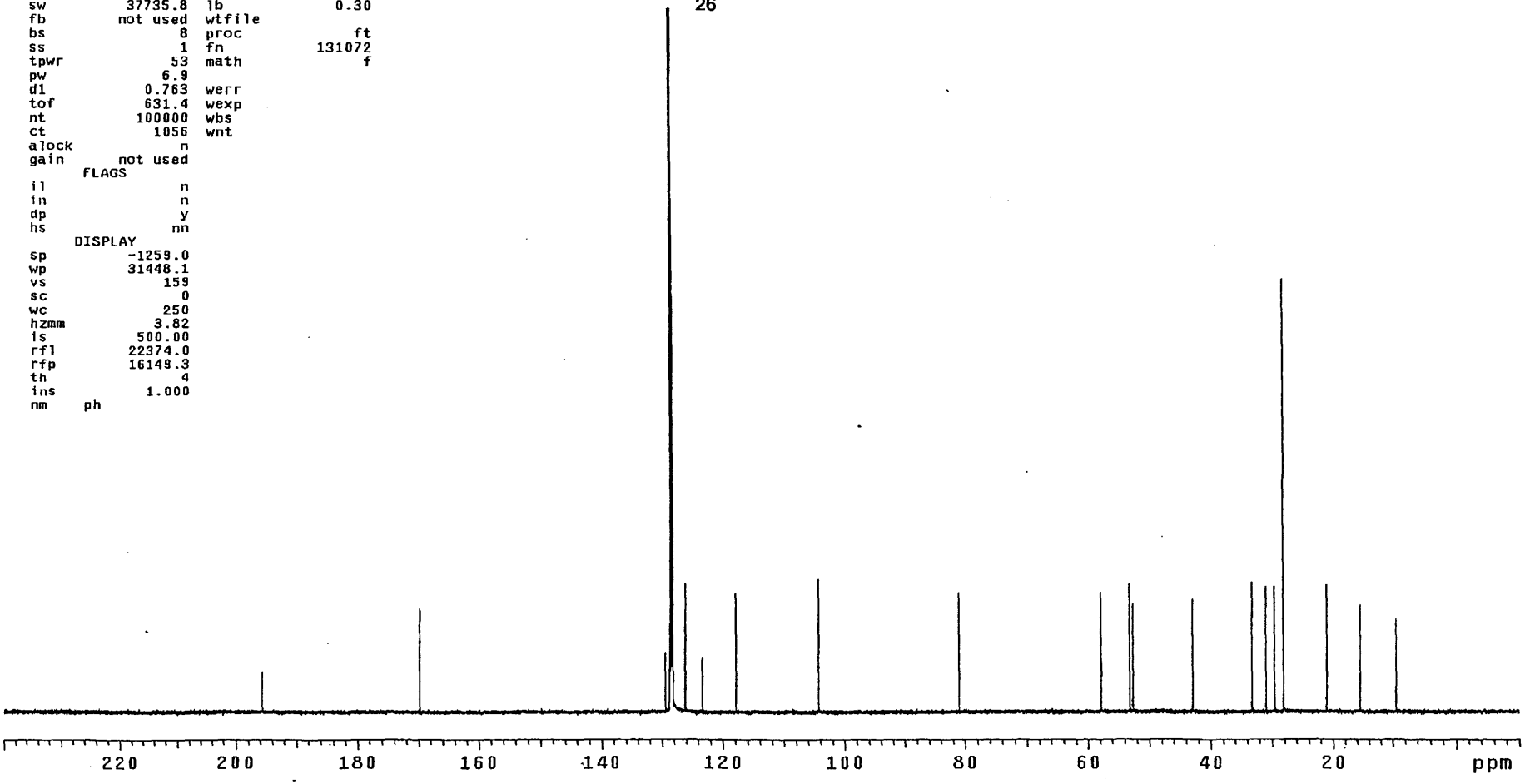

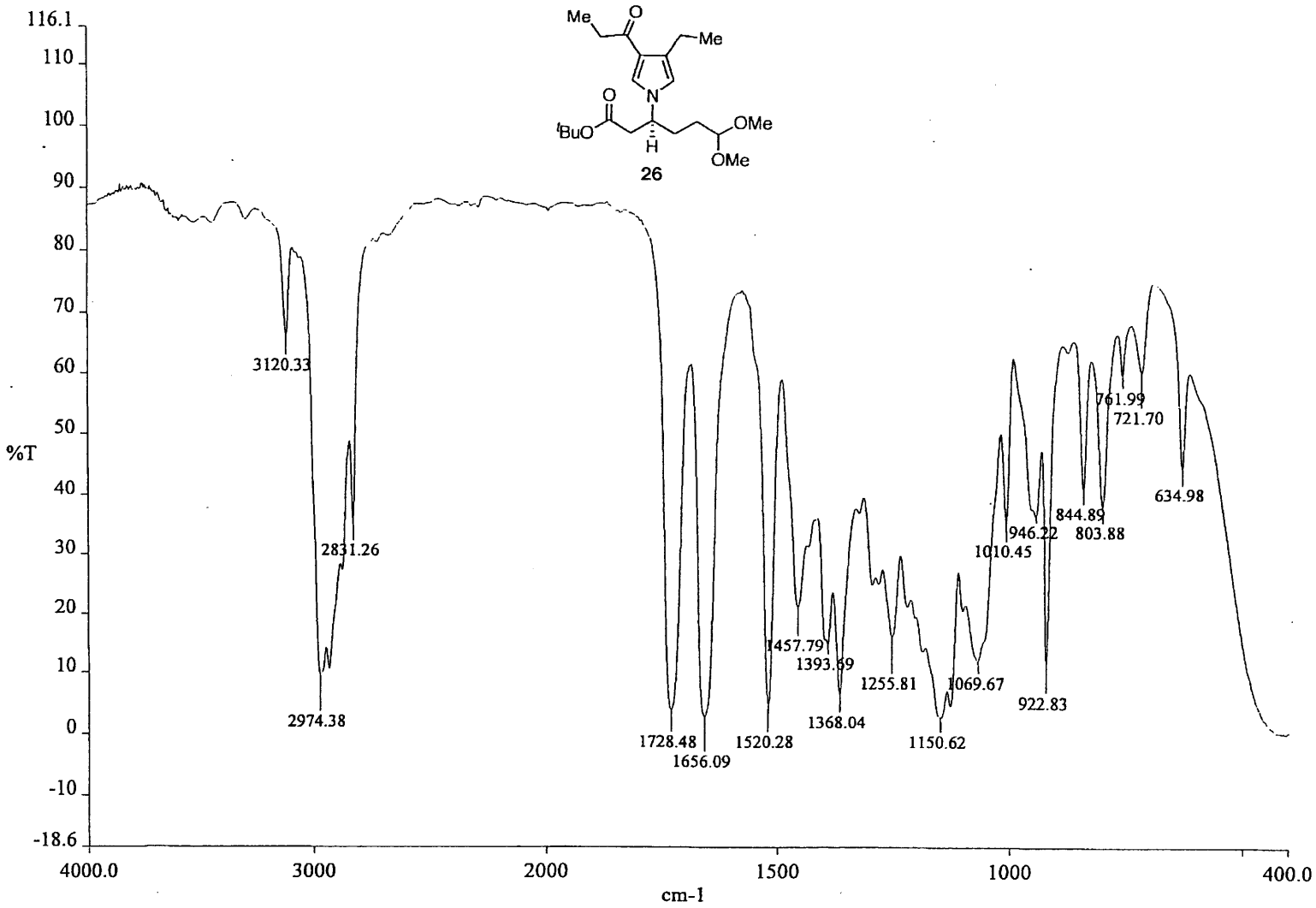
Me
O
Me
N
O
tBuO
OMe
H
OMe
26
116.1
110
100
90
80
70
60
50
%T
40
30
20
10
0
-10
-18.6
3120.33
2831.26
2974.38
1728.48
1656.09
1520.28
1457.79
1393.59
1368.04
1255.81
1150.62
1069.67
1010.45
946.22
922.83
844.89
803.88
761.99
721.70
634.98
4000.0
3000
2000
1500
1000
400.0
cm-1

ACQUISITION	
sfrq	499.758
tn	H1
at	3.277
np	65536
sw	9998.8
fb	not used
bs	4
tpwr	56
pw	8.2
d1	2.000
tof	1498.1
nt	24
ct	24
alock	n
gain	not used
FLAGS	
il	n
in	n
dp	y
hs	nn
DISPLAY	
sp	-250.2
wp	6246.5
vs	372
sc	0
wc	250
hzmm	3.15
is	198.29
rfl	4563.8
rfp	3578.2
th	7
ins	1.000
nm cdc ph	

DEC. & VT	
dfrq	125.677
dn	C13
dpwr	34
dof	1498.1
dm	nnn
dmm	w
dmf	10000
dseq	
dres	1.0
homo	n
PROCESSING	
wtfile	
proc	ft
fn	65536
math	f
werr	
wexp	
wbs	
wnt	

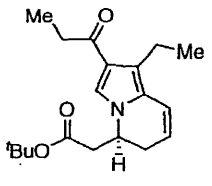

25

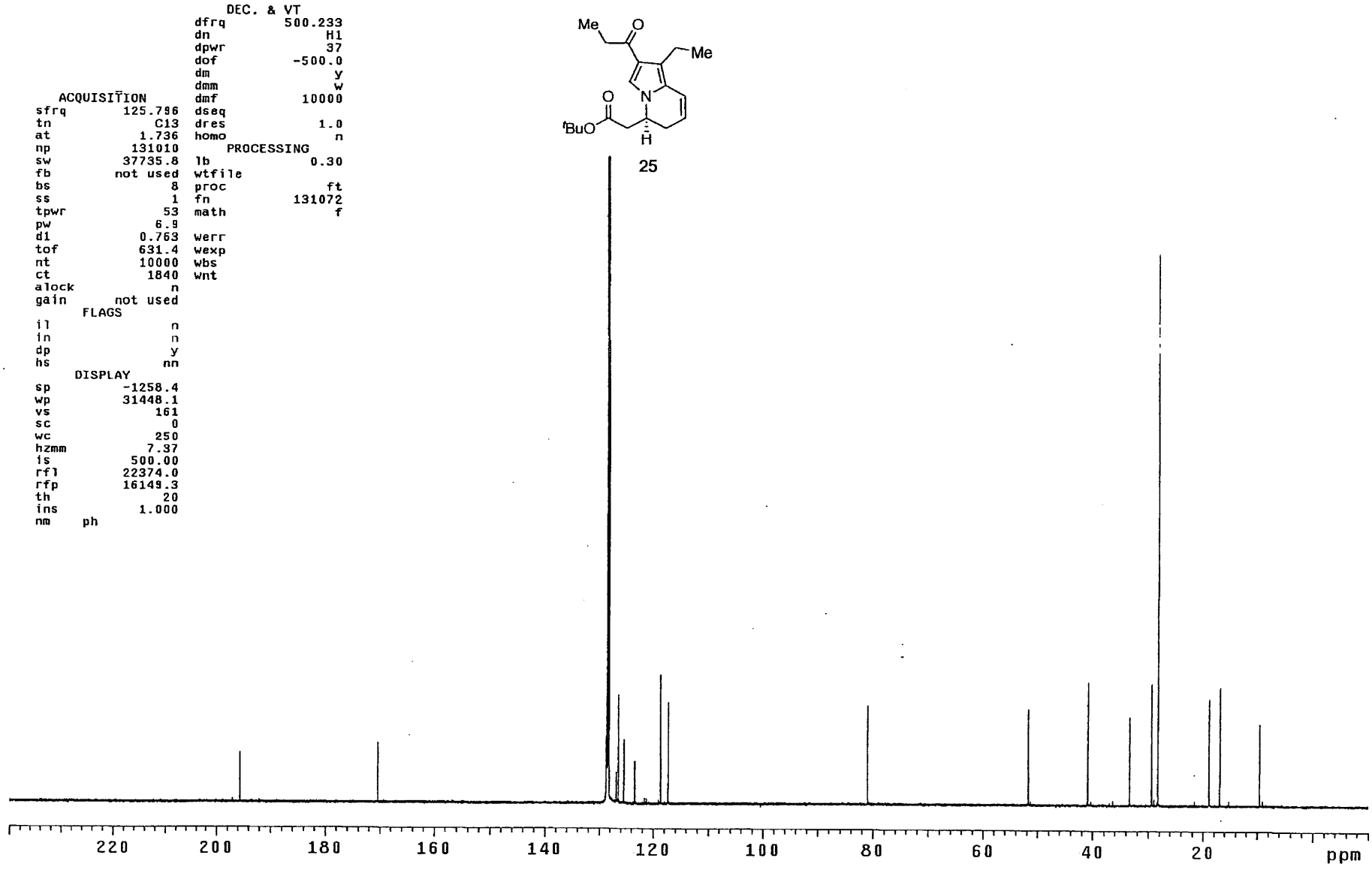
ACQUISITION
sfrq 125.786
tn C13
at 1.736
np 131010
sw 37735.8
fb not used
bs 8
ss 1
tpwr 53
pw 6.9
d1 0.763
tof 631.4
nt 10000
ct 1840
alock n
gain not used
FLAGS
il n
in n
dp y
hs nn
DISPLAY
sp -1258.4
wp 31448.1
vs 161
sc 0
wc 250
hzmm 7.37
is 500.00
rfl 22374.0
rfp 16149.3
th 20
ins 1.000
nm ph
DEC. & VT
dfrq 500.233
dn H1
dpwr 37
dof -500.0
dm y
dmm w
dmf 10000
dseq
dres 1.0
homo n
PROCESSING
lb 0.30
wtfile
proc ft
fn 131072
math f
werr
wexp
wbs
wnt
Me
O
Me
O
N
tBuO
H
25
220
200
180
160
140
120
100
80
60
40
20
ppm

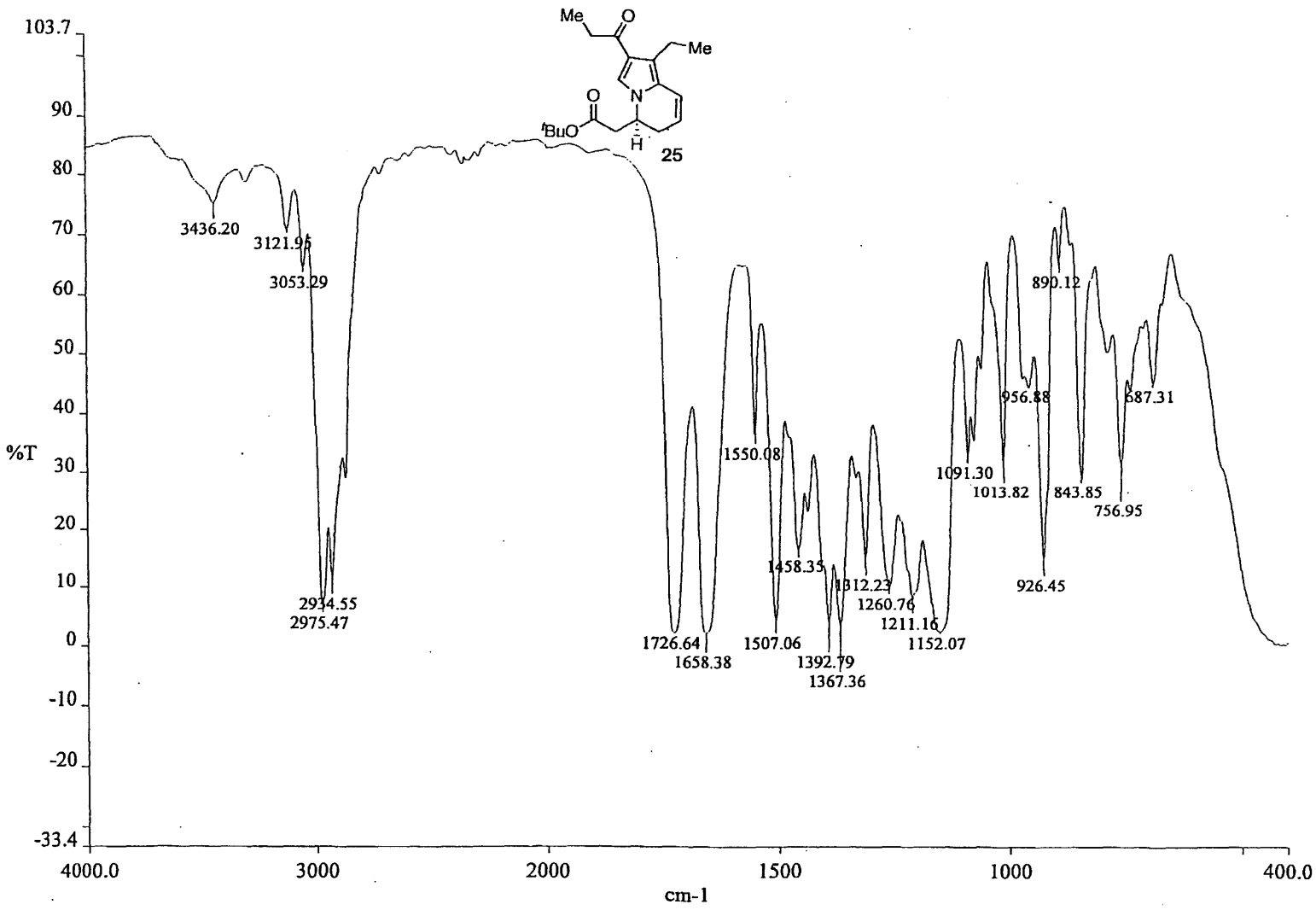
Me
O
Me
N
O
tBuO
H
25
103.7
90
80
70
60
50
40
%T
30
20
10
0
-10
-20
-33.4
3436.20
3121.95
3053.29
2934.55
2975.47
1726.64
1658.38
1550.08
1507.06
1458.35
1392.79
1367.36
1312.23
1260.76
1211.16
1152.07
1091.30
1013.82
956.88
926.45
890.12
843.85
756.95
687.31
4000.0
3000
2000
1500
1000
400.0
cm-1

ACQUISITION		DEC. & VT	
sfrq	499.758	dfrq	125.677
tn	H1	dn	C13
at	3.277	dpwr	34
np	65536	dof	1498.1
sw	9998.8	dm	nnn
fb	not used	dmm	w
bs	4	dmf	10000
tpwr	56	dseq	
pw	8.2	dres	1.0
d1	3.000	homo	n
tof	1498.1	PROCESSING	
nt	24	wtfile	
ct	24	proc	ft
alock	n	fn	65536
gain	not used	math	f
FLAGS		werr	
il	n	wexp	
in	n	wbs	
dp	y	wnt	
hs	nn		
DISPLAY			
sp	-250.2		
wp	6246.5		
vs	412		
sc	0		
wc	250		
hzmm	40.00		
is	33.57		
rfl	4564.4		
rfp	3578.2		
th	7		
ins	1.000		

nm cdc ph

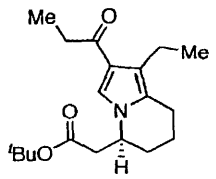

33

ACQUISITION	
sfrq	125.796
tn	C13
at	1.736
np	131010
sw	37735.8
fb	not used
bs	8
ss	1
tpwr	53
pw	6.9
d1	0.763
tof	631.4
nt	10000
ct	1152
alock	n
gain	not used
FLAGS	
il	n
in	n
dp	y
hs	nn
DISPLAY	
sp	-1258.4
wp	31448.1
vs	2134
sc	0
wc	250
hzmm	2.63
is	500.00
rfl	22374.0
rfp	16149.3
th	7
ins	1.000
ai	ph

DEC. & VT	
dfrq	500.233
dn	H1
dpwr	37
dof	-500.0
dm	y
dmm	w
dmf	10000
dseq	
dres	1.0
homo	n
PROCESSING	
lb	0.30
wtfile	
proc	ft
fn	131072
math	f
werr	
wexp	
wbs	
wnt	

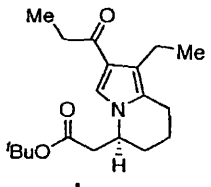

33

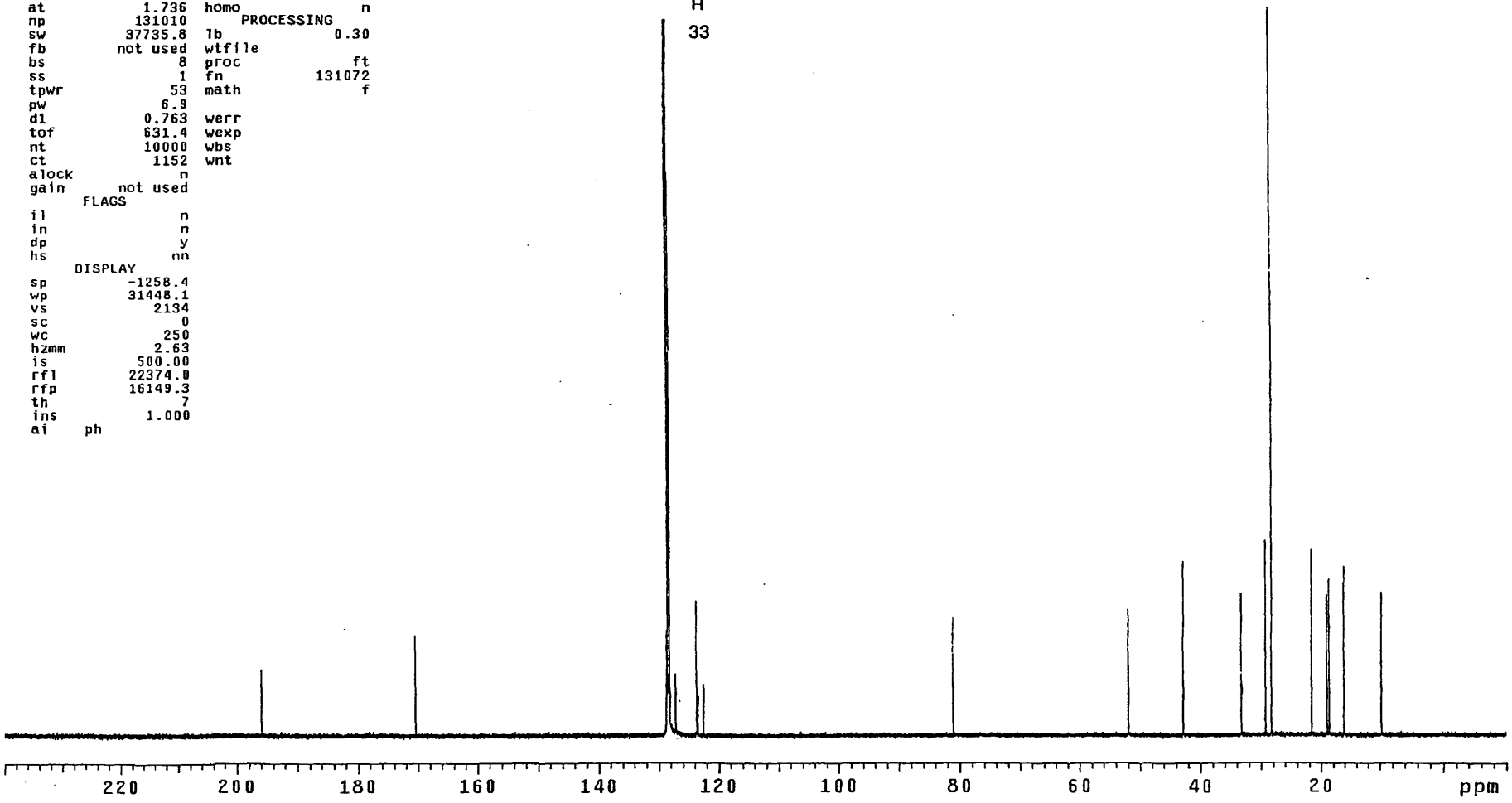

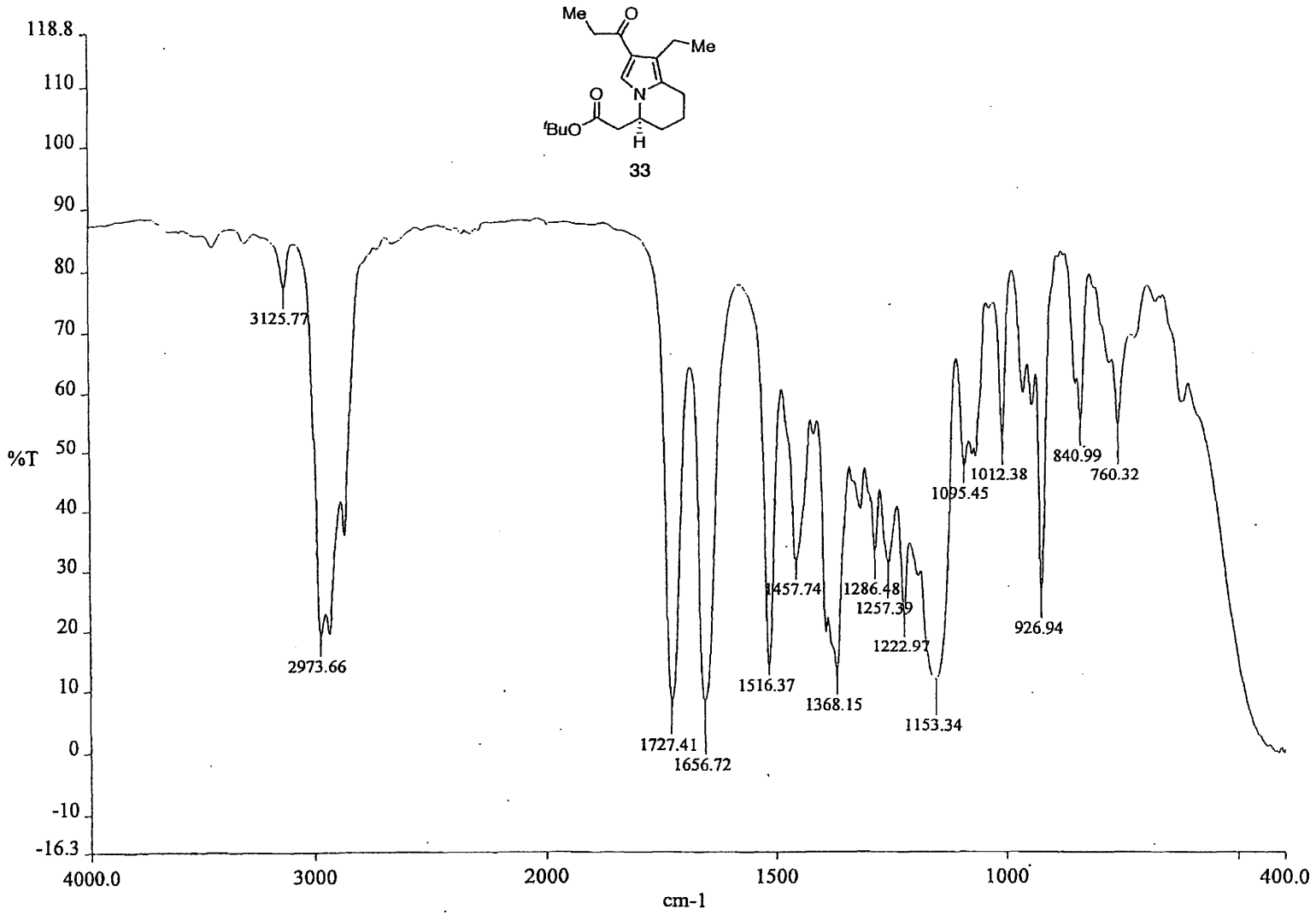
Me
O
Me
N
O
tBuO
H
33
118.8
110
100
90
80
70
60
50
40
30
20
10
0
-10
-16.3
%T
3125.77
2973.66
1727.41
1656.72
1516.37
1457.74
1368.15
1286.48
1257.39
1222.97
1153.34
1095.45
1012.38
926.94
840.99
760.32
4000.0
3000
2000
1500
1000
400.0
cm-1

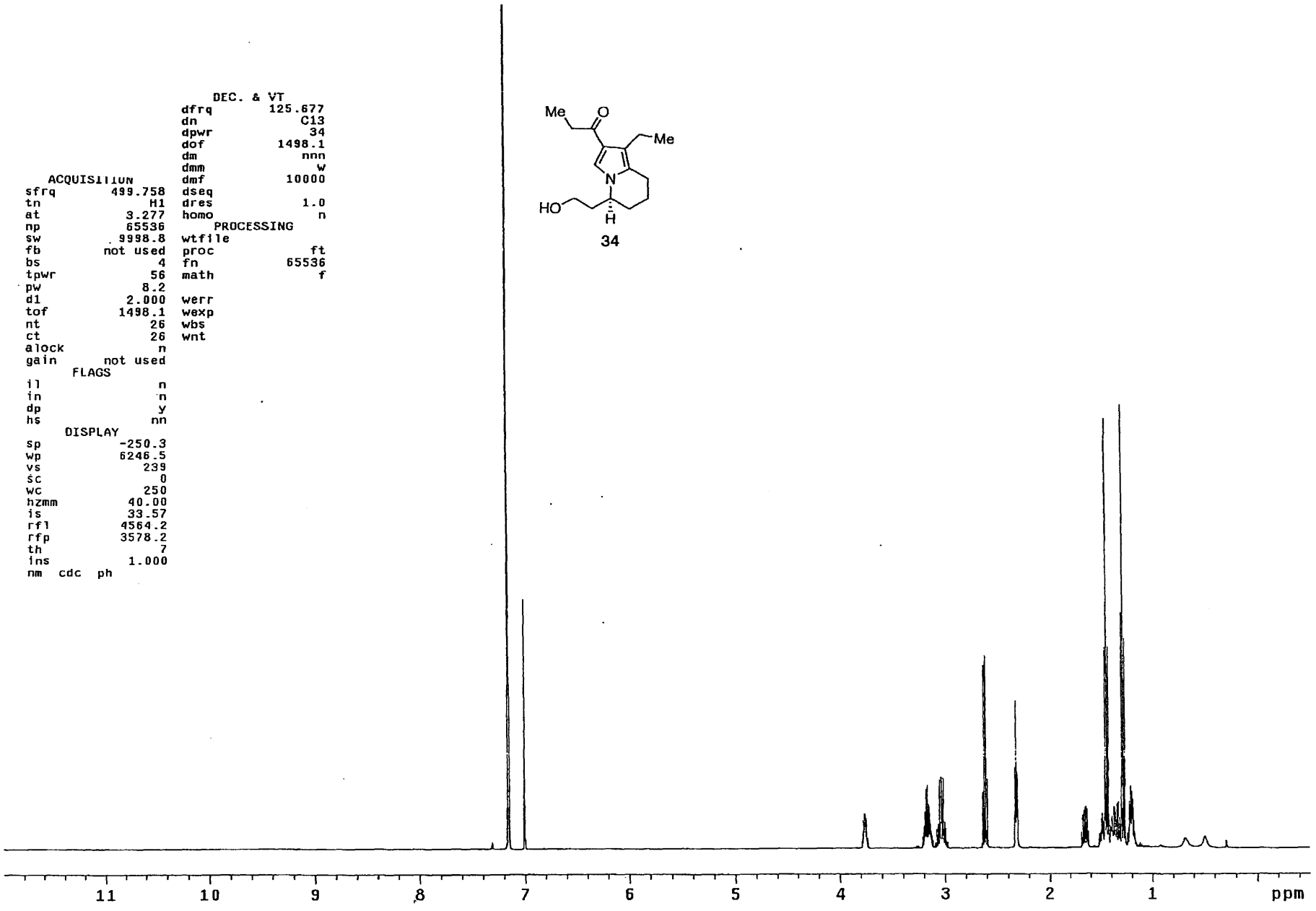
ACQUISITION
sfrq 499.758
tn H1
at 3.277
np 65536
sw 9998.8
fb not used
bs 4
tpwr 56
pw 8.2
d1 2.000
tof 1498.1
nt 26
ct 26
alock n
gain not used
FLAGS
il n
in n
dp y
hs nn
DISPLAY
sp -250.3
wp 6246.5
vs 239
sc 0
wc 250
hzmm 40.00
is 33.57
rfl 4564.2
rfp 3578.2
th 7
ins 1.000
nm cdc ph
DEC. & VT
dfrq 125.677
dn C13
dpwr 34
dof 1498.1
dm nnn
dmm w
dmf 10000
dseq
dres 1.0
homo n
PROCESSING
wtfile
proc ft
fn 65536
math f
werr
wexp
wbs
wnt
Me
O
Me
N
HO
H
34
11
10
9
8
7
6
5
4
3
2
1
ppm

ACQUISITION		DEC. & VT	
sfrq	125.796	dfrq	500.233
tn	C13	dn	H1
at	1.736	dpwr	37
np	131010	dof	-500.0
sw	37735.8	dm	y
fb	not used	dmm	w
bs	8	dmf	10000
ss	1	dseq	
tpwr	53	dres	1.0
pw	6.9	homo	n
d1	0.763	PROCESSING	
tof	631.4	lb	0.30
nt	100000	wtfile	
ct	1832	proc	ft
alock	n	fn	131072
gain	not used	math	f
FLAGS		werr	
il	n	wexp	
in	n	wbs	
dp	y	wnt	
hs	nn		
DISPLAY			
sp	-1258.4		
wp	31445.8		
vs	4179		
sc	0		
wc	250		
hzmm	125.78		
is	500.00		
rfl	22374.6		
rfp	16149.3		
th	20		
ins	1.000		
ai	ph		

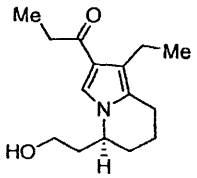

34

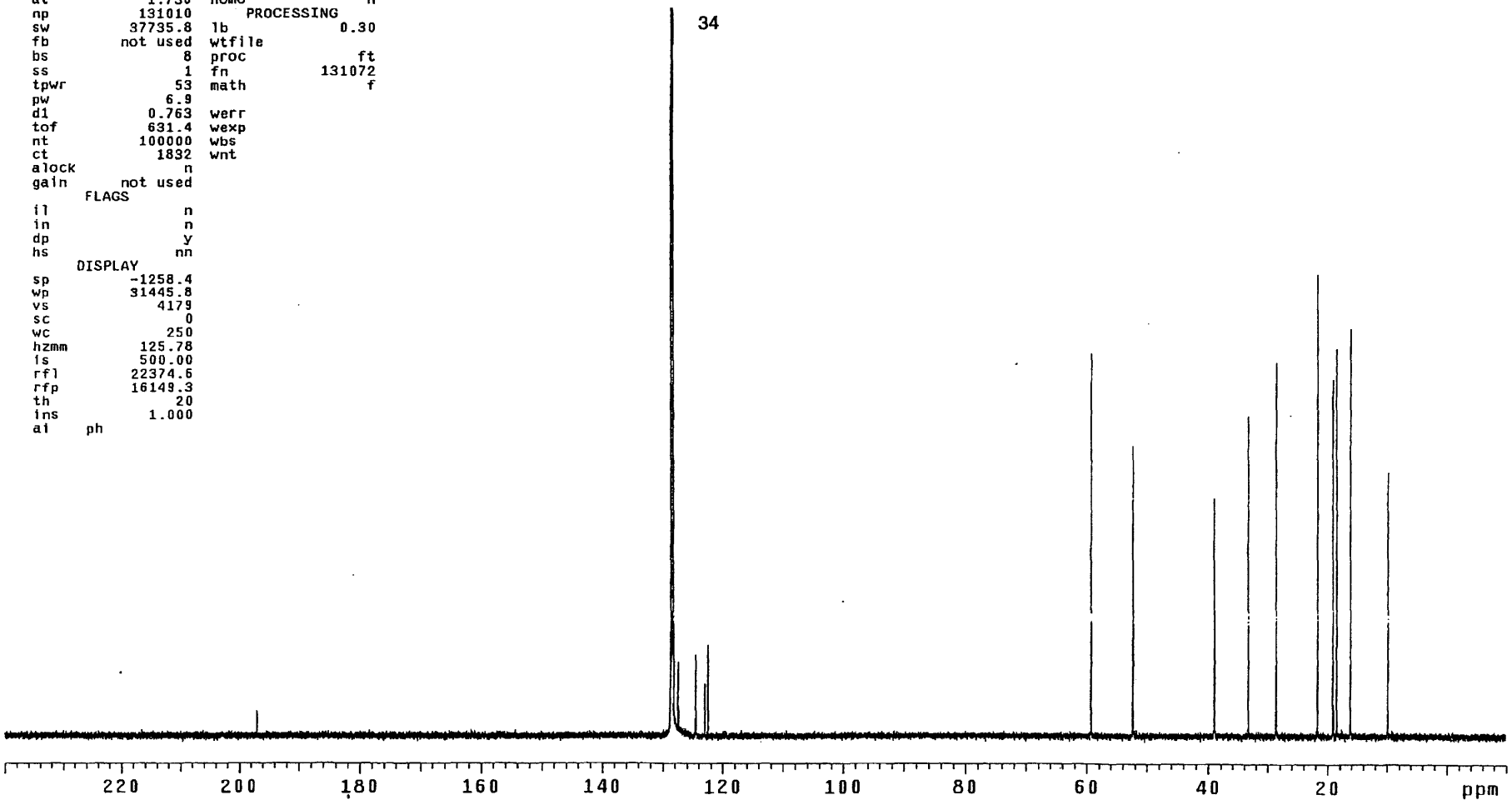

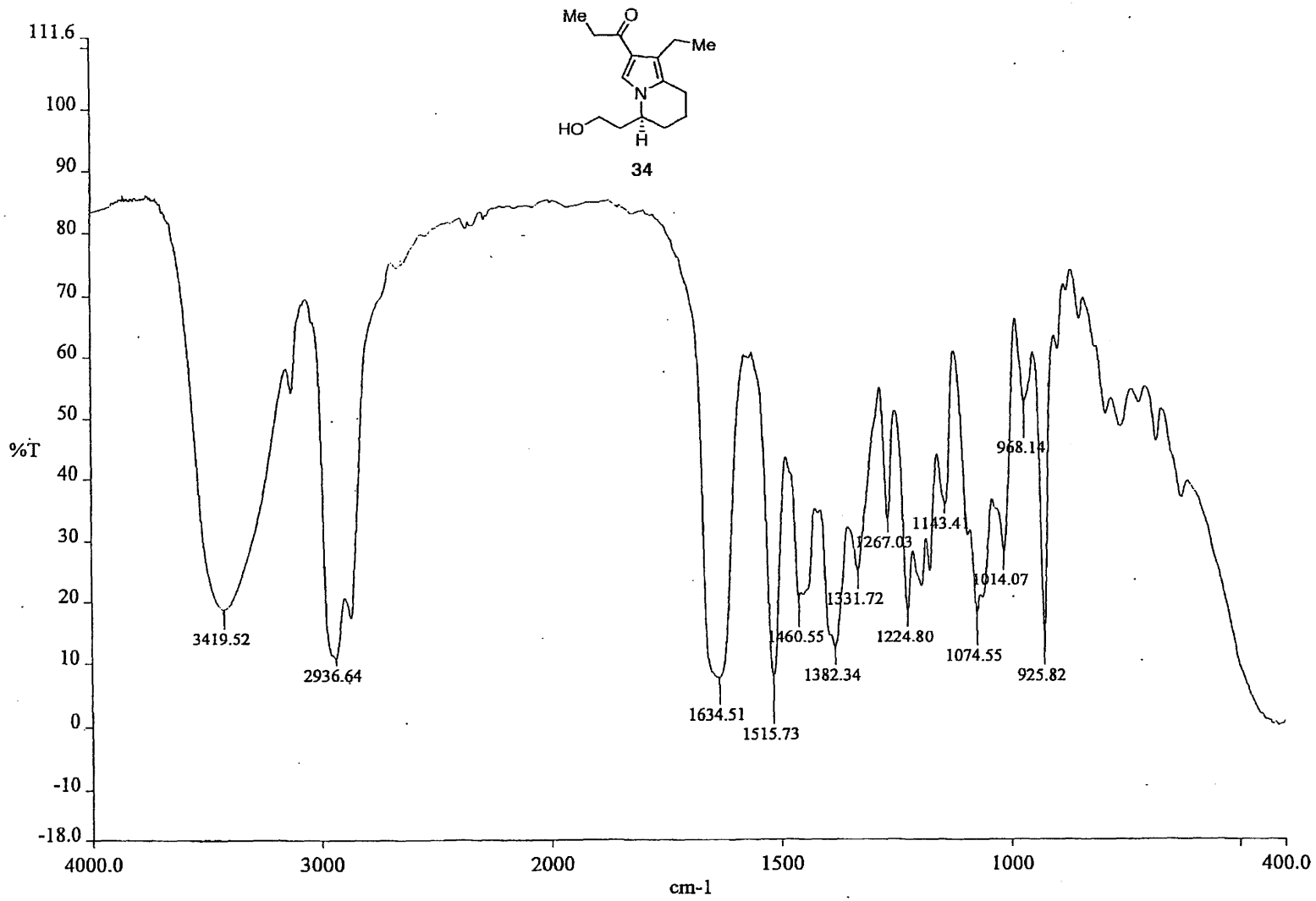
Me
O
Me
N
HO
H
34
111.6
100
90
80
70
60
50
40
30
20
10
0
-10
-18.0
%T
3419.52
2936.64
1634.51
1515.73
1460.55
1382.34
1331.72
1267.03
1224.80
1143.41
1074.55
1014.07
968.14
925.82
4000.0
3000
2000
1500
1000
400.0
cm-1

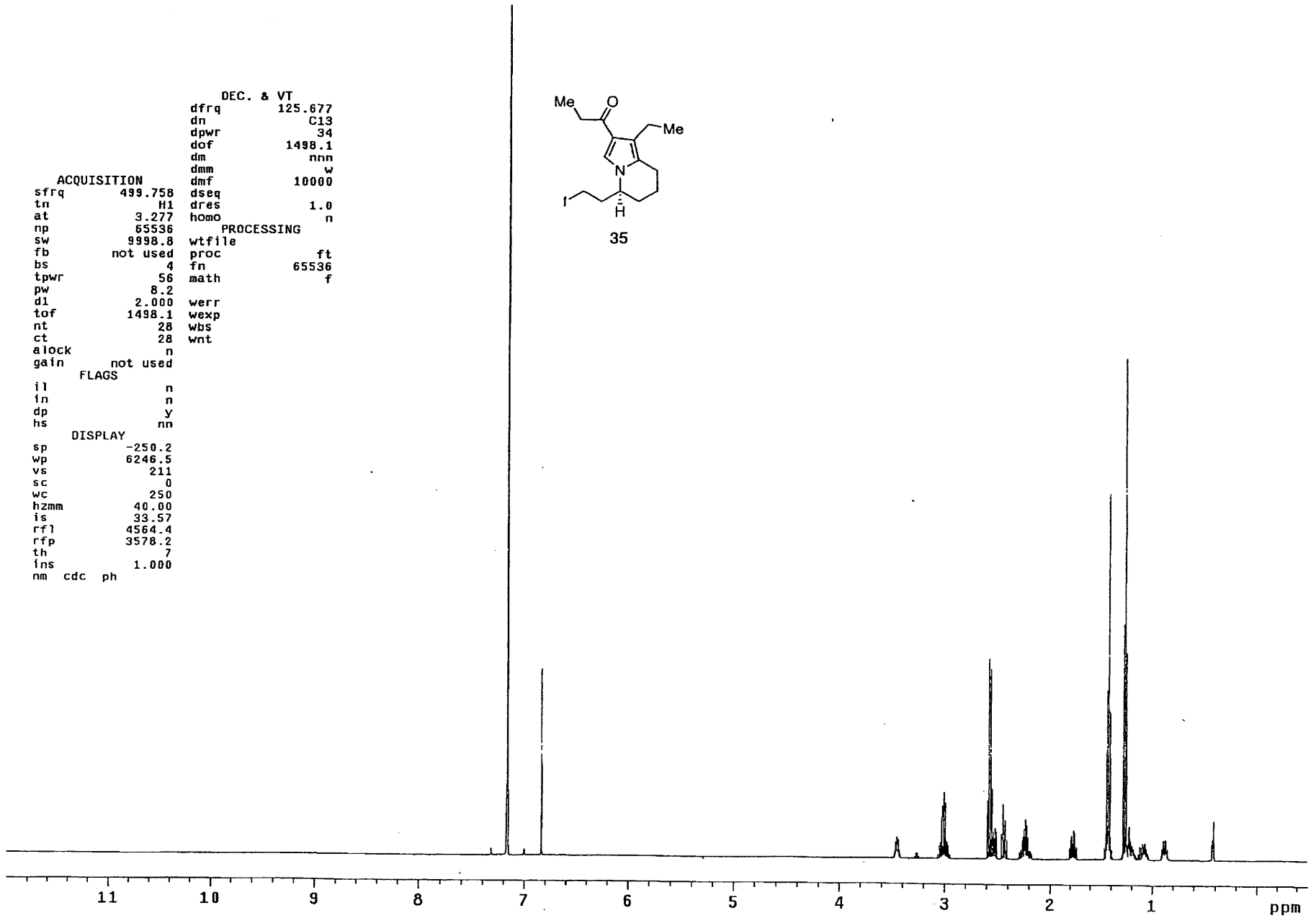
ACQUISITION
sfrq 499.758
tn H1
at 3.277
np 65536
sw 9998.8
fb not used
bs 4
tpwr 56
pw 8.2
d1 2.000
tof 1498.1
nt 28
ct 28
alock n
gain not used
FLAGS
il n
in n
dp y
hs nn
DISPLAY
sp -250.2
wp 6246.5
vs 211
sc 0
wc 250
hzmm 40.00
is 33.57
rfl 4564.4
rfp 3578.2
th 7
ins 1.000
nm cdc ph
DEC. & VT
dfrq 125.677
dn C13
dpwr 34
dof 1498.1
dm nnn
dmm w
dmf 10000
dseq
dres 1.0
homo n
PROCESSING
wtfile
proc ft
fn 65536
math f
werr
wexp
wbs
wnt
Me
O
Me
N
I
H
35
11
10
9
8
7
6
5
4
3
2
1
ppm

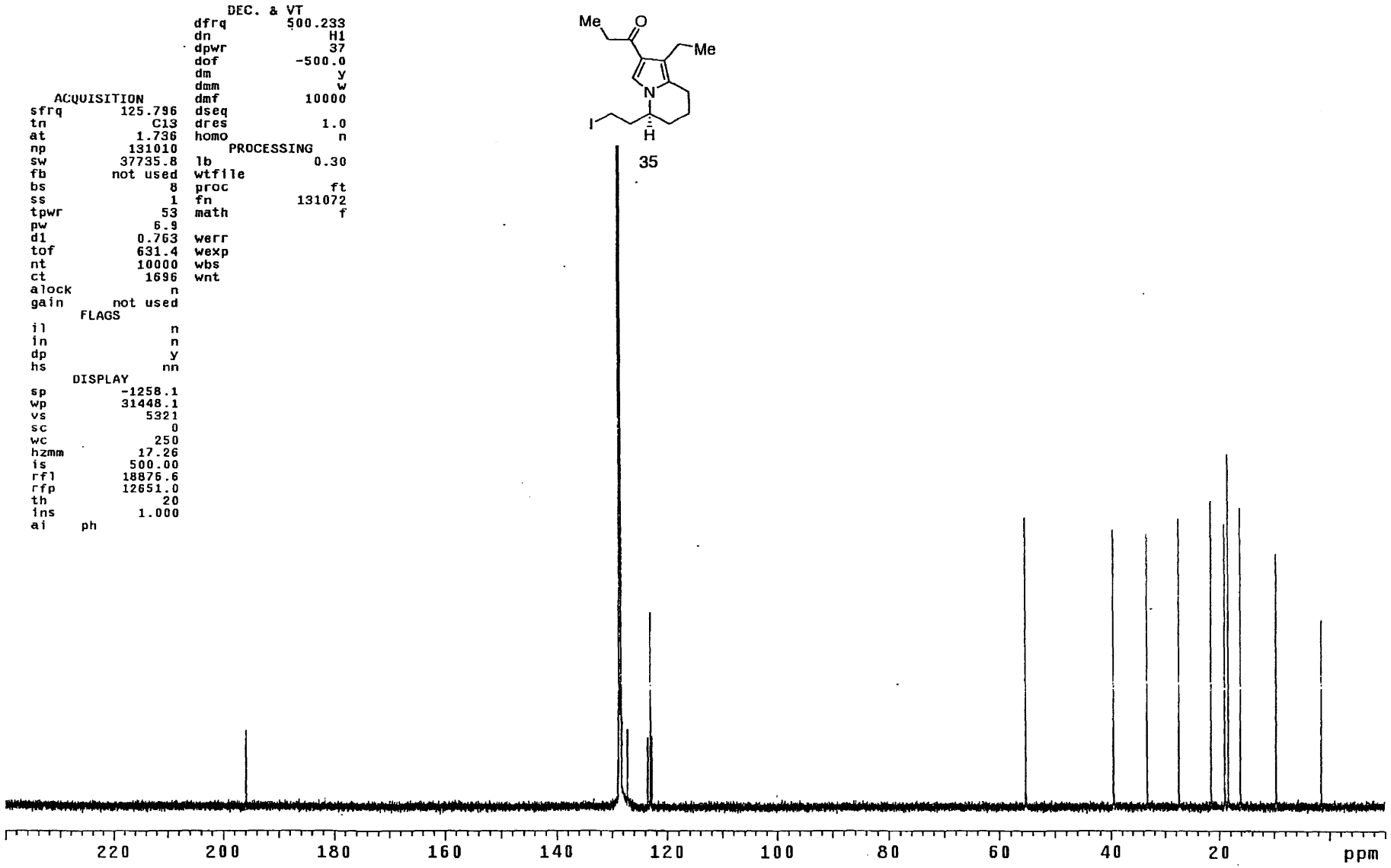
ACQUISITION
sfrq 125.796
tn C13
at 1.736
np 131010
sw 37735.8
fb not used
bs 8
ss 1
tpwr 53
pw 6.9
d1 0.763
tof 631.4
nt 10000
ct 1696
alock n
gain not used
FLAGS
il n
in n
dp y
hs nn
DISPLAY
sp -1258.1
wp 31448.1
vs 5321
sc 0
wc 250
hzmm 17.26
is 500.00
rfl 18876.6
rfp 12651.0
th 20
ins 1.000
ai ph
DEC. & VT
dfrq 500.233
dn H1
dpwr 37
dof -500.0
dm y
dmm w
dmf 10000
dseq
dres 1.0
homo n
PROCESSING
lb 0.30
wtfile
proc ft
fn 131072
math f
werr
wexp
wbs
wnt
Me
O
Me
N
I
H
35
220
200
180
160
140
120
100
80
60
40
20
ppm

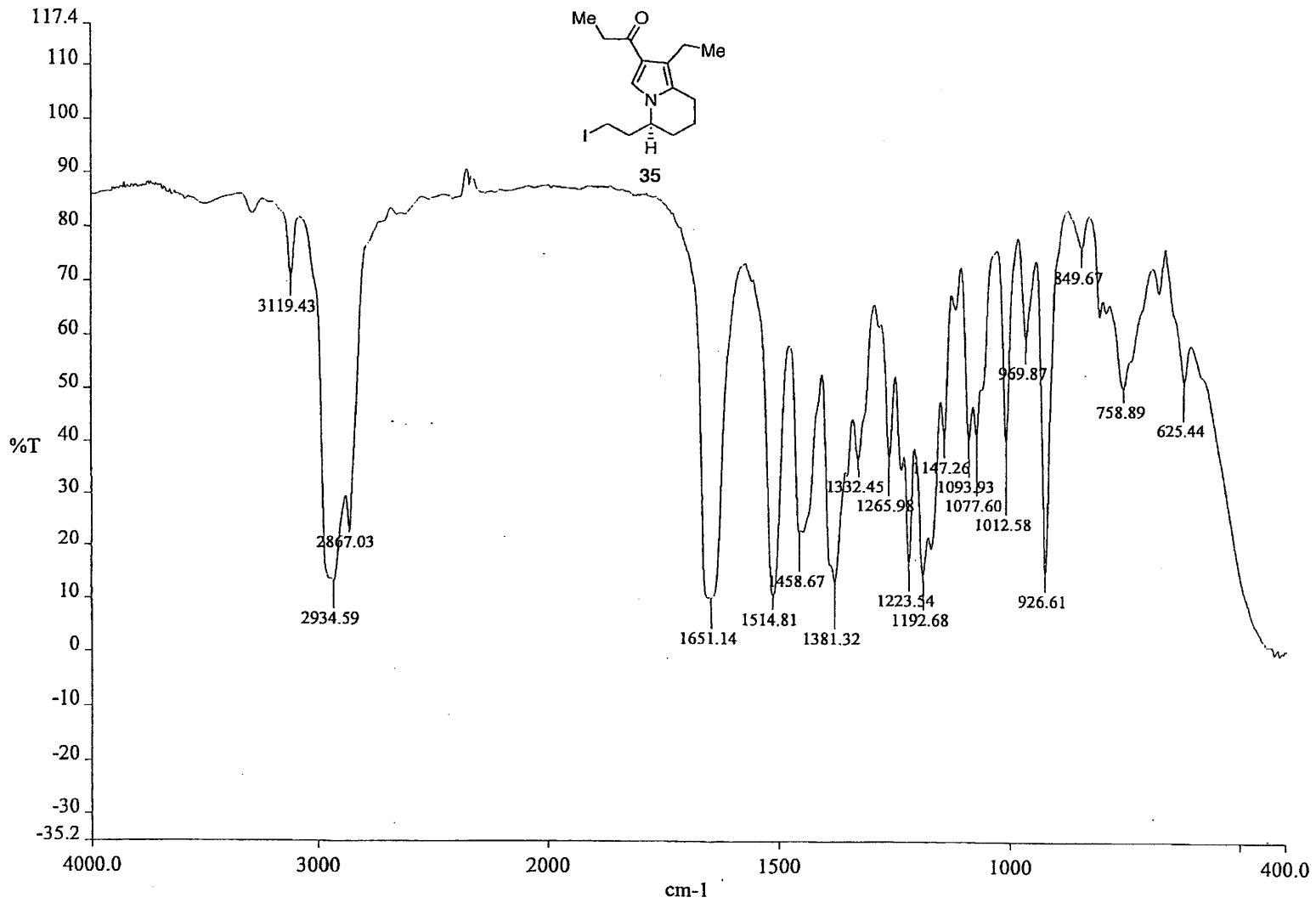
117.4
110
100
90
80
70
60
50
40
30
20
10
0
-10
-20
-30
-35.2
%T
4000.0
3000
2000
1500
1000
400.0
cm-1
Me
O
Me
N
I
H
35
3119.43
2867.03
2934.59
1651.14
1514.81
1458.67
1381.32
1332.45
1265.98
1223.54
1192.68
1147.26
1093.93
1077.60
1012.58
969.87
926.61
849.67
758.89
625.44

Data File C:\HPCHEM\2\DATA\.

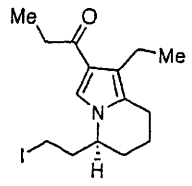

35

```
==========================================================================
Injection Date  :                                  Seq. Line :   1
Sample Name     :                                   Location : Vial 1
Acq. Operator   :                                        Inj :   1
                                                 Inj Volume : 1 µl

Acq. Method     : C:\HPCHEM\2\METHODS\
Last changed    :
Analysis Method : C:\HPCHEM\2\METHODS\.
Last changed    :
                  (modified after loading)
2.5% ipa-hexanes 3 mL/min
```

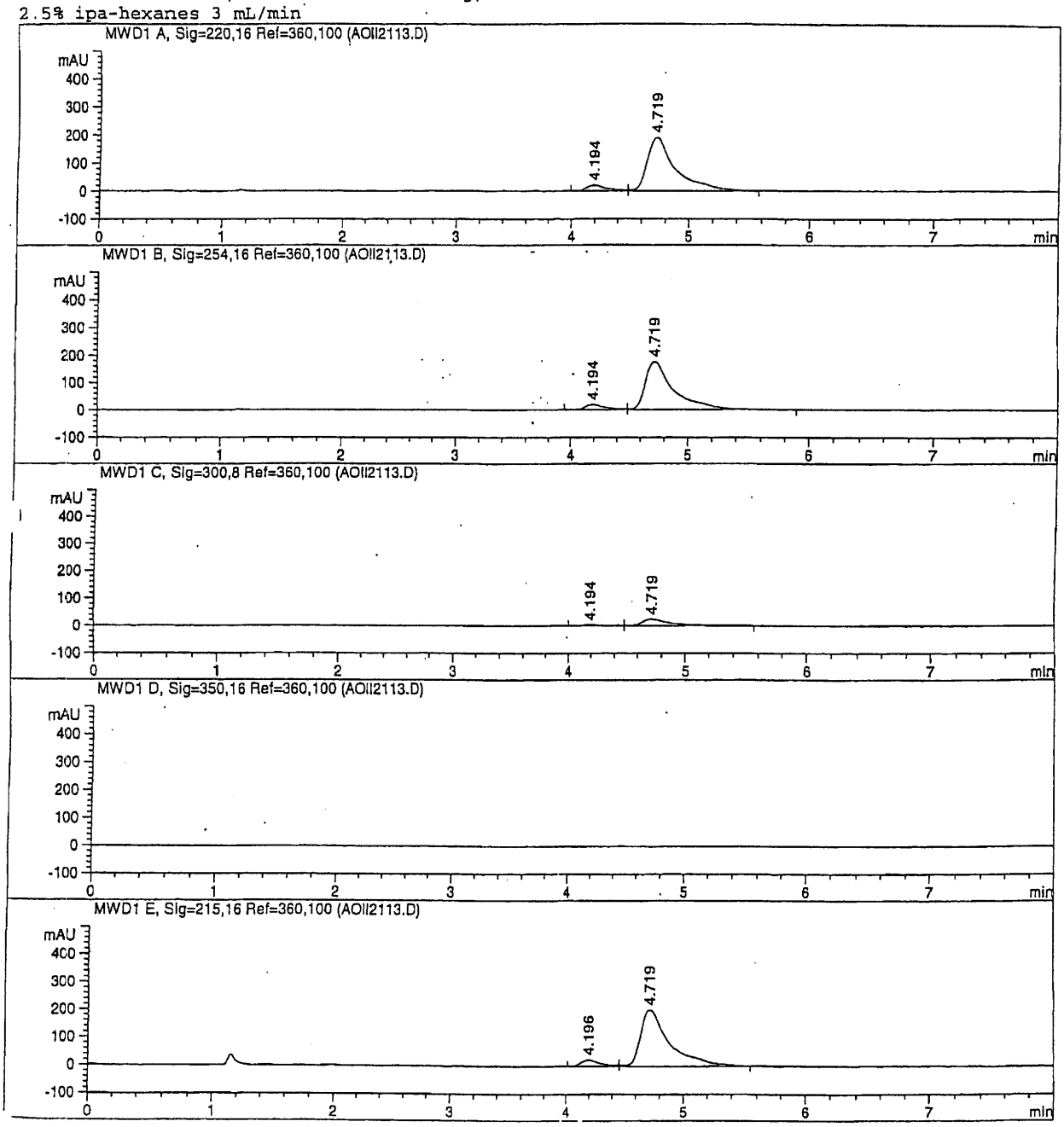

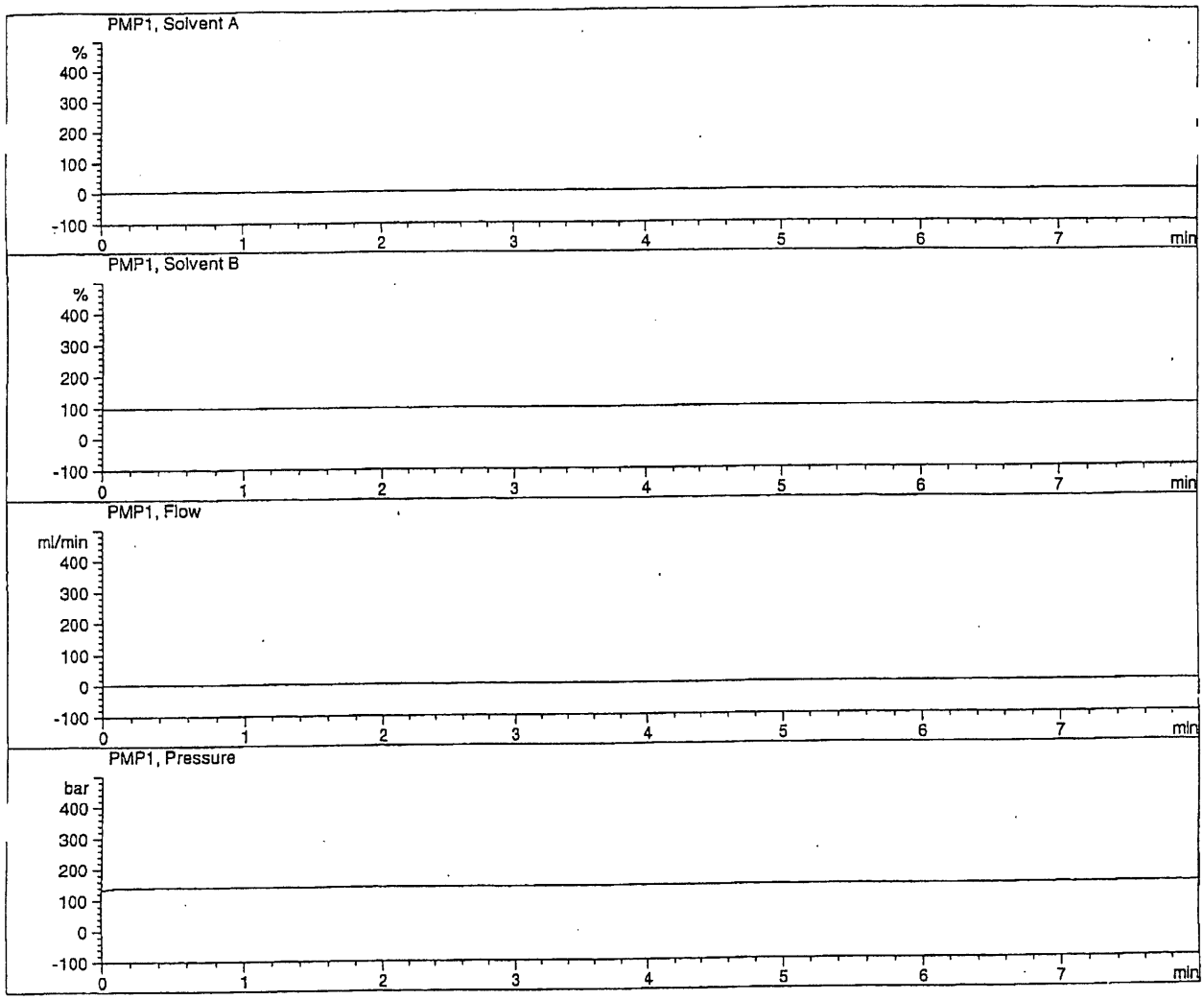

==========

Area Percent Report

==========

Sorted By : Signal
Multiplier : 1.0000
Dilution : 1.0000
Use Multiplier & Dilution Factor with ISTDs

Signal 1: MWD1 A, Sig=220,16 Ref=360,100

Peak #	RetTime [min]	Type	Width [min]	Area [mAU*s]	Height [mAU]	Area %
1	4.194	VV	0.1792	256.73700	20.91166	7.4632
2	4.719	VV	0.2383	3183.32153	191.15761	92.5368
Totals :				3440.05853	212.06927	

Results obtained with enhanced integrator!

Data File C:\HPCHEM\2\DATA\ Sample Name:

Signal 2: MWD1 B, Sig=254,16 Ref=360,100

Peak #	RetTime [min]	Type	Width [min]	Area [mAU*s]	Height [mAU]	Area %
1	4.194	PV	0.1750	227.27029	18.80288	7.3077
2	4.719	VB	0.2358	2882.74707	175.37024	92.6923
Totals :				3110.01736	194.17312	

Results obtained with enhanced integrator!

Signal 3: MWD1 C, Sig=300,8 Ref=360,100

Peak #	RetTime [min]	Type	Width [min]	Area [mAU*s]	Height [mAU]	Area %
1	4.194	BV	0.1728	29.93626	2.51618	7.2961
2	4.719	VB	0.2337	380.36707	23.39379	92.7039
Totals :				410.30333	25.90997	

Results obtained with enhanced integrator!

Signal 4: MWD1 D, Sig=350,16 Ref=360,100

Signal 5: MWD1 E, Sig=215,16 Ref=360,100

Peak #	RetTime [min]	Type	Width [min]	Area [mAU*s]	Height [mAU]	Area %
1	4.196	VV	0.1762	271.47430	22.59101	7.2723
2	4.719	VV	0.2398	3388.25854	201.93718	90.7654
3	11.005	VV	0.1430	16.85956	1.71089	0.4516
4	11.574	VV	0.1341	20.44657	1.98692	0.5477
5	18.327	VV	0.1578	18.15042	1.73816	0.4862
6	20.315	VV	0.1524	17.79565	1.78367	0.4767
Totals :				3732.98505	231.74783	

Results obtained with enhanced integrator!

*** End of Report ***

ACQUISITION	
sfrq	499.758
tn	H1
at	3.277
np	65536
sw	9998.8
fb	not used
bs	4
tpwr	56
pw	8.2
d1	2.000
tof	1498.1
nt	28
ct	28
alock	n
gain	not used
FLAGS	
il	n
in	n
dp	y
hs	nn
DISPLAY	
sp	-250.2
wp	6246.5
vs	135
sc	0
wc	250
hzmm	40.00
is	33.57
rfl	4564.7
rfp	3578.2
th	7
ins	1.000

nm cdc ph

DEC. & VT	
dfrq	125.677
dn	C13
dpwr	34
dof	1498.1
dm	nnn
dmm	w
dmf	10000
dseq	
dres	1.0
homo	n
PROCESSING	
wtfile	
proc	ft
fn	65536
math	f
werr	
wexp	
wbs	
wnt	

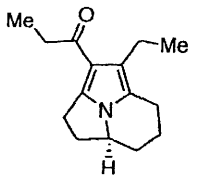

19

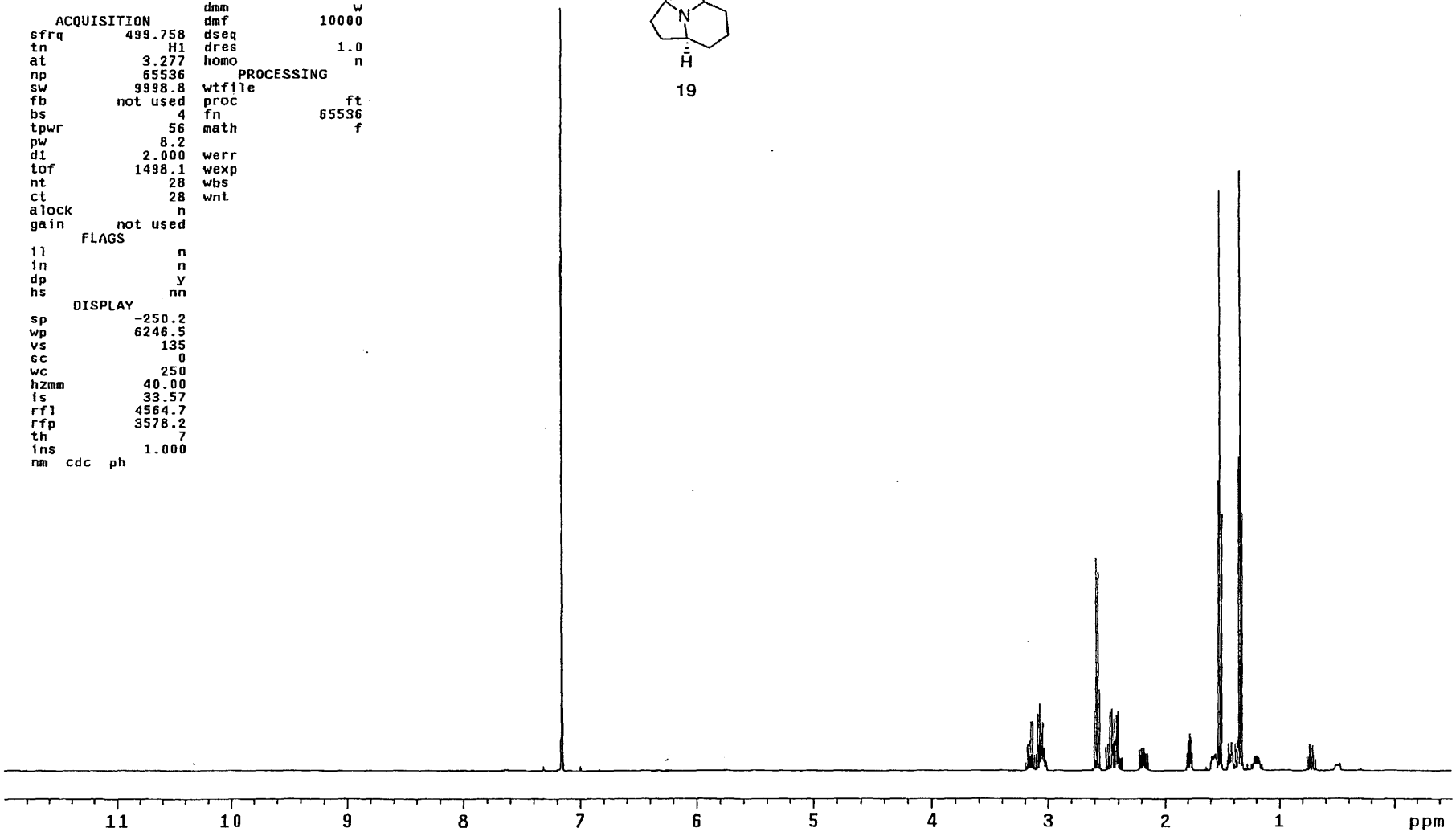

ACQUISITION	
sfrq	125.796
tn	C13
at	1.736
np	131010
sw	37735.8
fb	not used
bs	8
ss	1
tpwr	53
pw	6.9
d1	0.763
tof	631.4
nt	1e+06
ct	5520
alock	n
gain	not used

FLAGS	
il	n
in	n
dp	y
hs	nn

DISPLAY	
sp	-1258.4
wp	31448.1
vs	1403
sc	0
wc	250
hzmm	3.69
is	500.00
rfl	22373.4
rfp	16149.3
th	20
ins	1.000
ai	ph

DEC. & VT	
dfrq	500.233
dn	H1
dpwr	37
dof	-500.0
dm	y
dmm	w
dmf	10000
dseq	
dres	1.0
homo	n

PROCESSING	
lb	0.30
wtfile	
proc	ft
fn	131072
math	f
werr	
wexp	
wbs	
wnt	

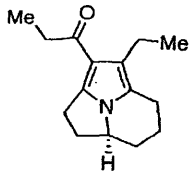

19

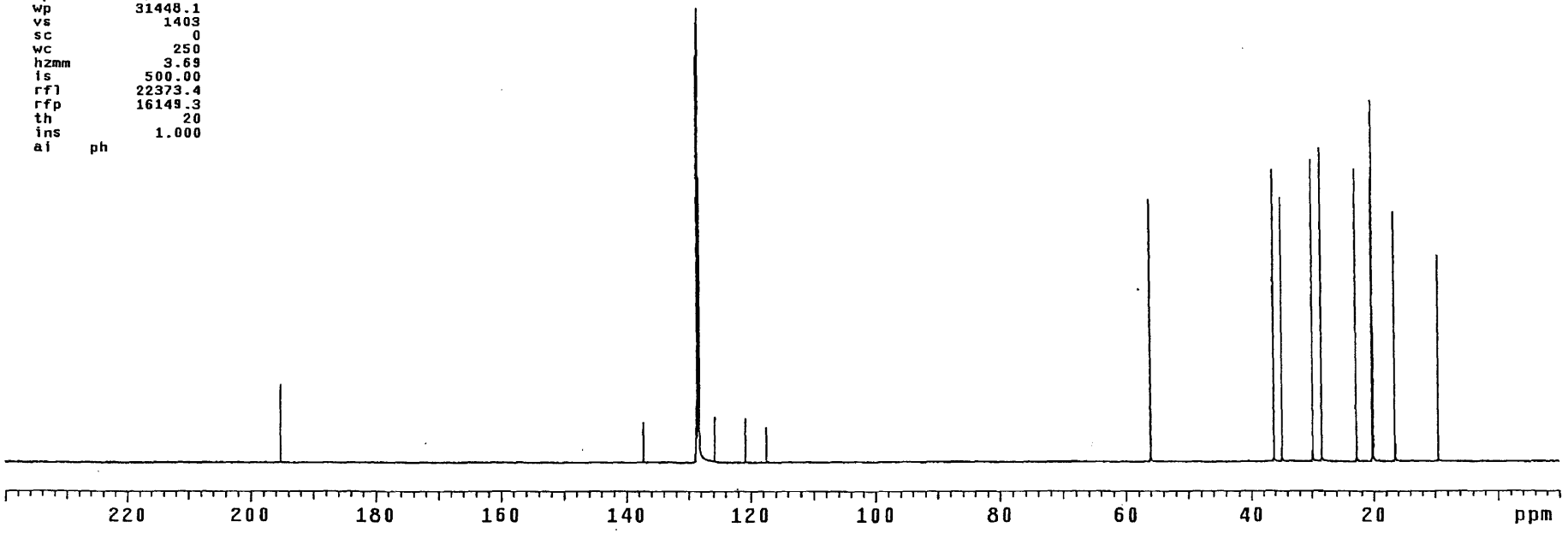

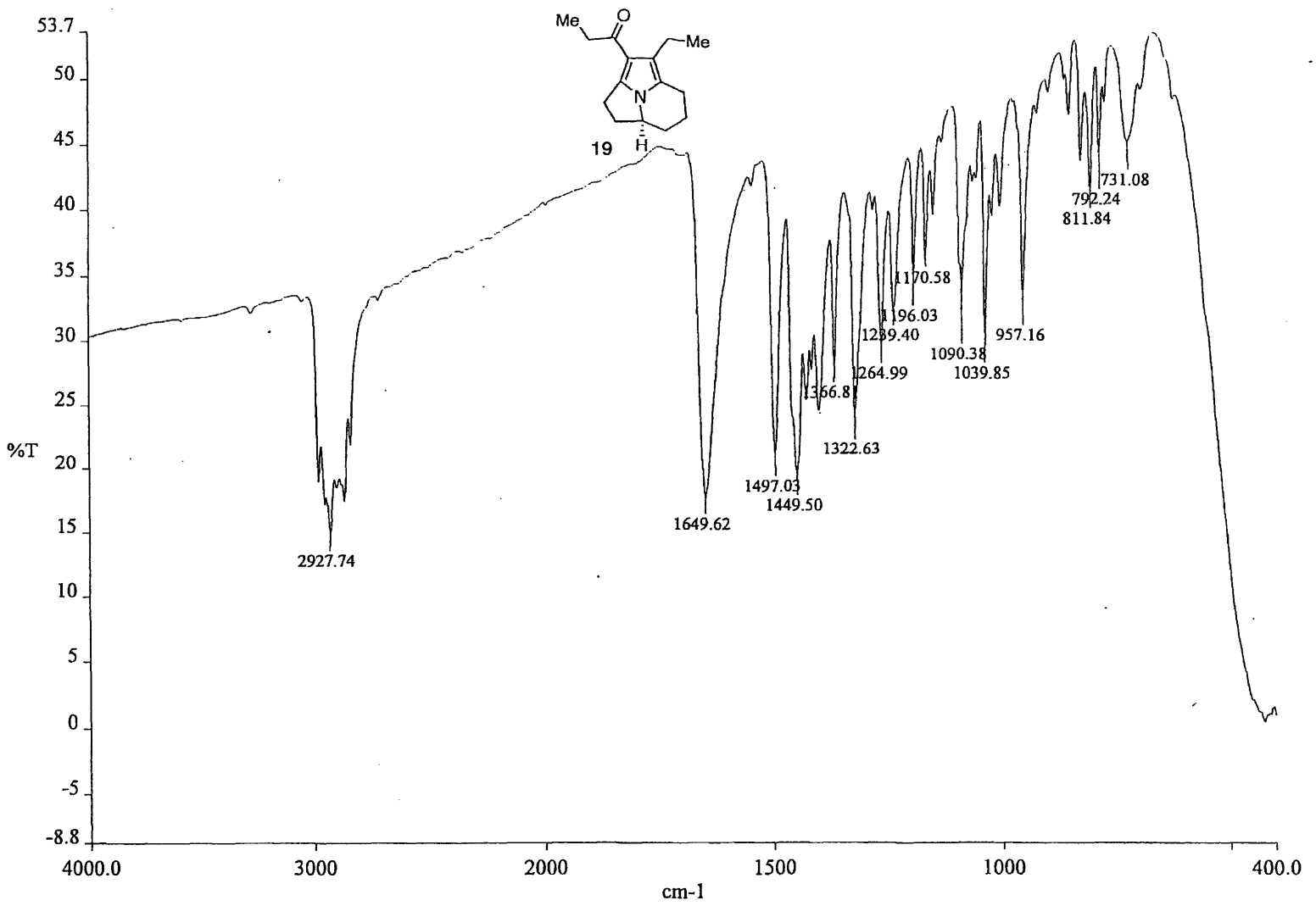
Me
O
Me
N
19
H
53.7
50
45
40
35
30
25
%T
20
15
10
5
0
-5
-8.8
4000.0
3000
2000
1500
1000
400.0
cm-1
2927.74
1649.62
1497.03
1449.50
1366.8
1322.63
1264.99
1239.40
1196.03
1170.58
1090.38
1039.85
957.16
811.84
792.24
731.08

ACQUISITION	
sfrq	499.758
tn	H1
at	3.277
np	65536
sw	9998.8
fb	not used
bs	4
tpwr	56
pw	8.2
d1	3.000
tof	1498.1
nt	36
ct	36
alock	n
gain	not used

FLAGS	
il	n
in	n
dp	y
hs	nn

DISPLAY	
sp	-250.2
wp	6246.5
vs	72
sc	0
wc	250
hzmm	7.52
is	33.57
rfl	4564.4
rfp	3578.2
th	7
ins	3.000

nm cdc ph

DEC. & VT	
dfrq	125.677
dn	C13
dpwr	34
dof	1498.1
dm	nnn
dmm	w
dmf	10000
dseq	
dres	1.0
homo	n

PROCESSING	
wtfile	
proc	ft
fn	65536
math	f
werr	
wexp	
wbs	
wnt	

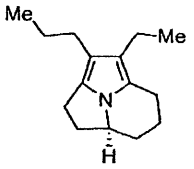

ent-6

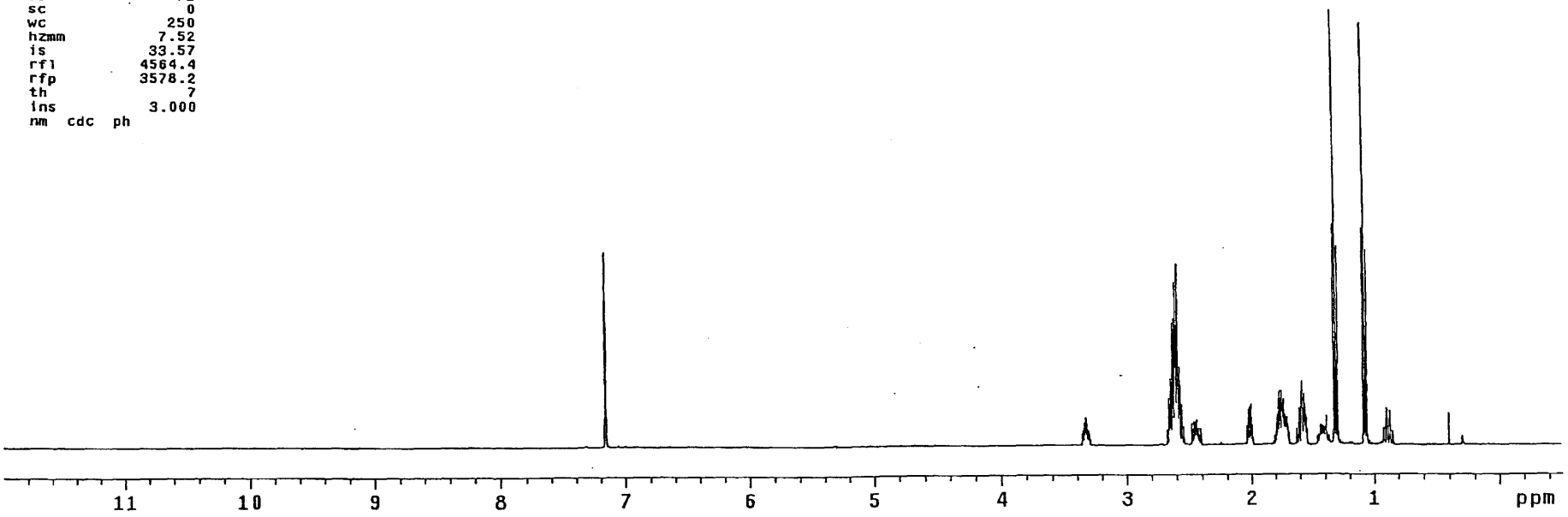

ACQUISITION		DEC. & VT	
sfrq	125.796	dfrq	500.233
tn	C13	dn	H1
at	1.736	dpwr	37
np	131010	dof	-500.0
sw	37735.8	dm	y
fb	not used	dmm	w
bs	8	dmf	10000
ss	1	dseq	
tpwr	53	dres	1.0
pw	6.9	homo	n
d1	0.763	PROCESSING	
tof	631.4	lb	0.30
nt	4e+07	wtfile	
ct	19872	proc	ft
alock	n	fn	131072
gain	not used	math	f
FLAGS		werr	
il	n	wexp	
in	n	wbs	
dp	y	wnt	
hs	nn		
DISPLAY			
sp	-1258.4		
wp	31448.1		
vs	2138		
sc	0		
wc	250		
hzmm	8.06		
is	500.00		
rfl	22373.4		
rfp	16149.3		
th	20		
ins	1.000		
ai	ph		

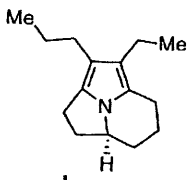

ent-6

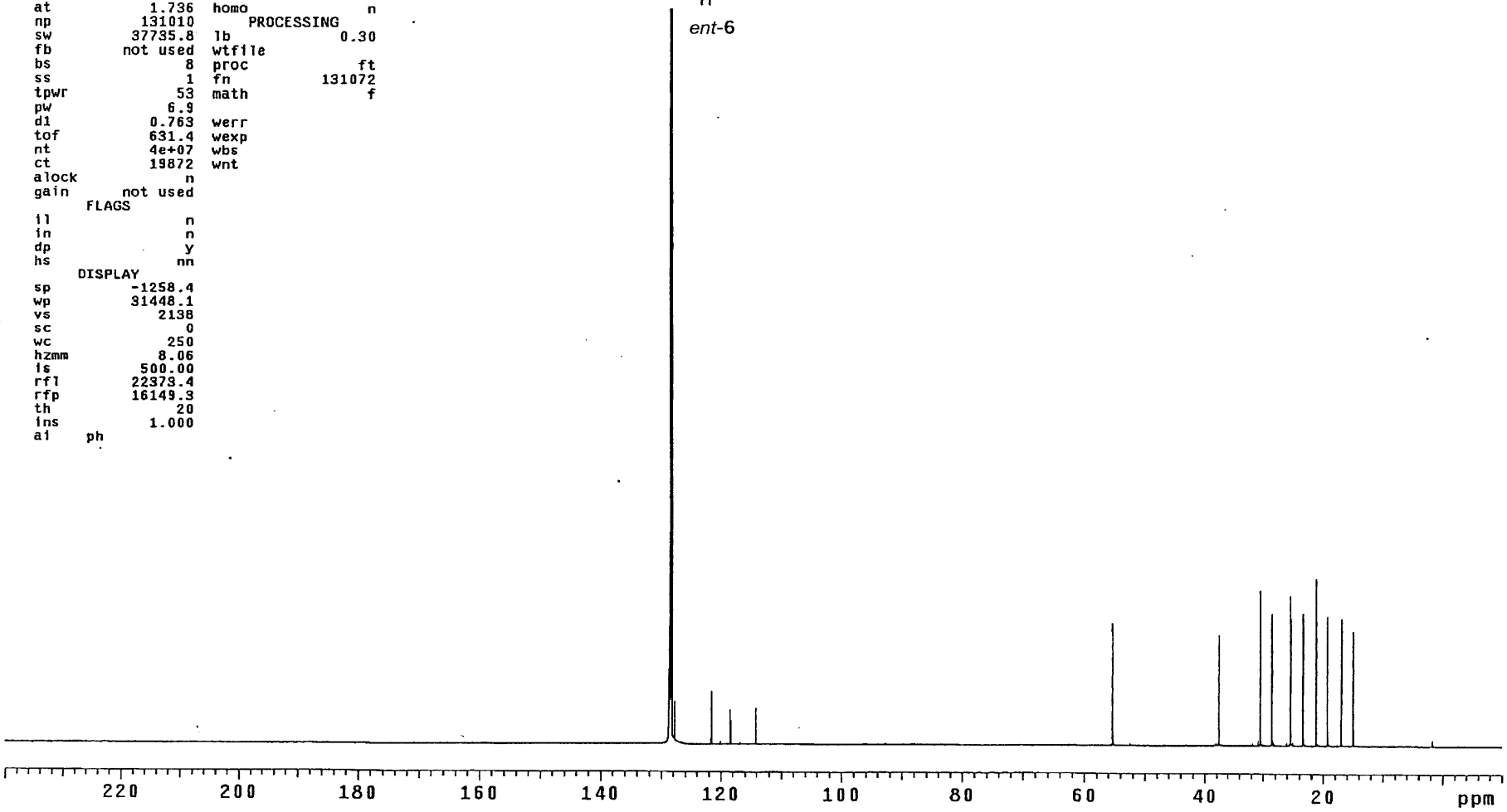

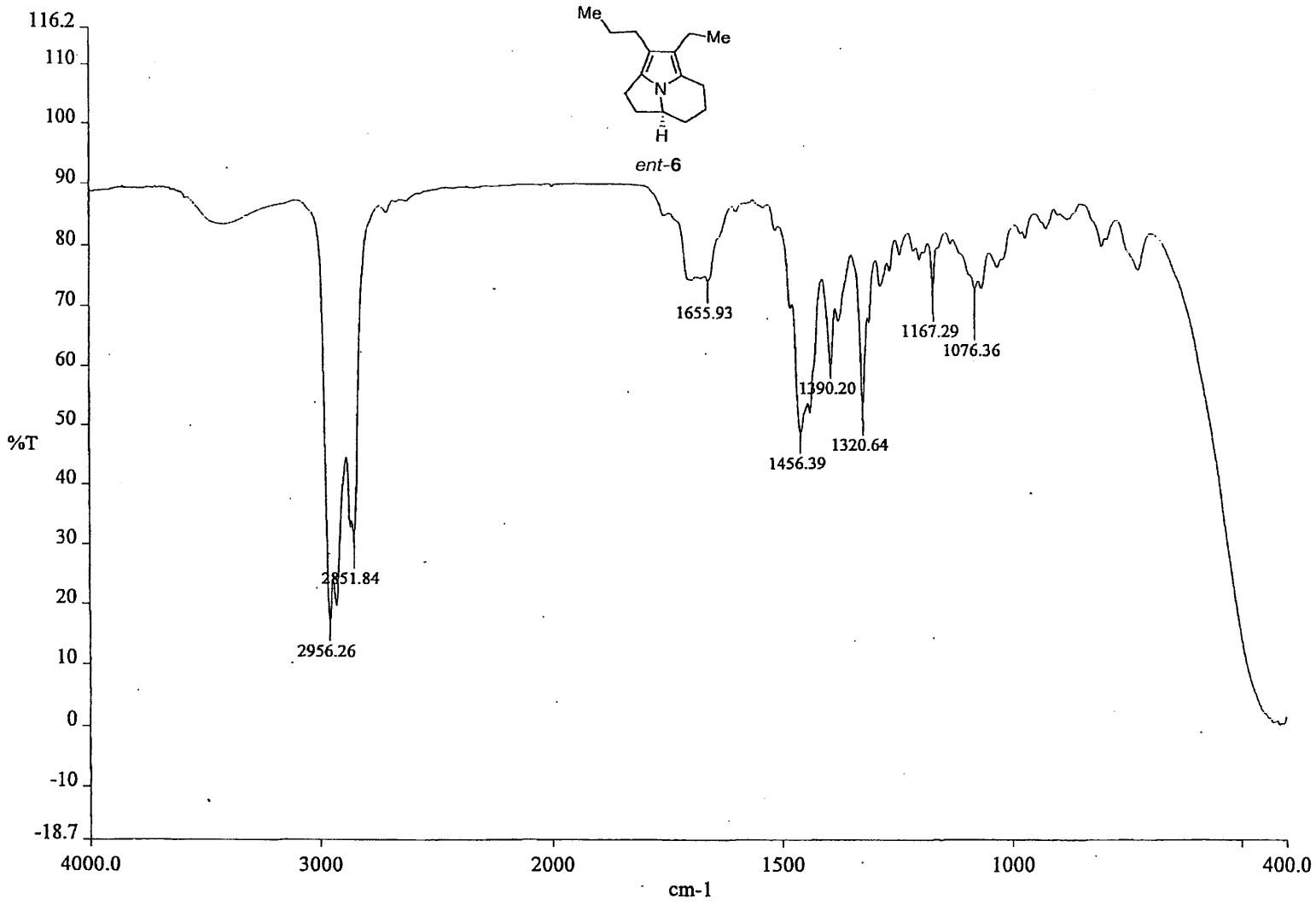
Me
Me
N
H
ent-6
116.2
110
100
90
80
70
60
50
40
30
20
10
0
-10
-18.7
%T
1655.93
1167.29
1076.36
1390.20
1320.64
1456.39
2851.84
2956.26
4000.0
3000
2000
1500
1000
400.0
cm-1

ACQUISITION	
sfrq	499.749
tn	H1
at	3.277
np	65536
sw	9998.8
fb	not used
bs	4
tpwr	56
pw	8.2
d1	2.000
tof	1498.1
nt	24
ct	24
alock	n
gain	not used

FLAGS	
il	n
in	n
dp	y
hs	nn

DISPLAY	
sp	-250.2
wp	6246.5
vs	90
sc	0
wc	250
hzmm	40.00
is	33.57
rfl	4567.1
rfp	3578.2
th	7
ins	1.000

nm cdc ph

DEC. & VT	
dfrq	125.674
dn	C13
dpwr	34
dof	1498.1
dm	nnn
dmm	w
dmf	10000
dseq	
dres	1.0
homo	n

PROCESSING	
wtfile	
proc	ft
fn	65536
math	f
werr	
wexp	
wbs	
wnt	

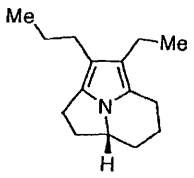

6

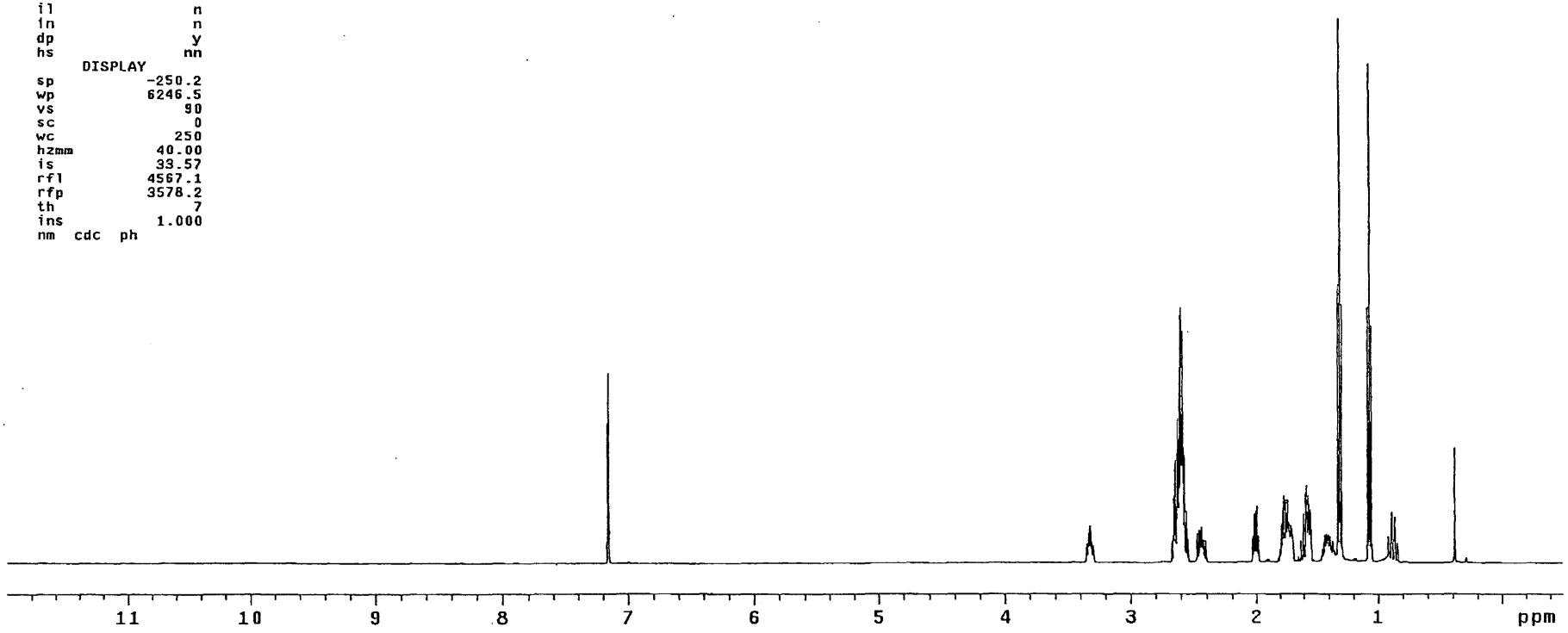

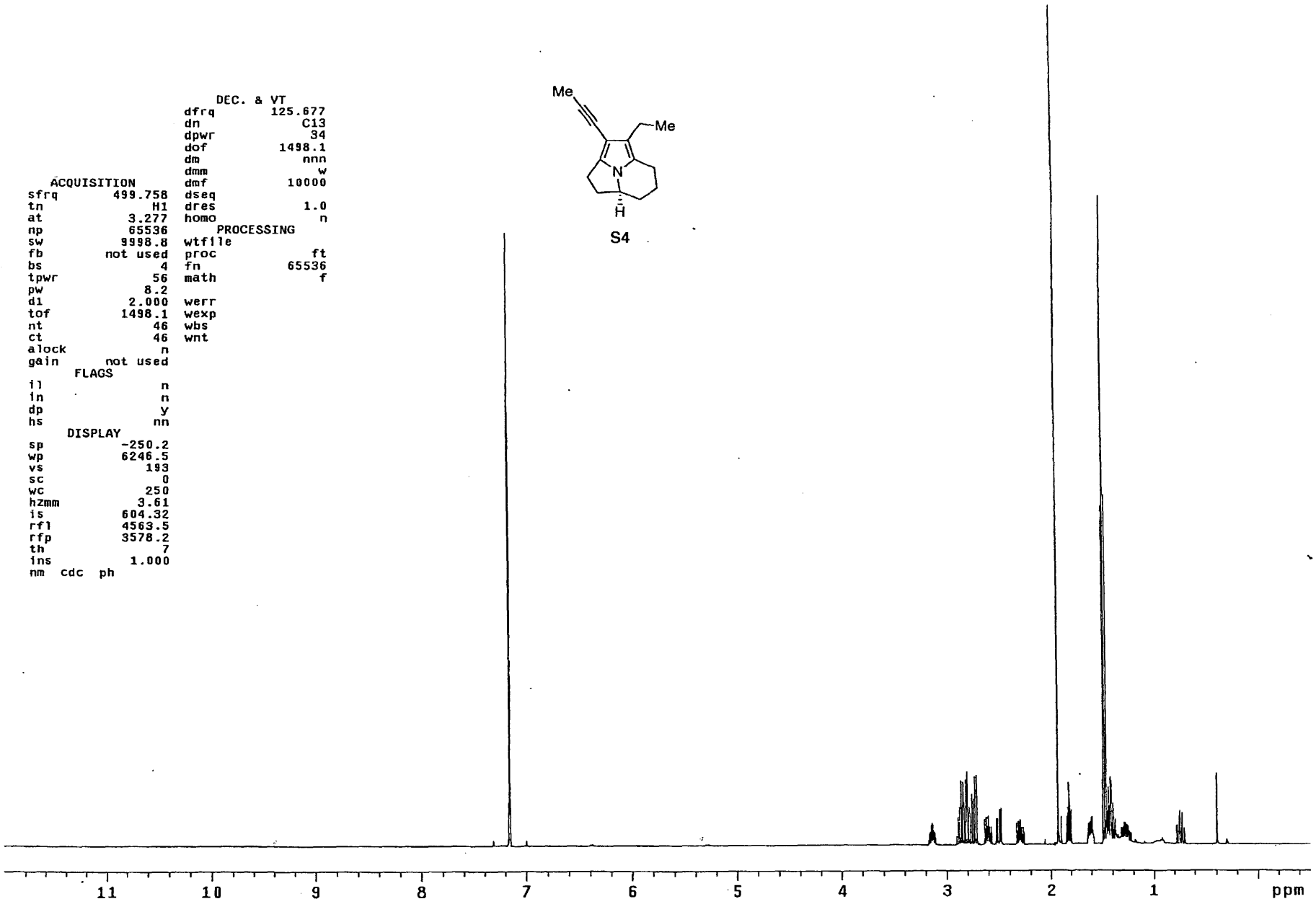
ACQUISITION
sfrq 499.758
tn H1
at 3.277
np 65536
sw 9998.8
fb not used
bs 4
tpwr 56
pw 8.2
d1 2.000
tof 1498.1
nt 46
ct 46
alock n
gain not used
FLAGS
il n
in n
dp y
hs nn
DISPLAY
sp -250.2
wp 6246.5
vs 193
sc 0
wc 250
hzmm 3.61
is 604.32
rfl 4563.5
rfp 3578.2
th 7
ins 1.000
nm cdc ph
DEC. & VT
dfrq 125.677
dn C13
dpwr 34
dof 1498.1
dm nnn
dmm w
dmf 10000
dseq
dres 1.0
homo n
PROCESSING
wtfile
proc ft
fn 65536
math f
werr
wexp
wbs
wnt
Me
Me
N
H
S4
11
10
9
8
7
6
5
4
3
2
1
ppm

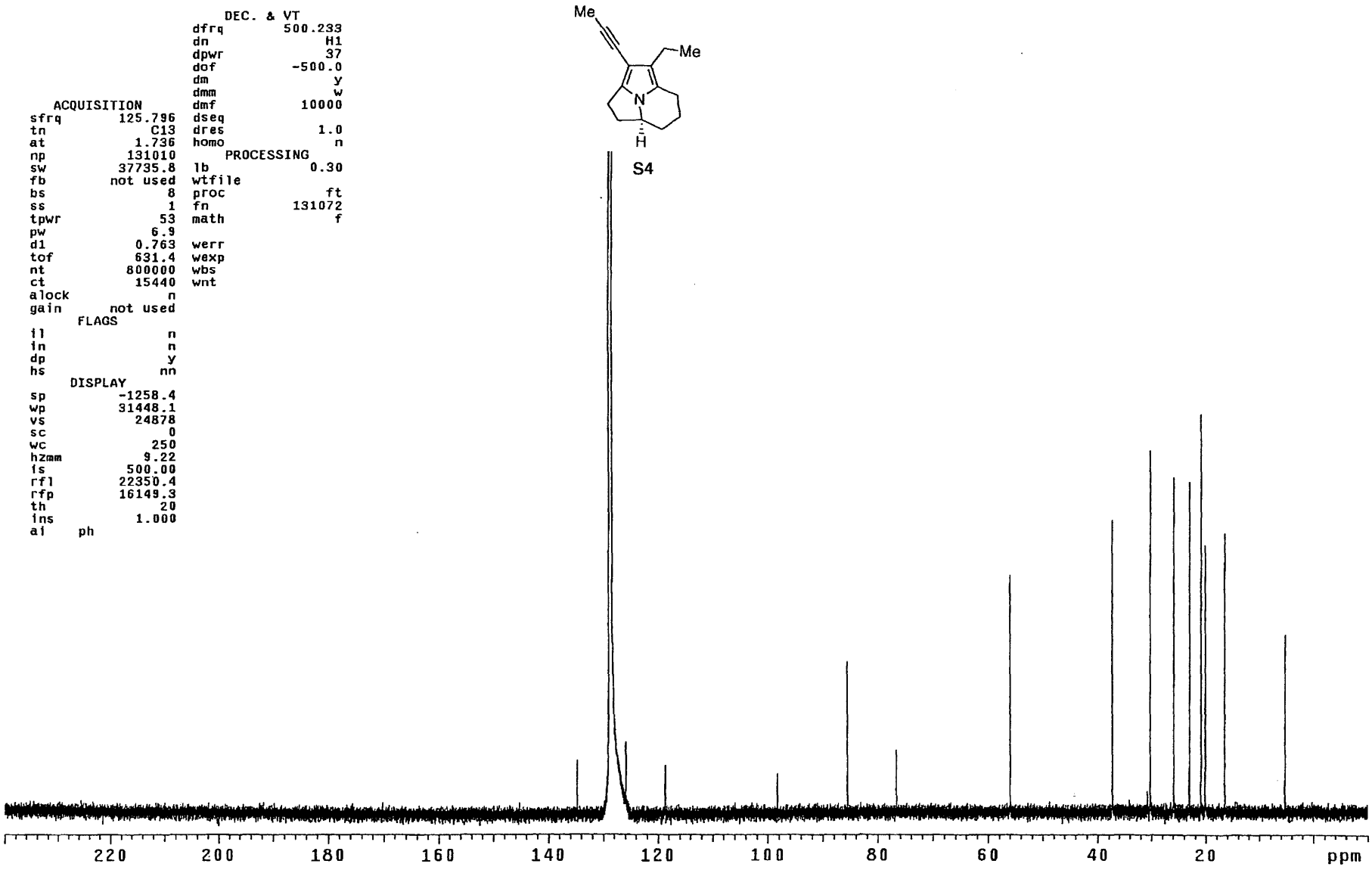
ACQUISITION
sfrq 125.796
tn C13
at 1.736
np 131010
sw 37735.8
fb not used
bs 8
ss 1
tpwr 53
pw 6.9
d1 0.763
tof 631.4
nt 800000
ct 15440
alock n
gain not used
FLAGS
il n
in n
dp y
hs nn
DISPLAY
sp -1258.4
wp 31448.1
vs 24878
sc 0
wc 250
hzmm 9.22
is 500.00
rfl 22350.4
rfp 16149.3
th 20
ins 1.000
ai ph
DEC. & VT
dfrq 500.233
dn H1
dpwr 37
dof -500.0
dm y
dmm w
dmf 10000
dseq
dres 1.0
homo n
PROCESSING
lb 0.30
wtfile
proc ft
fn 131072
math f
werr
wexp
wbs
wnt
Me
Me
N
H
S4
220
200
180
160
140
120
100
80
60
40
20
ppm

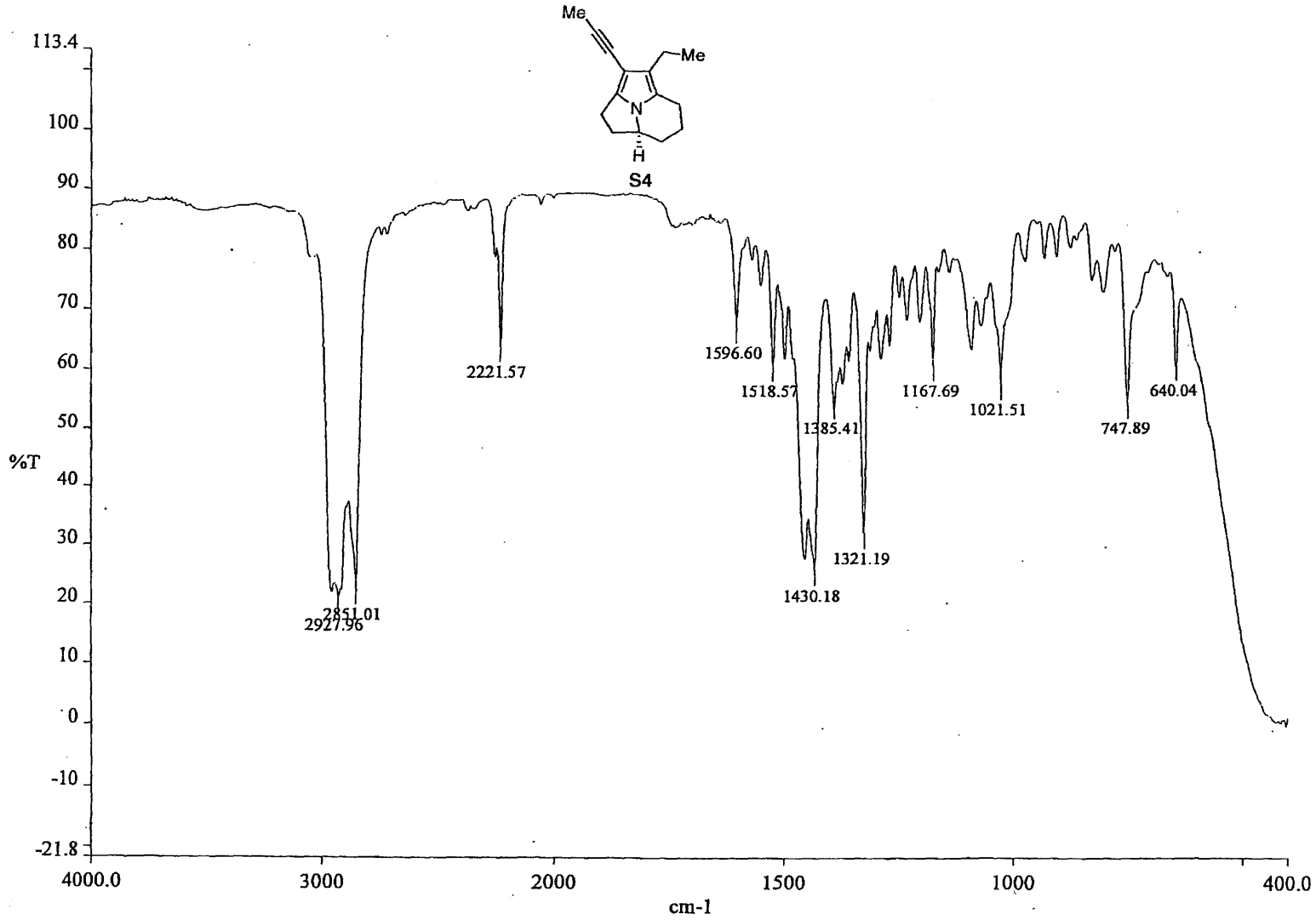
Me
Me
N
H
S4
113.4
100
90
80
70
60
50
40
30
20
10
0
-10
-21.8
%T
2927.96
2851.01
2221.57
1596.60
1518.57
1430.18
1385.41
1321.19
1167.69
1021.51
747.89
640.04
4000.0
3000
2000
1500
1000
400.0
cm-1

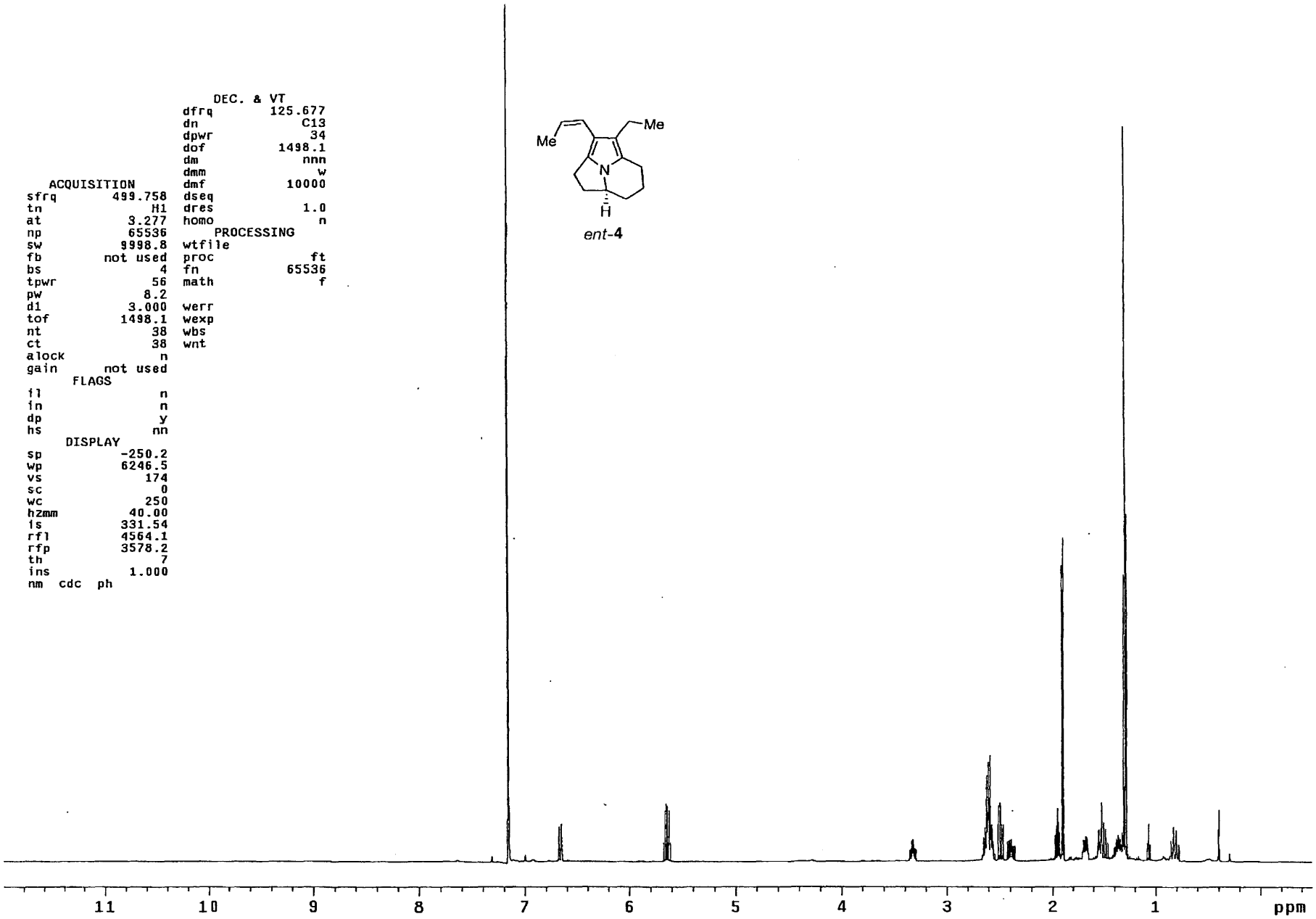
ACQUISITION
sfrq 499.758
tn H1
at 3.277
np 65536
sw 9998.8
fb not used
bs 4
tpwr 56
pw 8.2
d1 3.000
tof 1498.1
nt 38
ct 38
alock n
gain not used
FLAGS
il n
in n
dp y
hs nn
DISPLAY
sp -250.2
wp 6246.5
vs 174
sc 0
wc 250
hzmm 40.00
is 331.54
rfl 4564.1
rfp 3578.2
th 7
ins 1.000
nm cdc ph
DEC. & VT
dfrq 125.677
dn C13
dpwr 34
dof 1498.1
dm nnn
dmm w
dmf 10000
dseq
dres 1.0
homo n
PROCESSING
wtfile
proc ft
fn 65536
math f
werr
wexp
wbs
wnt
Me
Me
N
H
ent-4
11
10
9
8
7
6
5
4
3
2
1
ppm

ACQUISITION	
sfrq	125.796
tn	C13
at	1.736
np	131010
sw	37735.8
fb	not used
bs	8
ss	1
tpwr	53
pw	6.9
d1	0.763
tof	631.4
nt	80000
ct	20472
alock	n
gain	not used

FLAGS	
il	n
in	n
dp	y
hs	nn

DISPLAY	
sp	-1258.4
wp	31448.1
vs	1413
sc	0
wc	250
hzmm	2.00
is	500.00
rfl	22374.0
rfp	16149.3
th	20
ins	1.000
nm	ph

DEC. & VT	
dfrq	500.233
dn	H1
dpwr	37
dof	-500.0
dm	y
dmm	w
dmf	10000
dseq	
dres	1.0
homo	n

PROCESSING	
lb	0.30
wtfile	
proc	ft
fn	131072
math	f
werr	
wexp	
wbs	
wnt	

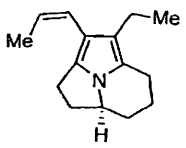

ent-4

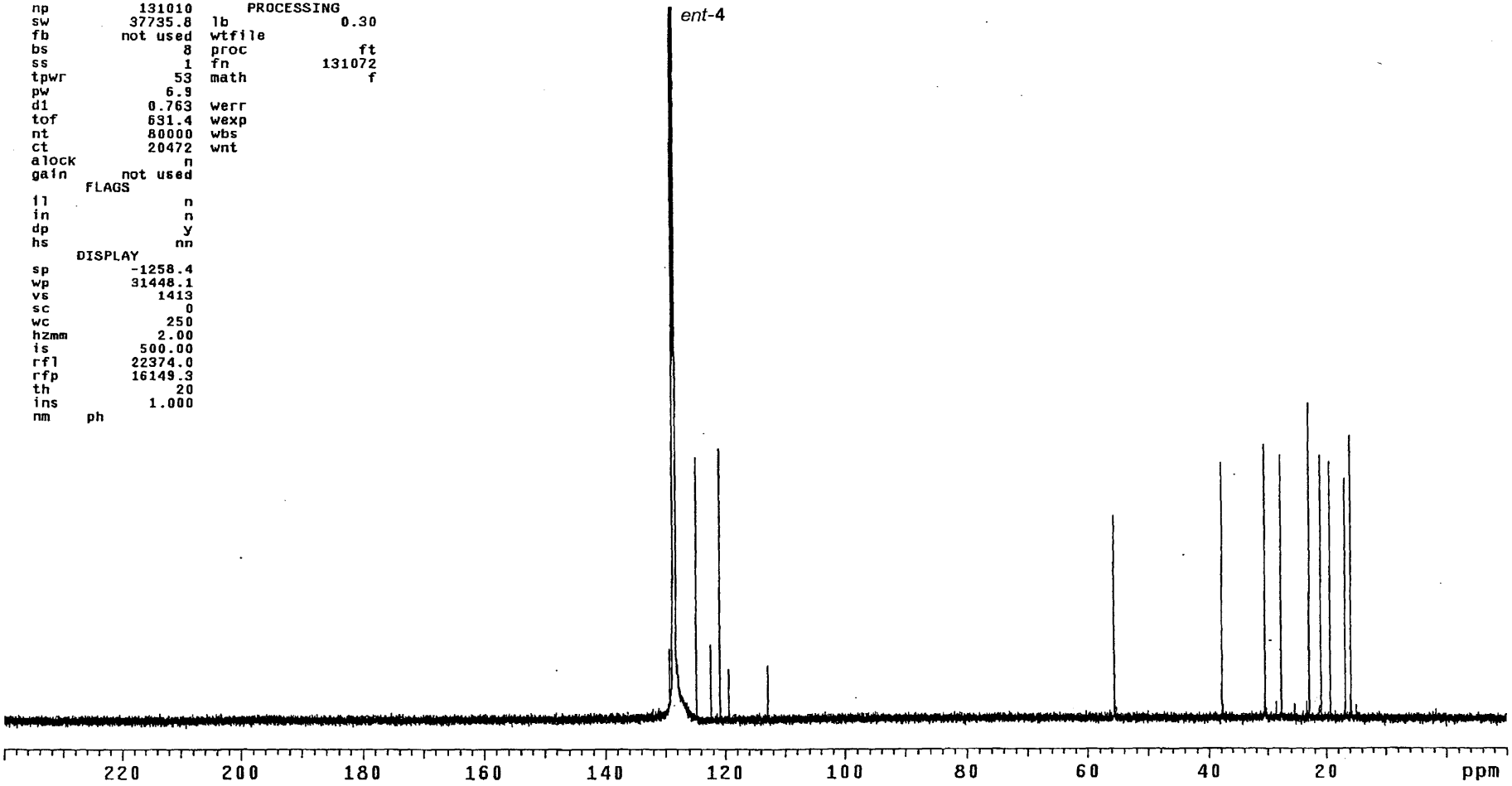

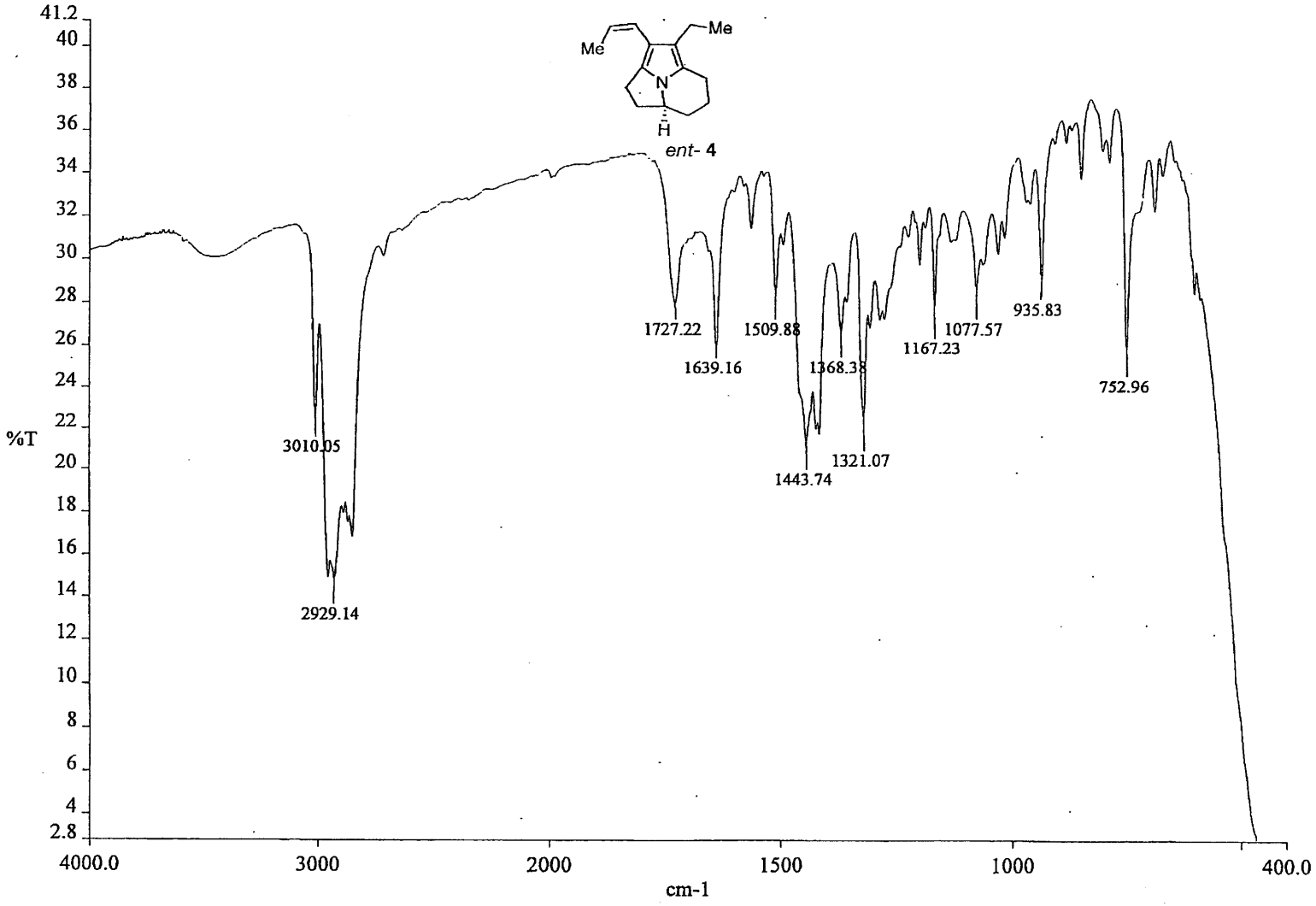
Me
Me
N
H
ent- 4
%T
41.2
40
38
36
34
32
30
28
26
24
22
20
18
16
14
12
10
8
6
4
2.8
3010.05
2929.14
1727.22
1639.16
1509.88
1443.74
1368.38
1321.07
1167.23
1077.57
935.83
752.96
4000.0
3000
2000
1500
1000
400.0
cm-1

ACQUISITION	
sfrq	499.749
tn	H1
at	3.277
np	65536
sw	9998.8
fb	not used
bs	4
tpwr	56
pw	8.2
d1	2.000
tof	1498.1
nt	100000
ct	64
alock	n
gain	not used

FLAGS	
il	n
in	n
dp	y
hs	nn

DISPLAY	
sp	-249.9
wp	6246.5
vs	96
sc	0
wc	250
hzmm	40.00
is	33.57
rfl	4567.4
rfp	3578.2
th	7
ins	1.000
nm	cdc ph

DEC. & VT	
dfrq	125.674
dn	C13
dpwr	34
dof	1498.1
dm	nnn
dmm	w
dmf	10000
dseq	
dres	1.0
homo	n

PROCESSING	
wtfile	
proc	ft
fn	65536
math	f
werr	
wexp	
wbs	
wnt	

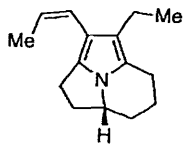

4

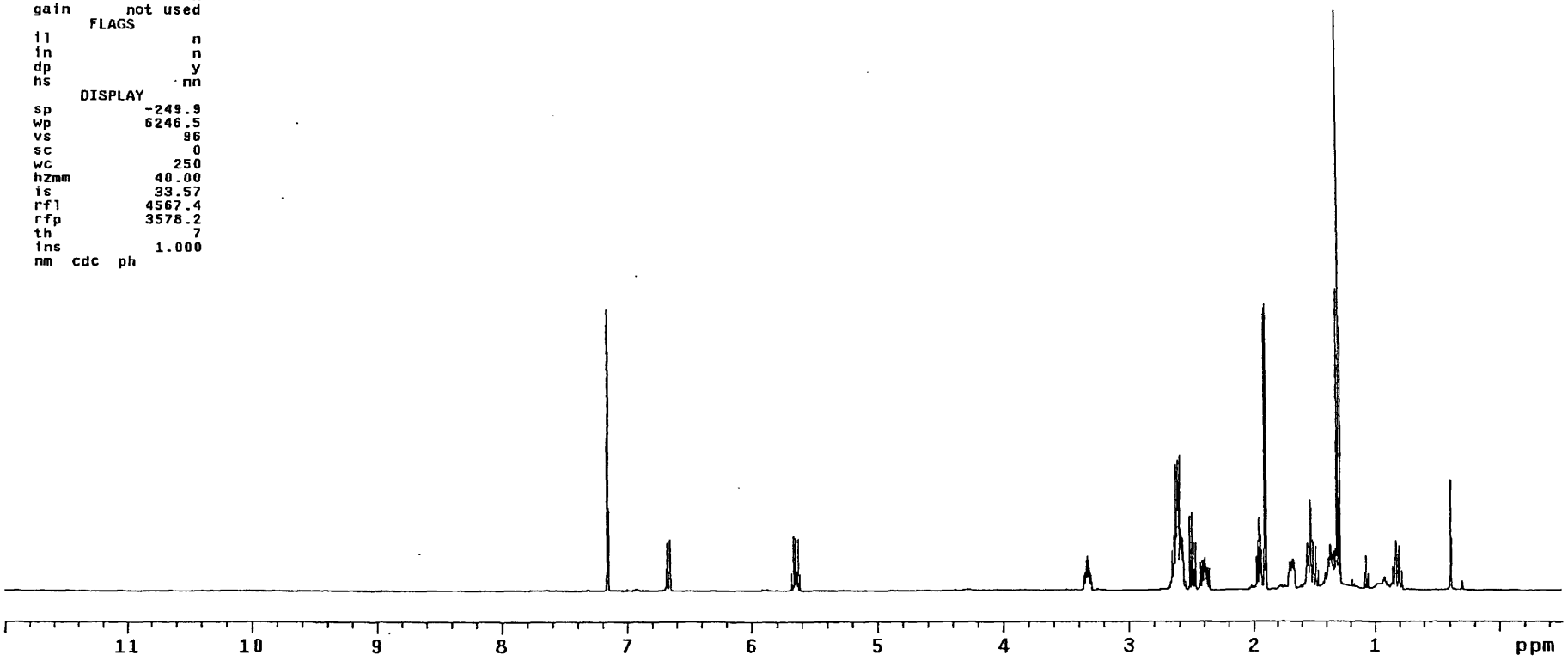

ACQUISITION	
sfrq	499.758
tn	H1
at	3.277
np	65536
sw	9998.8
fb	not used
bs	4
tpwr	56
pw	8.2
d1	2.000
tof	1498.1
nt	36
ct	36
alock	n
gain	not used
FLAGS	
il	n
in	n
dp	y
hs	nn
DISPLAY	
sp	-250.2
wp	6246.5
vs	225
sc	0
wc	250
hzmm	24.99
is	33.57
rfl	4564.4
rfp	3578.2
th	7
ins	1.000
nm cdc ph	

DEC. & VT	
dfrq	125.677
dn	C13
dpwr	34
dof	1498.1
dm	nnn
dmm	w
dmf	10000
dseq	
dres	1.0
homo	n
PROCESSING	
wtfile	
proc	ft
fn	65536
math	f
werr	
wexp	
wbs	
wnt	

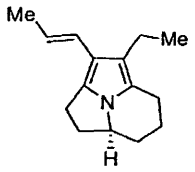

ent-5

ACQUISITION	
sfrq	125.796
tn	C13
at	1.736
np	131010
sw	37735.8
fb	not used
bs	10
ss	1
tpwr	53
pw	6.9
d1	0.763
tof	631.4
nt	100000
ct	2710
alock	n
gain	not used
FLAGS	
fl	n
in	n
dp	y
hs	nn
DISPLAY	
sp	-1258.4
wp	31448.1
vs	270
sc	0
wc	250
hzmm	4.48
is	500.00
rfl	22374.0
rfp	16149.3
th	20
ins	1.000
nm	ph

DEC. & VT	
dfrq	500.233
dn	H1
dpwr	37
dof	-500.0
dm	y
dmm	w
dmf	10000
dseq	
dres	1.0
homo	n
PROCESSING	
lb	0.30
wtfile	
proc	ft
fn	131072
math	f
werr	
wexp	
wbs	
wnt	

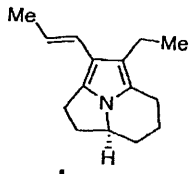

ent-5

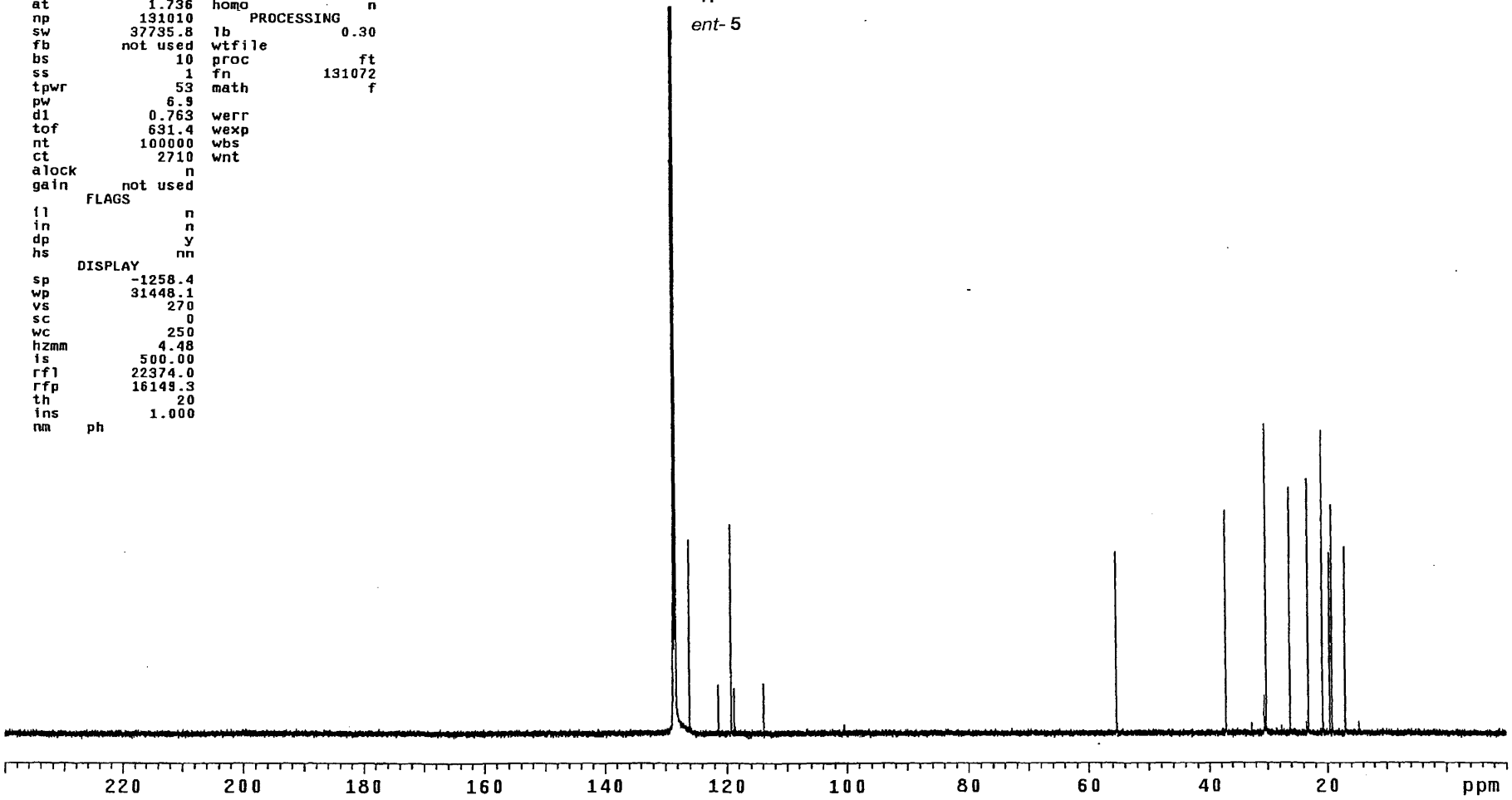

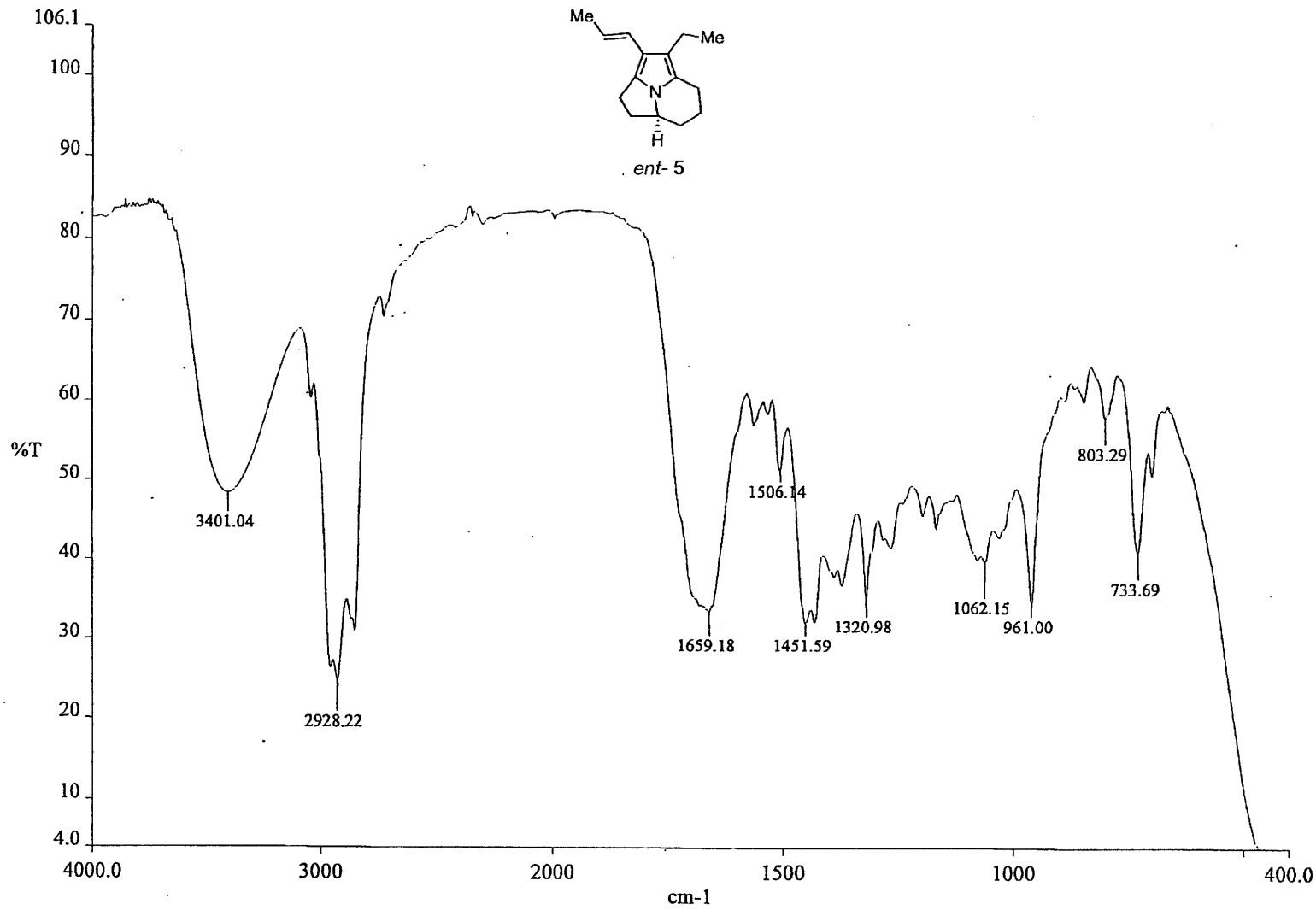
Me
Me
N
H
. ent- 5
106.1
100
90
80
70
60
50
40
30
20
10
4.0
%T
3401.04
2928.22
1659.18
1506.14
1451.59
1320.98
1062.15
961.00
803.29
733.69
4000.0
3000
2000
1500
1000
400.0
cm-1

ACQUISITION	
sfrq	499.749
tn	H1
at	3.277
np	65536
sw	9998.8
fb	not used
bs	4
tpwr	56
pw	8.2
d1	2.000
tof	1498.1
nt	24
ct	24
alock	n
gain	not used

FLAGS	
il	n
in	n
dp	y
hs	nn

DISPLAY	
sp	-250.5
wp	6246.5
vs	92
sc	0
wc	250
hzmm	40.00
is	33.57
rfl	4567.1
rfp	3578.2
th	7
ins	1.000

nm cdc ph

DEC. & VT	
dfrq	125.674
dn	C13
dpwr	34
dof	1498.1
dm	nnn
dmm	w
dmf	10000
dseq	
dres	1.0
homo	n

PROCESSING	
wtfile	
proc	ft
fn	65536
math	f
werr	
wexp	
wbs	
wnt	

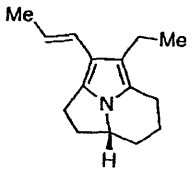

5

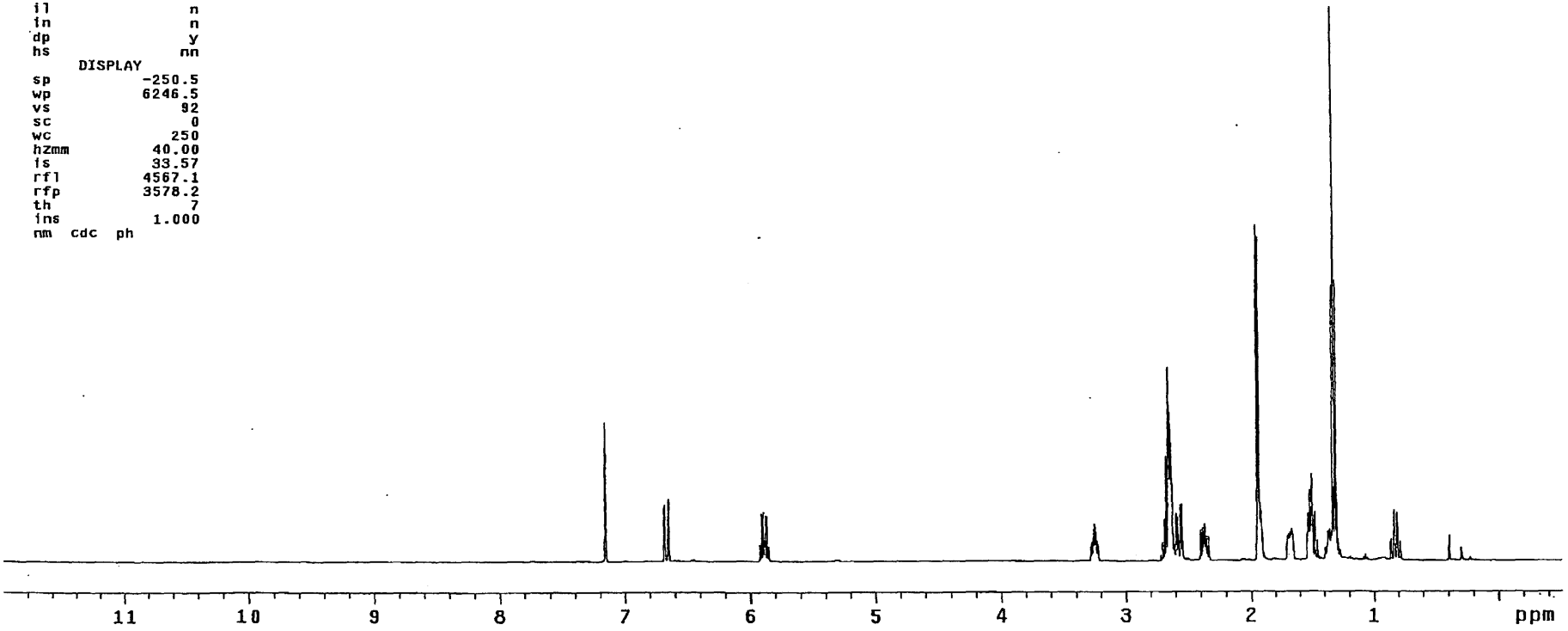

Appendix B.

Spectra for Chapter II

ACQUISITION	
sfrq	499.749
tn	H1
at	3.277
np	65536
sw	9998.8
fb	not used
bs	4
tpwr	56
pw	8.2
d1	2.000
tof	1498.1
nt	18
ct	18
alock	n
gain	not used
FLAGS	
il	n
in	n
dp	y
hs	nn
DISPLAY	
sp	-250.1
wp	6246.5
vs	71
sc	0
wc	250
hzmm	6.88
is	840.27
rfl	4638.5
rfp	3623.1
th	7
ins	2.000
nm	cdc ph

DEC. & VT	
dfrq	125.674
dn	C13
dpwr	34
dof	1498.1
dm	nnn
dmm	w
dmf	10000
dseq	
dres	1.0
homo	n
PROCESSING	
wtfile	
proc	ft
fn	65536
math	f
werr	
wexp	
wbs	
wnt	

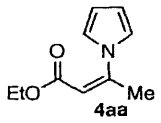

4aa

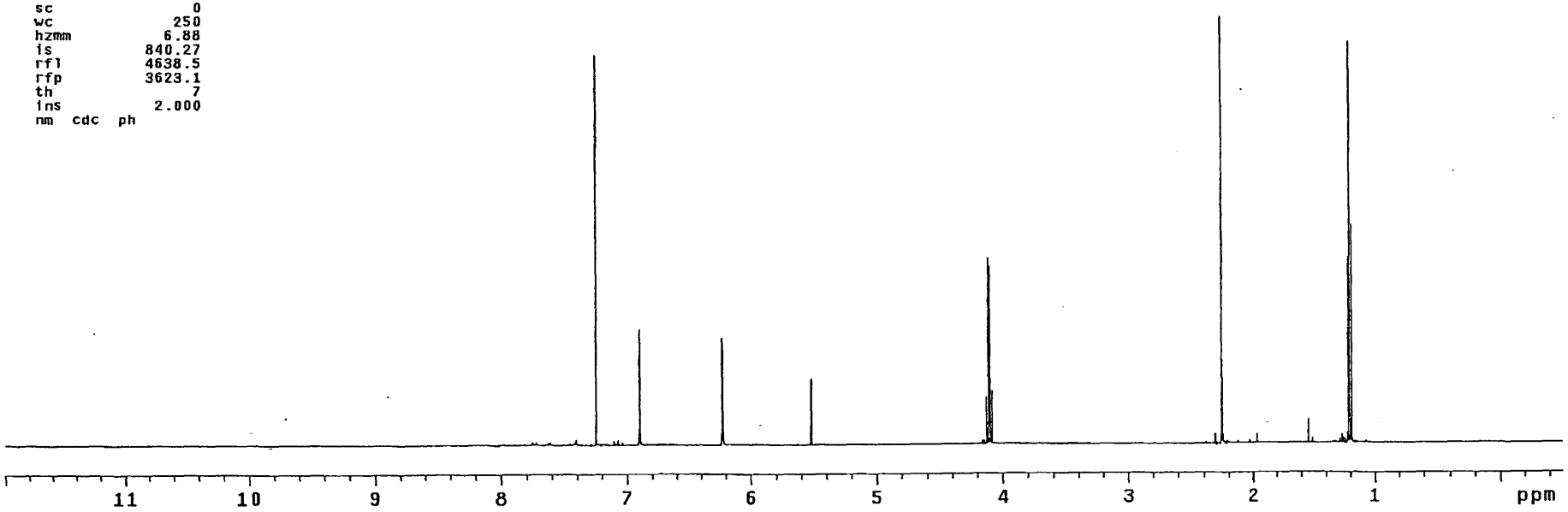

ACQUISITION		DEC. & VT	
sfrq	125.673	dfrq	499.747
tn	C13	dn	H1
at	0.869	dpwr	34
np	65536	dof	0
sw	37718.1	dm	yyy
fb	not used	dmm	w
bs	16	dmf	10000
ss	1	dseq	
tpwr	58	dres	1.0
pw	7.5	homo	n
d1	3.000	PROCESSING	
tof	615.5	lb	1.00
nt	10000	wtfile	
ct	336	proc	ft
alock	n.	fn	131072
gain	not used	math	f
FLAGS		werr	
il	n	wexp	
in	n	wbs	
dp	y	wnt	
hs	nn		
DISPLAY			
sp	-1256.8		
wp	31414.8		
vs	295		
sc	0		
wc	250		
hzmm	125.66		
is	500.00		
rfl	6304.2		
rfp	0		
th	68		
ins	1.000		
ai cdc ph			

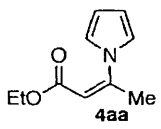

4aa

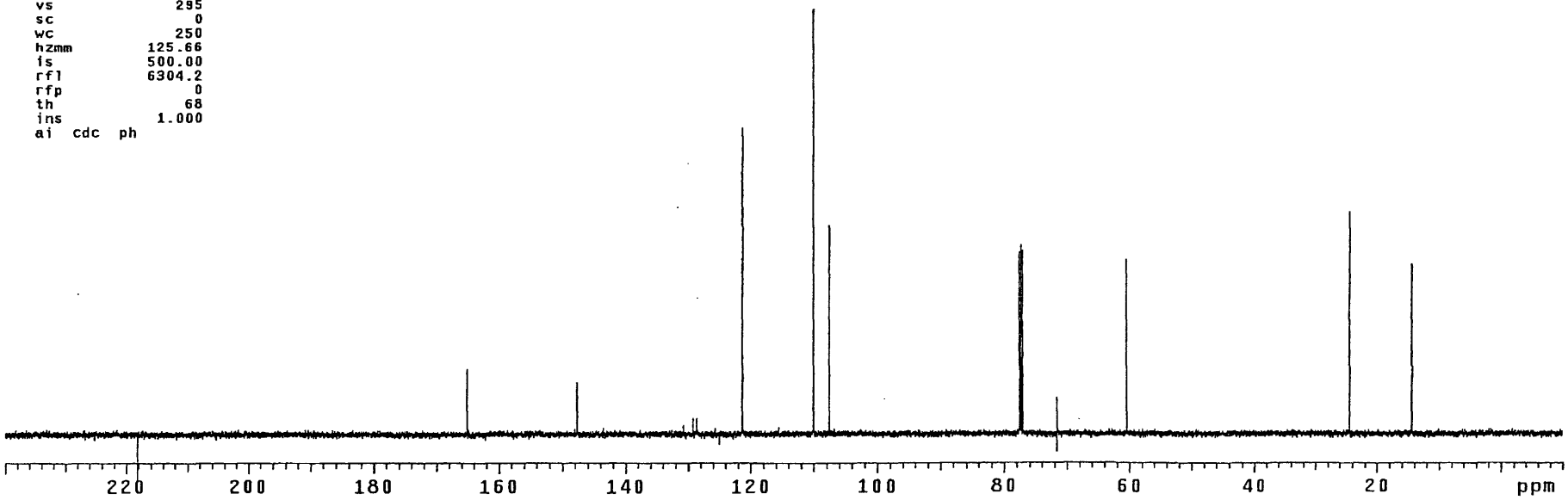

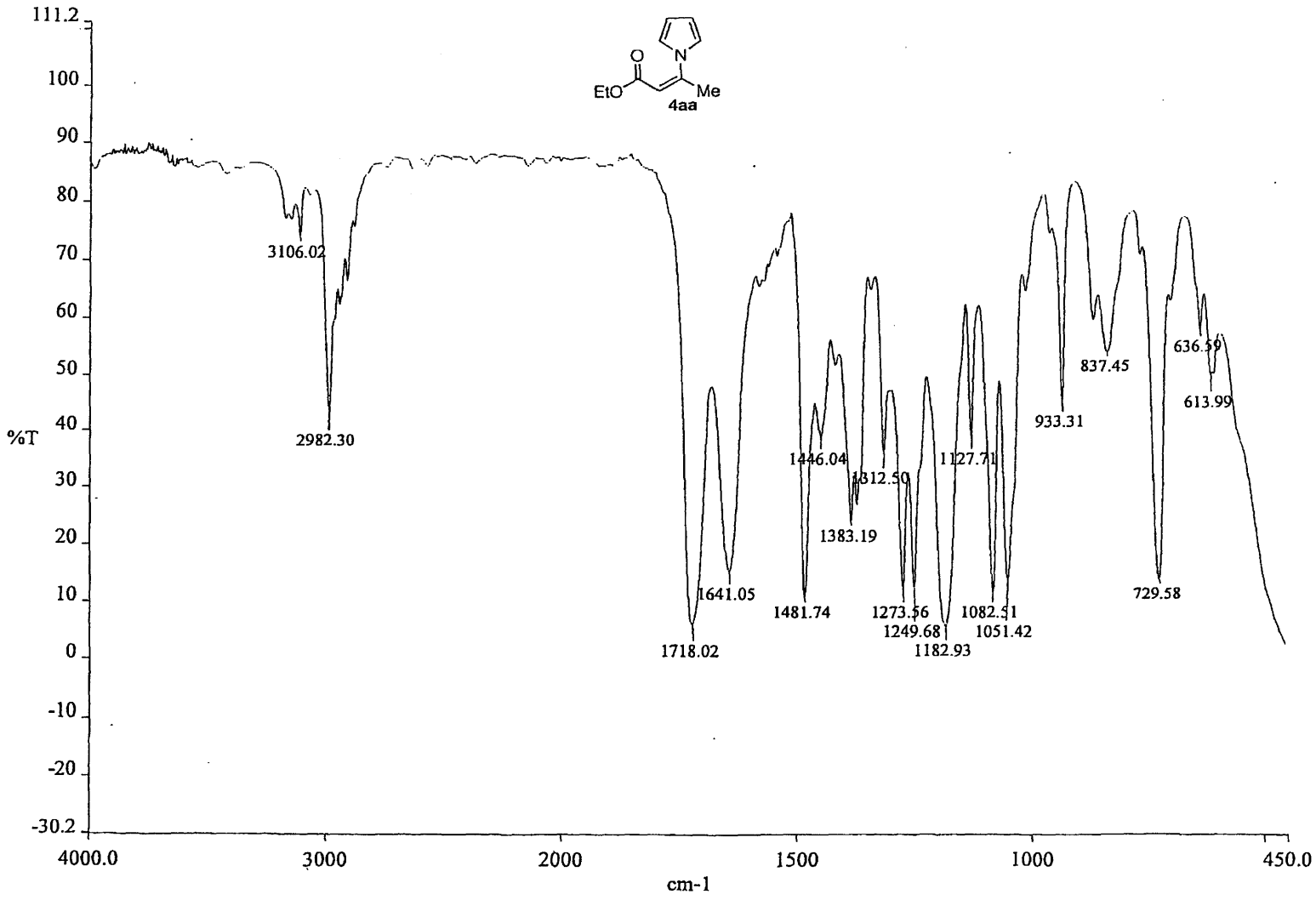
111.2
100
90
80
70
60
50
40
30
20
10
0
-10
-20
-30.2
%T
4000.0
3000
2000
1500
1000
450.0
cm-1
O
N
EtO
Me
4aa
3106.02
2982.30
1718.02
1641.05
1481.74
1446.04
1383.19
1312.50
1273.56
1249.68
1182.93
1127.71
1082.51
1051.42
933.31
837.45
729.58
636.59
613.99

ACQUISITION		DEC. & VT	
sfrq	499.758	dfrq	125.677
tn	H1	dn	C13
at	3.277	dpwr	34
np	65536	dof	1498.1
sw	9998.8	dm	nnn
fb	not used	dmm	w
bs	4	dmf	10000
tpwr	56	dseq	
pw	8.2	dres	1.0
d1	2.000	homo	n
tof	1498.1	PROCESSING	
nt	18	wtfile	
ct	18	proc	ft
alock	n	fn	65536
gain	not used	math	f
FLAGS		werr	
il	n	wexp	
in	n	wbs	
dp	y	wnt	
hs	nn		
DISPLAY			
sp	-250.4		
wp	6246.5		
vs	35		
sc	0		
wc	250		
hzmm	40.00		
is	33.57		
rfl	1002.5		
rfp	0		
th	7		
ins	2.000		
nm cdc ph			

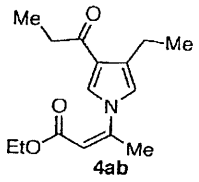

4ab

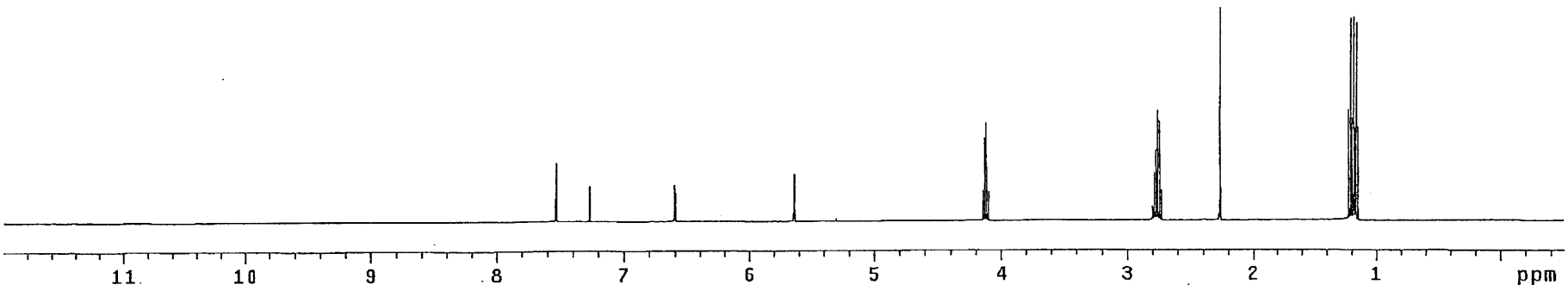

ACQUISITION	
sfrq	125.676
tn	C13
at	0.869
np	65536
sw	37718.1
fb	not used
bs	16
ss	1
tpwr	58
pw	7.5
d1	3.000
tof	615.5
nt	100000
ct	576
alock	n
gain	not used

FLAGS	
il	n
in	n
dp	y
hs	nn

DISPLAY	
sp	-1256.7
wp	31415.4
vs	63
sc	0
wc	250
hzmm	125.66
is	500.00
rfl	6304.1
rfp	0
th	6
ins	1.000

nm cdc ph

DEC. & VT	
dfrq	499.756
dn	H1
dpwr	34
dof	0
dm	yyy
dmm	w
dmf	10000
dseq	
dres	1.0
homo	n

PROCESSING	
lb	1.00
wtfile	
proc	ft
fn	131072
math	f
werr	
wexp	
wbs	
wnt	

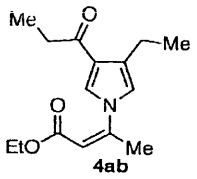

4ab

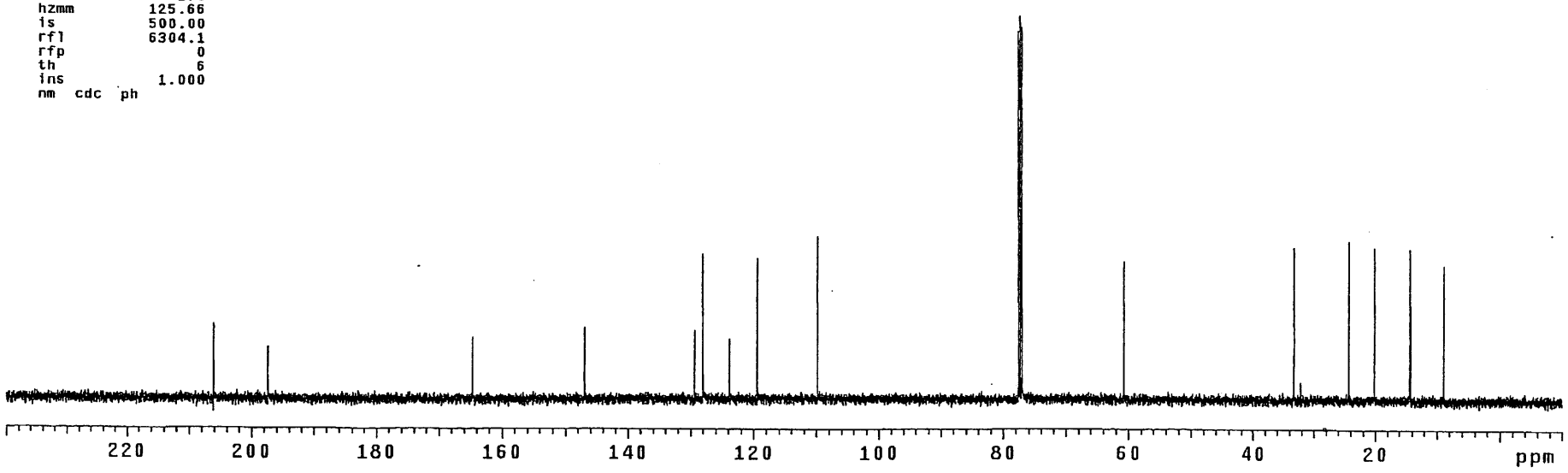

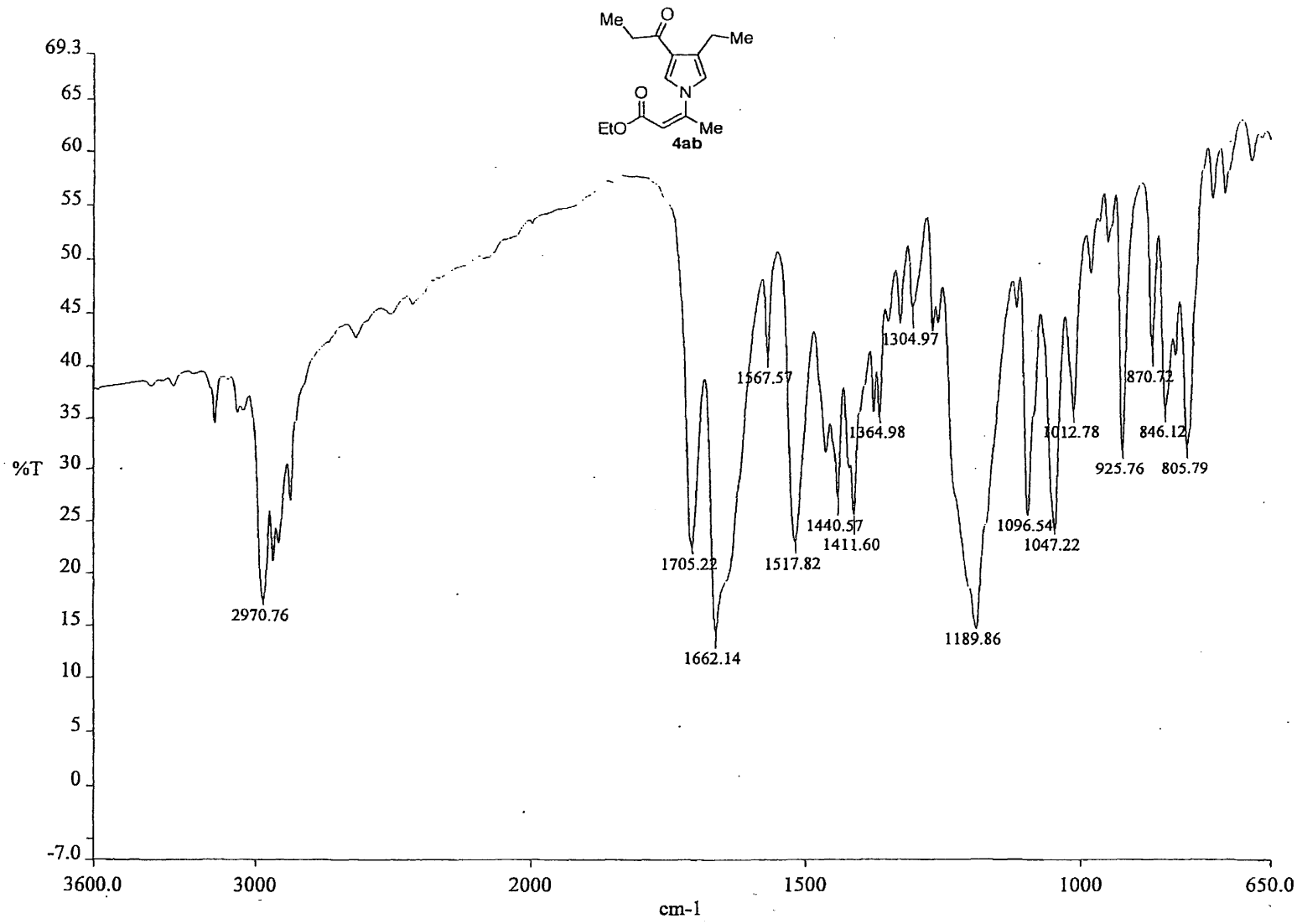
Me
O
Me
O
N
EtO
Me
4ab
69.3
65
60
55
50
45
40
35
%T 30
25
20
15
10
5
0
-7.0
3600.0
3000
2000
1500
1000
650.0
cm-1
2970.76
1705.22
1662.14
1567.57
1517.82
1440.57
1411.60
1364.98
1304.97
1189.86
1096.54
1047.22
1012.78
925.76
870.72
846.12
805.79

ACQUISITION	
sfrq	499.758
tn	H1
at	3.277
np	65536
sw	9998.8
fb	not used
bs	4
tpwr	56
pw	8.2
d1	2.000
tof	1498.1
nt	20
ct	20
alock	n
gain	not used

FLAGS	
il	n
in	n
dp	y
hs	nn

DISPLAY	
sp	-250.1
wp	6246.8
vs	11
sc	0
wc	250
hzmm	40.00
is	33.57
rfl	1002.5
rfp	0
th	7
ins	2.000
ai cdc ph	

DEC. & VT	
dfrq	125.677
dn	C13
dpwr	34
dof	1498.1
dm	nnn
dmm	w
dmf	10000
dseq	
dres	1.0
homo	n

PROCESSING	
wtfile	
proc	ft
fn	65536
math	f
werr	
wexp	
wbs	
wnt	

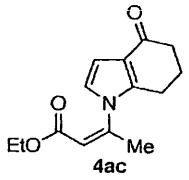

4ac

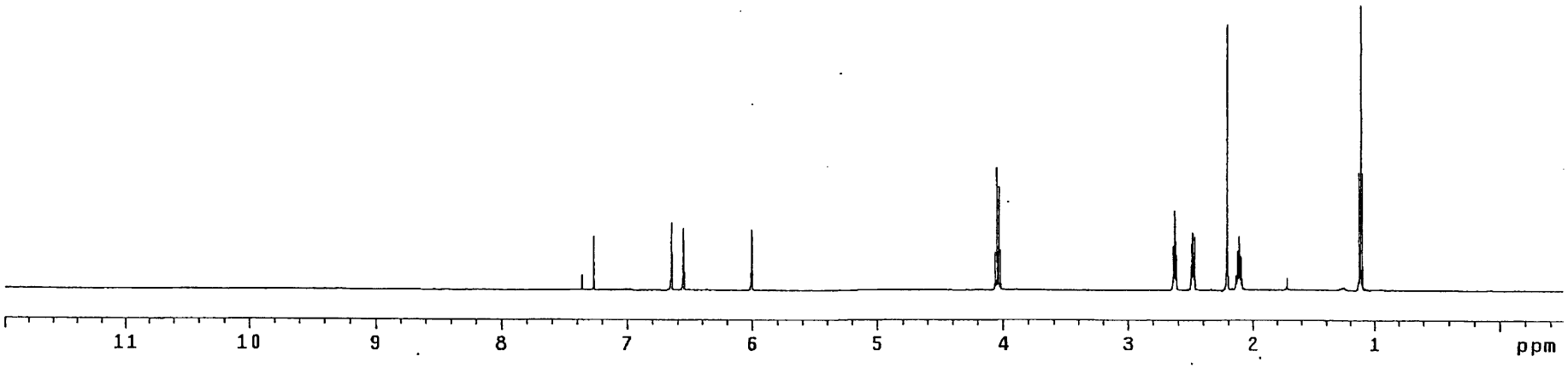

ACQUISITION	
sfrq	125.676
tn	C13
at	0.869
np	65536
sw	37718.1
fb	not used
bs	16
ss	1
tpwr	58
pw	7.5
d1	3.000
tof	615.5
nt	10000
ct	672
alock	n
gain	not used

FLAGS	
il	n
in	n
dp	y
hs	nn

DISPLAY	
sp	-1256.7
wp	31415.4
vs	917
sc	0
wc	250
hzmm	125.66
is	500.00
rfl	6304.1
rfp	0
th	7
ins	1.000

ai cdc ph

DEC. & VT	
dfrq	499.756
dn	H1
dpwr	34
dof	0
dm	yyy
dmm	w
dmf	10000
dseq	
dres	1.0
homo	n

PROCESSING	
lb	1.00
wtfile	
proc	ft
fn	131072
math	f
werr	
wexp	
wbs	
wnt	

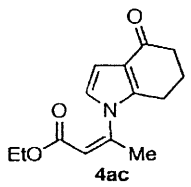

4ac

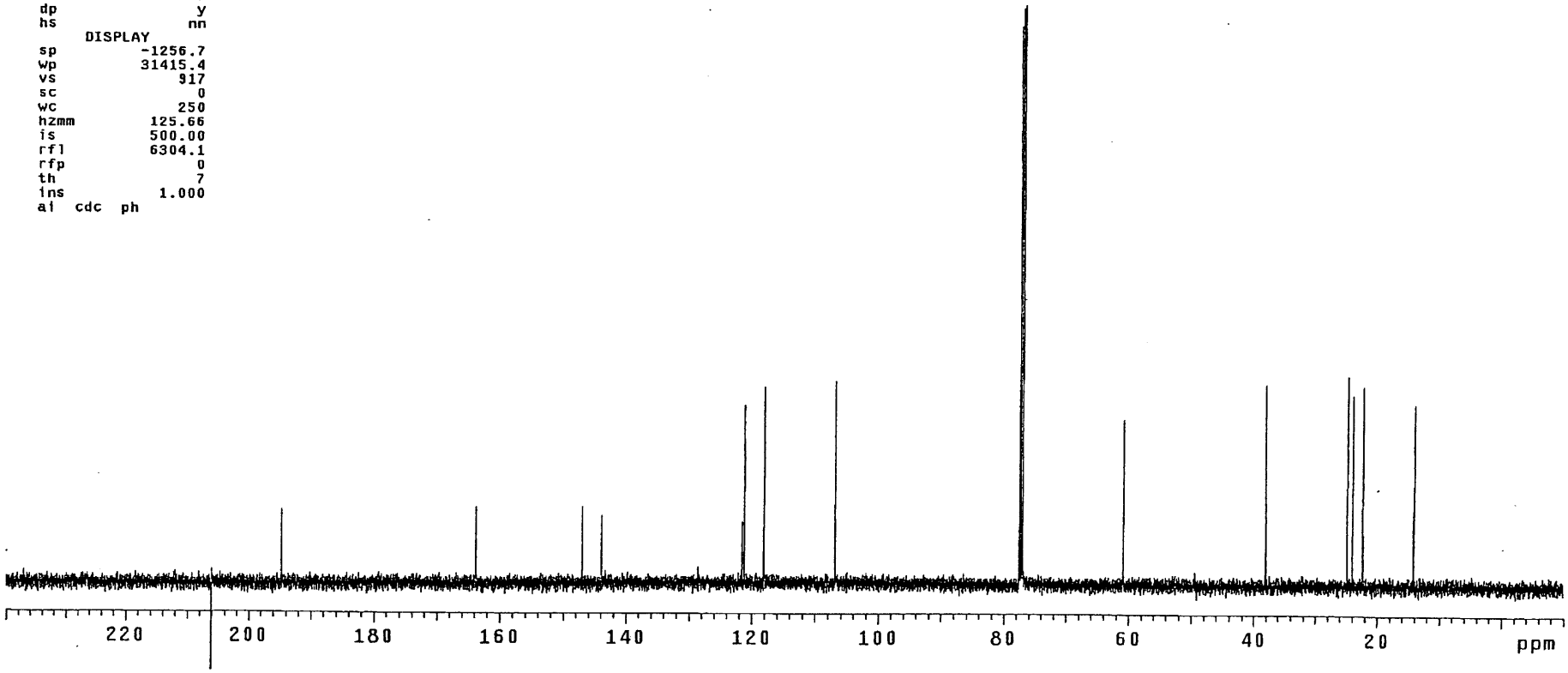

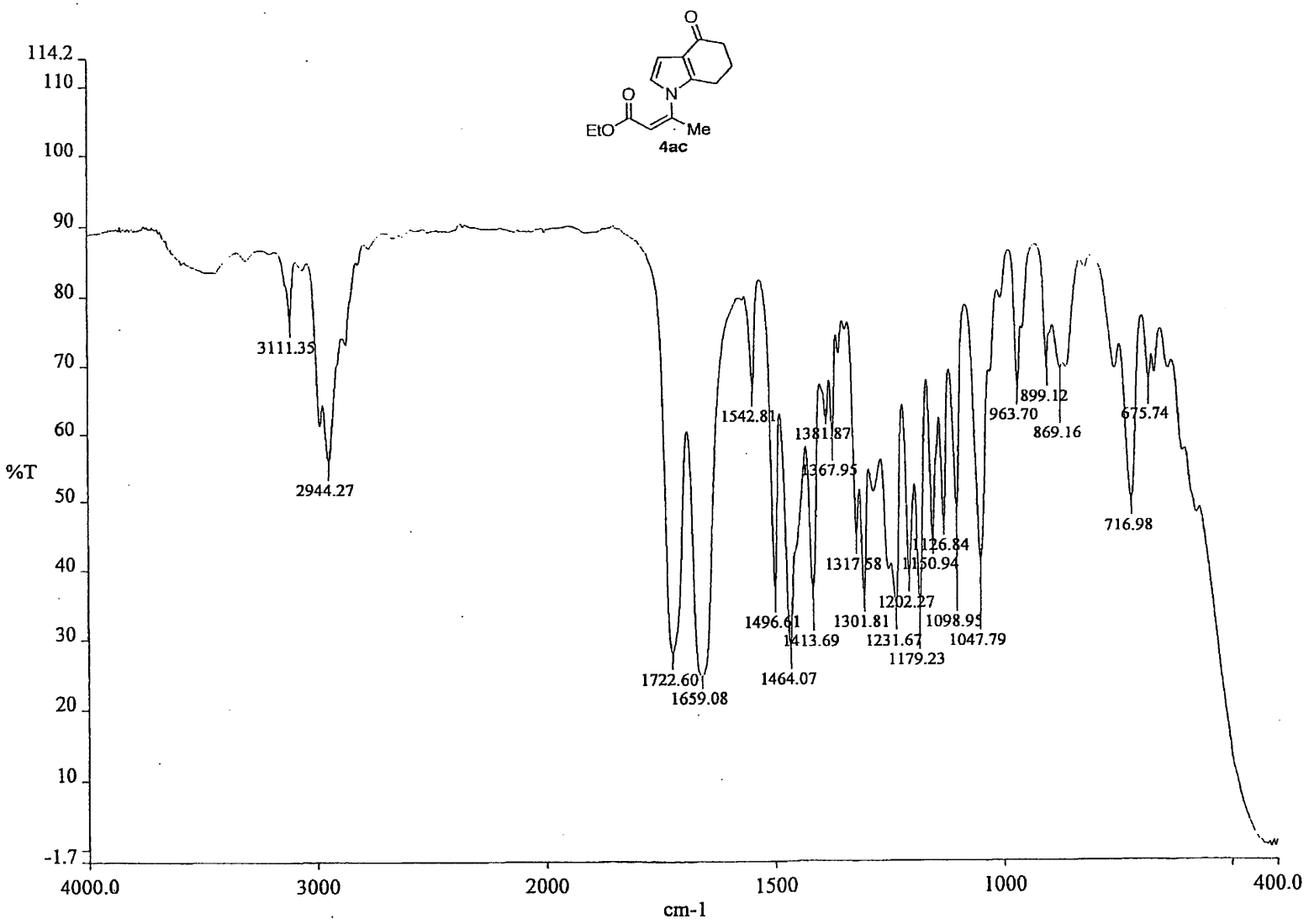
4ac
%T
cm-1
114.2
110
100
90
80
70
60
50
40
30
20
10
-1.7
4000.0
3000
2000
1500
1000
400.0
3111.35
2944.27
1722.60
1659.08
1542.81
1496.61
1464.07
1413.69
1381.87
1367.95
1317.58
1301.81
1231.67
1202.27
1179.23
1150.94
1126.84
1098.95
1047.79
963.70
899.12
869.16
716.98
675.74

ACQUISITION	
sfrq	500.235
tn	H1
at	3.200
np	64000
sw	10000.0
fb	not used
bs	4
ss	1
tpwr	59
pw	9.8
d1	2.000
tof	1498.2
nt	20
ct	20
alock	n
gain	not used
FLAGS	
il	n
in	n
dp	y
hs	nn
DISPLAY	
sp	-250.1
wp	6246.6
vs	45
sc	0
wc	250
hzmm	40.00
is	100.00
rfl	4632.9
rfp	3636.7
th	7
ins	2.000
ai	ph

DEC. & VT	
dfrq	125.795
dn	C13
dpwr	37
dof	0
dm	nnn
dmm	c
dmf	10000
dseq	
dres	1.0
homo	n
PROCESSING	
wtfile	
proc	ft
fn	131072
math	f
werr	
wexp	
wbs	
wnt	

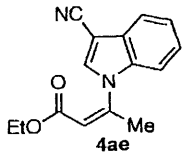

4ae

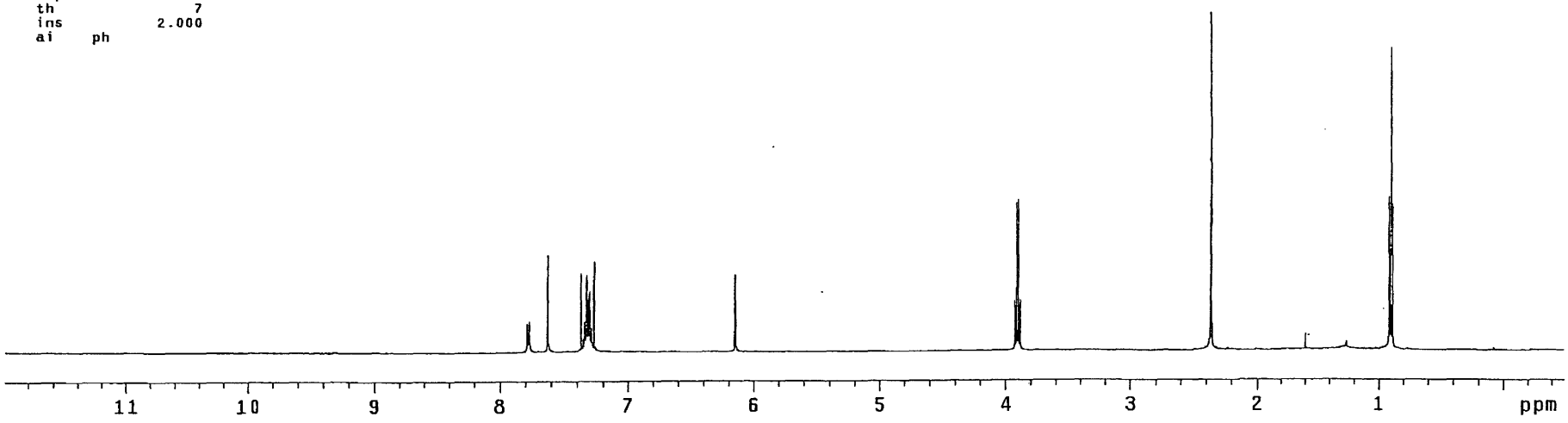

ACQUISITION	
sfrq	125.796
tn	C13
at	1.736
np	131010
sw	37735.8
fb	not used
bs	8
ss	1
tpwr	53
pw	6.9
d1	0.763
tof	631.4
nt	10000
ct	968
alock	n
gain	not used

FLAGS	
il	n
in	n
dp	y
hs	nn

DISPLAY	
sp	-1258.3
wp	31448.1
vs	4325
sc	0
wc	250
hzmm	125.79
is	500.00
rfl	15911.8
rfp	9686.0
th	4
ins	1.000
ai	ph

DEC. & VT	
dfrq	500.233
dn	H1
dpwr	37
dof	-500.0
dm	y
dmm	w
dmf	10000
dseq	
dres	1.0
homo	n

PROCESSING	
lb	0.30
wtfile	
proc	ft
fn	131072
math	f
werr	
wexp	
wbs	
wnt	

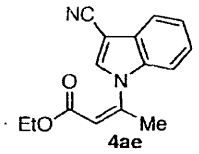

4ae

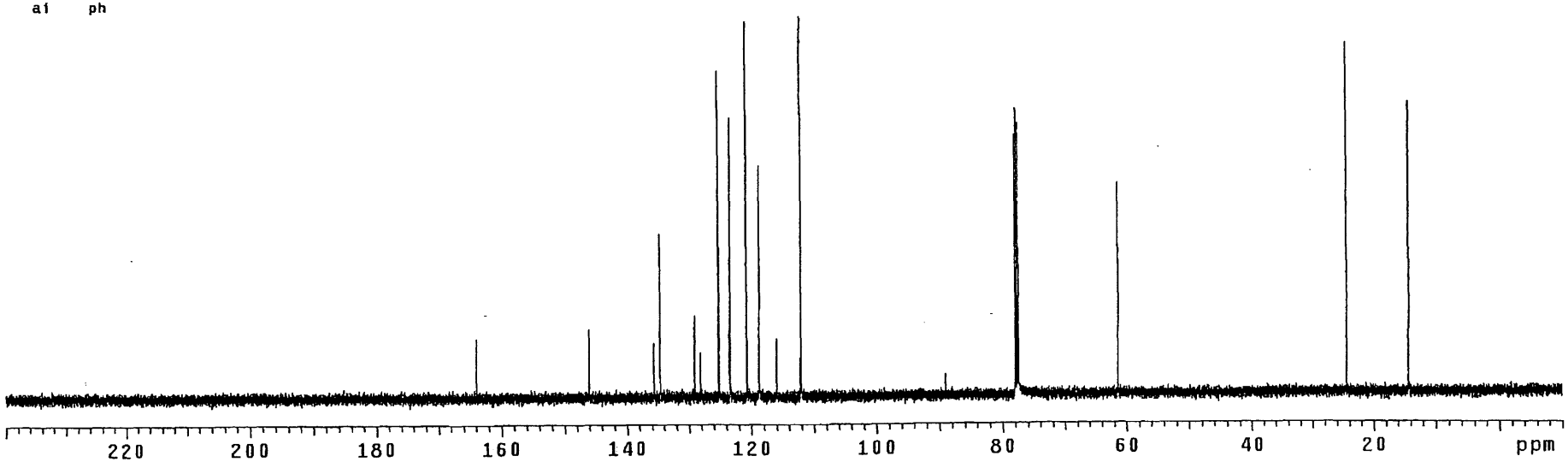

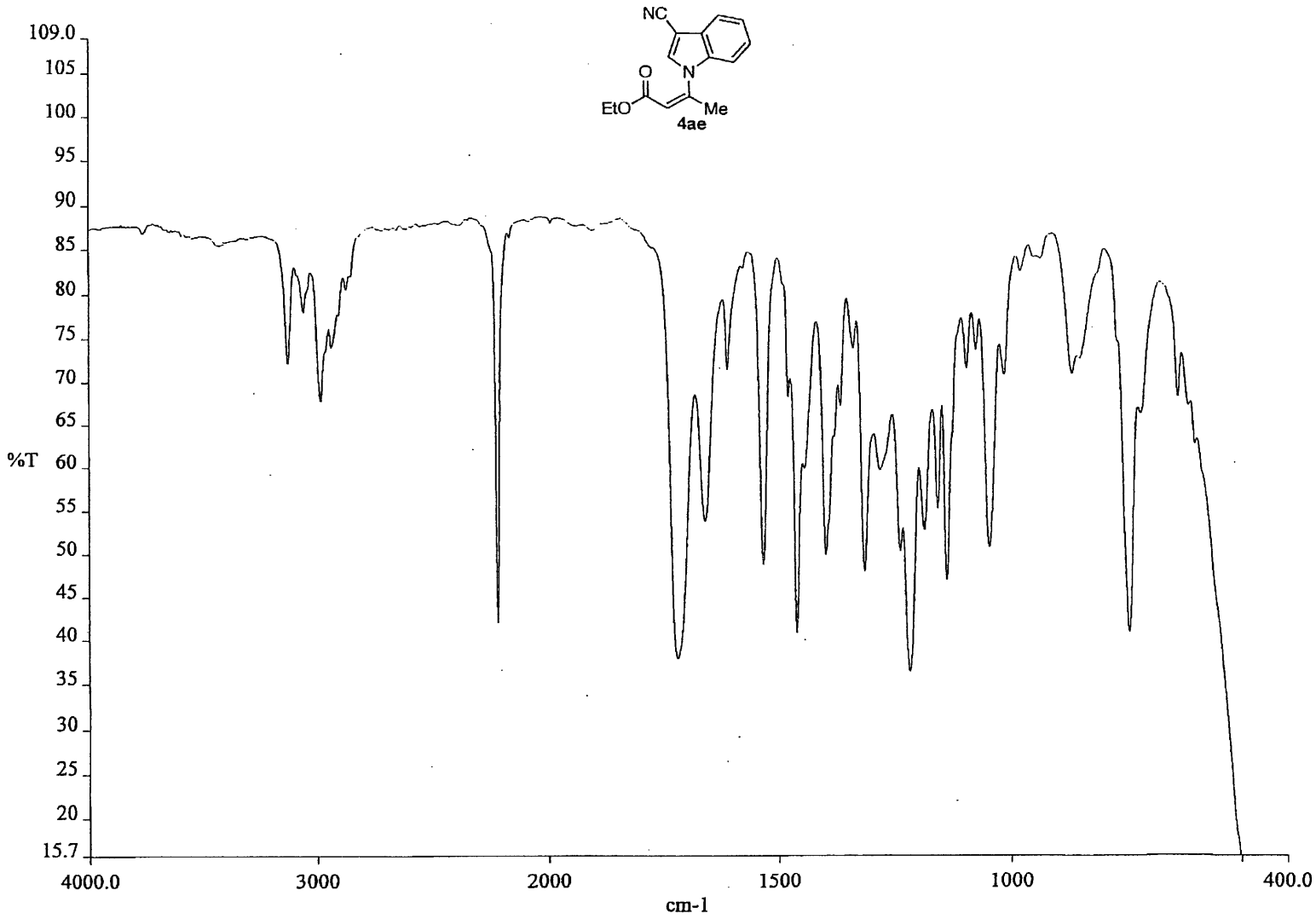
NC
O
N
EtO
Me
4ae
109.0
105
100
95
90
85
80
75
70
65
%T
60
55
50
45
40
35
30
25
20
15.7
4000.0
3000
2000
1500
1000
400.0
cm-1

ACQUISITION	
sfrq	499.749
tn	H1
at	3.277
np	65536
sw	9998.8
fb	not used
bs	4
tpwr	56
pw	8.2
d1	2.000
tof	1498.1
nt	20
ct	20
alock	n
gain	not used
FLAGS	
il	n
in	n
dp	y
hs	nn
DISPLAY	
sp	-250.1
wp	6246.5
vs	101
sc	0
wc	250
hzmm	40.00
is	33.57
rfl	4638.2
rfp	3623.1
th	7
ins	1.000
nm	cdc ph

DEC. & VT	
dfrq	125.674
dn	C13
dpwr	34
dof	1498.1
dm	nnn
dmm	w
dmf	10000
dseq	
dres	1.0
homo	n
PROCESSING	
wtfile	
proc	ft
fn	65536
math	f
werr	
wexp	
wbs	
wnt	

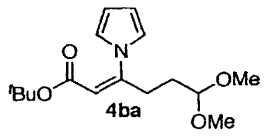

4ba

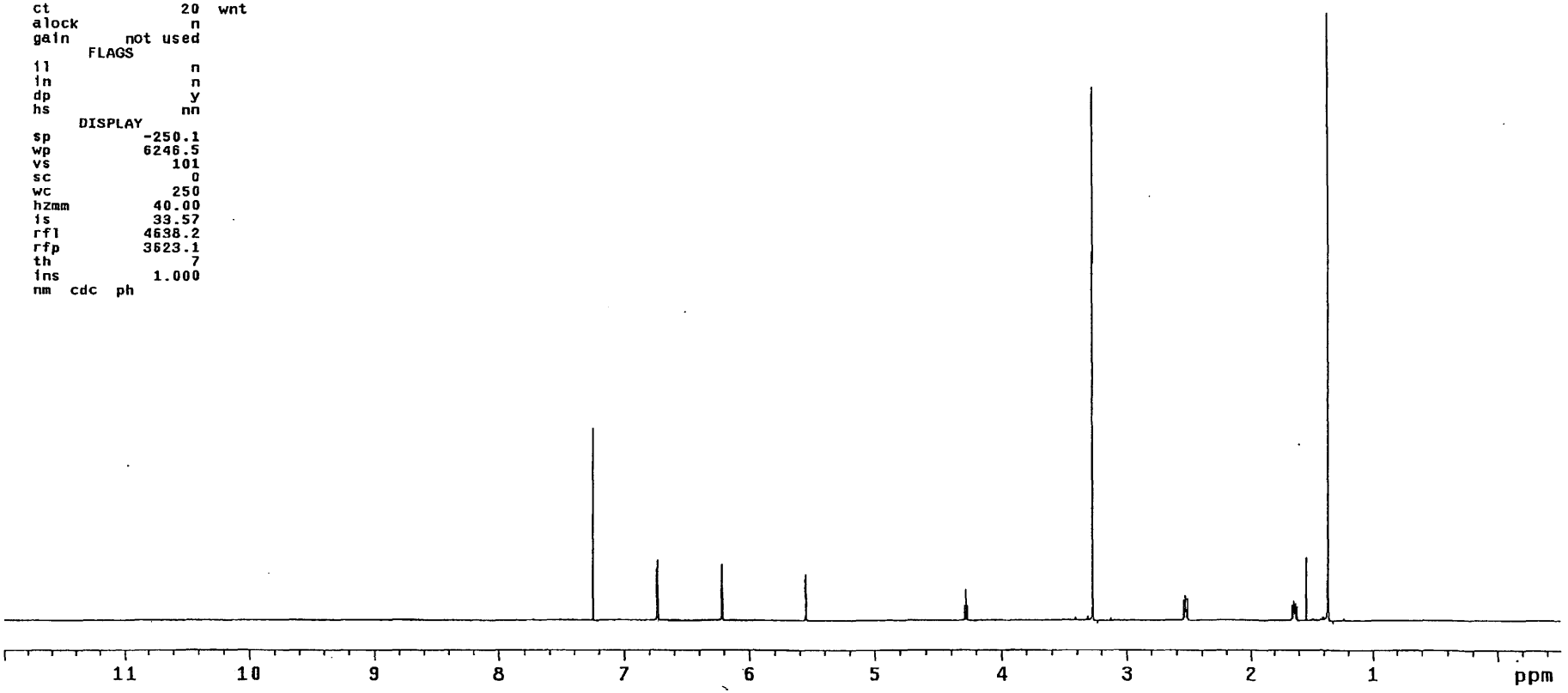

ACQUISITION		DEC. & VT	
sfrq	125.673	dfrq	499.747
tn	C13	dn	H1
at	0.869	dpwr	34
np	65536	dof	0
sw	37718.1	dm	yyy
fb	not used	dmm	w
bs	16	dmf	10000
ss	1	dseq	
tpwr	58	dres	1.0
pw	7.5	homo	n
d1	3.000	PROCESSING	
tof	615.5	lb	1.00
nt	10000	wtfile	
ct	752	proc	ft
alock	n	fn	131072
gain	not used	math	f
FLAGS			
il	n	werr	
in	n	wexp	
dp	y	wbs	
hs	nn	wnt	
DISPLAY			
sp	-1256.8		
wp	31414.3		
vs	423		
sc	0		
wc	250		
hzmm	125.66		
is	500.00		
rfl	6304.2		
rfp	0		
th	68		
ins	1.000		
ai cdc ph			

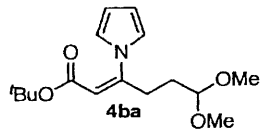

4ba

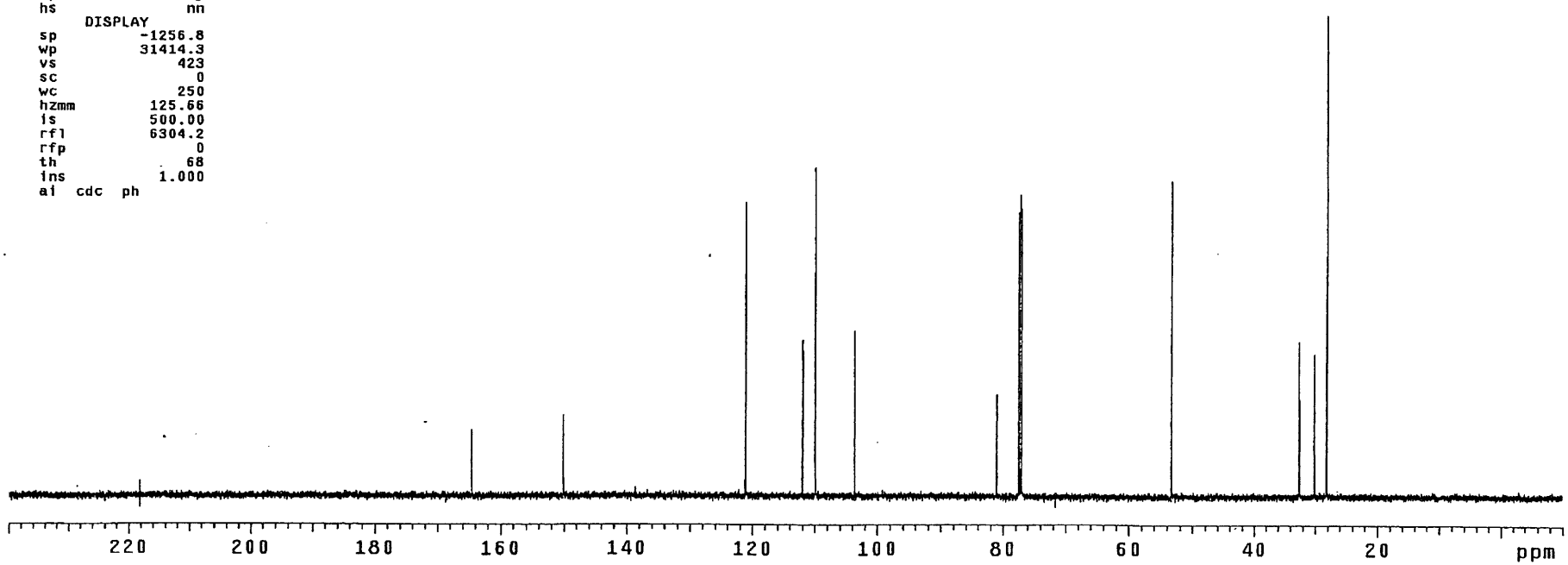

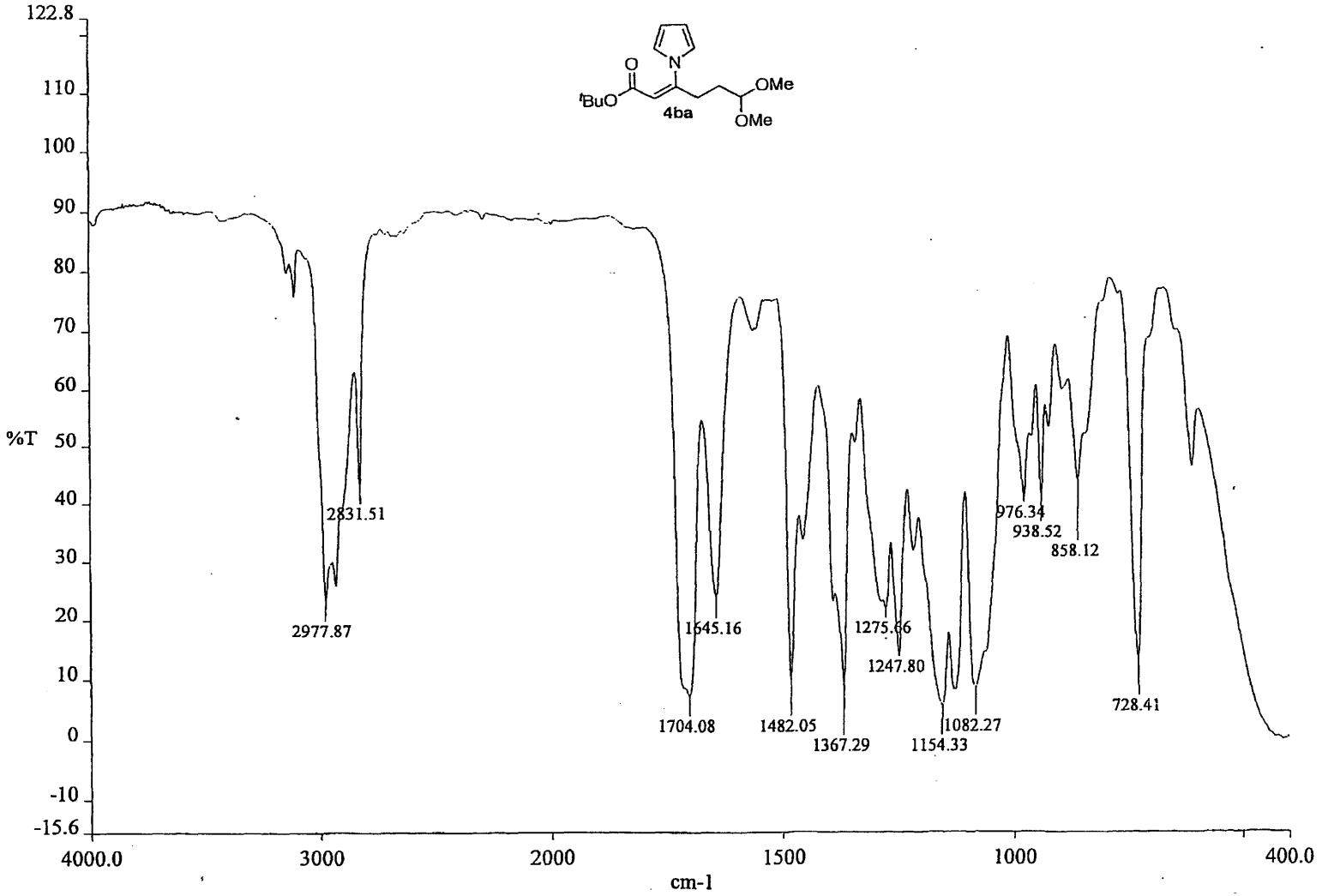
4ba
%T
cm-1
2977.87
2831.51
1704.08
1645.16
1482.05
1367.29
1275.66
1247.80
1154.33
1082.27
976.34
938.52
858.12
728.41

ACQUISITION		DEC. & VT	
sfrq	500.235	dfrq	125.795
tn	H1	dn	C13
at	3.200	dpwr	37
np	64000	dof	0
sw	10000.0	dm	nnn
fb	not used	dmm	c
bs	4	dmf	10000
ss	1	dseq	
tpwr	59	dres	1.0
pw	9.8	homo	n
d1	2.000	PROCESSING	
tof	1498.2	wtfile	
nt	20	proc	ft
ct	20	fn	131072
alock	n	math	f
gain	not used	werr	
FLAGS		wexp	
il	n	wbs	
in	n	wnt	
dp	y		
hs	nn		
DISPLAY			
sp	-250.2		
wp	6252.8		
vs	62		
sc	0		
wc	250		
hzmm	40.00		
is	119.21		
rfl	4632.8		
rfp	3636.7		
th	23		
ins	2.000		
nm	ph		

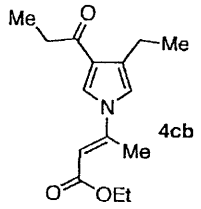

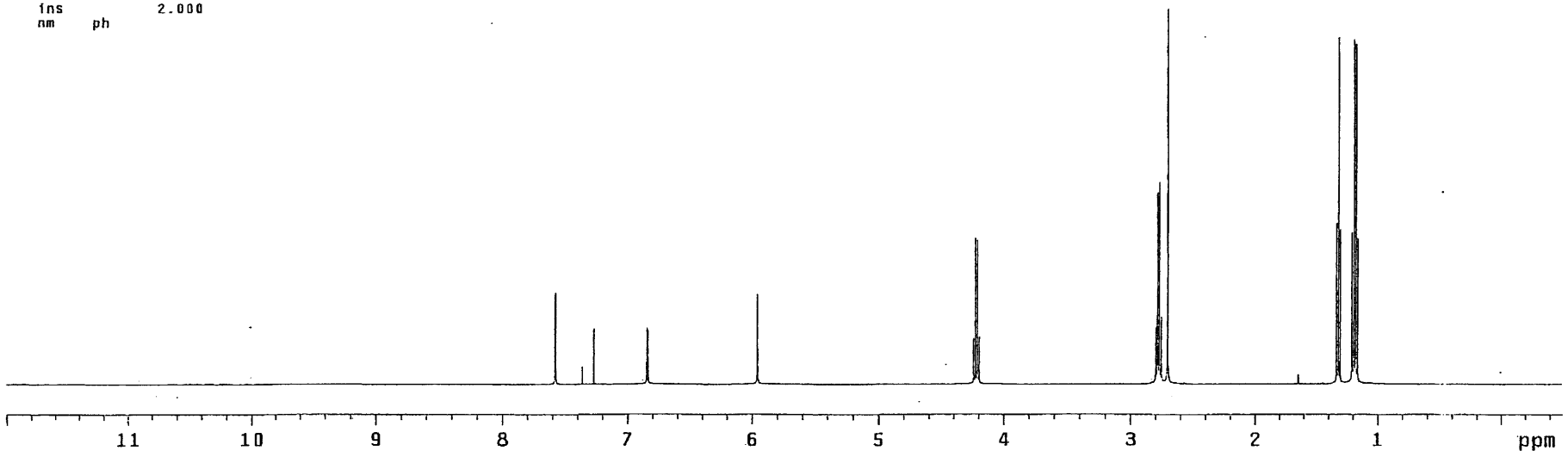

solvent	CDCl3
file	exp
ACQUISITION	
sfrq	125.796
tn	C13
at	1.736
np	131010
sw	37735.8
fb	not used
bs	8
ss	1
tpwr	53
pw	6.9
d1	0.763
tof	631.4
nt	10000
ct	904
alock	n
gain	not used
FLAGS	
il	n
in	n
dp	y
hs	nn
DISPLAY	
sp	-1258.3
wp	31448.0
vs	60
sc	0
wc	250
hzmm	125.79
is	500.00
rfl	15911.8
rfp	9686.0
th	5
ins	1.000
nm	ph

DEC. & VT	
dfrq	500.233
dn	H1
dpwr	37
dof	-500.0
dm	y
dmm	w
dmf	10000
dseq	
dres	1.0
homo	n
PROCESSING	
lb	0.30
wtfile	
proc	ft
fn	131072
math	f
werr	
wexp	
wbs	
wnt	

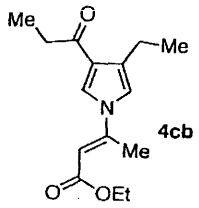

4cb

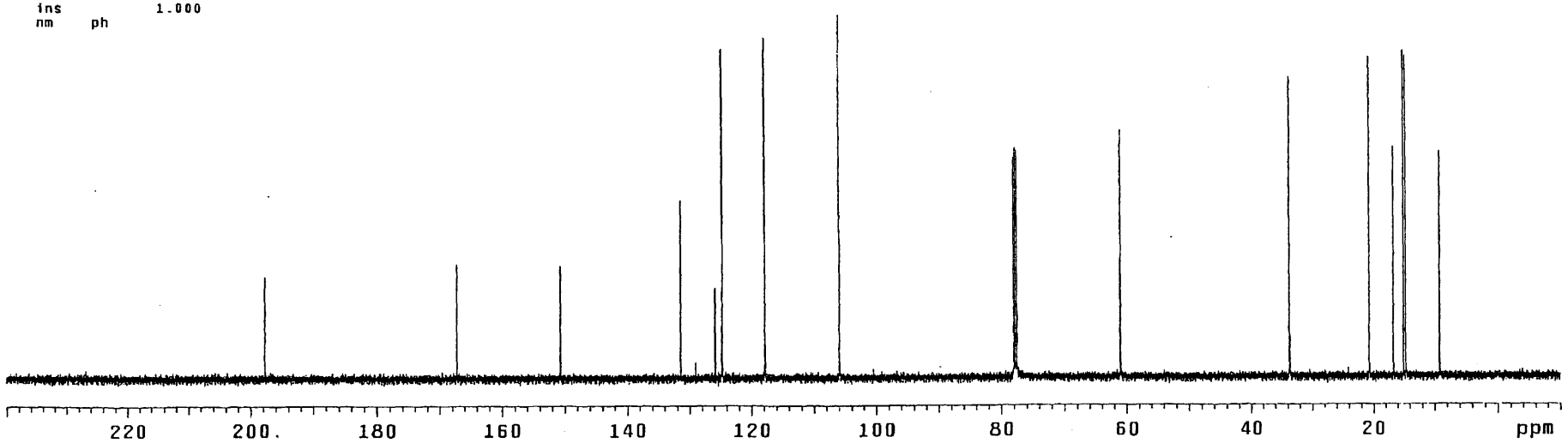

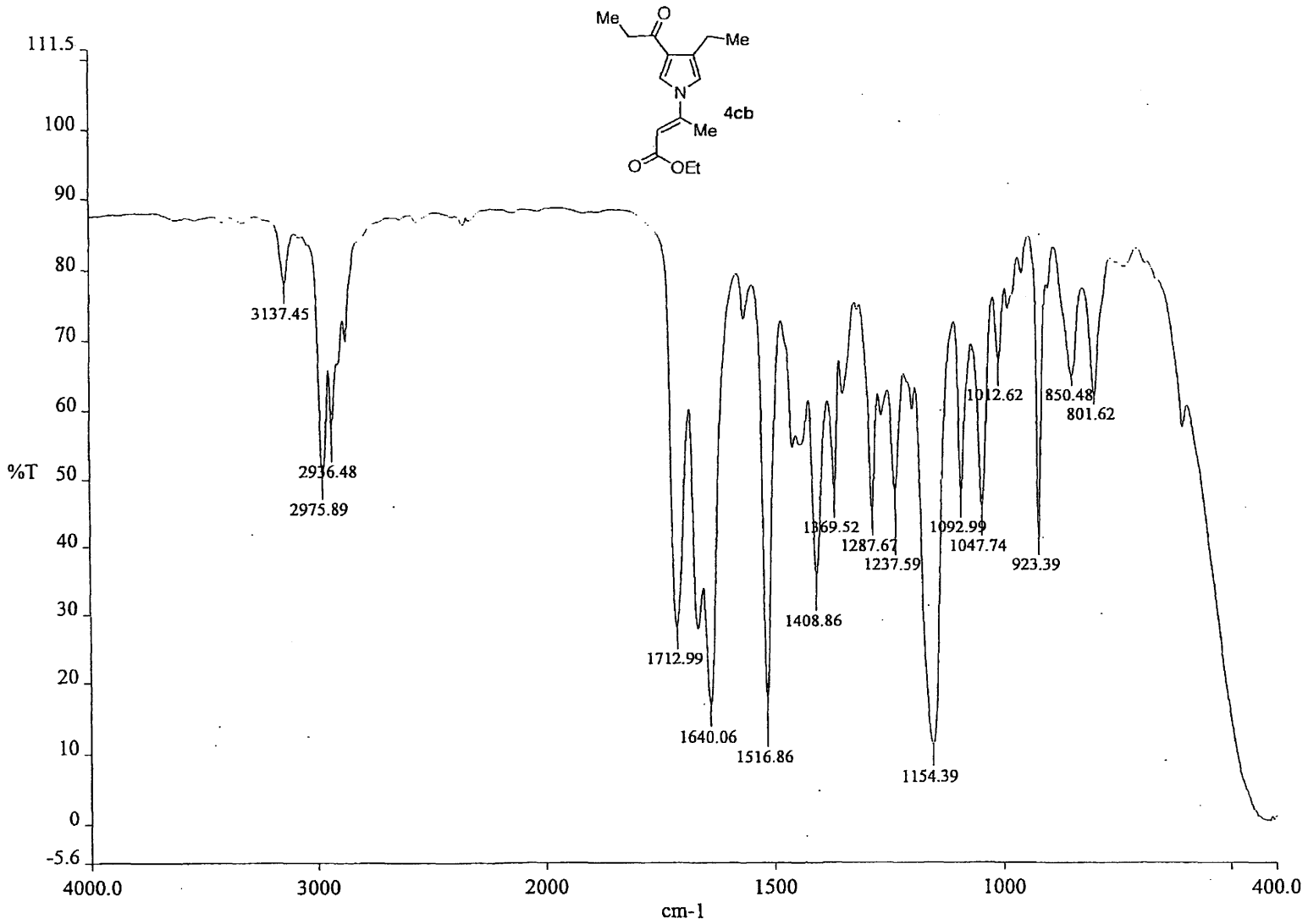
Me
O
Me
N
Me
4cb
O
OEt
111.5
100
90
80
70
60
%T 50
40
30
20
10
0
-5.6
3137.45
2936.48
2975.89
1712.99
1640.06
1516.86
1408.86
1369.52
1287.67
1237.59
1154.39
1092.99
1047.74
1012.62
923.39
850.48
801.62
4000.0
3000
2000
1500
1000
400.0
cm-1

ACQUISITION	
sfrq	500.235
tn	H1
at	3.200
np	64000
sw	10000.0
fb	not used
bs	4
ss	1
tpwr	59
pw	9.8
d1	2.000
tof	1498.2
nt	20
ct	20
alock	n
gain	not used

FLAGS	
il	n
in	n
dp	y
hs	nn

DISPLAY	
sp	-250.4
wp	6246.3
vs	46
sc	0
wc	250
hzmm	2.00
is	100.00
rfl	4632.9
rfp	3636.7
th	7
ins	2.000
nm	ph

DEC. & VT	
dfrq	125.795
dn	C13
dpwr	37
dof	0
dm	nnn
dmm	c
dmf	10000
dseq	
dres	1.0
homo	n

PROCESSING	
wtfile	
proc	ft
fn	131072
math	f
werr	
wexp	
wbs	
wnt	

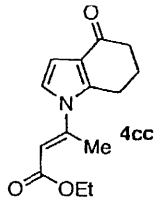

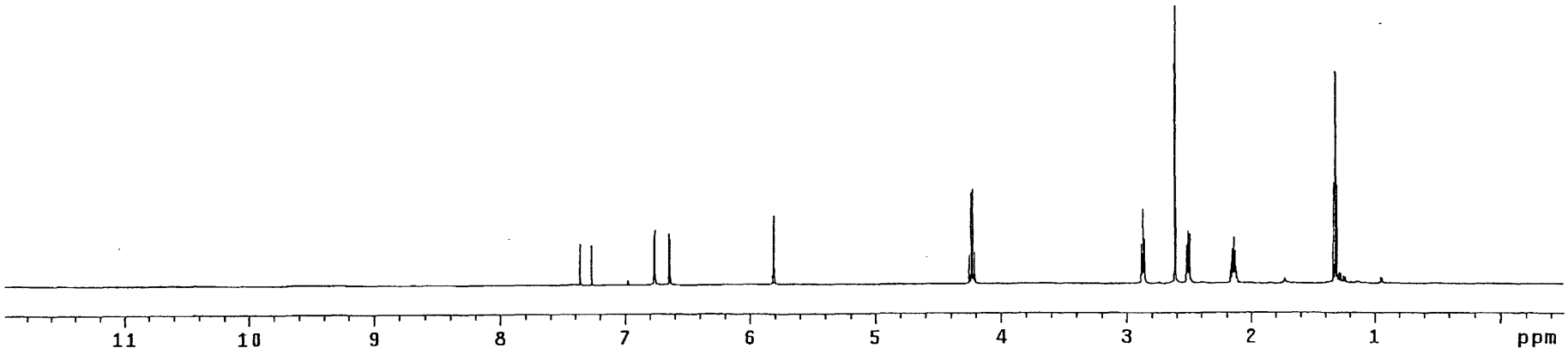

ACQUISITION		DEC. & VT	
sfrq	125.796	dfrq	500.233
tn	C13	dn	H1
at	1.736	dpwr	37
np	131010	dof	-500.0
sw	37735.8	dm	y
fb	not used	dmm	w
bs	8	dmf	10000
ss	1	dseq	
tpwr	53	dres	1.0
pw	6.9	homo	n
d1	0.763	PROCESSING	
tof	631.4	lb	0.30
nt	1e+06	wtfile	
ct	616	proc	ft
alock	n	fn	131072
gain	not used	math	f
FLAGS		werr	
il	n	wexp	
in	n	wbs	
dp	y	wnt	
hs	nn		
DISPLAY			
sp	-1258.3		
wp	31448.1		
vs	3026		
sc	0		
wc	250		
hzmm	125.79		
is	500.00		
rfl	15911.8		
rfp	9686.0		
th	4		
ins	1.000		
al	ph		

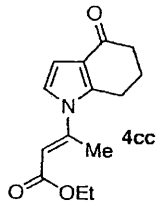

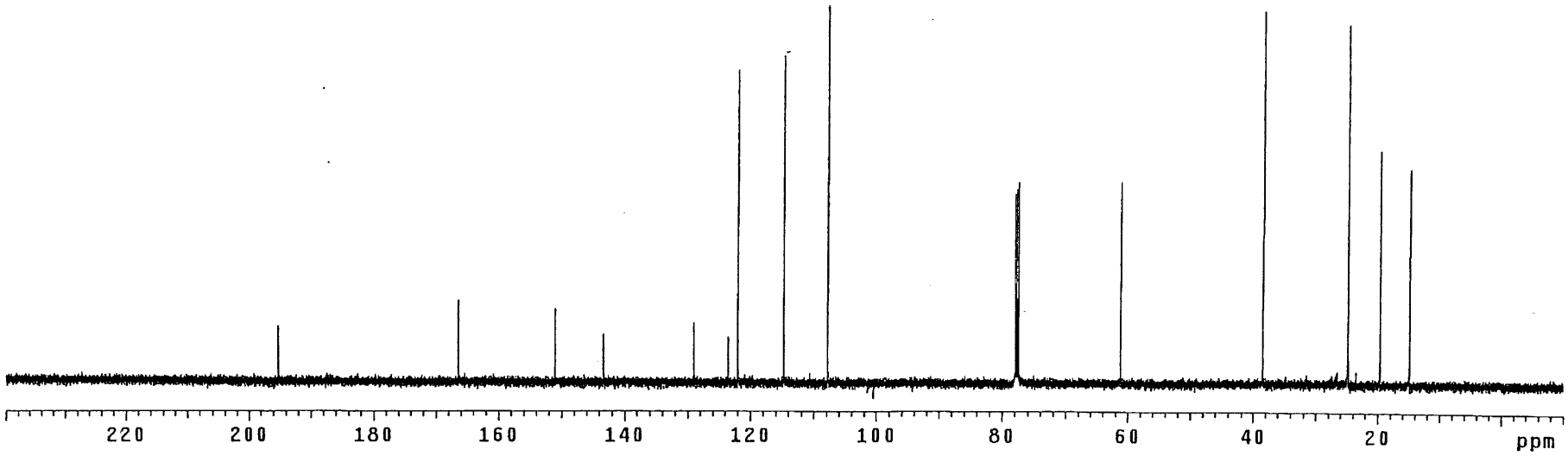

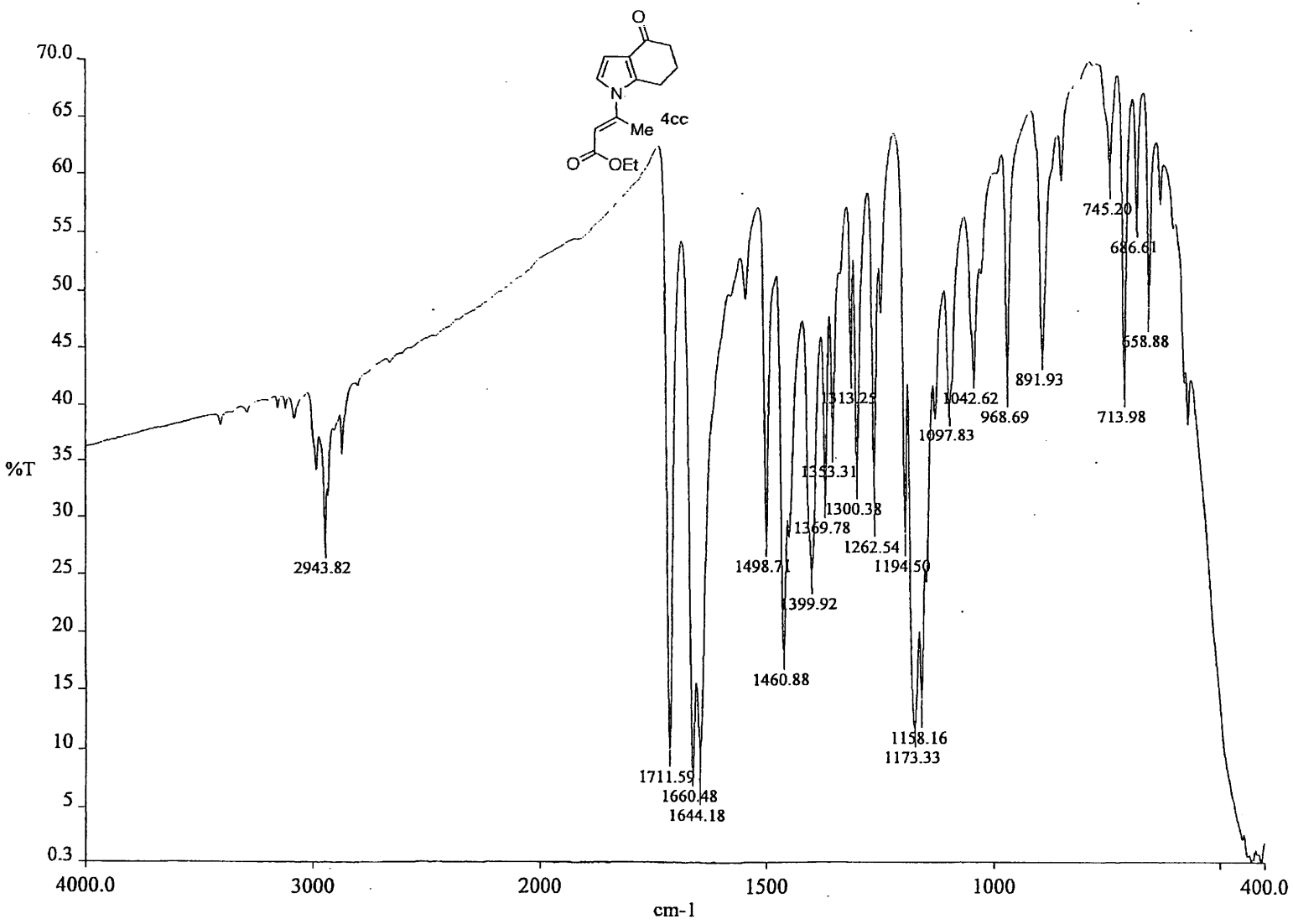
4cc
%T
cm-1
2943.82
1711.59
1660.48
1644.18
1498.71
1460.88
1399.92
1369.78
1353.31
1313.25
1300.38
1262.54
1194.50
1173.33
1158.16
1097.83
1042.62
968.69
891.93
745.20
713.98
686.61
658.88

ACQUISITION	
sfrq	499.749
tn	H1
at	3.277
np	65536
sw	9998.8
fb	not used
bs	4
tpwr	56
pw	8.2
d1	2.000
tof	1498.1
nt	18
ct	18
alock	n
gain	not used

FLAGS	
il	n
in	n
dp	y
hs	nn

DISPLAY	
sp	-250.1
wp	6248.8
vs	32
sc	0
wc	250
hzmm	4.87
is	840.27
rfl	1015.4
rfp	0
th	7
ins	2.000

ai cdc ph

DEC. & VT	
dfrq	125.674
dn	C13
dpwr	34
dof	1498.1
dm	nnn
dmm	w
dmf	10000
dseq	
dres	1.0
homo	n

PROCESSING	
wtfile	
proc	ft
fn	65536
math	f
werr	
wexp	
wbs	
wnt	

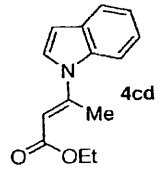

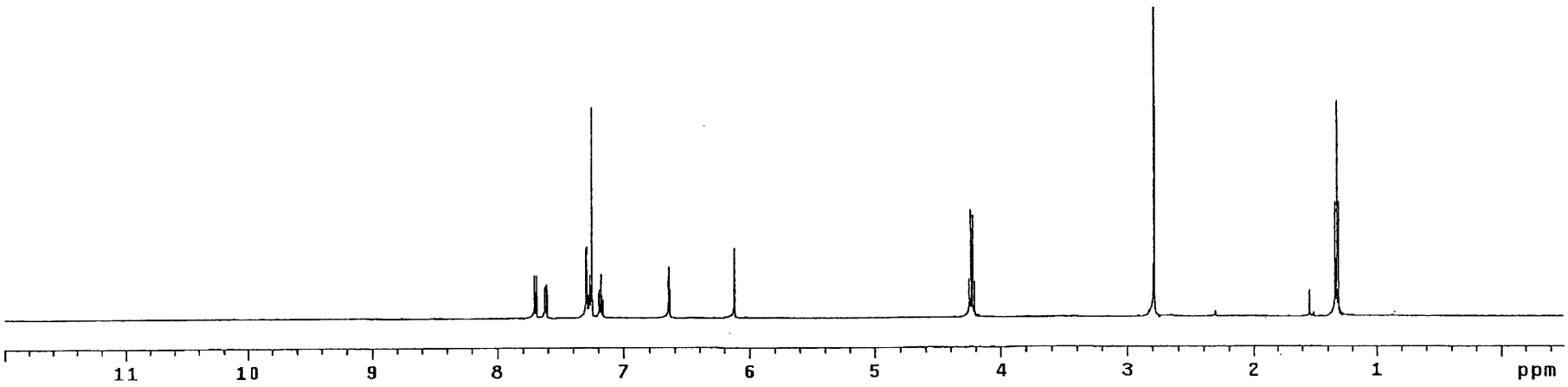

ACQUISITION	
sfrq	125.673
tn	C13
at	0.869
np	65536
sw	37718.1
fb	not used
bs	16
ss	1
tpwr	58
pw	7.5
d1	3.000
tof	615.5
nt	10000
ct	1168
alock	n
gain	not used

FLAGS	
il	n
in	n
dp	y
hs	nn

DISPLAY	
sp	-1256.8
wp	31414.3
vs	447
sc	0
wc	250
hzmm	150.87
is	500.00
rfl	6304.2
rfp	0
th	8
ins	1.000

ai cdc ph

DEC. & VT	
dfrq	499.747
dn	H1
dpwr	34
dof	0
dm	yyy
dmm	w
dmf	10000
dseq	
dres	1.0
homo	n

PROCESSING	
lb	1.00
wtfile	
proc	ft
fn	131072
math	f
werr	
wexp	
wbs	
wnt	

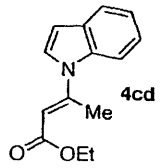

4cd

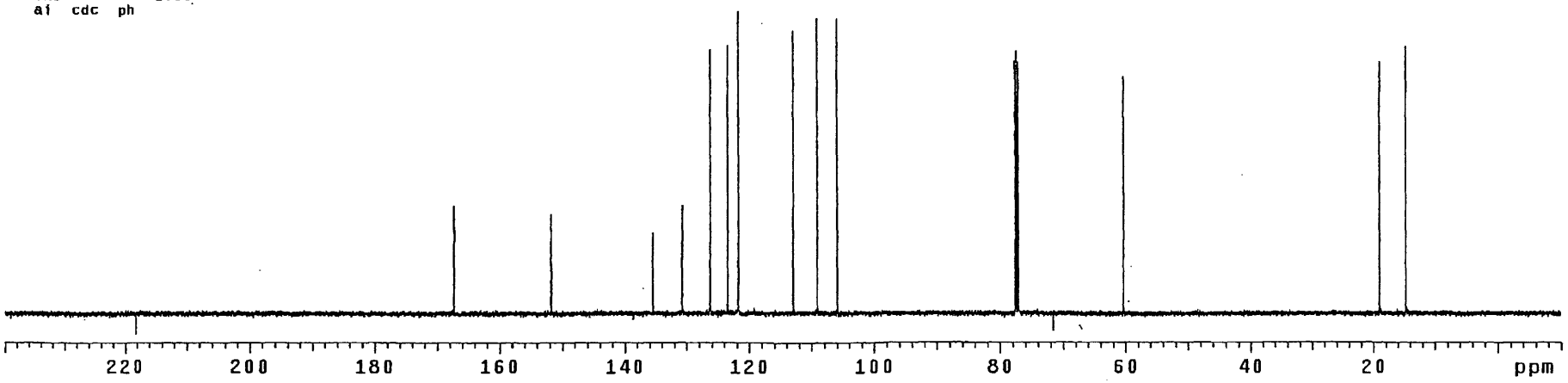

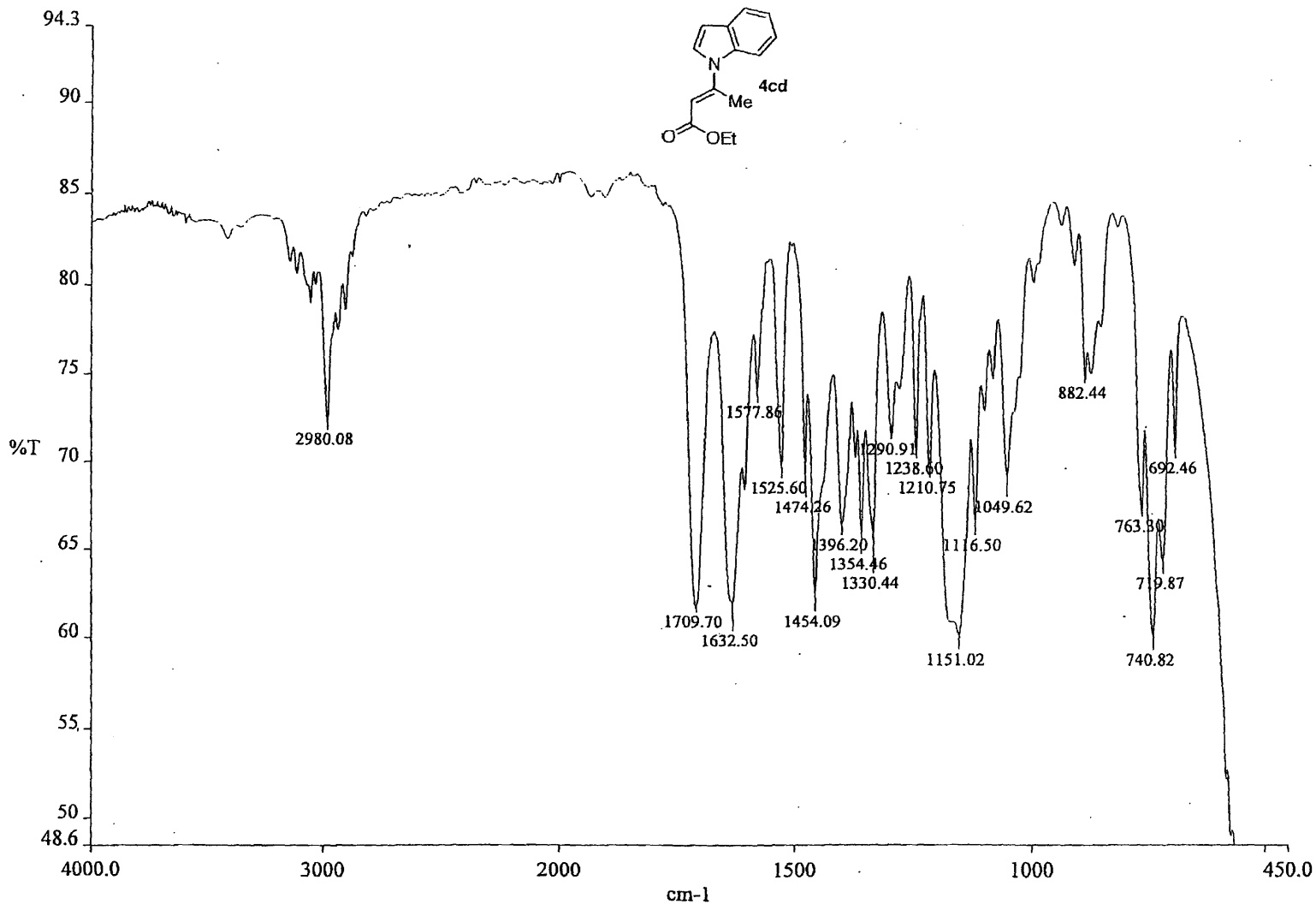
4cd
Me
OEt
%T
94.3
90
85
80
75
70
65
60
55
50
48.6
4000.0
3000
2000
1500
1000
450.0
cm-1
2980.08
1709.70
1632.50
1577.86
1525.60
1474.26
1454.09
1396.20
1354.46
1330.44
1290.91
1238.60
1210.75
1151.02
1116.50
1049.62
882.44
763.30
740.82
719.87
692.46

ACQUISITION	
sfrq	499.758
tn	H1
at	3.277
np	65536
sw	9998.8
fb	not used
bs	4
tpwr	56
pw	8.2
d1	2.000
tof	1498.1
nt	18
ct	18
alock	n
gain	not used

FLAGS	
il	n
in	n
dp	y
hs	nn

DISPLAY	
sp	-250.1
wp	6246.8
vs	59
sc	0
wc	250
hzmm	2.36
is	33.57
rfl	1002.0
rfp	0
th	7
ins	2.000

nm cdc ph

DEC. & VT	
dfrq	125.677
dn	C13
dpwr	34
dof	1498.1
dm	nnn
dmm	w
dmf	10000
dseq	
dres	1.0
homo	n

PROCESSING	
wtfile	
proc	ft
fn	65536
math	f
werr	
wexp	
wbs	
wnt	

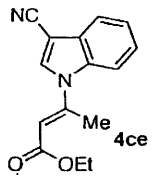

4ce

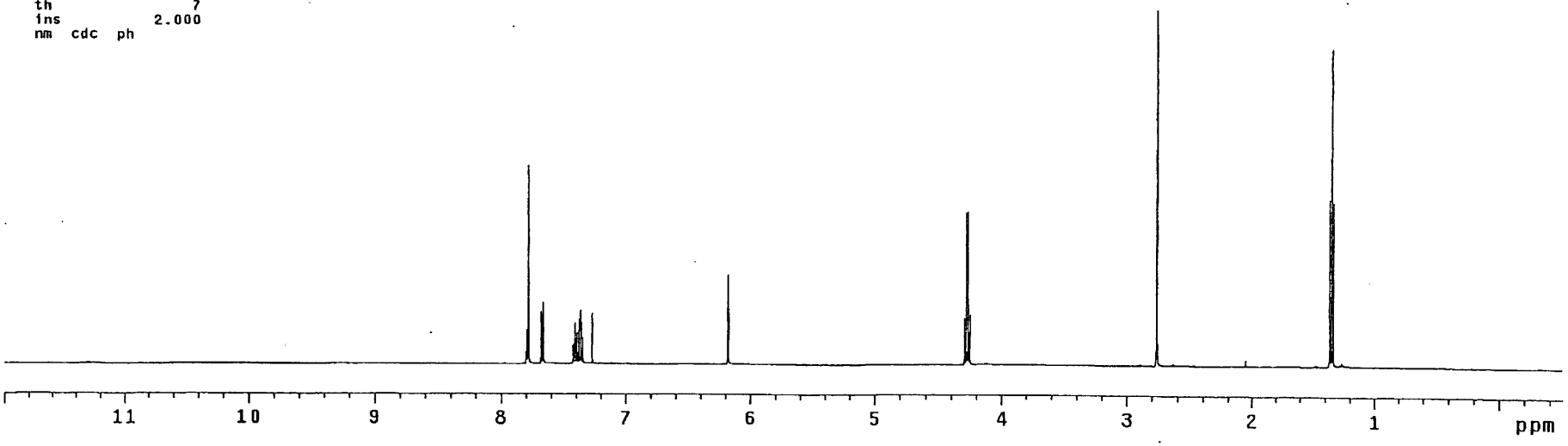

ACQUISITION	
sfrq	125.796
tn	C13
at	1.736
np	131010
sw	37735.8
fb	not used
bs	8
ss	1
tpwr	53
pw	6.9
d1	0.763
tof	631.4
nt	10000
ct	896
alock	n
gain	not used

FLAGS	
il	n
in	n
dp	y
hs	nn

DISPLAY	
sp	-1258.3
wp	31448.1
vs	3159
sc	0
wc	250
hzmm	125.79
is	500.00
rfl	15911.8
rfp	9686.0
th	6
ins	1.000
ai	ph

DEC. & VT	
dfrq	500.233
dn	H1
dpwr	37
dof	-500.0
dm	y
dmm	w
dmf	10000
dseq	
dres	1.0
homo	n

PROCESSING	
lb	0.30
wtfile	
proc	ft
fn	131072
math	f
werr	
wexp	
wbs	
wnt	

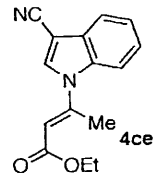

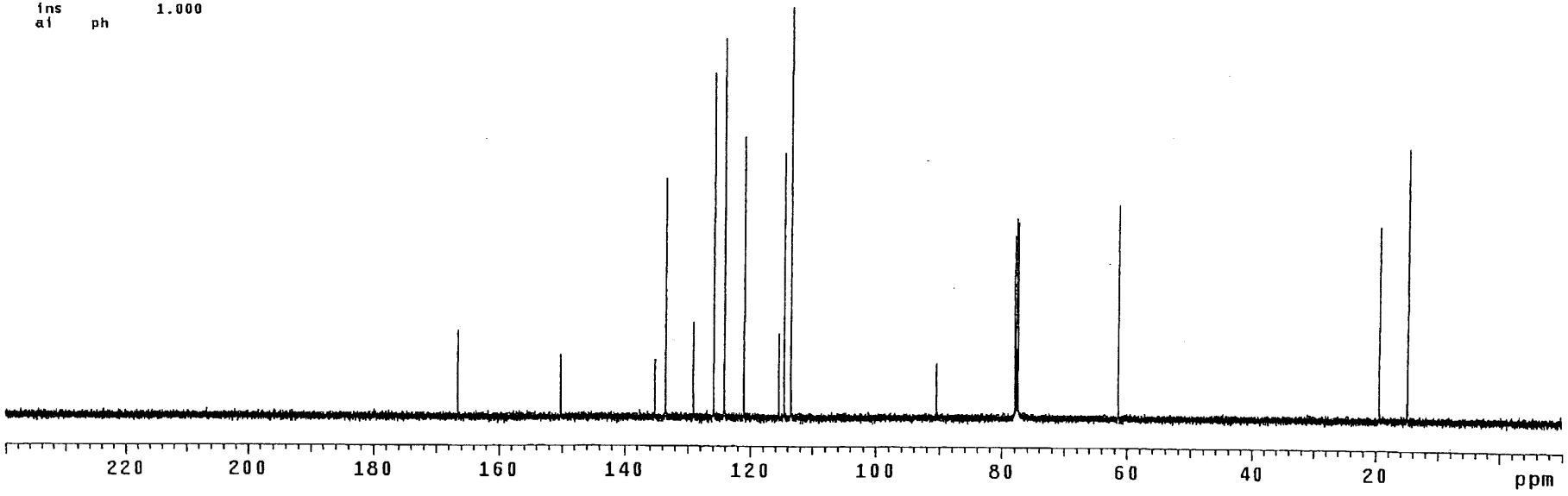

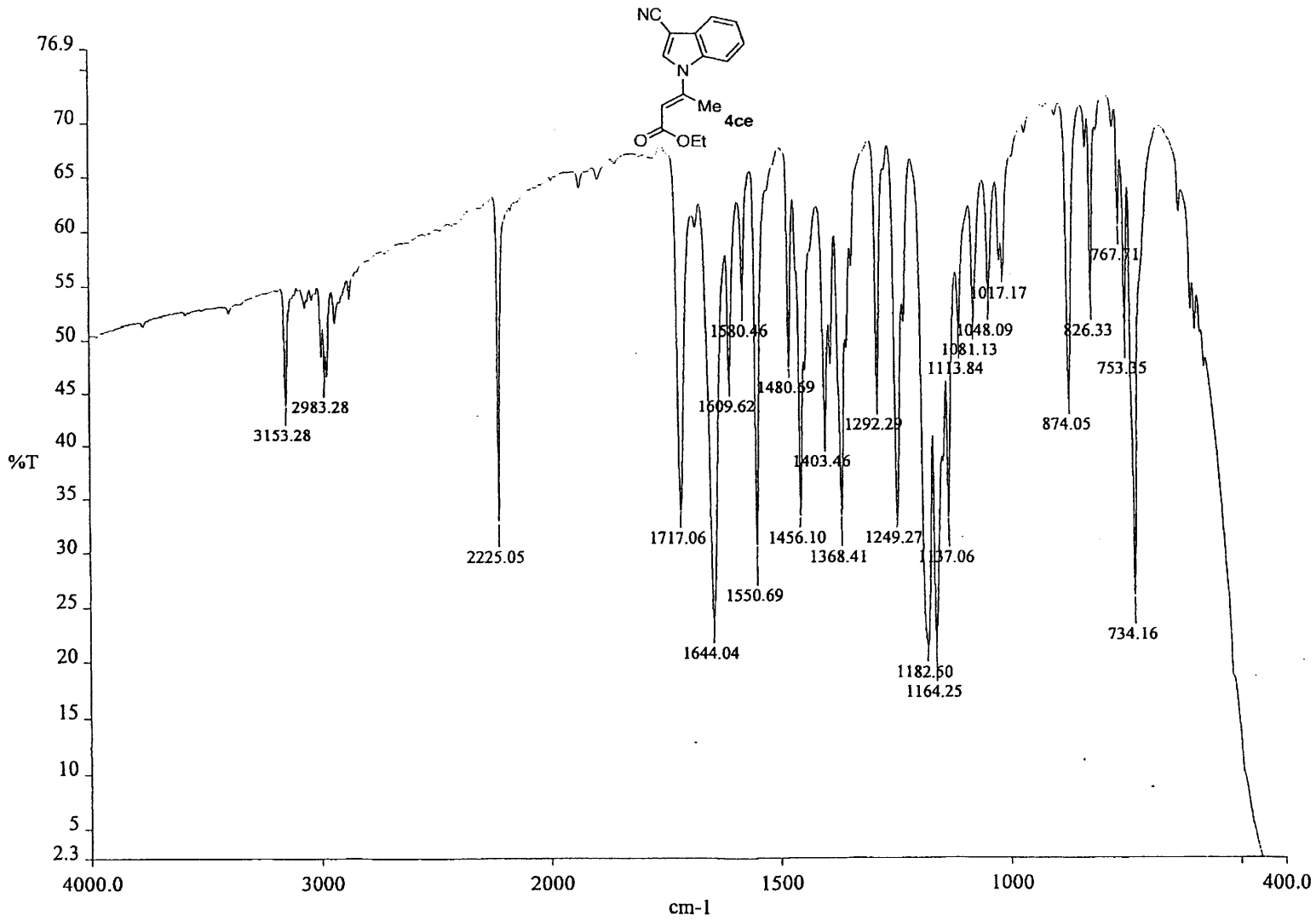
NC
N
Me
4ce
O
OEt
76.9
70
65
60
55
50
45
40
35
30
25
20
15
10
5
2.3
%T
4000.0
3000
2000
1500
1000
400.0
cm-1
3153.28
2983.28
2225.05
1717.06
1644.04
1609.62
1580.46
1550.69
1480.59
1456.10
1403.46
1368.41
1292.29
1249.27
1182.50
1164.25
1137.06
1113.84
1081.13
1048.09
1017.17
874.05
826.33
767.71
753.35
734.16

ACQUISITION	
sfrq	500.235
tn	H1
at	3.200
np	64000
sw	10000.0
fb	not used
bs	4
ss	1
tpwr	59
pw	9.8
d1	2.000
tof	1498.2
nt	20
ct	20
alock	n
gain	not used

FLAGS	
il	n
in	n
dp	y
hs	nn

DISPLAY	
sp	-250.4
wp	6246.3
vs	61
sc	0
wc	250
hzmm	3.57
is	119.21
rfl	4632.8
rfp	3636.7
th	23
ins	2.000
nm	ph

DEC. & VT	
dfrq	125.795
dn	C13
dpwr	37
dof	0
dm	nnn
dmm	c
dmf	10000
dseq	
dres	1.0
homo	n

PROCESSING	
wtfile	
proc	ft
fn	131072
math	f
werr	
wexp	
wbs	
wnt	

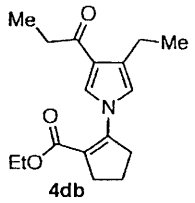

4db

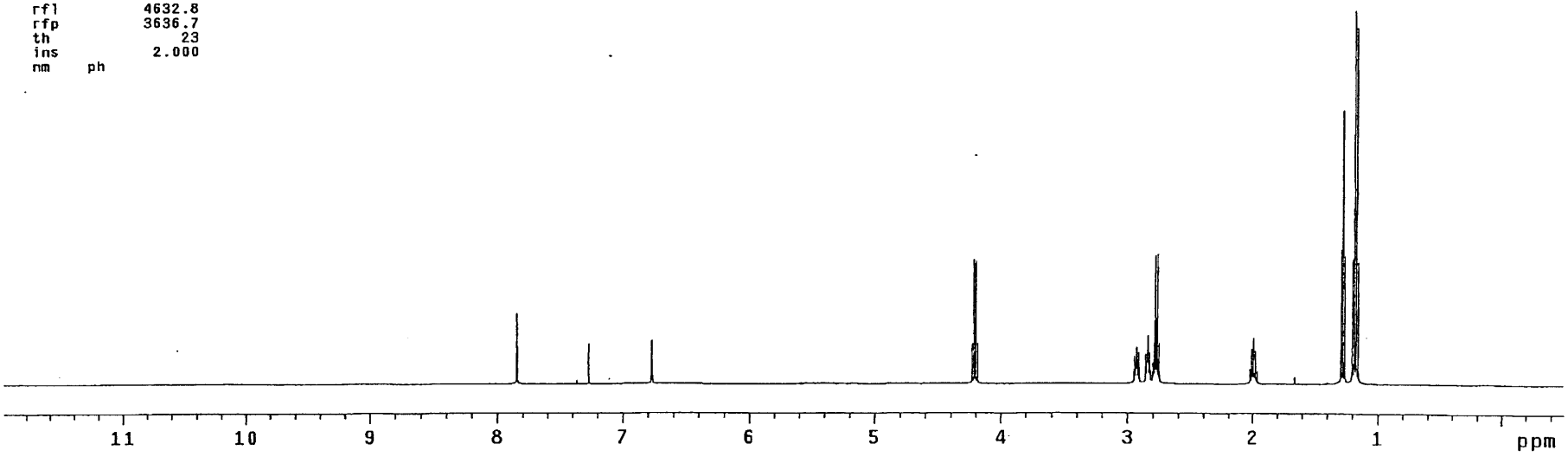

ACQUISITION		DEC. & VT	
sfrq	125.796	dfrq	500.233
tn	C13	dn	H1
at	1.736	dpwr	37
np	131010	dof	-500.0
sw	37735.8	dm	y
fb	not used	dmm	w
bs	8	dmf	10000
ss	1	dseq	
tpwr	53	dres	1.0
pw	6.9	homo	n
d1	0.763	PROCESSING	
tof	631.4	lb	0.30
nt	10000	wtfile	
ct	584	proc	ft
alock	n	fn	131072
gain	not used	math	f
FLAGS		werr	
il	n	wexp	
in	n	wbs	
dp	y	wnt	
hs	nn		
DISPLAY			
sp	-1258.3		
wp	31448.1		
vs	35		
sc	0		
wc	250		
hzmm	125.79		
is	500.00		
rfl	15911.8		
rfp	9686.0		
th	5		
ins	1.000		
nm	ph		

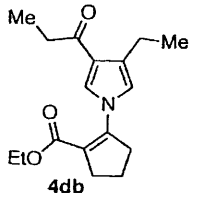

4db

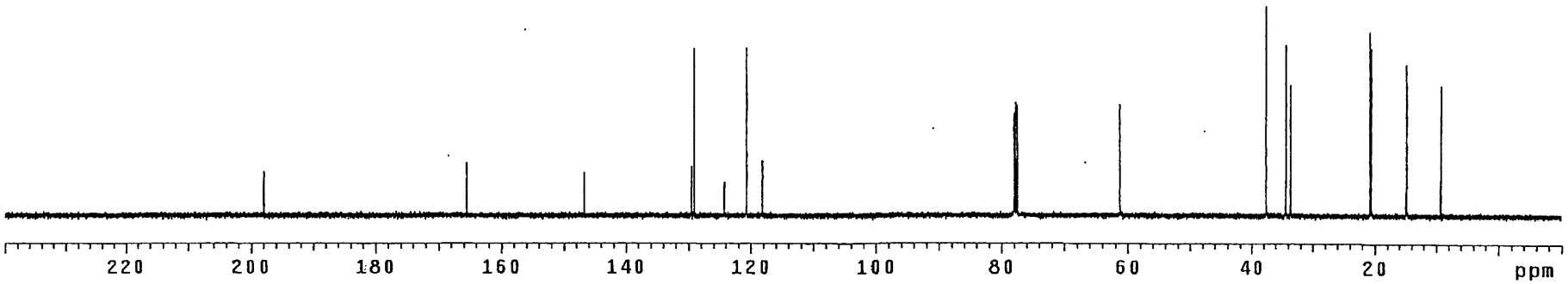

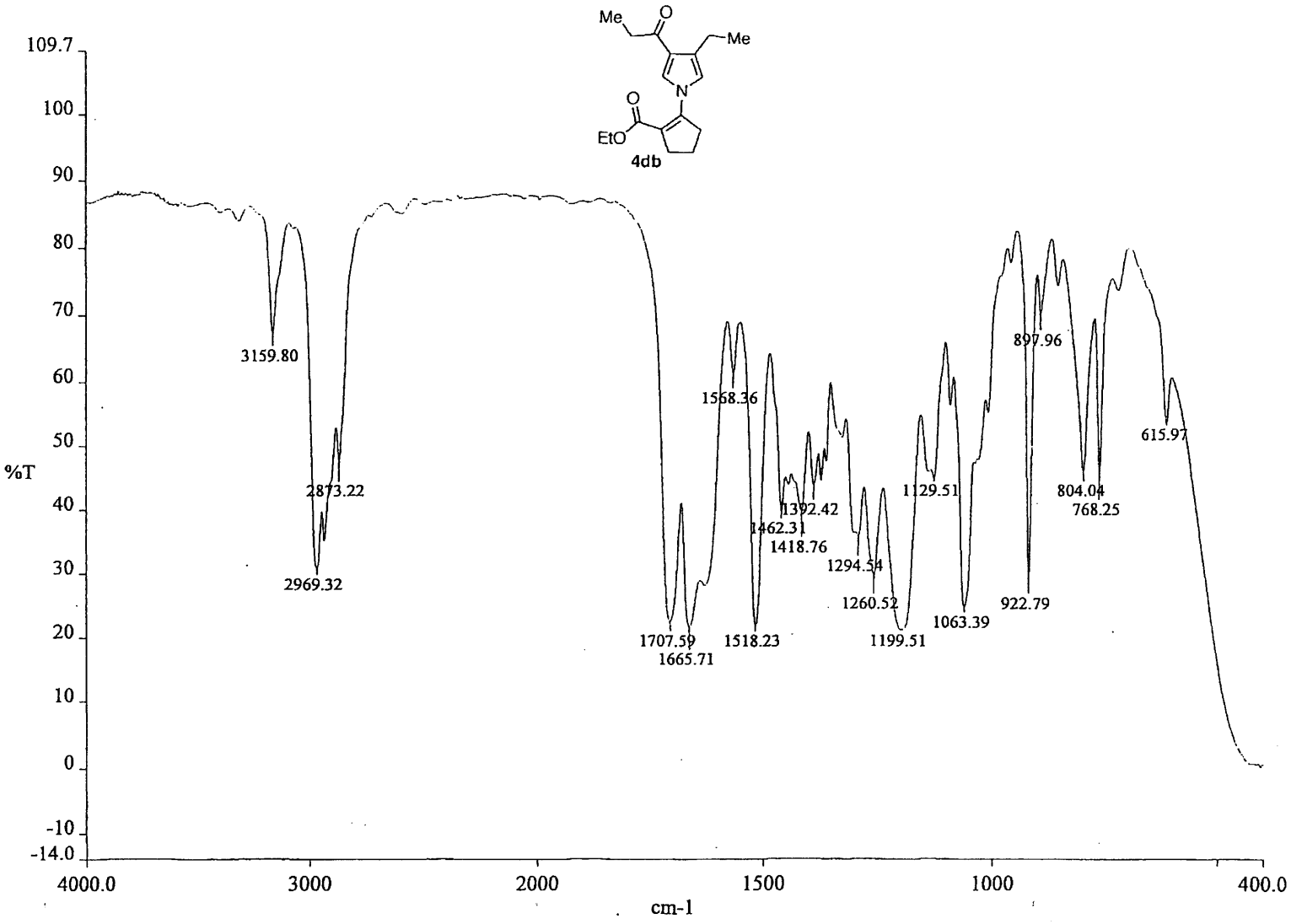
Me
O
Me
N
O
EtO
4db
109.7
100
90
80
70
60
50
40
30
20
10
0
-10
-14.0
%T
3159.80
2873.22
2969.32
1568.36
1707.59
1665.71
1518.23
1462.31
1418.76
1392.42
1294.54
1260.52
1199.51
1129.51
1063.39
922.79
897.96
804.04
768.25
615.97
4000.0
3000
2000
1500
1000
400.0
cm-1

ACQUISITION		DEC. & VT	
sfrq	499.758	dfrq	125.677
tn	H1	dn	C13
at	3.277	dpwr	34
np	65536	dof	1498.1
sw	9998.8	dm	nnn
fb	not used	dmm	w
bs	4	dmf	10000
tpwr	56	dseq	
pw	8.2	dres	1.0
d1	2.000	homo	n
tof	1498.1	PROCESSING	
nt	18	wtfile	
ct	18	proc	ft
alock	n	fn	65536
gain	not used	math	f
FLAGS		werr	
il	n	wexp	
in	n	wbs	
dp	y	wnt	
hs	nn		
DISPLAY			
sp	-250.4		
wp	6246.5		
vs	45		
sc	0		
wc	250		
hzmm	40.00		
is	33.57		
rfl	1002.5		
rfp	0		
th	7		
ins	2.000		
nm cdc ph			

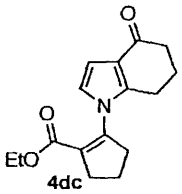

4dc

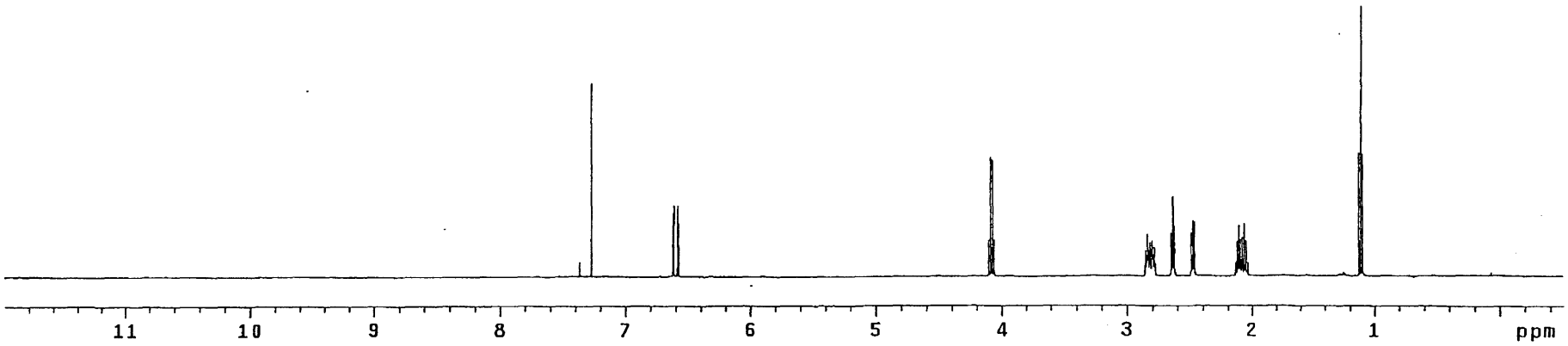

ACQUISITION	
sfrq	125.676
tn	C13
at	0.869
np	65536
sw	37718.1
fb	not used
bs	16
ss	1
tpwr	58
pw	7.5
d1	3.000
tof	615.5
nt	10000
ct	832
alock	n
gain	not used

FLAGS	
il	n
in	n
dp	y
hs	nn

DISPLAY	
sp	-1257.2
wp	31415.3
vs	677
sc	0
wc	250
hzmm	125.66
is	500.00
rfl	6304.1
rfp	0
th	7
ins	1.000
al cdc ph	

DEC. & VT	
dfrq	499.756
dn	H1
pwr	34
dof	0
dm	yyy
dmm	w
dmf	10000
dseq	
dres	1.0
homo	n

DEC2	
dfrq2	0
dn2	
dpwr2	1
dof2	0
dm2	n
dmm2	c
dmf2	10000
dseq2	
dres2	1.0
homo2	n

DEC3	
dfrq3	0
dn3	
dpwr3	1
dof3	0
dm3	n
dmm3	c
dmf3	10000
dseq3	
dres3	1.0
homo3	n

PROCESSING	
lb	1.00
wtfile	
proc	ft
fn	131072
math	f
werr	
wexp	
wbs	
wnt	

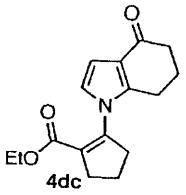

4dc

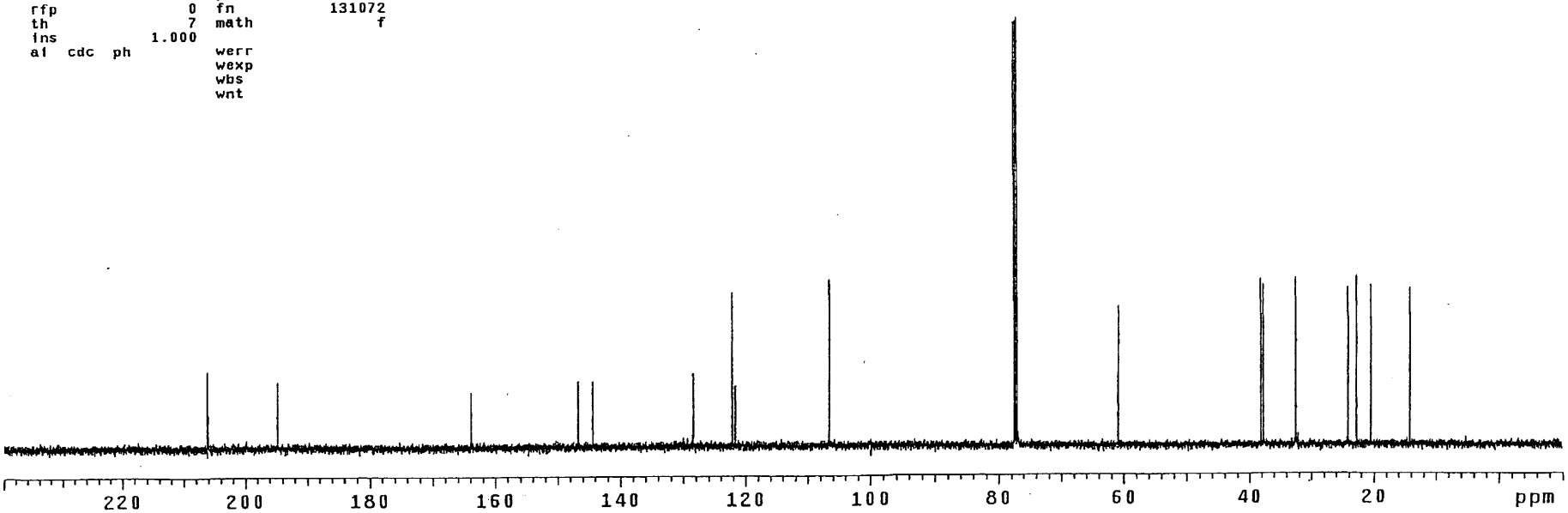

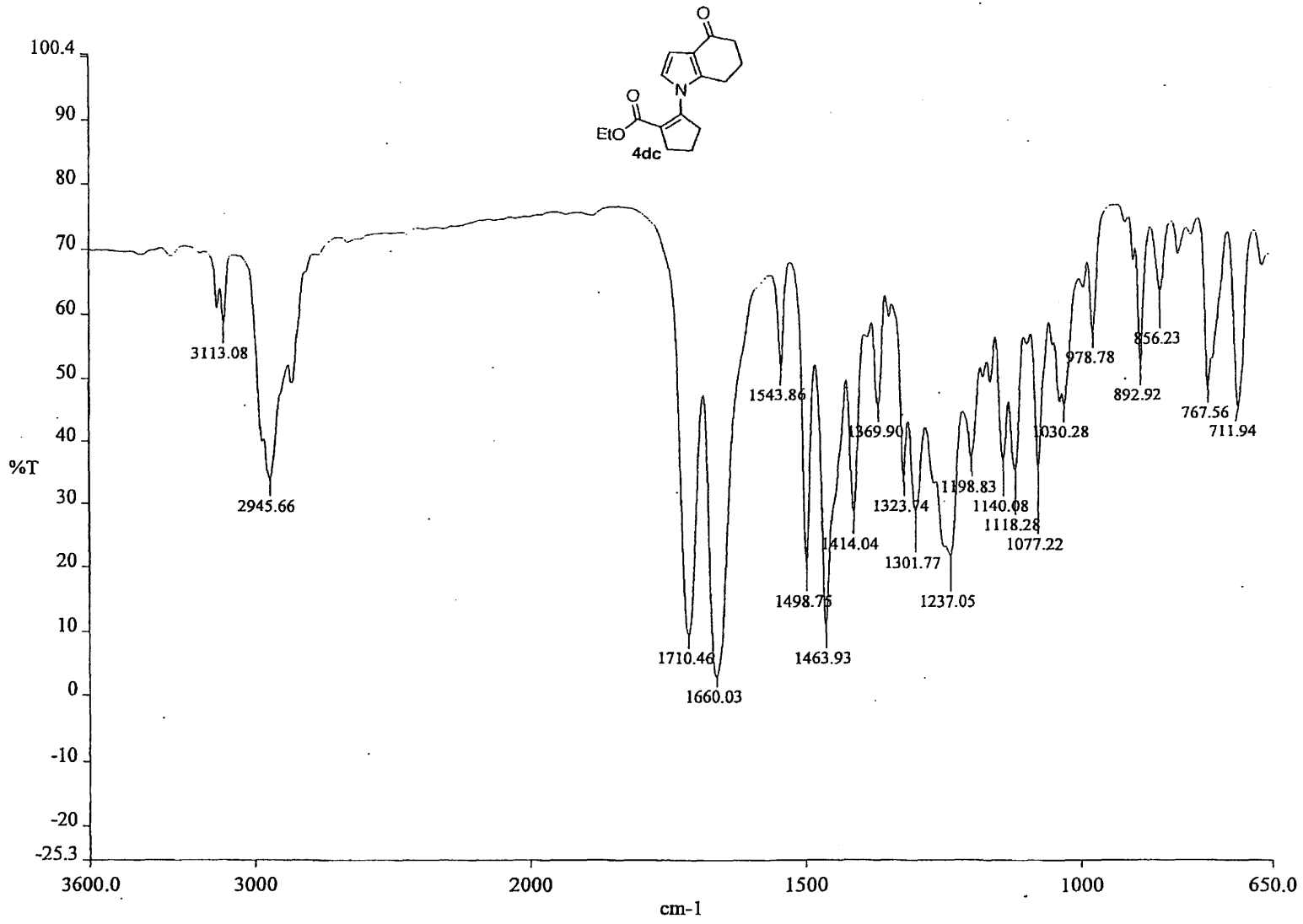
4dc
100.4
90
80
70
60
50
40
30
20
10
0
-10
-20
-25.3
%T
3600.0
3000
2000
1500
1000
650.0
cm-1
3113.08
2945.66
1710.46
1660.03
1543.86
1498.75
1463.93
1414.04
1369.90
1323.74
1301.77
1237.05
1198.83
1140.08
1118.28
1077.22
1030.28
978.78
892.92
856.23
767.56
711.94

ACQUISITION		DEC. & VT	
sfrq	499.758	dfrq	125.677
tn	H1	dn	C13
at	3.277	dpwr	34
np	65536	dof	1498.1
sw	9998.8	dm	nnn
fb	not used	dmm	w
bs	4	dmf	10000
tpwr	56	dseq	
pw	8.2	dres	1.0
d1	2.000	homo	n
tof	1498.1	PROCESSING	
nt	18	wtfile	
ct	18	proc	ft
alock	n	fn	65536
gain	not used	math	f
FLAGS		werr	
il	n	wexp	
in	n	wbs	
dp	y	wnt	
hs	nn		
DISPLAY			
sp	-250.4		
wp	6246.5		
vs	35		
sc	0		
wc	250		
hzmm	40.00		
is	33.57		
rfl	4635.5		
rfp	3633.2		
th	7		
ins	2.000		
nm cdc ph			

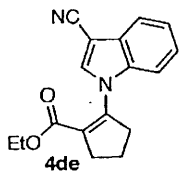

4de

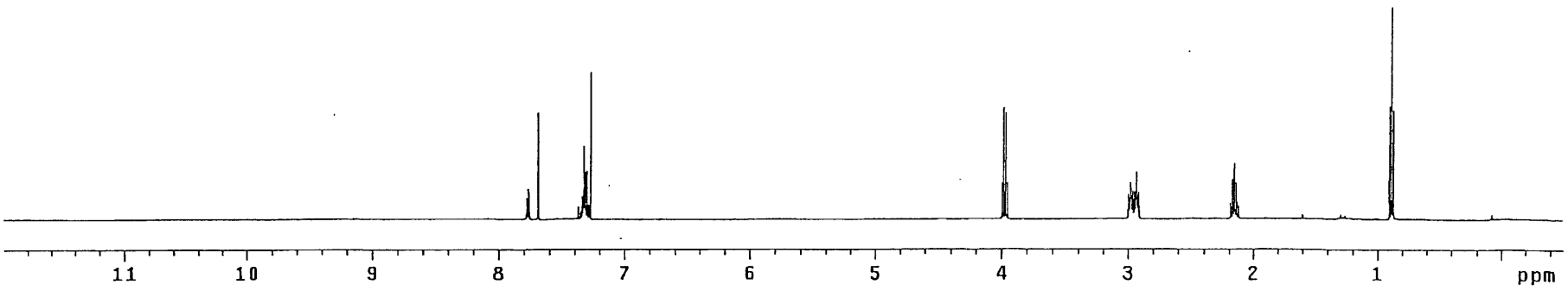

ACQUISITION		DEC. & VT			
sfrq	125.676	dfrq	499.756		
tn	C13	dn	H1		
at	0.869	dpwr	34		
np	65536	dof	0		
sw	37718.1	dm	yyy		
fb	not used	dmm	w		
bs	16	dmf	10000		
ss	1	dseq			
tpwr	58	dres	1.0		
pw	7.5	homo	n		
d1	3.000	DEC2			
tof	615.5	dfrq2	0		
nt	10000	dn2			
ct	800	dpwr2	1		
alock	n	dof2	0		
gain	not used	dm2	n		
FLAGS		dmm2	c		
il	n	dmf2	10000		
in	n	dseq2			
dp	y	dres2	1.0		
hs	nn	homo2	n		
DISPLAY		DEC3			
sp	-1257.2	dfrq3	0		
wp	31415.3	dn3			
vs	1030	dpwr3	1		
sc	0	dof3	0		
wc	250	dm3	n		
hzmm	125.66	dmm3	c		
is	500.00	dmf3	10000		
rfl	6304.1	dseq3			
rfp	0	dres3	1.0		
th	10	homo3	n		
ins	1.000	PROCESSING			
ai cdc ph		lb	1.00		
		wtfile			
		proc	ft		
		fn	131072		
		math	f		
		werr			
		wexp			
		wbs			
		wnt			

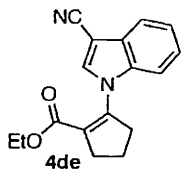

4de

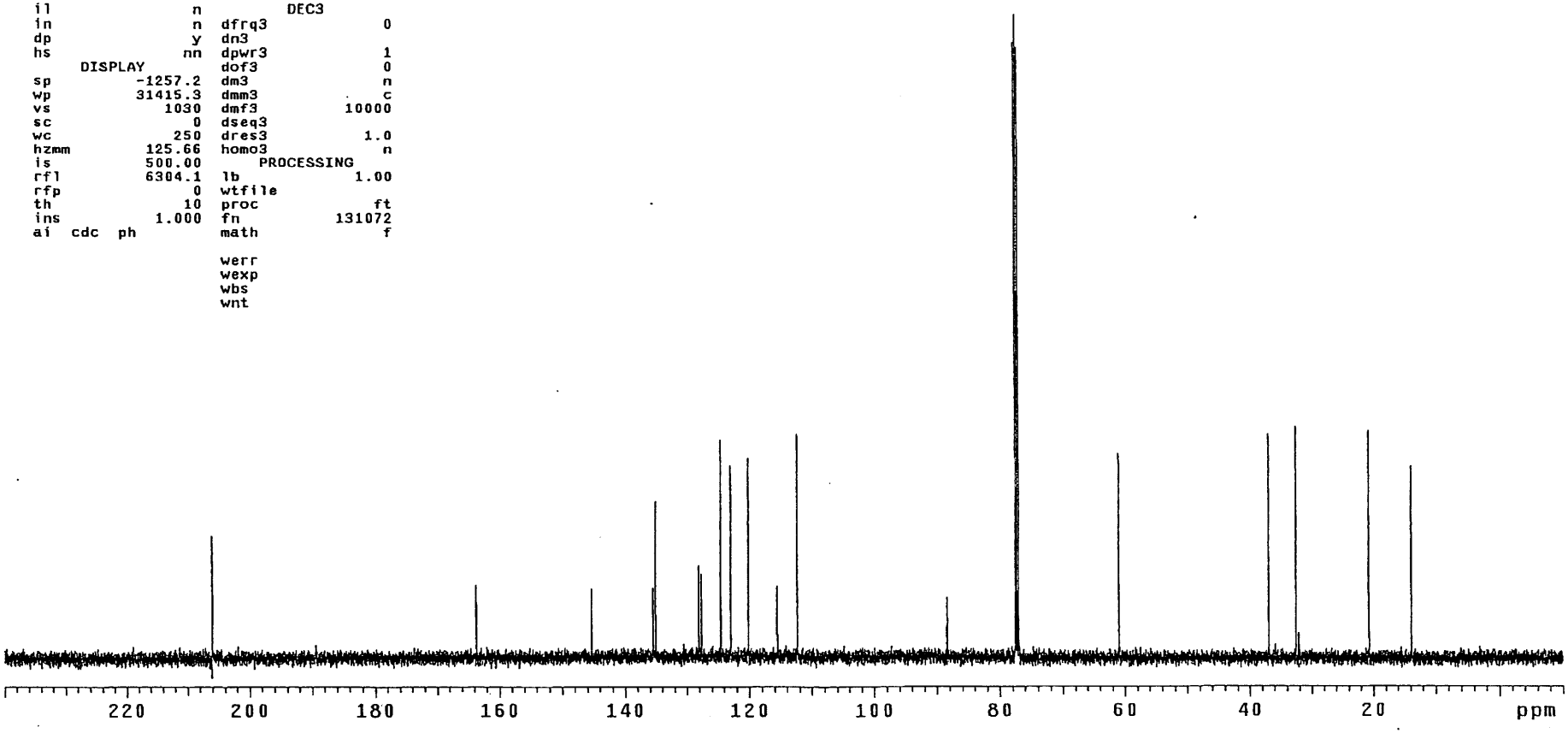

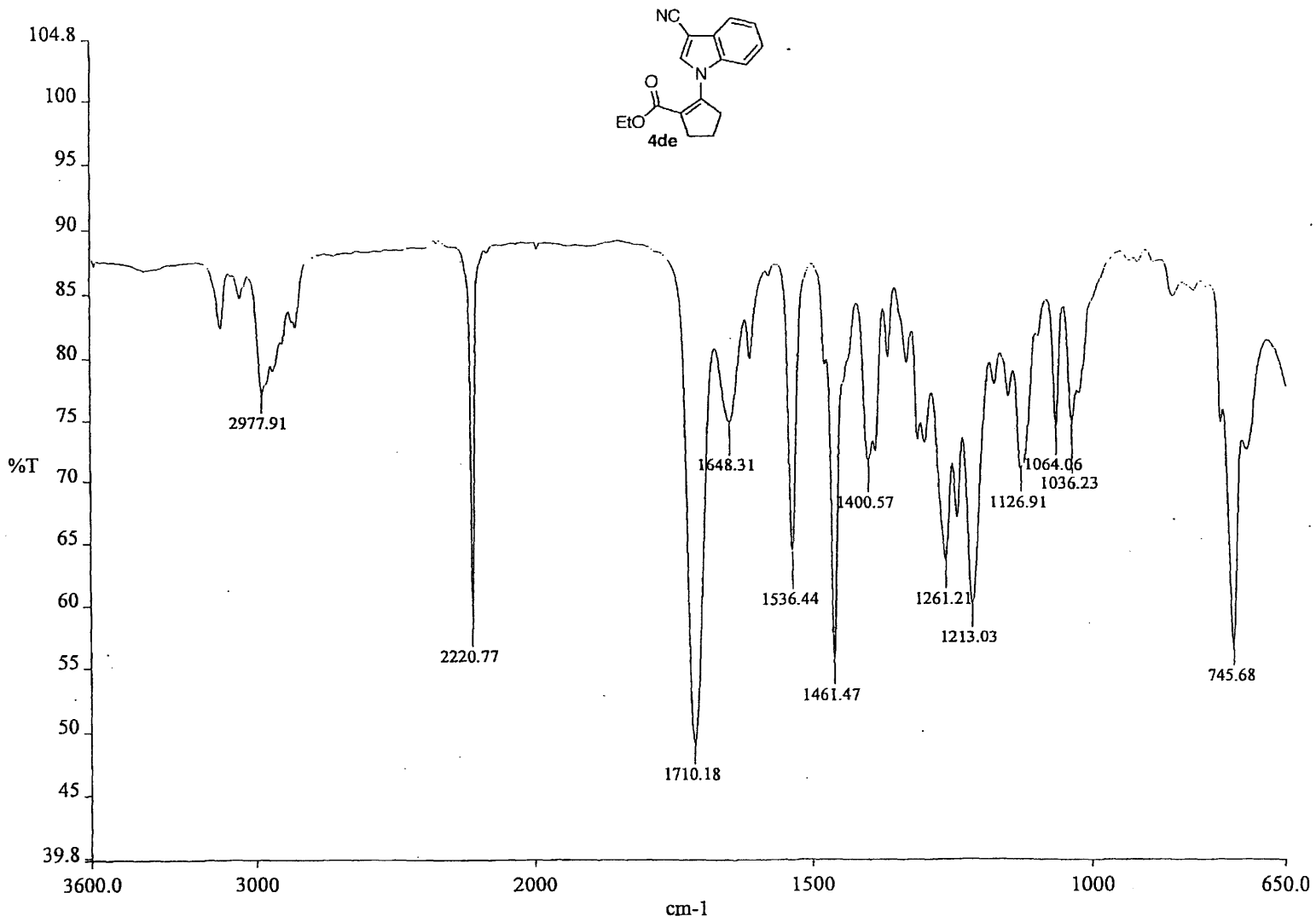
NC
N
O
EtO
4de
104.8
100
95
90
85
80
75
70
65
60
55
50
45
39.8
%T
2977.91
2220.77
1710.18
1648.31
1536.44
1461.47
1400.57
1261.21
1213.03
1126.91
1064.06
1036.23
745.68
3600.0
3000
2000
1500
1000
650.0
cm-1

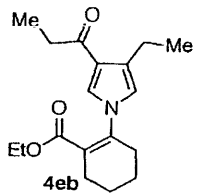

ACQUISITION	
sfrq	500.235
tn	H1
at	3.200
np	64000
sw	10000.0
fb	not used
bs	4
ss	1
tpwr	59
pw	9.8
d1	2.000
tof	1498.2
nt	20
ct	20
alock	n
gain	not used
FLAGS	
il	n
in	n
dp	y
hs	nn
DISPLAY	
sp	-250.1
wp	6246.6
vs	37
sc	0
wc	250
hzmm	7.04
is	119.21
rfl	4632.9
rfp	3636.7
th	15
ins	2.000
ai	ph

DEC. & VT	
dfrq	125.795
dn	C13
dpwr	37
dof	0
dm	nnn
dmm	c
dmf	10000
dseq	
dres	1.0
homo	n
PROCESSING	
wtfile	
proc	ft
fn	131072
math	f
werr	
wexp	
wbs	
wnt	

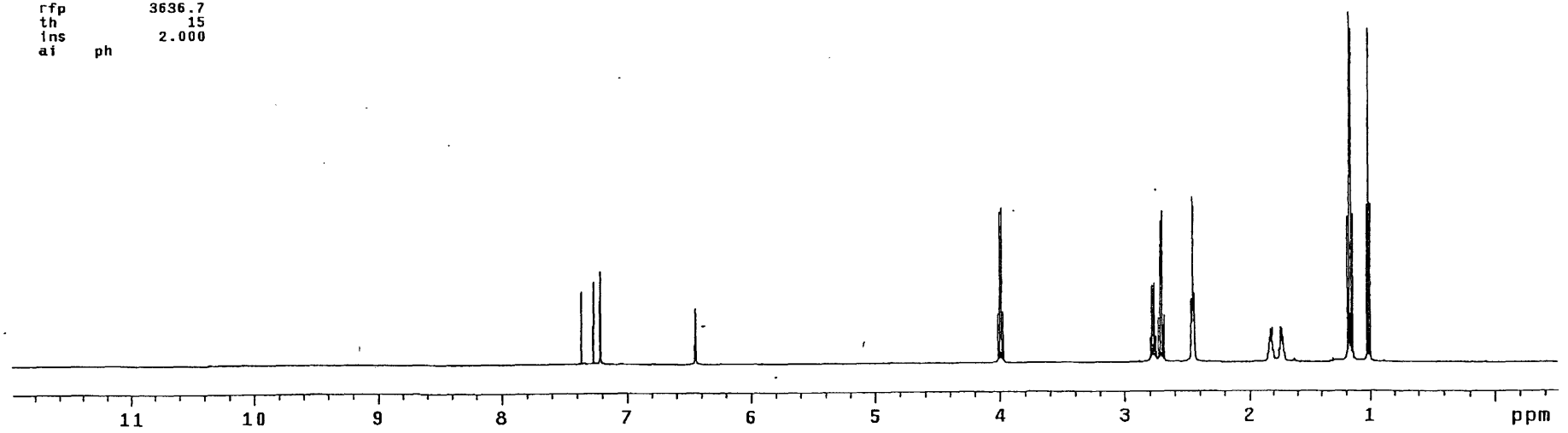

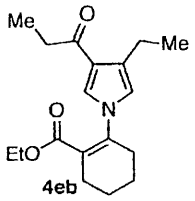

ACQUISITION		DEC. & VT	
sfrq	125.796	dfrq	500.233
tn	C13	dn	H1
at	1.736	dpwr	37
np	131010	dof	-500.0
sw	37735.8	dm	y
fb	not used	dmm	w
bs	8	dmf	10000
ss	1	dseq	
tpwr	53	dres	1.0
pw	6.9	homo	n
d1	0.763	PROCESSING	
tof	631.4	lb	0.30
nt	10000	wtfile	
ct	736	proc	ft
alock	n	fn	131072
gain	not used	math	f
FLAGS		werr	
il	n	wexp	
in	n	wbs	
dp	y	wnt	
hs	nn		
DISPLAY			
sp	-1258.3		
wp	31448.1		
vs	39		
sc	0		
wc	250		
hzmm	125.79		
is	500.00		
rfl	15911.8		
rfp	9686.0		
th	6		
ins	1.000		
nm	ph		

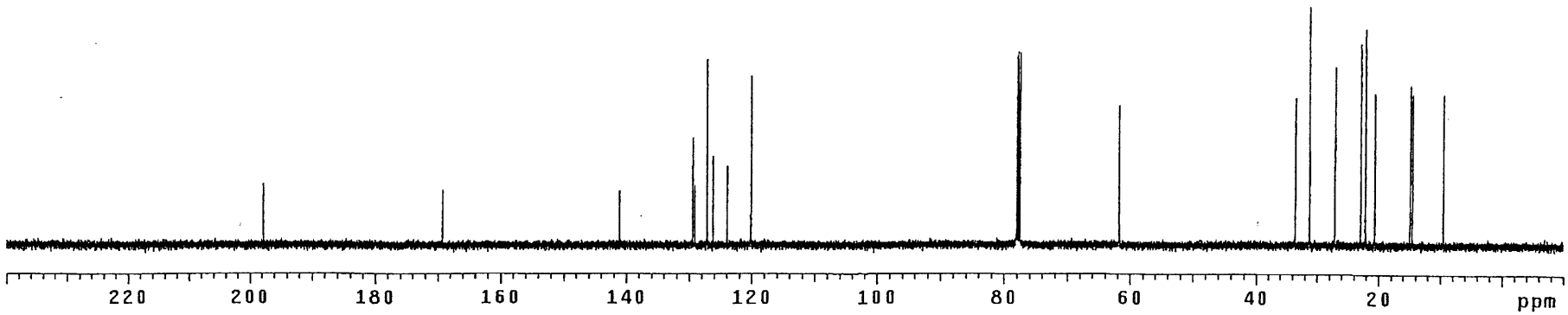

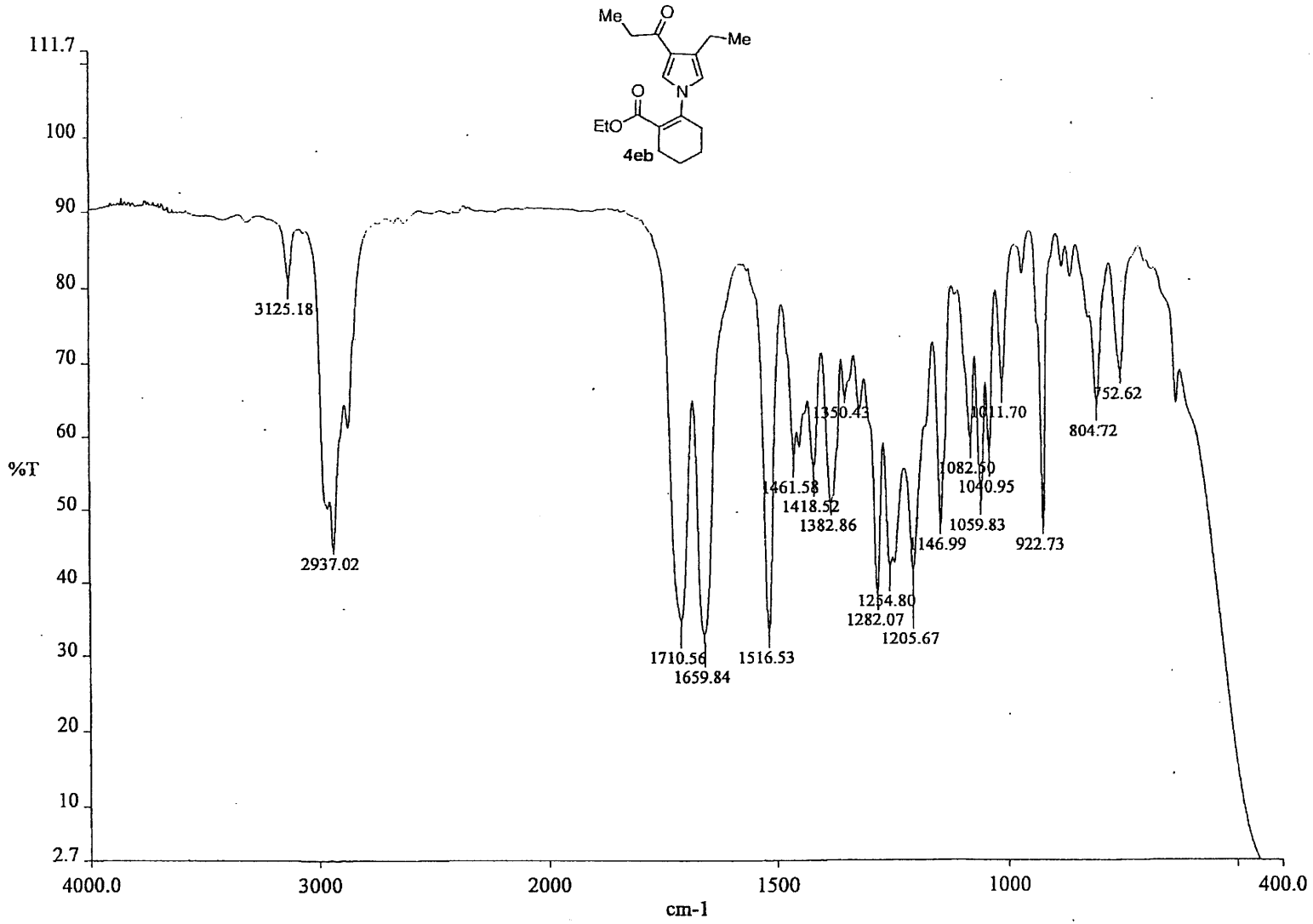
Me
O
Me
N
O
EtO
4eb
111.7
100
90
80
70
60
50
40
30
20
10
2.7
%T
3125.18
2937.02
1710.56
1659.84
1516.53
1461.58
1418.52
1382.86
1350.43
1254.80
1282.07
1205.67
1146.99
1082.50
1040.95
1059.83
1011.70
922.73
804.72
752.62
4000.0
3000
2000
1500
1000
400.0
cm-1

ACQUISITION	
sfrq	499.749
tn	H1
at	3.277
np	65536
sw	9998.8
fb	not used
bs	4
tpwr	56
pw	8.2
d1	2.000
tof	1498.1
nt	20
ct	20
alock	n
gain	not used

FLAGS	
il	n
in	n
dp	y
hs	nn

DISPLAY	
sp	-250.1
wp	6246.5
vs	69
sc	0
wc	250
hzmm	5.47
is	33.57
rfl	4638.5
rfp	3623.1
th	7
ins	1.000

nm cdc ph

DEC. & VT	
dfrq	125.674
dn	C13
dpwr	34
dof	1498.1
dm	nnn
dmm	w
dmf	10000
dseq	
dres	1.0
homo	n

PROCESSING	
wtfile	
proc	ft
fn	65536
math	f
werr	
wexp	
wbs	
wnt	

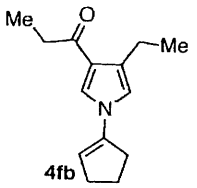

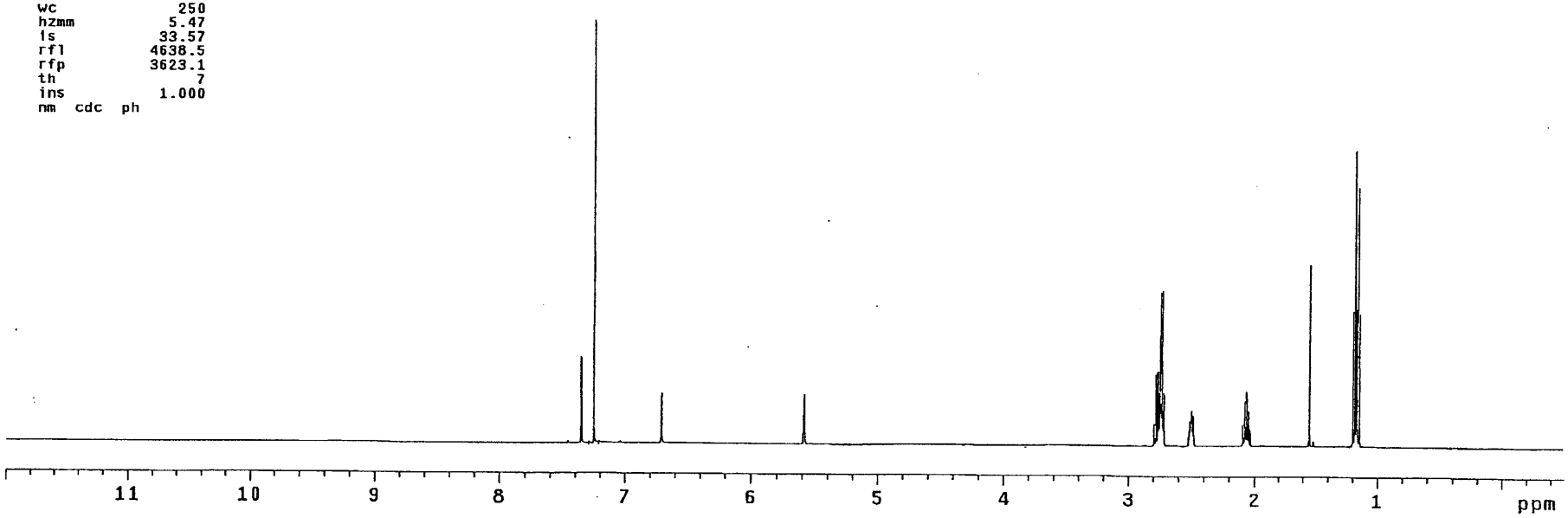

ACQUISITION	
sfrq	125.673
tn	C13
at	0.869
np	65536
sw	37718.1
fb	not used
bs	16
ss	1
tpwr	58
pw	7.5
d1	3.000
tof	615.5
nt	100000
ct	432
alock	n
gain	not used

FLAGS	
il	n
in	n
dp	y
hs	nn

DISPLAY	
sp	-1256.8
wp	31414.3
vs	328
sc	0
wc	250
hzmm	125.66
is	500.00
rfl	6304.2
rfp	0
th	10
ins	1.000
ai cdc ph	

DEC. & VT	
dfrq	499.747
dn	H1
dpwr	34
dof	0
dm	yyy
dmm	w
dmf	10000
dseq	
dres	1.0
homo	n

PROCESSING	
lb	1.00
wtfile	
proc	ft
fn	131072
math	f
werr	
wexp	
wbs	
wnt	

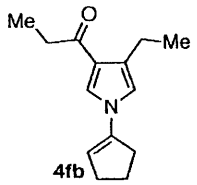

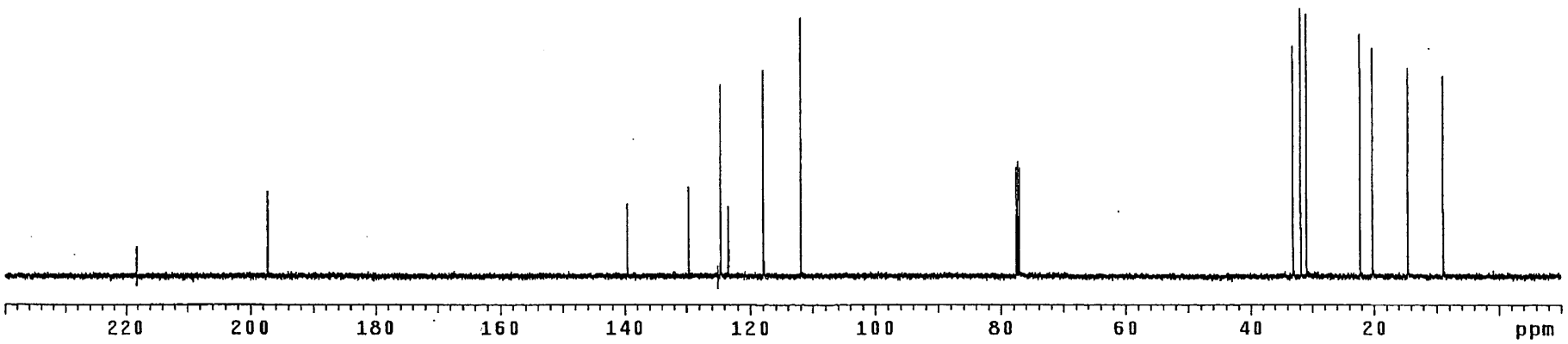

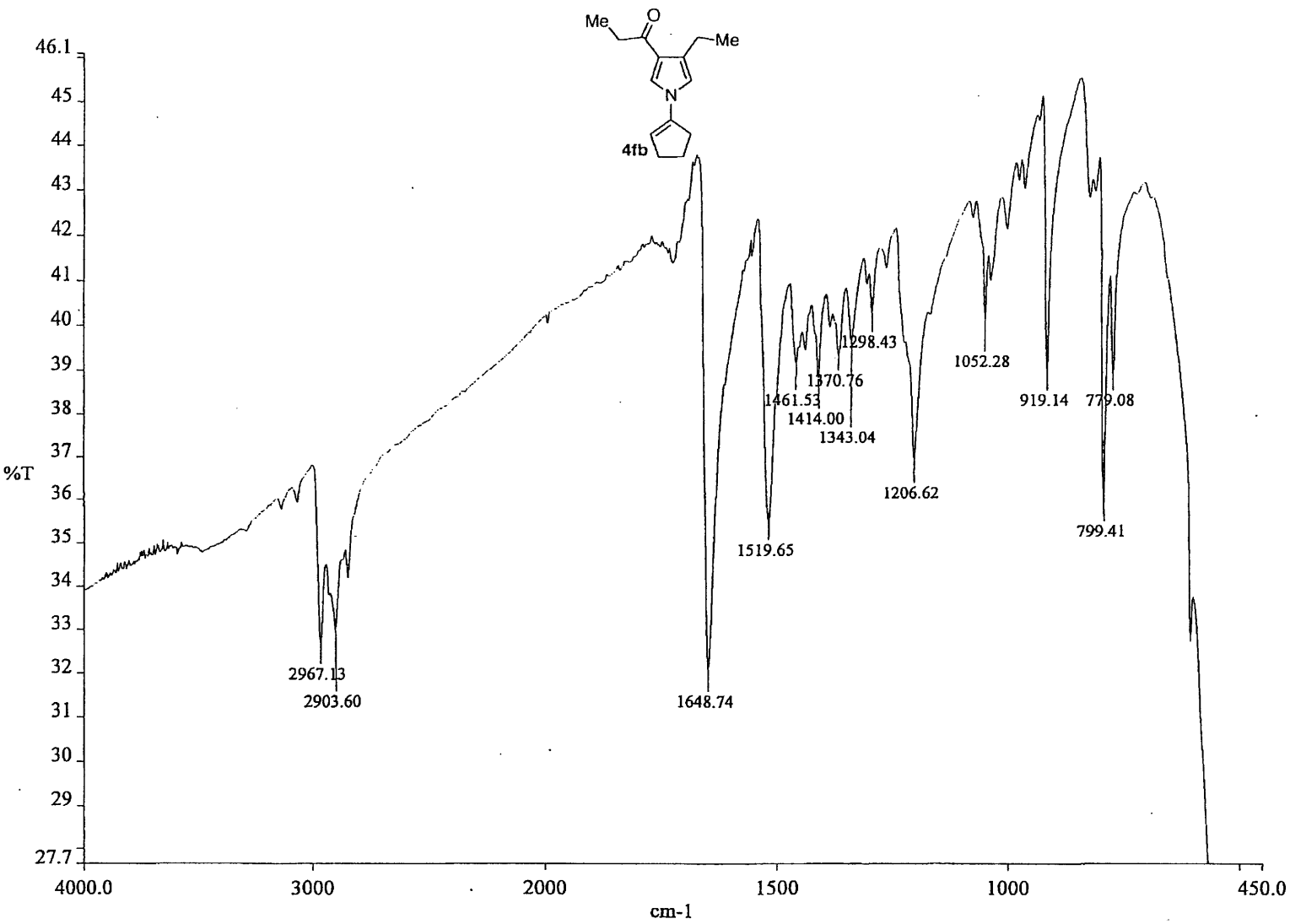
Me
O
Me
N
4fb
46.1
45
44
43
42
41
40
39
38
37
36
35
34
33
32
31
30
29
27.7
%T
2967.13
2903.60
1648.74
1519.65
1461.53
1414.00
1370.76
1343.04
1298.43
1206.62
1052.28
919.14
799.41
779.08
4000.0
3000
2000
1500
1000
450.0
cm-1

Appendix C.

Spectra for Chapter III

ACQUISITION	
sfrq	499.758
tn	H1
at	3.277
np	65536
sw	9998.8
fb	not used
bs	4
tpwr	56
pw	8.2
d1	2.000
tof	1498.1
nt	36
ct	36
alock	n
gain	not used

FLAGS	
il	n
in	n
dp	y
hs	nn

DISPLAY	
sp	-250.2
wp	6246.5
vs	107
sc	0
wc	250
hzmm	3.47
is	33.57
rfl	4564.4
rfp	3578.2
th	7
ins	2.000
nm	cdc ph

DEC. & VT	
dfrq	125.677
dn	C13
dpwr	34
dof	1498.1
dm	nnn
dmm	w
dmf	10000
dseq	
dres	1.0
homo	n

PROCESSING	
wtfile	
proc	ft
fn	65536
math	f
werr	
wexp	
wbs	
wnt	

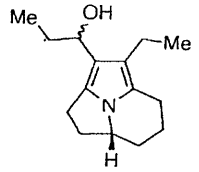

21

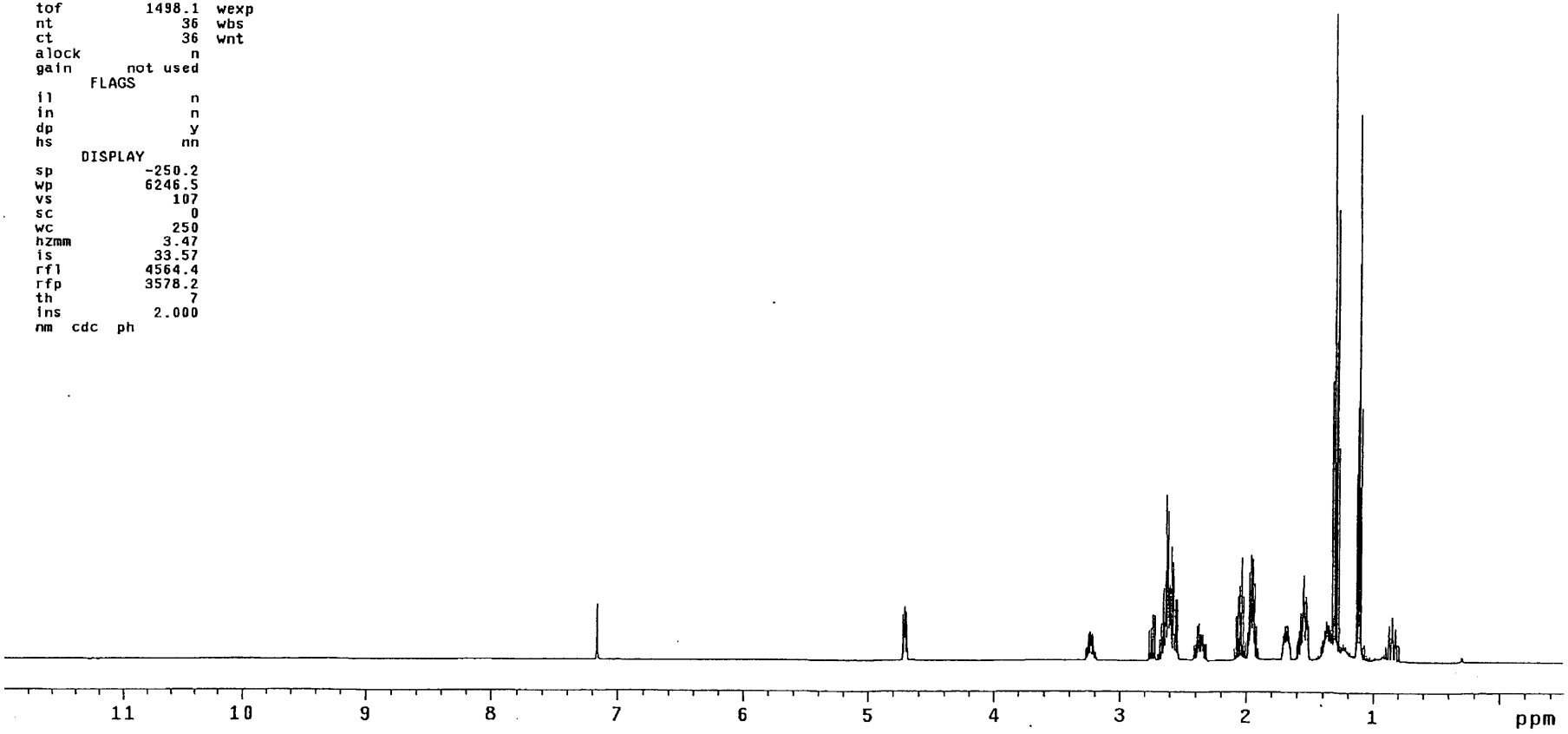

ACQUISITION	
sfrq	125.796
tn	C13
at	1.736
np	131010
sw	37735.8
fb	not used
bs	8
ss	1
tpwr	53
pw	6.9
d1	0.763
tof	631.4
nt	10000
ct	1888
alock	n
gain	not used

FLAGS	
il	n
in	n
dp	y
hs	nn

DISPLAY	
sp	-1258.1
wp	31448.7
vs	11085
sc	0
wc	250
hzmm	125.79
is	500.00
rfl	18876.6
rfp	12651.0
th	5
ins	1.000
ai	ph

DEC. & VT	
dfrq	500.233
dn	H1
dpwr	37
dof	-500.0
dm	y
dmm	w
dmf	10000
dseq	
dres	1.0
homo	n

PROCESSING	
lb	0.30
wtfile	
proc	ft
fn	131072
math	f
werr	
wexp	
wbs	
wnt	

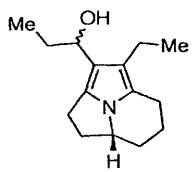

21

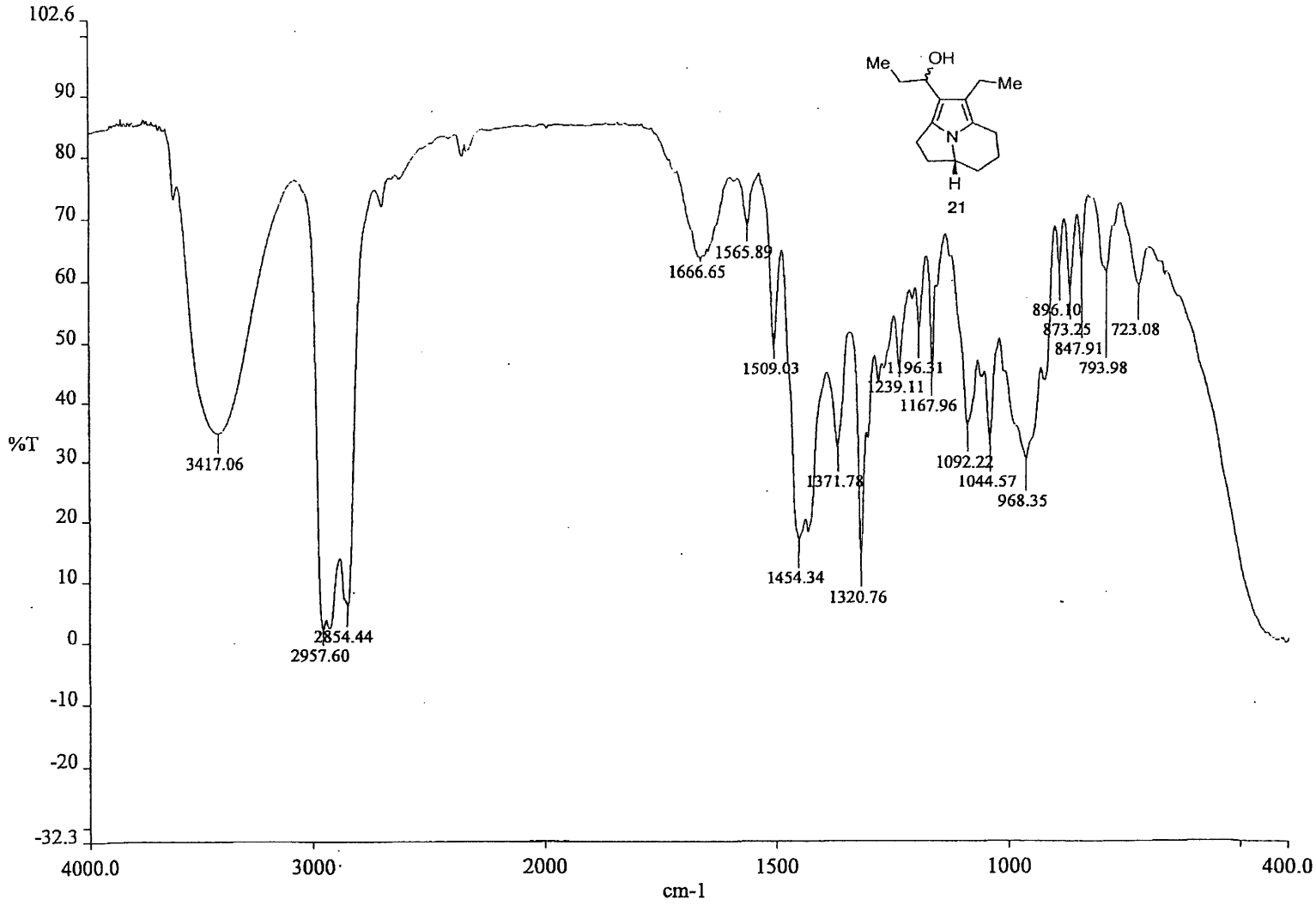
102.6
90
80
70
60
50
40
30
20
10
0
-10
-20
-32.3
%T
4000.0
3000
2000
1500
1000
400.0
cm-1
3417.06
2957.60
2854.44
1666.65
1565.89
1509.03
1454.34
1371.78
1320.76
1239.11
1196.31
1167.96
1092.22
1044.57
968.35
896.10
873.25
847.91
793.98
723.08
Me
OH
Me
N
H
21

ACQUISITION		DEC. & VT	
sfrq	499.758	dfrq	125.677
tn	H1	dn	C13
at	3.277	dpwr	34
np	65536	dof	1498.1
sw	9998.8	dm	nnn
fb	not used	dmm	w
bs	4	dmf	10000
tpwr	56	dseq	
pw	8.2	dres	1.0
d1	2.000	homo	n
tof	1498.1	DEC2	
nt	24	dfrq2	0
ct	24	dn2	
alock	n	dpwr2	1
gain	not used	dof2	0
FLAGS		dm2	n
il	n	dmm2	c
in	n	dmf2	200
dp	y	dseq2	
hs	nn	dres2	1.0
DISPLAY		homo2	n
sp	-250.4	DEC3	
wp	6246.7	dfrq3	0
vs	65	dn3	
sc	0	dpwr3	1
wc	250	dof3	0
hzmm	40.00	dm3	n
is	33.57	dmm3	c
rfl	4562.3	dmf3	200
rfp	3578.2	dseq3	
th	7	dres3	1.0
ins	1.000	homo3	n
nm cdc ph		PROCESSING	
		wtfile	
		proc	ft
		fn	65536
		math	f
		werr	
		wexp	
		wbs	
		wnt	

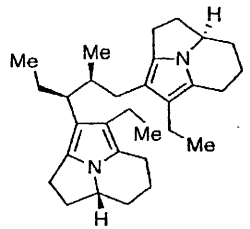

24

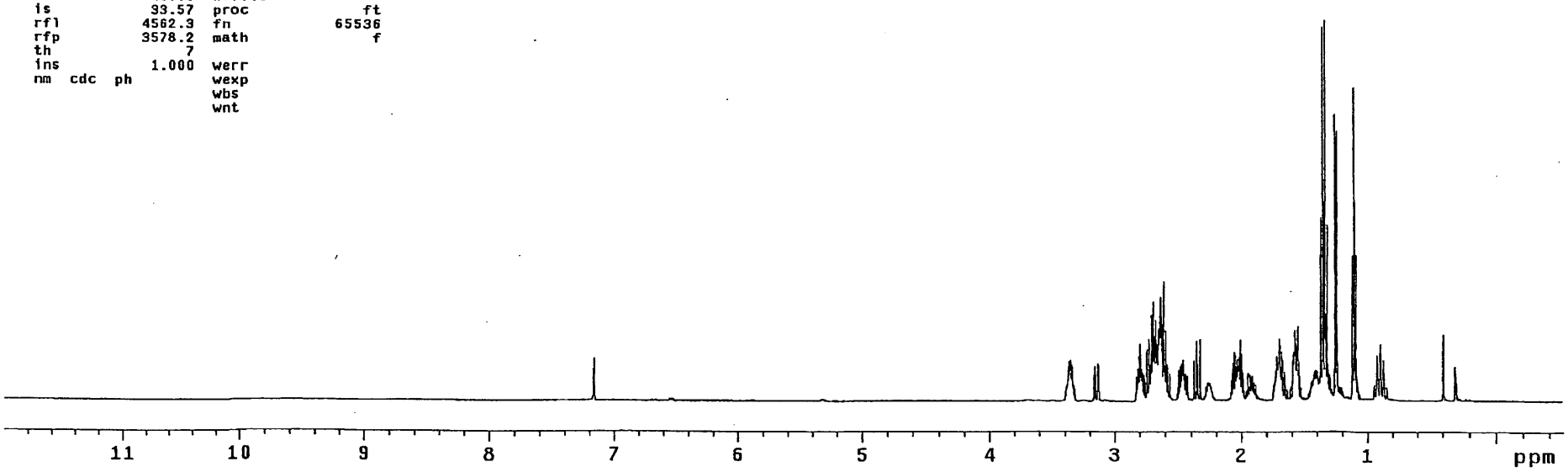

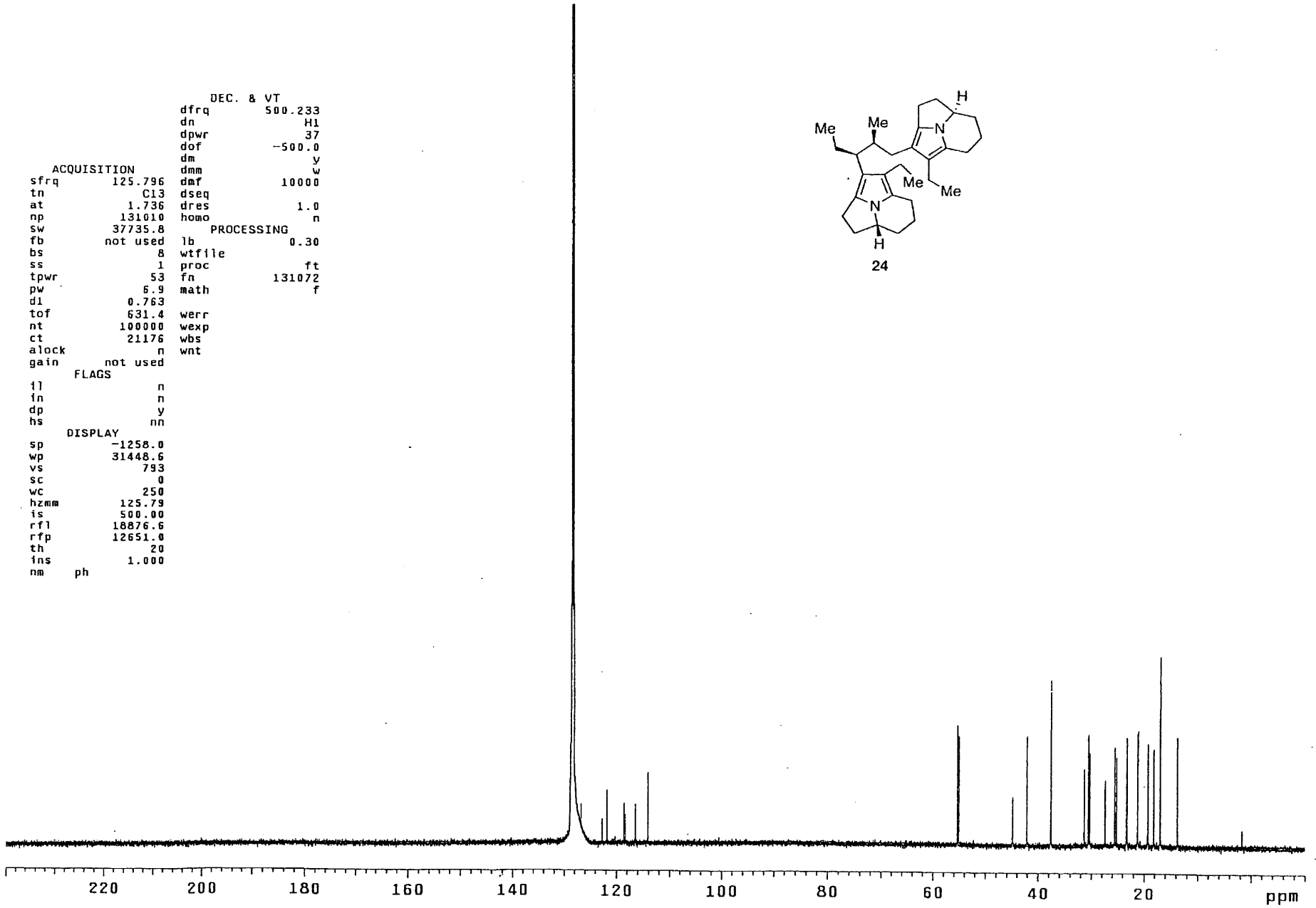
ACQUISITION
sfrq 125.796
tn C13
at 1.736
np 131010
sw 37735.8
fb not used
bs 8
ss 1
tpwr 53
pw 6.9
d1 0.763
tof 631.4
nt 100000
ct 21176
alock n
gain not used
FLAGS
il n
in n
dp y
hs nn
DISPLAY
sp -1258.0
wp 31448.6
vs 793
sc 0
wc 250
hzmm 125.79
is 500.00
rfl 18876.6
rfp 12651.0
th 20
ins 1.000
nm ph
DEC. & VT
dfrq 500.233
dn H1
dpwr 37
dof -500.0
dm y
dmm w
dmf 10000
dseq
dres 1.0
homo n
PROCESSING
lb 0.30
wtfile
proc ft
fn 131072
math f
werr
wexp
wbs
wnt
Me
Me
N
H
Me
Me
N
H
24
220
200
180
160
140
120
100
80
60
40
20
ppm

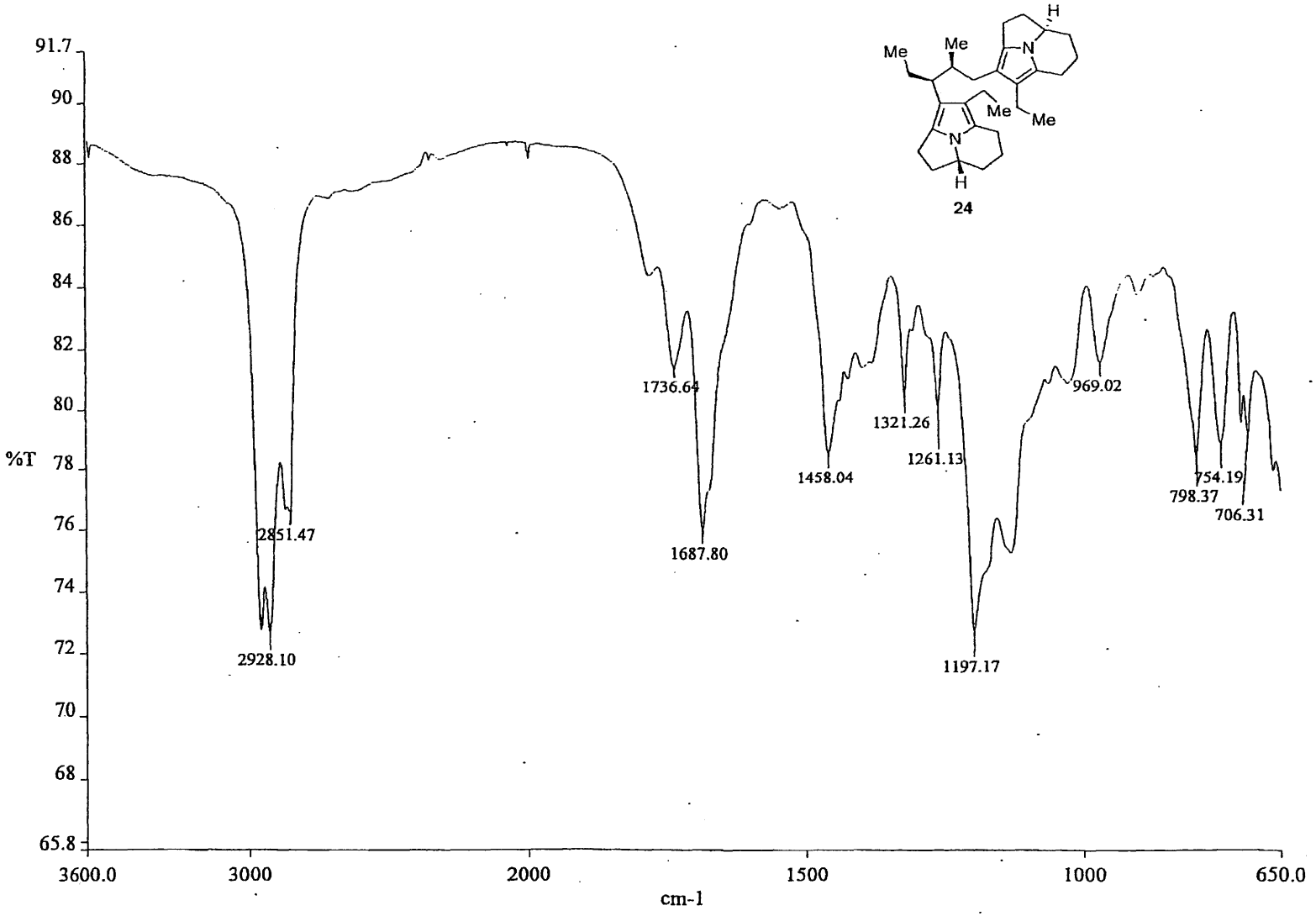
91.7
90
88
86
84
82
80
78
76
74
72
70
68
65.8
%T
3600.0
3000
2000
1500
1000
650.0
cm-1
2928.10
2851.47
1736.64
1687.80
1458.04
1321.26
1261.13
1197.17
969.02
798.37
754.19
706.31
Me
Me
Me
Me
N
N
H
H
24

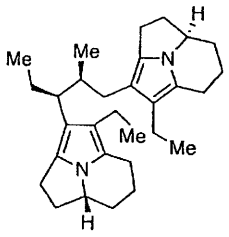
Me
Me
H
N
Me
Me
N
H

24

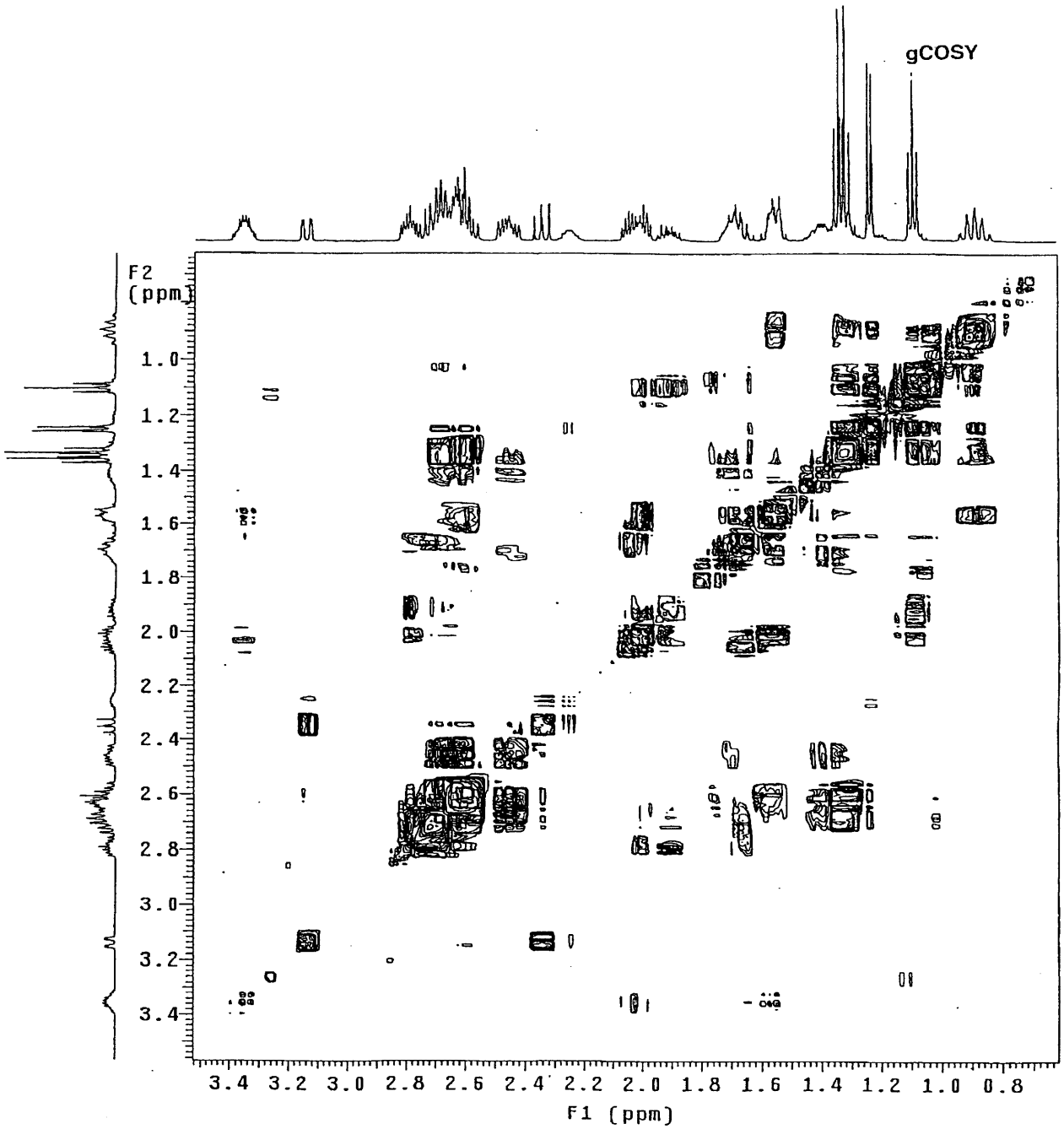
gCOSY
F2
(ppm)
1.0
1.2
1.4
1.6
1.8
2.0
2.2
2.4
2.6
2.8
3.0
3.2
3.4
3.4 3.2 3.0 2.8 2.6 2.4 2.2 2.0 1.8 1.6 1.4 1.2 1.0 0.8
F1 (ppm)

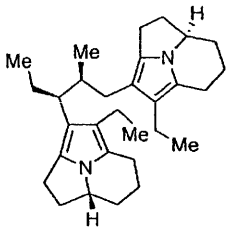
Me
Me
H
N
Me
Me
N
H

24

HSQC

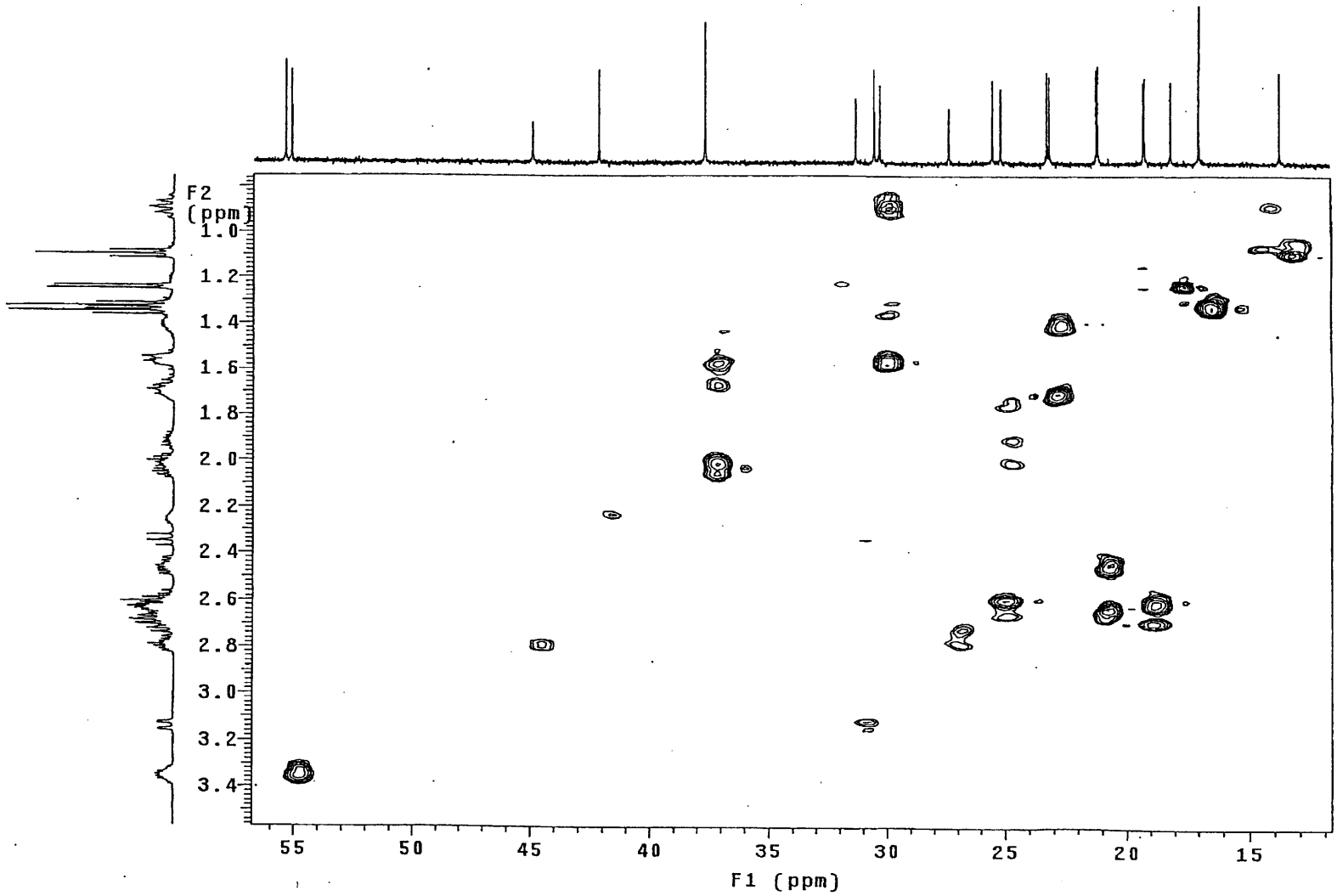
F2 (ppm)
1.0
1.2
1.4
1.6
1.8
2.0
2.2
2.4
2.6
2.8
3.0
3.2
3.4
55
50
45
40
35
30
25
20
15
F1 (ppm)

ACQUISITION		DEC. & VT			
sfrq	499.749	dfrq	125.674		
tn	H1	dn	C13		
at	3.277	dpwr	34		
np	65536	dof	1498.1		
sw	9998.8	dm	nnn		
fb	not used	dmm	w		
bs	4	dmf	10000		
tpwr	56	dseq			
pw	8.2	dres	1.0		
d1	2.000	homo	n		
tof	1498.1	DEC2			
nt	24	dfrq2	0		
ct	24	dn2			
alock	n	dpwr2	1		
gain	not used	dof2	0		
FLAGS		dm2	n		
il	n	dmm2	c		
in	n	dmf2	200		
dp	y	dseq2			
hs	nn	dres2	1.0		
DISPLAY		homo2	n		
sp	-249.9	DEC3			
wp	6246.7	dfrq3	0		
vs	250	dn3			
sc	0	dpwr3	1		
wc	250	dof3	0		
hzmm	24.99	dm3	n		
is	360.92	dmm3	c		
rfl	4567.4	dmf3	200		
rfp	3578.2	dseq3			
th	7	dres3	1.0		
ins	1.000	homo3	n		
nm cdc ph		PROCESSING			
		wtfile			
		proc	ft		
		fn	65536		
		math	f		
		werr			
		wexp			
		wbs			
		wnt			

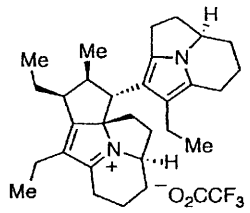

26

ACQUISITION		DEC. & VT	
sfrq	125.796	dfrq	500.233
tn	C13	dn	H1
at	1.736	dpwr	37
np	131010	dof	-500.0
sw	37735.8	dm	y
fb	not used	dmm	w
bs	8	dmf	10000
ss	1	dseq	
tpwr	53	dres	1.0
pw	6.9	homo	n
d1	0.763	PROCESSING	
tof	631.4	lb	0.30
nt	10000	wtfile	
ct	5512	proc	ft
alock	n	fn	131072
gain	not used	math	f
FLAGS		werr	
il	n	wexp	
in	n	wbs	
dp	y	wnt	
hs	nn		
DISPLAY			
sp	-1258.0		
wp	31448.6		
vs	1917		
sc	0		
wc	250		
hzmm	125.79		
is	500.00		
rfl	18876.6		
rfp	12651.0		
th	20		
ins	1.000		
nm	ph		

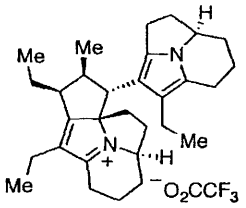

26

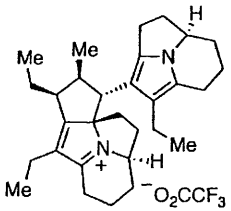
Me
Me
H
N
Me
N
+
H
Me
$^{-}O_2CCF_3$

26

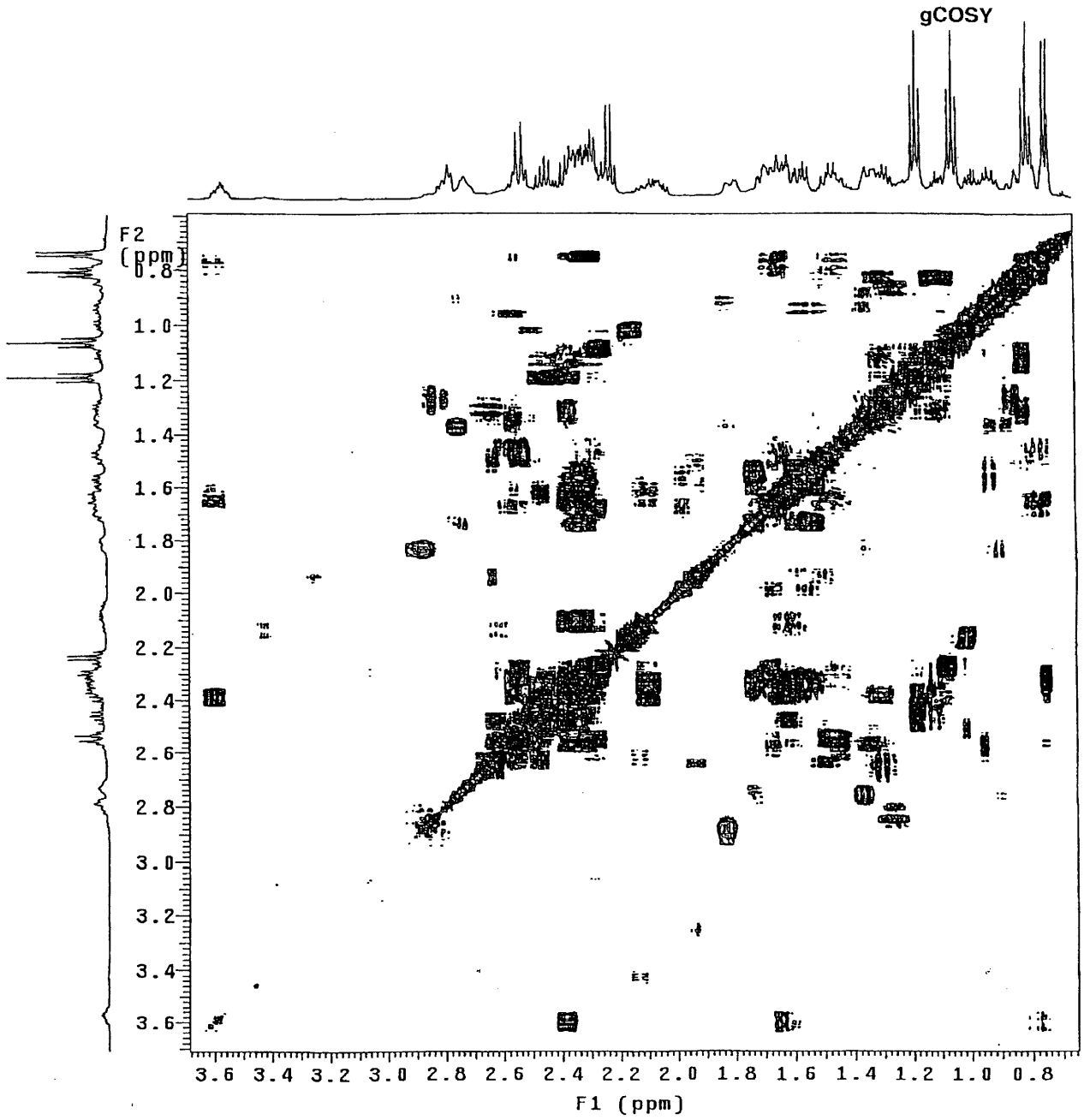
gCOSY
F2 (ppm)
0.8
1.0
1.2
1.4
1.6
1.8
2.0
2.2
2.4
2.6
2.8
3.0
3.2
3.4
3.6
3.6 3.4 3.2 3.0 2.8 2.6 2.4 2.2 2.0 1.8 1.6 1.4 1.2 1.0 0.8
F1 (ppm)

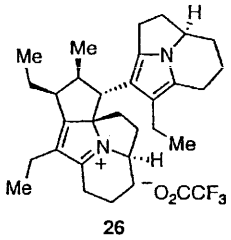
H
Me
Me
N
Me
N
H
Me
$^{-}O_2CCF_3$

26

HSQC

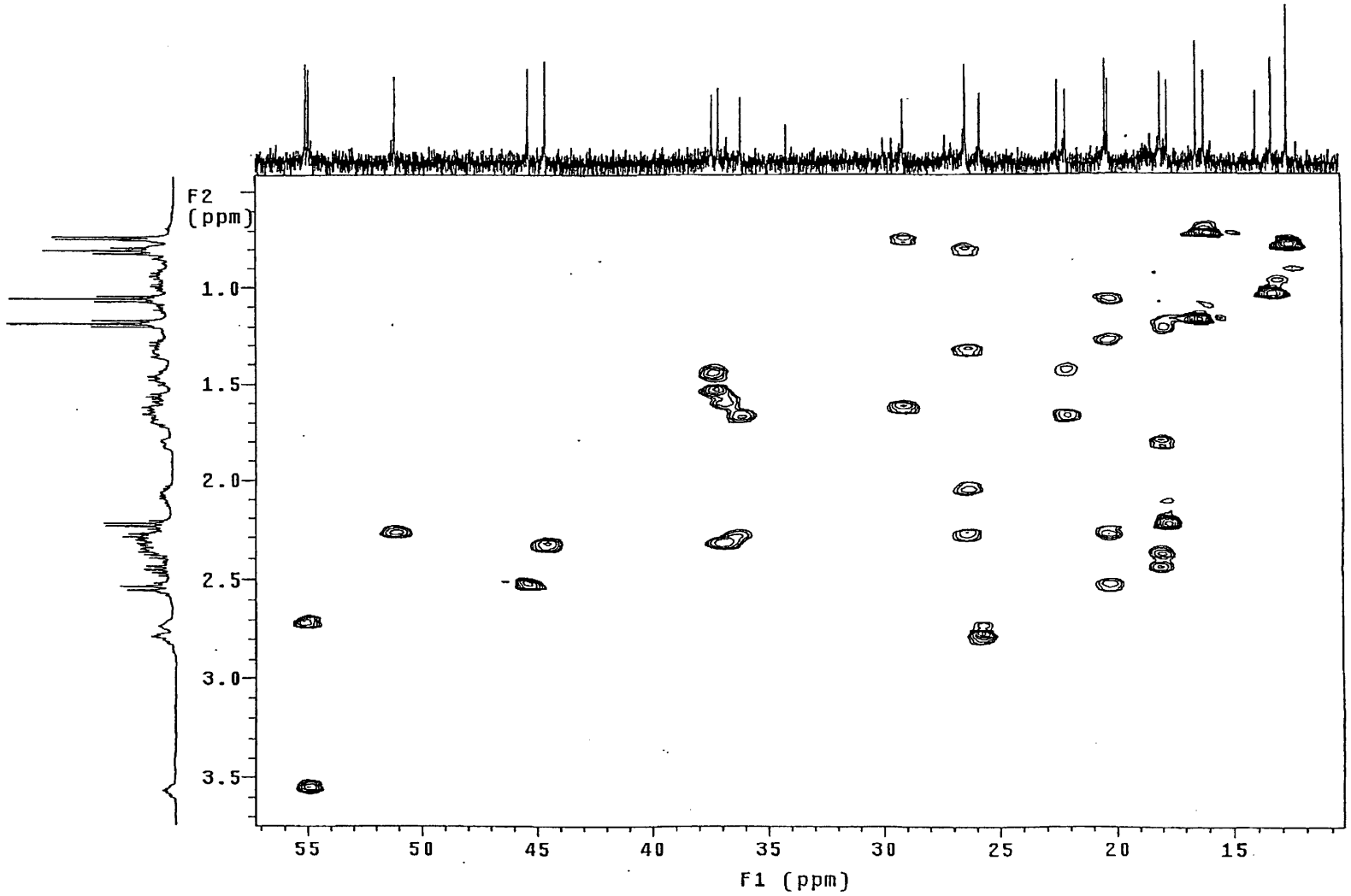
F2
(ppm)
1.0
1.5
2.0
2.5
3.0
3.5
55
50
45
40
35
30
25
20
15
F1 (ppm)

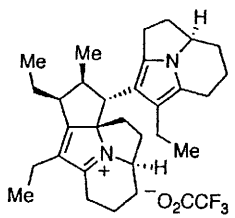
Me
Me
H
N
Me
N
+
H
Me
$^{-}O_2CCF_3$

26

gHMBC

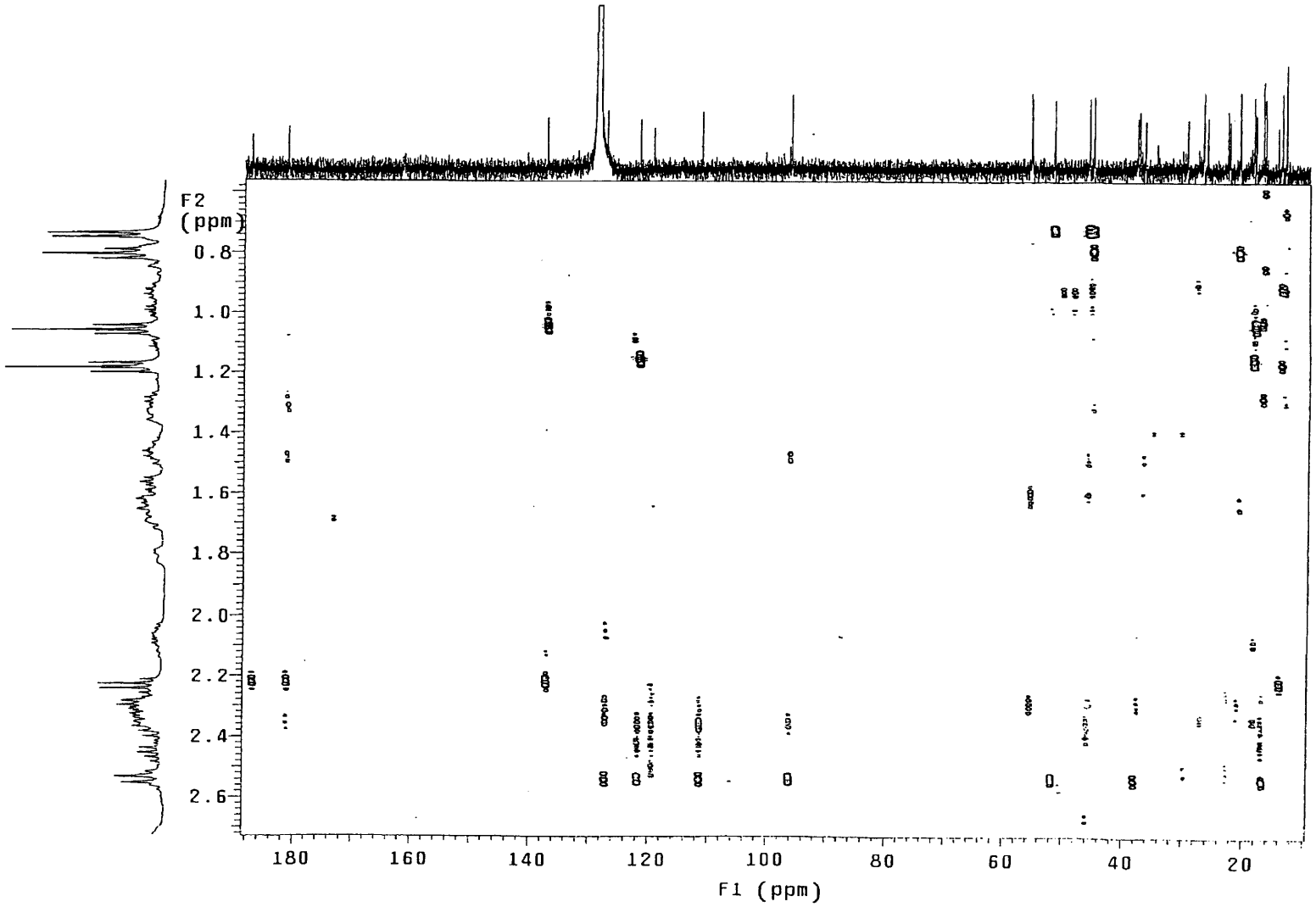
F2
(ppm)
0.8
1.0
1.2
1.4
1.6
1.8
2.0
2.2
2.4
2.6
180
160
140
120
100
80
60
40
20
F1 (ppm)

AO-II-142

exp301 s2pul

SAMPLE		DEC. & VT	
date	Apr 5 2005	dfrq	125.674
solvent	Benzene	dn	C13
file	/data/movassa~	dpwr	34
g/Mao/Mao_040505_A~		dof	1498.1
	OII142_2_1H.fid	dm	nnn
	ACQUISITION	dmm	w
sfrq	499.749	dmf	10000
tn	H1	dseq	
at	3.277	dres	1.0
np	65536	homo	n
sw	9998.8		DEC2
fb	not used	dfrq2	0
bs	4	dn2	
tpwr	56	dpwr2	1
pw	8.2	dof2	0
d1	2.000	dm2	n
tof	1498.1	dmm2	c
nt	24	dmf2	200
ct	24	dseq2	
alock	n	dres2	1.0
gain	not used	homo2	n
	FLAGS		DEC3
il	n	dfrq3	0
in	n	dn3	
dp	y	dpwr3	1
hs	nn	dof3	0
	DISPLAY	dm3	n
sp	-250.2	dmm3	c
wp	6246.7	dmf3	200
vs	96	dseq3	
sc	0	dres3	1.0
wc	250	homo3	n
hzmm	40.00		PROCESSING
is	33.57	wtfile	
rfl	4565.0	proc	ft
rfp	3578.2	fn	65536
th	7	math	f
ins	1.000		
nm cdc ph		werr	
		wexp	
		wbs	
		wnt	

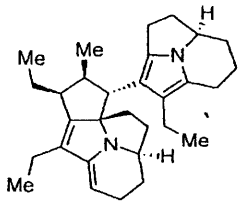

27

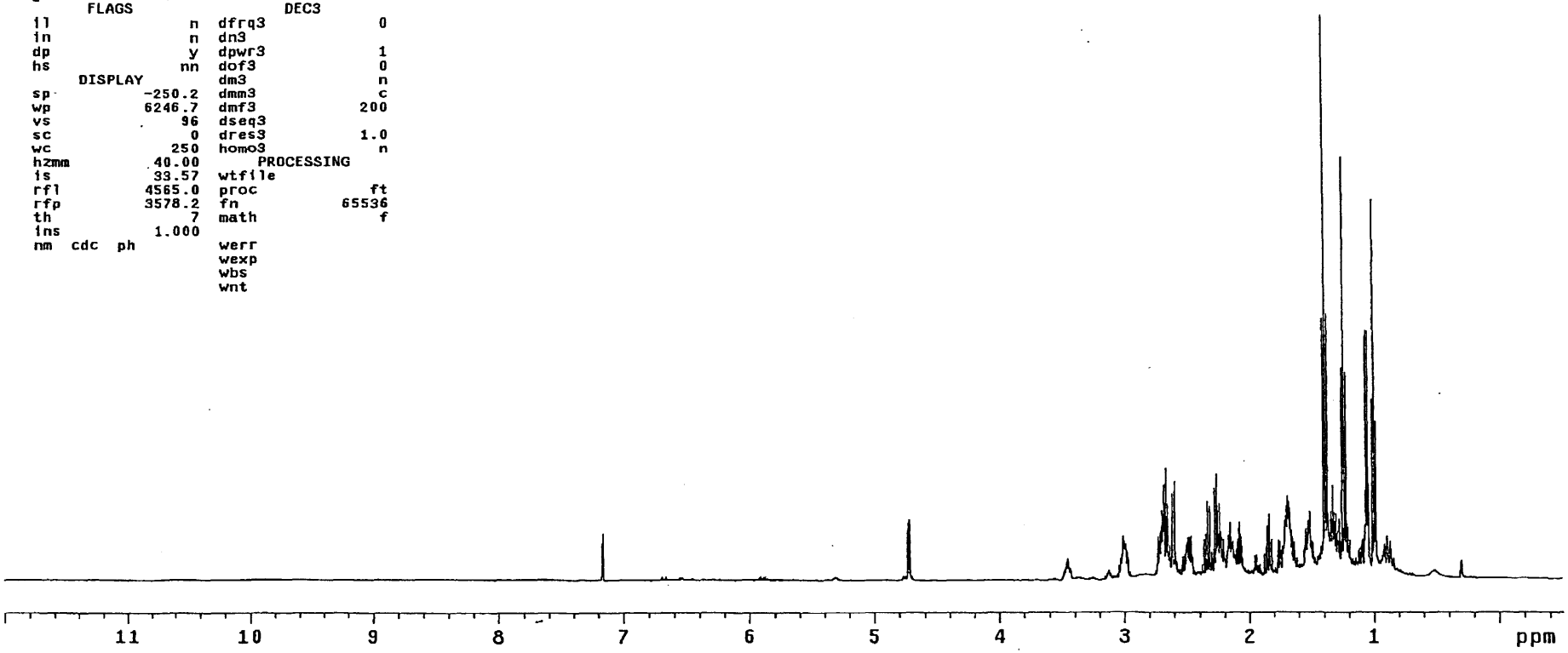

ACQUISITION	
sfrq	125.796
tn	C13
at	1.736
np	131010
sw	37735.8
fb	not used
bs	8
ss	1
tpwr	53
pw	6.9
d1	0.763
tof	631.4
nt	1e+07
ct	13008
alock	n
gain	not used

FLAGS	
il	n
in	n
dp	y
hs	nn

DISPLAY	
sp	-1258.0
wp	31448.6
vs	1322
sc	0
wc	250
hzmm	125.79
is	500.00
rfl	18876.6
rfp	12651.0
th	20
ins	1.000
nm	ph

DEC. & VT	
dfrq	500.233
dn	H1
dpwr	37
dof	-500.0
dm	y
dmm	w
dmf	10000
dseq	
dres	1.0
homo	n

PROCESSING	
lb	0.30
wtfile	
proc	ft
fn	131072
math	f
werr	
wexp	
wbs	
wnt	

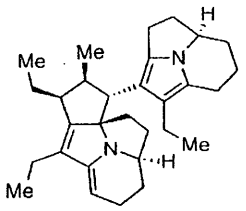

27

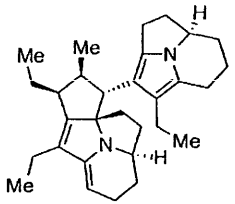
Me
Me
H
N
Me
N
H
Me

27

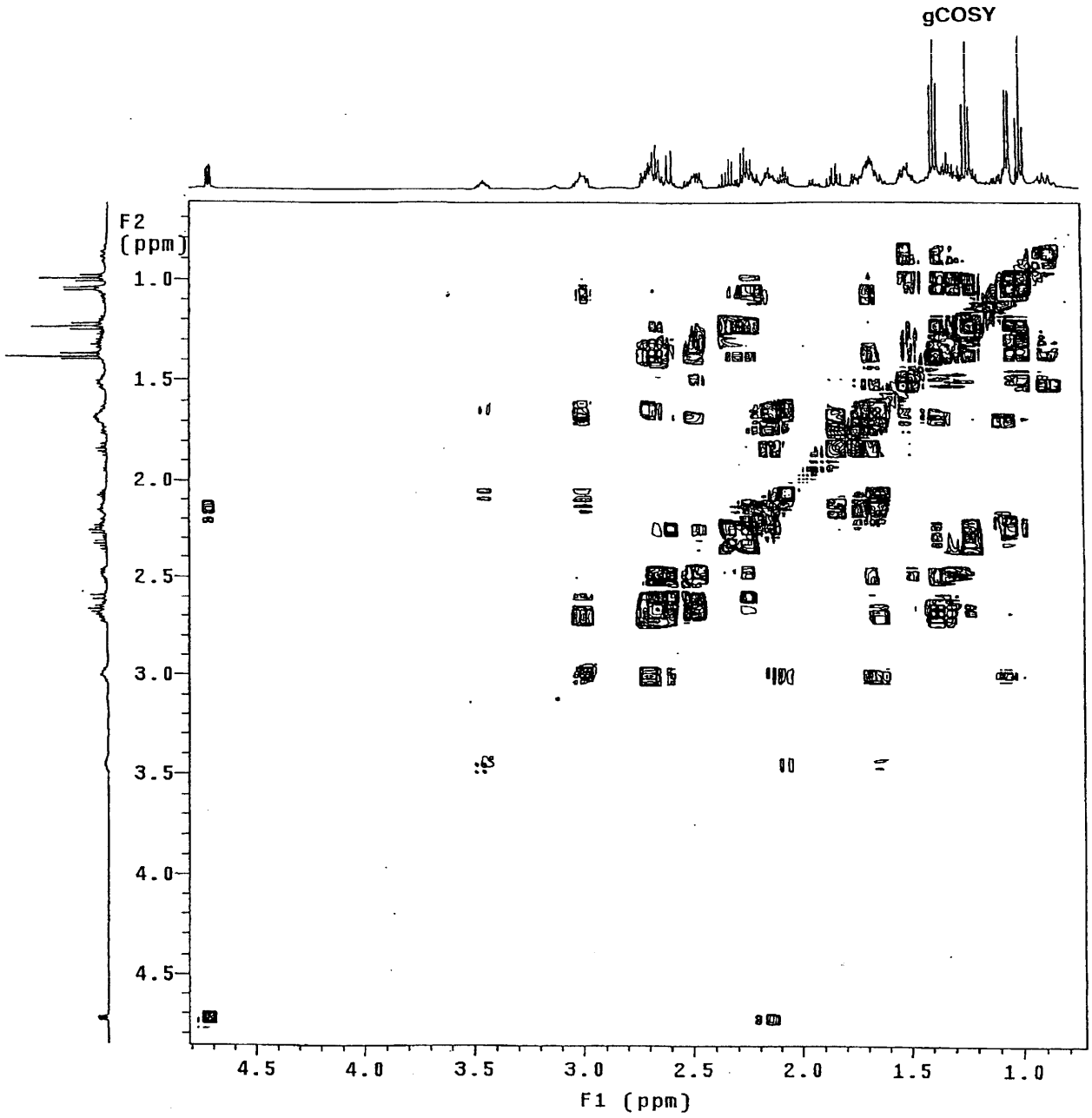
gCOSY
F2
(ppm)
1.0
1.5
2.0
2.5
3.0
3.5
4.0
4.5
4.5
4.0
3.5
3.0
2.5
2.0
1.5
1.0
F1 (ppm)

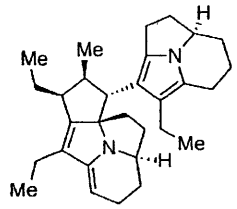
H
Me
Me
N
Me
N
H
Me

27

HSQC

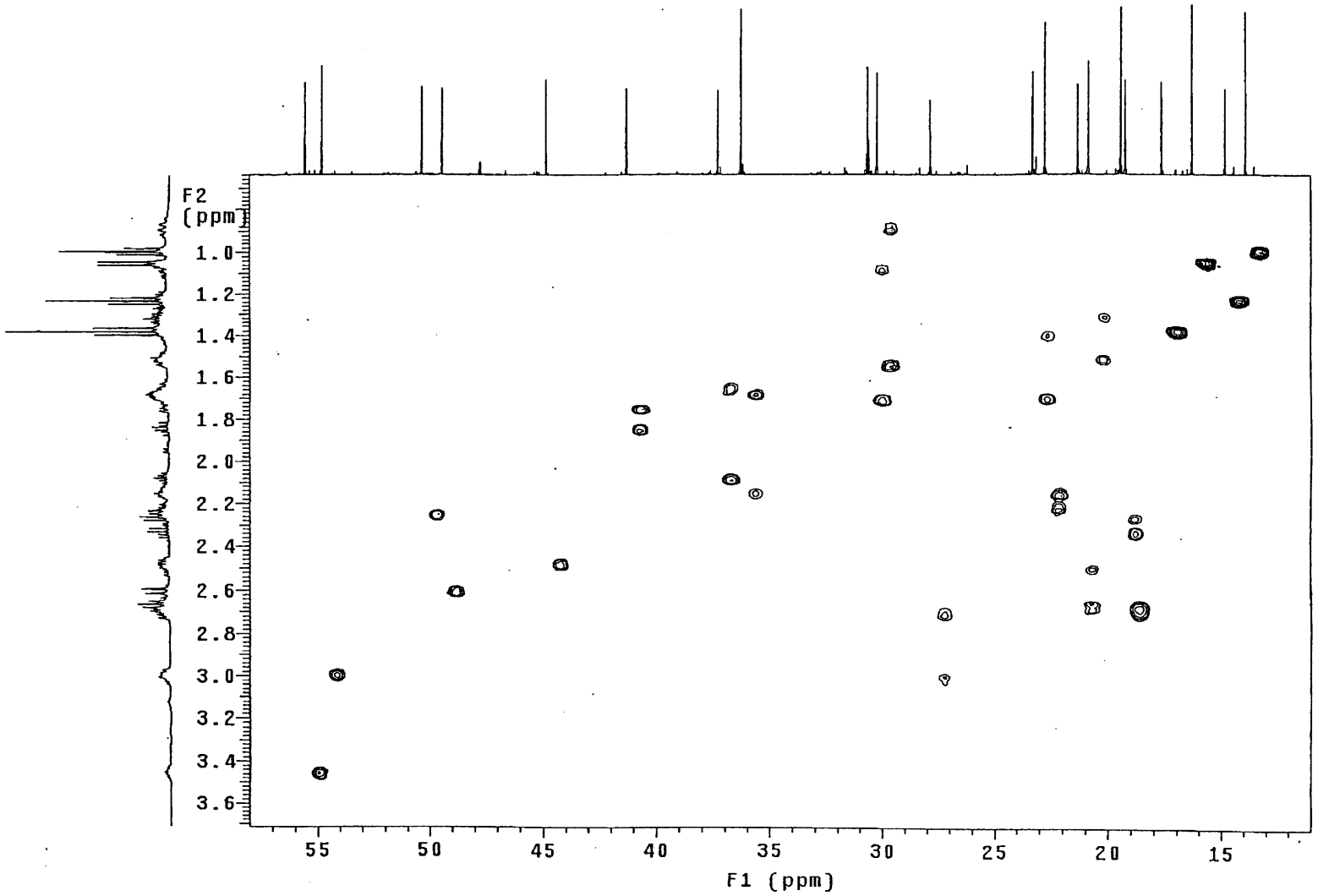
F2 (ppm)
1.0
1.2
1.4
1.6
1.8
2.0
2.2
2.4
2.6
2.8
3.0
3.2
3.4
3.6
55
50
45
40
35
30
25
20
15
F1 (ppm)

ACQUISITION		DEC. & VT	
sfrq	499.749	dfrq	125.674
tn	H1	dn	C13
at	3.277	dpwr	34
np	65536	dof	1498.1
sw	9998.8	dm	nnn
fb	not used	dmm	w
bs	4	dmf	10000
tpwr	56	dseq	
pw	8.2	dres	1.0
d1	2.000	homo	n
tof	1498.1	DEC2	
nt	18	dfrq2	0
ct	18	dn2	
alock	n	dpwr2	1
gain	not used	dof2	0
FLAGS		dm2	n
il	n	dmm2	c
in	n	dmf2	200
dp	y	dseq2	
hs	nn	dres2	1.0
DISPLAY		homo2	n
sp	-250.5	DEC3	
wp	6246.7	dfrq3	0
vs	99	dn3	
sc	0	dpwr3	1
wc	250	dof3	0
hzmm	40.00	dm3	n
is	33.57	dmm3	c
rfl	4565.6	dmf3	200
rfp	3578.2	dseq3	
th	7	dres3	1.0
ins	1.000	homo3	n
nm cdc ph		PROCESSING	
		wtfile	
		proc	ft
		fn	65536
		math	f
		werr	
		wexp	
		wbs	
		wnt	

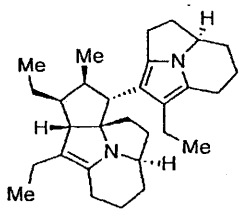

28

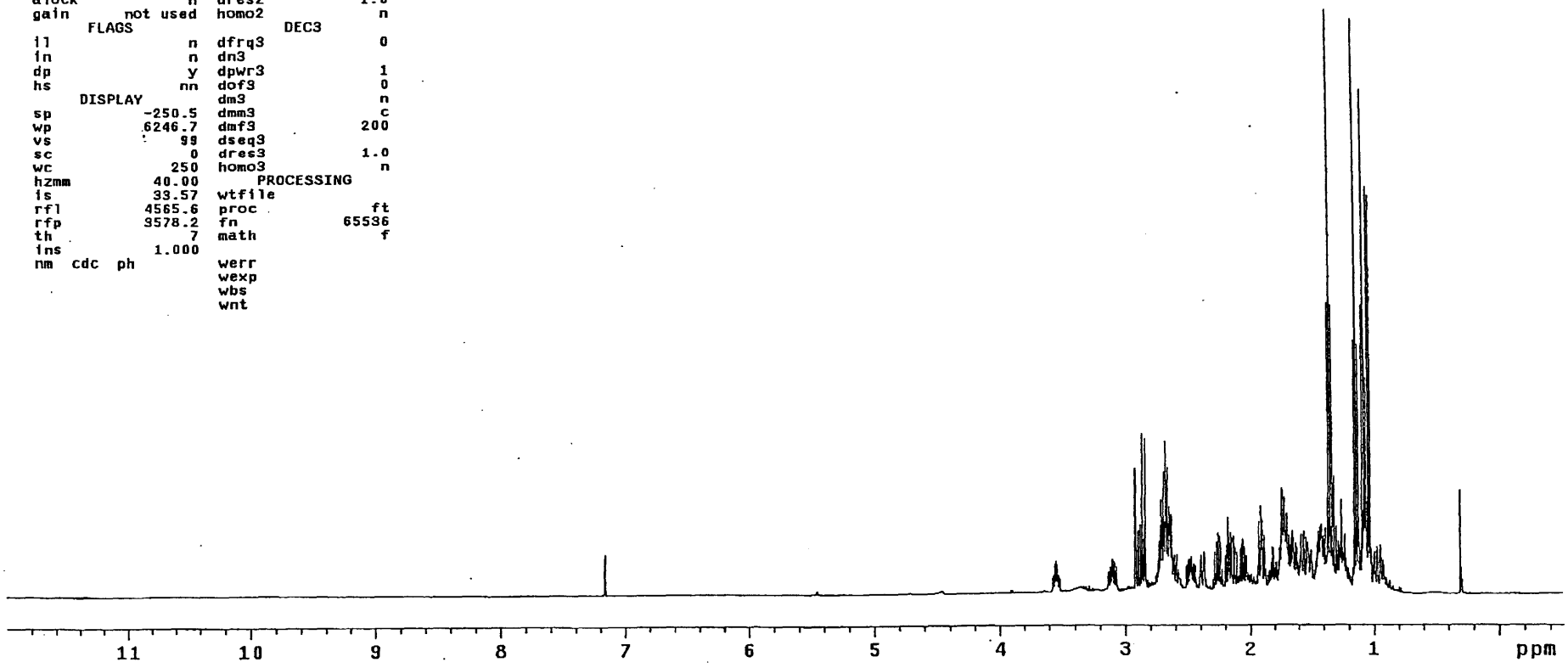

ACQUISITION		DEC. & VT	
sfrq	125.796	dfrq	500.233
tn	C13	dn	H1
at	1.736	dpwr	37
np	131010	dof	-500.0
sw	37735.8	dm	y
fb	not used	dmm	w
bs	8	dmf	10000
ss	1	dseq	
tpwr	53	dres	1.0
pw	6.9	homo	n
d1	0.763	PROCESSING	
tof	631.4	lb	0.30
nt	1e+06	wtfile	
ct	13264	proc	ft
alock	n	fn	131072
gain	not used	math	f
FLAGS		werr	
il	n	wexp	
in	n	wbs	
dp	y	wnt	
hs	nn		
DISPLAY			
sp	-1258.0		
wp	31448.6		
vs	649		
sc	0		
wc	250		
hzmm	125.79		
is	500.00		
rfl	18876.6		
rfp	12651.0		
th	20		
ins	1.000		
nm	ph		

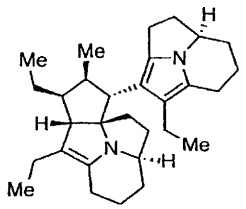

28

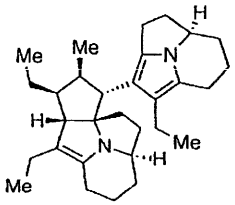
Me
Me
H
N
H
Me
H
N
Me

28

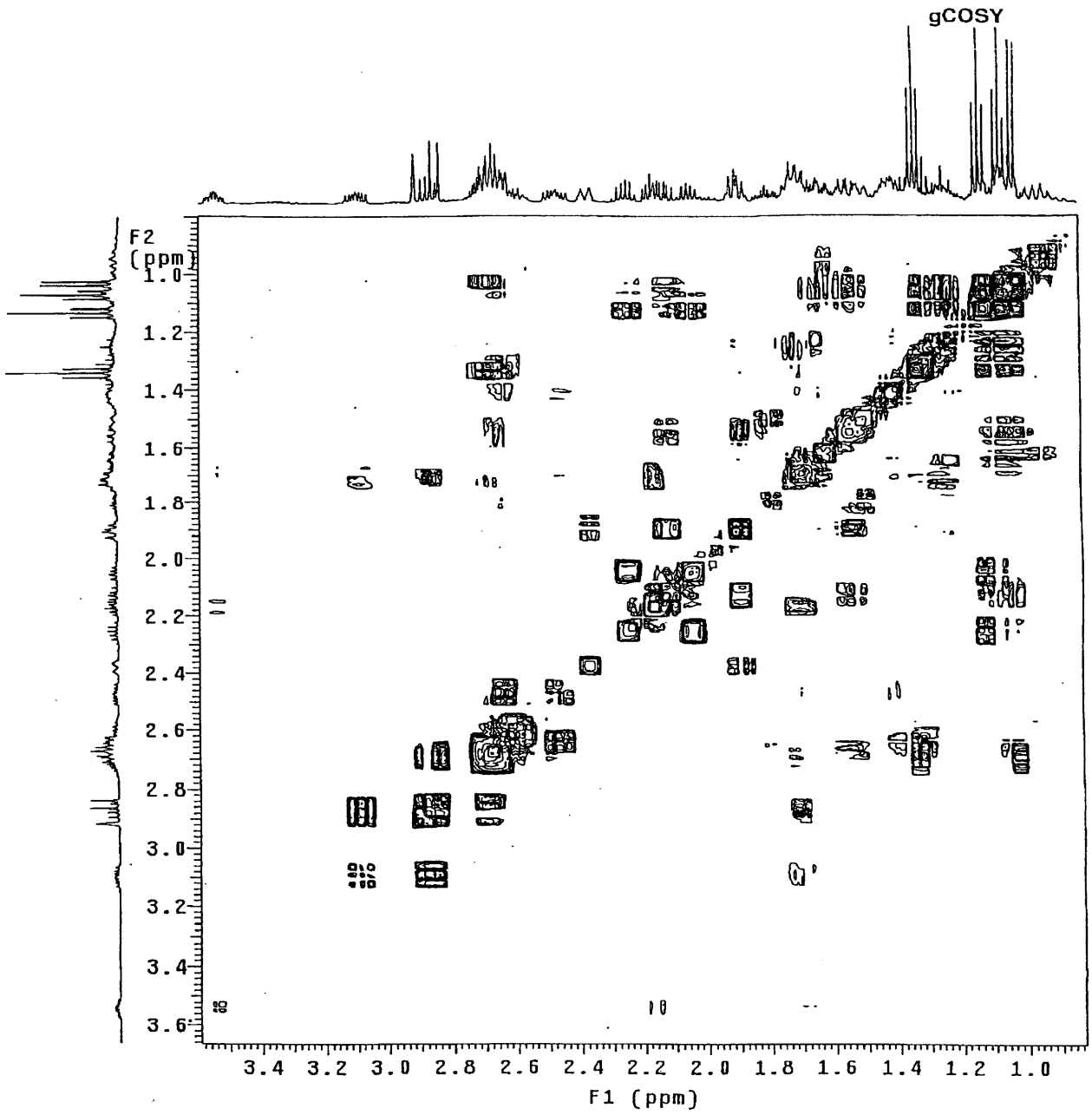
gCOSY
F2
(ppm)
1.0
1.2
1.4
1.6
1.8
2.0
2.2
2.4
2.6
2.8
3.0
3.2
3.4
3.6
3.4 3.2 3.0 2.8 2.6 2.4 2.2 2.0 1.8 1.6 1.4 1.2 1.0
F1 (ppm)

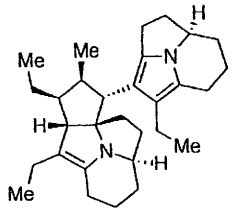
Me
Me
H
N
Me
H
N
H
Me

28

HSQC

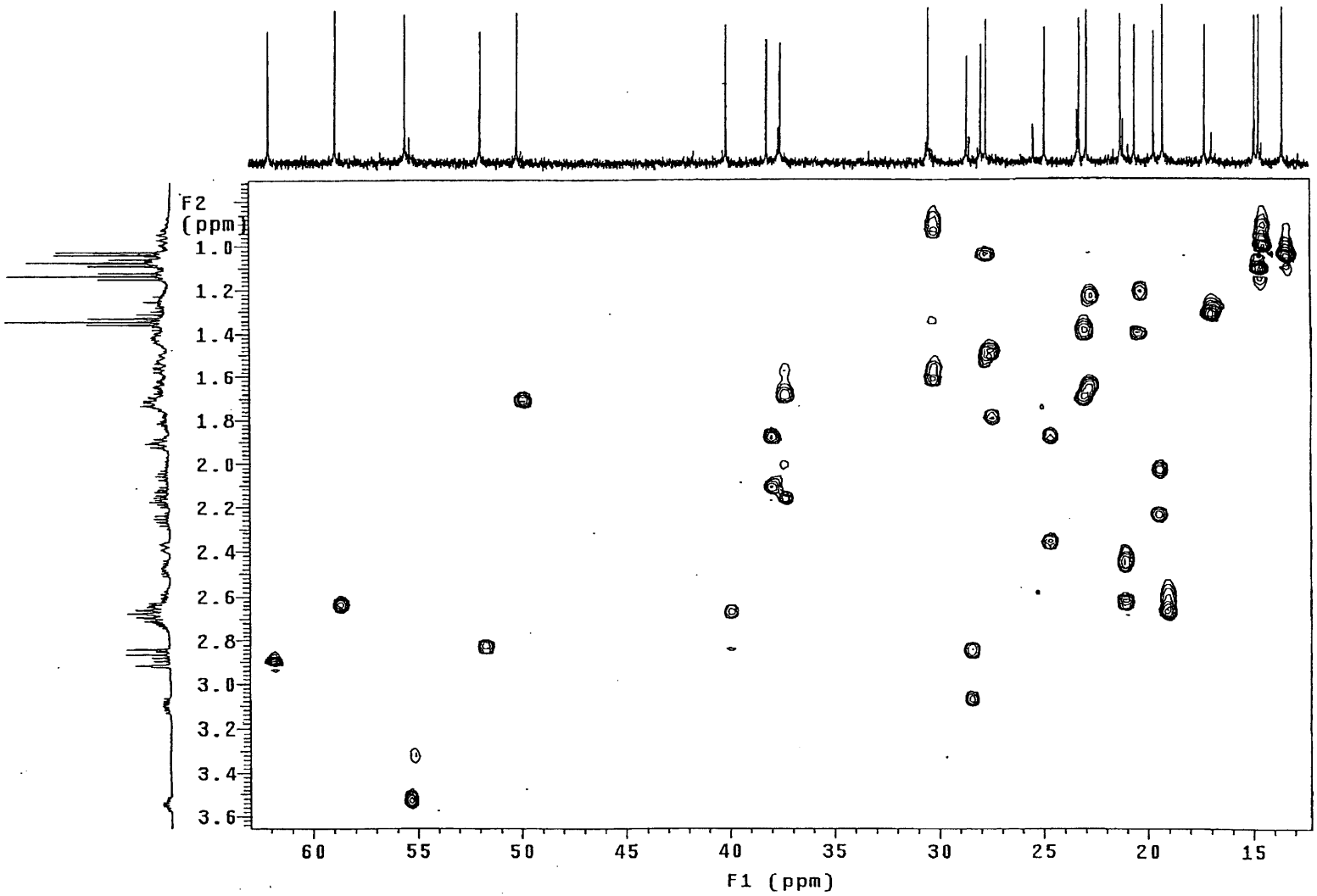
F2 (ppm)
1.0
1.2
1.4
1.6
1.8
2.0
2.2
2.4
2.6
2.8
3.0
3.2
3.4
3.6
60
55
50
45
40
35
30
25
20
15
F1 (ppm)

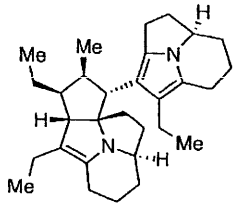
Me
Me
H
N
H
N
H
Me
Me

28

gHMBC

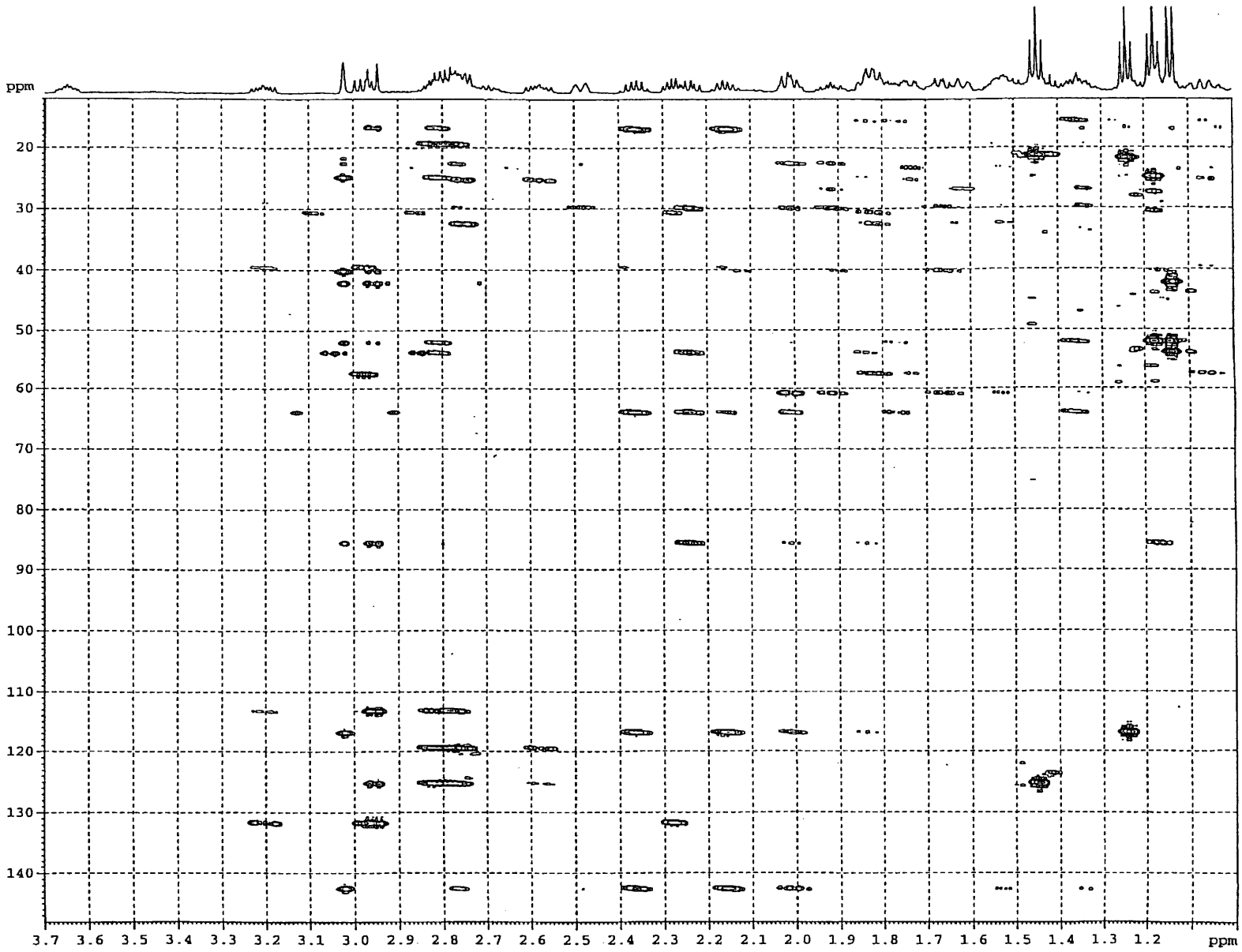
ppm
20
30
40
50
60
70
80
90
100
110
120
130
140
3.7 3.6 3.5 3.4 3.3 3.2 3.1 3.0 2.9 2.8 2.7 2.6 2.5 2.4 2.3 2.2 2.1 2.0 1.9 1.8 1.7 1.6 1.5 1.4 1.3 1.2
ppm

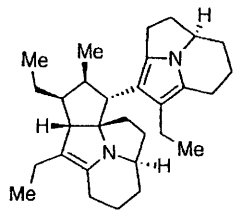
Me
Me
H
N
Me
H
N
H
Me

28

gNOESY

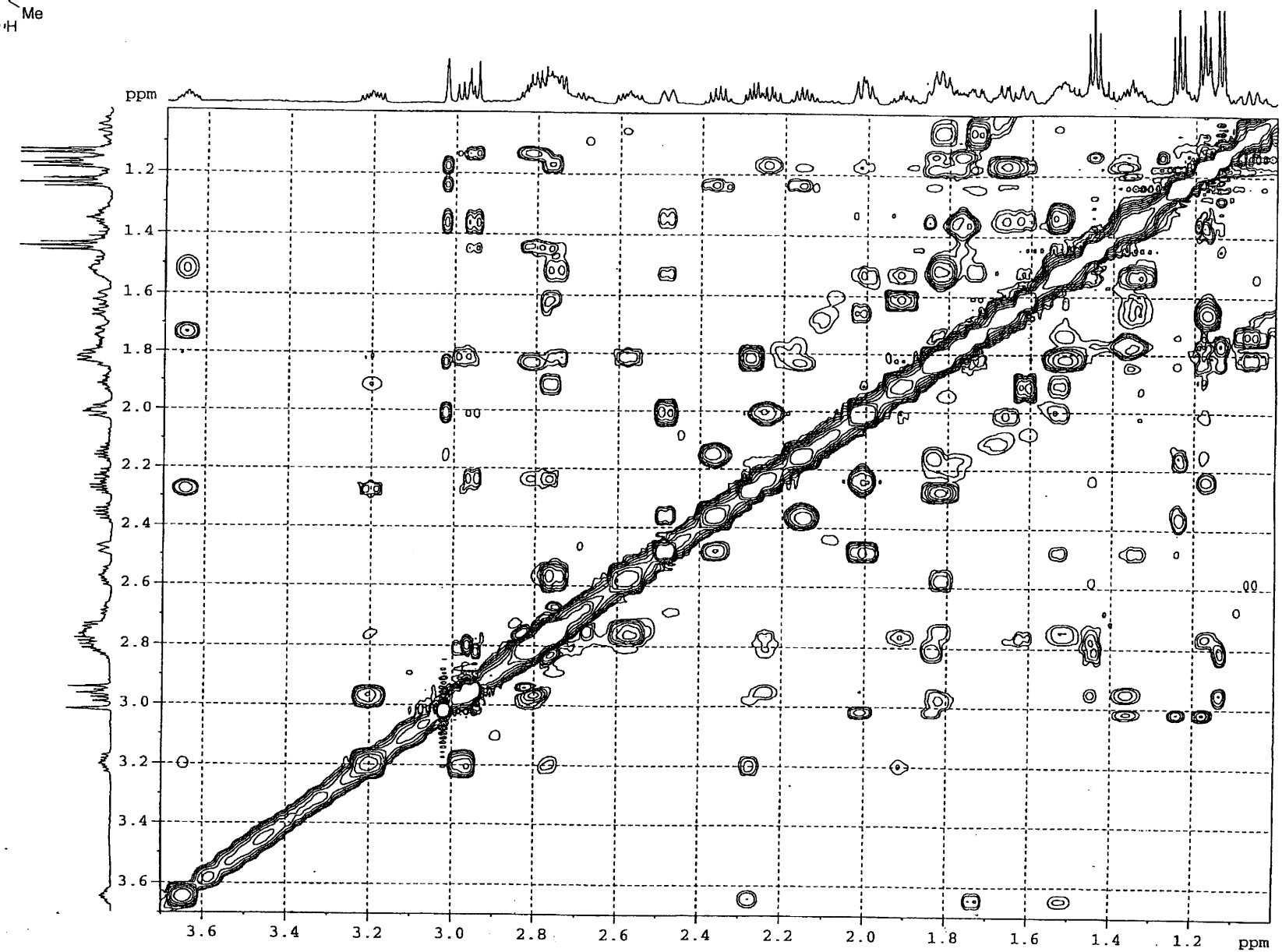
ppm
1.2
1.4
1.6
1.8
2.0
2.2
2.4
2.6
2.8
3.0
3.2
3.4
3.6
3.6
3.4
3.2
3.0
2.8
2.6
2.4
2.2
2.0
1.8
1.6
1.4
1.2
ppm

ACQUISITION		DEC. & VT	
sfrq	499.749	dfrq	125.674
tn	H1	dn	C13
at	3.277	dpwr	34
np	65536	dof	1498.1
sw	9998.8	dm	nnn
fb	not used	dmm	w
bs	4	dmf	10000
tpwr	56	dseq	
pw	8.2	dres	1.0
d1	2.000	homo	n
tof	1498.1	DEC2	
nt	32	dfrq2	0
ct	32	dn2	
alock	n	dpwr2	1
gain	not used	dof2	0
FLAGS		dm2	n
il	n	dmm2	c
in	n	dmf2	200
dp	y	dseq2	
hs	nn	dres2	1.0
DISPLAY		homo2	n
sp	-249.9	DEC3	
wp	6246.7	dfrq3	0
vs	79	dn3	
sc	0	dpwr3	1
wc	250	dof3	0
hzmm	0.21	dm3	n
is	33.57	dmm3	c
rfl	4567.4	dmf3	200
rfp	3578.2	dseq3	
th	7	dres3	1.0
ins	1.000	homo3	n
nm cdc ph		PROCESSING	
		wtfile	
		proc	ft
		fn	65536
		math	f
		werr	
		wexp	
		wbs	
		wnt	

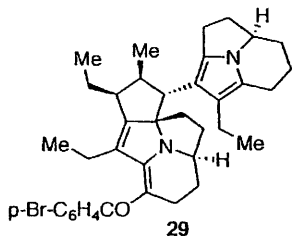

29

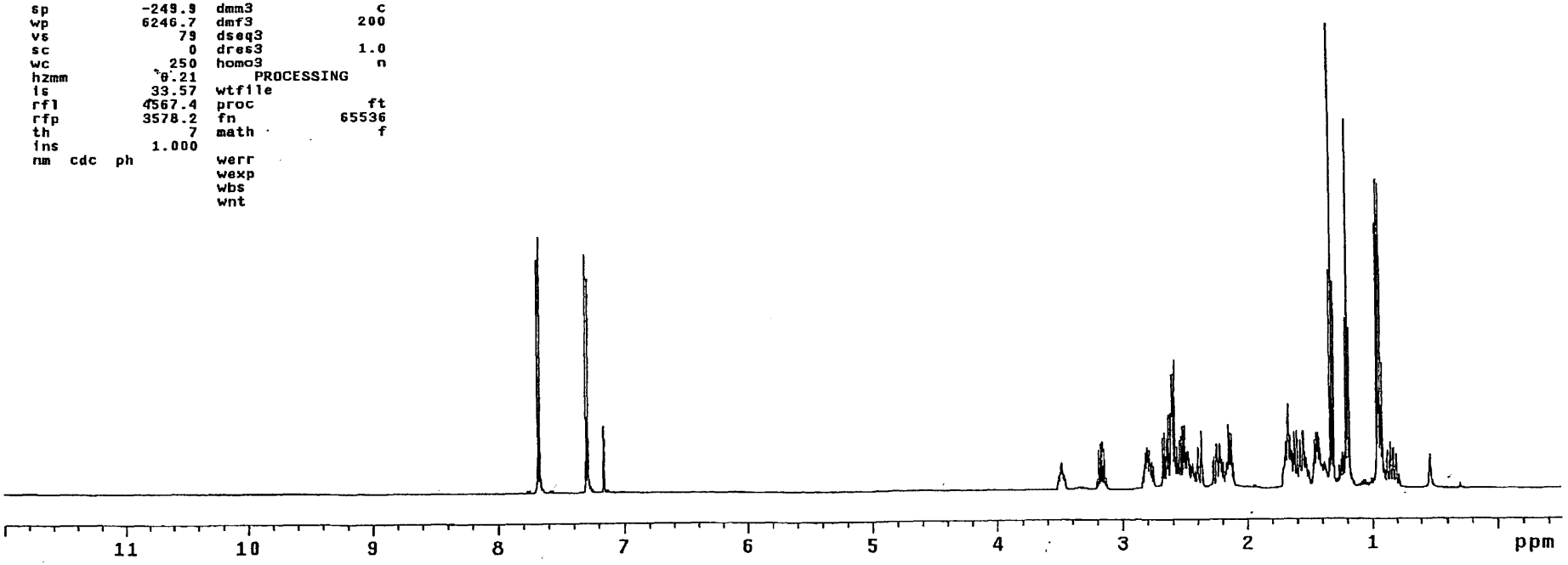

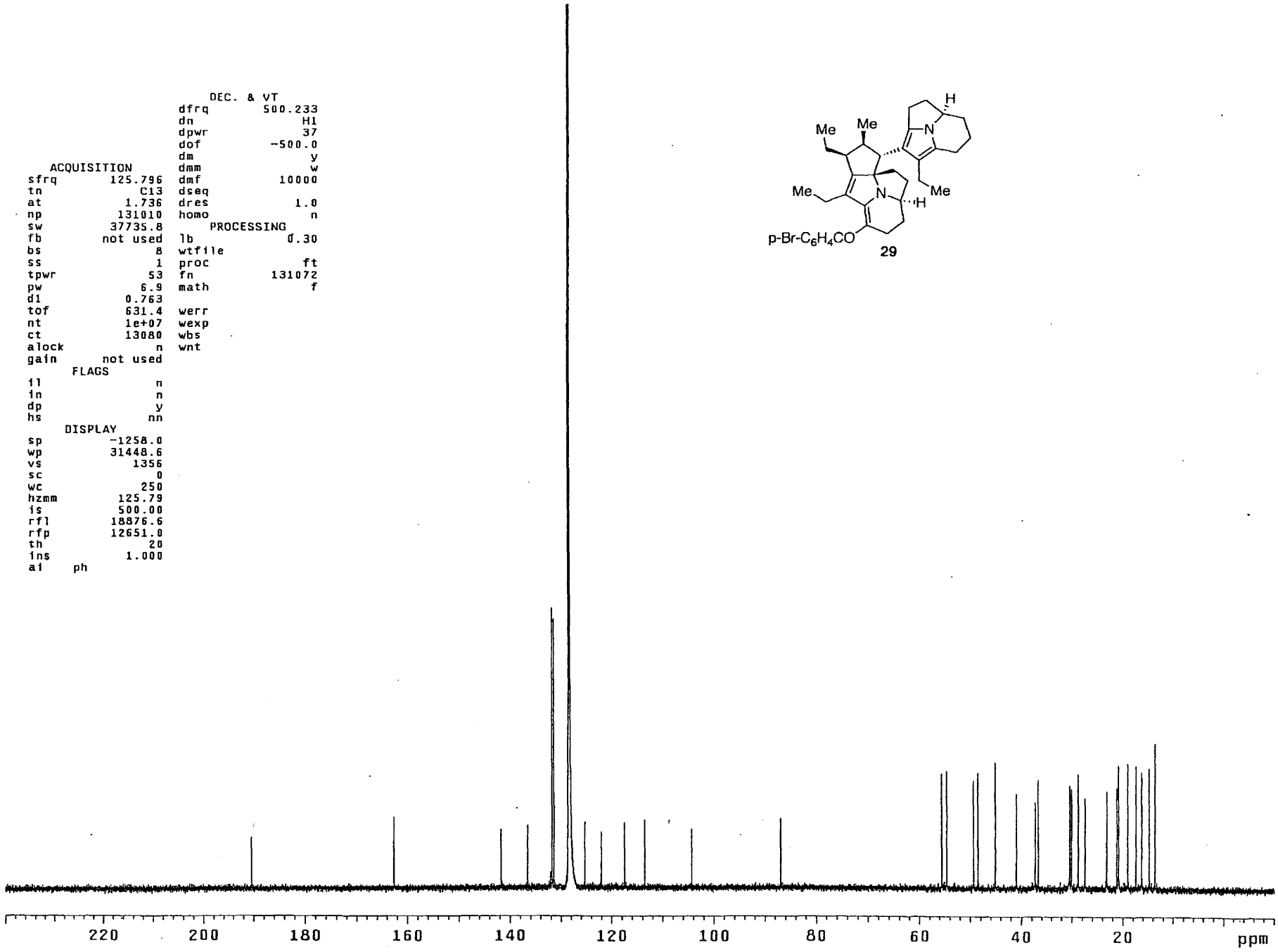
ACQUISITION
sfrq 125.796
tn C13
at 1.736
np 131010
sw 37735.8
fb not used
bs 8
ss 1
tpwr 53
pw 6.9
d1 0.763
tof 631.4
nt 1e+07
ct 13080
alock n
gain not used
FLAGS
il n
in n
dp y
hs nn
DISPLAY
sp -1258.0
wp 31448.6
vs 1356
sc 0
wc 250
hzmm 125.79
is 500.00
rfl 18876.6
rfp 12651.0
th 20
ins 1.000
ai ph
DEC. & VT
dfrq 500.233
dn H1
dpwr 37
dof -500.0
dm y
dmm w
dmf 10000
dseq
dres 1.0
homo n
PROCESSING
lb 0.30
wtfile
proc ft
fn 131072
math f
werr
wexp
wbs
wnt
Me
Me
Me
Me
H
N
N
H
p-Br-C6H4CO
29
220
200
180
160
140
120
100
80
60
40
20
ppm

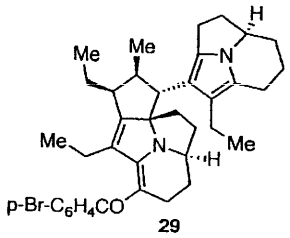
Me
Me
Me
Me
N
N
H
H
p-Br-C6H4CO

29

gCOSY

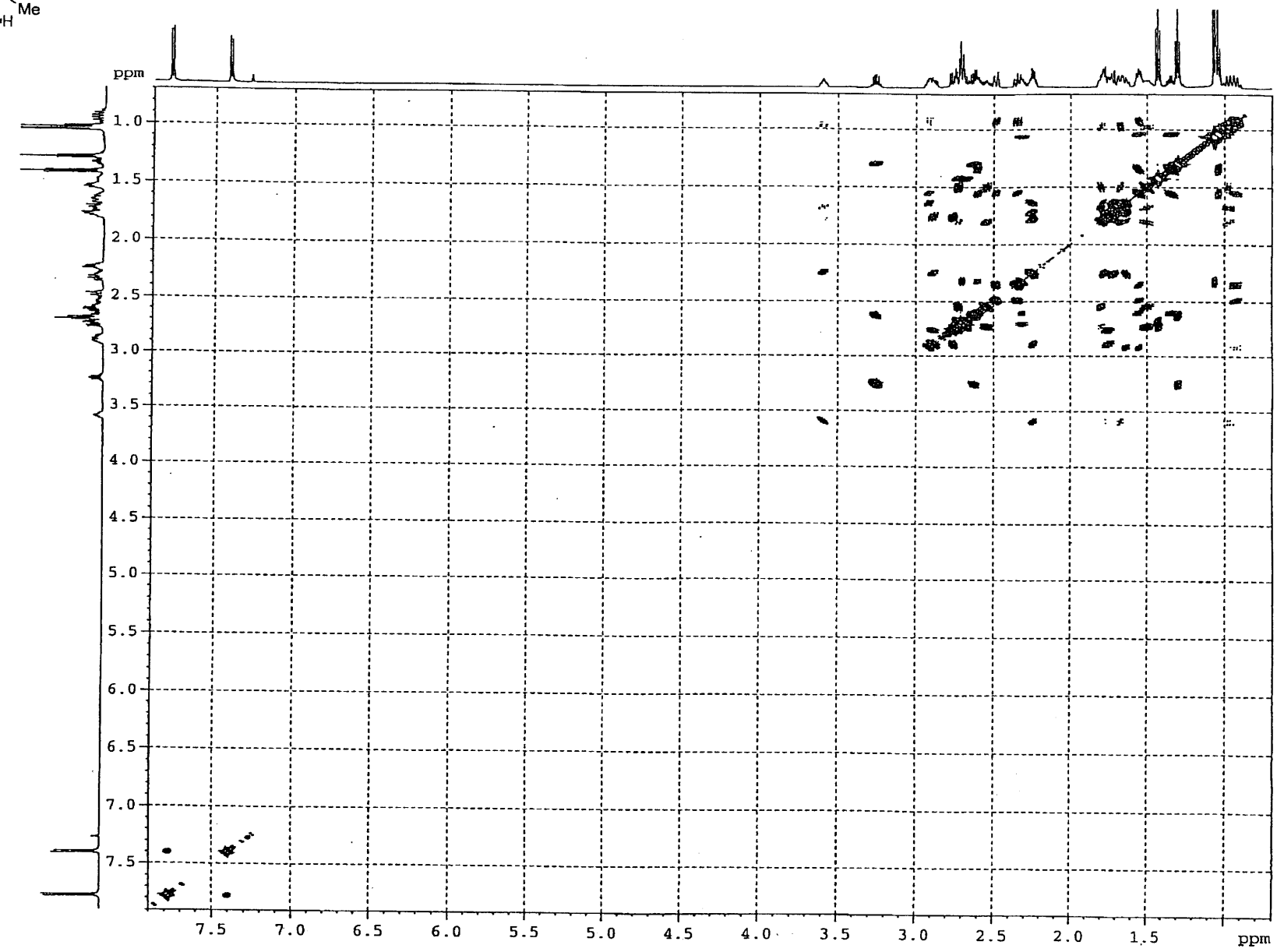
ppm
1.0
1.5
2.0
2.5
3.0
3.5
4.0
4.5
5.0
5.5
6.0
6.5
7.0
7.5
7.5
7.0
6.5
6.0
5.5
5.0
4.5
4.0
3.5
3.0
2.5
2.0
1.5
ppm

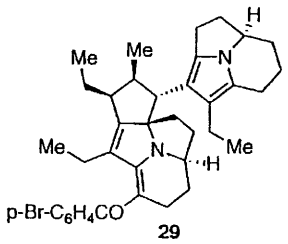
Me
Me
H
N
Me
N
Me
H
p-Br-C6H4CO

29

HSQC

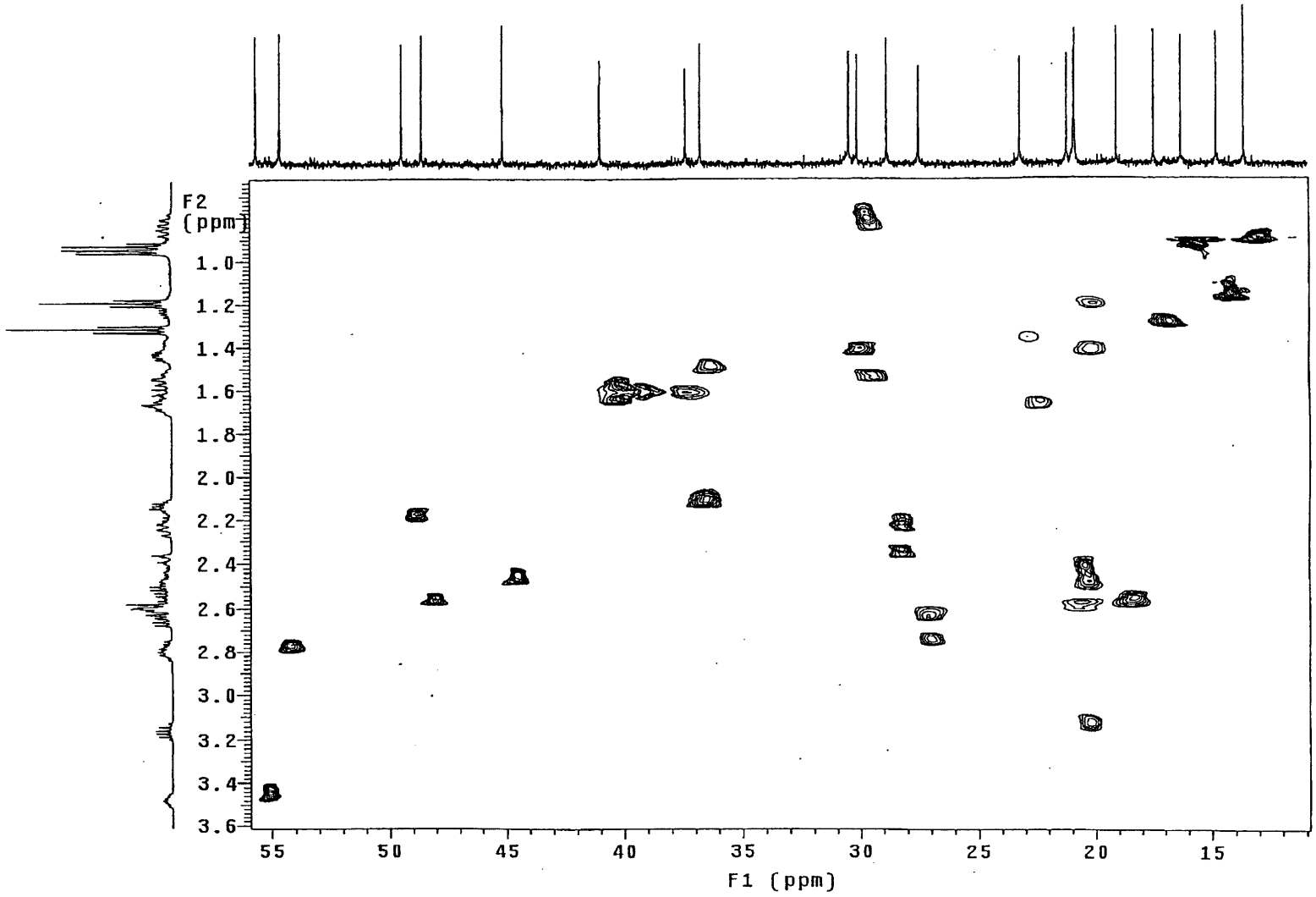
F2
(ppm)
1.0
1.2
1.4
1.6
1.8
2.0
2.2
2.4
2.6
2.8
3.0
3.2
3.4
3.6
55
50
45
40
35
30
25
20
15
F1 (ppm)

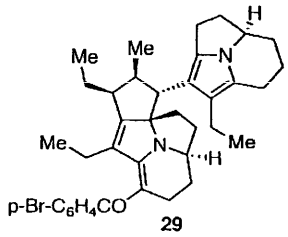
Me
Me
Me
Me
N
N
H
H
p-Br-C6H4CO

29

gHMBC

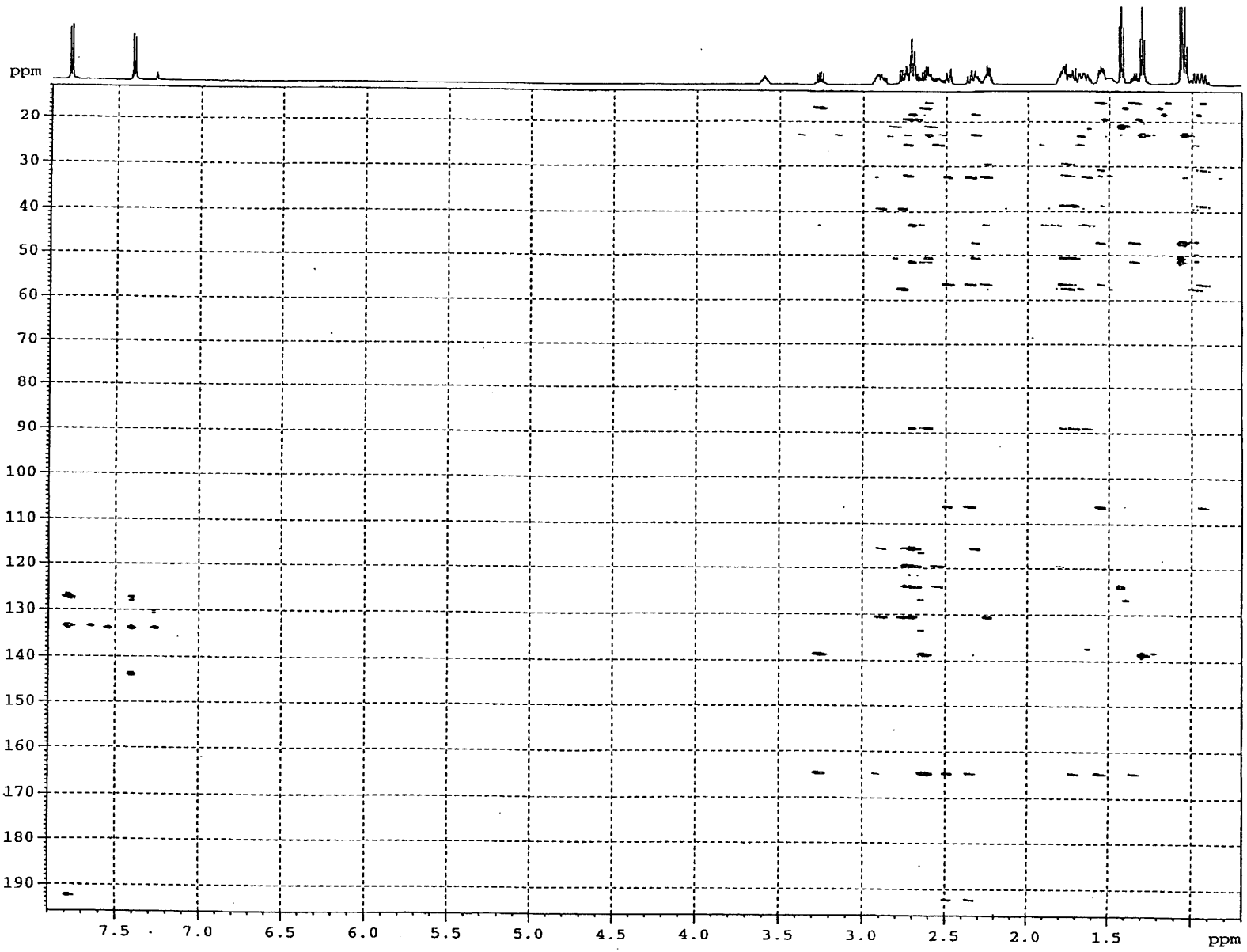
ppm
20
30
40
50
60
70
80
90
100
110
120
130
140
150
160
170
180
190
7.5
7.0
6.5
6.0
5.5
5.0
4.5
4.0
3.5
3.0
2.5
2.0
1.5
ppm

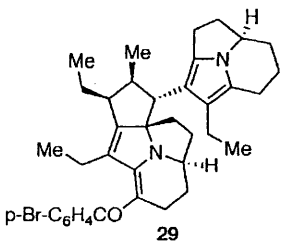
Me
Me
H
N
Me
N
Me
H
p-Br-C6H4CO

29

gNOESY

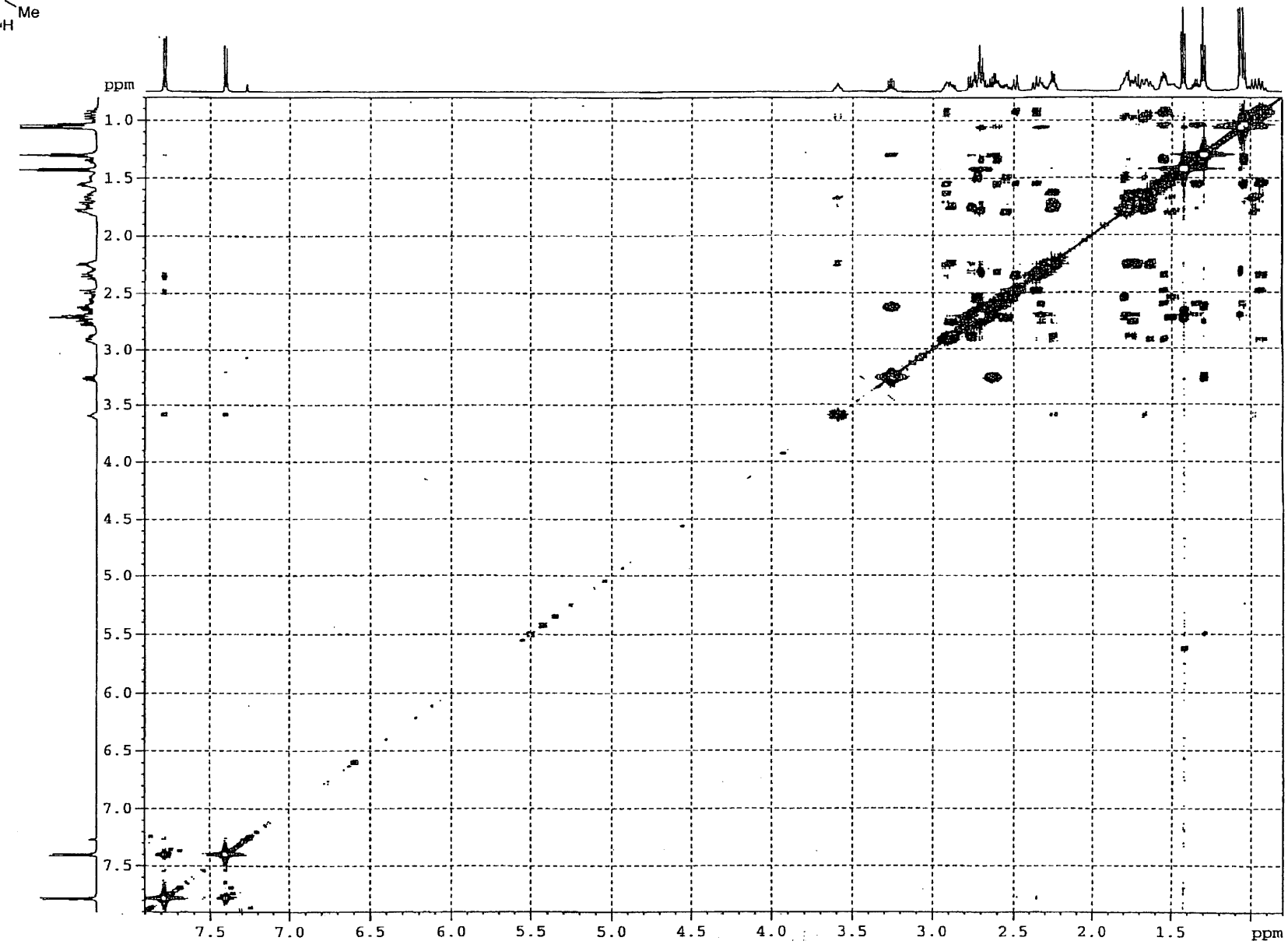
ppm
1.0
1.5
2.0
2.5
3.0
3.5
4.0
4.5
5.0
5.5
6.0
6.5
7.0
7.5
7.5
7.0
6.5
6.0
5.5
5.0
4.5
4.0
3.5
3.0
2.5
2.0
1.5
ppm

Appendix D.

Spectra for Chapter IV

ACQUISITION	
sfrq	499.749
tn	H1
at	3.277
np	65536
sw	9998.8
fb	not used
bs	4
tpwr	56
pw	8.2
d1	0
tof	1498.1
nt	36
ct	36
alock	n
gain	30
FLAGS	
il	n
in	n
dp	y
hs	nn
DISPLAY	
sp	-249.9
wp	6246.8
vs	75
sc	0
wc	250
hzmm	6.94
is	33.57
rfl	4567.4
rfp	3578.2
th	27
ins	1.000
nm cdc ph	

DEC. & VT	
dfrq	125.674
dn	C13
dpwr	34
dof	1498.1
dm	nnn
dmm	w
dmf	10000
dseq	
dres	1.0
homo	n
PROCESSING	
wtfile	
proc	ft
fn	65536
math	f
werr	
wexp	
wbs	
wnt	

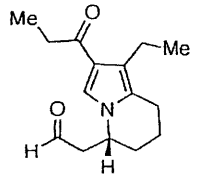

33

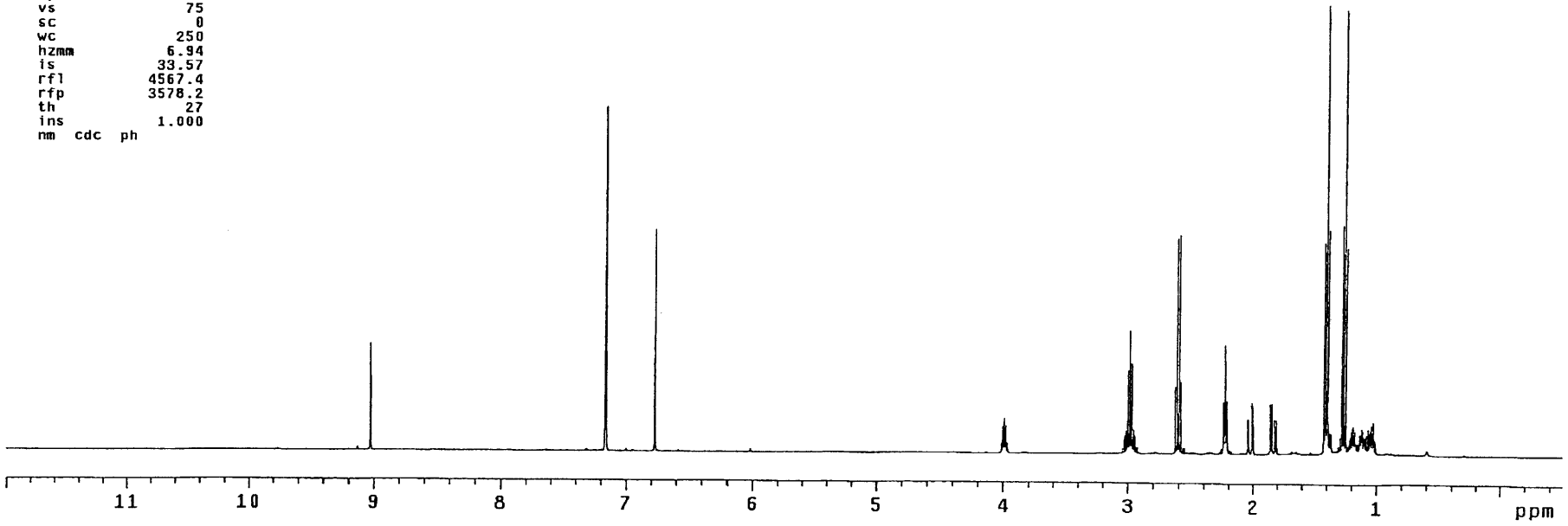

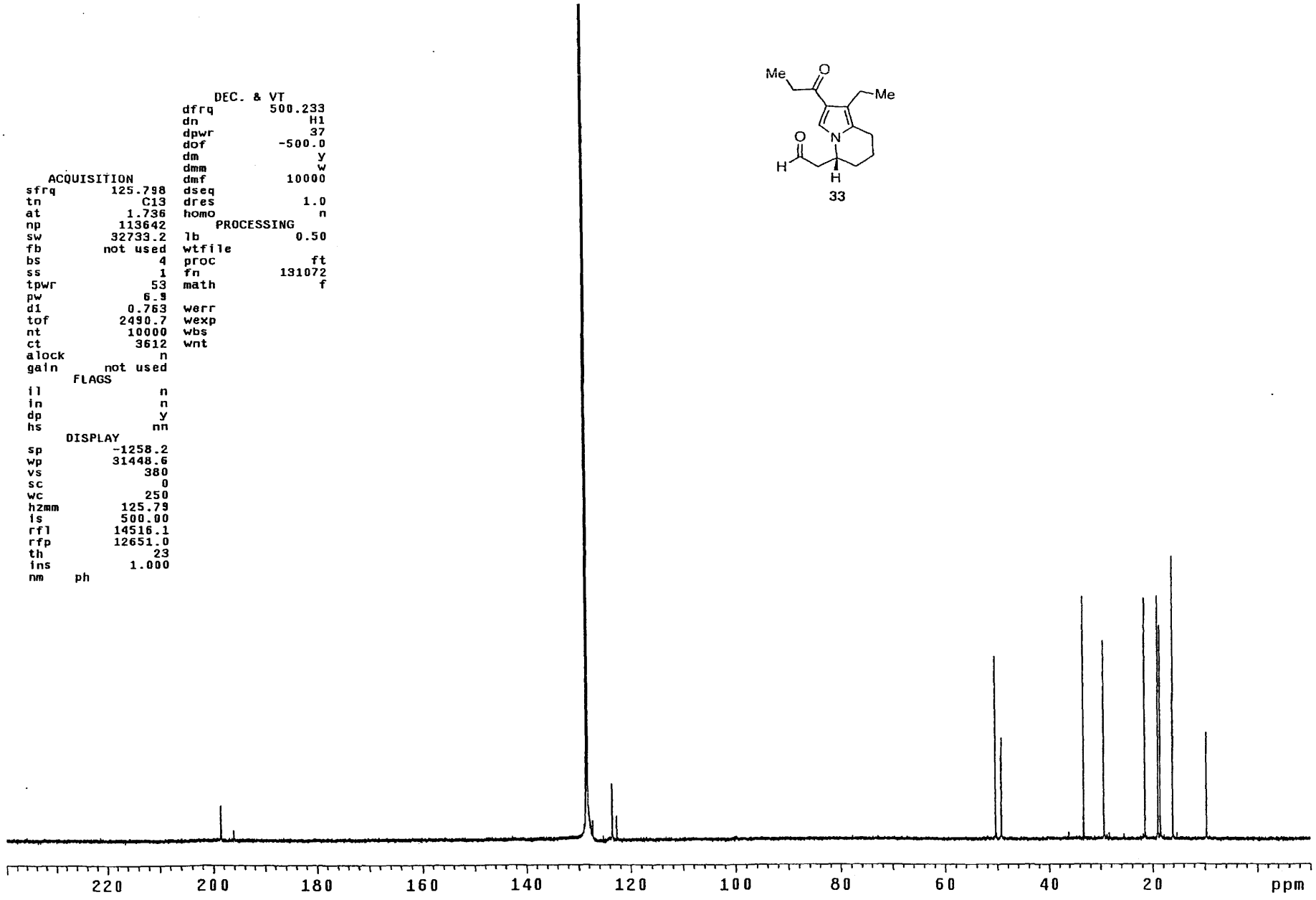
ACQUISITION
sfrq 125.798
tn C13
at 1.736
np 113642
sw 32733.2
fb not used
bs 4
ss 1
tpwr 53
pw 6.9
d1 0.763
tof 2490.7
nt 10000
ct 3612
alock n
gain not used
FLAGS
il n
in n
dp y
hs nn
DISPLAY
sp -1258.2
wp 31448.6
vs 380
sc 0
wc 250
hzmm 125.79
is 500.00
rfl 14516.1
rfp 12651.0
th 23
ins 1.000
nm ph
DEC. & VT
dfrq 500.233
dn H1
dpwr 37
dof -500.0
dm y
dmm w
dmf 10000
dseq
dres 1.0
homo n
PROCESSING
lb 0.50
wtfile
proc ft
fn 131072
math f
werr
wexp
wbs
wnt
Me
O
Me
O
N
H
H
33
220
200
180
160
140
120
100
80
60
40
20
ppm

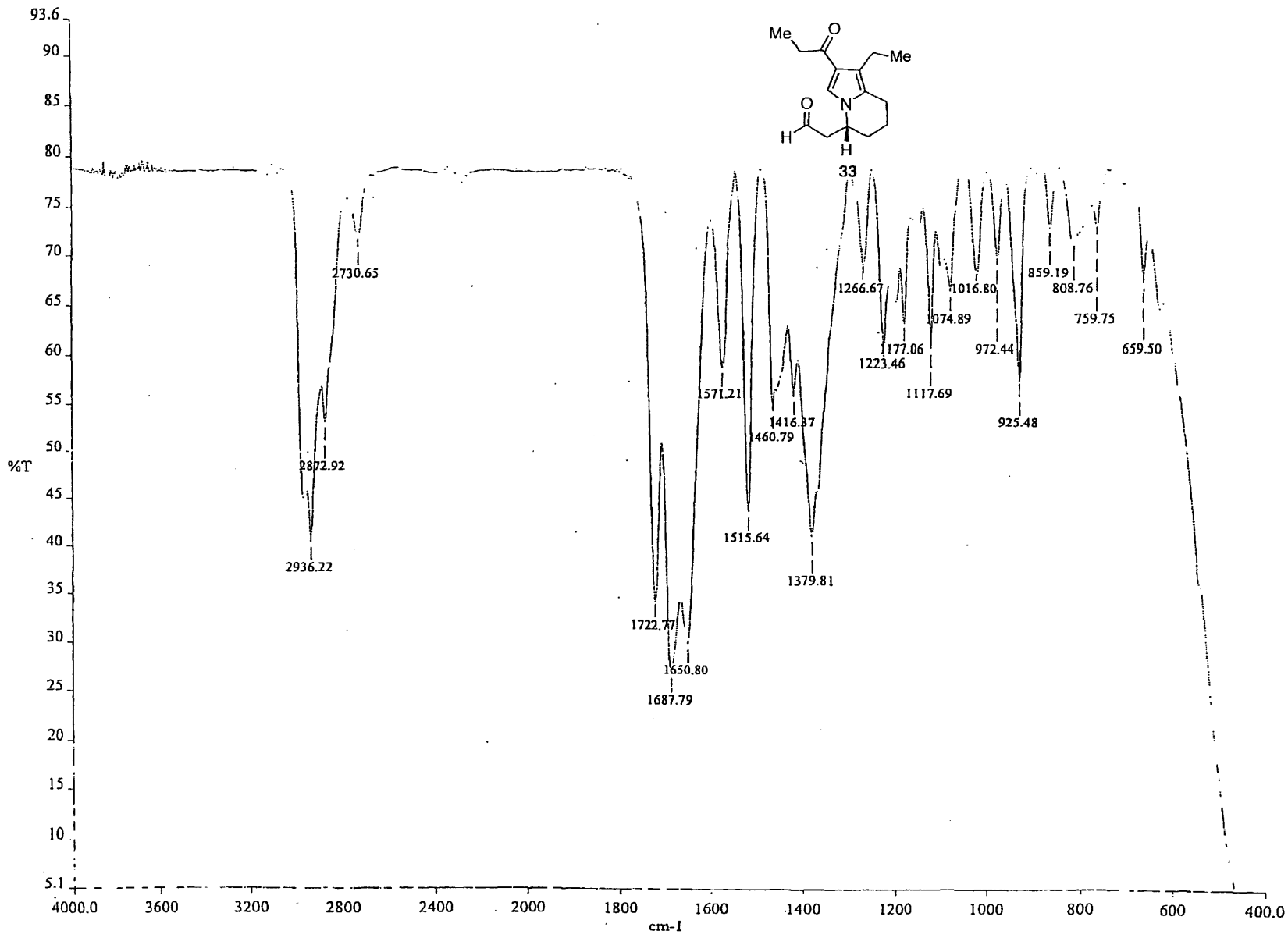
93.6
90
85
80
75
70
65
60
55
50
45
40
35
30
25
20
15
10
5.1
%T
4000.0
3600
3200
2800
2400
2000
1800
1600
1400
1200
1000
800
600
400.0
cm-1
Me
O
Me
O
N
H
H
33
2730.65
2872.92
2936.22
1722.77
1650.80
1687.79
1571.21
1515.64
1460.79
1416.37
1379.81
1266.67
1223.46
1177.06
1117.69
1074.89
1016.80
972.44
925.48
859.19
808.76
759.75
659.50

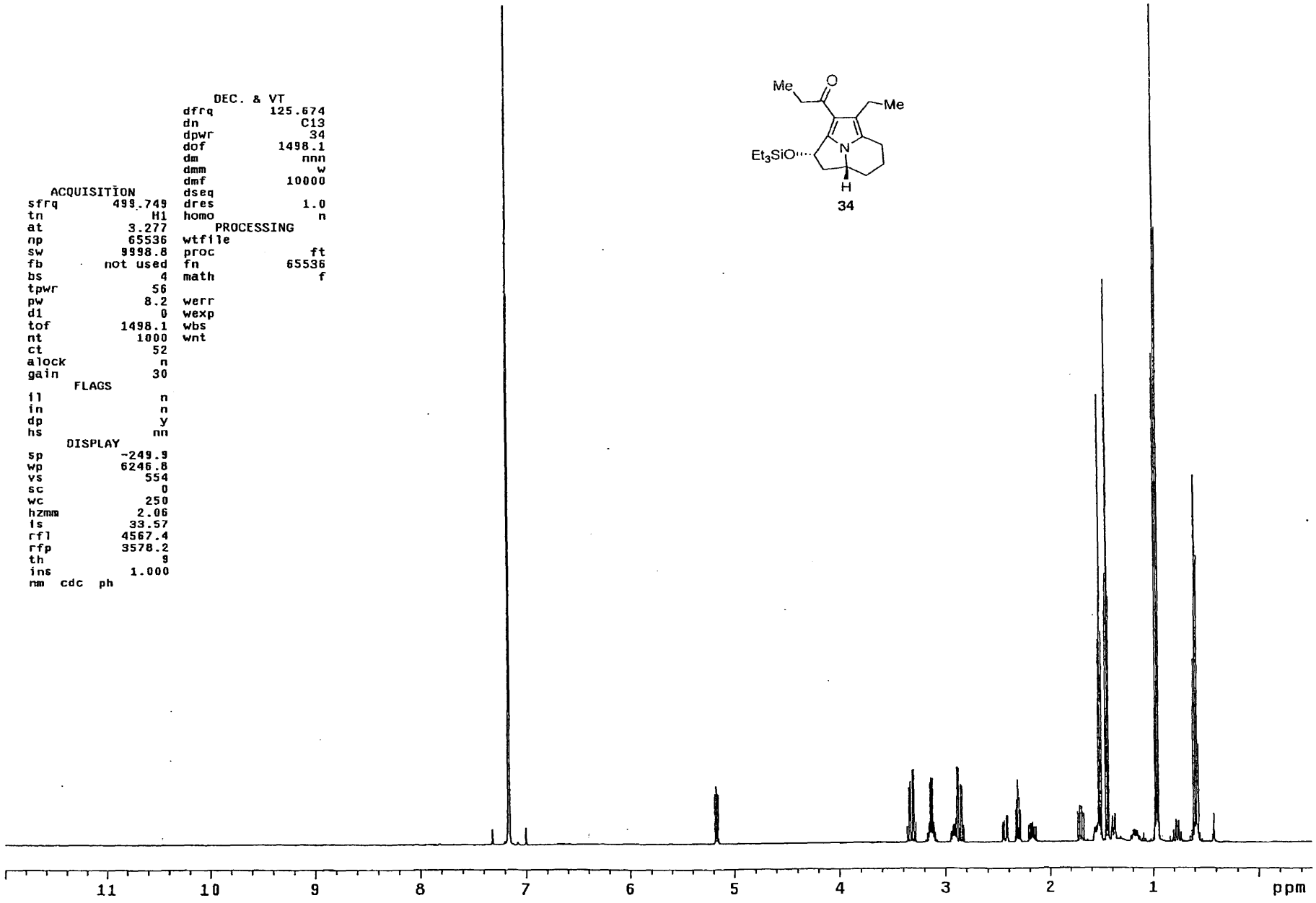
ACQUISITION
sfrq 499.749
tn H1
at 3.277
np 65536
sw 9998.8
fb not used
bs 4
tpwr 56
pw 8.2
d1 0
tof 1498.1
nt 1000
ct 52
alock n
gain 30
FLAGS
il n
in n
dp y
hs nn
DISPLAY
sp -249.9
wp 6246.8
vs 554
sc 0
wc 250
hzmm 2.06
is 33.57
rfl 4567.4
rfp 3578.2
th 9
ins 1.000
nm cdc ph
DEC. & VT
dfrq 125.674
dn C13
dpwr 34
dof 1498.1
dm nnn
dmm w
dmf 10000
dseq
dres 1.0
homo n
PROCESSING
wtfile
proc ft
fn 65536
math f
werr
wexp
wbs
wnt
Me
O
Me
Et3SiO
N
H
34
11
10
9
8
7
6
5
4
3
2
1
ppm

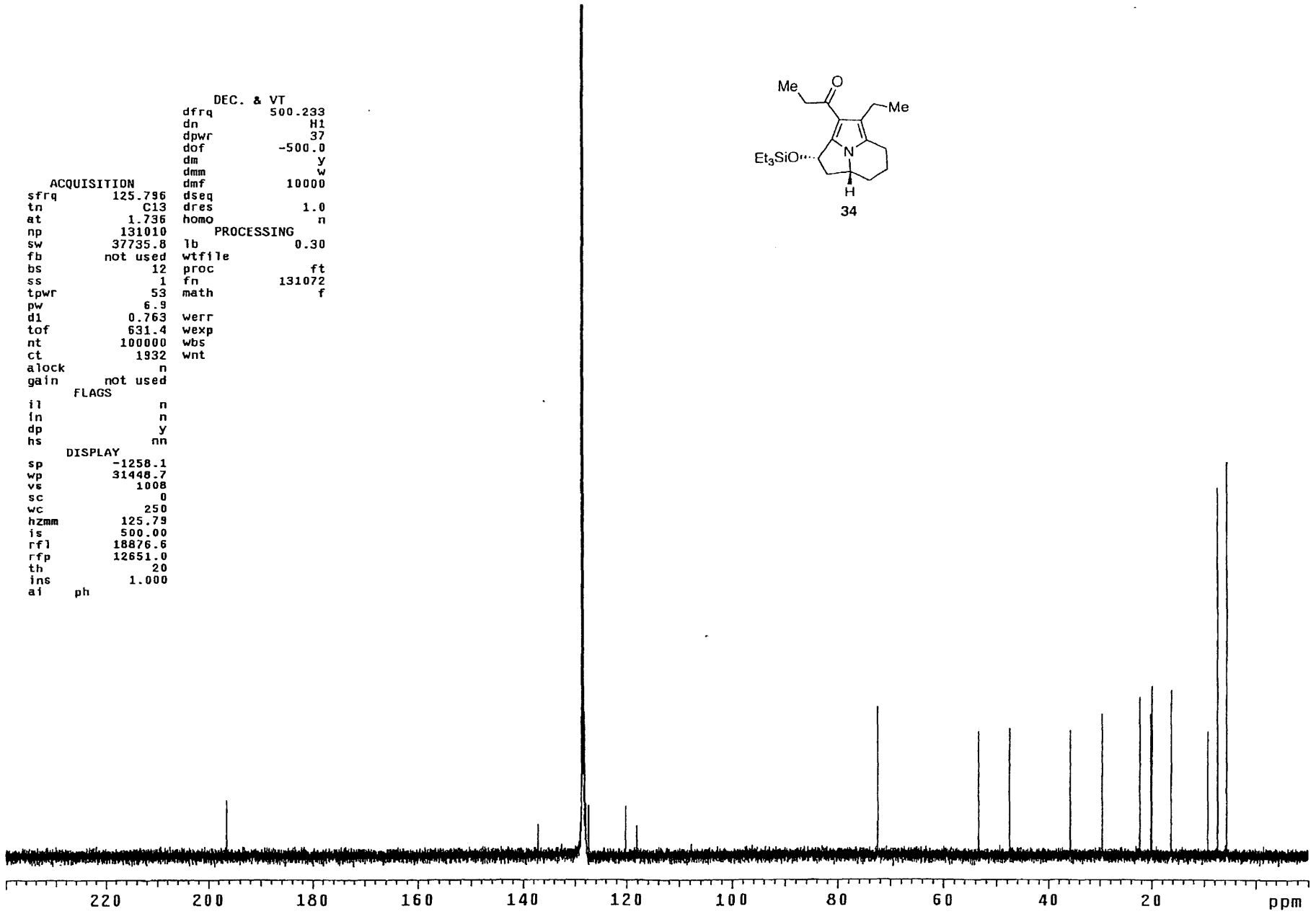
ACQUISITION
sfrq 125.796
tn C13
at 1.736
np 131010
sw 37735.8
fb not used
bs 12
ss 1
tpwr 53
pw 6.9
d1 0.763
tof 631.4
nt 100000
ct 1932
alock n
gain not used
FLAGS
il n
in n
dp y
hs nn
DISPLAY
sp -1258.1
wp 31448.7
vs 1008
sc 0
wc 250
hzmm 125.79
is 500.00
rfl 18876.6
rfp 12651.0
th 20
ins 1.000
ai ph
DEC. & VT
dfrq 500.233
dn H1
dpwr 37
dof -500.0
dm y
dmm w
dmf 10000
dseq
dres 1.0
homo n
PROCESSING
lb 0.30
wtfile
proc ft
fn 131072
math f
werr
wexp
wbs
wnt
Me
O
Me
Et3SiO
N
H
34
220
200
180
160
140
120
100
80
60
40
20
ppm

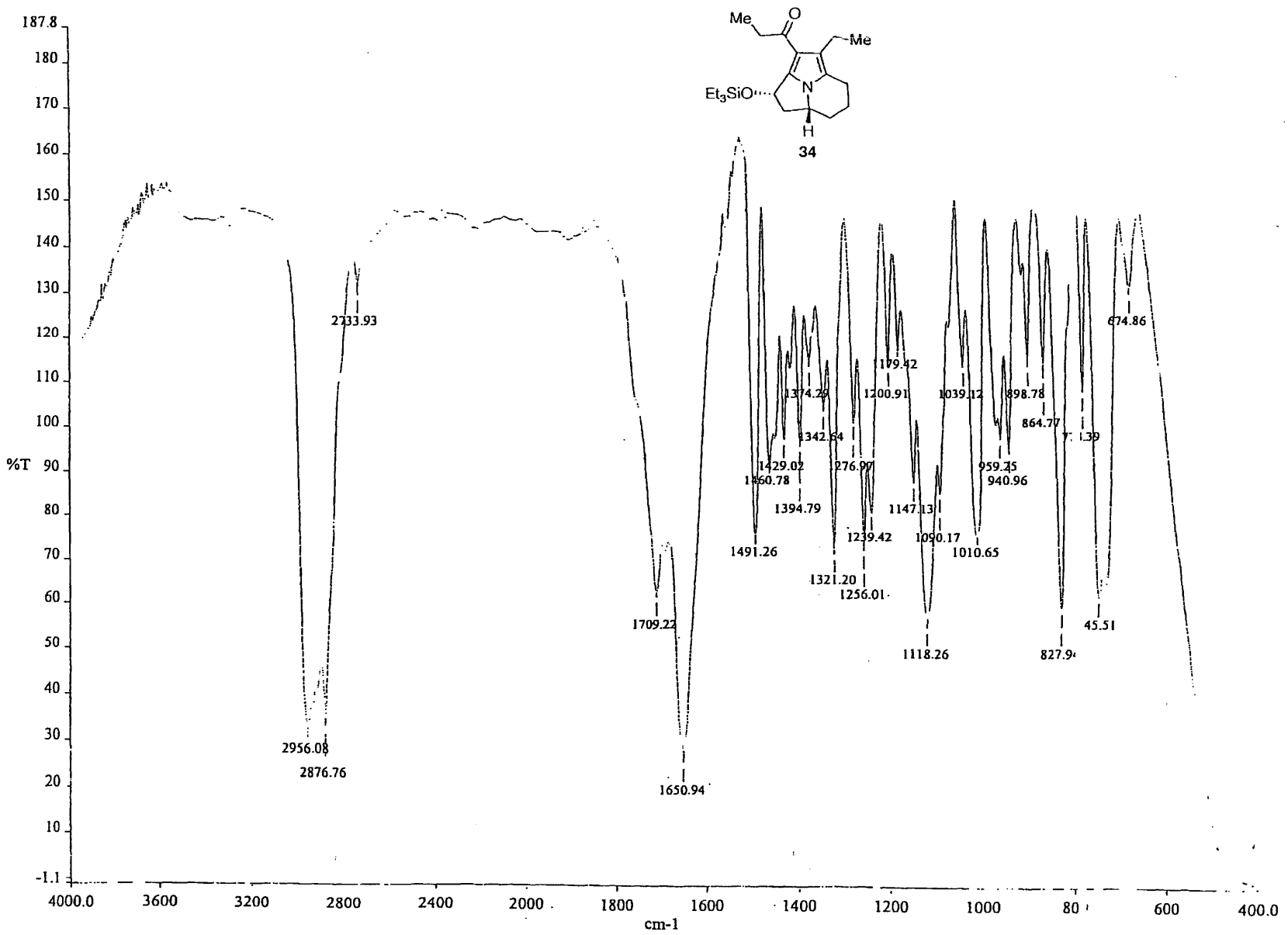
Me
O
Me
Et3SiO
N
H
34
%T
cm-1
2956.08
2876.76
2733.93
1709.22
1650.94
1491.26
1460.78
1429.02
1394.79
1374.29
1342.64
1321.20
1276.97
1256.01
1239.42
1200.91
1179.42
1147.13
1118.26
1090.17
1039.12
1010.65
959.25
940.96
898.78
864.77
827.9
745.39
674.86

ACQUISITION	
sfrq	499.749
tn	H1
at	3.277
np	65536
sw	9998.8
fb	not used
bs	4
tpwr	56
pw	8.2
d1	0
tof	1498.1
nt	48
ct	48
alock	n
gain	30
FLAGS	
il	n
in	n
dp	y
hs	nn
DISPLAY	
sp	-249.9
wp	6246.8
vs	137
sc	0
wc	250
hzmm	24.99
is	33.57
rfl	4567.1
rfp	3578.2
th	6
ins	1.000
nm cdc ph	

DEC. & VT	
dfrq	125.674
dn	C13
dpwr	34
dof	1498.1
dm	nnn
dmm	w
dmf	10000
dseq	
dres	1.0
homo	n
PROCESSING	
wtfile	
proc	ft
fn	65536
math	f
werr	
wexp	
wbs	
wnt	

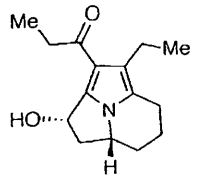

35

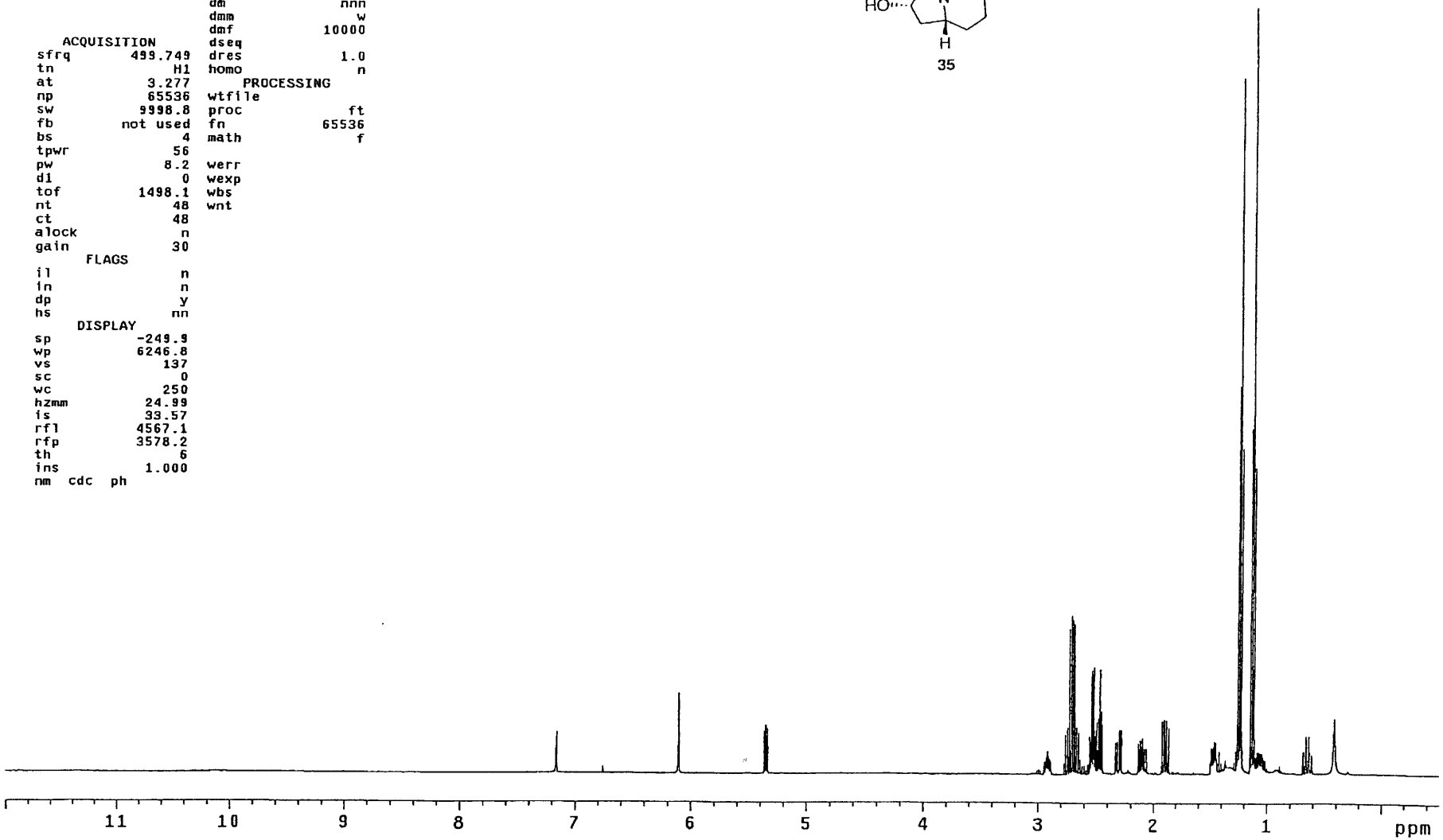

ACQUISITION		DEC. & VT	
sfrq	125.798	dfrq	500.233
tn	C13	dn	H1
at	1.735	dpwr	37
np	115870	dof	-500.0
sw	33389.0	dm	y
fb	not used	dmm	w
bs	4	dmf	10000
ss	1	dseq	
tpwr	53	dres	1.0
pw	6.9	homo	n
d1	0.763	PROCESSING	
tof	2763.4	lb	0.30
nt	10000	wtfile	
ct	2048	proc	ft
alock	n	fn	131072
gain	not used	math	f
FLAGS		werr	
il	n	wexp	
in	n	wbs	
dp	y	wnt	
hs	nn		
DISPLAY			
sp	-1258.0		
wp	31447.9		
vs	339		
sc	0		
wc	250		
hzmm	125.79		
is	500.00		
rfl	11606.4		
rfp	9686.0		
th	4		
ins	1.000		
ai	ph		

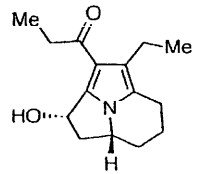

35

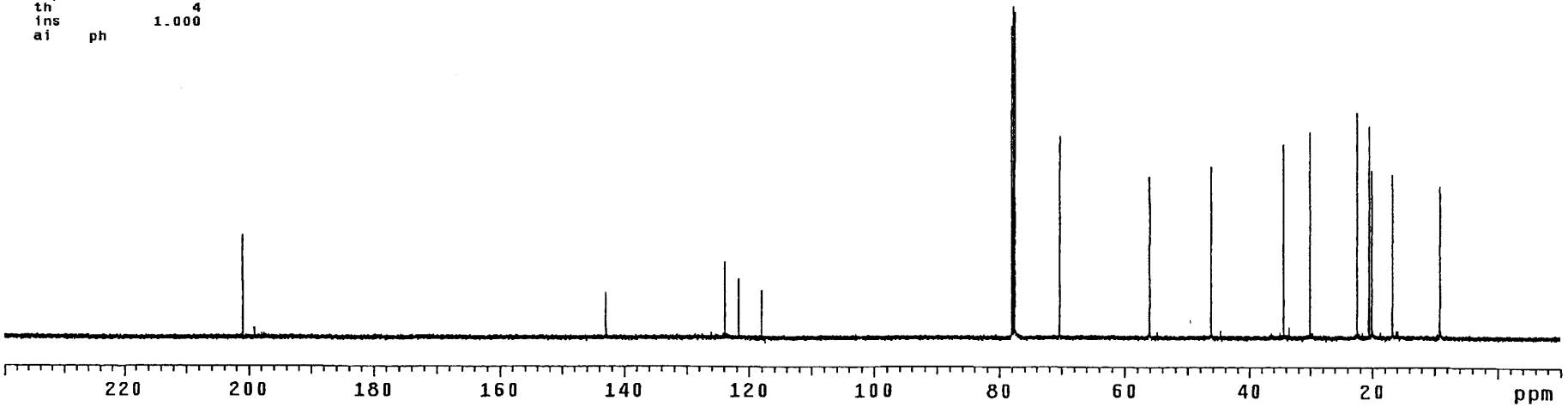

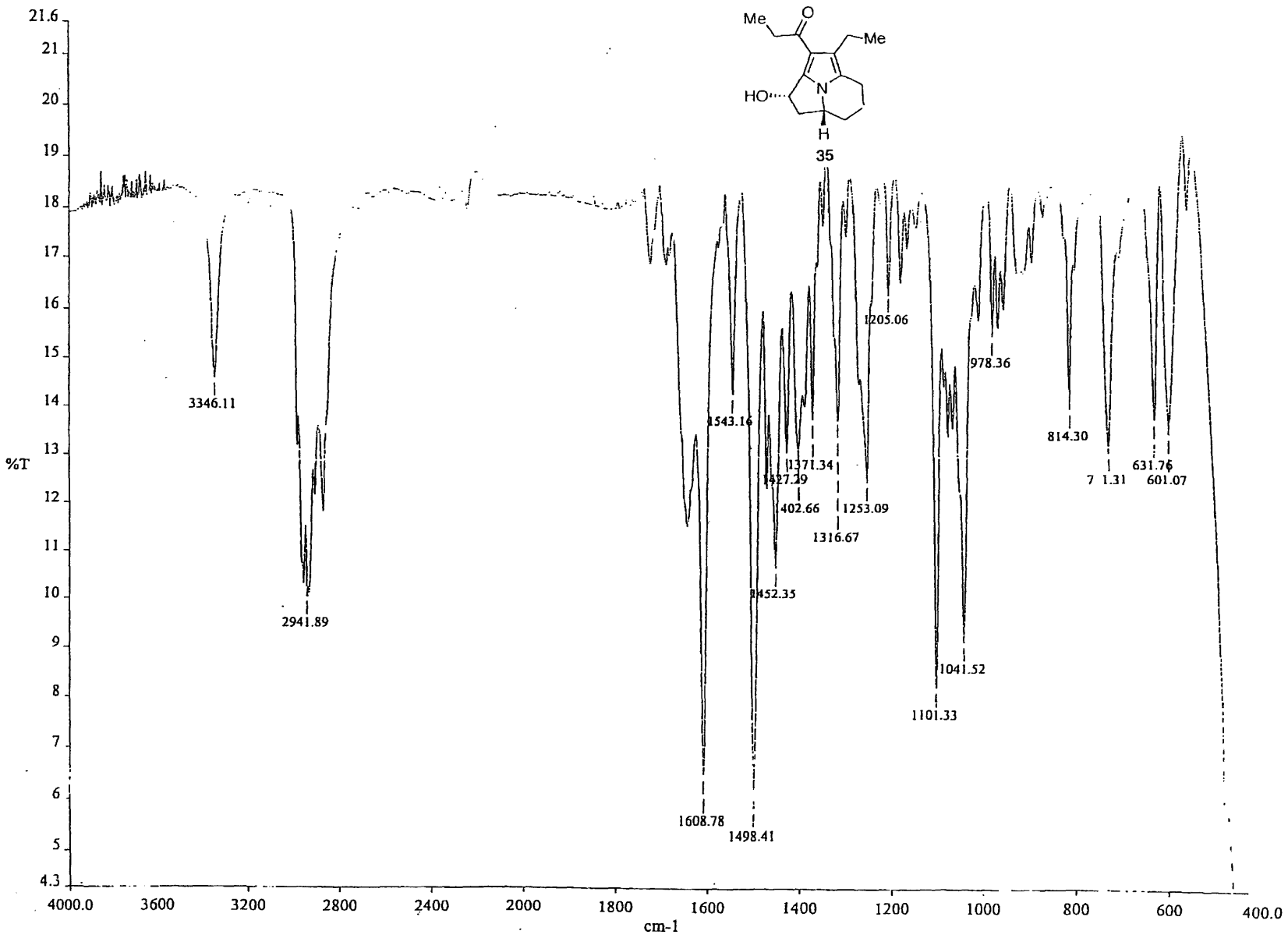
Me
O
Me
HO
N
H
35
%T
21.6
21
20
19
18
17
16
15
14
13
12
11
10
9
8
7
6
5
4.3
3346.11
2941.89
1608.78
1543.16
1498.41
1452.35
1427.29
1402.66
1371.34
1316.67
1253.09
1205.06
1101.33
1041.52
978.36
814.30
7 1.31
631.76
601.07
4000.0
3600
3200
2800
2400
2000
1800
1600
1400
1200
1000
800
600
400.0
cm-1

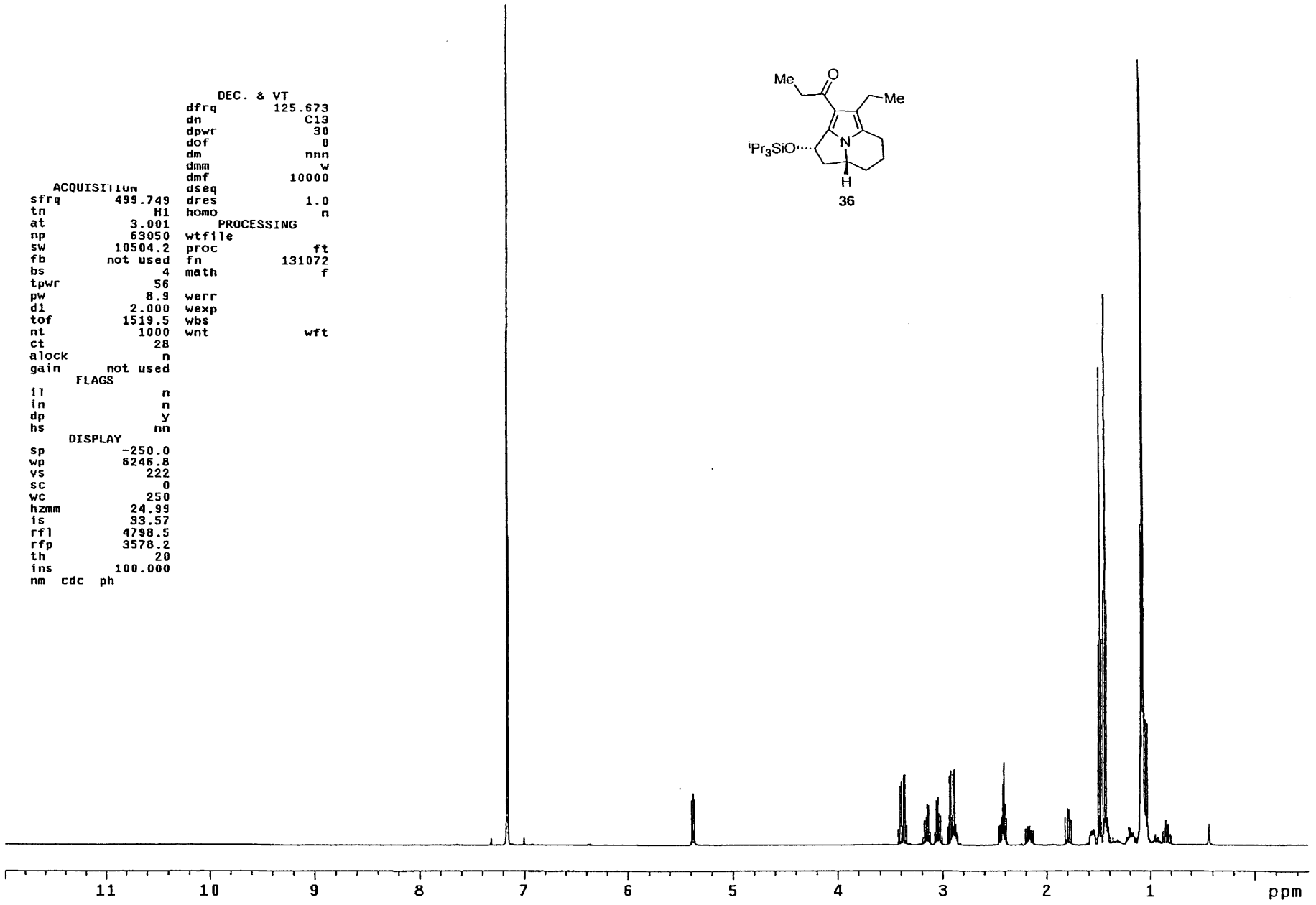
ACQUISITION
sfrq 499.749
tn H1
at 3.001
np 63050
sw 10504.2
fb not used
bs 4
tpwr 56
pw 8.9
d1 2.000
tof 1519.5
nt 1000
ct 28
alock n
gain not used
FLAGS
il n
in n
dp y
hs nn
DISPLAY
sp -250.0
wp 6246.8
vs 222
sc 0
wc 250
hzmm 24.99
is 33.57
rfl 4798.5
rfp 3578.2
th 20
ins 100.000
nm cdc ph
DEC. & VT
dfrq 125.673
dn C13
dpwr 30
dof 0
dm nnn
dmm w
dmf 10000
dseq
dres 1.0
homo n
PROCESSING
wtfile
proc ft
fn 131072
math f
werr
wexp
wbs
wnt wft
Me
O
Me
iPr3SiO
N
H
36
11
10
9
8
7
6
5
4
3
2
1
ppm

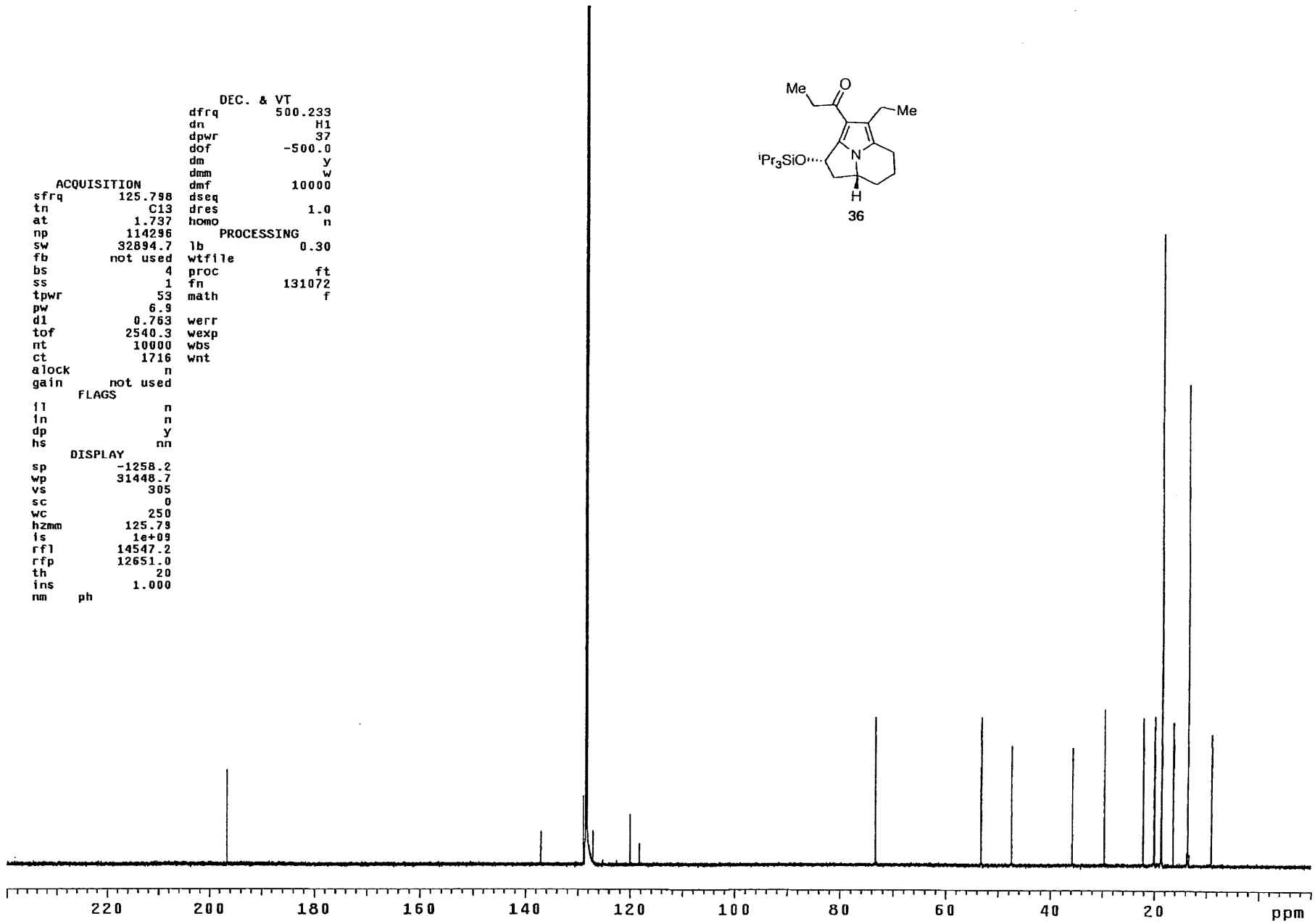
ACQUISITION
sfrq 125.798
tn C13
at 1.737
np 114296
sw 32894.7
fb not used
bs 4
ss 1
tpwr 53
pw 6.9
d1 0.763
tof 2540.3
nt 10000
ct 1716
alock n
gain not used
FLAGS
il n
in n
dp y
hs nn
DISPLAY
sp -1258.2
wp 31448.7
vs 305
sc 0
wc 250
hzmm 125.79
is 1e+09
rfl 14547.2
rfp 12651.0
th 20
ins 1.000
nm ph
DEC. & VT
dfrq 500.233
dn H1
dpwr 37
dof -500.0
dm y
dmm w
dmf 10000
dseq
dres 1.0
homo n
PROCESSING
lb 0.30
wtfile
proc ft
fn 131072
math f
werr
wexp
wbs
wnt
Me
O
Me
iPr3SiO
N
H
36
220
200
180
160
140
120
100
80
60
40
20
ppm

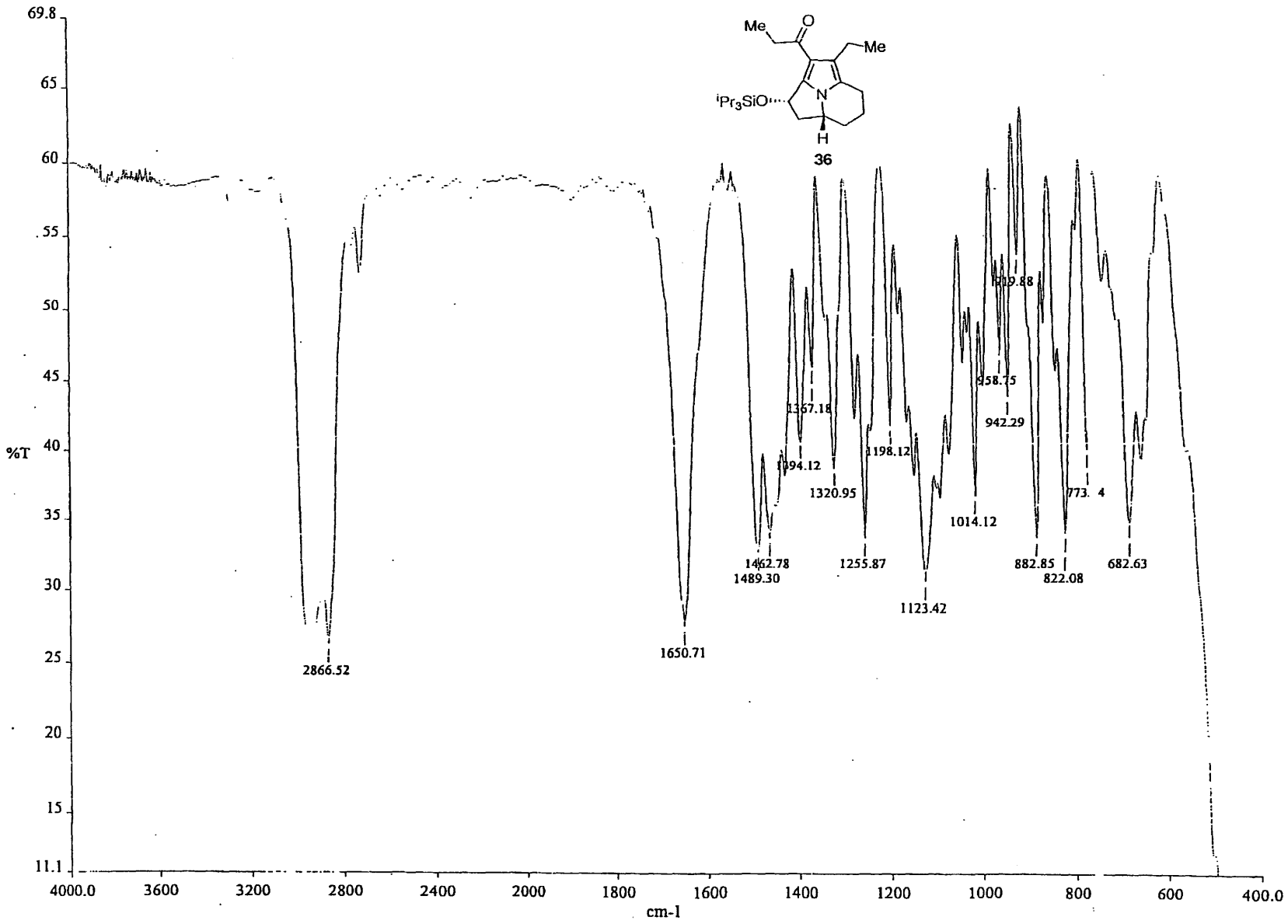
Me
O
Me
$^{i}Pr_3SiO$
N
H
36
%T
69.8
65
60
55
50
45
40
35
30
25
20
15
11.1
2866.52
1650.71
1489.30
1462.78
1394.12
1367.18
1320.95
1255.87
1198.12
1123.42
1014.12
958.75
942.29
919.88
882.85
822.08
773. 4
682.63
4000.0
3600
3200
2800
2400
2000
1800
1600
1400
1200
1000
800
600
400.0
cm-1

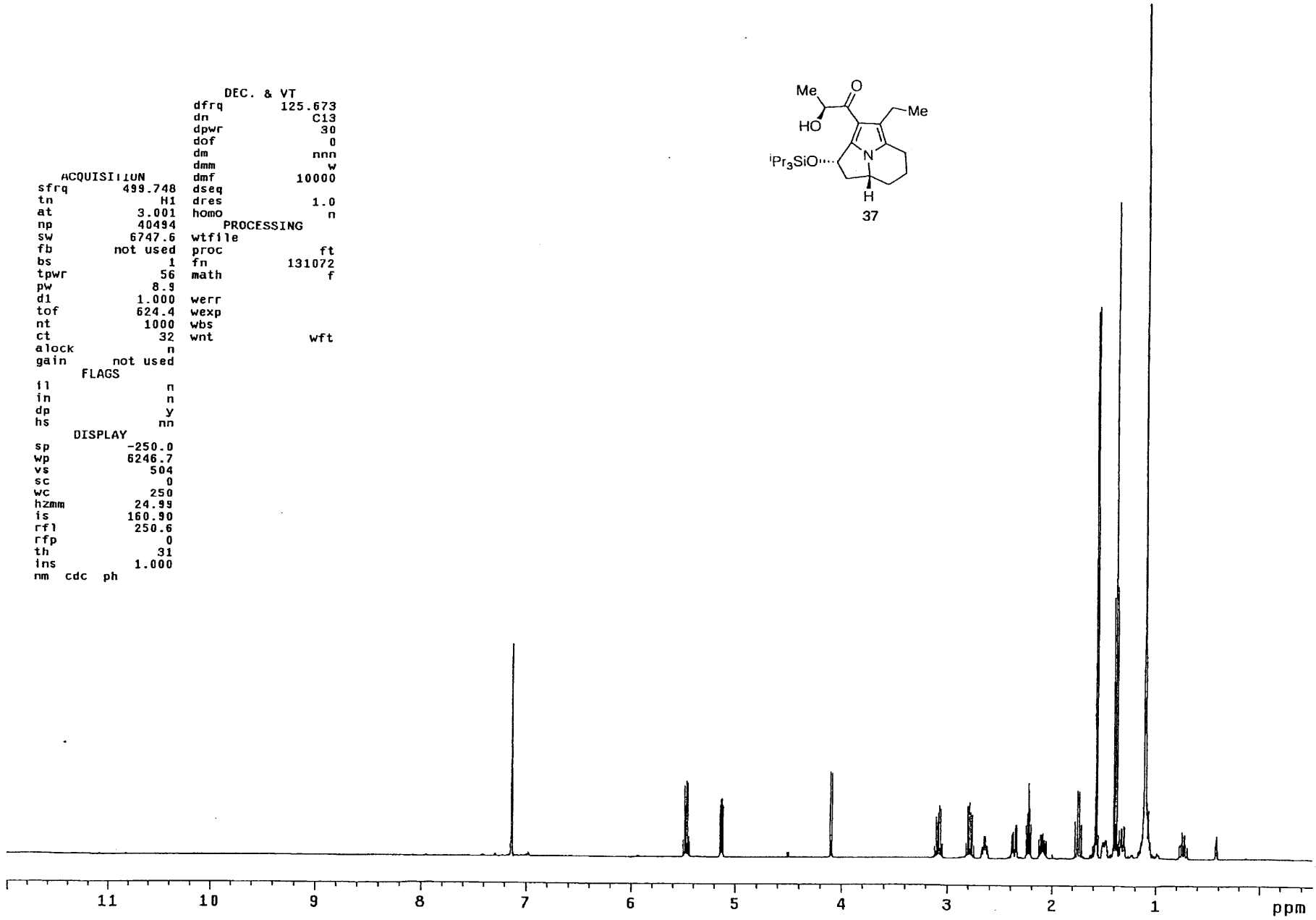
ACQUISITION
sfrq 499.748
tn H1
at 3.001
np 40494
sw 6747.6
fb not used
bs 1
tpwr 56
pw 8.9
d1 1.000
tof 624.4
nt 1000
ct 32
alock n
gain not used
FLAGS
il n
in n
dp y
hs nn
DISPLAY
sp -250.0
wp 6246.7
vs 504
sc 0
wc 250
hzmm 24.99
is 160.90
rfl 250.6
rfp 0
th 31
ins 1.000
nm cdc ph
DEC. & VT
dfrq 125.673
dn C13
dpwr 30
dof 0
dm nnn
dmm w
dmf 10000
dseq
dres 1.0
homo n
PROCESSING
wtfile
proc ft
fn 131072
math f
werr
wexp
wbs
wnt wft
Me
O
HO
Me
N
iPr3SiO
H
37
11
10
9
8
7
6
5
4
3
2
1
ppm

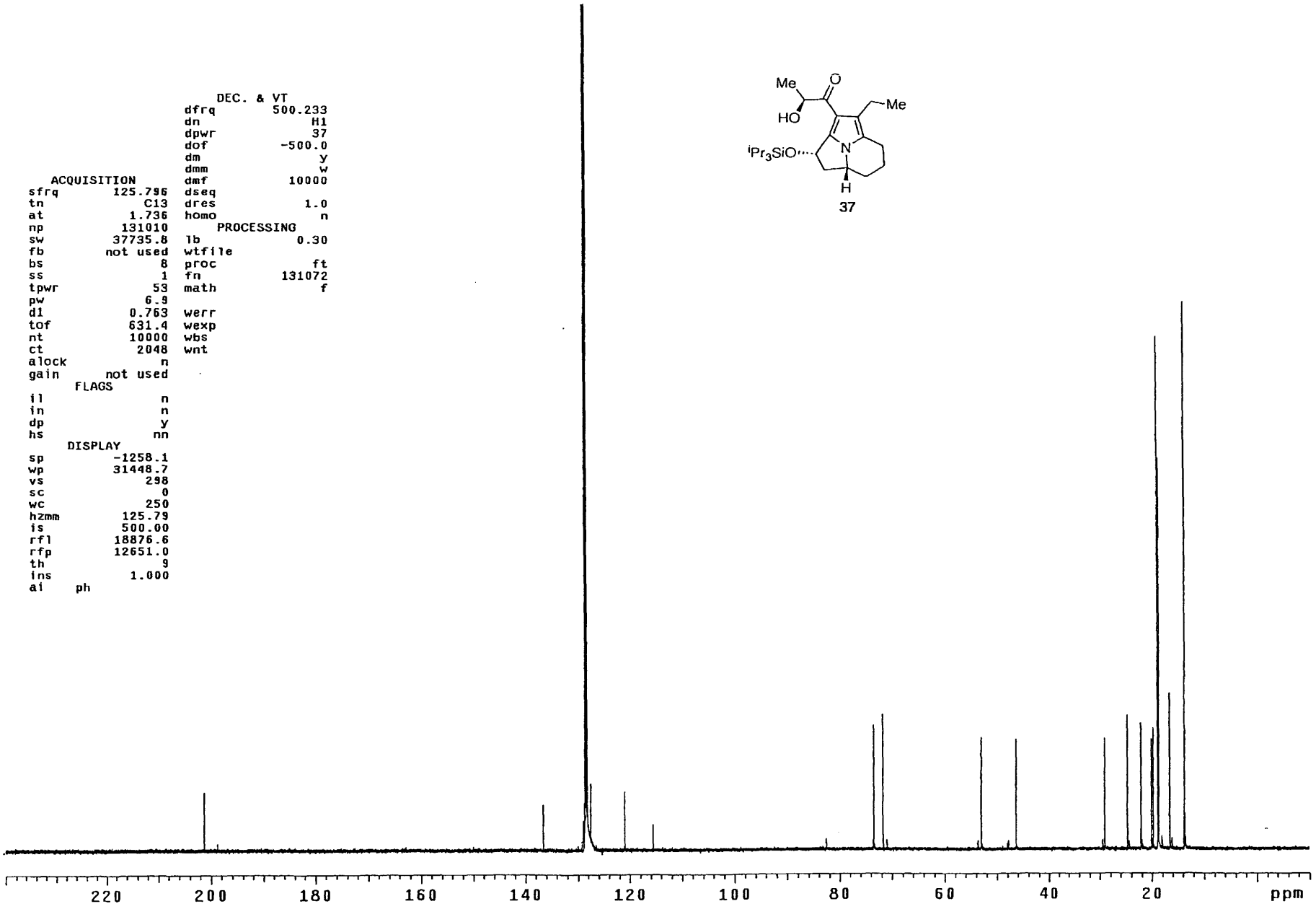
ACQUISITION
sfrq 125.796
tn C13
at 1.736
np 131010
sw 37735.8
fb not used
bs 8
ss 1
tpwr 53
pw 6.9
d1 0.763
tof 631.4
nt 10000
ct 2048
alock n
gain not used
FLAGS
il n
in n
dp y
hs nn
DISPLAY
sp -1258.1
wp 31448.7
vs 298
sc 0
wc 250
hzmm 125.79
is 500.00
rfl 18876.6
rfp 12651.0
th 9
ins 1.000
al ph
DEC. & VT
dfrq 500.233
dn H1
dpwr 37
dof -500.0
dm y
dmm w
dmf 10000
dseq
dres 1.0
homo n
PROCESSING
lb 0.30
wtfile
proc ft
fn 131072
math f
werr
wexp
wbs
wnt
Me
O
Me
HO
iPr3SiO
N
H
37
220
200
180
160
140
120
100
80
60
40
20
ppm

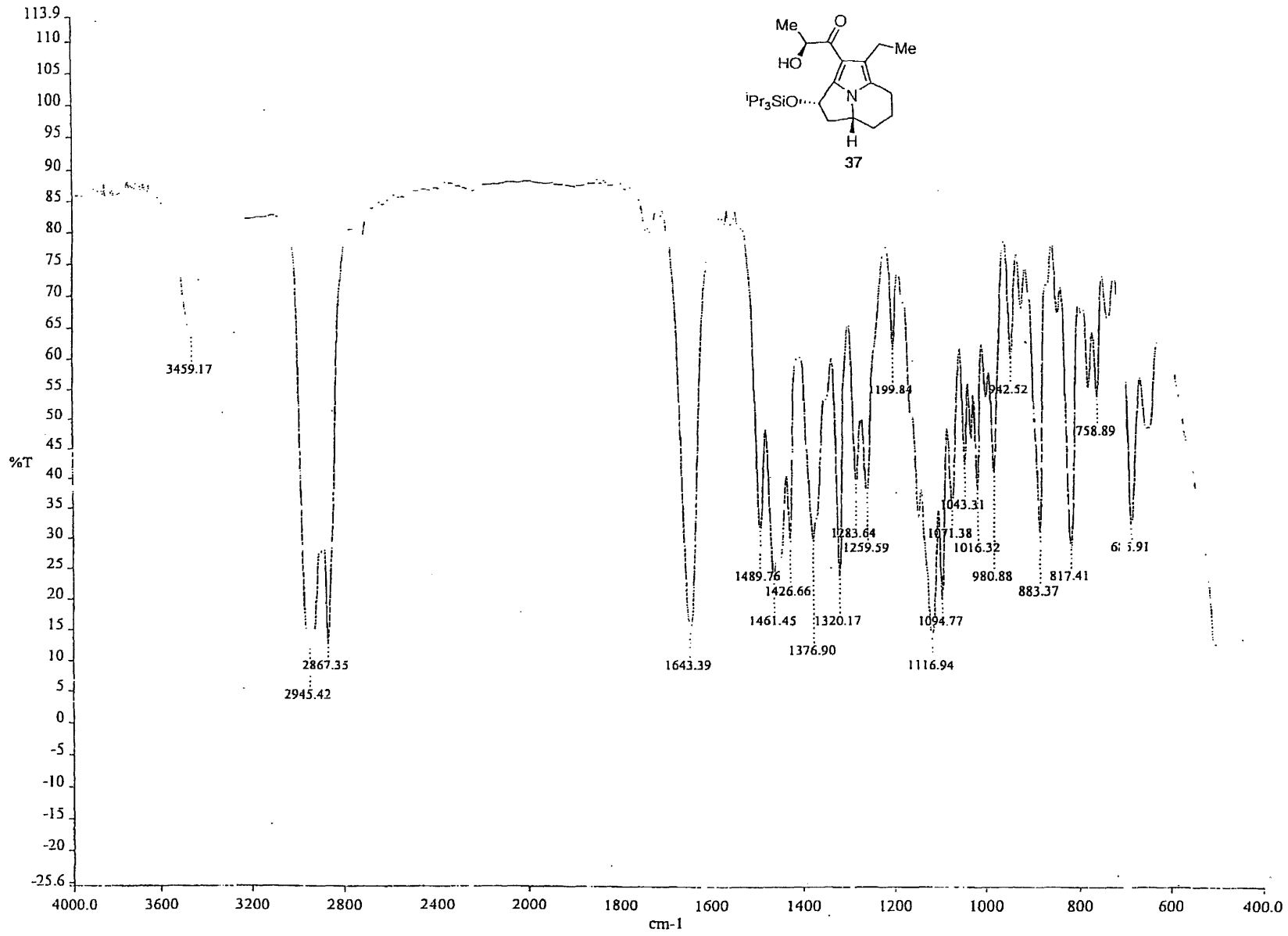
Me
O
HO
Me
$^{i}Pr_3SiO$
N
H
37
%T
cm-1
3459.17
2945.42
2867.35
1643.39
1489.76
1461.45
1426.66
1376.90
1320.17
1283.64
1259.59
1199.84
1116.94
1094.77
1071.38
1043.31
1016.32
980.88
942.52
883.37
817.41
758.89

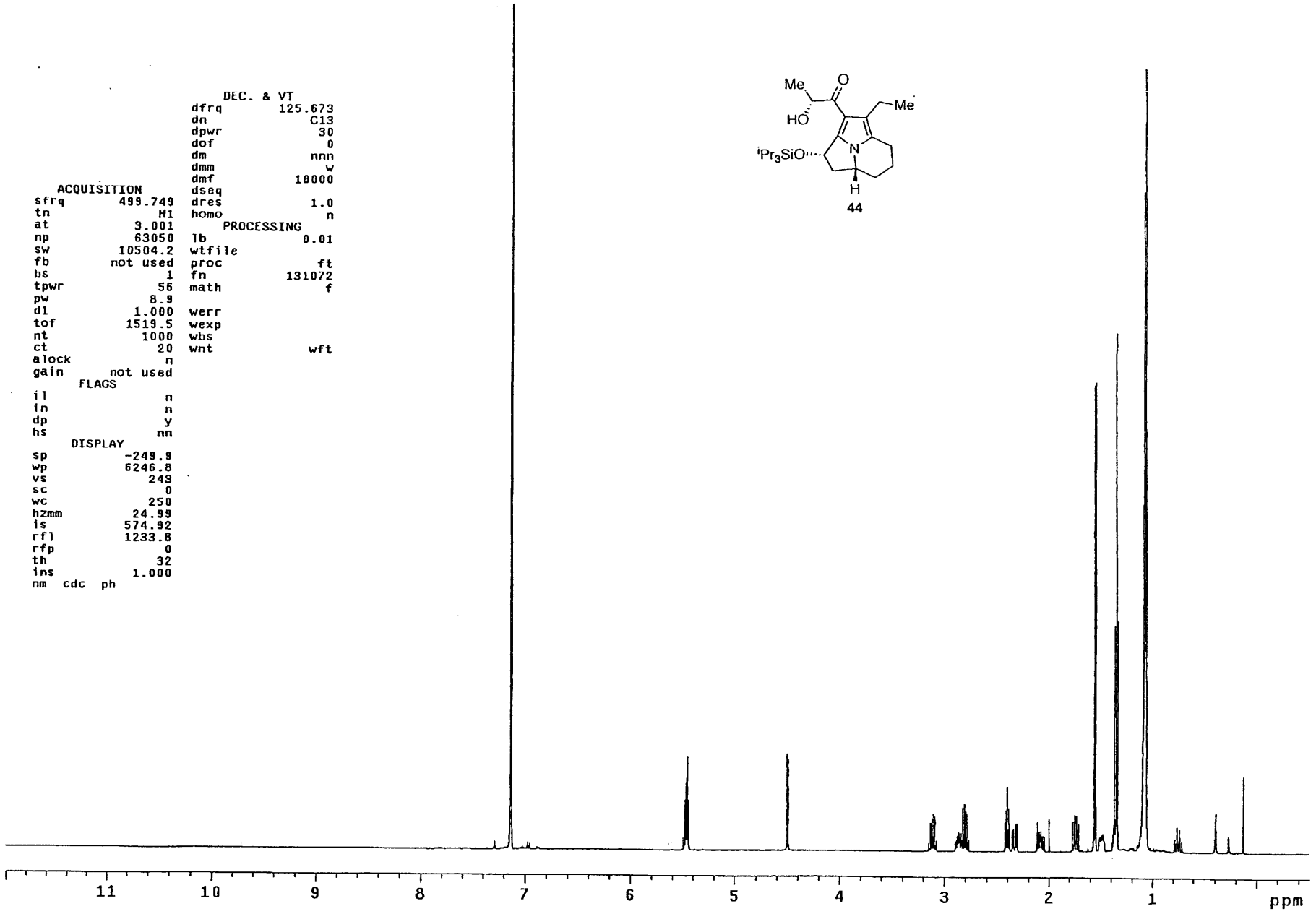
ACQUISITION
sfrq 499.749
tn H1
at 3.001
np 63050
sw 10504.2
fb not used
bs 1
tpwr 56
pw 8.9
d1 1.000
tof 1519.5
nt 1000
ct 20
alock n
gain not used
FLAGS
il n
in n
dp y
hs nn
DISPLAY
sp -249.9
wp 6246.8
vs 243
sc 0
wc 250
hzmm 24.99
is 574.92
rfl 1233.8
rfp 0
th 32
ins 1.000
nm cdc ph
DEC. & VT
dfrq 125.673
dn C13
dpwr 30
dof 0
dm nnn
dmm w
dmf 10000
dseq
dres 1.0
homo n
PROCESSING
lb 0.01
wtfile
proc ft
fn 131072
math f
werr
wexp
wbs
wnt wft
Me
O
HO
Me
iPr3SiO
N
H
44
11
10
9
8
7
6
5
4
3
2
1
ppm

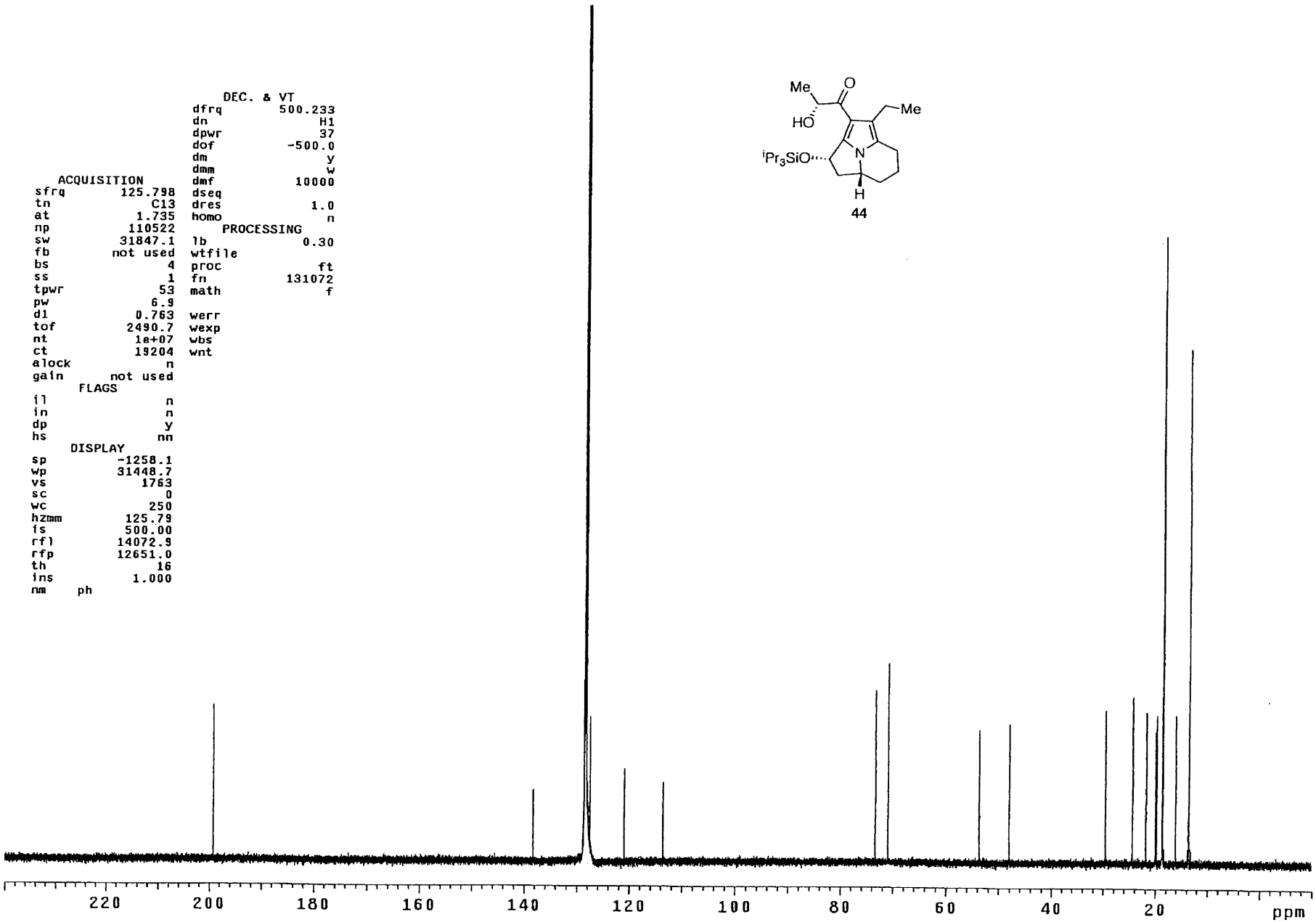
ACQUISITION
sfrq 125.798
tn C13
at 1.735
np 110522
sw 31847.1
fb not used
bs 4
ss 1
tpwr 53
pw 6.9
d1 0.763
tof 2490.7
nt 1e+07
ct 19204
alock n
gain not used
FLAGS
il n
in n
dp y
hs nn
DISPLAY
sp -1258.1
wp 31448.7
vs 1763
sc 0
wc 250
hzmm 125.79
is 500.00
rfl 14072.9
rfp 12651.0
th 16
ins 1.000
nm ph
DEC. & VT
dfrq 500.233
dn H1
dpwr 37
dof -500.0
dm y
dmm w
dmf 10000
dseq
dres 1.0
homo n
PROCESSING
lb 0.30
wtfile
proc ft
fn 131072
math f
werr
wexp
wbs
wnt
Me
O
HO
Me
iPr3SiO
N
H
44
220
200
180
160
140
120
100
80
60
40
20
ppm

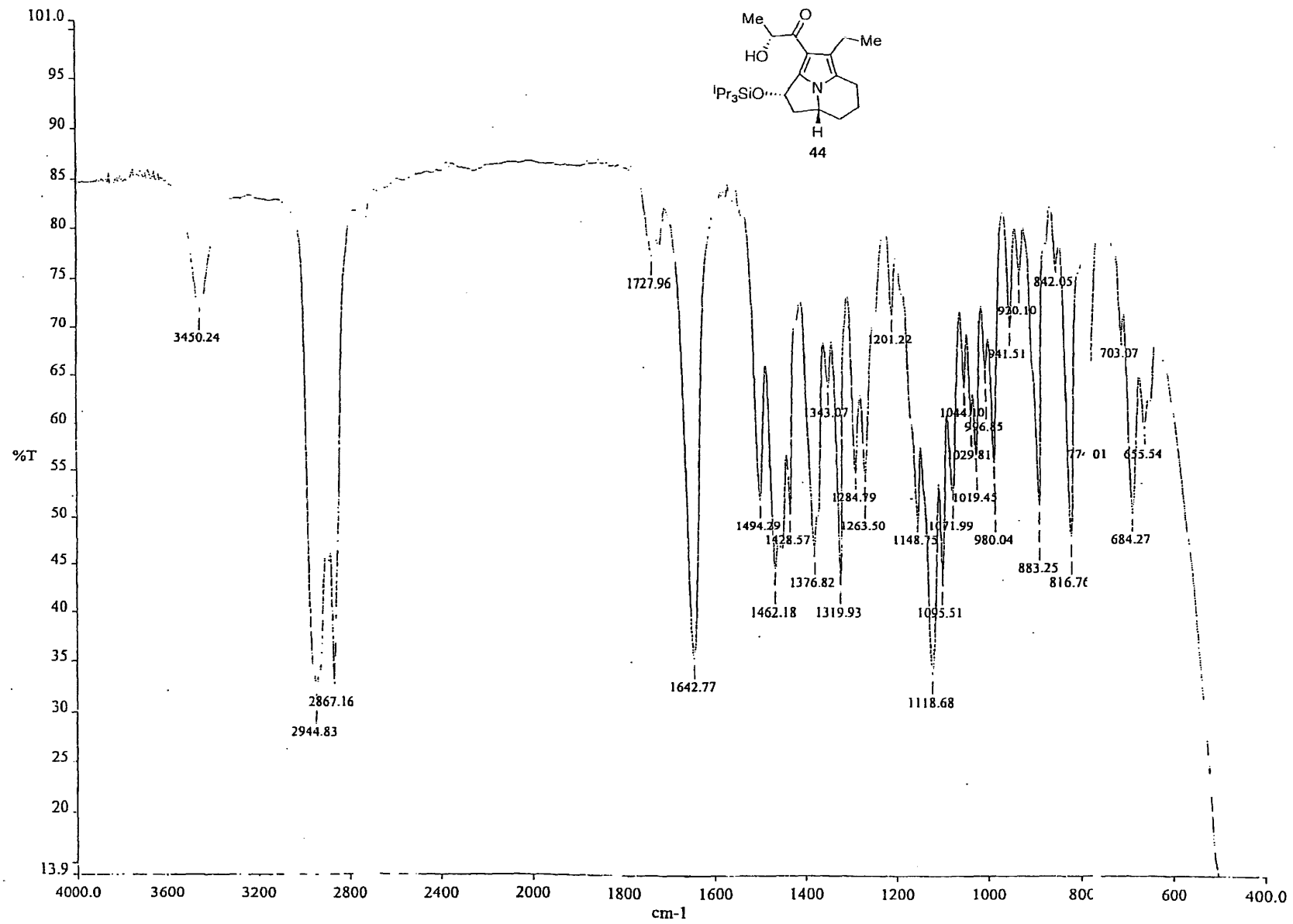
Me
O
Me
HO
$^{i}Pr_3SiO$
N
H
44
%T
cm-1
3450.24
2944.83
2867.16
1727.96
1642.77
1494.29
1462.18
1428.57
1376.82
1343.07
1319.93
1284.79
1263.50
1201.22
1148.75
1118.68
1095.51
1044.10
1019.45
980.04
941.51
920.10
883.25
842.05
816.76
703.07
684.27
655.54

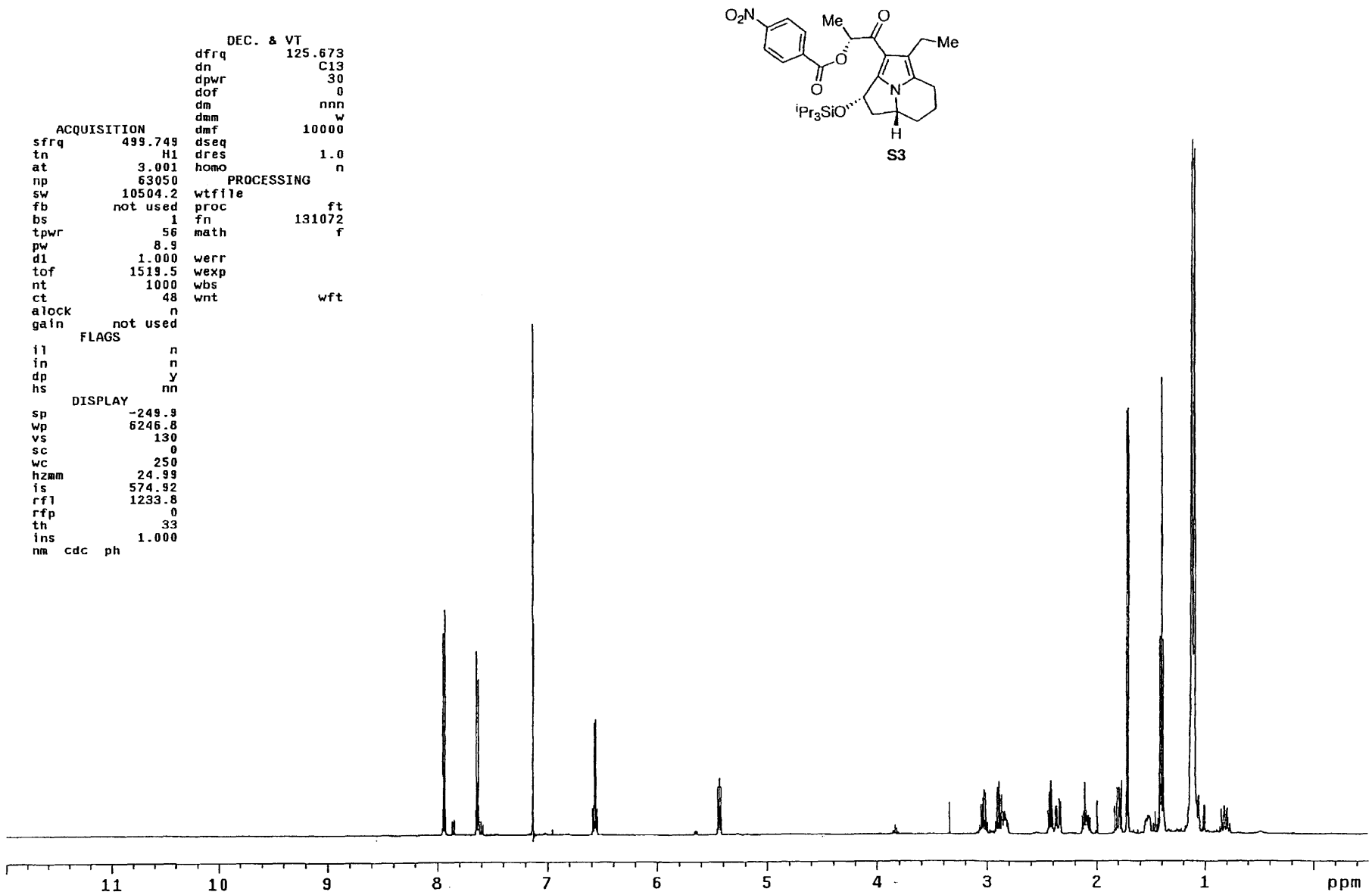
ACQUISITION
sfrq 499.749
tn H1
at 3.001
np 63050
sw 10504.2
fb not used
bs 1
tpwr 56
pw 8.9
d1 1.000
tof 1519.5
nt 1000
ct 48
alock n
gain not used
FLAGS
il n
in n
dp y
hs nn
DISPLAY
sp -249.9
wp 6246.8
vs 130
sc 0
wc 250
hzmm 24.99
is 574.92
rfl 1233.8
rfp 0
th 33
ins 1.000
nm cdc ph
DEC. & VT
dfrq 125.673
dn C13
dpwr 30
dof 0
dm nnn
dmm w
dmf 10000
dseq
dres 1.0
homo n
PROCESSING
wtfile
proc ft
fn 131072
math f
werr
wexp
wbs
wnt wft
O2N
Me
O
O
O
Me
N
iPr3SiO
H
S3
11
10
9
8
7
6
5
4
3
2
1
ppm

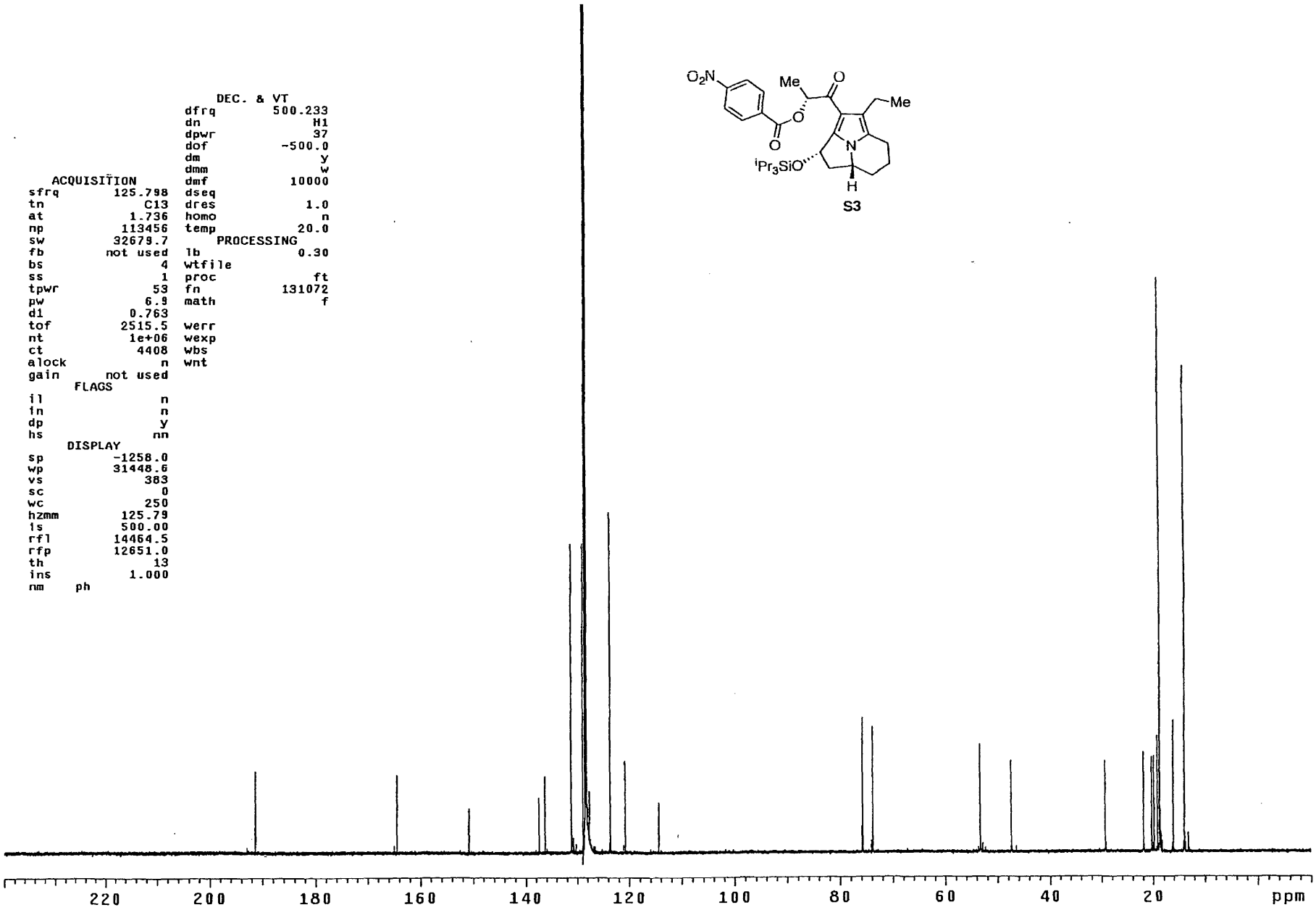
ACQUISITION
sfrq 125.798
tn C13
at 1.736
np 113456
sw 32679.7
fb not used
bs 4
ss 1
tpwr 53
pw 6.9
d1 0.763
tof 2515.5
nt 1e+06
ct 4408
alock n
gain not used
FLAGS
il n
in n
dp y
hs nn
DISPLAY
sp -1258.0
wp 31448.6
vs 383
sc 0
wc 250
hzmm 125.79
is 500.00
rfl 14464.5
rfp 12651.0
th 13
ins 1.000
nm ph
DEC. & VT
dfrq 500.233
dn H1
dpwr 37
dof -500.0
dm y
dmm w
dmf 10000
dseq
dres 1.0
homo n
temp 20.0
PROCESSING
lb 0.30
wtfile
proc ft
fn 131072
math f
werr
wexp
wbs
wnt
O2N
Me
O
Me
O
O
N
iPr3SiO
H
S3
220
200
180
160
140
120
100
80
60
40
20
ppm

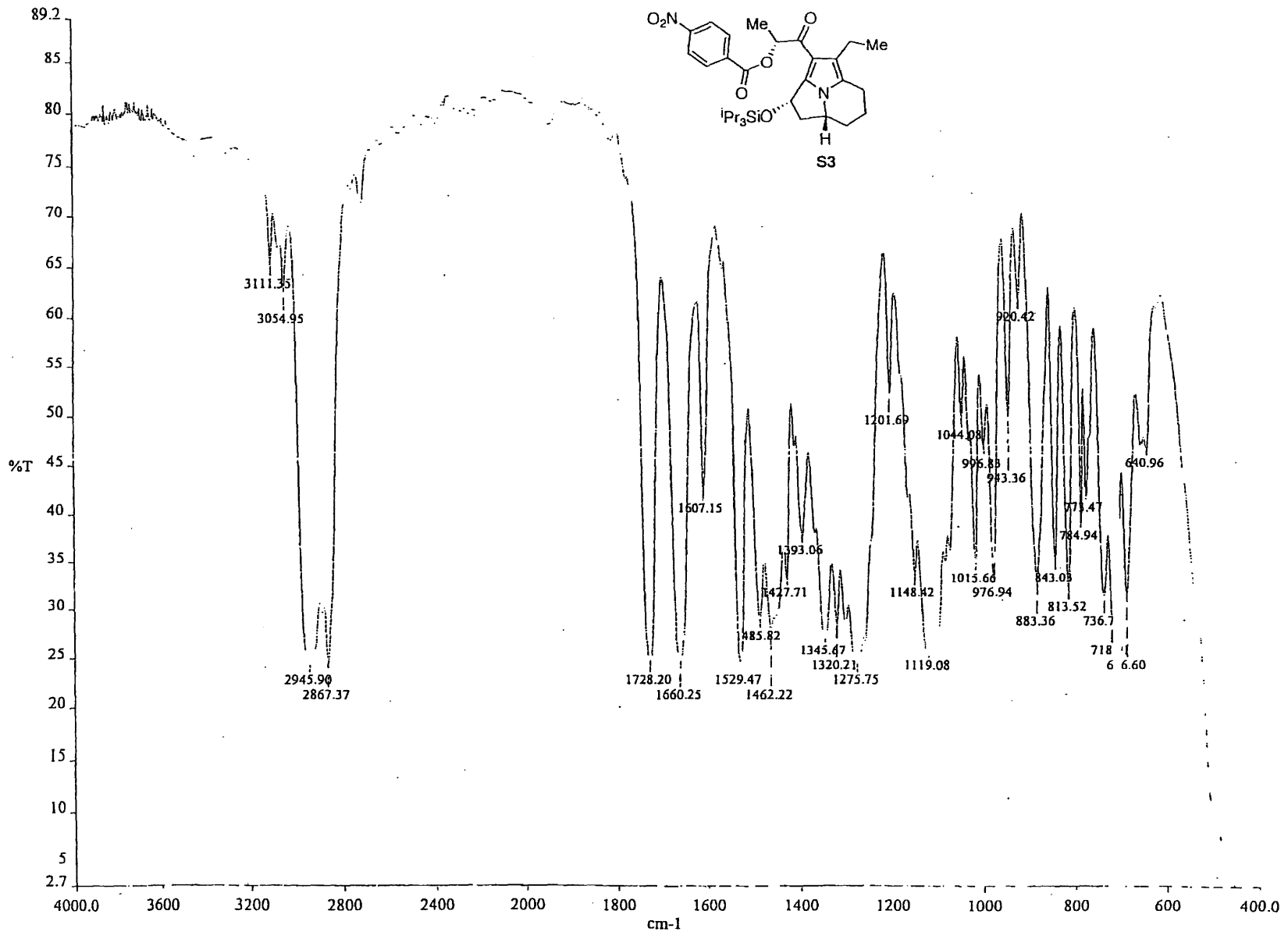
S3
%T
cm-1
89.2
85
80
75
70
65
60
55
50
45
40
35
30
25
20
15
10
5
2.7
4000.0
3600
3200
2800
2400
2000
1800
1600
1400
1200
1000
800
600
400.0
3111.35
3054.95
2945.90
2867.37
1728.20
1660.25
1607.15
1529.47
1462.22
1485.82
1427.71
1393.06
1345.67
1320.21
1275.75
1201.69
1148.42
1119.08
1044.08
1015.66
996.83
976.94
943.36
920.42
883.36
843.03
813.52
784.94
775.47
736.7
718
640.96

ACQUISITION	
sfrq	499.749
tn	H1
at	3.001
np	63050
sw	10504.2
fb	not used
bs	1
tpwr	56
pw	8.9
d1	1.000
tof	1519.5
nt	100
ct	12
alock	n
gain	not used

FLAGS	
il	n
in	n
dp	y
hs	nn

DISPLAY	
sp	-250.0
wp	6246.8
vs	90
sc	0
wc	250
hzmm	24.99
is	188.30
rfl	1233.8
rfp	0
th	25
ins	1.000

nm cdc ph

DEC. & VT	
dfrq	125.673
dn	C13
dpwr	30
dof	0
dm	nnn
dmm	w
dmf	10000
dseq	
dres	1.0
homo	n

PROCESSING	
lb	0.00
wtfile	
proc	ft
fn	131072
math	f
werr	
wexp	
wbs	
wnt	wft

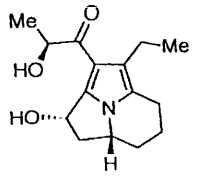

38

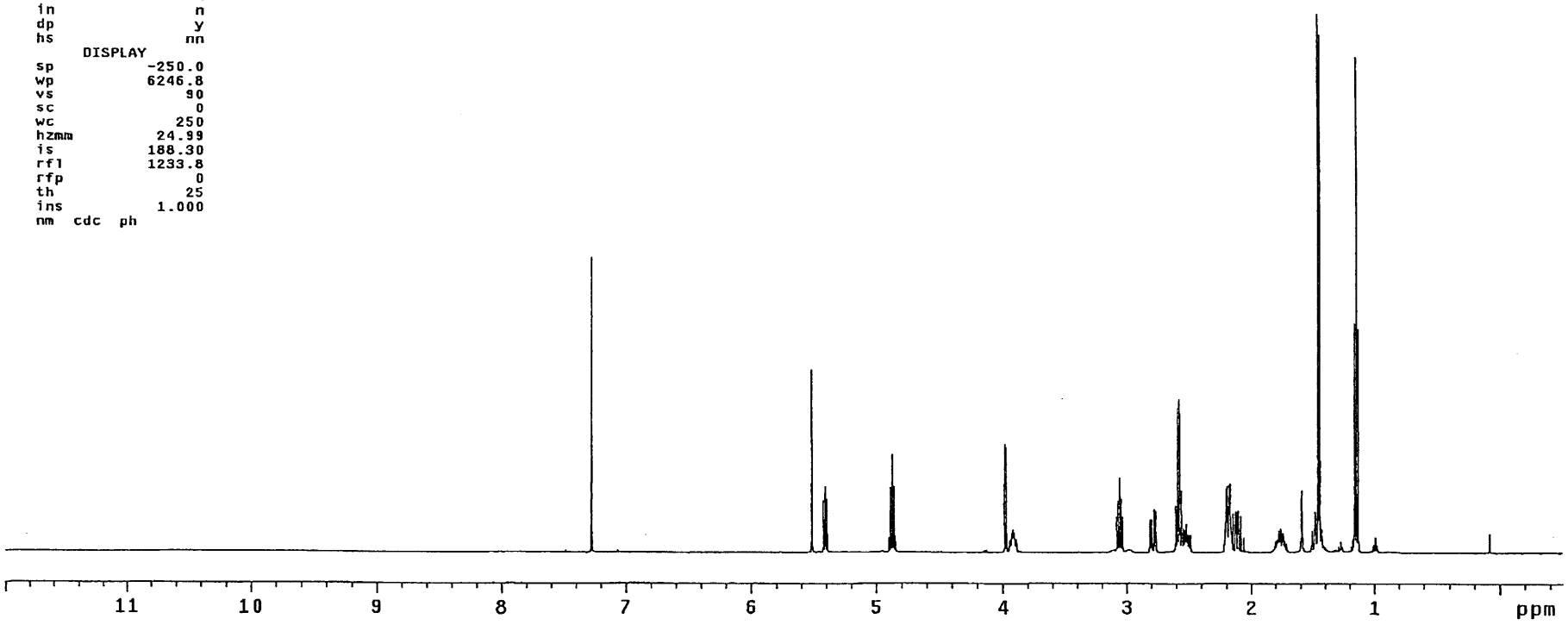

ACQUISITION		DEC. & VT	
sfrq	125.796	dfrq	500.233
tn	C13	dn	H1
at	1.736	dpwr	37
np	131010	dof	-500.0
sw	37735.8	dm	y
fb	not used	dmm	w
bs	4	dmf	10000
ss	1	dseq	
tpwr	53	dres	1.0
pw	6.9	homo	n
d1	0.763	PROCESSING	
tof	631.4	lb	0.30
nt	1e+07	wtfile	
ct	1168	proc	ft
alock	n	fn	131072
gain	not used	math	f
FLAGS		werr	
il	n	wexp	
in	n	wbs	
dp	y	wnt	
hs	nn		
DISPLAY			
sp	-1258.3		
wp	31448.1		
vs	65		
sc	0		
wc	250		
hzmm	125.79		
is	500.00		
rfl	15911.8		
rfp	9686.0		
th	6		
ins	1.000		
nm	ph		

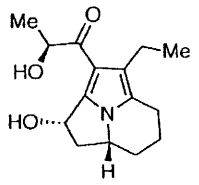

38

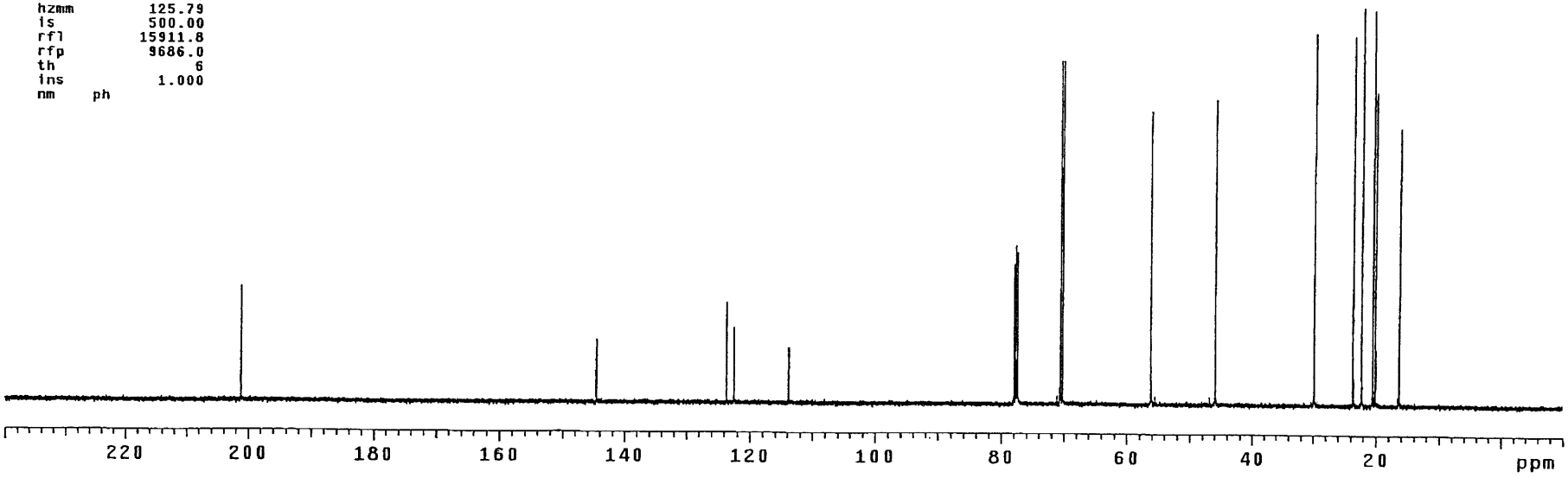

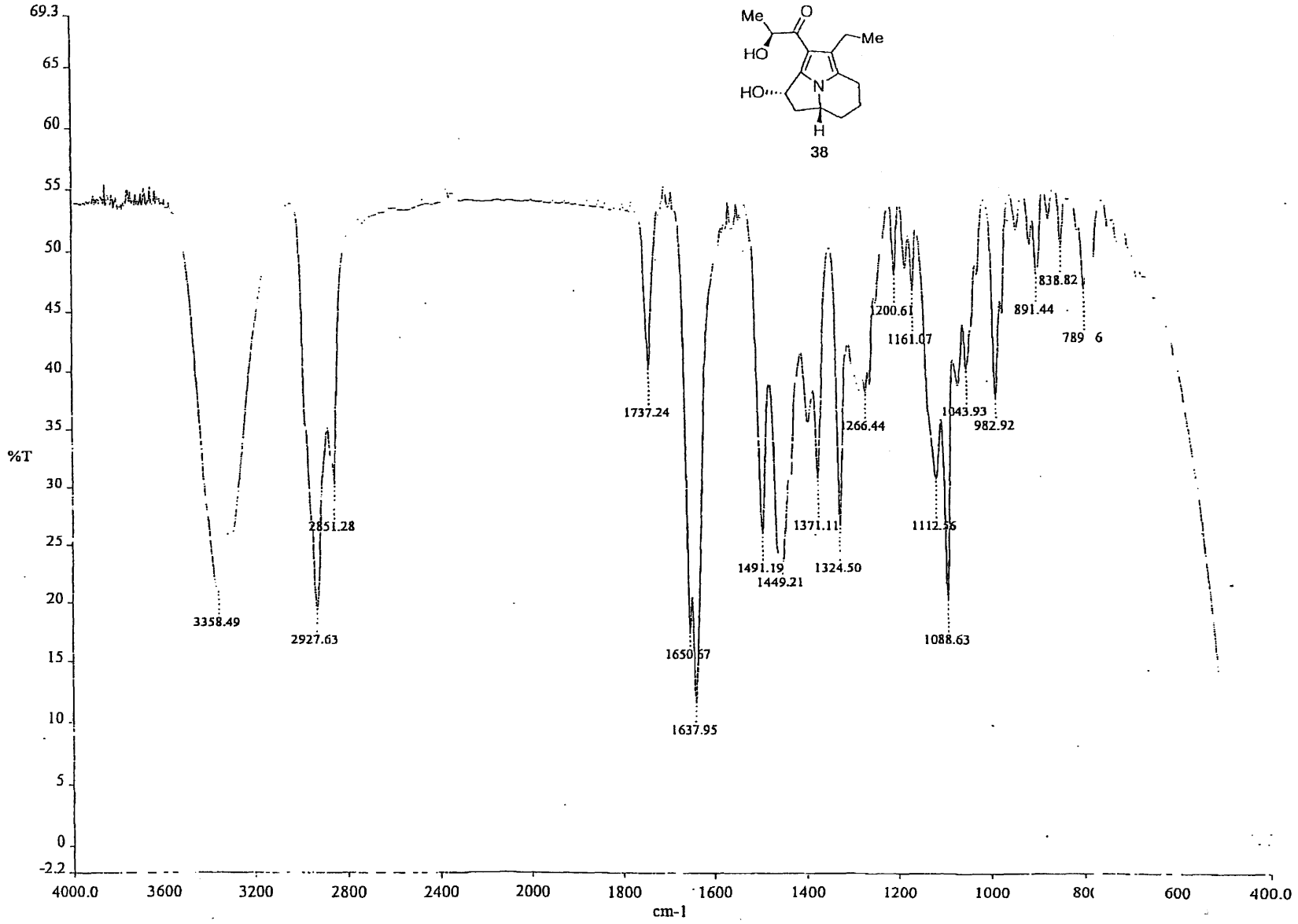
Me
O
Me
HO
HO
N
H
38
69.3
65
60
55
50
45
40
35
%T
30
25
20
15
10
5
0
-2.2
3358.49
2927.63
2851.28
1737.24
1650.67
1637.95
1491.19
1449.21
1371.11
1324.50
1266.44
1200.61
1161.07
1112.56
1088.63
1043.93
982.92
891.44
838.82
789.6
4000.0
3600
3200
2800
2400
2000
1800
1600
1400
1200
1000
800
600
400.0
cm-1

ACQUISITION		DEC. & VT	
sfrq	499.748	dfrq	125.673
tn	H1	dn	C13
at	3.001	dpwr	30
np	40494	dof	0
sw	6747.6	dm	nnn
fb	not used	dmm	w
bs	1	dmf	10000
tpwr	56	dseq	
pw	8.9	dres	1.0
d1	1.000	homo	n
tof	624.4	PROCESSING	
nt	1000	lb	0.05
ct	24	wtfile	
alock	n	proc	ft
gain	not used	fn	131072
FLAGS		math	f
il	n	werr	
in	n	wexp	
dp	y	wbs	
hs	nn	wnt	wft
DISPLAY			
sp	-208.6		
wp	6242.1		
vs	90		
sc	0		
wc	250		
hzmm	24.97		
is	321.72		
rfl	208.7		
rfp	0		
th	25		
ins	1.000		
nm cdc ph			

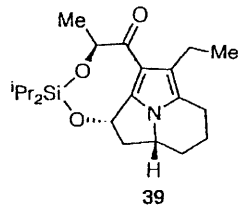

39

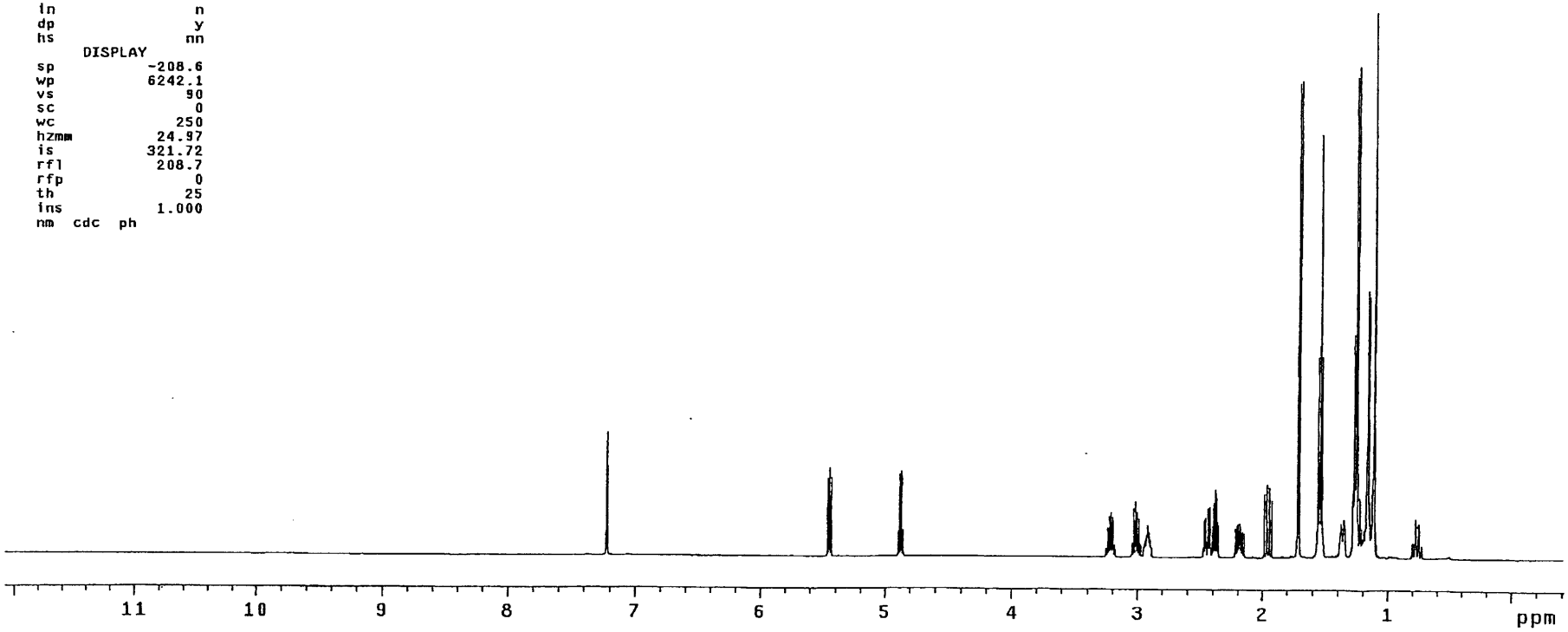

ACQUISITION		DEC. & VT	
sfrq	125.796	dfrq	500.233
tn	C13	dn	H1
at	1.736	dpwr	37
np	131010	dof	-500.0
sw	37735.8	dm	y
fb	not used	dmm	w
bs	4	dmf	10000
ss	1	dseq	
tpwr	53	dres	1.0
pw	6.9	homo	n
d1	0.763	PROCESSING	
tof	631.4	lb	0.30
nt	1e+09	wtfile	
ct	17872	proc	ft
alock	n	fn	131072
gain	not used	math	f
FLAGS		werr	
il	n	wexp	
in	n	wbs	
dp	y	wnt	
hs	nn		
DISPLAY			
sp	-1258.3		
wp	31448.1		
vs	711		
sc	0		
wc	250		
hzmm	125.79		
is	500.00		
rfl	15911.8		
rfp	9686.0		
th	20		
ins	1.000		
nm	ph		

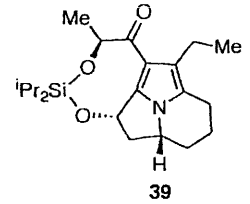

39

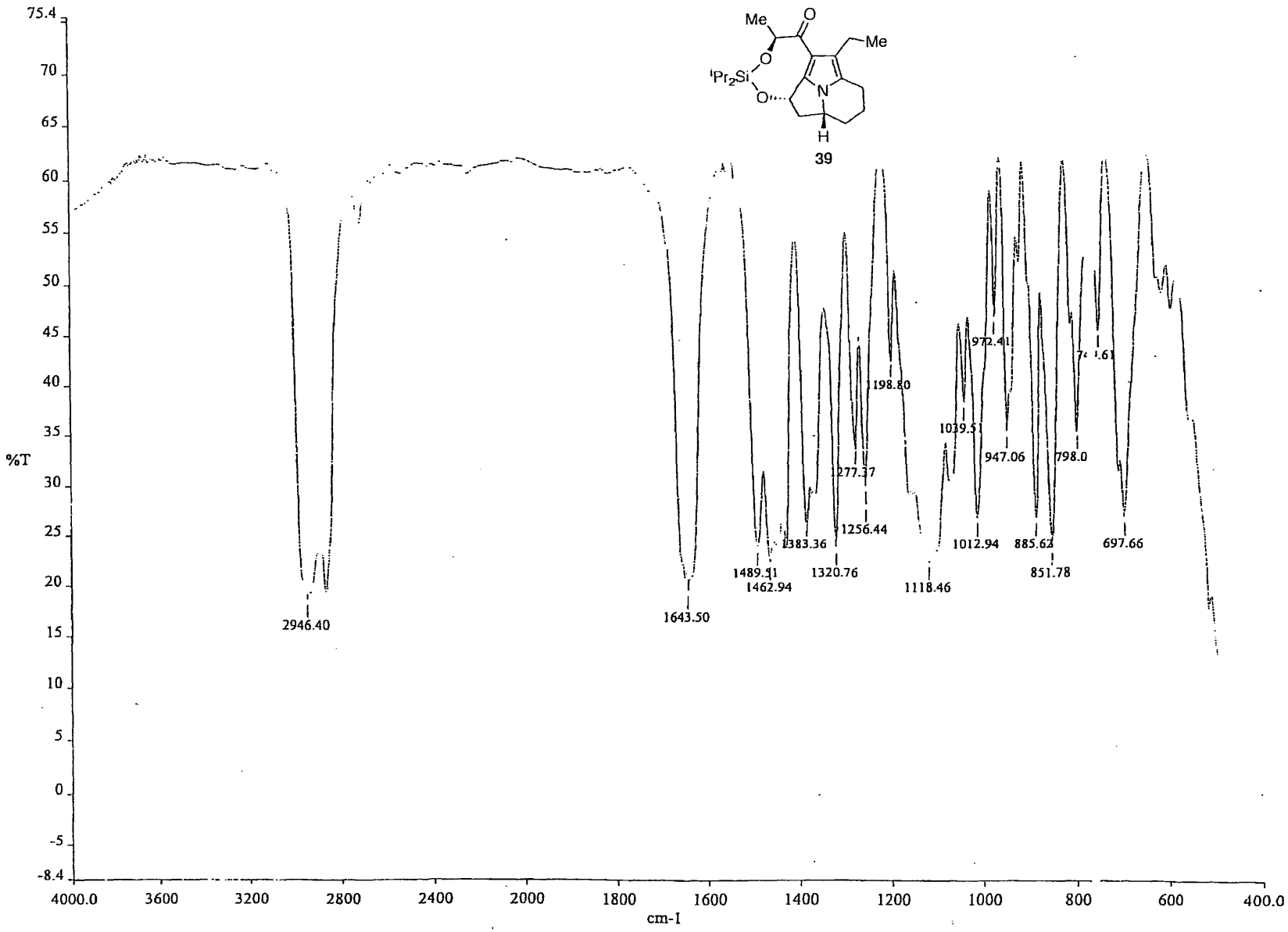
Me
O
Me
$^{i}Pr_2Si$
O
O
N
H
39
%T
75.4
70
65
60
55
50
45
40
35
30
25
20
15
10
5
0
-5
-8.4
2946.40
1643.50
1489.51
1462.94
1383.36
1320.76
1256.44
1277.37
1198.80
1118.46
1039.51
1012.94
972.41
947.06
885.62
851.78
798.0
697.66
4000.0
3600
3200
2800
2400
2000
1800
1600
1400
1200
1000
800
600
400.0
cm-1

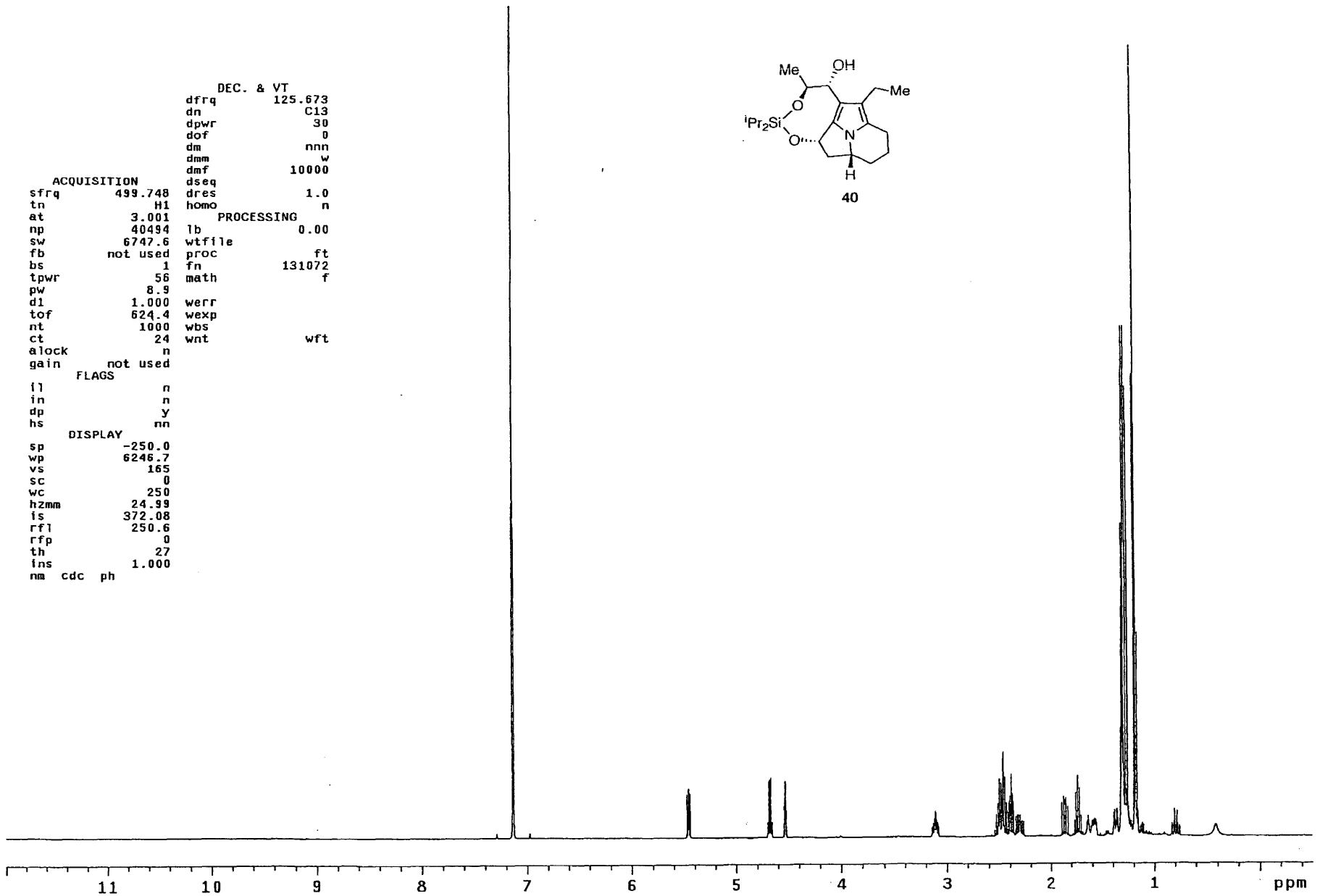
ACQUISITION
sfrq 499.748
tn H1
at 3.001
np 40494
sw 6747.6
fb not used
bs 1
tpwr 56
pw 8.9
d1 1.000
tof 624.4
nt 1000
ct 24
alock n
gain not used
FLAGS
il n
in n
dp y
hs nn
DISPLAY
sp -250.0
wp 6246.7
vs 165
sc 0
wc 250
hzmm 24.99
is 372.08
rfl 250.6
rfp 0
th 27
ins 1.000
nm cdc ph
DEC. & VT
dfrq 125.673
dn C13
dpwr 30
dof 0
dm nnn
dmm w
dmf 10000
dseq
dres 1.0
homo n
PROCESSING
lb 0.00
wtfile
proc ft
fn 131072
math f
werr
wexp
wbs
wnt wft
Me
OH
Me
iPr2Si
O
O
N
H
40
11
10
9
8
7
6
5
4
3
2
1
ppm

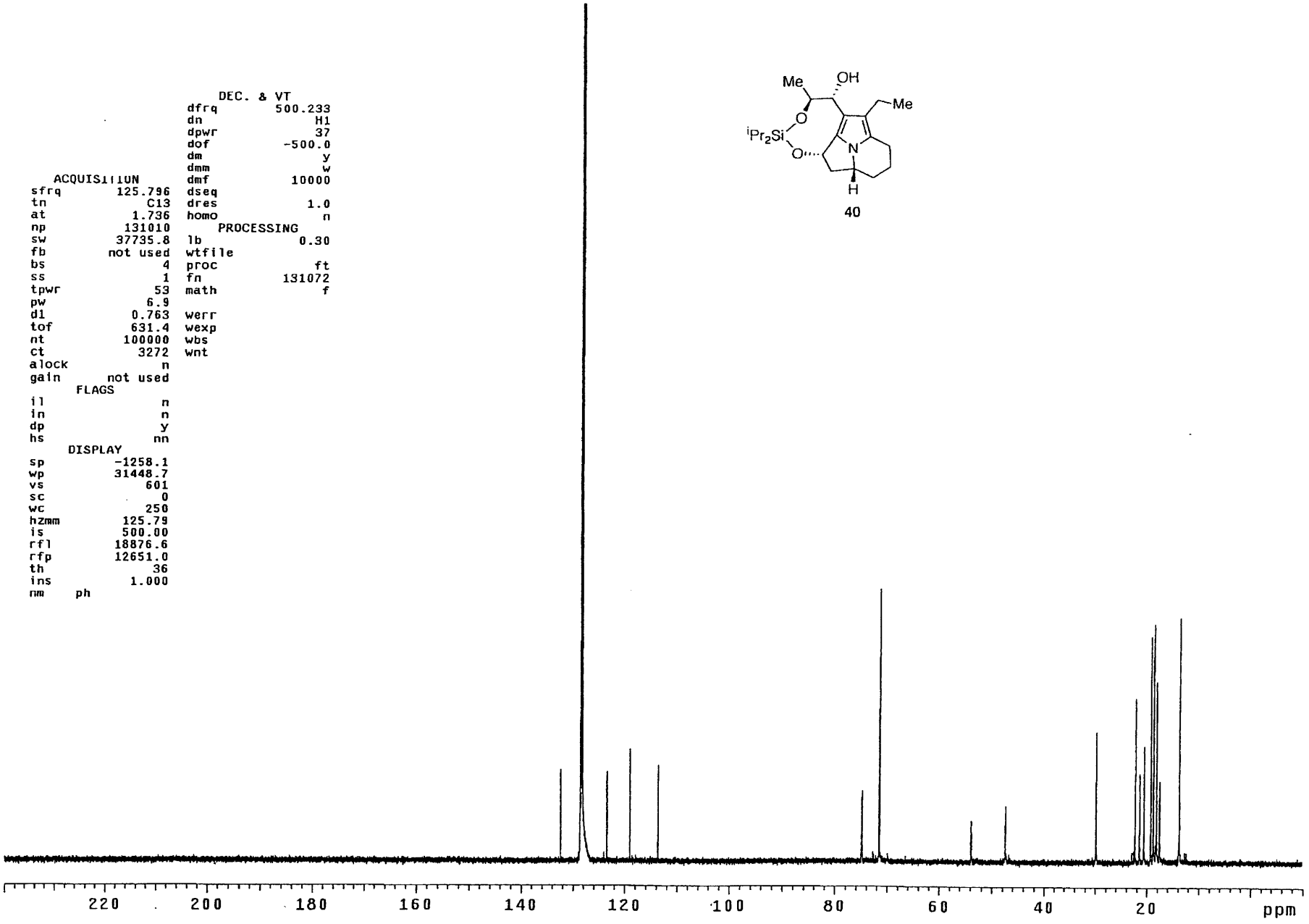
ACQUISITION
sfrq 125.796
tn C13
at 1.736
np 131010
sw 37735.8
fb not used
bs 4
ss 1
tpwr 53
pw 6.9
d1 0.763
tof 631.4
nt 100000
ct 3272
alock n
gain not used
FLAGS
il n
in n
dp y
hs nn
DISPLAY
sp -1258.1
wp 31448.7
vs 601
sc 0
wc 250
hzmm 125.79
is 500.00
rfl 18876.6
rfp 12651.0
th 36
ins 1.000
nm ph
DEC. & VT
dfrq 500.233
dn H1
dpwr 37
dof -500.0
dm y
dmm w
dmf 10000
dseq
dres 1.0
homo n
PROCESSING
lb 0.30
wtfile
proc ft
fn 131072
math f
werr
wexp
wbs
wnt
Me
OH
Me
O
iPr2Si
O
N
H
40
220
200
180
160
140
120
100
80
60
40
20
ppm

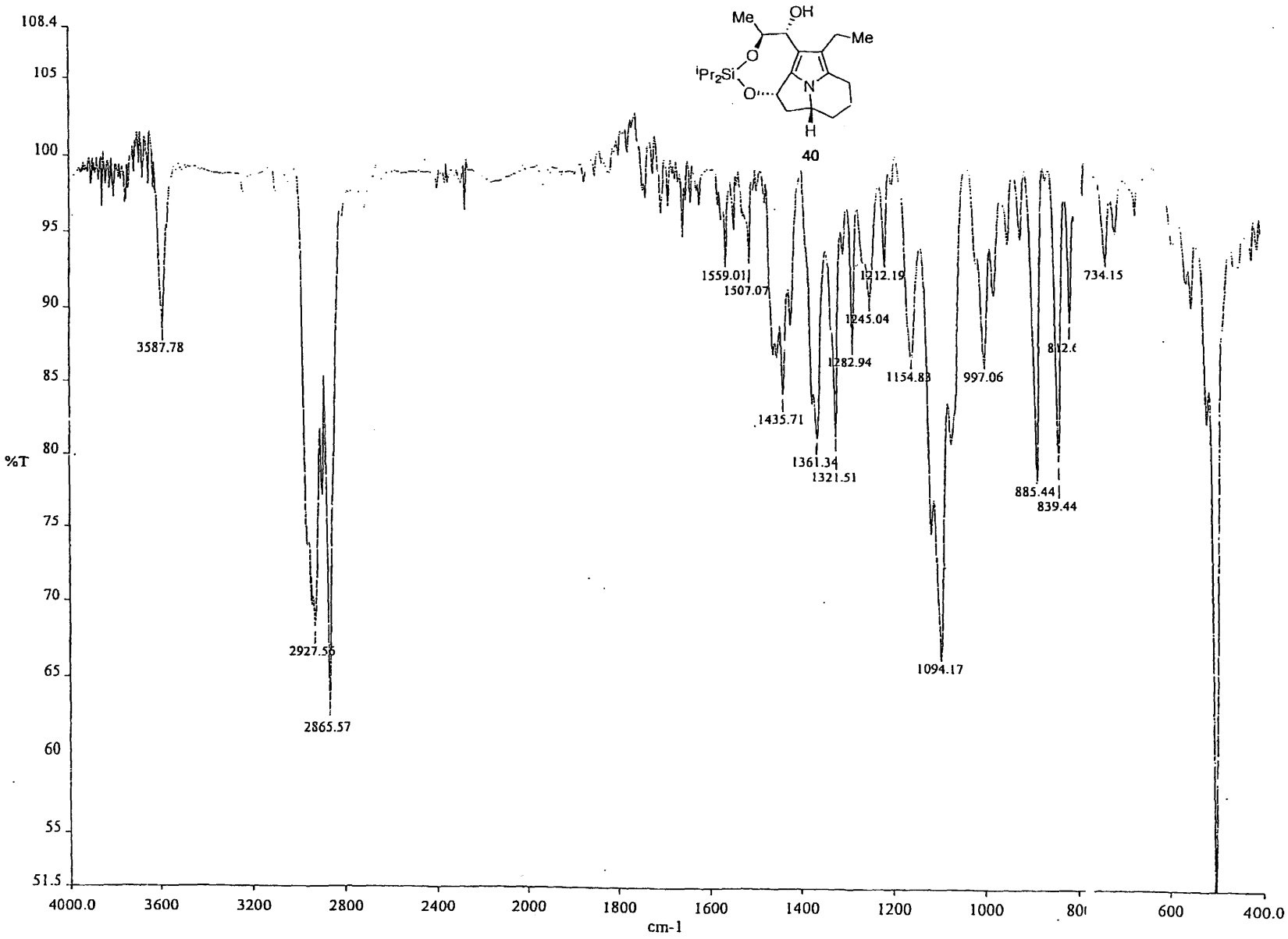
Me
OH
Me
$^{i}Pr_2Si$
O
O
N
H
40
%T
108.4
105
100
95
90
85
80
75
70
65
60
55
51.5
3587.78
2927.56
2865.57
1559.01
1507.07
1435.71
1361.34
1321.51
1282.94
1245.04
1212.19
1154.83
1094.17
997.06
885.44
839.44
734.15
4000.0
3600
3200
2800
2400
2000
1800
1600
1400
1200
1000
600
400.0
cm-1

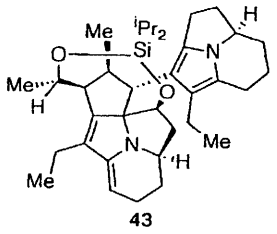

43

ACQUISITION	
sfrq	499.748
tn	H1
at	3.001
np	40494
sw	6747.6
fb	not used
bs	1
tpwr	56
pw	8.9
d1	1.000
tof	624.4
nt	1000
ct	80
alock	n
gain	not used

FLAGS	
il	n
in	n
dp	y
hs	nn

DISPLAY	
sp	-208.6
wp	6246.7
vs	135
sc	0
wc	250
hzmm	1.70
is	15.98
rfl	208.7
rfp	0
th	39
ins	3.000
nm	cdc ph

DEC. & VT	
dfrq	125.673
dn	C13
dpwr	30
dof	0
dm	nnn
dmm	w
dmf	10000
dseq	
dres	1.0
homo	n

PROCESSING	
wtfile	
proc	ft
fn	131072
math	f
werr	
wexp	
wbs	
wnt	wft

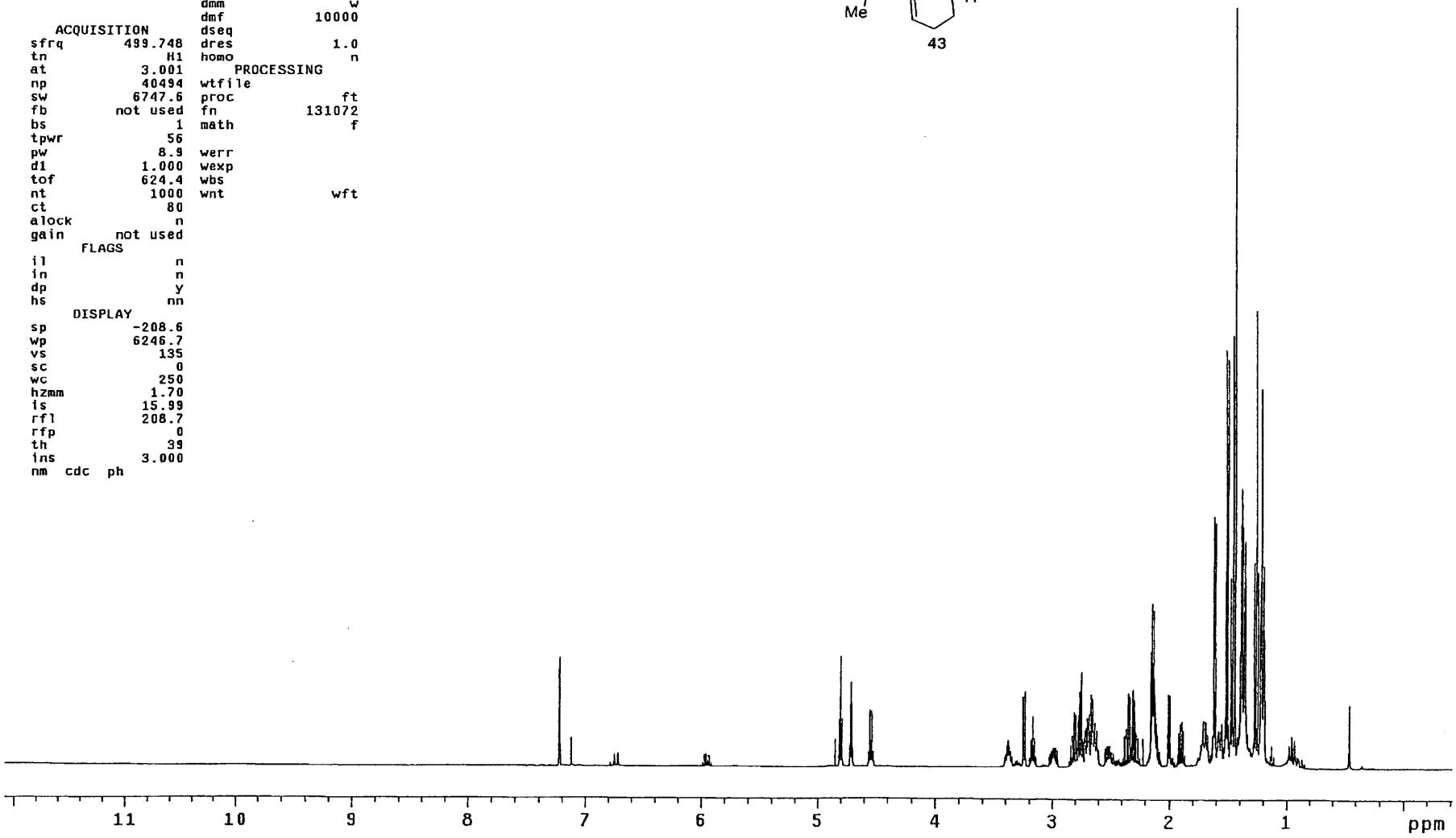

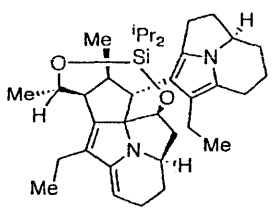

43

ACQUISITION		DEC. & VT	
sfrq	125.796	dfrq	500.233
tn	C13	dn	H1
at	1.736	dpwr	37
np	131010	dof	-500.0
sw	37735.8	dm	y
fb	not used	dmm	w
bs	4	dmf	10000
ss	1	dseq	
tpwr	53	dres	1.0
pw	6.9	homo	n
d1	0.763	PROCESSING	
tof	631.4	lb	0.30
nt	1e+08	wtfile	
ct	34176	proc	ft
alock	n	fn	131072
gain	not used	math	f
FLAGS		werr	
il	n	wexp	
in	n	wbs	
dp	y	wnt	
hs	nn		
DISPLAY			
sp	-1258.1		
wp	31448.7		
vs	3883		
sc	0		
wc	250		
hzmm	3.14		
is	500.00		
rfl	18876.6		
rfp	12651.0		
th	22		
ins	1.000		
ai	ph		

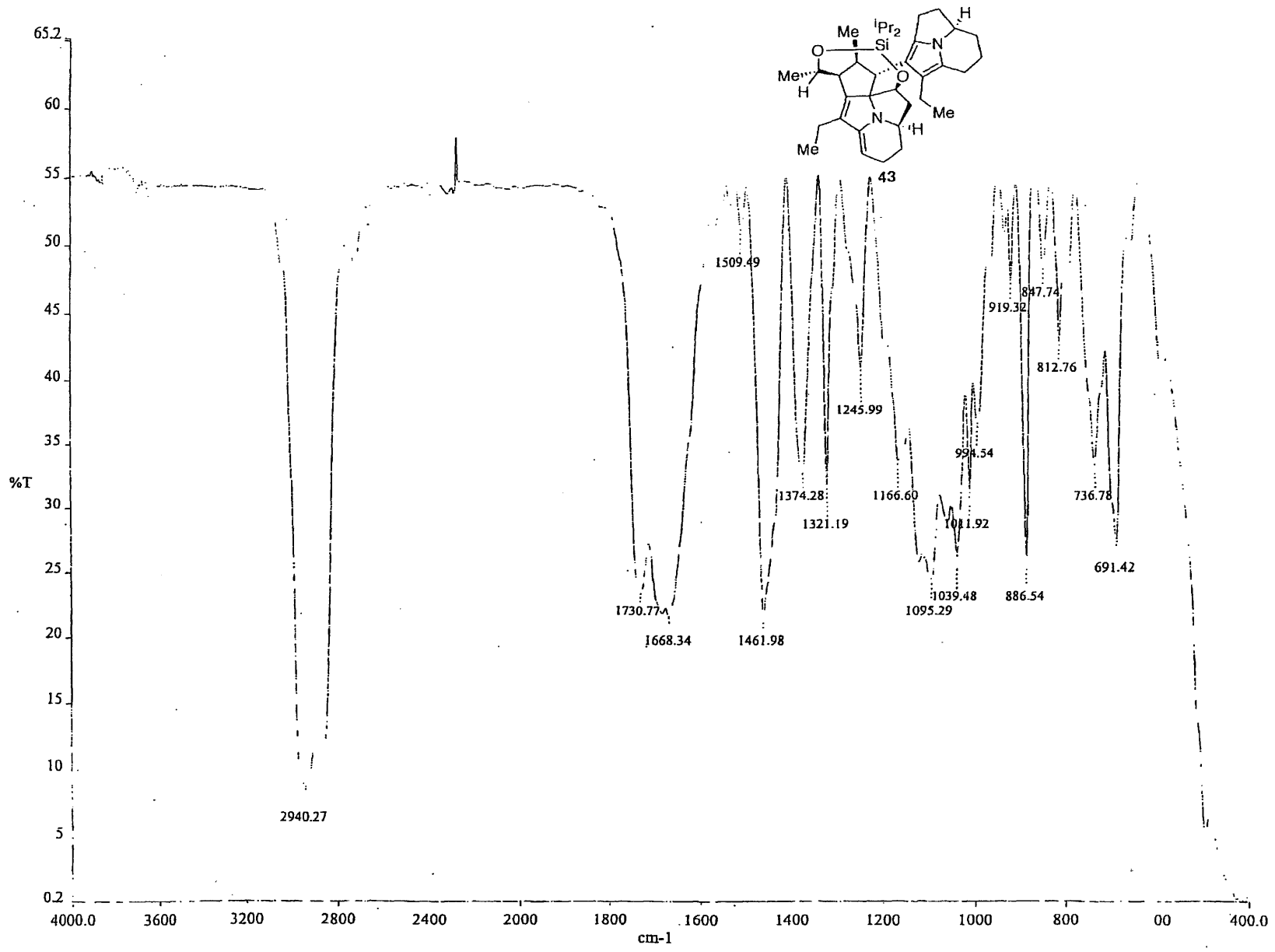
65.2
60
55
50
45
40
35
30
25
20
15
10
5
0.2
%T
4000.0
3600
3200
2800
2400
2000
1800
1600
1400
1200
1000
800
00
400.0
cm-1
2940.27
1730.77
1668.34
1509.49
1461.98
1374.28
1321.19
1245.99
1166.60
1095.29
1039.48
1011.92
994.54
919.32
886.54
847.74
812.76
736.78
691.42
Me
iPr2
Si
O
Me
H
O
N
H
Me
N
H
Me
43

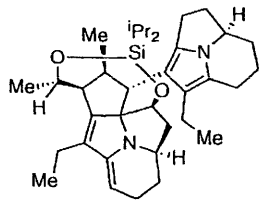
Me
iPr2
Si
O
Me
H
O
H
N
N
H
Me
Me

43

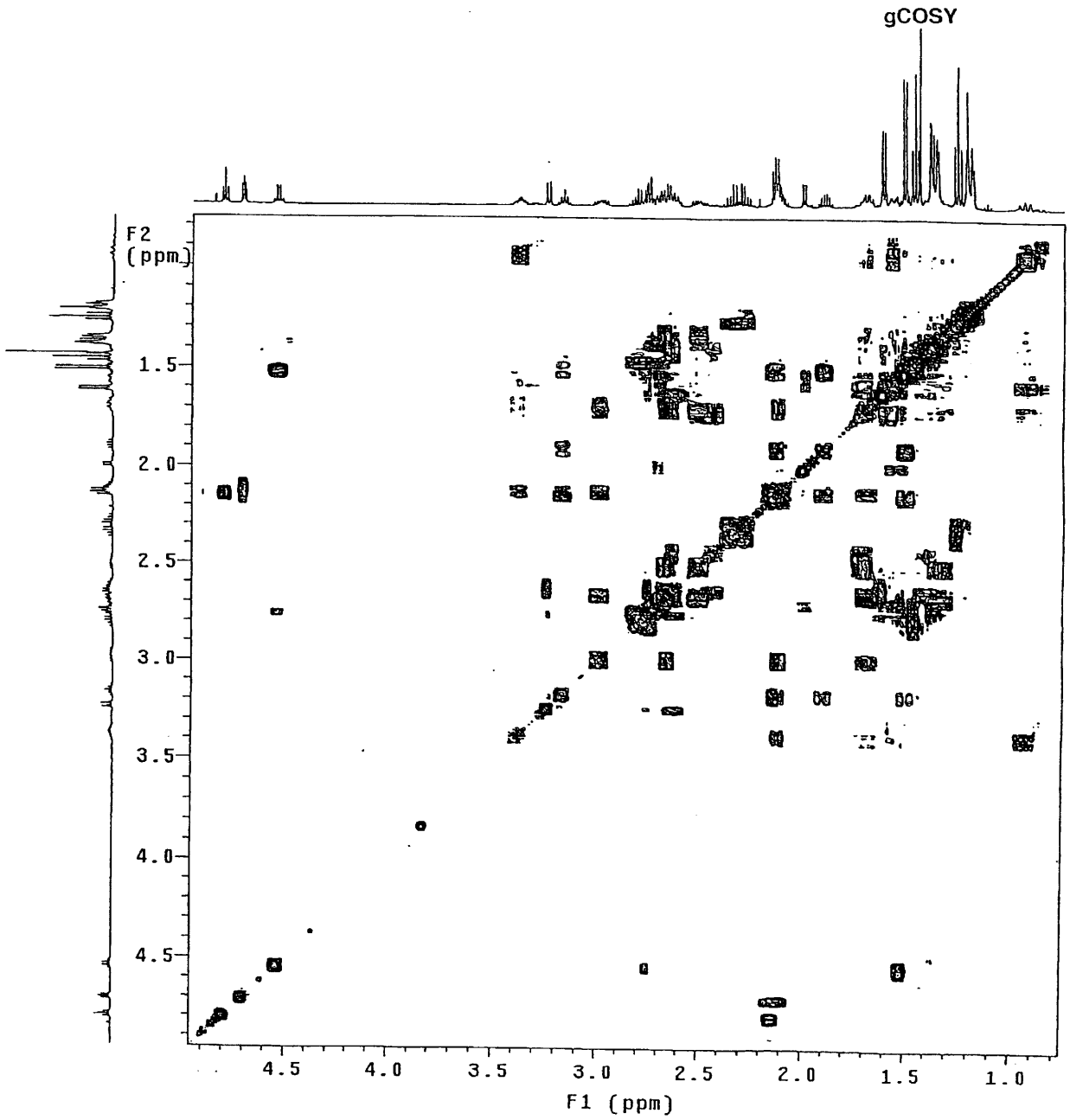
gCOSY
F2
(ppm)
1.5
2.0
2.5
3.0
3.5
4.0
4.5
4.5
4.0
3.5
3.0
2.5
2.0
1.5
1.0
F1 (ppm)

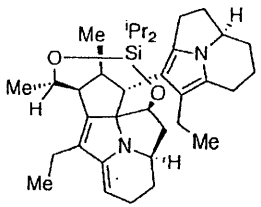
Me
iPr2
Si
O
Me
H
O
N
H
Me
N
H
Me

43

gNOESY

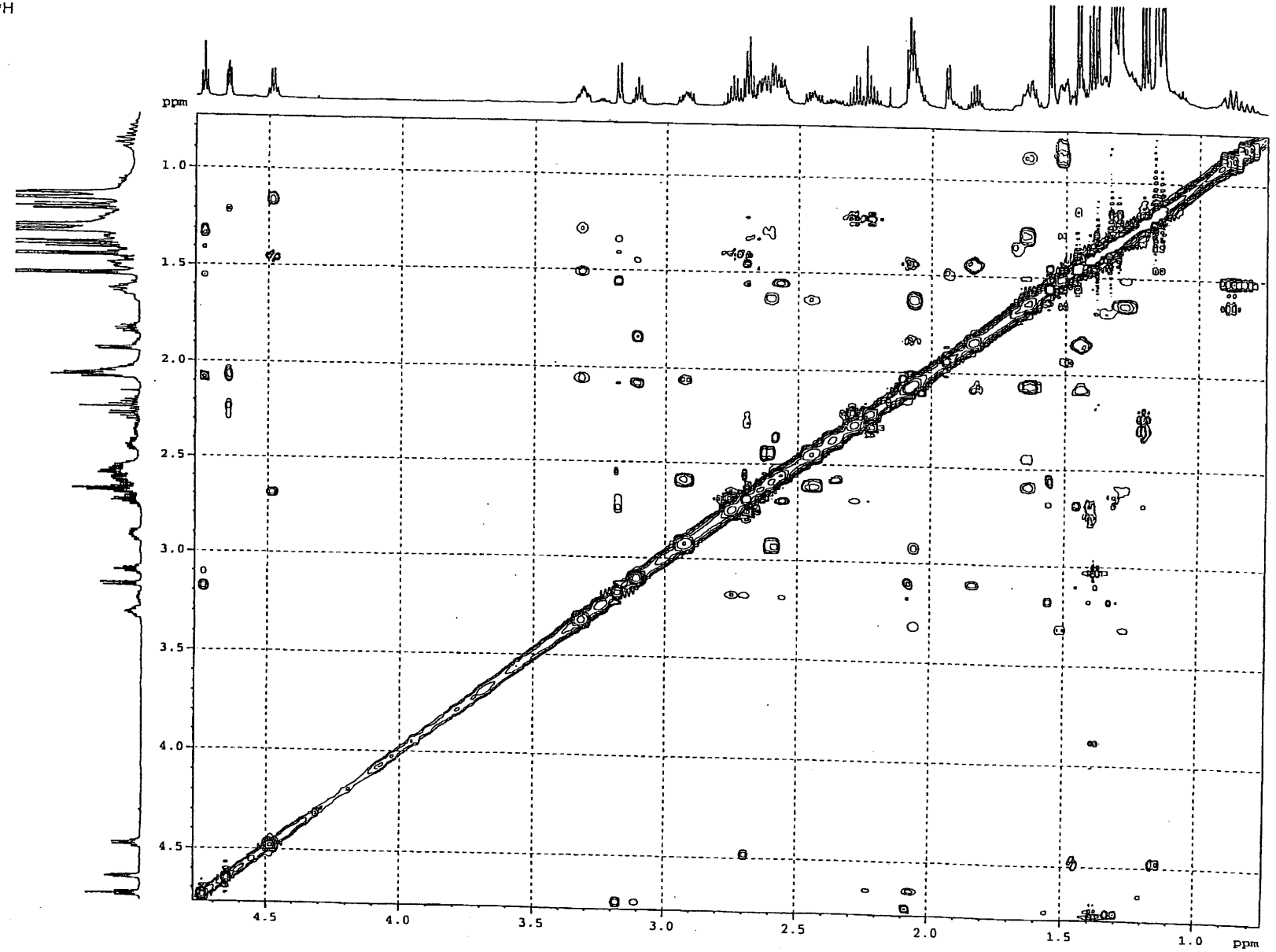
ppm
1.0
1.5
2.0
2.5
3.0
3.5
4.0
4.5
4.5
4.0
3.5
3.0
2.5
2.0
1.5
1.0
ppm

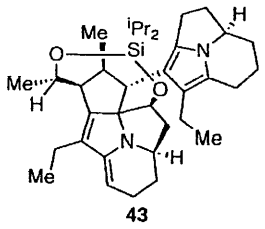
Me
iPr2
Si
O
Me
H
O
N
H
Me
N
H
Me

43

HSQC

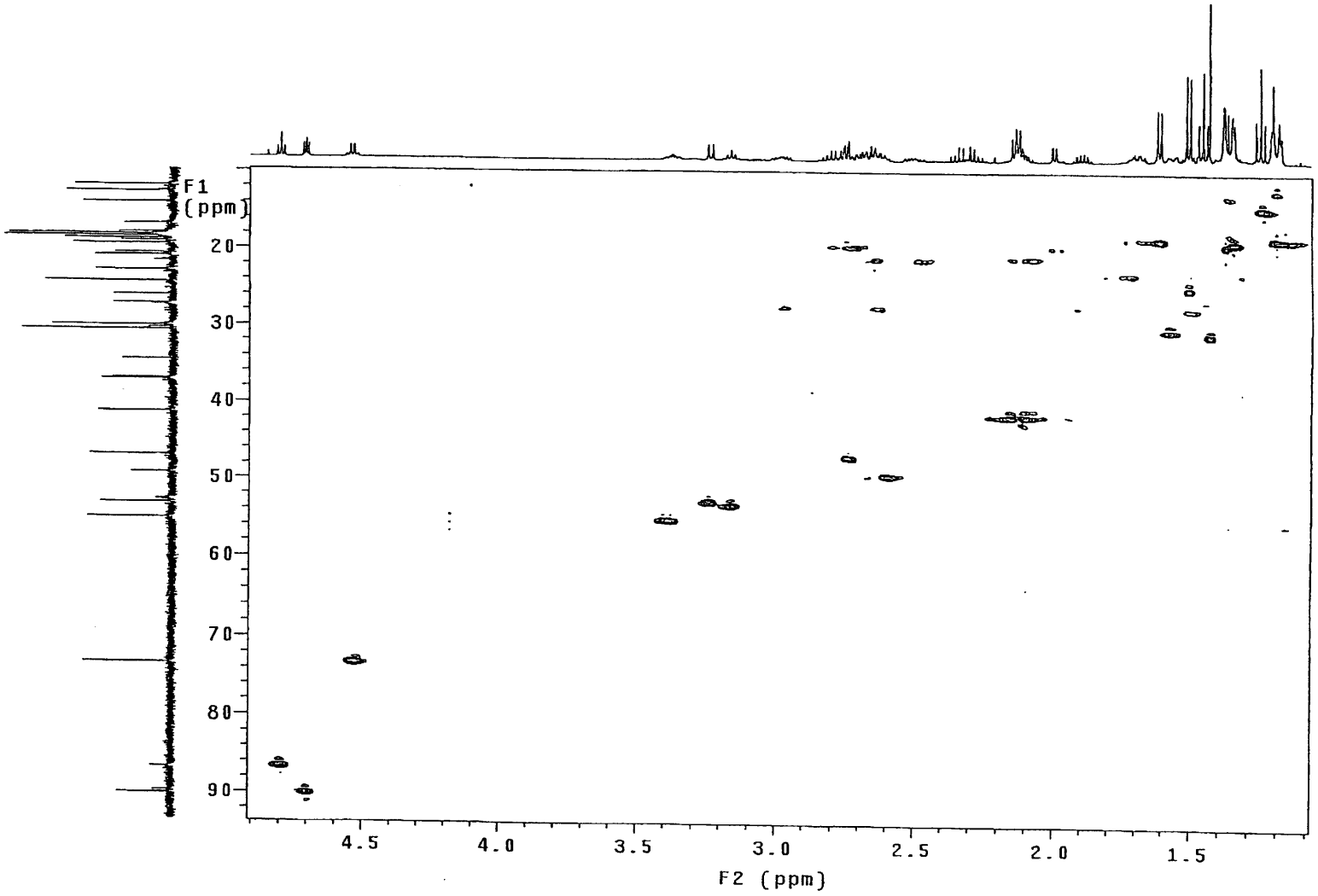
F1
(ppm)
20
30
40
50
60
70
80
90
4.5
4.0
3.5
3.0
2.5
2.0
1.5
F2 (ppm)

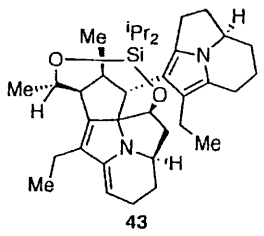
Me
iPr2
Si
O
H
Me
H
O
N
Me
N
H
Me

43

gHMBC

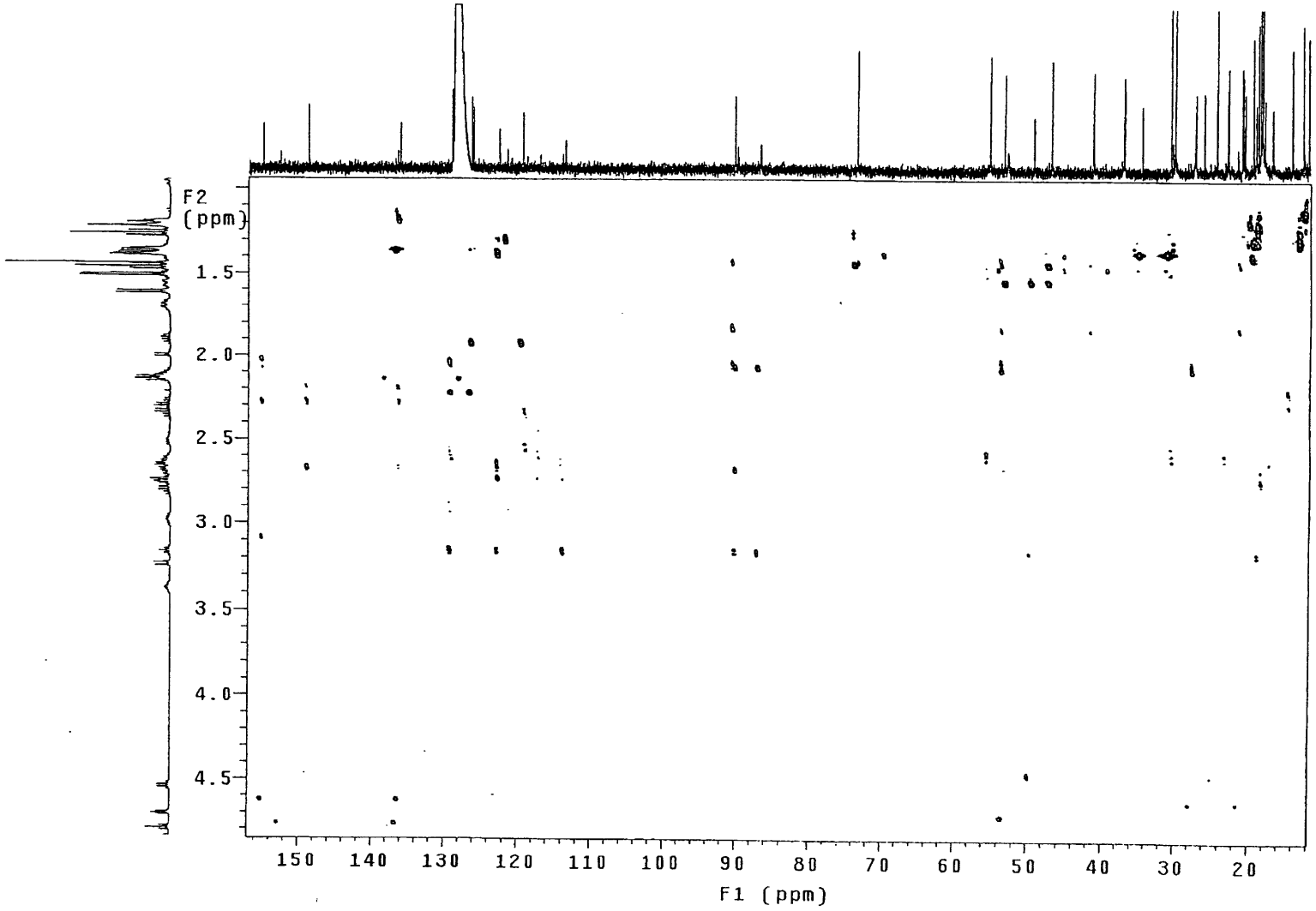
F2
(ppm)
1.5
2.0
2.5
3.0
3.5
4.0
4.5
150
140
130
120
110
100
90
80
70
60
50
40
30
20
F1 (ppm)

ACQUISITION	
sfrq	499.749
tn	H1
at	3.001
np	63050
sw	10504.2
fb	not used
bs	1
tpwr	56
pw	8.9
d1	1.000
tof	1519.5
nt	1000
ct	24
alock	n
gain	not used

FLAGS	
il	n
in	n
dp	y
hs	nn

DISPLAY	
sp	-250.0
wp	6246.8
vs	107
sc	0
wc	250
hzmm	24.99
is	33.57
rfl	1233.8
rfp	0
th	7
ins	1.000

nm cdc ph

DEC. & VT	
dfrq	125.673
dn	C13
dpwr	30
dof	0
dm	nnn
dmm	w
dmf	10000
dseq	
dres	1.0
homo	n

PROCESSING	
lb	0.01
wtfile	
proc	ft
fn	131072
math	f
werr	
wexp	
wbs	
wnt	wft

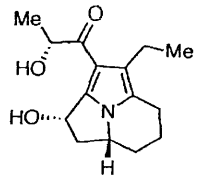

45

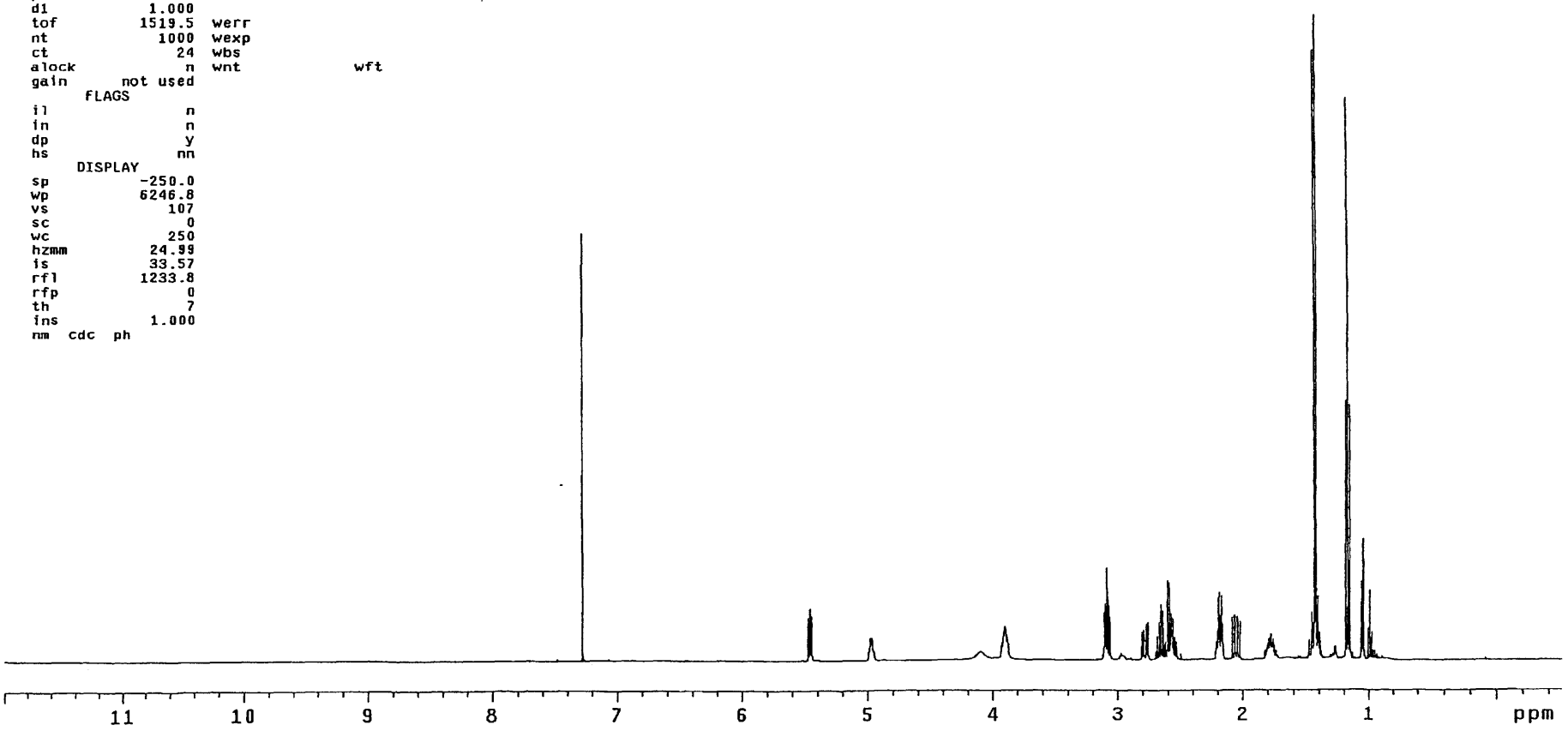

ACQUISITION		DEC. & VT	
sfrq	125.798	dfrq	500.233
tn	C13	dn	H1
at	1.736	dpwr	37
np	110920	dof	-500.0
sw	31948.9	dm	y
fb	not used	dmm	w
bs	8	dmf	10000
ss	1	dseq	
tpwr	53	dres	1.0
pw	6.9	homo	n
d1	0.763	PROCESSING	
tof	2455.2	lb	0.30
nt	1e+06	wtfile	
ct	1456	proc	ft
alock	n	fn	131072
gain	not used	math	f
FLAGS		werr	
il	n	wexp	
in	n	wbs	
dp	y	wnt	
hs	nn		
DISPLAY			
sp	-1258.3		
wp	31448.7		
vs	671		
sc	0		
wc	250		
hzmm	125.79		
is	500.00		
rfl	14159.4		
rfp	12651.0		
th	8		
ins	1.000		
ai	ph		

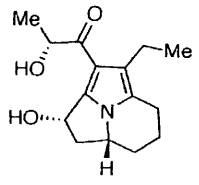

45

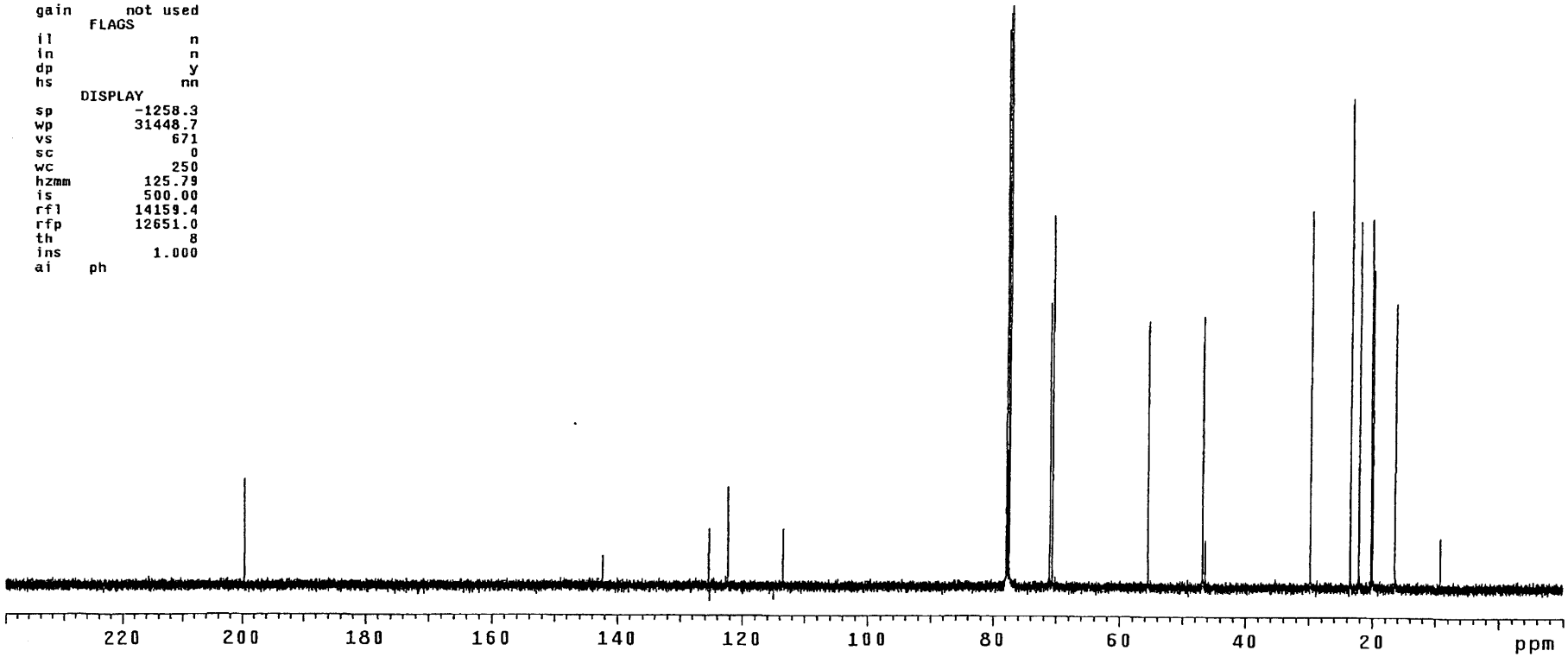

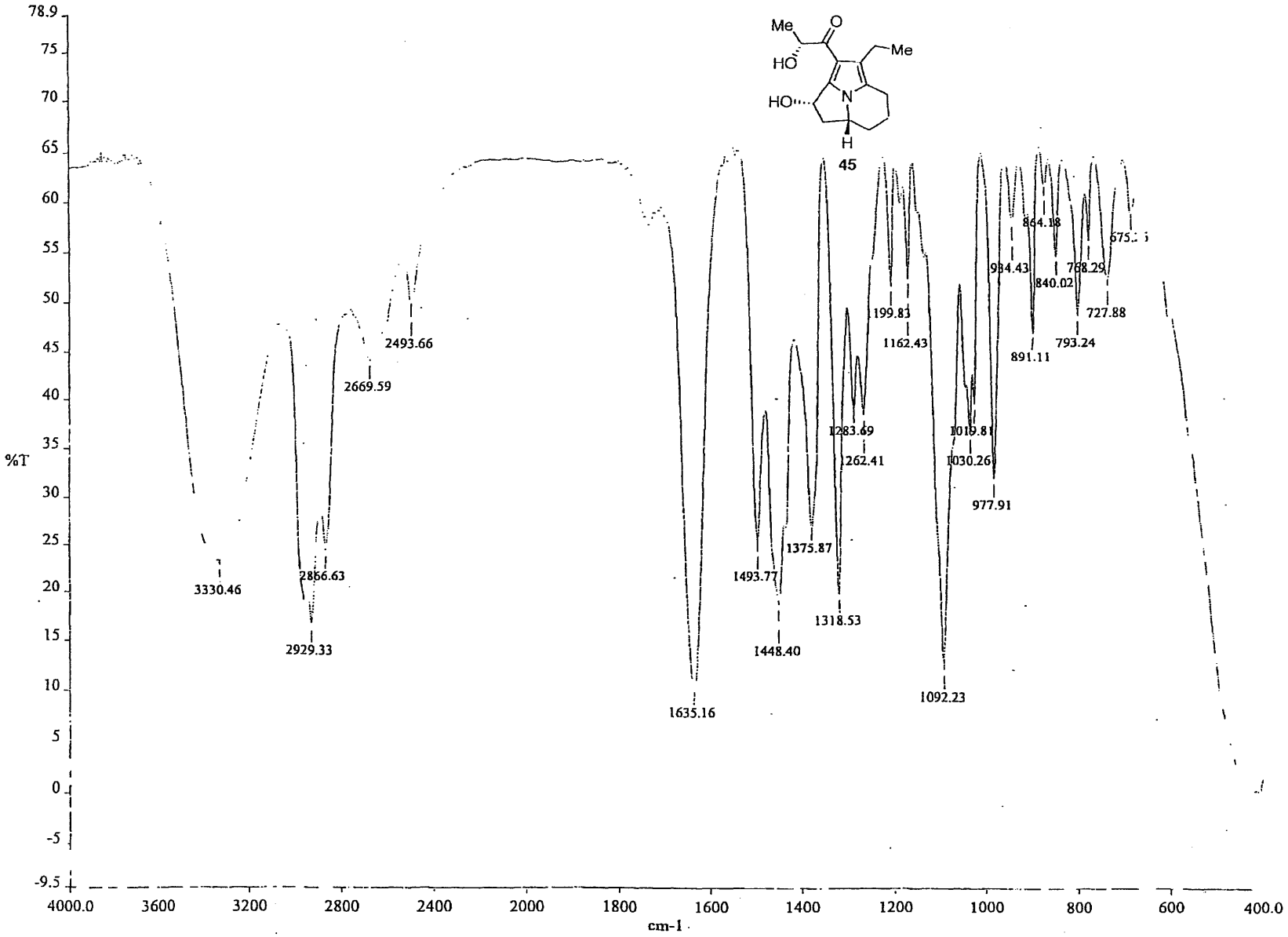
78.9
75
70
65
60
55
50
45
40
35
30
25
20
15
10
5
0
-5
-9.5
%T
4000.0
3600
3200
2800
2400
2000
1800
1600
1400
1200
1000
800
600
400.0
cm-1
Me
O
HO
Me
HO
N
H
45
3330.46
2929.33
2866.63
2669.59
2493.66
1635.16
1493.77
1448.40
1375.87
1318.53
1283.69
1262.41
1199.83
1162.43
1092.23
1019.81
1030.26
977.91
934.43
891.11
864.18
840.02
793.24
768.29
727.88

ACQUISITION		DEC. & VT	
sfrq	500.235	dfrq	125.795
tn	H1	dn	C13
at	3.200	dpwr	37
np	64000	dof	0
sw	10000.0	dm	nnn
fb	not used	dmm	c
bs	1	dmf	10000
ss	1	dseq	
tpwr	59	dres	1.0
pw	9.8	homo	n
d1	1.000	PROCESSING	
tof	1498.2	lb	0.00
nt	10	wtfile	
ct	10	proc	ft
alock	n	fn	131072
gain	not used	math	f
FLAGS		werr	
il	n	wexp	
in	n	wbs	
dp	y	wnt	
hs	nn		
DISPLAY			
sp	-250.2		
wp	6252.9		
vs	87		
sc	0		
wc	250		
hzmm	25.01		
is	100.00		
rfl	4577.3		
rfp	3576.7		
th	7		
ins	1.000		
nm cdc ph			

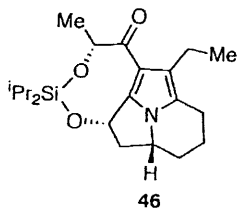

46

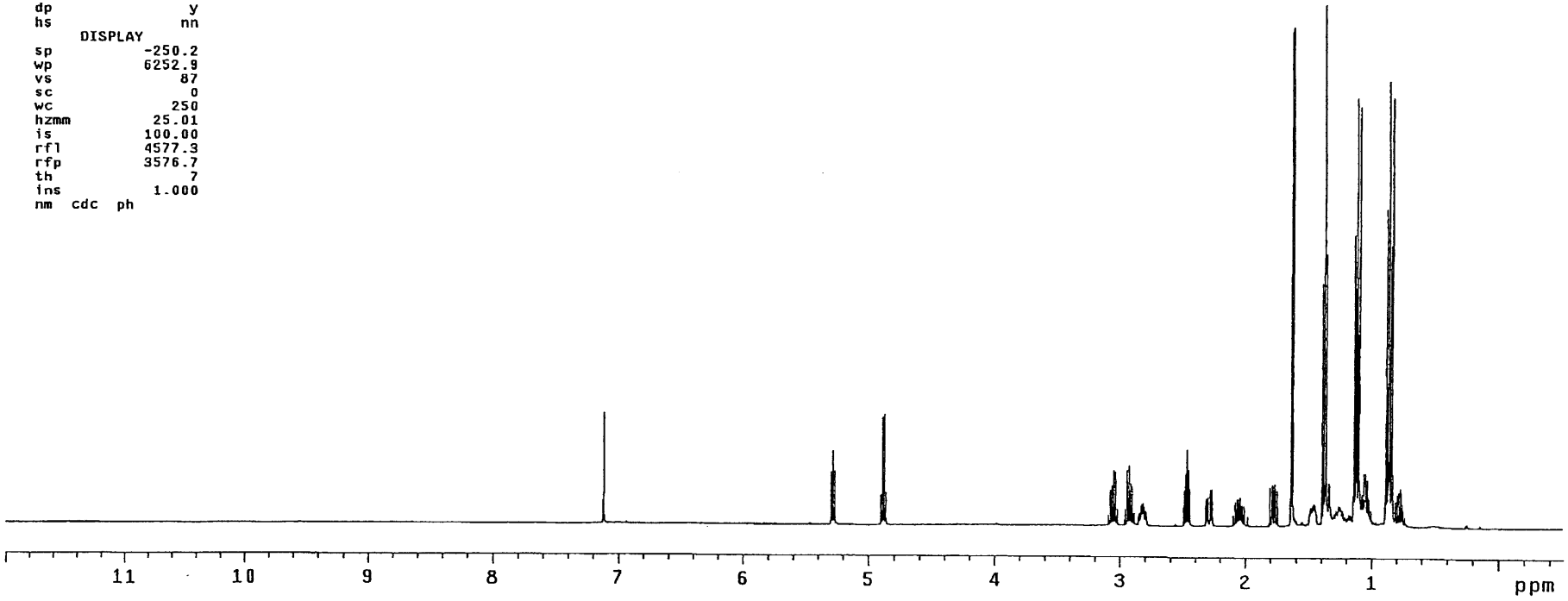

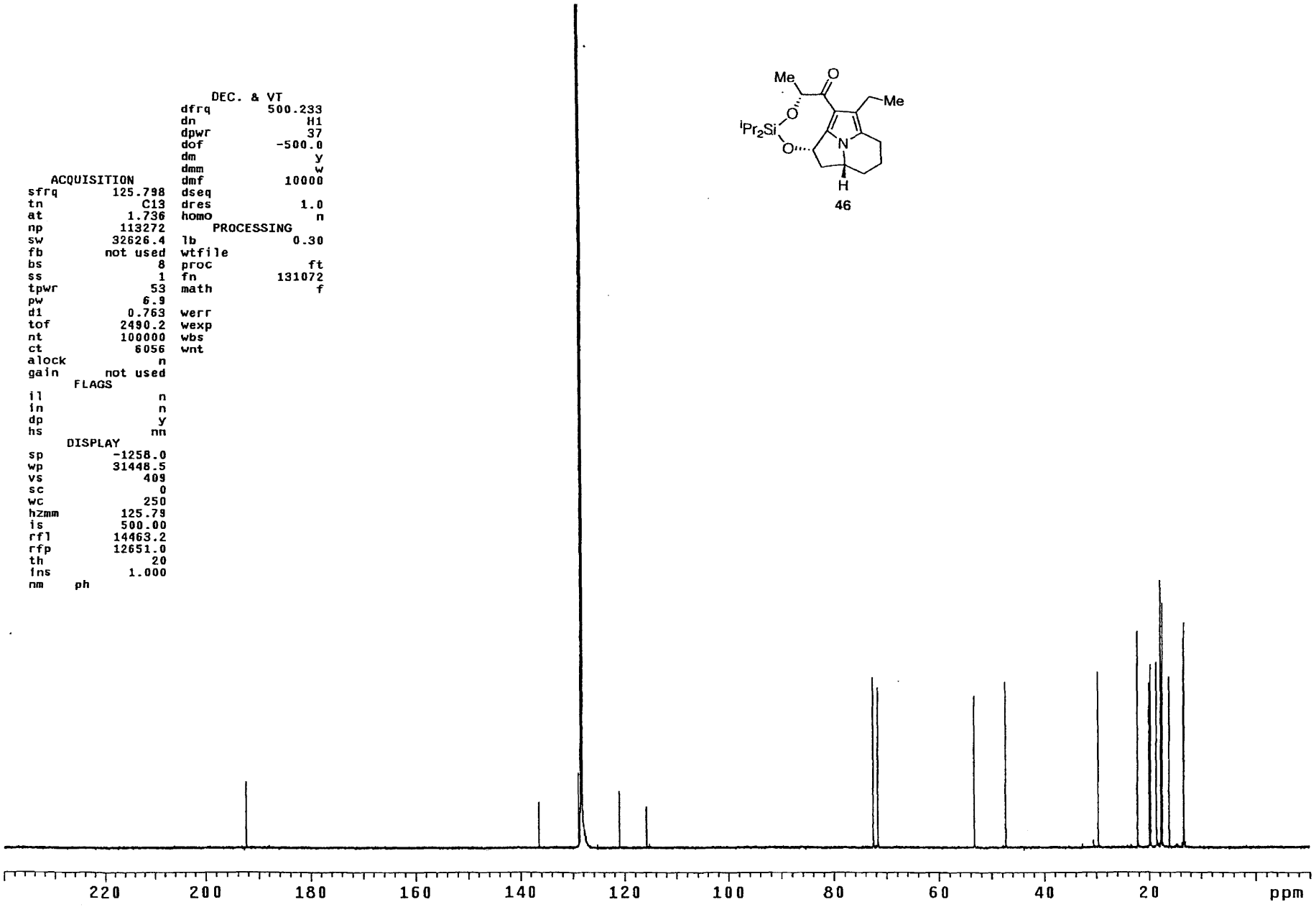
ACQUISITION
sfrq 125.798
tn C13
at 1.736
np 113272
sw 32626.4
fb not used
bs 8
ss 1
tpwr 53
pw 6.9
d1 0.763
tof 2490.2
nt 100000
ct 6056
alock n
gain not used
FLAGS
il n
in n
dp y
hs nn
DISPLAY
sp -1258.0
wp 31448.5
vs 409
sc 0
wc 250
hzmm 125.79
is 500.00
rfl 14463.2
rfp 12651.0
th 20
ins 1.000
nm ph
DEC. & VT
dfrq 500.233
dn H1
dpwr 37
dof -500.0
dm y
dmm w
dmf 10000
dseq
dres 1.0
homo n
PROCESSING
lb 0.30
wtfile
proc ft
fn 131072
math f
werr
wexp
wbs
wnt
Me
O
Me
iPr2Si
O
O
N
H
46
220
200
180
160
140
120
100
80
60
40
20
ppm

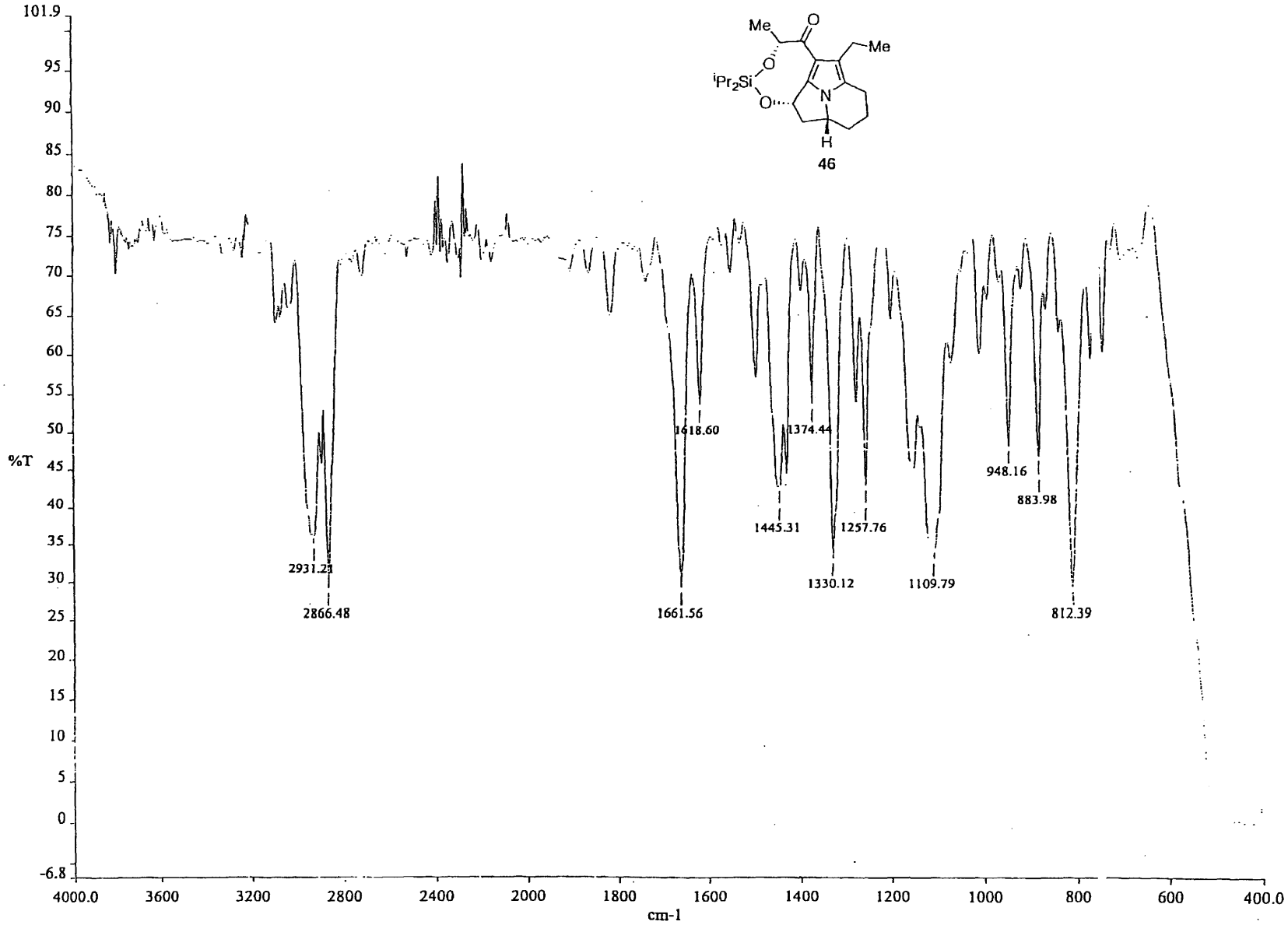
Me
O
Me
O
iPr2Si
O
N
H
46
%T
101.9
95
90
85
80
75
70
65
60
55
50
45
40
35
30
25
20
15
10
5
0
-6.8
2931.23
2866.48
1661.56
1618.60
1445.31
1374.44
1330.12
1257.76
1109.79
948.16
883.98
812.39
4000.0
3600
3200
2800
2400
2000
1800
1600
1400
1200
1000
800
600
400.0
cm-1

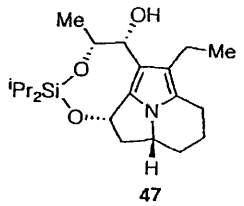

47

ACQUISITION		DEC. & VT	
sfrq	499.749	dfrq	125.673
tn	H1	dn	C13
at	3.001	dpwr	30
np	63050	dof	0
sw	10504.2	dm	nnn
fb	not used	dmm	w
bs	1	dmf	10000
tpwr	56	dseq	
pw	8.9	dres	1.0
d1	1.000	homo	n
tof	1519.5	PROCESSING	
nt	1000	lb	0.01
ct	72	wtfile	
alock	n	proc	ft
gain	not used	fn	131072
FLAGS		math	f
il	n	werr	
in	n	wexp	
dp	y	wbs	
hs	nn	wnt	wft
DISPLAY			
sp	-208.8		
wp	6246.6		
vs	116		
sc	0		
wc	250		
hzmm	7.75		
is	112.47		
rfl	1233.8		
rfp	0		
th	29		
ins	1.000		
nm cdc ph			

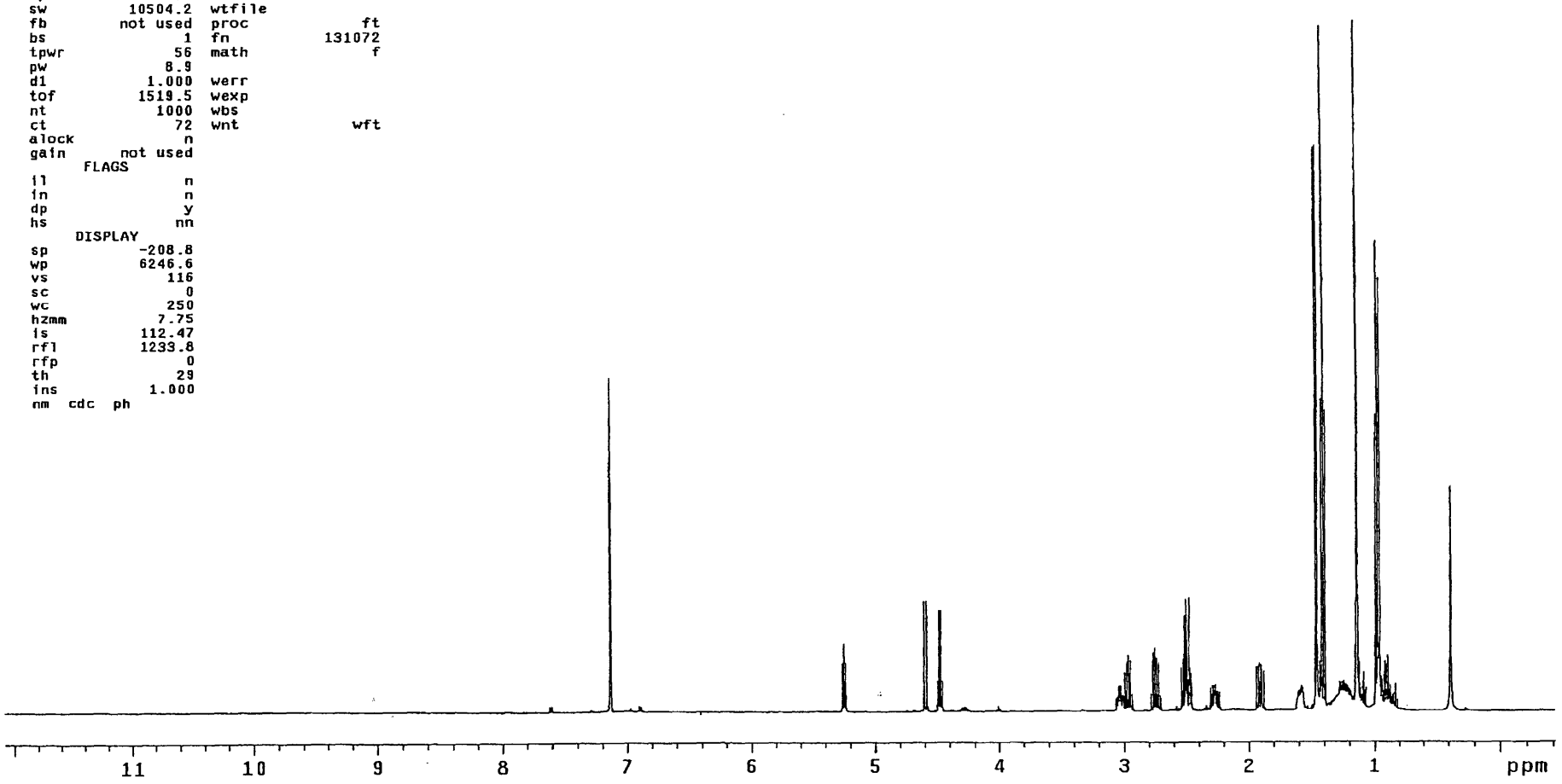

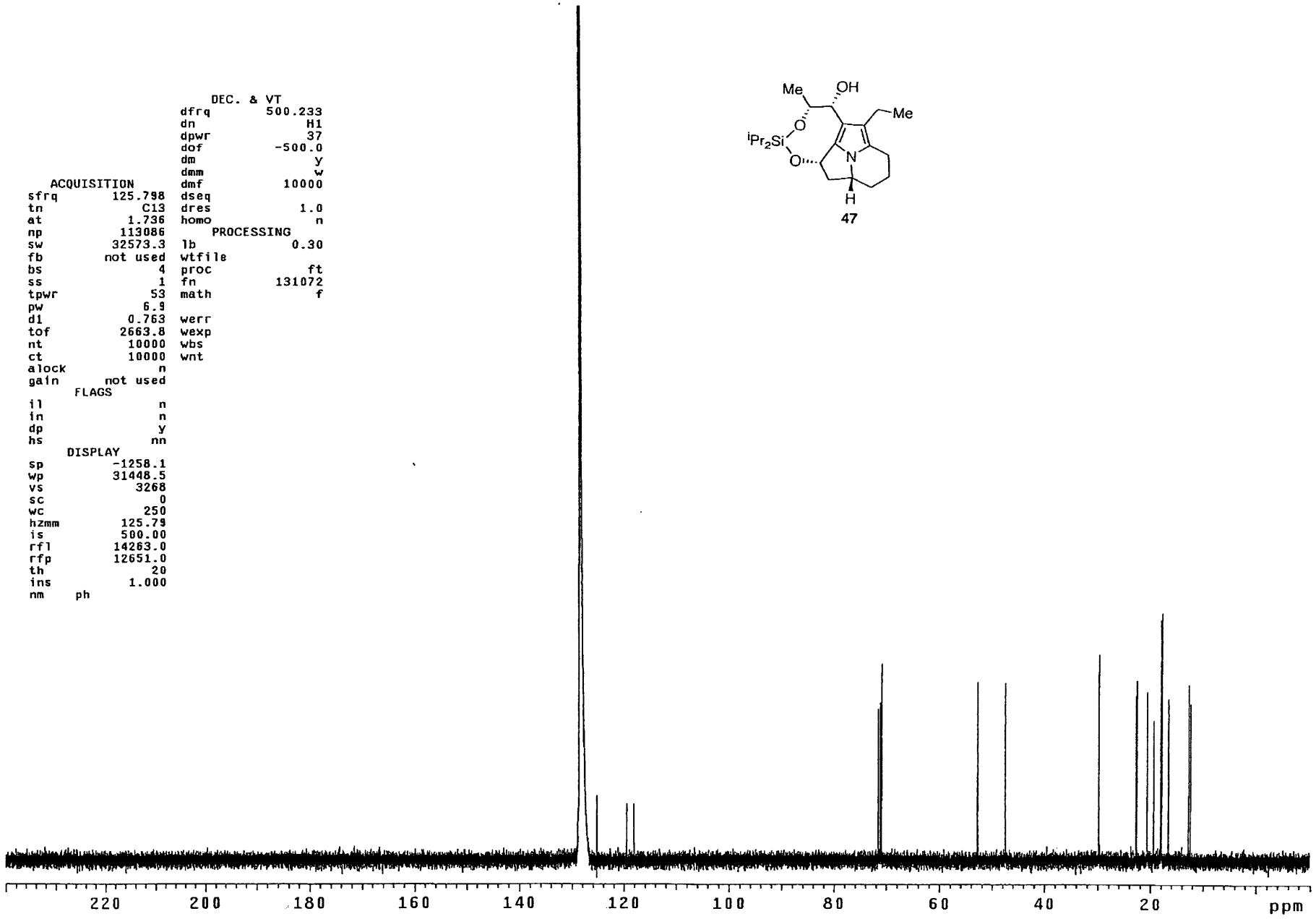
ACQUISITION
sfrq 125.798
tn C13
at 1.736
np 113086
sw 32573.3
fb not used
bs 4
ss 1
tpwr 53
pw 6.9
d1 0.763
tof 2663.8
nt 10000
ct 10000
alock n
gain not used
FLAGS
il n
in n
dp y
hs nn
DISPLAY
sp -1258.1
wp 31448.5
vs 3268
sc 0
wc 250
hzmm 125.79
is 500.00
rfl 14263.0
rfp 12651.0
th 20
ins 1.000
nm ph
DEC. & VT
dfrq 500.233
dn H1
dpwr 37
dof -500.0
dm y
dmm w
dmf 10000
dseq
dres 1.0
homo n
PROCESSING
lb 0.30
wtfile
proc ft
fn 131072
math f
werr
wexp
wbs
wnt
Me
OH
Me
iPr2Si
O
O
N
H
47
220
200
180
160
140
120
100
80
60
40
20
ppm

ACQUISITION	
sfrq	499.749
tn	H1
at	3.001
np	63050
sw	10504.2
fb	not used
bs	1
tpwr	56
pw	8.9
d1	1.000
tof	1519.5
nt	1000
ct	121
alock	n
gain	not used

FLAGS	
il	n
in	n
dp	y
hs	nn

DISPLAY	
sp	-249.9
wp	6246.8
vs	108
sc	0
wc	250
hzmm	2.03
is	112.47
rfl	1233.8
rfp	0
th	45
ins	3.000
nm	cdc ph

DEC. & VT	
dfrq	125.673
dn	C13
dpwr	30
dof	0
dm	nnn
dmm	w
dmf	10000
dseq	
dres	1.0
homo	n

PROCESSING	
wtfile	
proc	ft
fn	131072
math	f
werr	
wexp	
wbs	
wnt	wft

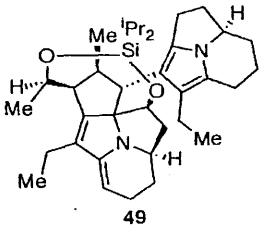

49

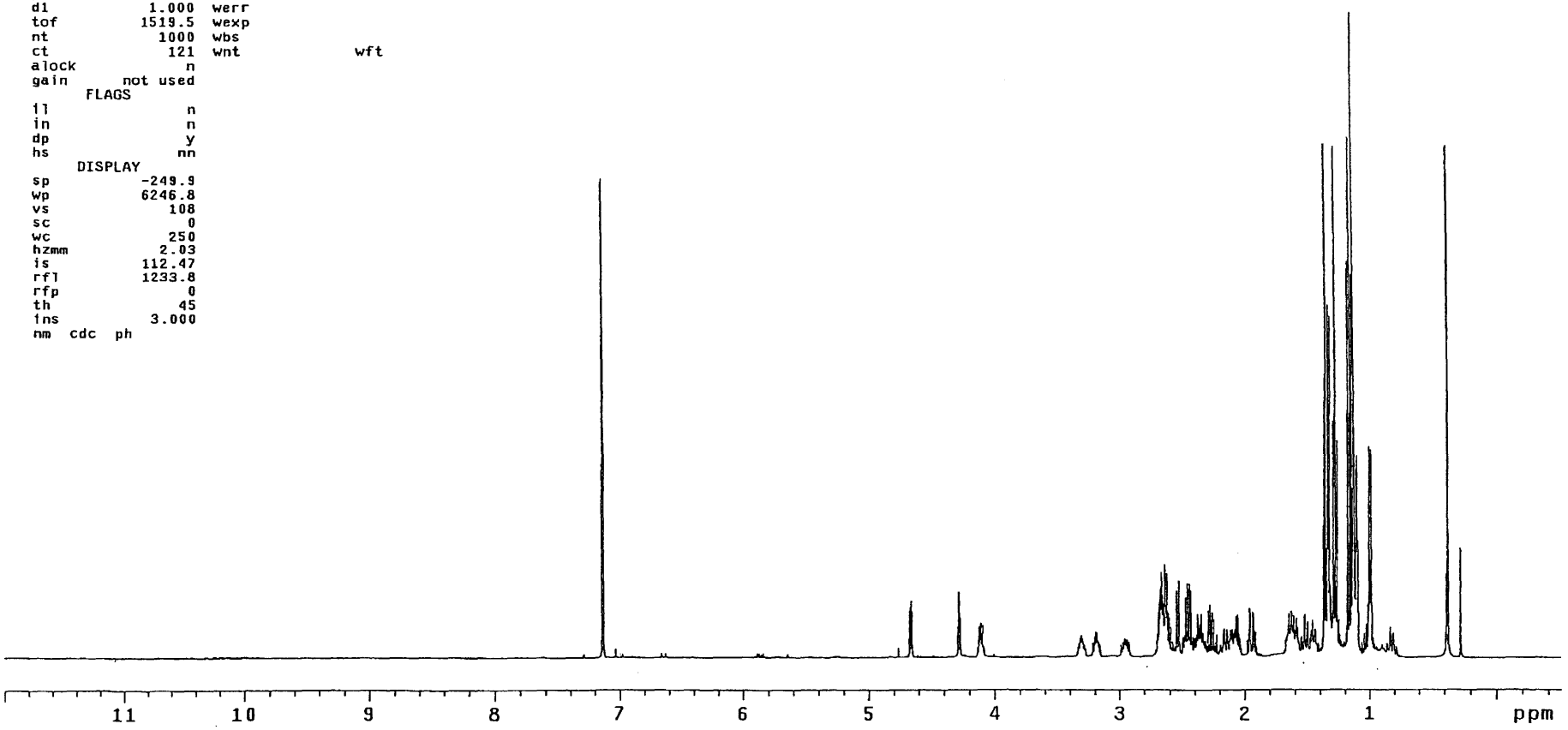

ACQUISITION		DEC. & VT	
sfrq	125.798	dfrq	500.233
tn	C13	dn	H1
at	1.737	dpwr	37
np	111364	dof	-500.0
sw	32051.3	dm	y
fb	not used	dmm	w
bs	4	dmf	10000
ss	1	dseq	
tpwr	53	dres	1.0
pw	6.9	homo	n
dl	0.763	PROCESSING	
tof	2466.0	lb	0.30
nt	1e+08	wtfile	
ct	41308	proc	ft
alock	n	fn	131072
gain	not used	math	f
FLAGS		werr	
fl	n	wexp	
in	n	wbs	
dp	y	wnt	
hs	nn		
DISPLAY			
sp	-1544.7		
wp	32050.8		
vs	18433		
sc	0		
wc	250		
hzmm	2.70		
is	500.00		
rfl	17696.6		
rfp	16151.4		
th	45		
ins	1.000		
al ph			

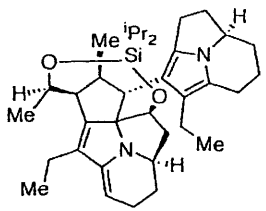

49

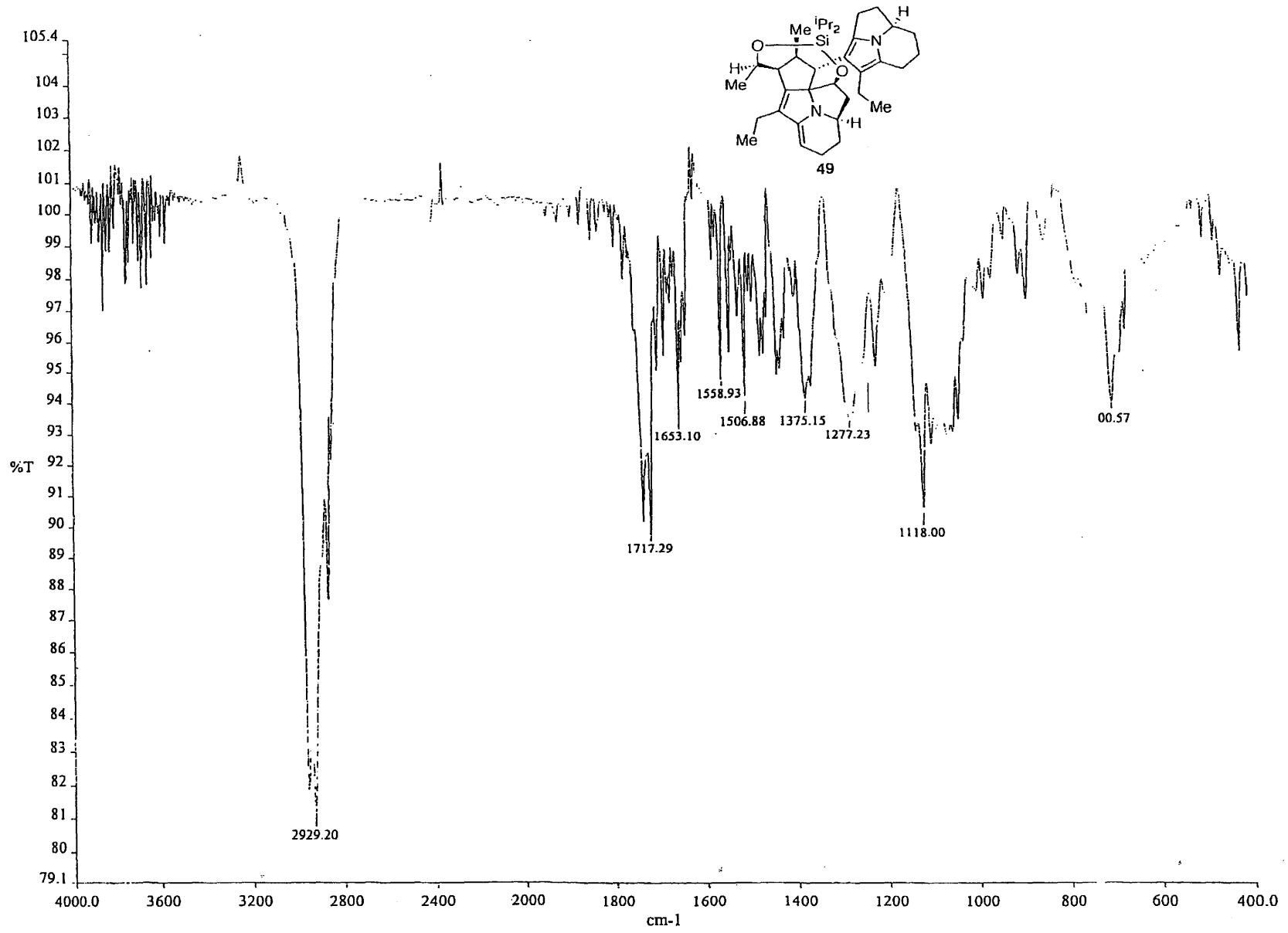
105.4
104
103
102
101
100
99
98
97
96
95
94
93
92
91
90
89
88
87
86
85
84
83
82
81
80
79.1
%T
2929.20
1717.29
1653.10
1558.93
1506.88
1375.15
1277.23
1118.00
00.57
4000.0
3600
3200
2800
2400
2000
1800
1600
1400
1200
1000
800
600
400.0
cm-1
Me
iPr2
Si
O
H
Me
O
N
H
Me
Me
N
H
H
49

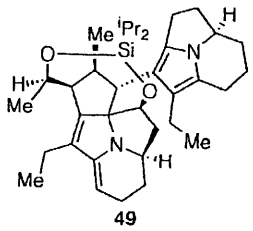
Me
iPr2
Si
O
H
Me
O
H
N
N
Me
Me
H

49

gCOSY

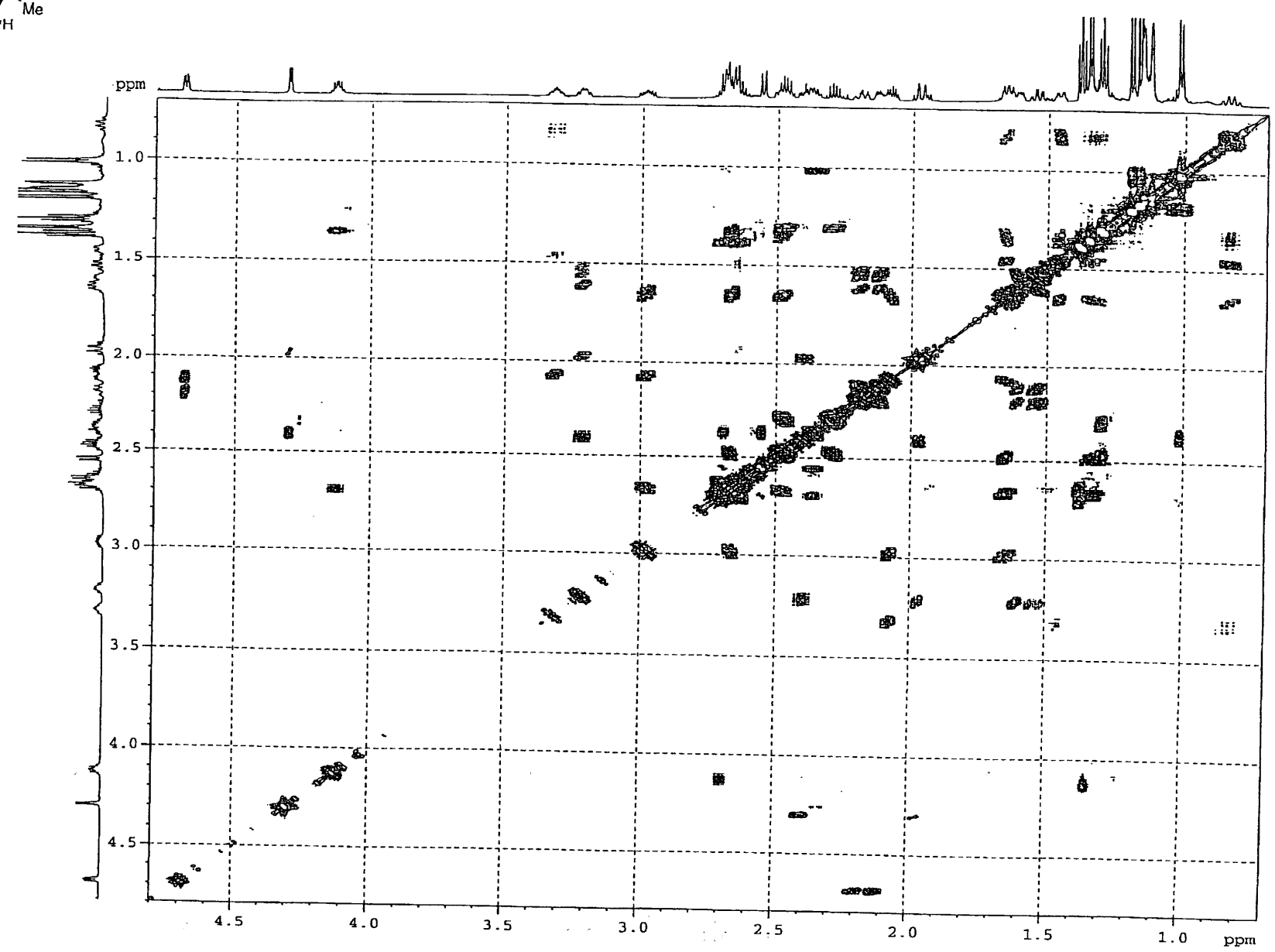
ppm
1.0
1.5
2.0
2.5
3.0
3.5
4.0
4.5
4.5
4.0
3.5
3.0
2.5
2.0
1.5
1.0
ppm

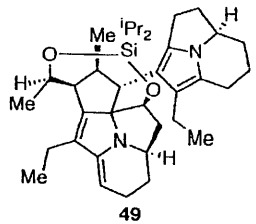
Me
iPr2
Si
O
H
Me
O
N
H
Me
N
H
Me
Me

49

gHSQC

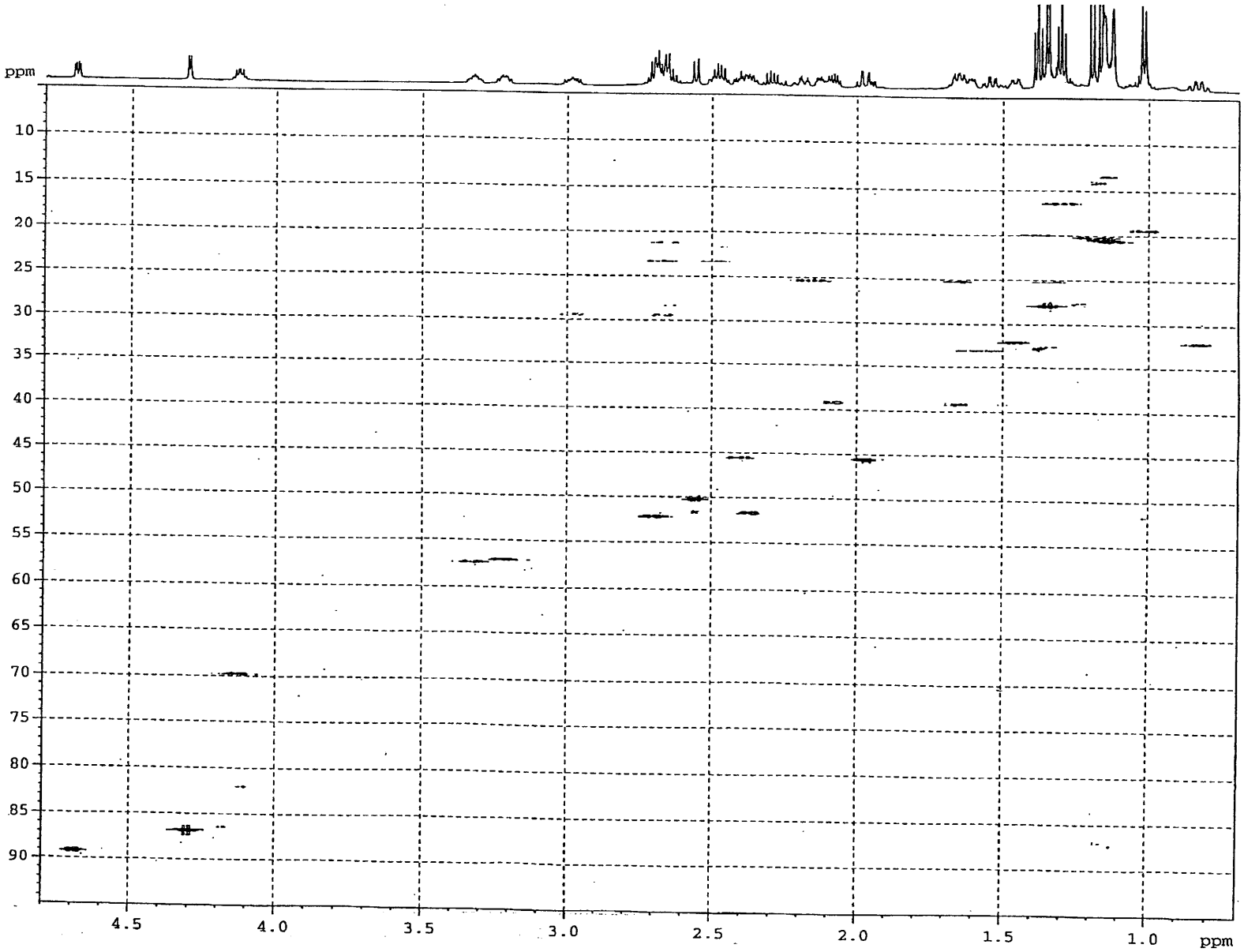
ppm
10
15
20
25
30
35
40
45
50
55
60
65
70
75
80
85
90
4.5
4.0
3.5
3.0
2.5
2.0
1.5
1.0
ppm

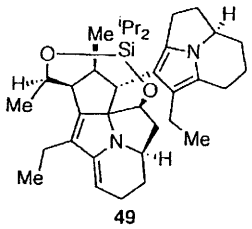
Me
iPr2
Si
O
H
Me
O
N
H
Me
N
H
Me

49

gHMBC

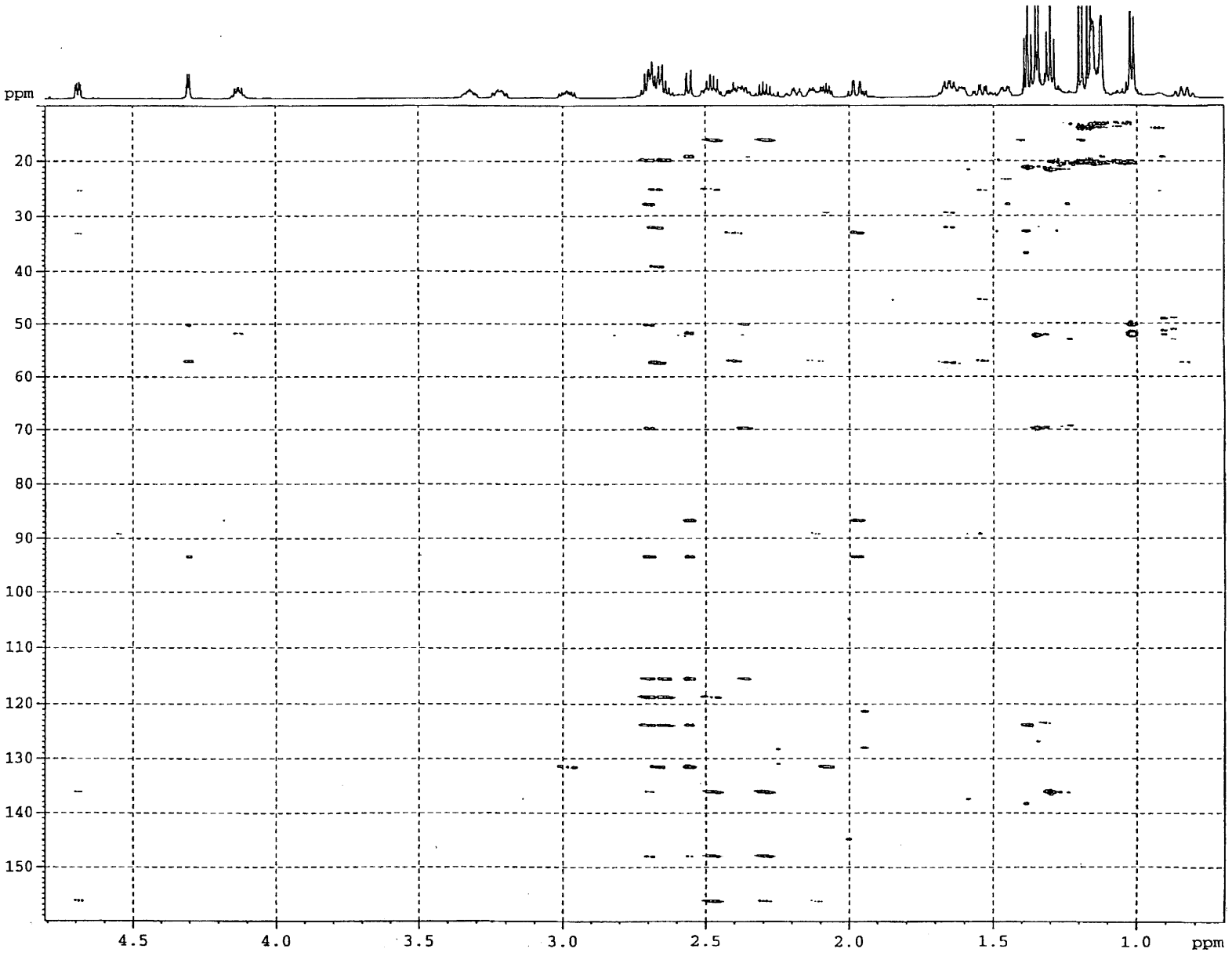
ppm
20
30
40
50
60
70
80
90
100
110
120
130
140
150
4.5
4.0
3.5
3.0
2.5
2.0
1.5
1.0
ppm

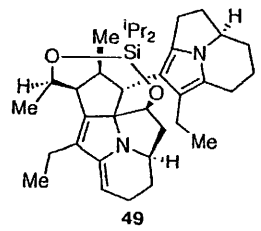
Me
iPr2
Si
O
O
H
Me
N
H
Me
N
H
Me
Me

49

gNOESY

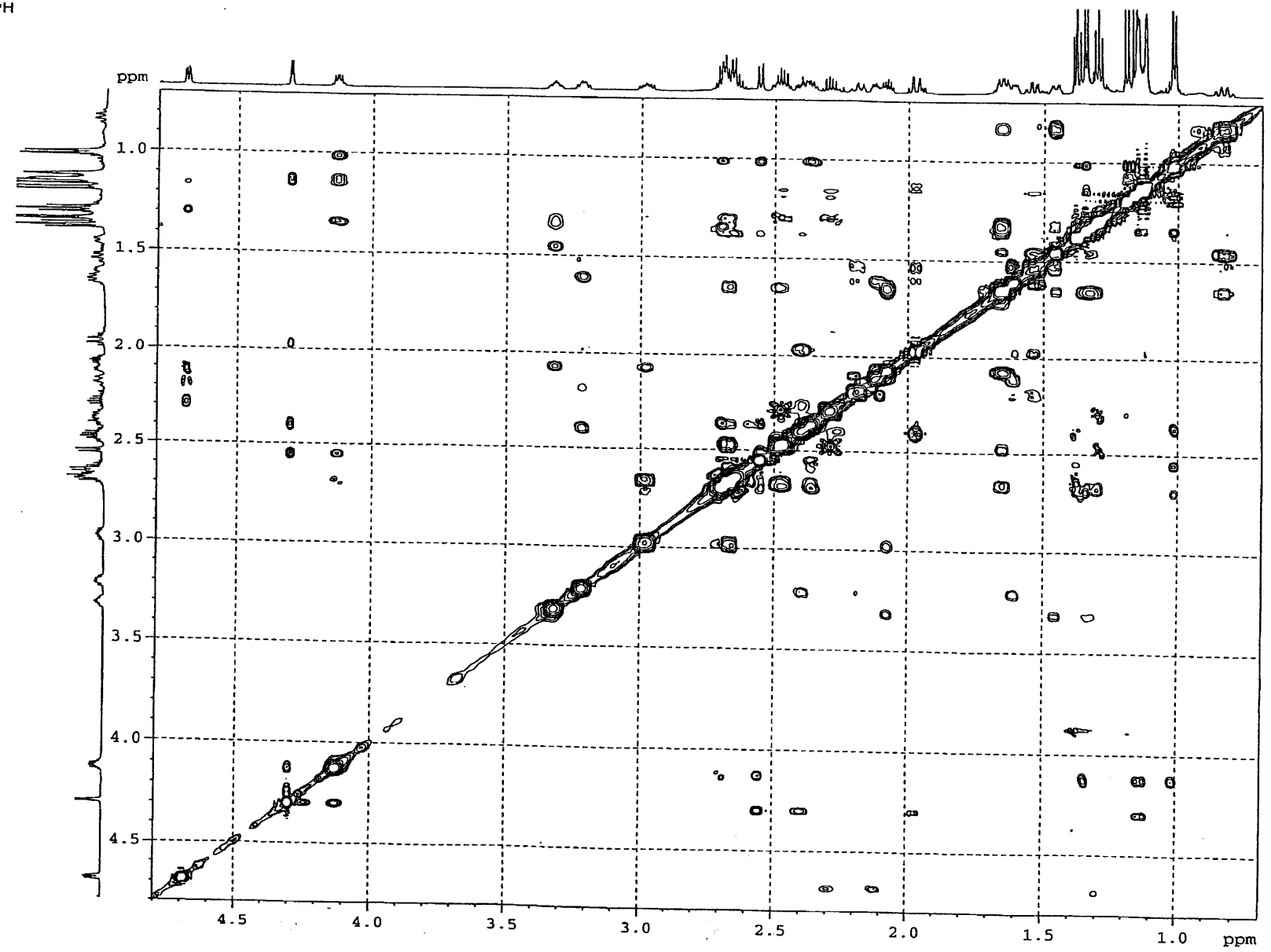
ppm
1.0
1.5
2.0
2.5
3.0
3.5
4.0
4.5
4.5
4.0
3.5
3.0
2.5
2.0
1.5
1.0
ppm

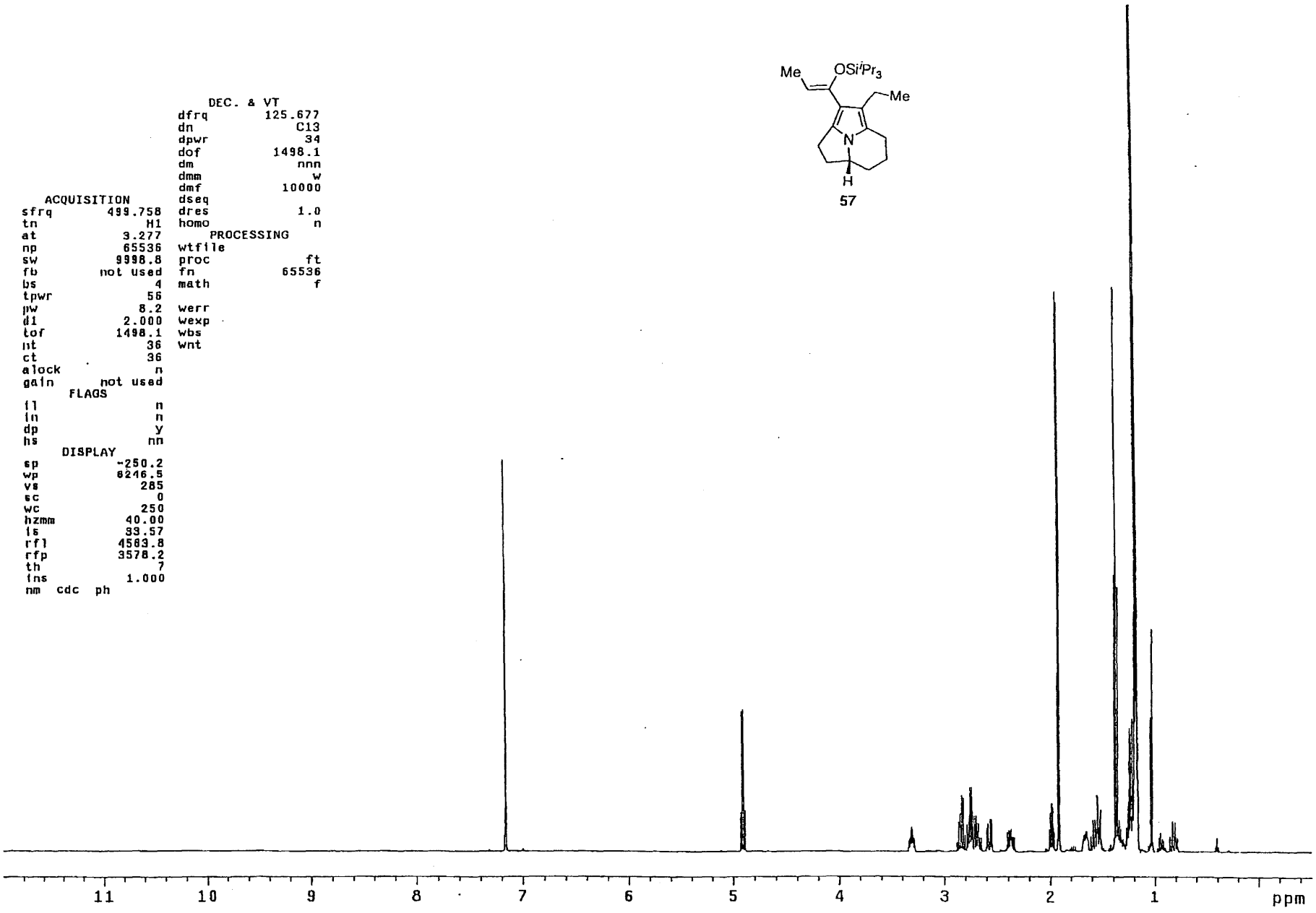
ACQUISITION
sfrq 499.758
tn H1
at 3.277
np 65536
sw 9998.8
fb not used
bs 4
tpwr 56
pw 8.2
d1 2.000
tof 1498.1
nt 36
ct 36
alock n
gain not used
FLAGS
fl n
in n
dp y
hs nn
DISPLAY
sp -250.2
wp 8246.5
vs 285
sc 0
wc 250
hzmm 40.00
is 33.57
rfl 4563.8
rfp 3578.2
th 7
ins 1.000
nm cdc ph
DEC. & VT
dfrq 125.677
dn C13
dpwr 34
dof 1498.1
dm nnn
dmm w
dmf 10000
dseq
dres 1.0
homo n
PROCESSING
wtfile
proc ft
fn 65536
math f
werr
wexp
wbs
wnt
Me
OSi'Pr3
Me
N
H
57
11
10
9
8
7
6
5
4
3
2
1
ppm

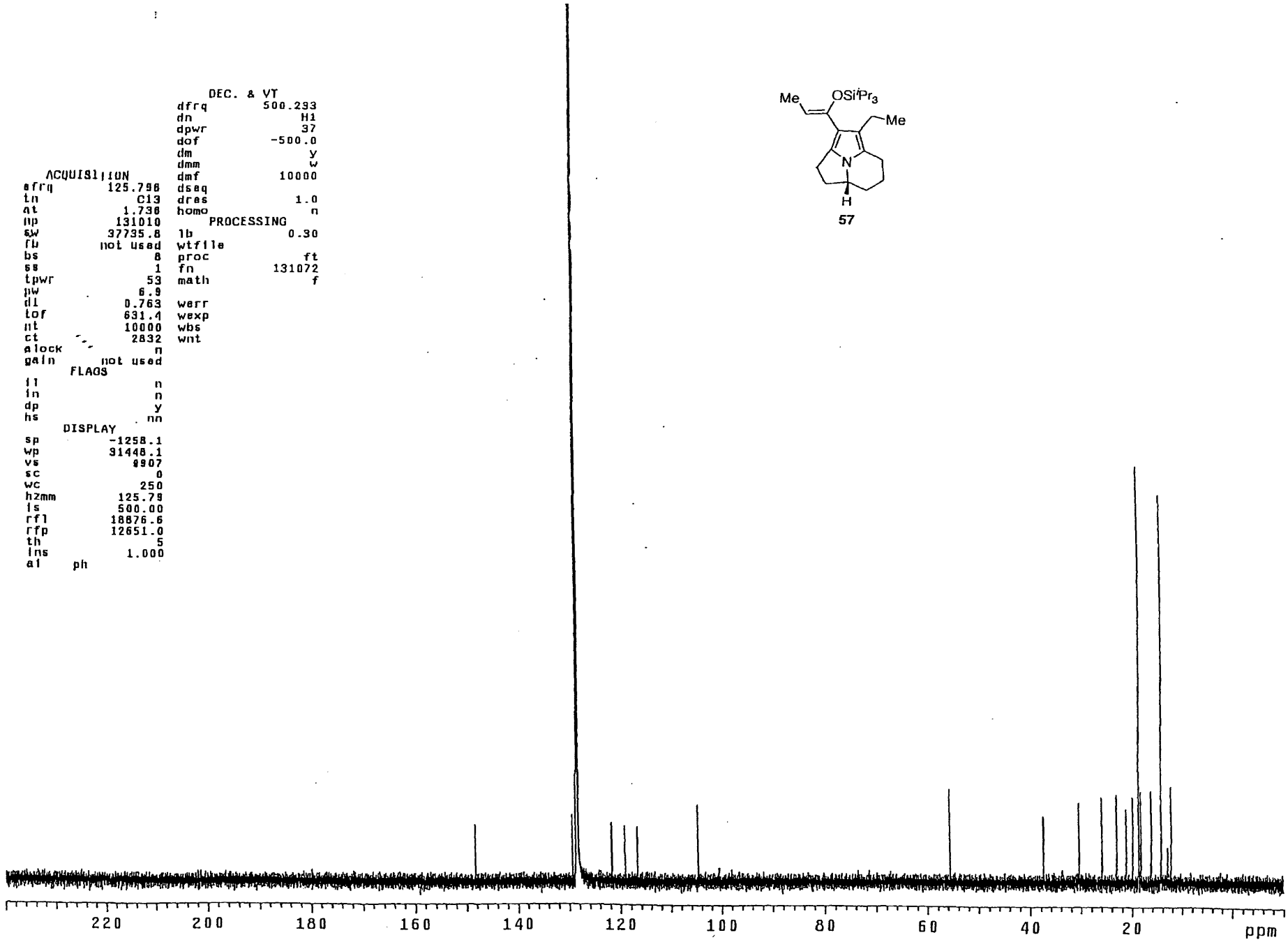
ACQUISITION
sfrq 125.798
tn C13
at 1.736
np 131010
sw 37735.8
fb not used
bs 8
ss 1
tpwr 53
pw 6.9
dl 0.763
tof 631.4
nt 10000
ct 2832
alock n
gain not used
FLAGS
il n
in n
dp y
hs nn
DISPLAY
sp -1258.1
wp 31448.1
vs 8907
sc 0
wc 250
hzmm 125.79
is 500.00
rfl 18876.6
rfp 12651.0
th 5
ins 1.000
al ph
DEC. & VT
dfrq 500.293
dn H1
dpwr 37
dof -500.0
dm y
dmm w
dmf 10000
dseq
dres 1.0
homo n
PROCESSING
lb 0.30
wtfile
proc ft
fn 131072
math f
werr
wexp
wbs
wnt
Me
OSi^{i}Pr$_3$
Me
N
H
57
220
200
180
160
140
120
100
80
60
40
20
ppm

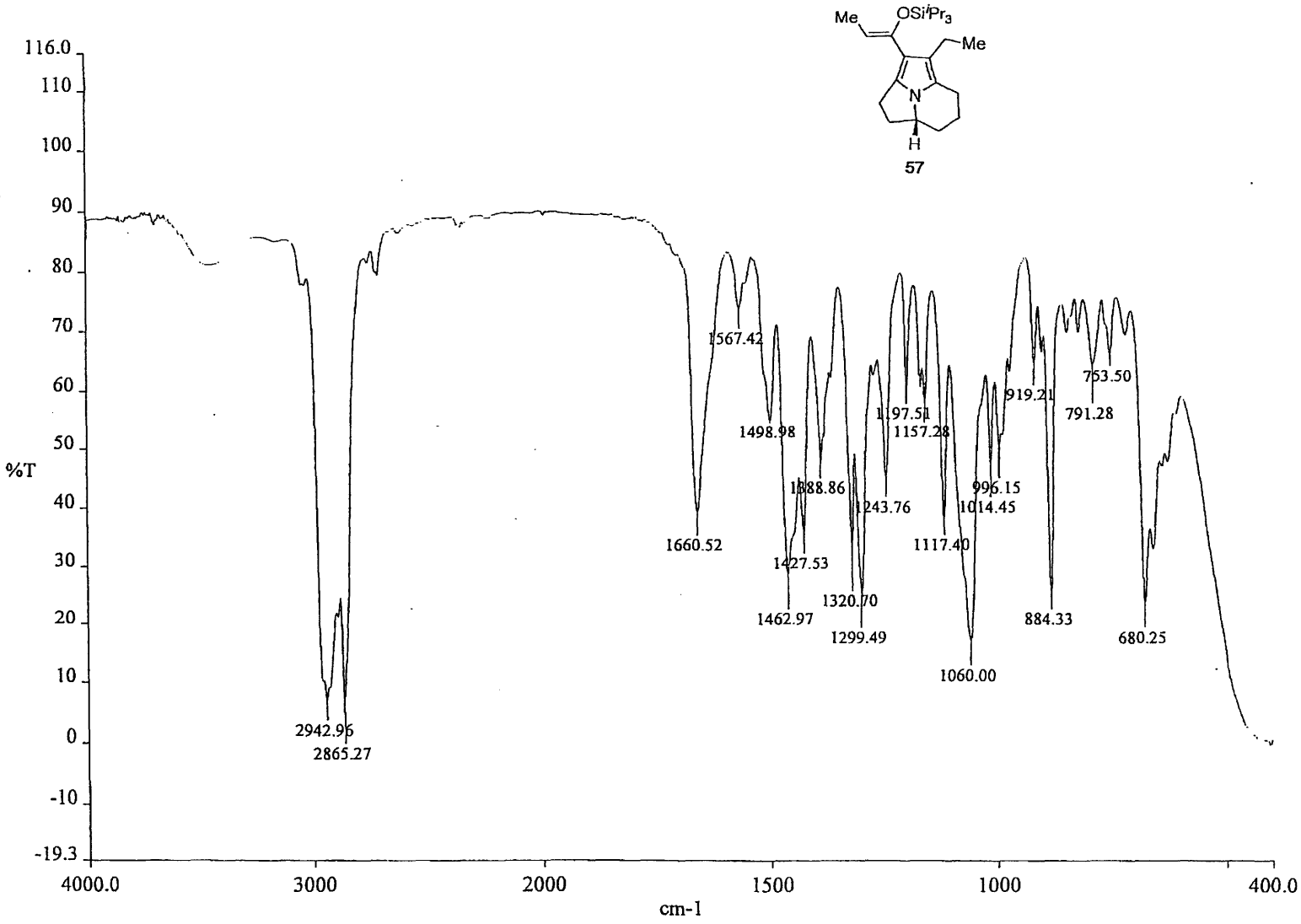
Me
OSi^{i}Pr$_3$
Me
N
H
57
116.0
110
100
90
80
70
60
50
40
30
20
10
0
-10
-19.3
%T
4000.0
3000
2000
1500
1000
400.0
cm-1
2942.96
2865.27
1660.52
1567.42
1498.98
1462.97
1427.53
1388.86
1320.70
1299.49
1243.76
1197.51
1157.28
1117.40
1060.00
1014.45
996.15
919.21
884.33
791.28
753.50
680.25

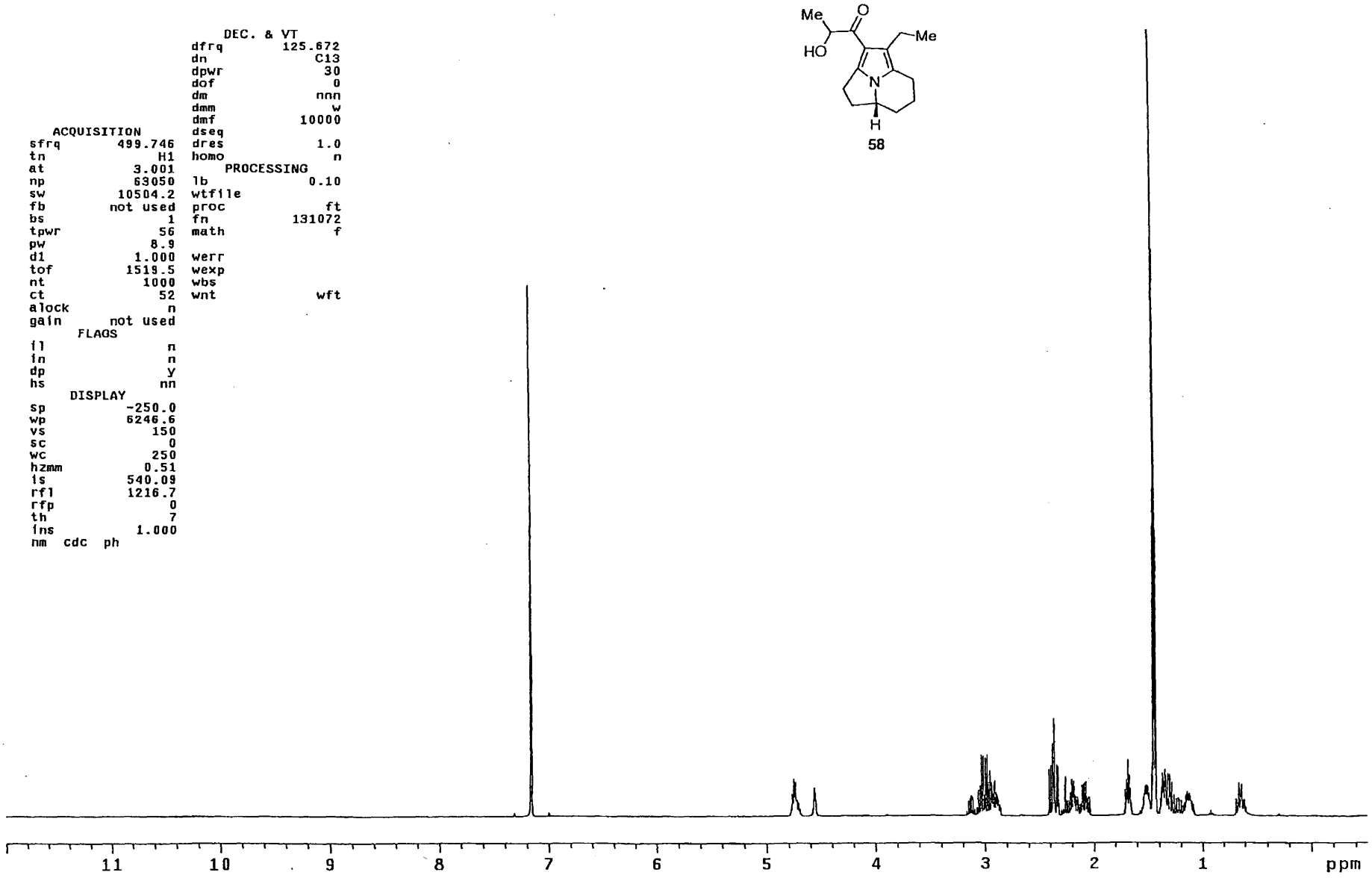
ACQUISITION
sfrq 499.746
tn H1
at 3.001
np 63050
sw 10504.2
fb not used
bs 1
tpwr 56
pw 8.9
d1 1.000
tof 1519.5
nt 1000
ct 52
alock n
gain not used
FLAGS
il n
in n
dp y
hs nn
DISPLAY
sp -250.0
wp 6246.6
vs 150
sc 0
wc 250
hzmm 0.51
is 540.09
rfl 1216.7
rfp 0
th 7
ins 1.000
nm cdc ph
DEC. & VT
dfrq 125.672
dn C13
dpwr 30
dof 0
dm nnn
dmm w
dmf 10000
dseq
dres 1.0
homo n
PROCESSING
lb 0.10
wtfile
proc ft
fn 131072
math f
werr
wexp
wbs
wnt wft
Me
O
HO
Me
N
H
58
11
10
9
8
7
6
5
4
3
2
1
ppm

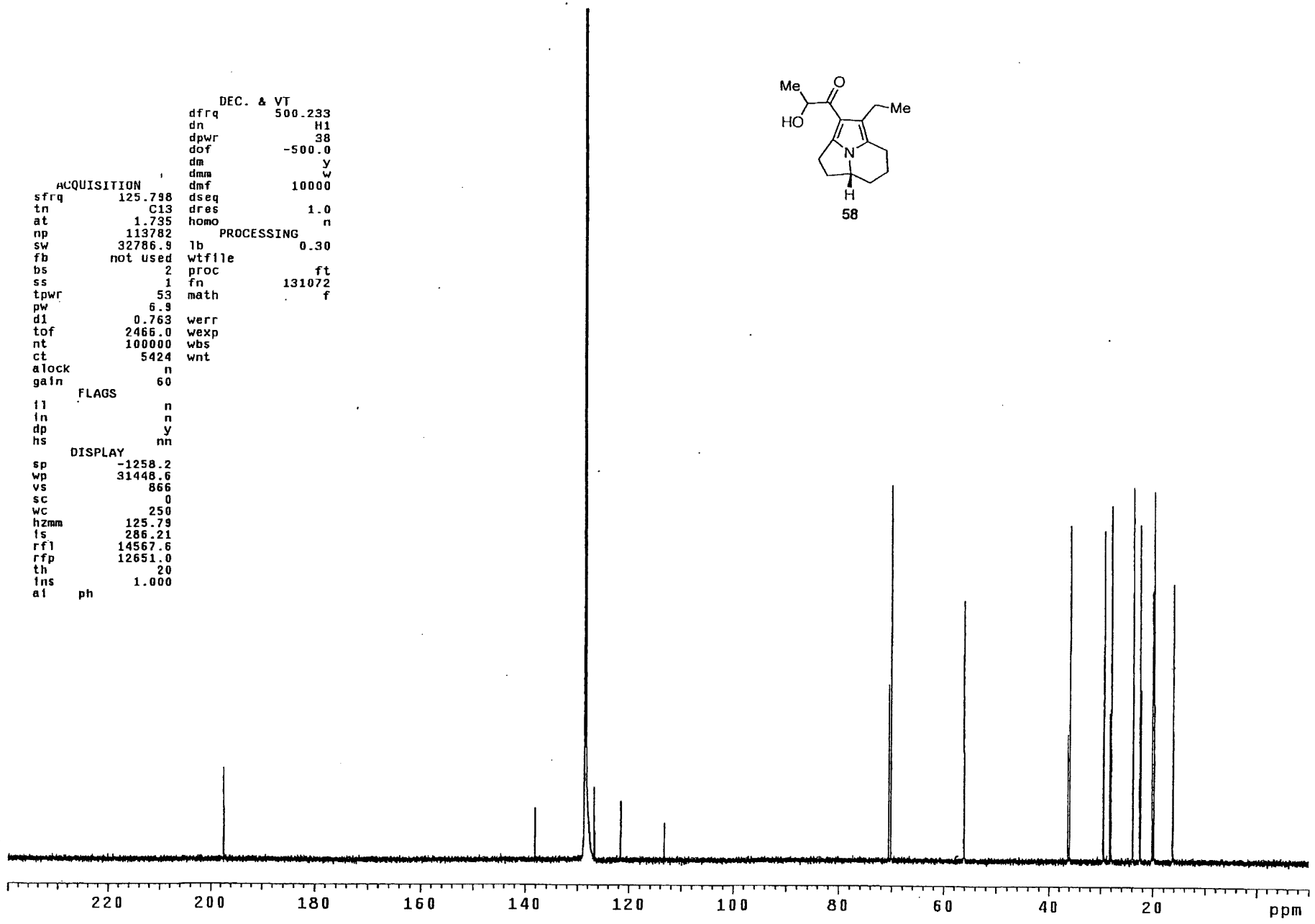
ACQUISITION
sfrq 125.798
tn C13
at 1.735
np 113782
sw 32786.9
fb not used
bs 2
ss 1
tpwr 53
pw 6.9
d1 0.763
tof 2466.0
nt 100000
ct 5424
alock n
gain 60
FLAGS
il n
in n
dp y
hs nn
DISPLAY
sp -1258.2
wp 31448.6
vs 866
sc 0
wc 250
hzmm 125.79
fs 286.21
rfl 14567.6
rfp 12651.0
th 20
ins 1.000
ai ph
DEC. & VT
dfrq 500.233
dn H1
dpwr 38
dof -500.0
dm y
dmm w
dmf 10000
dseq
dres 1.0
homo n
PROCESSING
lb 0.30
wtfile
proc ft
fn 131072
math f
werr
wexp
wbs
wnt
Me
O
HO
Me
N
H
58
220
200
180
160
140
120
100
80
60
40
20
ppm

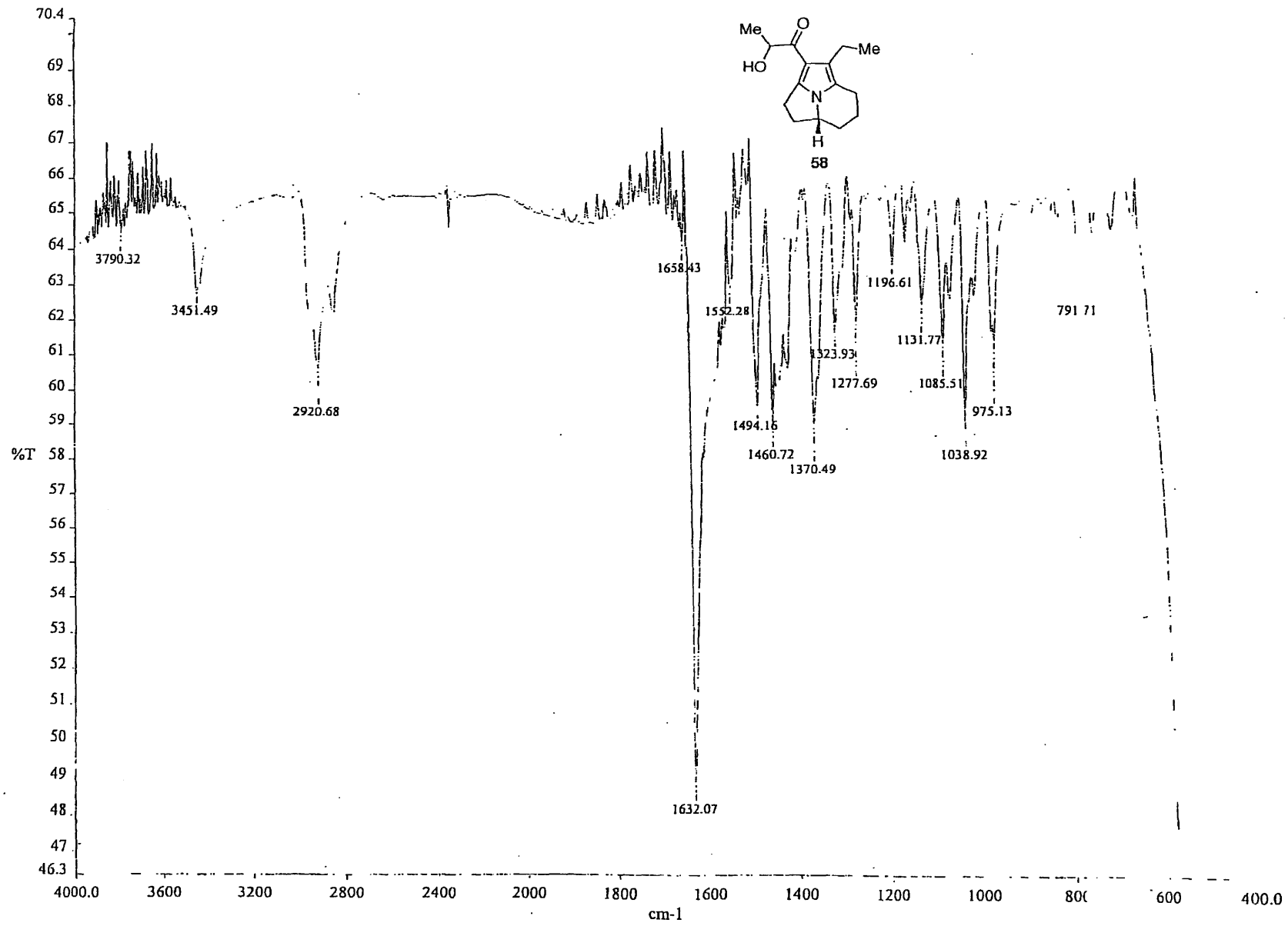
Me
O
HO
Me
N
H
58
3790.32
3451.49
2920.68
1658.43
1552.28
1494.16
1460.72
1370.49
1323.93
1277.69
1196.61
1131.77
1085.51
1038.92
975.13
791.71
1632.07
%T
cm-1
4000.0
3600
3200
2800
2400
2000
1800
1600
1400
1200
1000
800
600
400.0
70.4
69
68
67
66
65
64
63
62
61
60
59
58
57
56
55
54
53
52
51
50
49
48
47
46.3

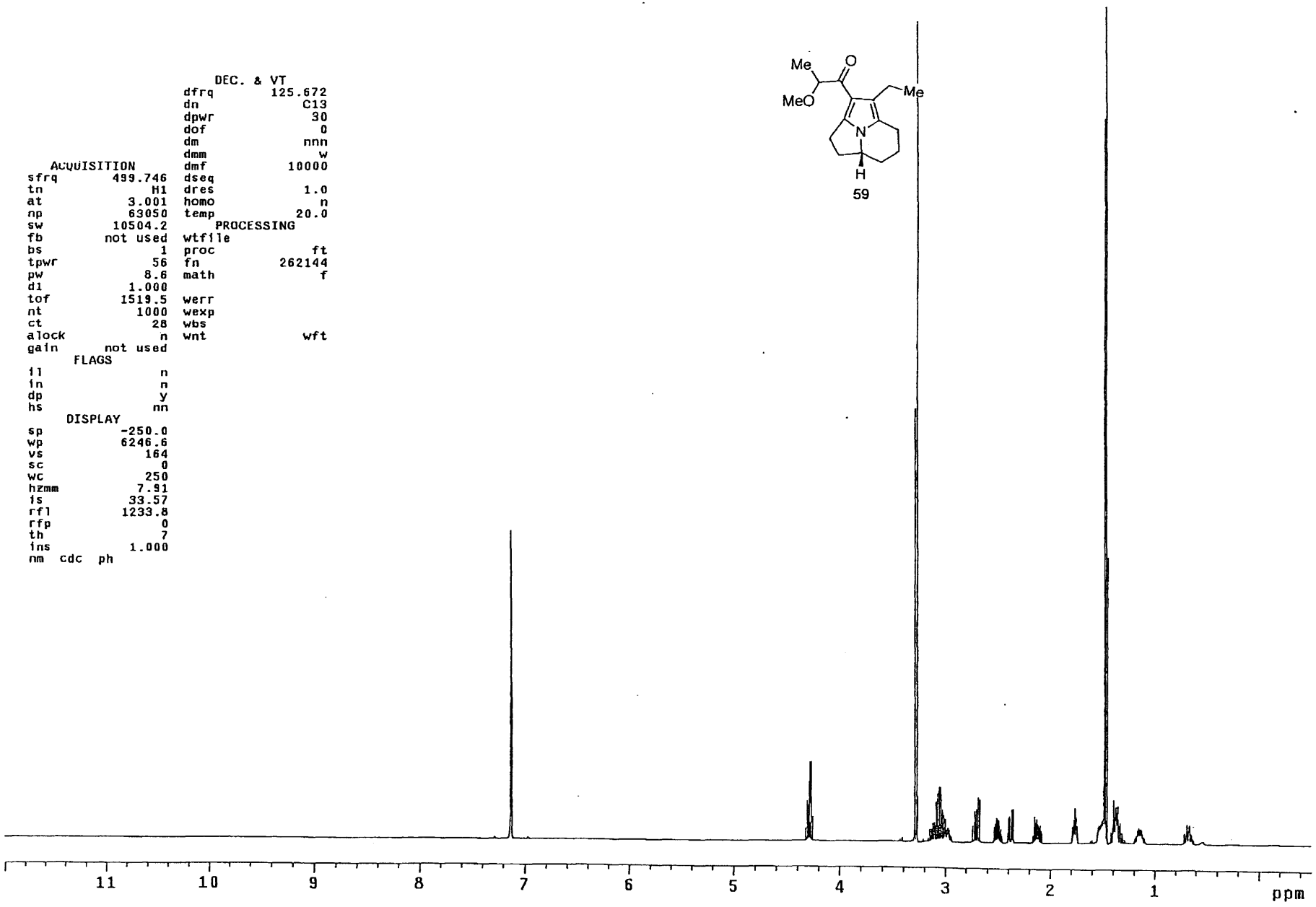
ACQUISITION
sfrq 499.746
tn H1
at 3.001
np 63050
sw 10504.2
fb not used
bs 1
tpwr 56
pw 8.6
d1 1.000
tof 1519.5
nt 1000
ct 28
alock n
gain not used
FLAGS
il n
in n
dp y
hs nn
DISPLAY
sp -250.0
wp 6246.6
vs 164
sc 0
wc 250
hzmm 7.91
is 33.57
rfl 1233.8
rfp 0
th 7
ins 1.000
nm cdc ph
DEC. & VT
dfrq 125.672
dn C13
dpwr 30
dof 0
dm nnn
dmm w
dmf 10000
dseq
dres 1.0
homo n
temp 20.0
PROCESSING
wtfile
proc ft
fn 262144
math f
werr
wexp
wbs
wnt wft
Me
O
MeO
Me
N
H
59
11
10
9
8
7
6
5
4
3
2
1
ppm

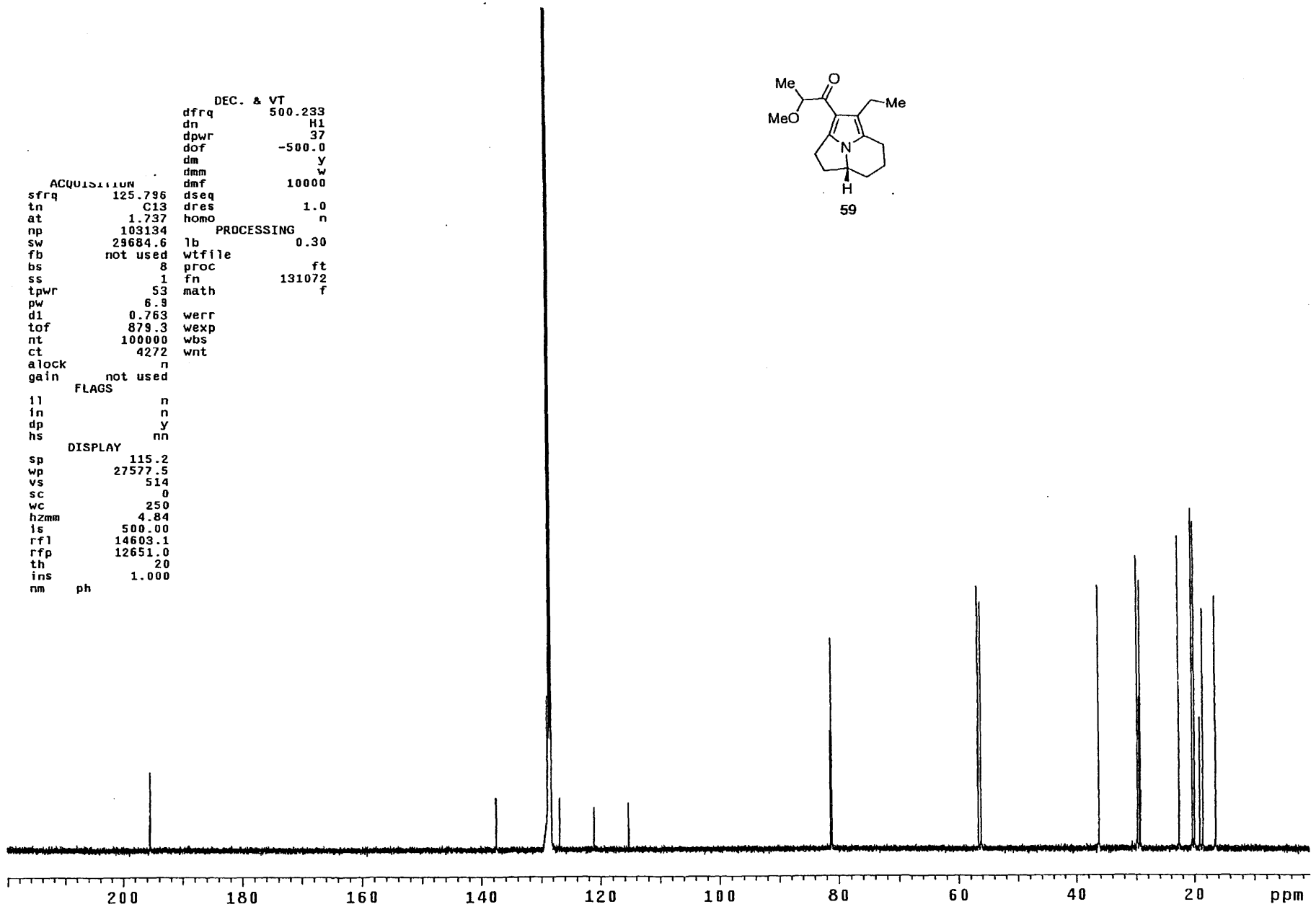
ACQUISITION
sfrq 125.796
tn C13
at 1.737
np 103134
sw 29684.6
fb not used
bs 8
ss 1
tpwr 53
pw 6.9
d1 0.763
tof 879.3
nt 100000
ct 4272
alock n
gain not used
FLAGS
il n
in n
dp y
hs nn
DISPLAY
sp 115.2
wp 27577.5
vs 514
sc 0
wc 250
hzmm 4.84
is 500.00
rfl 14603.1
rfp 12651.0
th 20
ins 1.000
nm ph
DEC. & VT
dfrq 500.233
dn H1
dpwr 37
dof -500.0
dm y
dmm w
dmf 10000
dseq
dres 1.0
homo n
PROCESSING
lb 0.30
wtfile
proc ft
fn 131072
math f
werr
wexp
wbs
wnt
Me
O
MeO
Me
N
H
59
200
180
160
140
120
100
80
60
40
20
ppm

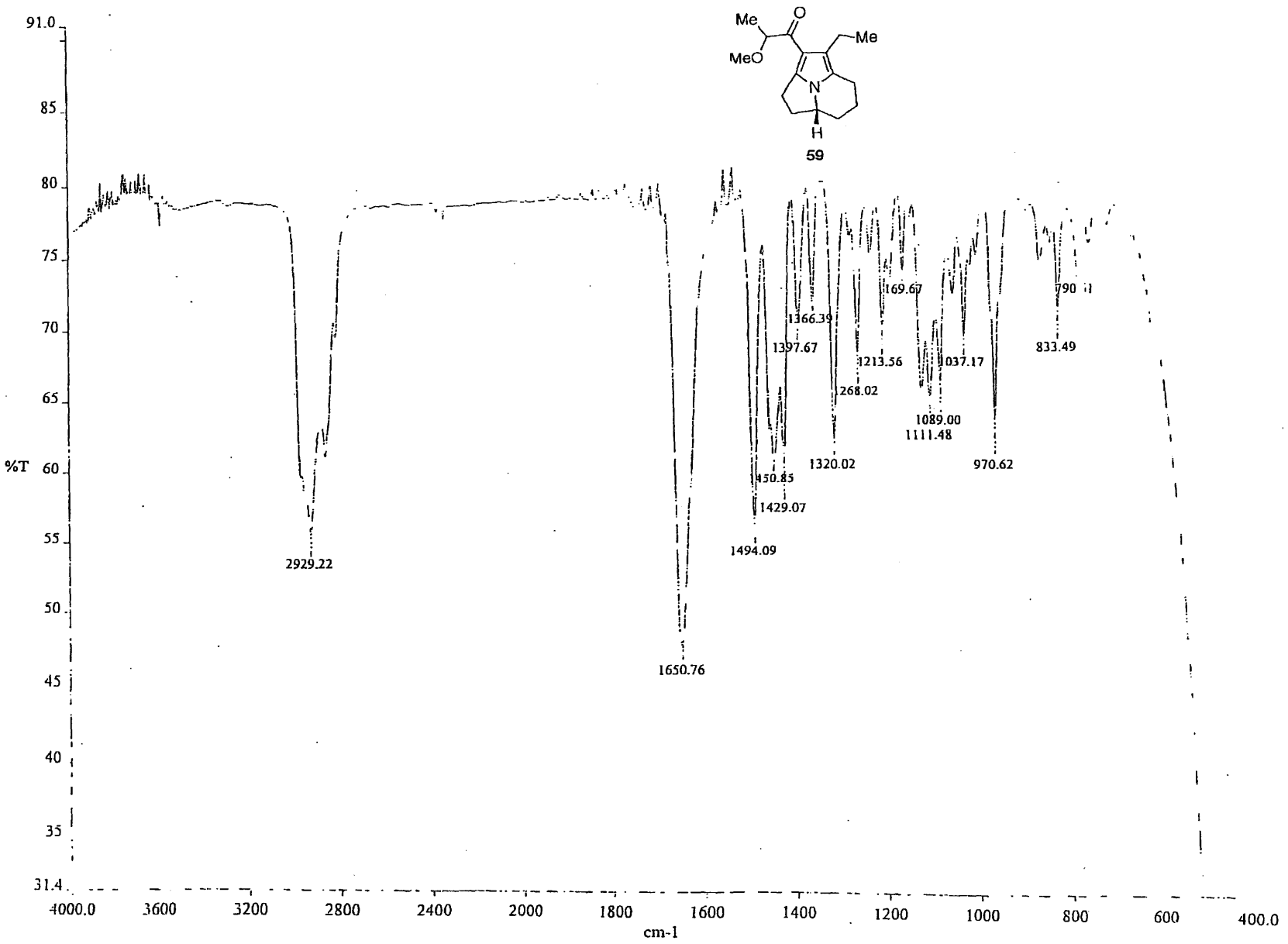
Me
O
MeO
Me
N
H
59
91.0
85
80
75
70
65
%T 60
55
50
45
40
35
31.4
2929.22
1650.76
1494.09
1450.85
1429.07
1397.67
1366.39
1320.02
1268.02
1213.56
1169.67
1111.48
1089.00
1037.17
970.62
833.49
790.11
4000.0
3600
3200
2800
2400
2000
1800
1600
1400
1200
1000
800
600
400.0
cm-1

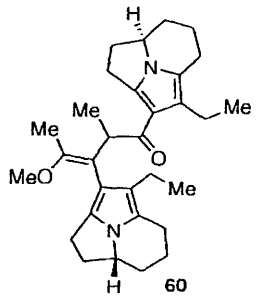

ACQUISITION		DEC. & VT	
sfrq	499.745	dfrq	125.674
tn	H1	dn	C13
at	3.000	dpwr	30
np	41840	dof	1519.5
sw	6973.5	dm	nnn
fb	not used	dmm	w
bs	1	dmf	10000
tpwr	56	dseq	
pw	8.9	dres	1.0
d1	1.000	homo	n
tof	291.0	PROCESSING	
nt	100000	lb	0.01
ct	65	wtfile	
alock	n	proc	ft
gain	not used	fn	131072
FLAGS		math	f
fl	n	werr	
in	n	wexp	
dp	y	wbs	
hs	nn	wnt	wft
DISPLAY			
sp	-250.0		
wp	6246.7		
vs	106		
sc	0		
wc	250		
hzmm	1.04		
is	53.01		
rfl	680.1		
rfp	0		
th	7		
ins	1.000		
nm cdc ph			

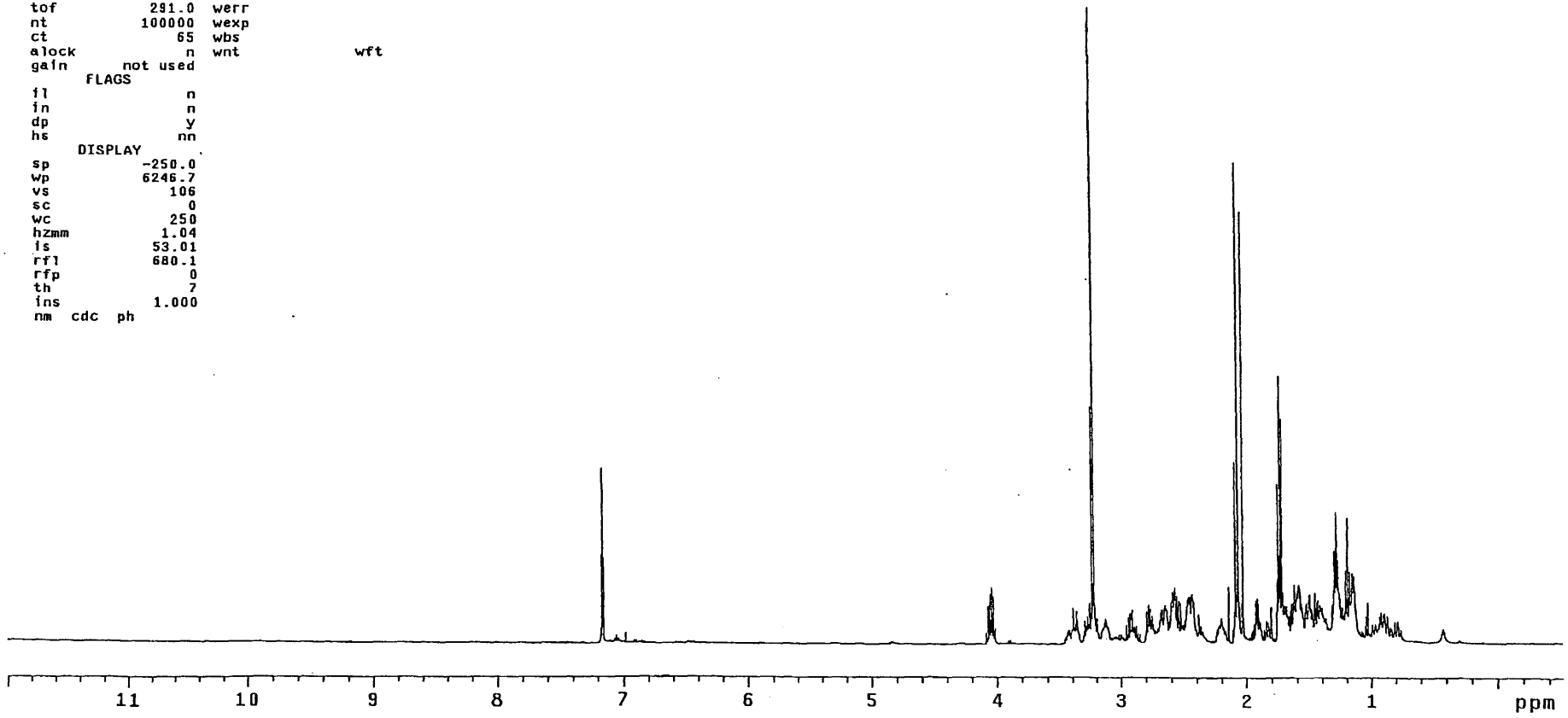

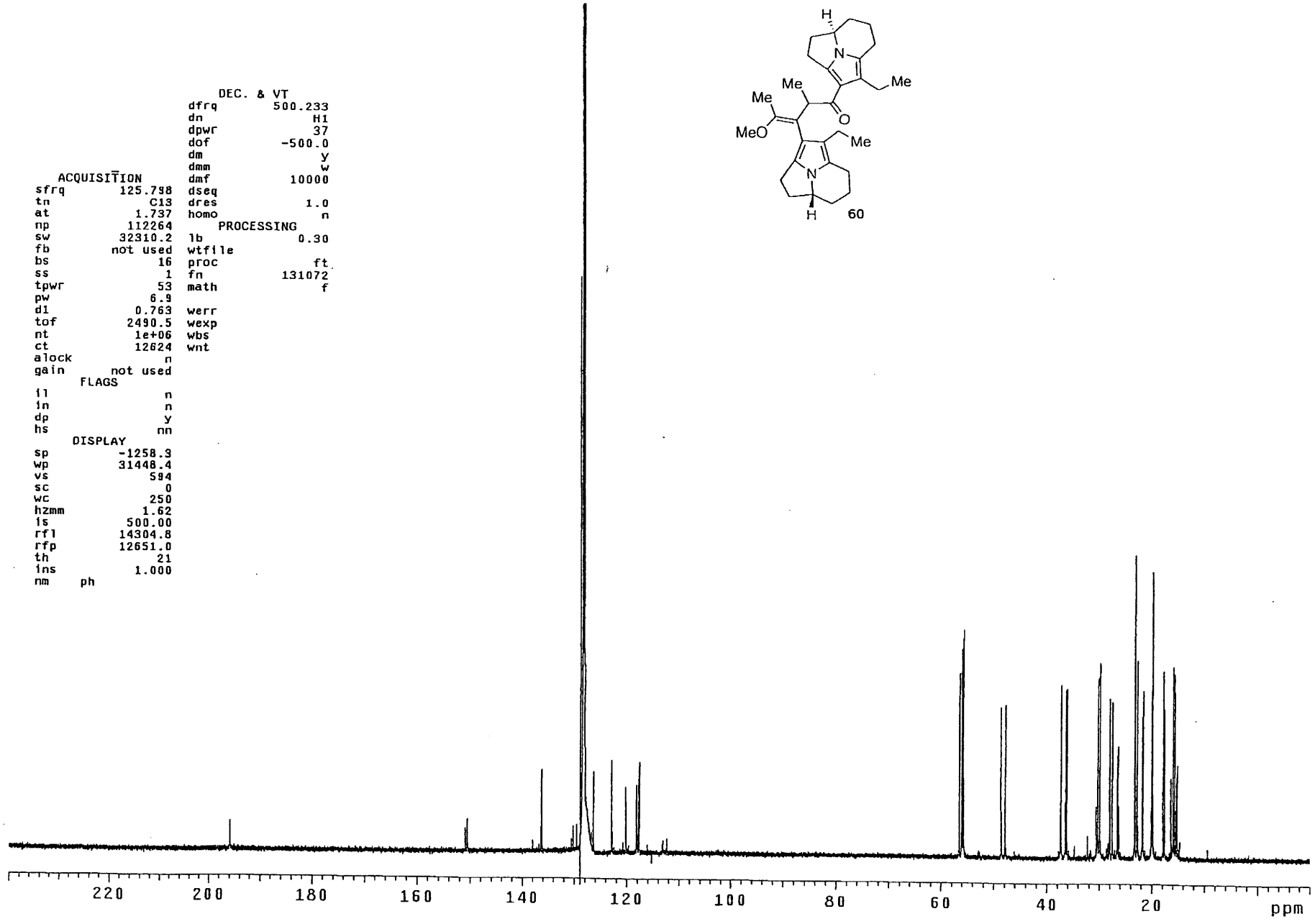
ACQUISITION
sfrq 125.798
tn C13
at 1.737
np 112264
sw 32310.2
fb not used
bs 16
ss 1
tpwr 53
pw 6.9
d1 0.763
tof 2490.5
nt 1e+06
ct 12624
alock n
gain not used
FLAGS
il n
in n
dp y
hs nn
DISPLAY
sp -1258.9
wp 31448.4
vs 594
sc 0
wc 250
hzmm 1.62
is 500.00
rfl 14304.8
rfp 12651.0
th 21
ins 1.000
nm ph
DEC. & VT
dfrq 500.233
dn H1
dpwr 37
dof -500.0
dm y
dmm w
dmf 10000
dseq
dres 1.0
homo n
PROCESSING
lb 0.30
wtfile
proc ft
fn 131072
math f
werr
wexp
wbs
wnt
H
N
Me
Me
Me
O
MeO
Me
N
H
60
220
200
180
160
140
120
100
80
60
40
20
ppm

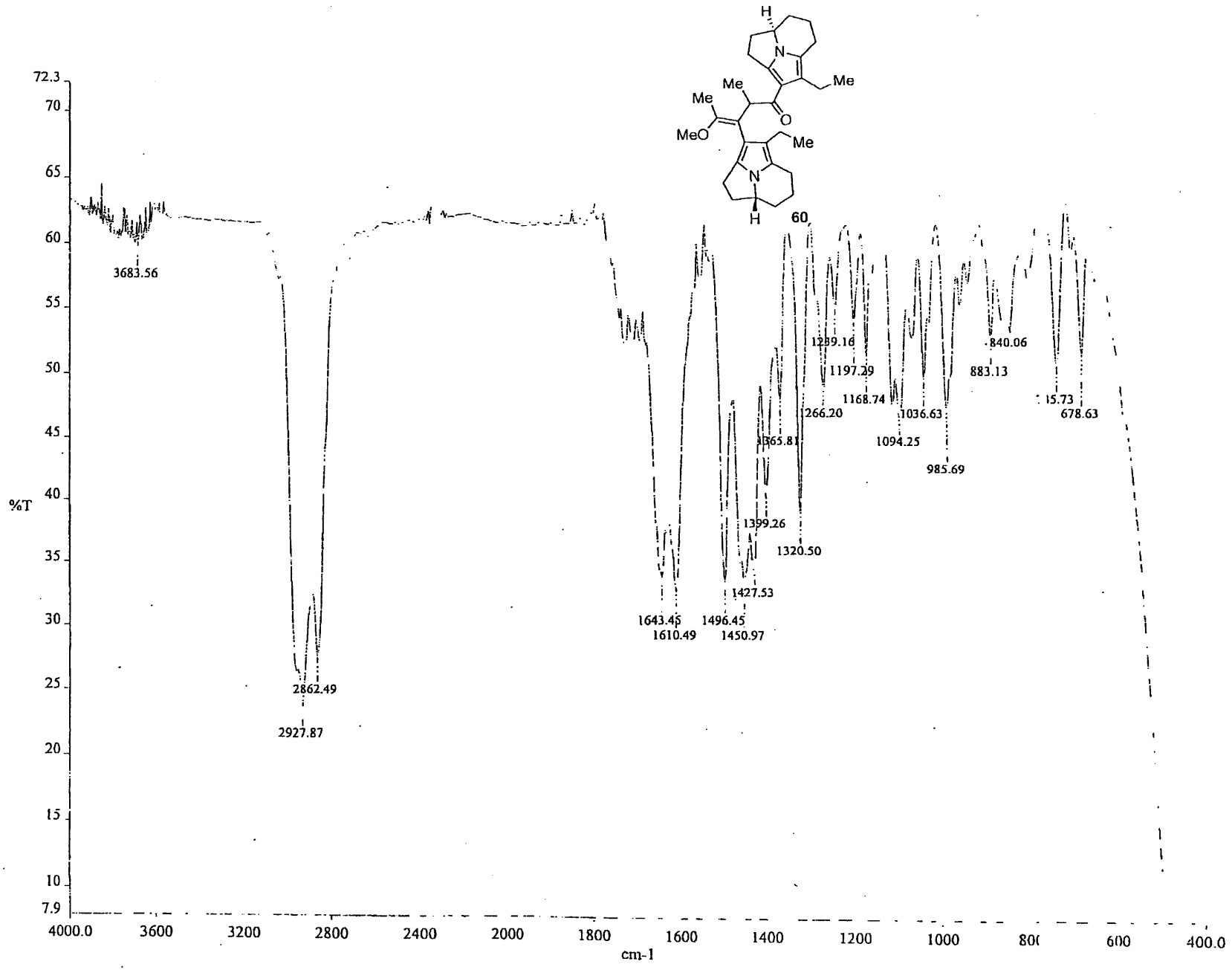
H
N
Me
Me
Me
MeO
O
Me
N
H
60
%T
72.3
70
65
60
55
50
45
40
35
30
25
20
15
10
7.9
3683.56
2927.87
2862.49
1643.45
1610.49
1496.45
1450.97
1427.53
1399.26
1365.81
1320.50
1266.20
1239.16
1197.29
1168.74
1094.25
1036.63
985.69
883.13
840.06
715.73
678.63
4000.0
3600
3200
2800
2400
2000
1800
1600
1400
1200
1000
800
600
400.0
cm-1

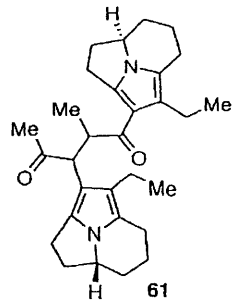

61

ACQUISITION		DEC. & VT	
sfrq	500.235	dfrq	125.795
tn	H1	dn	C13
at	3.200	dpwr	37
np	64000	dof	0
sw	10000.0	dm	nnn
fb	not used	dmm	c
bs	1	dmf	10000
ss	1	dseq	
tpwr	59	dres	1.0
pw	9.0	homo	n
d1	0	PROCESSING	
tof	1498.2	wtfile	
nt	16	proc	ft
ct	14	fn	131072
alock	n	math	f
gain	not used	werr	
FLAGS		wexp	
il	n	wbs	
in	n	wnt	
dp	y		
hs	nn		
DISPLAY			
sp	-250.2		
wp	6252.7		
vs	94		
sc	0		
wc	250		
hzmm	9.33		
is	100.00		
rfl	4577.3		
rfp	3576.7		
th	7		
ins	1.000		
nm	cdc ph		

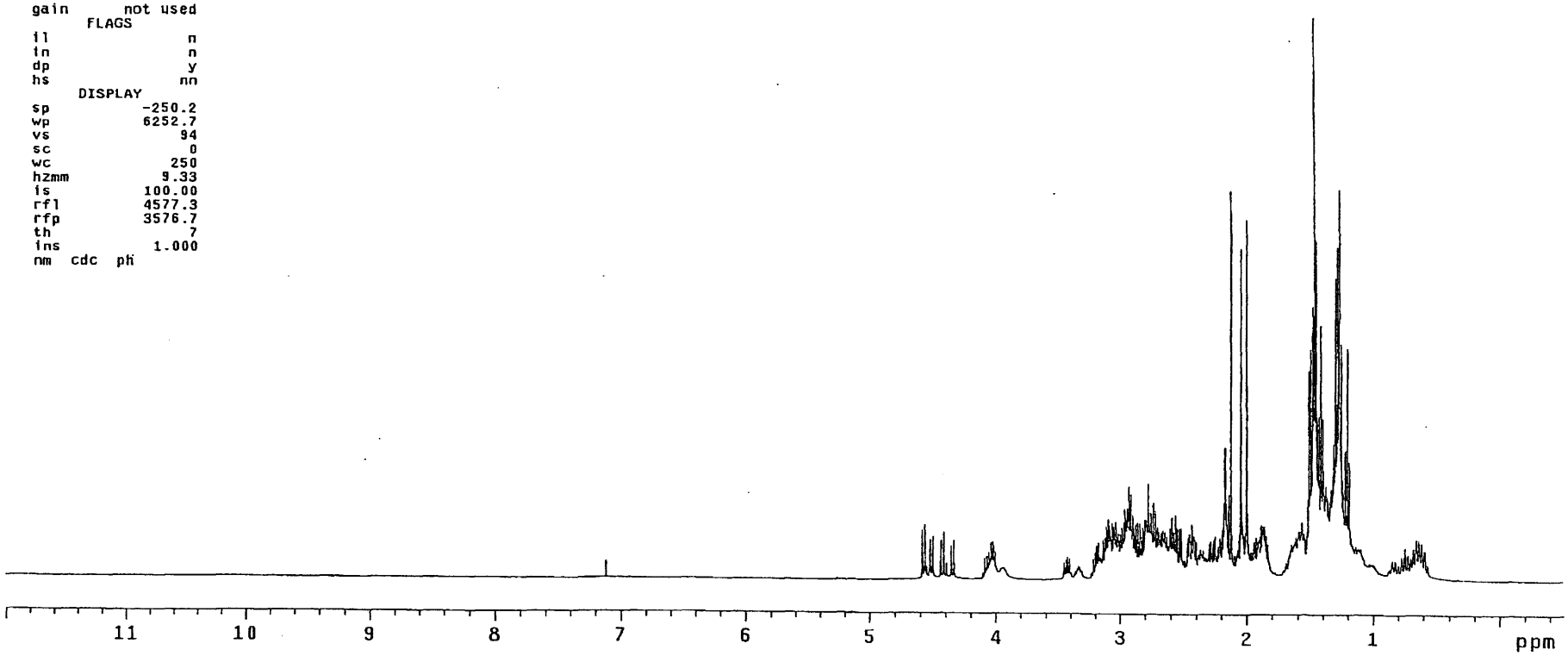

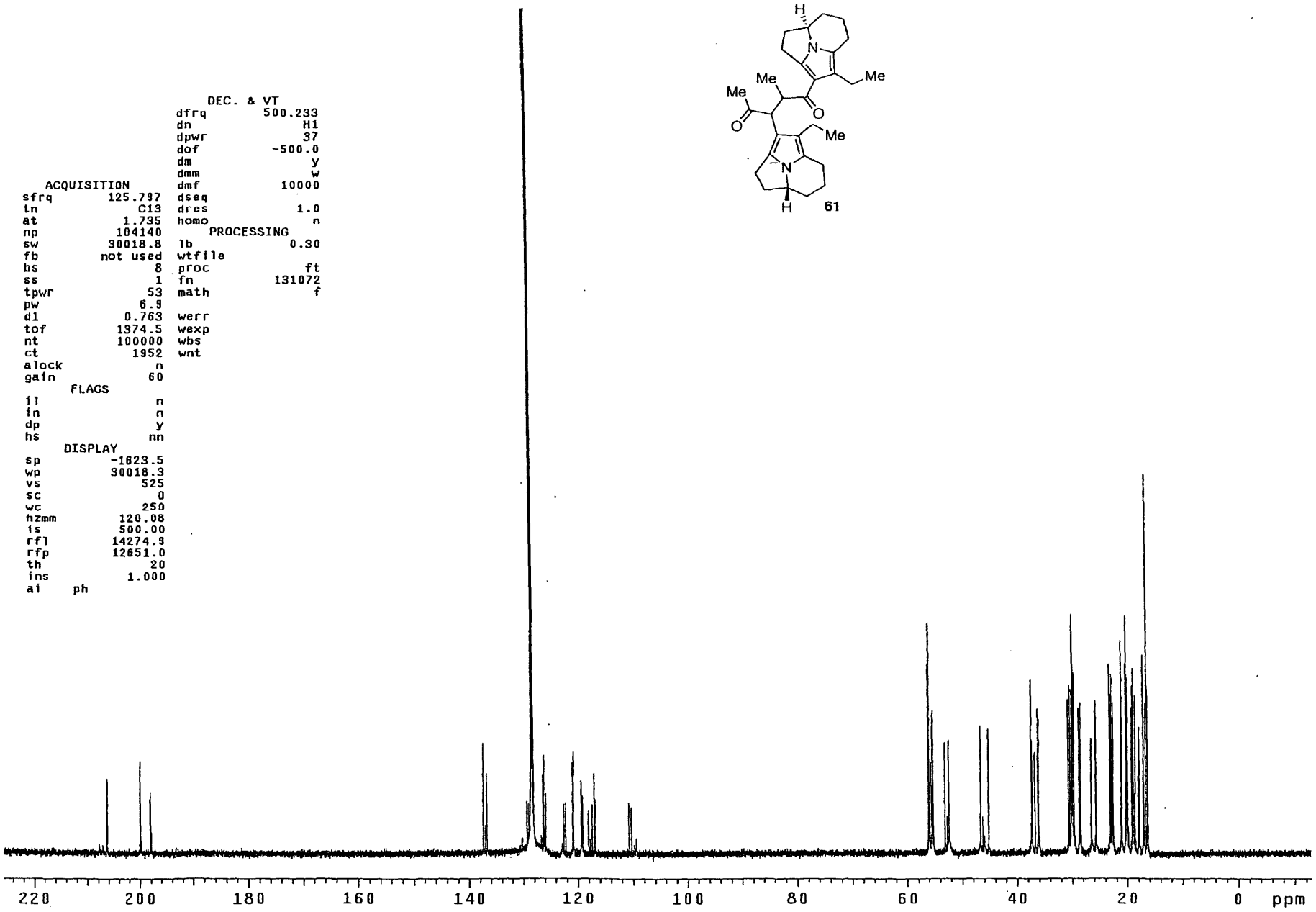
ACQUISITION
sfrq 125.797
tn C13
at 1.735
np 104140
sw 30018.8
fb not used
bs 8
ss 1
tpwr 53
pw 6.9
d1 0.763
tof 1374.5
nt 100000
ct 1952
alock n
gain 60
FLAGS
il n
in n
dp y
hs nn
DISPLAY
sp -1623.5
wp 30018.3
vs 525
sc 0
wc 250
hzmm 120.08
is 500.00
rfl 14274.9
rfp 12651.0
th 20
ins 1.000
ai ph
DEC. & VT
dfrq 500.233
dn H1
dpwr 37
dof -500.0
dm y
dmm w
dmf 10000
dseq
dres 1.0
homo n
PROCESSING
lb 0.30
wtfile
proc ft
fn 131072
math f
werr
wexp
wbs
wnt
H
N
Me
Me
Me
O
O
Me
N
H
61
220
200
180
160
140
120
100
80
60
40
20
0
ppm

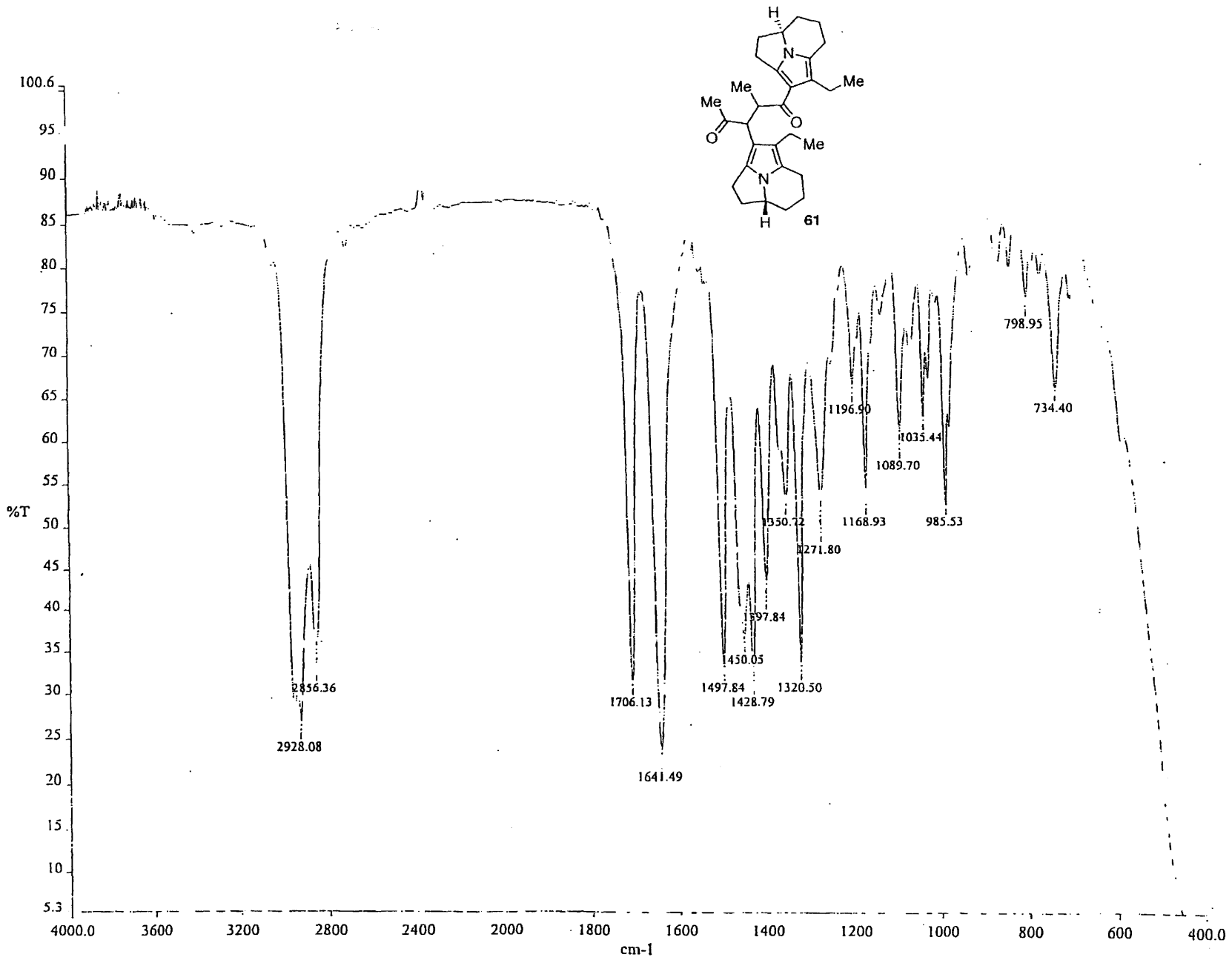
100.6
95
90
85
80
75
70
65
60
55
%T
50
45
40
35
30
25
20
15
10
5.3
4000.0
3600
3200
2800
2400
2000
1800
1600
1400
1200
1000
800
600
400.0
cm-1
2928.08
2856.36
1706.13
1641.49
1497.84
1450.05
1428.79
1397.84
1350.22
1320.50
1271.80
1196.90
1168.93
1089.70
1035.44
985.53
798.95
734.40
H
N
Me
Me
Me
O
O
Me
N
H
61

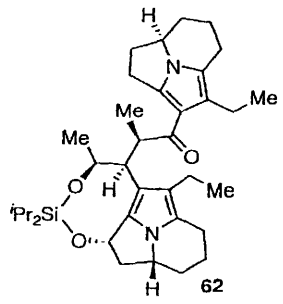

ACQUISITION		DEC. & VT	
sfrq	499.748	dfrq	125.673
tn	H1	dn	C13
at	3.001	dpwr	30
np	40494	dof	0
sw	6747.6	dm	nnn
fb	not used	dmm	w
bs	1	dmf	10000
tpwr	56	dseq	
pw	8.9	dres	1.0
d1	1.000	homo	n
tof	624.4	PROCESSING	
nt	1000	wtfile	
ct	57	proc	ft
alock	n	fn	131072
gain	not used	math	f
FLAGS		werr	
il	n	wexp	
in	n	wbs	
dp	y	wnt	wft
hs	nn		
DISPLAY			
sp	-250.0		
wp	6246.7		
vs	193		
sc	0		
wc	250		
hzmm	24.99		
is	372.08		
rfl	250.6		
rfp	0		
th	7		
ins	1.000		
nm cdc ph			

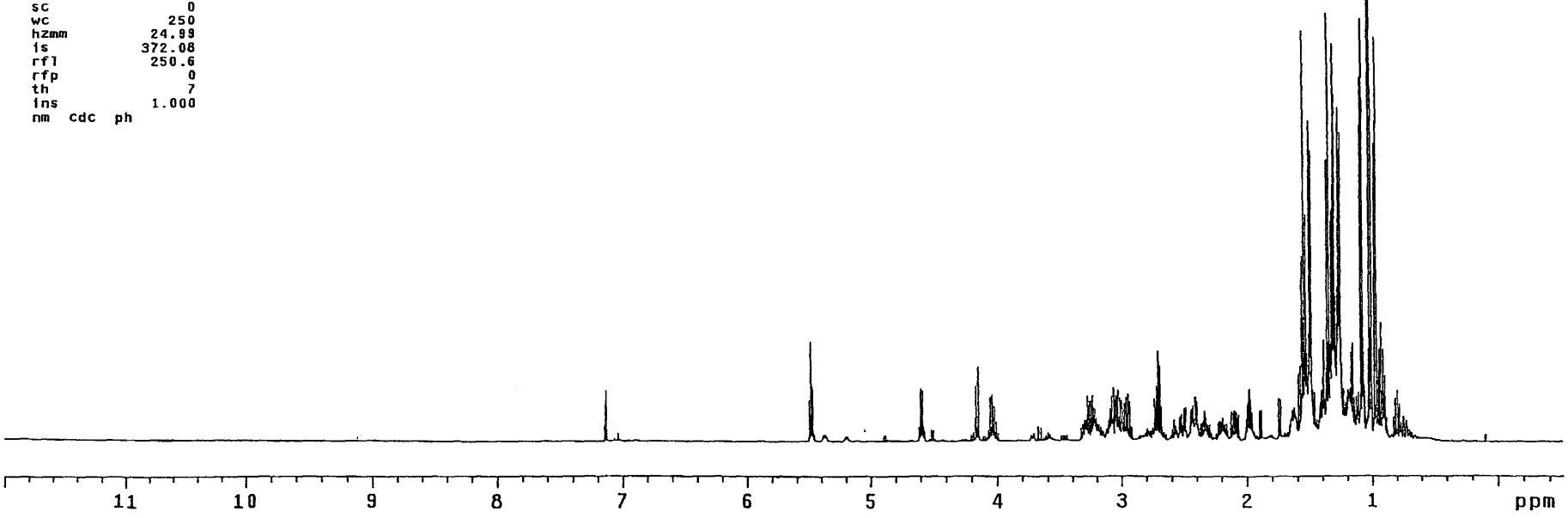

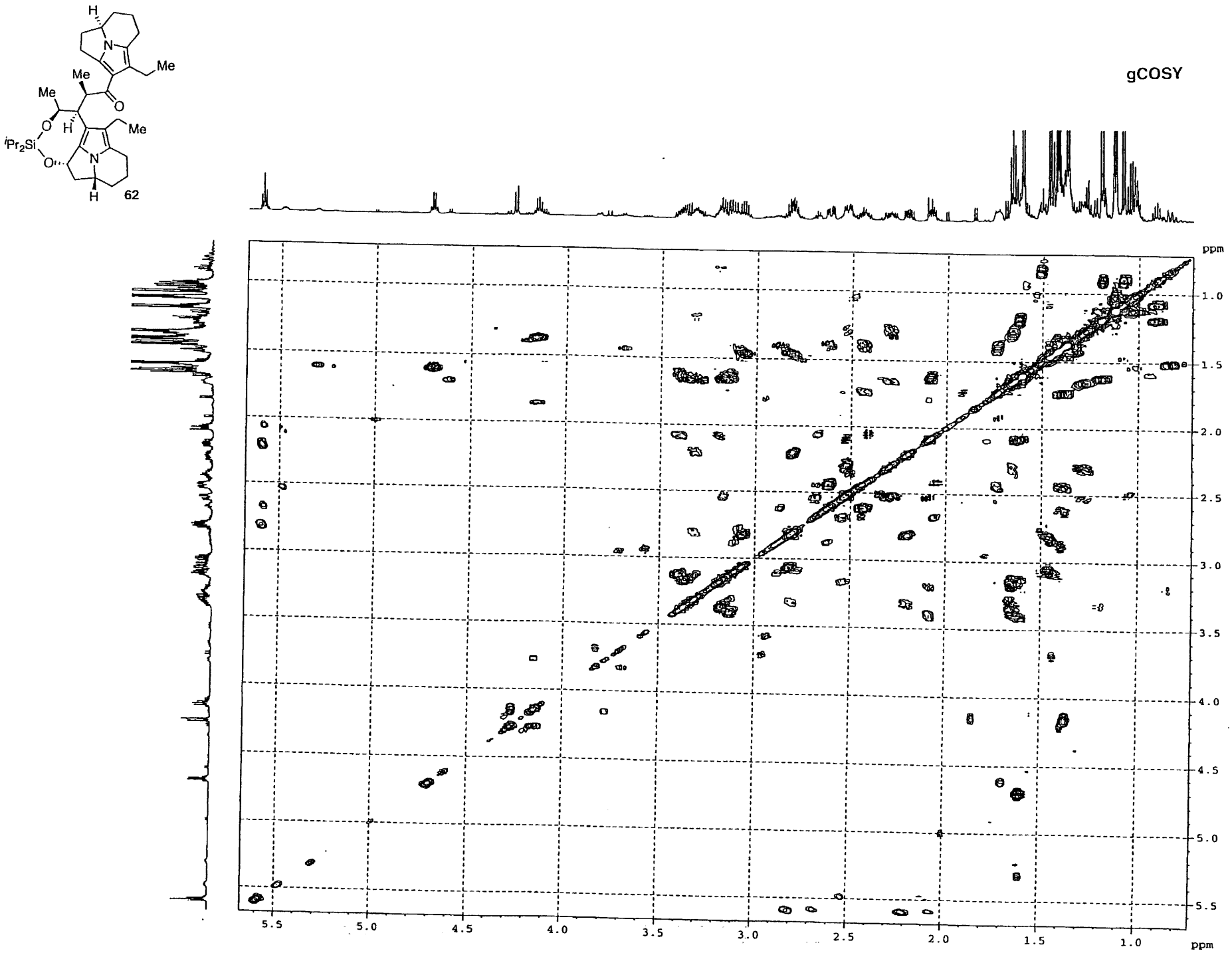
gCOSY
62
ppm
5.5
5.0
4.5
4.0
3.5
3.0
2.5
2.0
1.5
1.0

Appendix E.

Spectra for Chapter V

ACQUISITION		DEC. & VT	
sfrq	499.745	lfrq	125.672
tn	H1	dn	C13
at	3.001	dpwr	30
np	41342	dof	0
sw	6887.1	dm	nnn
fb	not used	dmm	w
bs	1	dmf	10000
tpwr	56	dseq	
pw	8.6	dres	1.0
d1	1.000	homo	n
tof	263.4	PROCESSING	
nt	10000	wtfile	
ct	10	proc	ft
alock	n	fn	262144
gain	not used	math	f
FLAGS		werr	
il	n	wexp	
in	n	wbs	
dp	y	wnt	wft
hs	nn		
DISPLAY			
sp	-249.9		
wp	6246.8		
vs	164		
sc	0		
wc	250		
hzmm	24.99		
is	161.11		
rfl	681.3		
rfp	0		
th	32		
ins	1.000		
ai cdc ph			

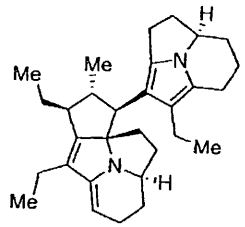

isoM430B

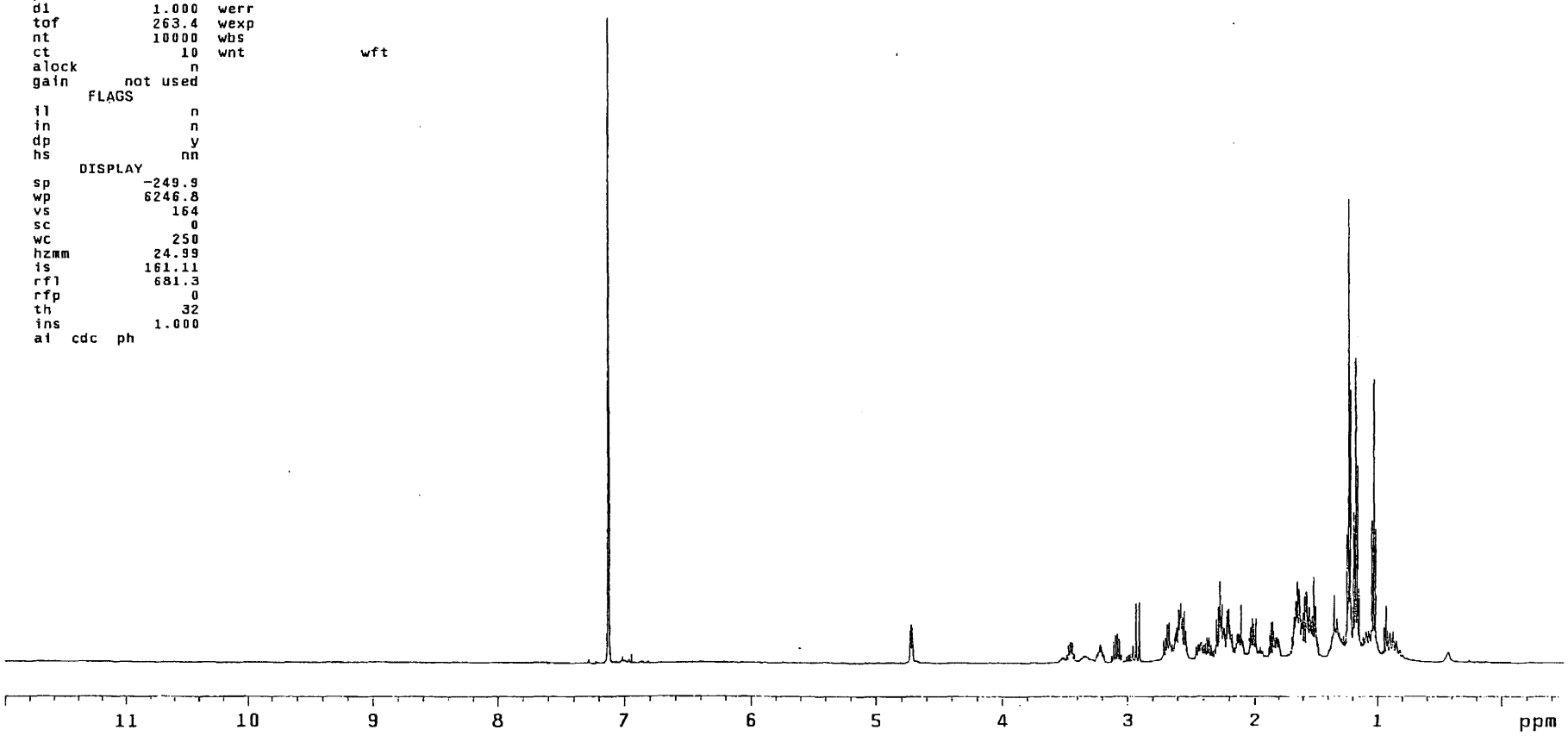

ACQUISITION		DEC. & VT	
sfrq	125.796	dfrq	500.233
tn	C13	dn	H1
at	1.735	dpwr	44
np	102450	dof	-500.0
sw	29520.3	dm	y
fb	not used	dmm	w
bs	8	dmf	10000
ss	1	dseq	
tpwr	54	dres	1.0
pw	6.9	homo	n
d1	0.763	PROCESSING	
tof	1027.4	lb	1.00
nt	1e+06	wtfile	
ct	848	proc	ft
alock	n	fn	131072
gain	not used	math	f
FLAGS		werr	
il	n	wexp	
in	n	wbs	
dp	y	wnt	
hs	nn		
DISPLAY			
sp	-629.0		
wp	28303.6		
vs	866		
sc	0		
wc	250		
hzmm	113.21		
is	500.00		
rfl	14372.8		
rfp	12651.0		
th	40		
ins	1.000		
ai	ph		

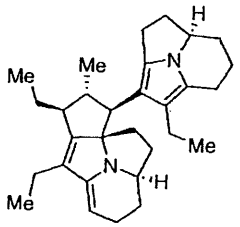

isoM430B

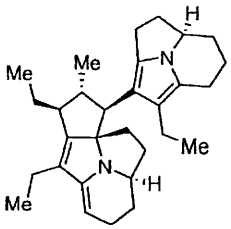

IsoM430B

gCOSY

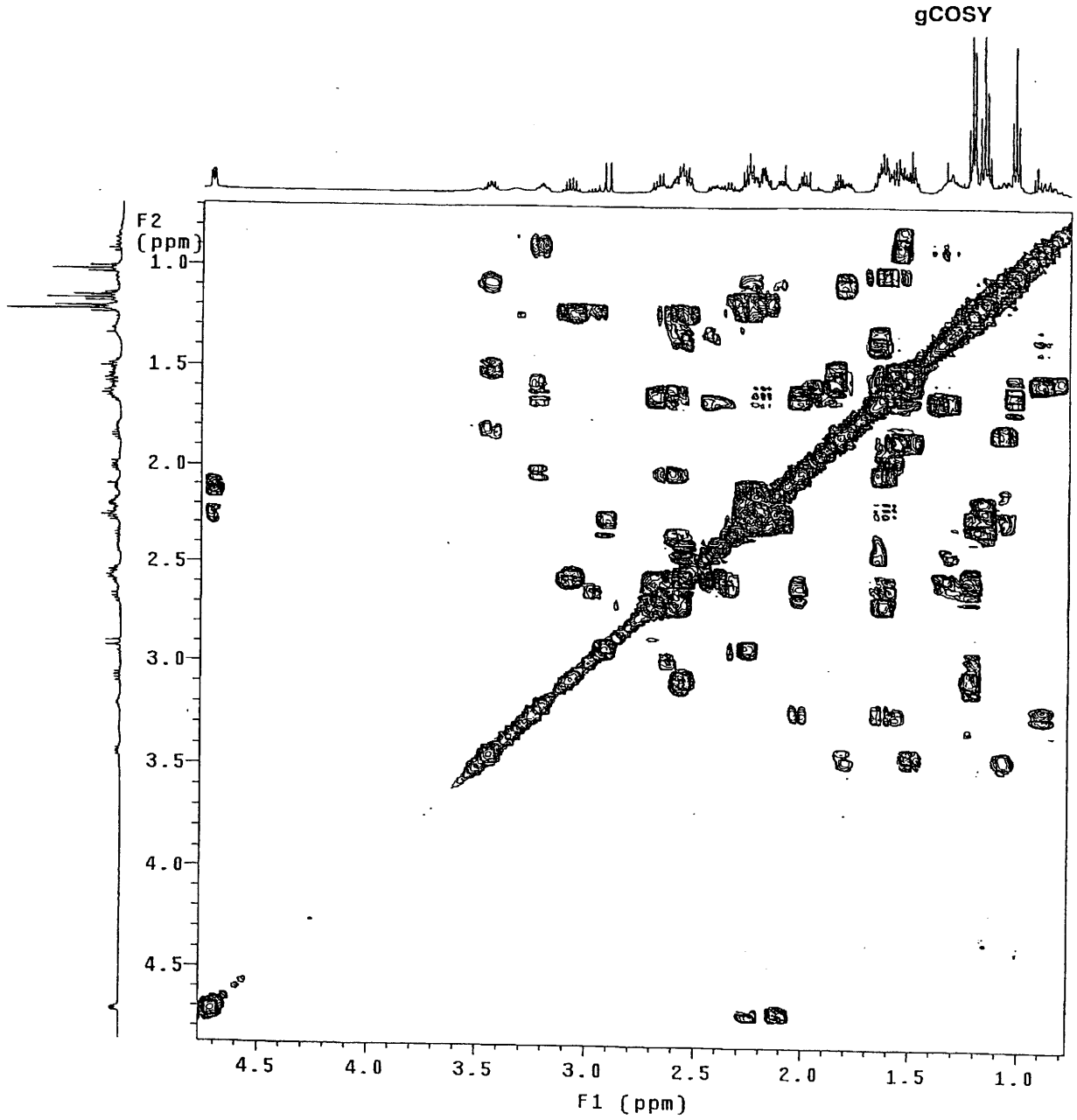

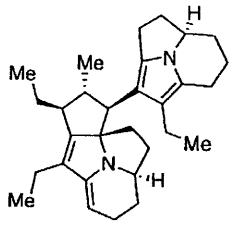

IsoM430B

HSQC

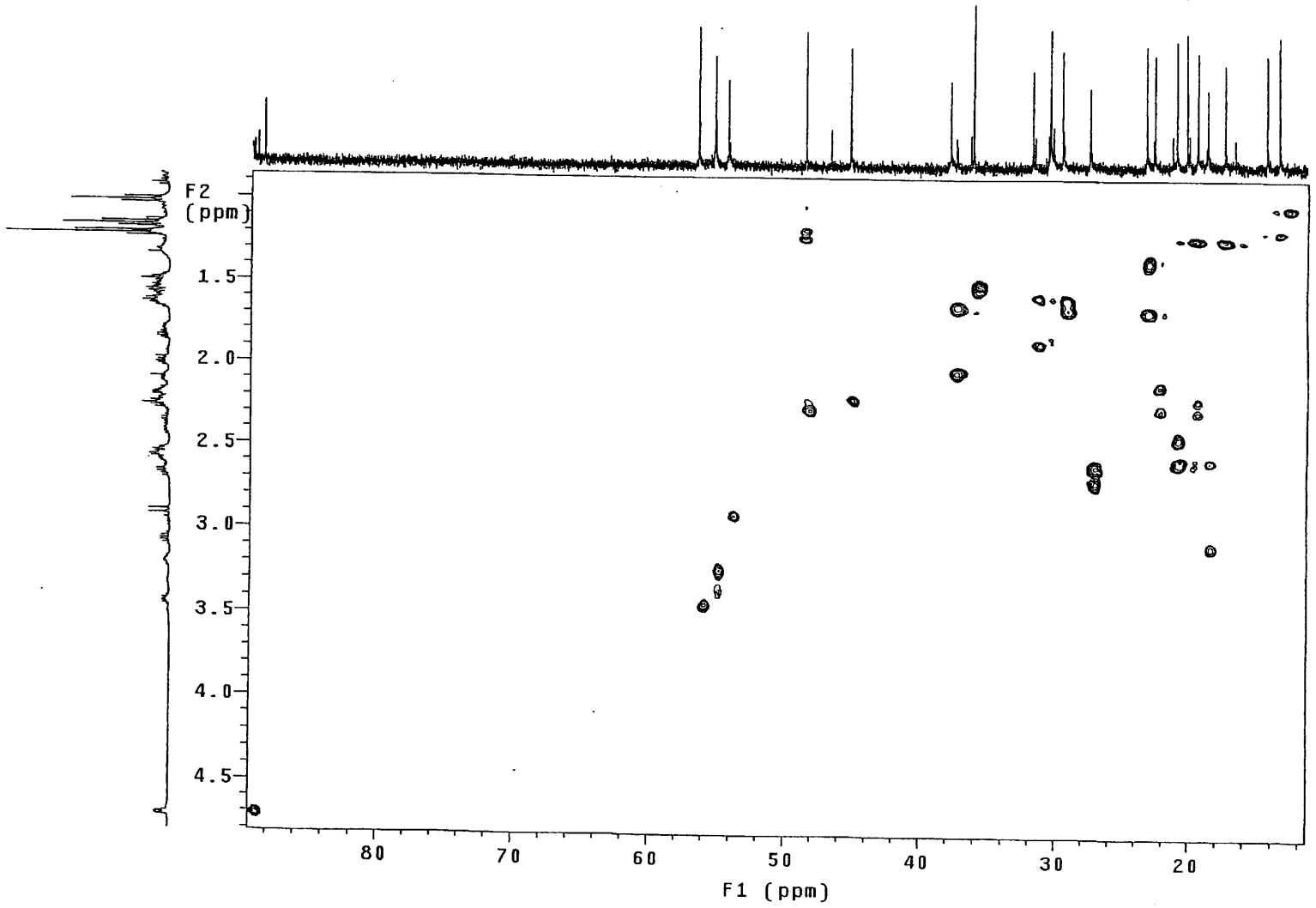

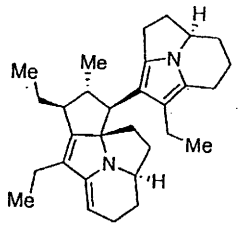

IsoM430B

gHMBC

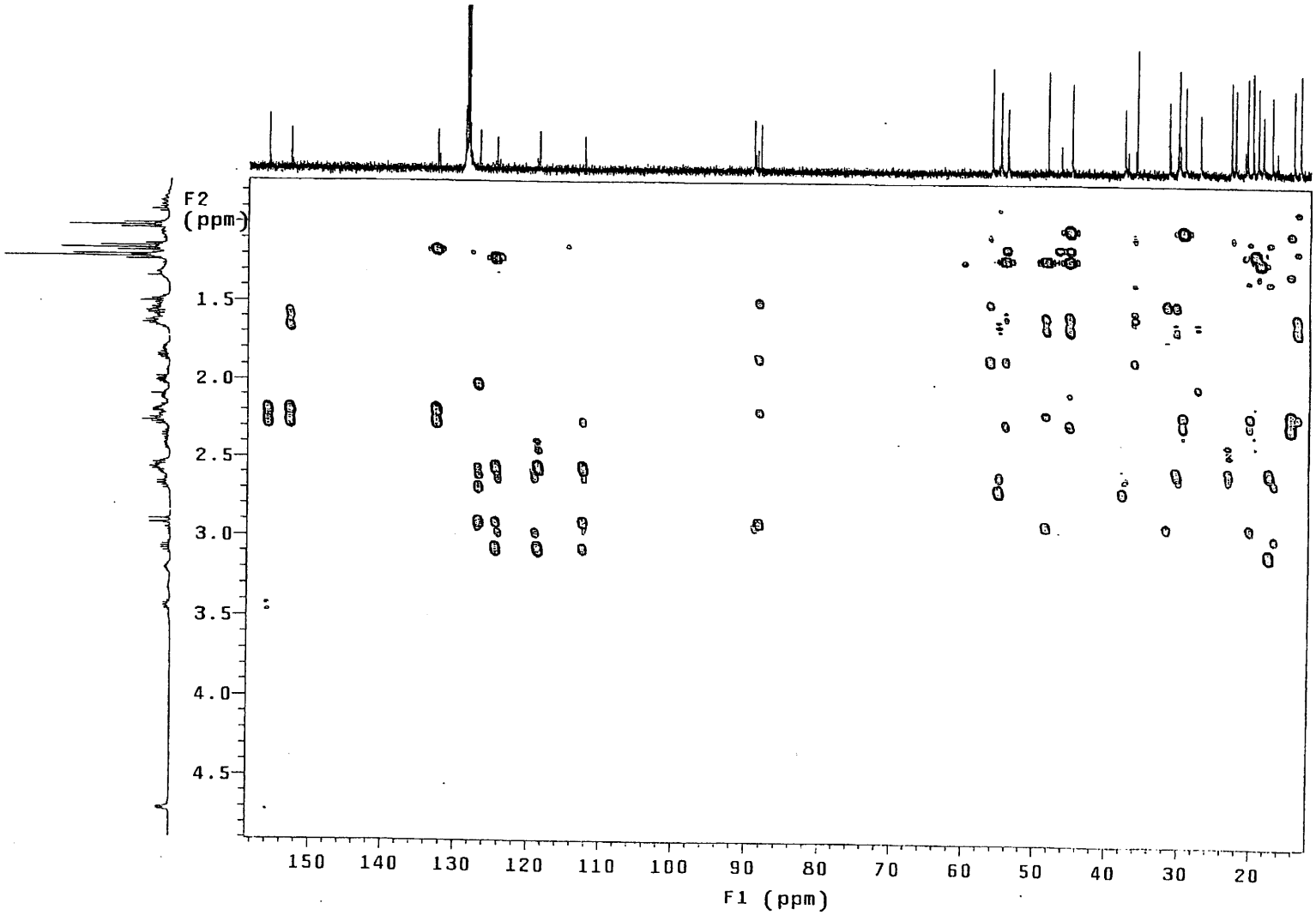

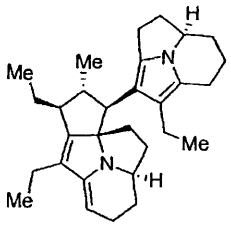

isoM430B

NOESY

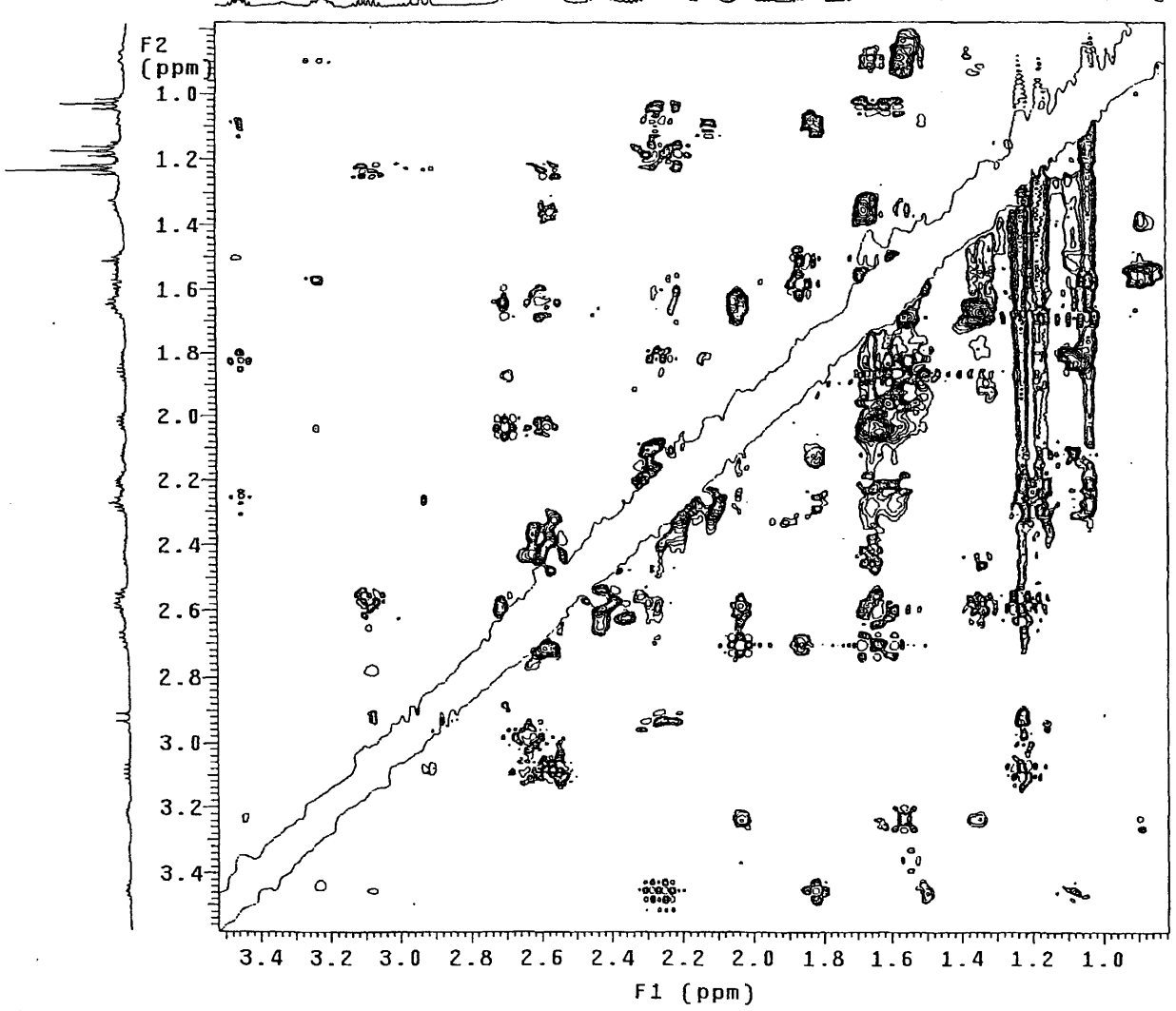

F2 - Acquisition Parameters

INSTRUM	spect	
PROBHD	5 mm CPTXI Z-G	
PULPROG	zg	
TD	32768	
SOLVENT	C6D6	
NS	8	
DS	2	
SWH	6009.615	Hz
FIDRES	0.183399	Hz
AQ	2.7263477	sec
RG	16	
DW	83.200	usec
DE	6.00	usec
TE	293.0	K
D1	1.00000000	sec
MCREST	0.00000000	sec
MCWRK	0.01500000	sec
======== CHANNEL f1 ========		
NUC1	1H	
P1	8.15	usec
PL1	-6.00	dB
SFO1	600.4674019	MHz

F2 - Processing parameters

SI	65536	
SF	600.4650662	MHz
WDW	EM	
SSB	0	
LB	0.00	Hz
GB	0	
PC	1.00	

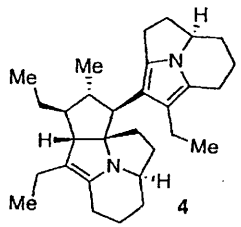

4

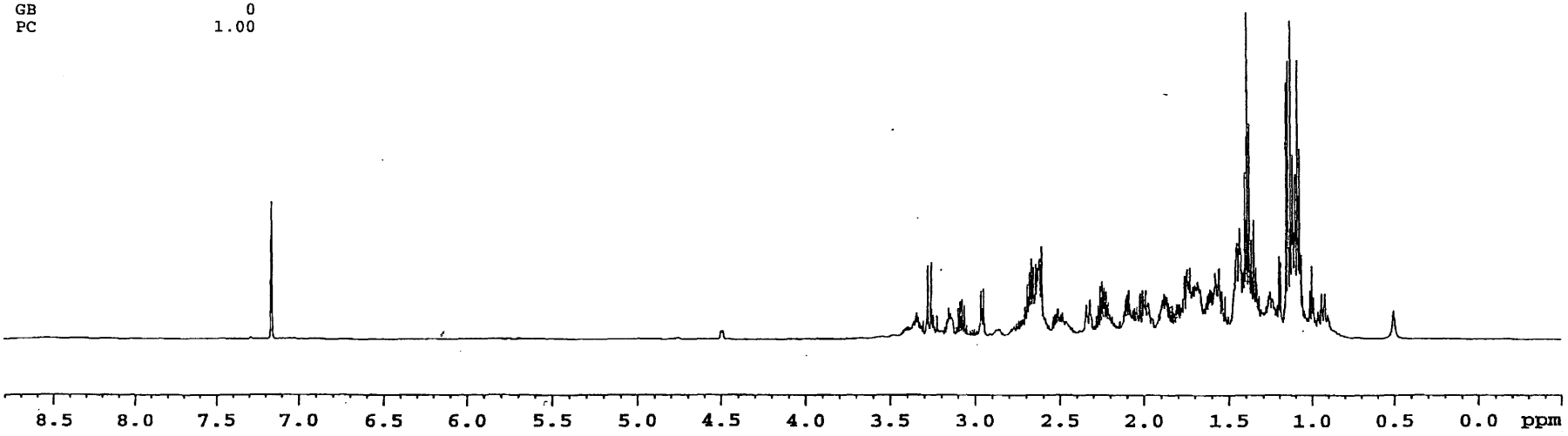

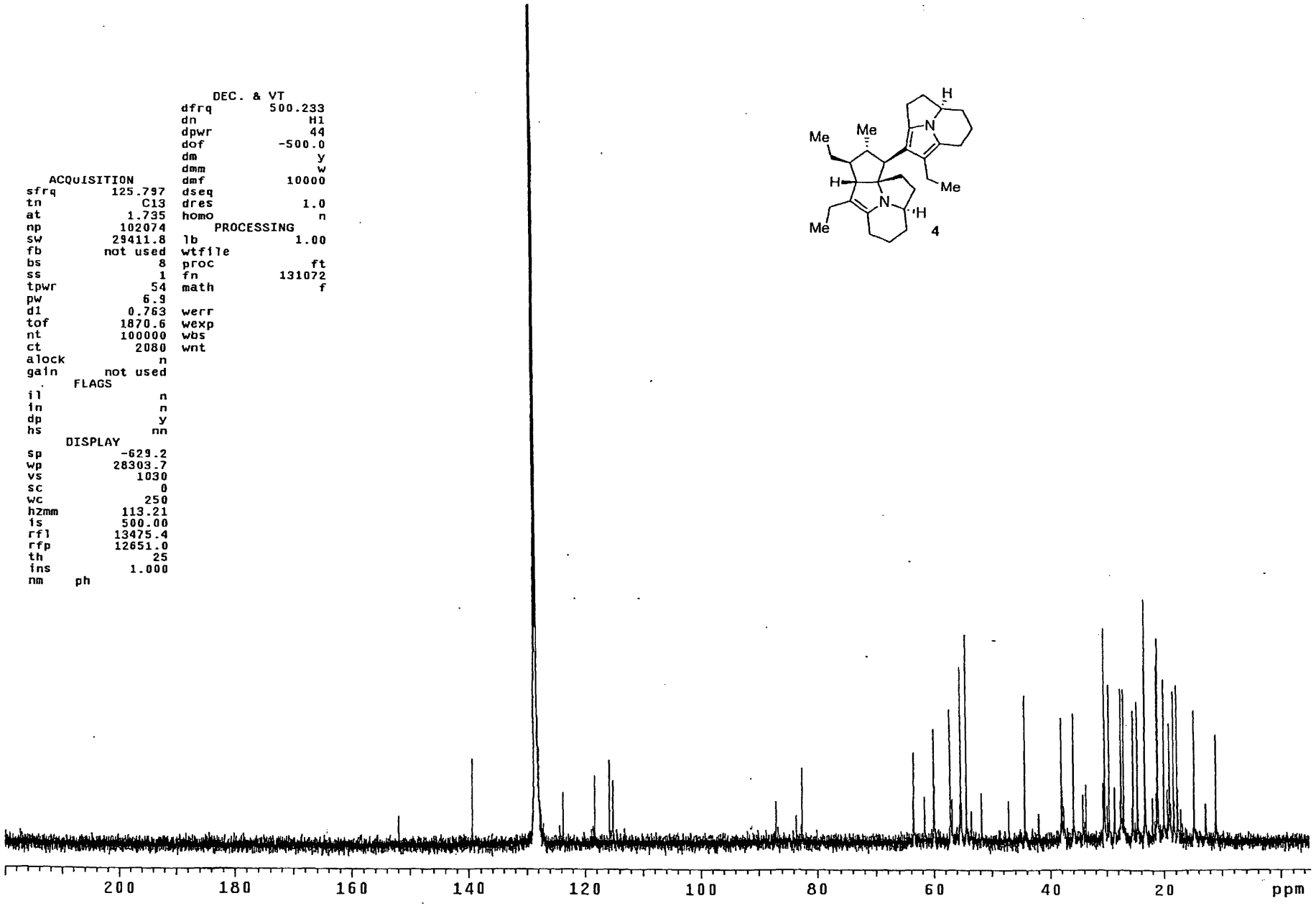
ACQUISITION
sfrq 125.797
tn C13
at 1.735
np 102074
sw 29411.8
fb not used
bs 8
ss 1
tpwr 54
pw 6.9
d1 0.763
tof 1870.6
nt 100000
ct 2080
alock n
gain not used
FLAGS
il n
in n
dp y
hs nn
DISPLAY
sp -629.2
wp 28303.7
vs 1030
sc 0
wc 250
hzmm 113.21
is 500.00
rfl 13475.4
rfp 12651.0
th 25
ins 1.000
nm ph
DEC. & VT
dfrq 500.233
dn H1
dpwr 44
dof -500.0
dm y
dmm w
dmf 10000
dseq
dres 1.0
homo n
PROCESSING
lb 1.00
wtfile
proc ft
fn 131072
math f
werr
wexp
wbs
wnt
Me
Me
H
N
Me
H
N
H
Me
4
200
180
160
140
120
100
80
60
40
20
ppm

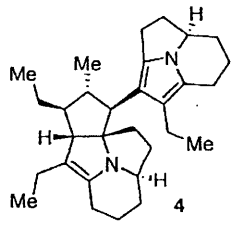
H
Me
Me
N
H
Me
N
H
Me
4

gCOSY

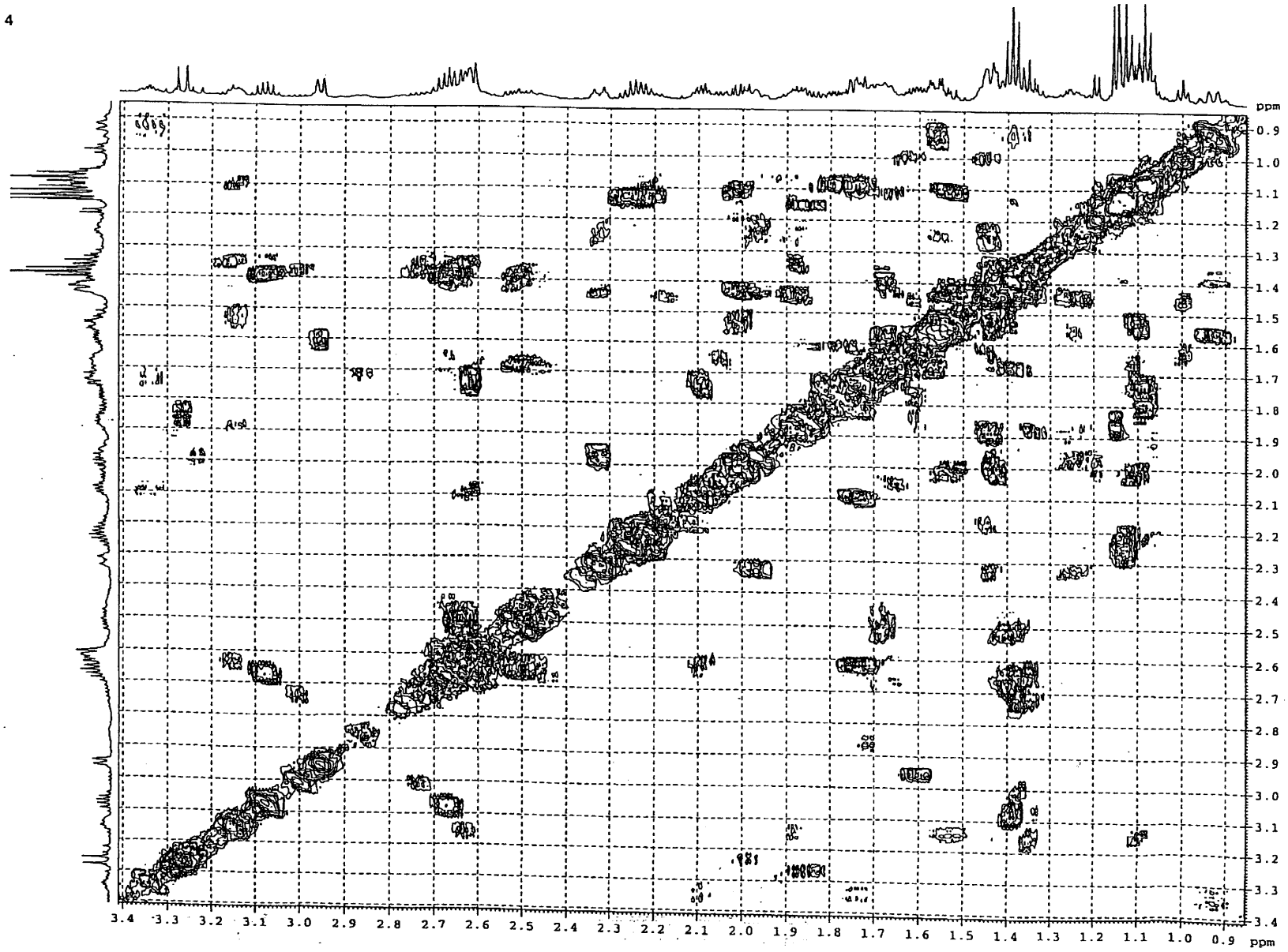
ppm
0.9
1.0
1.1
1.2
1.3
1.4
1.5
1.6
1.7
1.8
1.9
2.0
2.1
2.2
2.3
2.4
2.5
2.6
2.7
2.8
2.9
3.0
3.1
3.2
3.3
3.4
3.4 3.3 3.2 3.1 3.0 2.9 2.8 2.7 2.6 2.5 2.4 2.3 2.2 2.1 2.0 1.9 1.8 1.7 1.6 1.5 1.4 1.3 1.2 1.1 1.0 0.9 ppm

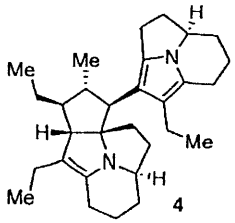
Me
Me
H
N
Me
H
N
H
Me
4

gHSQC

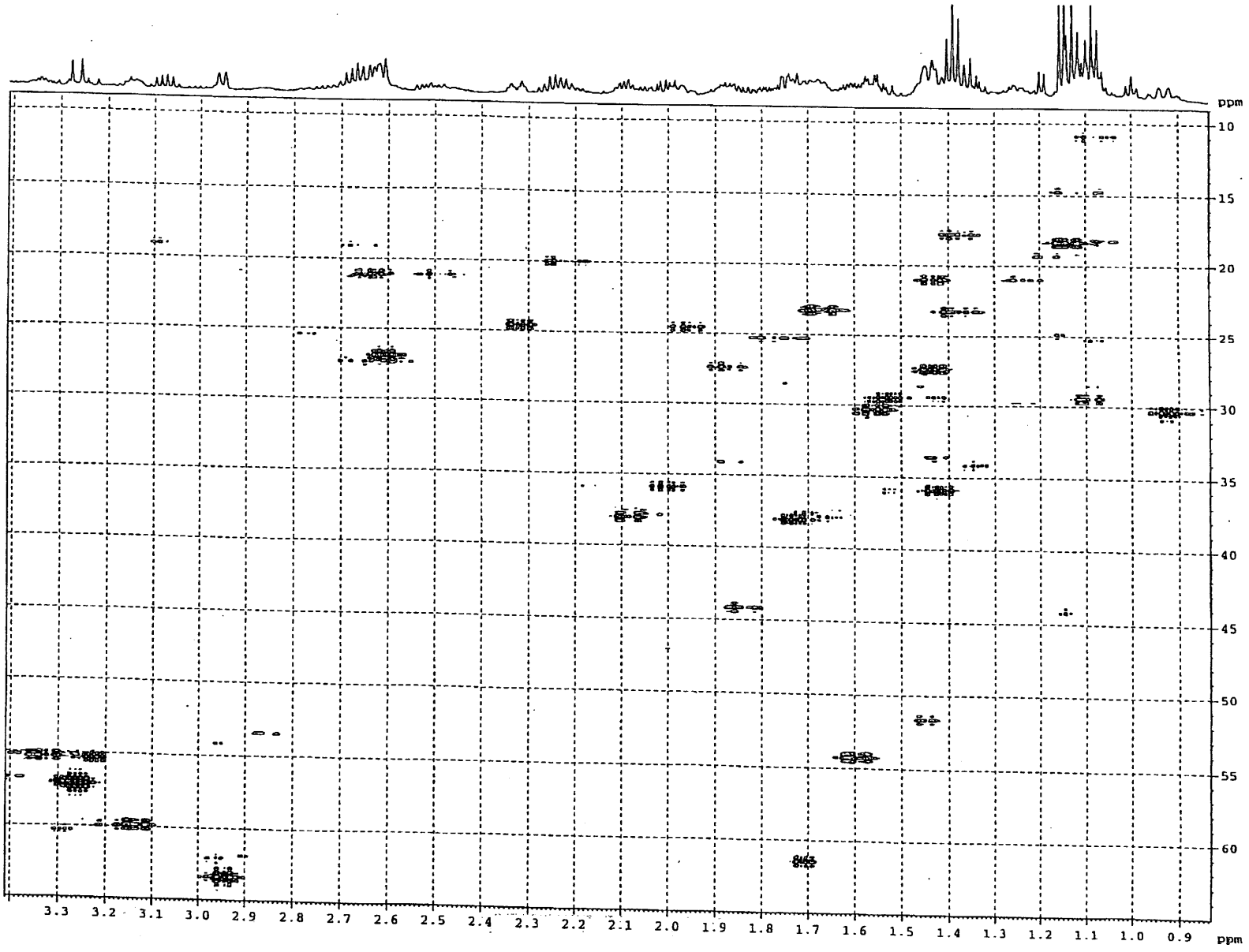
ppm
10
15
20
25
30
35
40
45
50
55
60
3.3
3.2
3.1
3.0
2.9
2.8
2.7
2.6
2.5
2.4
2.3
2.2
2.1
2.0
1.9
1.8
1.7
1.6
1.5
1.4
1.3
1.2
1.1
1.0
0.9
ppm

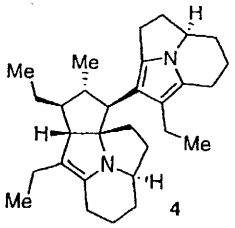
H
Me
Me
N
H
Me
Me
N
H
Me
4

gHMBC

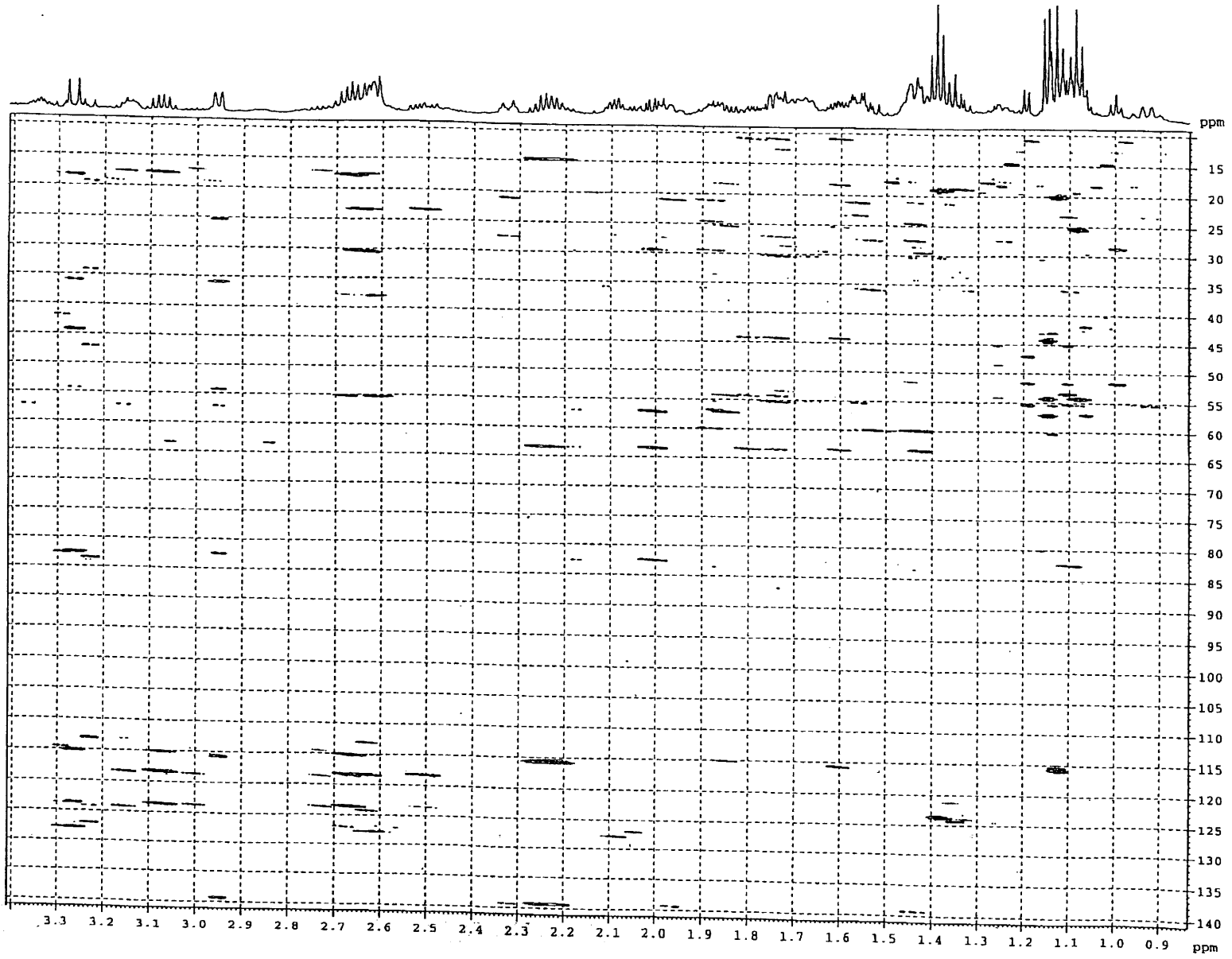
ppm
15
20
25
30
35
40
45
50
55
60
65
70
75
80
85
90
95
100
105
110
115
120
125
130
135
140
3.3
3.2
3.1
3.0
2.9
2.8
2.7
2.6
2.5
2.4
2.3
2.2
2.1
2.0
1.9
1.8
1.7
1.6
1.5
1.4
1.3
1.2
1.1
1.0
0.9
ppm

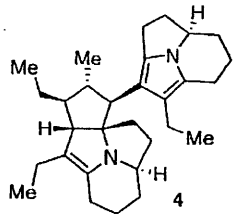
Me
Me
H
N
H
Me
Me
N
H
Me
4

gNOESY

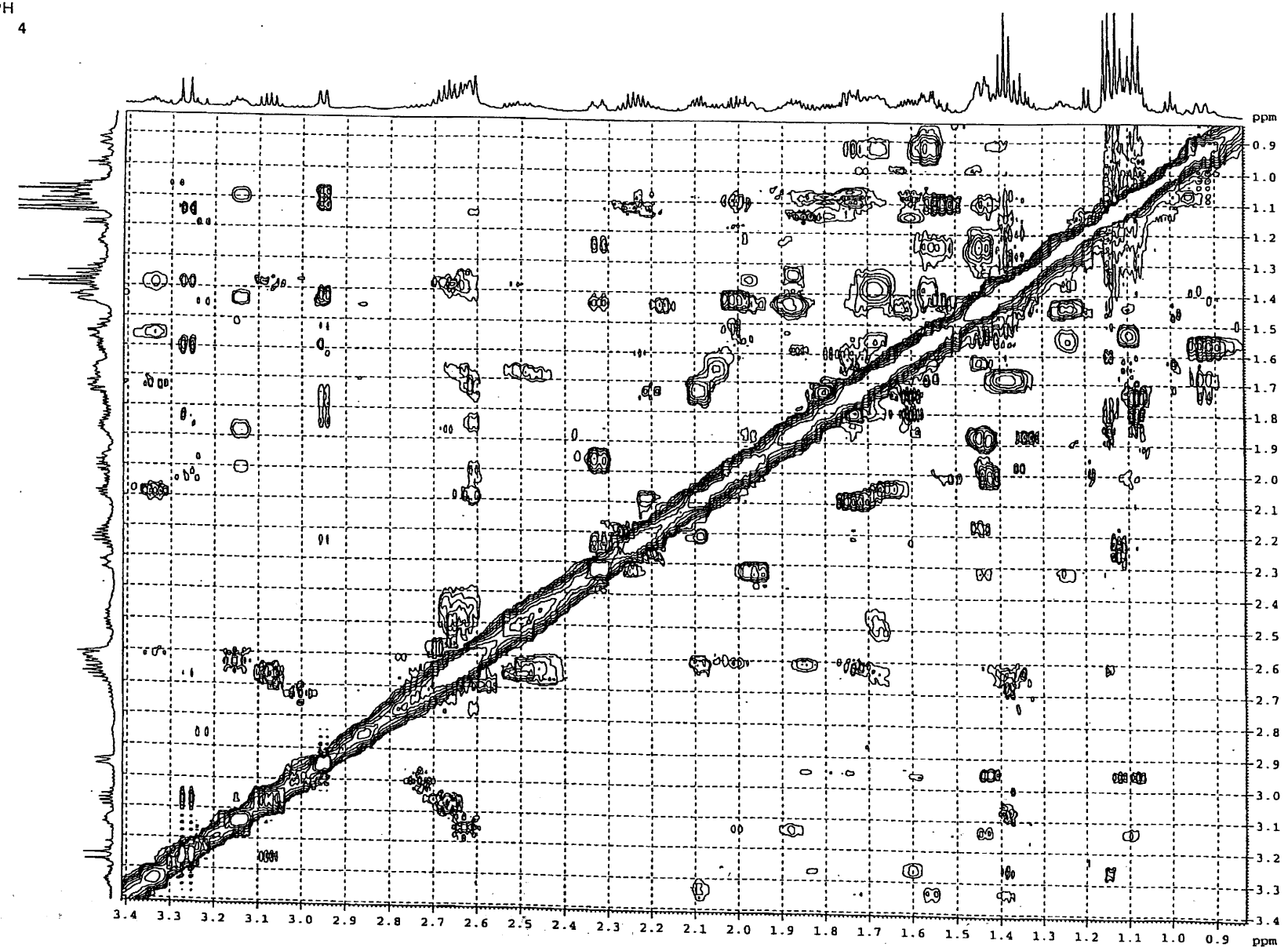
ppm
0.9
1.0
1.1
1.2
1.3
1.4
1.5
1.6
1.7
1.8
1.9
2.0
2.1
2.2
2.3
2.4
2.5
2.6
2.7
2.8
2.9
3.0
3.1
3.2
3.3
3.4
3.4 3.3 3.2 3.1 3.0 2.9 2.8 2.7 2.6 2.5 2.4 2.3 2.2 2.1 2.0 1.9 1.8 1.7 1.6 1.5 1.4 1.3 1.2 1.1 1.0 0.9
ppm

ACQUISITION	
sfrq	499.746
tn	H1
at	3.001
np	63050
sw	10504.2
fb	not used
bs	1
tpwr	56
pw	8.6
d1	1.000
tof	1519.5
nt	10000
ct	17
alock	n
gain	not used
FLAGS	
il	n
in	n
dp	y
hs	nn
DISPLAY	
sp	-249.9
wp	6246.7
vs	88
sc	0
wc	250
hzmm	24.99
is	161.11
rfl	1233.8
rfp	0
th	19
ins	1.000
ai cdc ph	

DEC. & VT	
dfrq	125.672
dn	C13
dpwr	30
dof	0
dm	nnn
dmm	w
dmf	10000
dseq	
dres	1.0
homo	n
PROCESSING	
wtfile	
proc	ft
fn	262144
math	f
werr	
wexp	
wbs	
wnt	wft

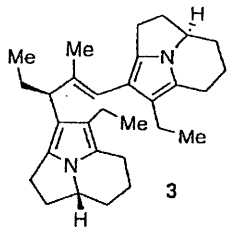

3

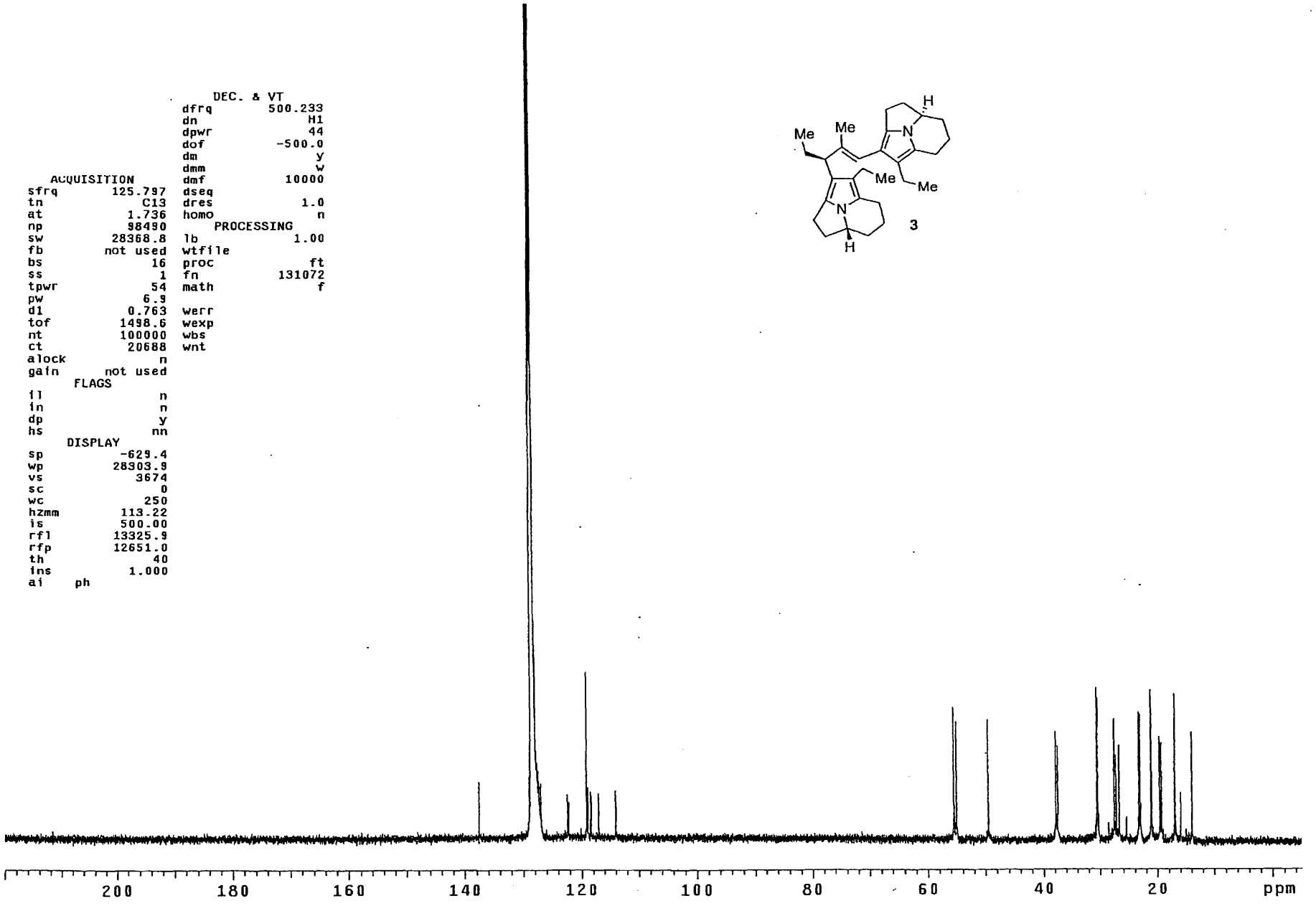
ACQUISITION
sfrq 125.797
tn C13
at 1.736
np 98490
sw 28368.8
fb not used
bs 16
ss 1
tpwr 54
pw 6.9
d1 0.763
tof 1498.6
nt 100000
ct 20688
alock n
gain not used
FLAGS
il n
in n
dp y
hs nn
DISPLAY
sp -629.4
wp 28303.9
vs 3674
sc 0
wc 250
hzmm 113.22
is 500.00
rfl 13325.9
rfp 12651.0
th 40
ins 1.000
ai ph
DEC. & VT
dfrq 500.233
dn H1
dpwr 44
dof -500.0
dm y
dmm w
dmf 10000
dseq
dres 1.0
homo n
PROCESSING
lb 1.00
wtfile
proc ft
fn 131072
math f
werr
wexp
wbs
wnt
Me
Me
Me
Me
N
N
H
H
3
200
180
160
140
120
100
80
60
40
20
ppm

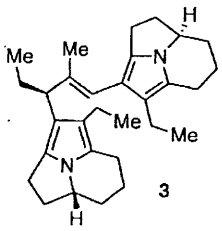
Me
Me
N
H
Me
Me
N
H

3

gCOSY

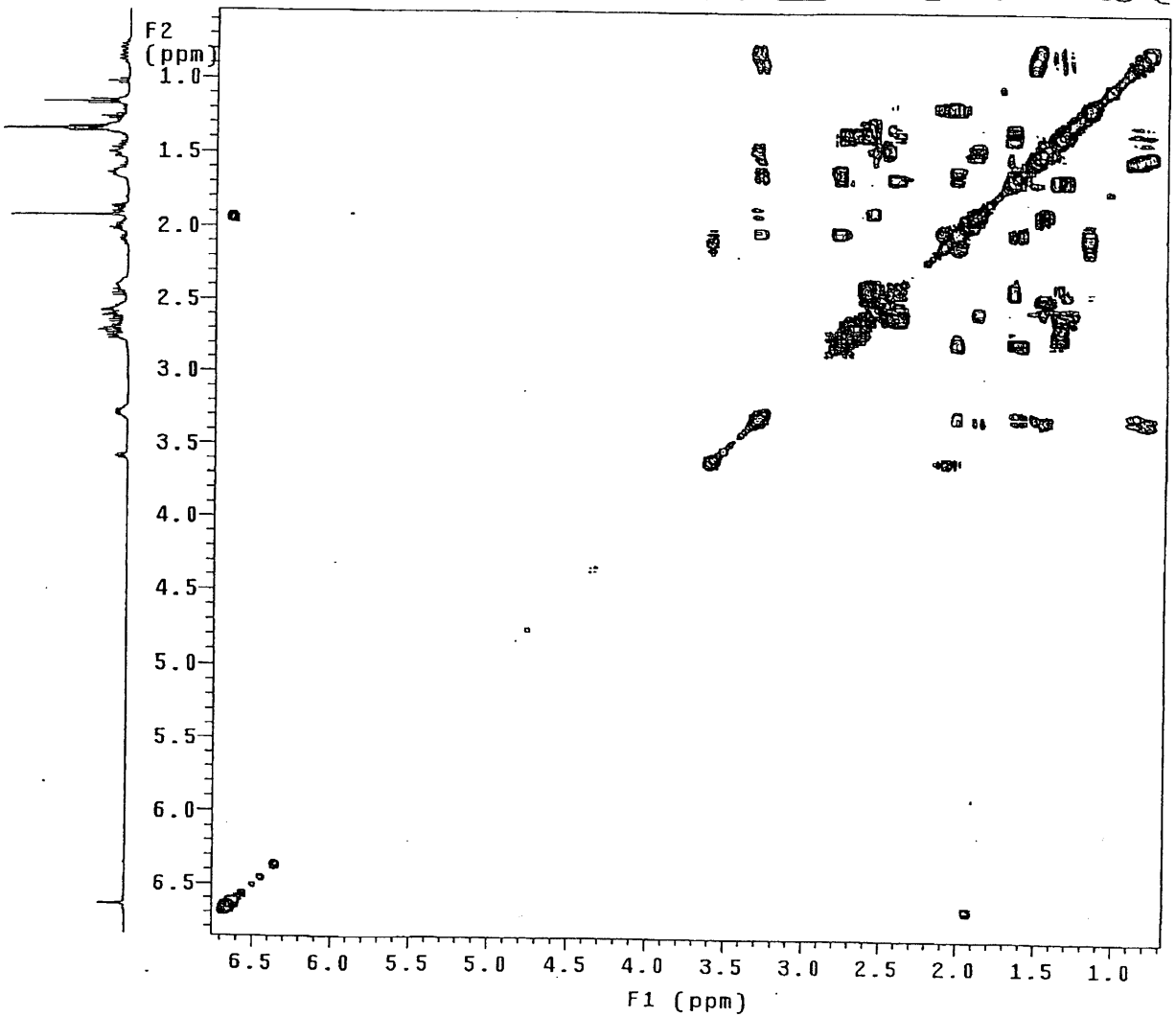
F2 (ppm)
1.0
1.5
2.0
2.5
3.0
3.5
4.0
4.5
5.0
5.5
6.0
6.5
6.5 6.0 5.5 5.0 4.5 4.0 3.5 3.0 2.5 2.0 1.5 1.0
F1 (ppm)

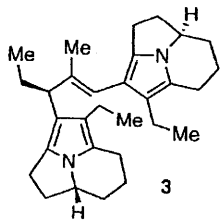
H
Me
Me
N
Me
Me
N
H

3

HSQC

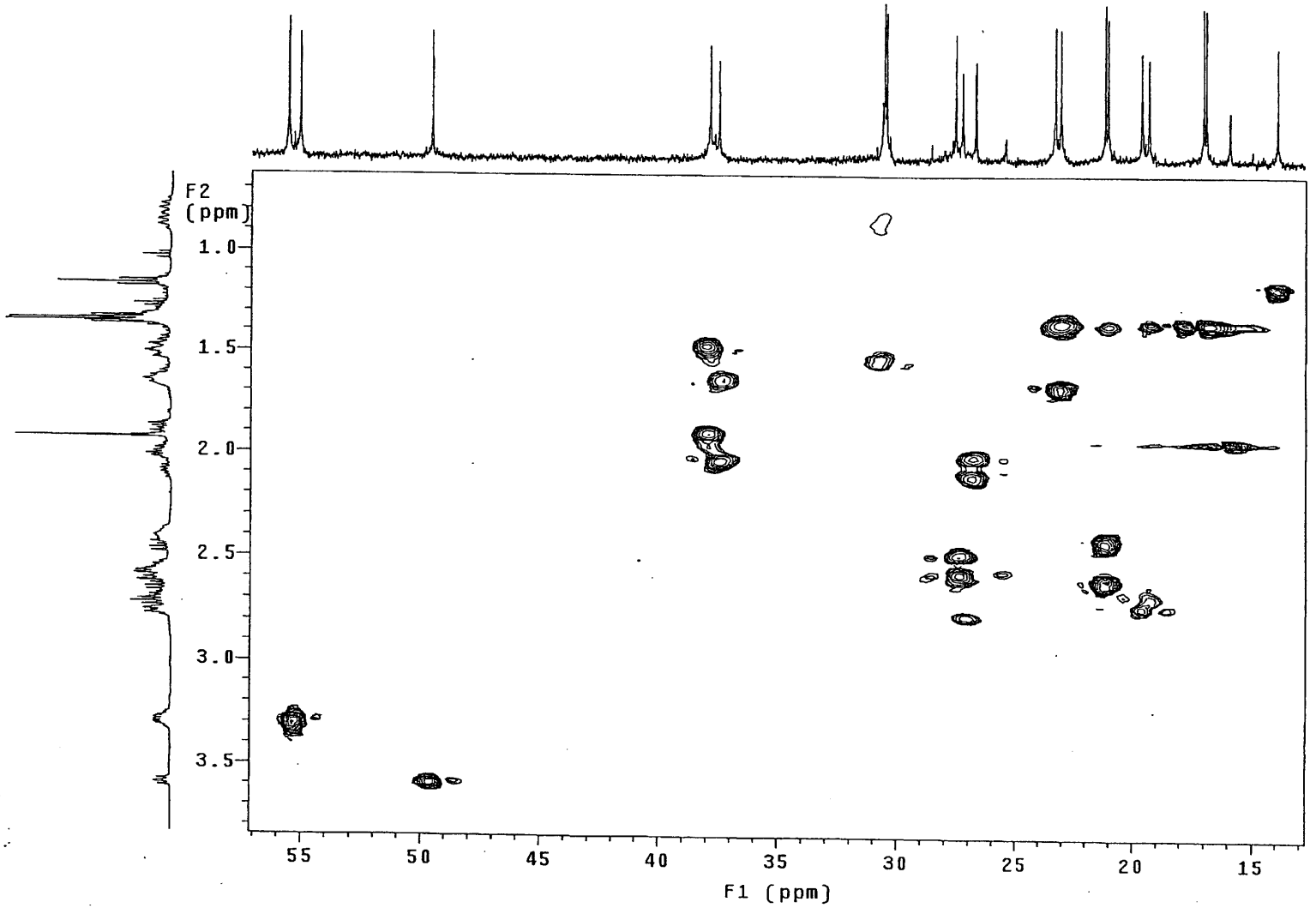
F2
(ppm)
1.0
1.5
2.0
2.5
3.0
3.5
55
50
45
40
35
30
25
20
15
F1 (ppm)

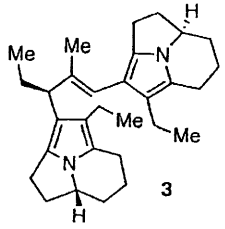
Me
Me
H
N
Me
Me
N
H

3

gHMBC

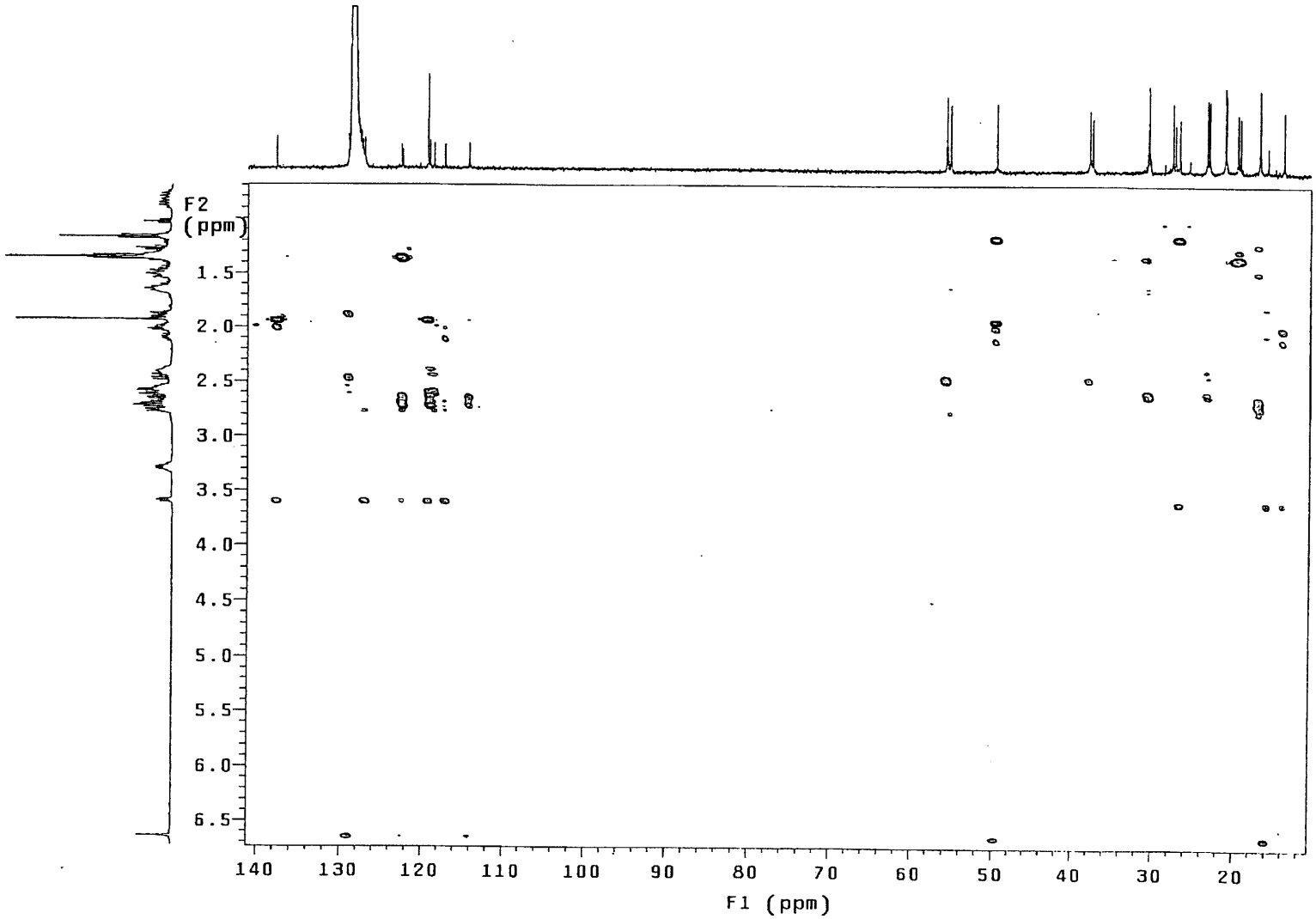
F2
(ppm)
1.5
2.0
2.5
3.0
3.5
4.0
4.5
5.0
5.5
6.0
6.5
140
130
120
110
100
90
80
70
60
50
40
30
20
F1 (ppm)

ACQUISITION		DEC. & VT	
sfrq	499.746	dfrq	125.672
tn	H1	dn	C13
at	3.001	dpwr	30
np	63050	dof	0
sw	10504.2	dm	nnn
fb	not used	dmm	w
bs	1	dmf	10000
tpwr	56	dseq	
pw	8.6	dres	1.0
d1	1.000	homo	n
tof	1519.5	temp	20.0
nt	1000	PROCESSING	
ct	26	wtfile	
alock	n	proc	ft
gain	not used	fn	262144
FLAGS		math	f
il	n	werr	
in	n	wexp	
dp	y	wbs	
hs	nn	wnt	wft
DISPLAY			
sp	-249.9		
wp	6246.7		
vs	152		
sc	0		
wc	250		
hzmm	24.99		
is	33.57		
rfl	1233.8		
rfp	0		
th	35		
ins	1.000		
ai cdc ph			

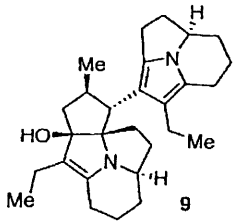

9

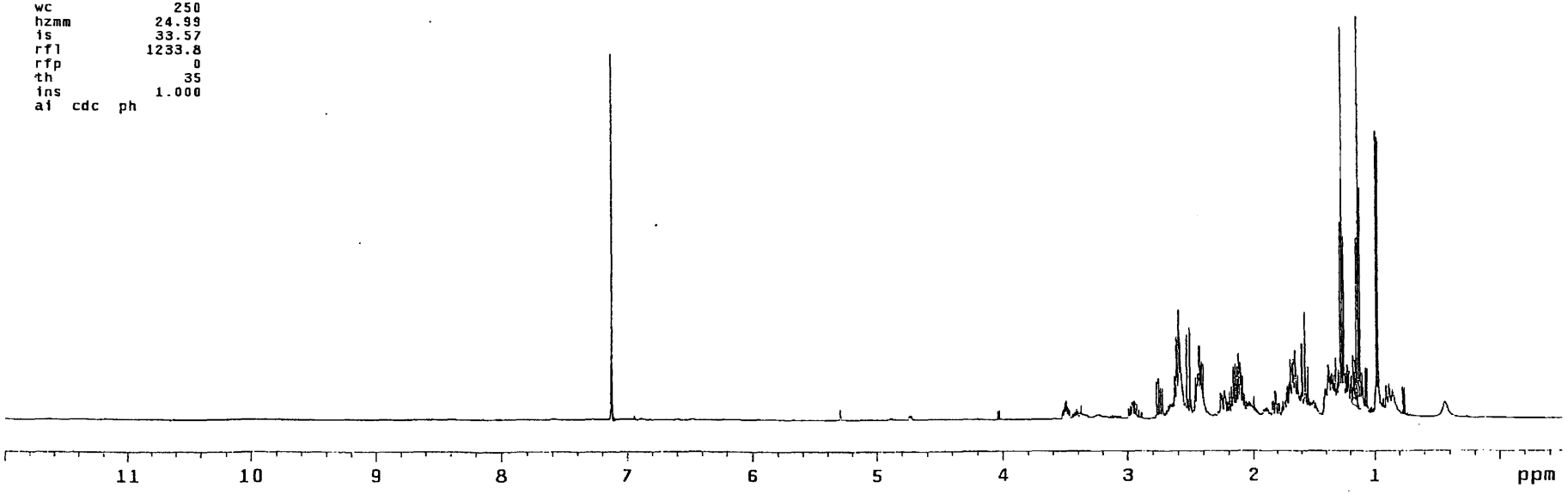

ACQUISITION	
sfrq	125.796
tn	C13
at	1.737
np	87810
sw	25276.5
fb	not used
bs	8
ss	1
tpwr	54
pw	6.9
d1	0.763
tof	556.4
nt	1e+06
ct	17584
alock	n
gain	not used

FLAGS	
il	n
in	n
dp	y
hs	nn

DISPLAY	
sp	-27.4
wp	25232.5
vs	1563
sc	0
wc	250
hzmm	100.93
is	500.00
rfl	12722.0
rfp	12651.0
th	32
ins	1.000
nm	ph

DEC. & VT	
dfrq	500.233
dn	H1
dpwr	44
dof	-500.0
dm	y
dmm	w
dmf	10000
dseq	
dres	1.0
homo	n

PROCESSING	
lb	1.00
wtfile	
proc	ft
fn	131072
math	f
werr	
wexp	
wbs	
wnt	

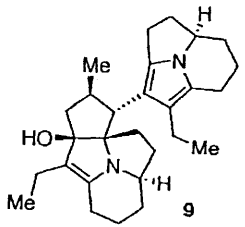

g

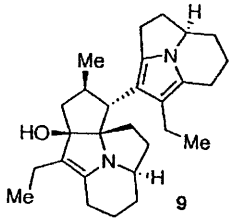
H
N
Me
HO
Me
N
H
Me

9

gCOSY

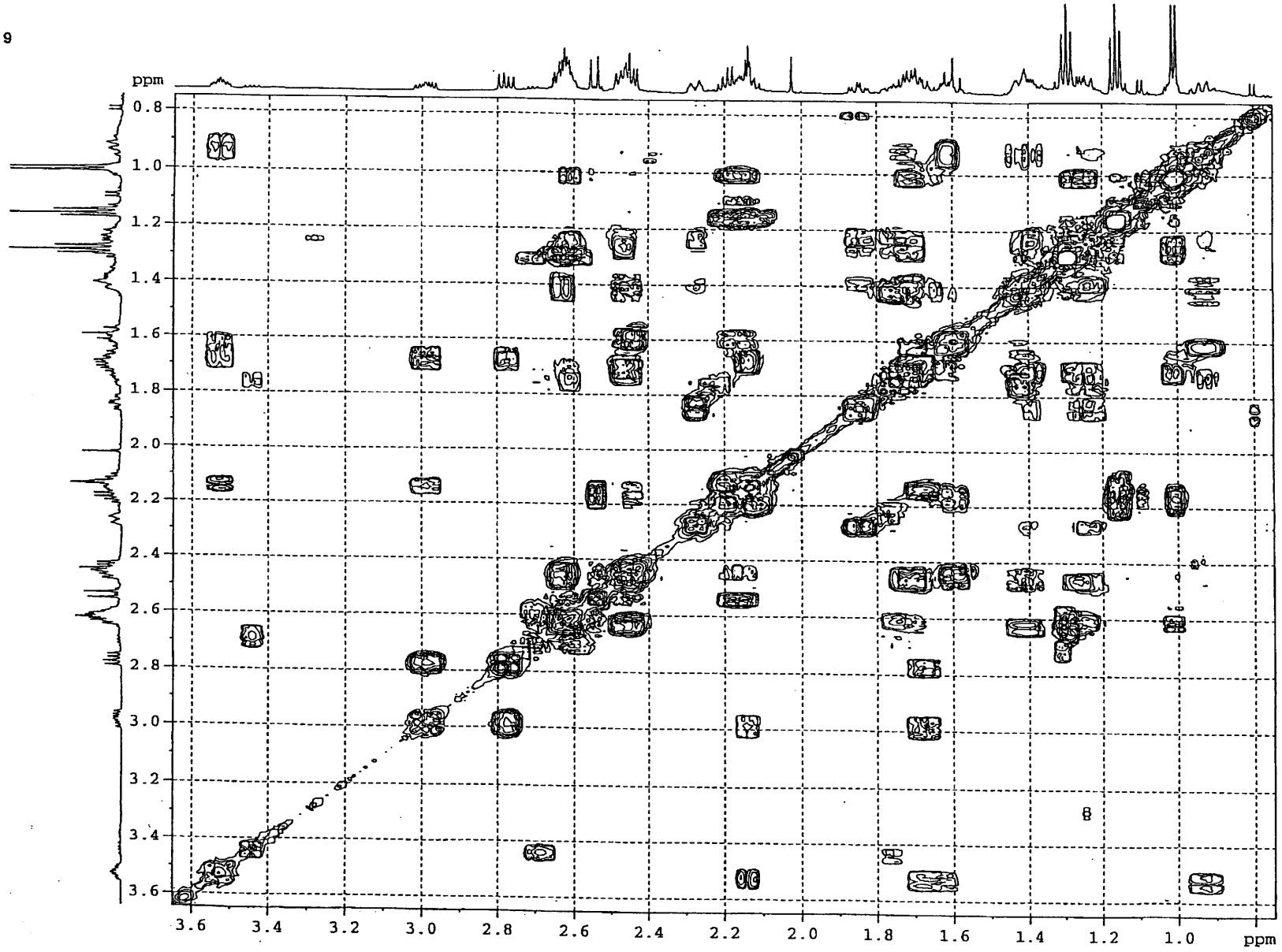
ppm
0.8
1.0
1.2
1.4
1.6
1.8
2.0
2.2
2.4
2.6
2.8
3.0
3.2
3.4
3.6
3.6
3.4
3.2
3.0
2.8
2.6
2.4
2.2
2.0
1.8
1.6
1.4
1.2
1.0
ppm

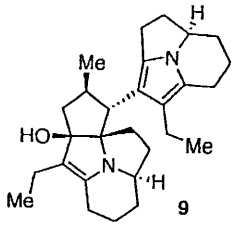
H
Me
N
HO
Me
N
H
Me

9

gHSQC

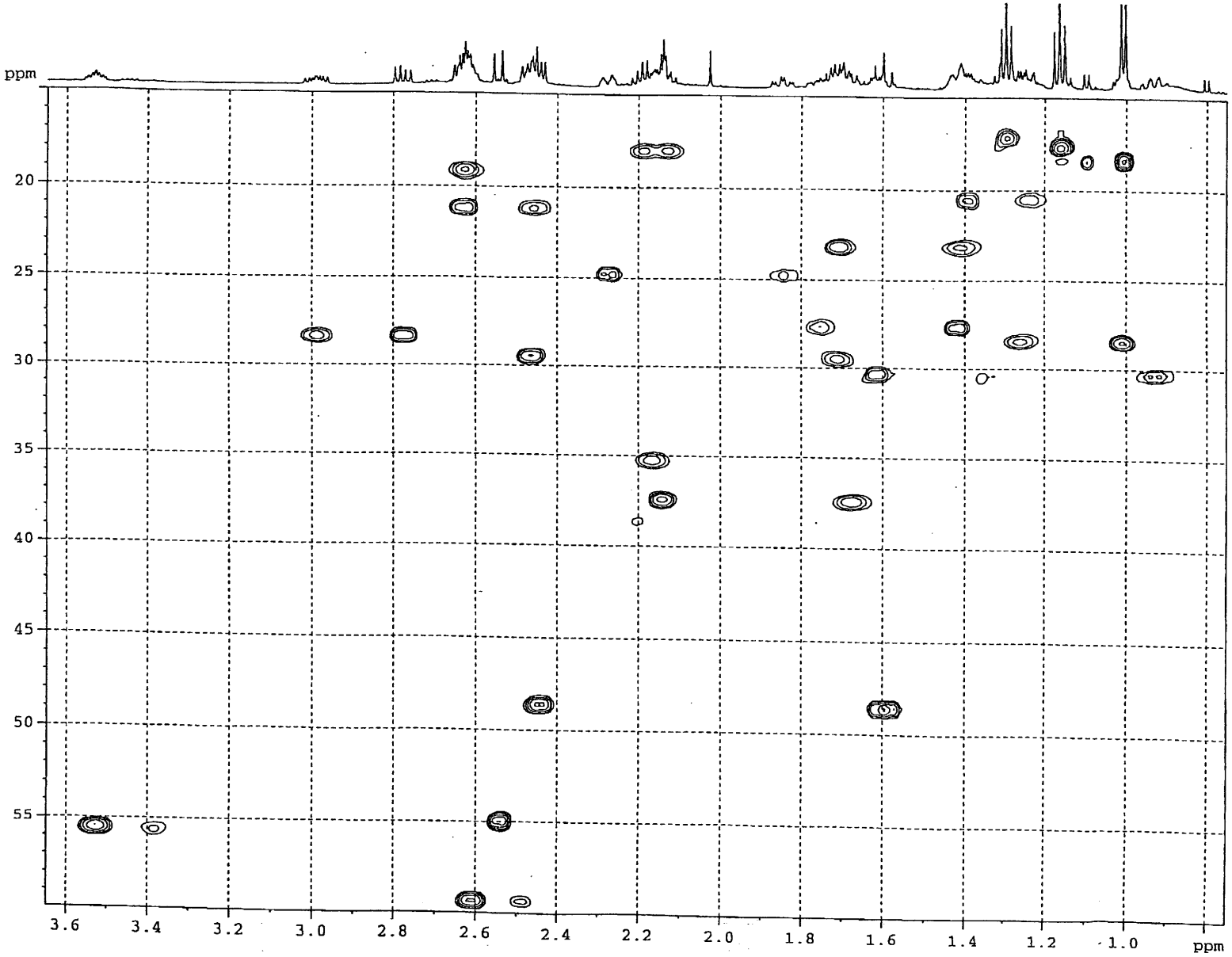
ppm
20
25
30
35
40
45
50
55
3.6
3.4
3.2
3.0
2.8
2.6
2.4
2.2
2.0
1.8
1.6
1.4
1.2
1.0
ppm

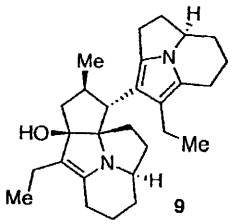
H
Me
N
HO
Me
N
H
Me

9

gHMBC

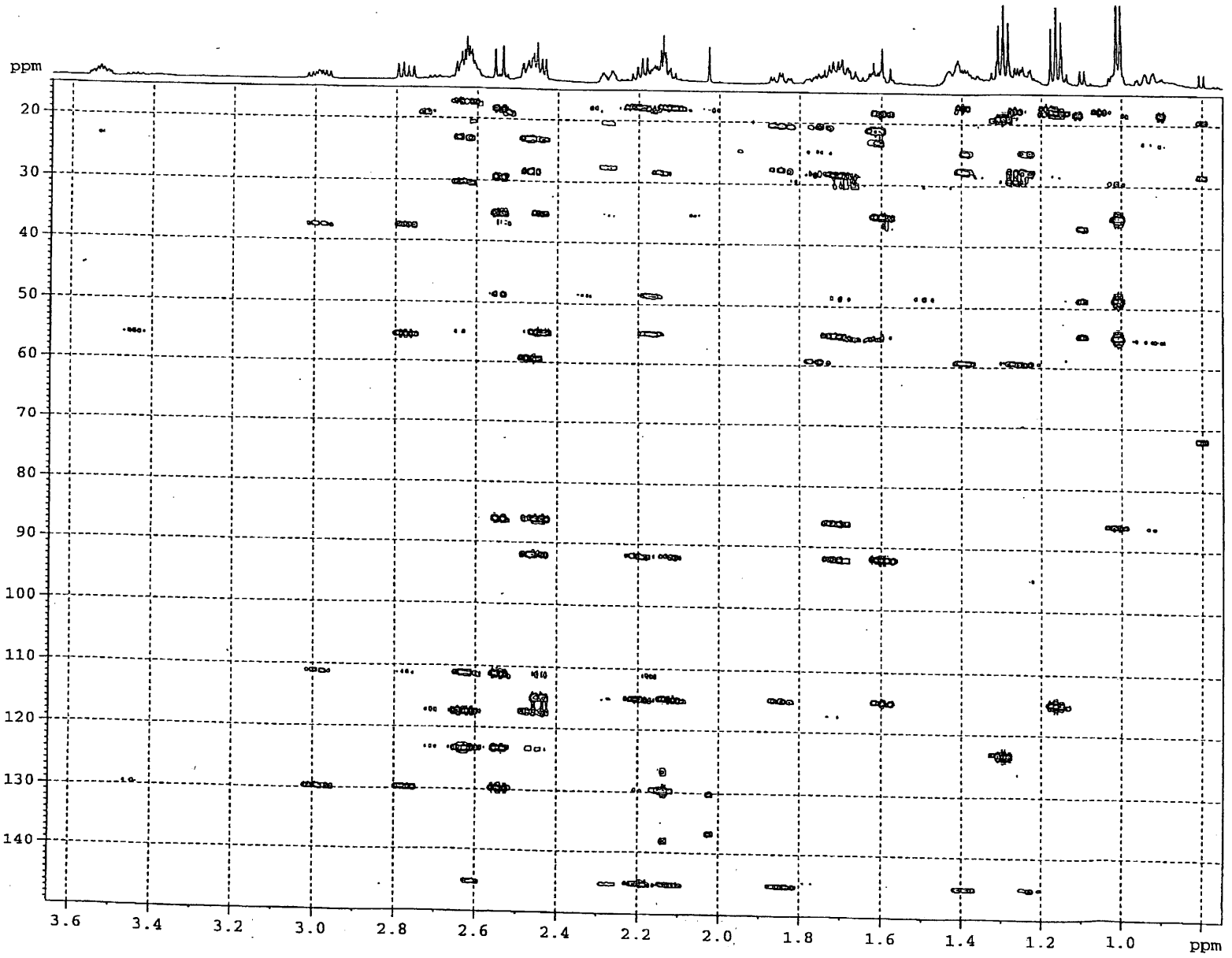
ppm
20
30
40
50
60
70
80
90
100
110
120
130
140
3.6
3.4
3.2
3.0
2.8
2.6
2.4
2.2
2.0
1.8
1.6
1.4
1.2
1.0
ppm

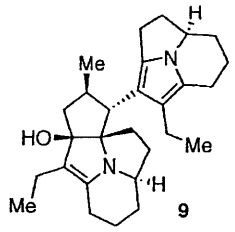
H
Me
N
HO
Me
N
H
Me

9

gNOESY

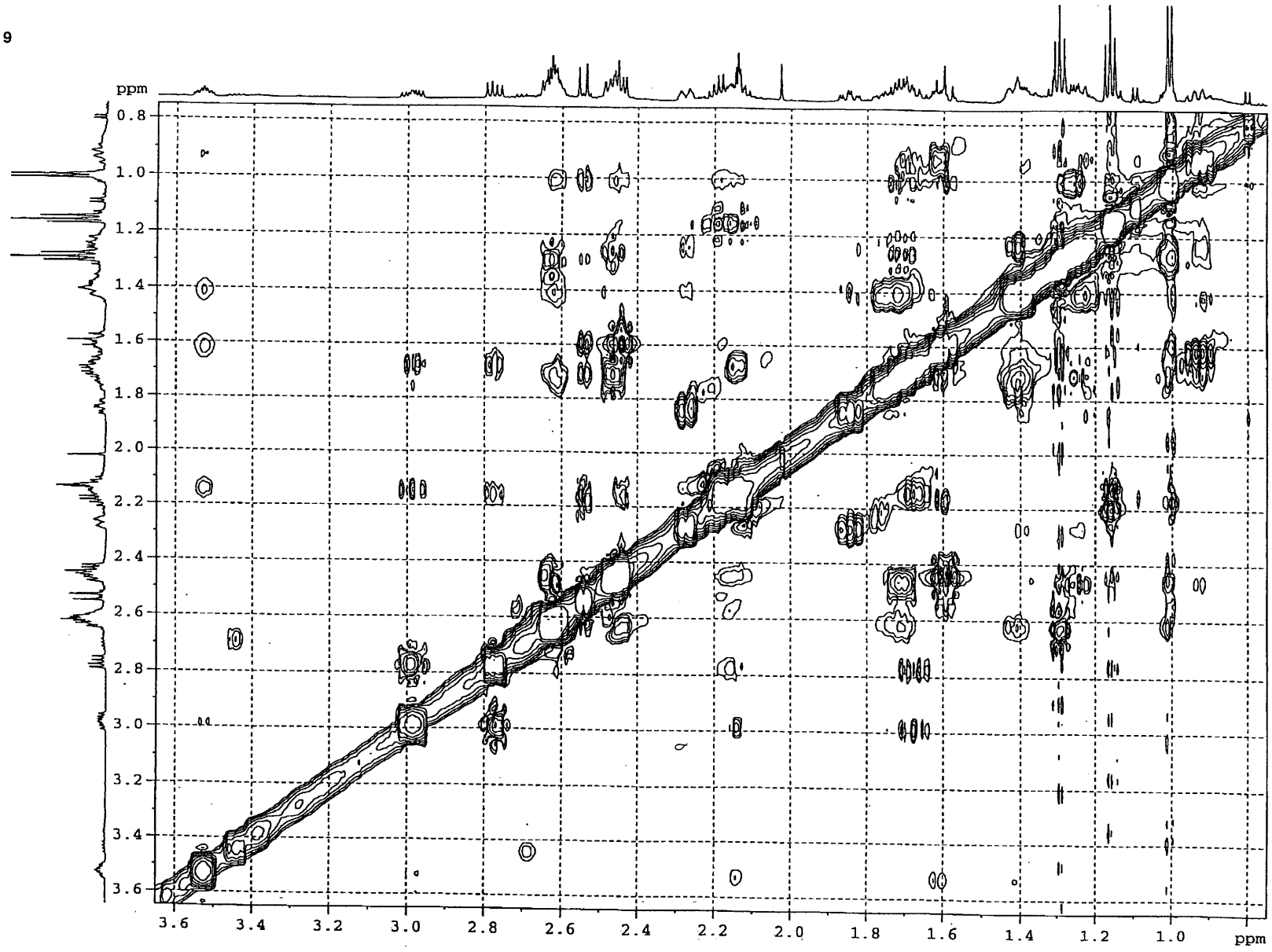
ppm
0.8
1.0
1.2
1.4
1.6
1.8
2.0
2.2
2.4
2.6
2.8
3.0
3.2
3.4
3.6
3.6
3.4
3.2
3.0
2.8
2.6
2.4
2.2
2.0
1.8
1.6
1.4
1.2
1.0
ppm

ACQUISITION		DEC. & VT	
sfrq	499.746	ifrq	125.672
tn	H1	in	C13
at	3.001	dpwr	30
np	63050	dof	0
sw	10504.2	dm	nnn
fb	not used	dmm	w
bs	1	dmf	10000
tpwr	56	dseq	
pw	8.6	dres	1.0
d1	1.000	homo	n
tof	1519.5	temp	20.0
nt	1000	PROCESSING	
ct	33	wtfile	
alock	n	proc	ft
gain	not used	fn	262144
FLAGS		math	f
il	n	werr	
in	n	wexp	
dp	y	wbs	
hs	nn	wnt	wft
DISPLAY			
sp	-249.9		
wp	6246.7		
vs	48		
sc	0		
wc	250		
hzmm	24.99		
is	33.57		
rfl	1233.8		
rfp	0		
th	22		
ins	1.000		
ai cdc ph			

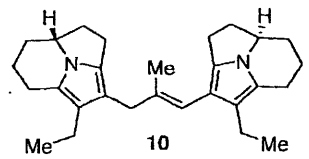

10

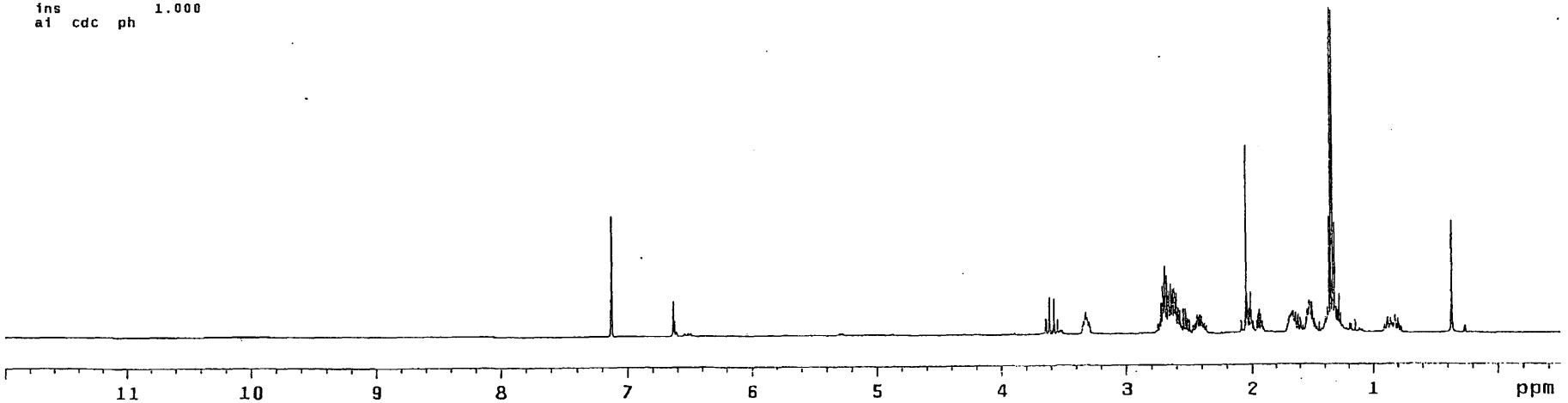

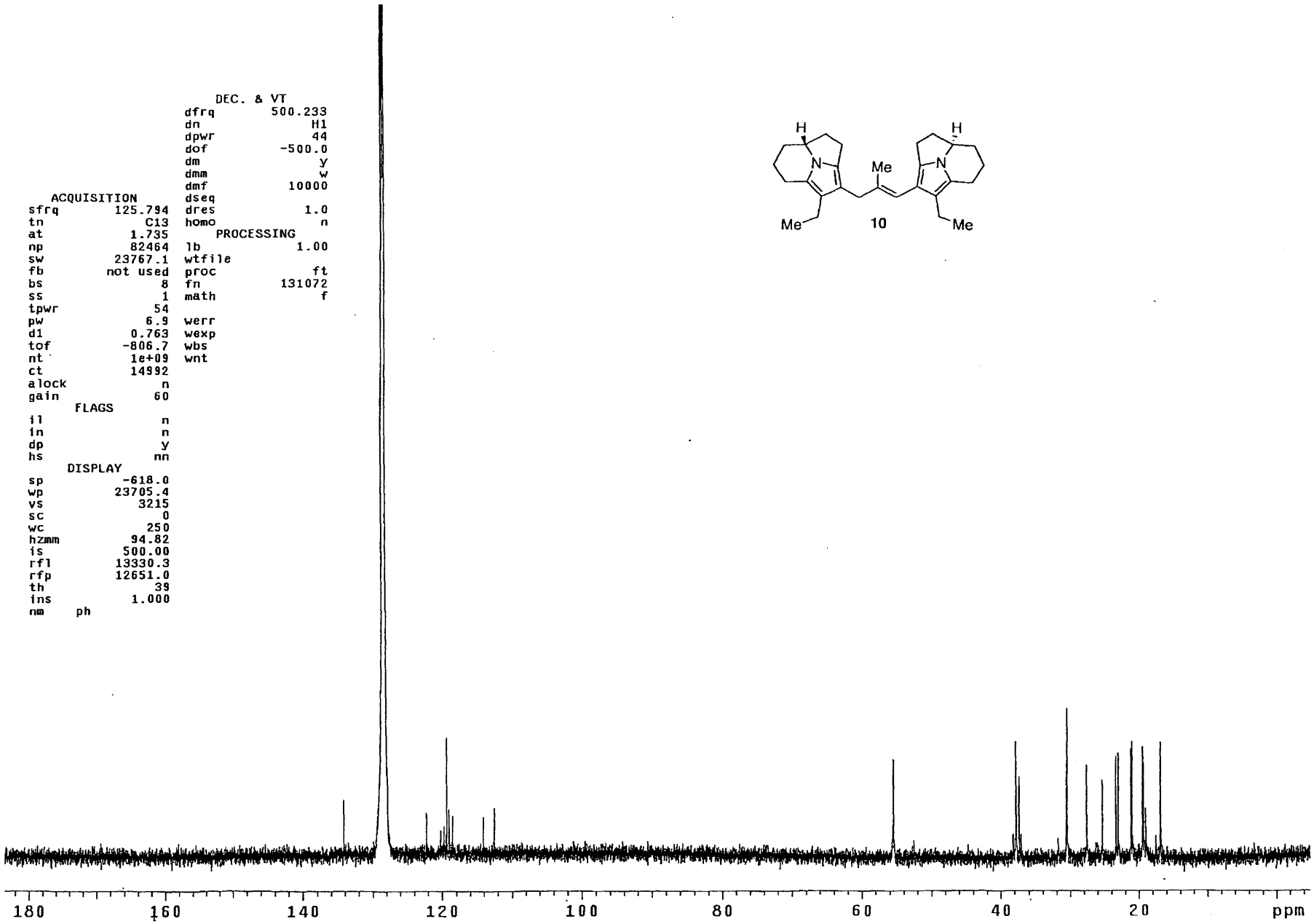
ACQUISITION
sfrq 125.794
tn C13
at 1.735
np 82464
sw 23767.1
fb not used
bs 8
ss 1
tpwr 54
pw 6.9
d1 0.763
tof -806.7
nt 1e+09
ct 14992
alock n
gain 60
FLAGS
il n
in n
dp y
hs nn
DISPLAY
sp -618.0
wp 23705.4
vs 3215
sc 0
wc 250
hzmm 94.82
is 500.00
rfl 13330.3
rfp 12651.0
th 39
ins 1.000
nm ph
DEC. & VT
dfrq 500.233
dn H1
dpwr 44
dof -500.0
dm y
dmm w
dmf 10000
dseq
dres 1.0
homo n
PROCESSING
lb 1.00
wtfile
proc ft
fn 131072
math f
werr
wexp
wbs
wnt
H
N
Me
H
N
Me
Me
10
180
160
140
120
100
80
60
40
20
ppm

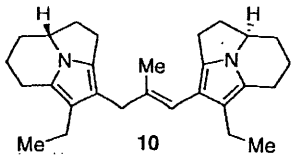

10

gCOSY

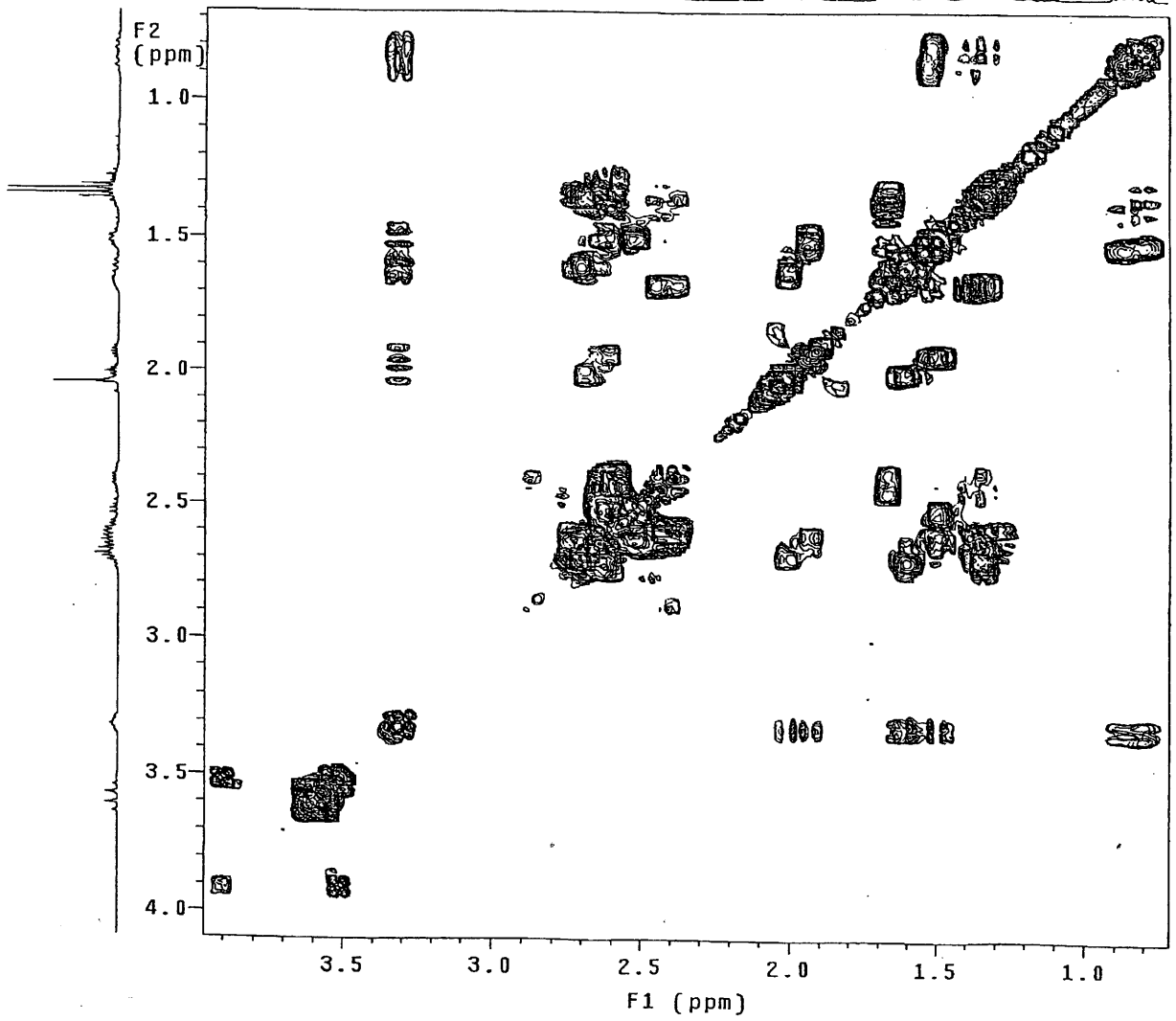

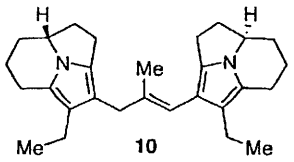
H
N
Me
H
N
Me
Me
10
Me

HSQC

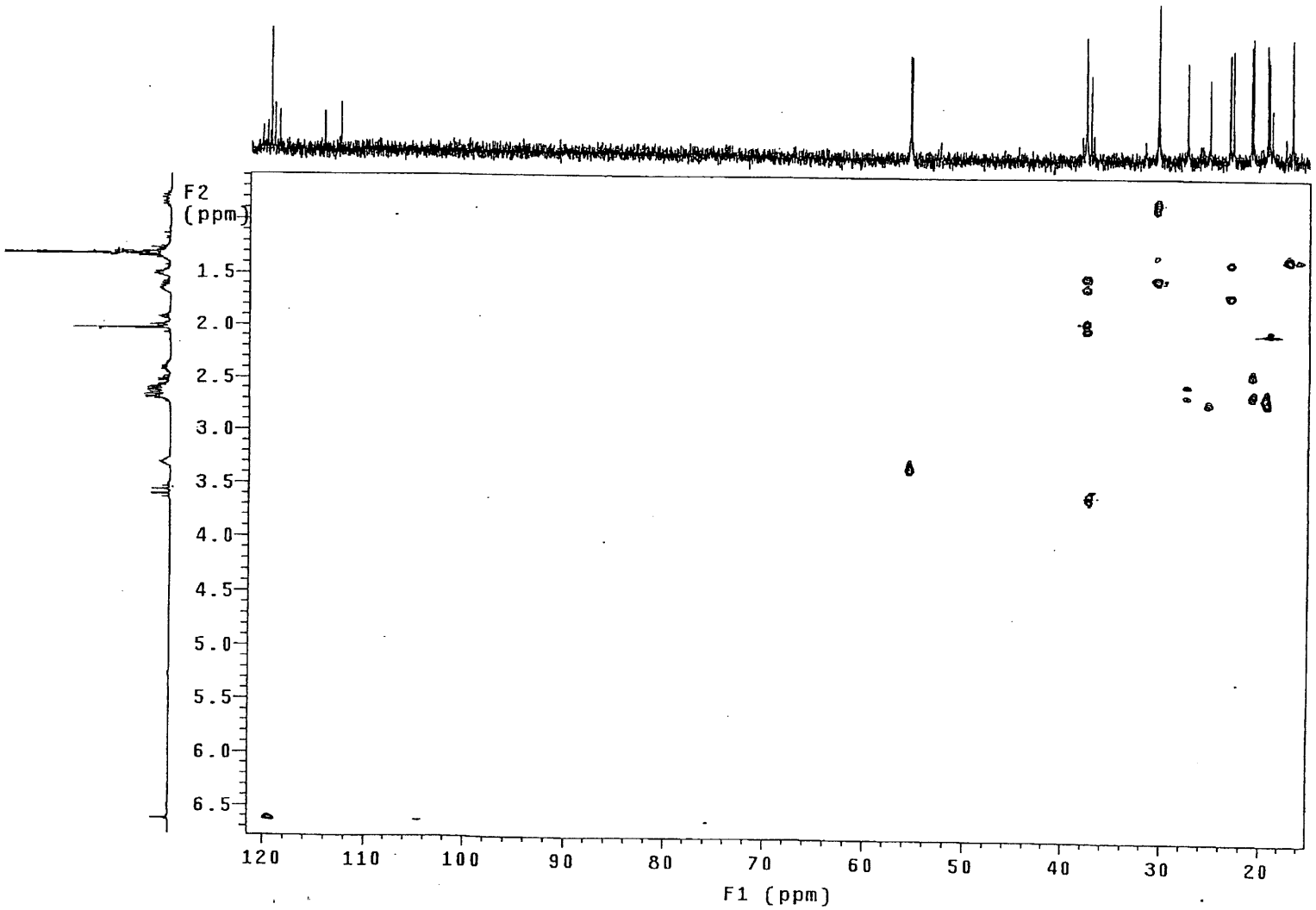
F2
(ppm)
1.5
2.0
2.5
3.0
3.5
4.0
4.5
5.0
5.5
6.0
6.5
120
110
100
90
80
70
60
50
40
30
20
F1 (ppm)

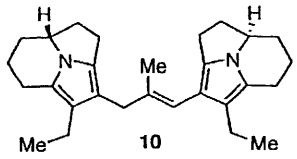
H
H
N
N
Me
Me
Me
10

gHMBC

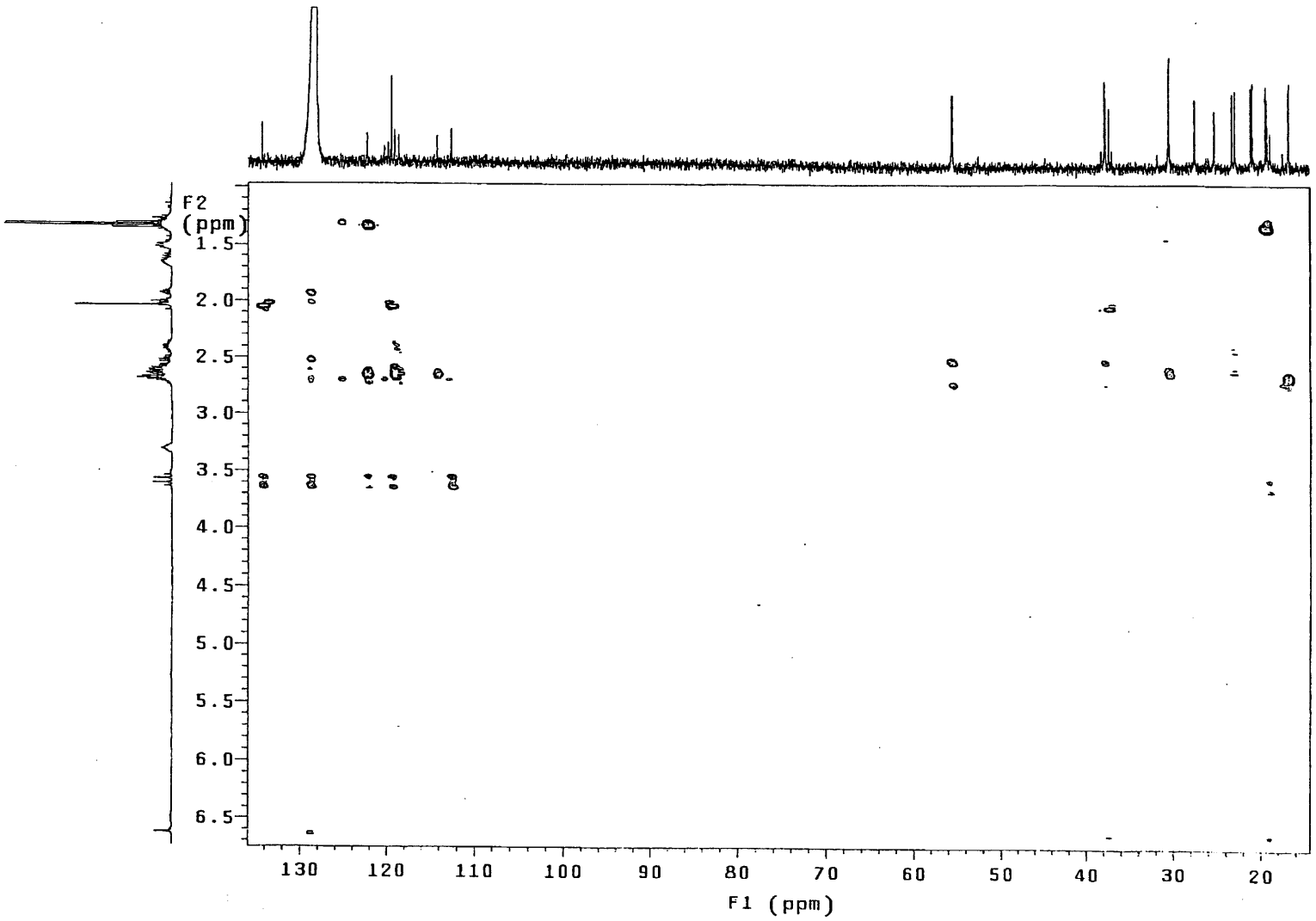
F2
(ppm)
1.5
2.0
2.5
3.0
3.5
4.0
4.5
5.0
5.5
6.0
6.5
130
120
110
100
90
80
70
60
50
40
30
20
F1 (ppm)

ALISON E. ONDRUS

Massachusetts Institute of Technology
Department of Chemistry, 18-225
Cambridge, Massachusetts 02139
aondrus@mit.edu
(617) 258-8806 (work)

Personal

Born August 13, 1981

Education

2003-present **Massachusetts Institute of Technology**, Cambridge, MA, USA
Ph.D. Candidate, Department of Chemistry. Graduation: May 2009
• Thesis: Total Synthesis and Study of Myrmicarin Alkaloids.
Advisor: Professor Mohammad Movassaghi. GPA: 5.0/5.0

2003 **University of Alberta**, Edmonton, Alberta, Canada
BSc Chemistry. Advisor: Margaret-Ann Armour. GPA: 9.0/9.0

Research Experience

2003-present ***Massachusetts Institute of Technology***
Department of Chemistry, Advisor: Professor Mohammad Movassaghi
Graduate Research Assistant
• Total synthesis and study of Myrmicarin alkaloids.

2001-2003 ***University of Alberta***
Summer 2003 Department of Chemistry, Advisor: Professor Dennis Hall
Undergraduate Research Assistant
• Transition-metal catalysts for alkene hydroboration.
Summer 2002 Department of Chemistry, Advisor: Professor Frederick G. West
Undergraduate Research Assistant
• Cascade approaches for the synthesis of marine polyether toxins.
Summer 2001 Department of Chemistry, Advisor: Professor Derrick L. G. Clive
Undergraduate Research Assistant
• Total synthesis of the anti-cancer compound (+)-puraquinonic acid.

Teaching Experience

2008 One semester of teaching assistantship for an undergraduate chemistry class at MIT. (Professor G. C. Fu)
2004 One semester of teaching assistantship for a graduate chemistry class at MIT. (Professor M. Movassaghi)
2003 One semester of teaching assistantship for an undergraduate chemistry class at MIT. (Professors S. T. Ceyer and C. C. Cummins)

Academic Honors and Awards

2007	Roche Symposium: Excellence in Chemistry Award
2007	Morse Travel Grant for Graduate Students (MIT), for research accomplishments
2005	Novartis Graduate Fellowship for Women and Minorities in Chemistry
2004	Award for Outstanding Teaching (MIT)
2004	SYNLETT Star Journal Award, for academic excellence
2003	Robert T. Haslam Presidential Graduate Fellow (MIT), for academic excellence
2003	Gold Medal in Chemistry (University of Alberta), for academic excellence
2002-2001	Two-time recipient of the NSERC Undergraduate Student Research Award
2002-2001	Two-time recipient of the Alberta Heritage Medical Research Foundation Summer Studentship
2002-2001	Two-time recipient of the Jason Lang Scholarship (Government of Alberta), for academic excellence
2002	AstraZeneca Undergraduate Scholarship
2002	Mar Prize in Inorganic Chemistry (University of Alberta)
2002	Pfizer Summer Undergraduate Research Fellowship
2001	Raylo Chemicals Prize in Carbohydrate Chemistry
2001	Fred H. Irwin Memorial Prize in Organic Chemistry (University of Alberta)
2001	Arthur Scroggie Scholarship (University of Alberta), for academic excellence
2001	Faculty of Science Undergraduate Scholarship for Students Entering Second Year (University of Alberta), for academic excellence
2000	Louise McKinney Scholarship (Government of Alberta), for academic excellence

Publications

• Ondrus, A. E.; Movassaghi, M. "Reversible Dimerization of (+)–Myrmicarin 215B." *Org. Lett.* **2009**, *submitted.*

• Ondrus, A. E.; Movassaghi, M. "Total Synthesis and Study of Myrmicarin Alkaloids." *Chem. Commun.* **2009**, *accepted.*

• Guggenheim, E. R.; Ondrus, A. E.; Movassaghi, M.; Lippard, S. J. "Poly(ADP-ribose) Polymerase-1 Activity Facilitates the Dissociation of Nuclear Proteins From Platinum-Modified DNA." *Bioorg. Med. Chem.* **2008**, *16*, 10121–10128.

• Movassaghi, M.; Ondrus, A. E.; Chen, B. "Efficient and Stereoselective Dimerization of Pyrroloindolizine Derivatives Inspired by a Hypothesis for the Biosynthesis of Complex Myrmicarin Alkaloids." *J. Org. Chem.* **2007**, *72*, 10065–10074.

• Ondrus, A. E.; Movassaghi, M. "Dimerization of (+)-Myrmicarin 215B. A Potential Biomimetic Approach to Complex Myrmicarin Alkaloids." *Tetrahedron* **2006**, *62*, 5287–5297.

• Movassaghi, M.; Ondrus, A. E. "Enantioselective Total Synthesis of Tricyclic Myrmicarin Alkaloids." *Org. Lett.* **2005**, *7*, 4423–4426.

• Movassaghi, M.; Ondrus, A. E. "Palladium-Catalyzed Synthesis of *N*-Vinyl Pyrroles and Indoles." *J. Org. Chem.* **2005**, *70*, 8638–8641.

Presentations

- "Total Synthesis and Study of Myrmicarin Alkaloids." Mohammad Movassaghi and Alison Ondrus. Presented by Alison Ondrus at the 234th ACS National Meeting, Boston, MA, August 2007.
- "Total Synthesis and Study of Myrmicarin Alkaloids." Presented by Alison Ondrus at the 2007 Roche Excellence in Chemistry Fellowship Recipient Conference, Nutley, NJ, May 2007.
- "Total Synthesis and Study of Myrmicarin Alkaloids." Mohammad Movassaghi and Alison Ondrus. Presented by Alison Ondrus at the Gordon Research Conference, Newport, RI, June 2007.
- "Total Synthesis and Study of Myrmicarin Alkaloids." Presented by Alison Ondrus at the Massachusetts Institute of Technology Fourth Year Graduate Symposium, Cambridge, MA, May 2007.
- "Studies Toward Enantioselective Total Synthesis of the Complex Myrmicarin Alkaloids." Presented by Alison Ondrus at the 2005 Novartis Graduate Fellowship Recipient Conference, Cambridge, MA, October 2005.
- "A Cascade Approach to the Polyether Toxins." Alison Ondrus, and Frederick G. West. Presented by Alison Ondrus at the Pfizer Student Undergraduate Research Award Conference, La Jolla, CA, September 2002.

References

Professor Mohammad Movassaghi
Massachusetts Institute of Technology
Department of Chemistry
77 Massachusetts Avenue
18-292
Cambridge, MA 02139
Phone: (617) 253-3986
movassag@mit.edu

Professor Rick L. Danheiser
Massachusetts Institute of Technology
Department of Chemistry
77 Massachusetts Avenue
18-298
Cambridge, MA 02139
Phone: (617) 253-1842
danheisr@mit.edu

Professor Gregory C. Fu
Massachusetts Institute of Technology
Department of Chemistry
77 Massachusetts Avenue
18-290
Cambridge, MA 02139
Phone: (617) 253-2664
gcf@mit.edu